

SOLAR PHOTO RATES FOR PLANETARY ATMOSPHERES AND ATMOSPHERIC POLLUTANTS

W. F. HUEBNER

Southwest Research Institute, San Antonio, Texas, U.S.A.

and

Los Alamos National Laboratory, Los Alamos, NM, U.S.A.

and

J. J. KEADY and S. P. LYON

Los Alamos National Laboratory, Los Alamos, NM, U.S.A.

(Received 8 April, 1991)

Abstract. Unattenuated solar photo rate coefficients and excess energies for dissociation, ionization, and dissociative ionization are presented for atomic and molecular species that have been identified or are suspected to exist in the atmospheres of planets, satellites (moons), comets, or as pollutants in the Earth atmosphere. The branching ratios and cross sections with resonances have been tabulated to the greatest detail possible and the rate coefficients and excess energies have been calculated from them on a grid of small wavelength bins for the quiet and the active Sun at 1 AU heliocentric distance.

1. Introduction

Photo rate coefficients for atomic and molecular species that have been identified or are suspected to exist in the atmospheres of planets, satellites (moons), and comets, or as pollutants in the Earth atmosphere are needed for analysis and modeling. Lifetimes (reciprocals of rate coefficients) for possible mother molecules of observed radicals in comets were determined by Potter and del Duca (1964) and by Jackson (1976a, b). Some rate coefficients for several atomic and simple molecular constituents of lunar and planetary atmospheres have been calculated by Siscoe and Mukherjee (1972), McElroy and Hunten (1970), McElroy and McConnell (1971), and McElroy *et al.* (1976), for Io by Kumar (1982), for Earth thermospheric constituents by Banks and Kockarts (1973) and Torr *et al.* (1979), and for solar wind physics by Axford (1972). In addition, lifetimes for some isolated species or rate coefficients in very limited wavelength bands – e.g., the solar hydrogen L α line – have been obtained by various investigators for special situations and applications. The compilation presented by Whipple and Huebner (1976), showed little overlap of calculated and observed lifetimes of molecules in the solar radiation field. The calculation of rate coefficients for 26 atomic and molecular species made by Huebner and Carpenter (1979) increased the overlap somewhat. Their work has been extended here to over 80 species.

If the chief concern is the prediction of potential mother molecules of observed radicals, then only the main decay branch needs to be considered. For molecules the main branch is almost always a dissociation, very seldom ionization, and never photo-

TABLE I
Solar photon flux (photons cm⁻² s⁻¹ bin⁻¹) bracketed by wavelengths (Å)

Wavelength	Flux								
0	1.00E-01	520	2.42E+08	1090	1.31E+08	1351	3.09E+09	1961	1.01E+12
2	3.00E+01	540	3.62E+08	1100	1.31E+08	1360	2.57E+09	1980	1.20E+12
4	2.50E+03	560	5.17E+07	1110	1.31E+08	1370	2.74E+09	2000	1.44E+12
6	2.80E+04	580	1.02E+09	1120	6.21E+08	1379	3.10E+09	2020	1.80E+12
8	1.80E+05	600	5.52E+08	1130	1.31E+08	1389	7.60E+09	2041	2.08E+12
10	4.00E+06	620	1.20E+09	1140	1.31E+08	1408	1.01E+10	2062	2.45E+12
40	4.70E+07	630	1.15E+08	1150	9.15E+07	1428	1.30E+10	2083	5.09E+12
50	8.30E+07	680	3.39E+08	1157	7.84E+07	1449	1.82E+10	2105	7.12E+12
60	1.03E+08	710	1.59E+08	1163	1.03E+08	1470	2.33E+10	2128	9.23E+12
70	9.40E+07	740	5.19E+08	1170	2.66E+08	1492	2.66E+10	2150	8.42E+12
80	1.20E+08	770	1.28E+09	1176	1.12E+08	1515	2.90E+10	2174	1.20E+13
90	9.90E+07	800	8.07E+08	1183	1.24E+08	1538	3.60E+10	2198	1.22E+13
100	5.60E+07	830	2.05E+09	1190	1.82E+08	1562	4.75E+10	2222	1.77E+13
110	2.50E+07	860	2.73E+09	1198	1.90E+08	1587	6.40E+10	2247	1.60E+13
120	1.20E+07	890	3.34E+09	1205	7.40E+08	1613	5.49E+10	2273	1.96E+13
128	3.07E+08	911	9.39E+07	1212	3.02E+11	1639	1.19E+11	2299	2.40E+13
153	9.00E+08	920	2.34E+08	1220	3.67E+09	1667	1.76E+11	2326	2.25E+13
176	3.70E+09	930	5.84E+08	1227	1.36E+09	1695	2.32E+11	2353	2.21E+13
205	1.40E+09	940	5.94E+08	1235	1.61E+09	1724	1.44E+11	2381	2.32E+13
231	2.65E+09	950	1.04E+08	1242	1.32E+09	1739	1.83E+11	2410	2.50E+13
270	4.50E+08	960	1.04E+08	1250	1.41E+09	1754	2.34E+11	2439	2.73E+13
280	1.54E+09	970	5.30E+09	1258	3.11E+09	1770	2.62E+11	2469	2.88E+13
300	5.84E+09	980	7.56E+08	1266	1.06E+09	1786	2.88E+11	2500	3.02E+13
320	1.16E+09	995	1.25E+08	1274	1.37E+09	1802	3.14E+11	2532	3.97E+13
340	4.50E+08	1007	1.04E+08	1282	1.02E+09	1818	3.81E+11	2564	7.13E+13
360	1.31E+09	1017	3.60E+09	1290	1.14E+09	1835	4.43E+11	2597	4.37E+13
370	1.77E+08	1027	2.46E+09	1299	7.29E+09	1852	4.95E+11	2632	1.12E+14
400	2.76E+08	1035	1.83E+09	1307	2.20E+09	1869	5.94E+11	2667	1.25E+14
430	1.77E+08	1045	1.57E+08	1316	1.59E+09	1887	6.59E+11	2703	1.16E+14
460	2.12E+08	1057	1.70E+08	1324	2.21E+09	1905	7.26E+11	2740	1.19E+14
480	4.32E+08	1070	1.31E+08	1333	1.24E+10	1923	9.85E+11	2778	1.38E+14
500	6.32E+08	1080	7.21E+08	1342	1.99E+09	1942	1.27E+12	2817	1.70E+14

Table I (continued)

Wavelength	Flux								
2857	2.46E+14	4475	2.48E+15	6125	2.70E+15	9050	4.01E+15	23500	6.83E+15
2899	3.90E+14	4525	2.49E+15	6175	2.70E+15	9150	3.89E+15	24500	6.07E+15
2941	3.99E+14	4575	2.48E+15	6225	2.69E+15	9250	3.88E+15	25500	5.50E+15
2985	3.86E+14	4625	2.50E+15	6275	2.68E+15	9350	3.78E+15	26500	4.96E+15
3030	5.08E+14	4675	2.55E+15	6325	2.67E+15	9450	3.76E+15	27500	4.51E+15
3077	5.92E+14	4725	2.61E+15	6375	2.66E+15	9550	3.72E+15	28500	4.09E+15
3125	6.05E+14	4775	2.59E+15	6425	2.65E+15	9650	3.72E+15	29500	3.74E+15
3175	6.94E+14	4825	2.46E+15	6475	3.95E+15	9750	3.79E+15	30500	3.40E+15
3225	8.12E+14	4875	2.44E+15	6550	5.22E+15	9850	3.79E+15	31500	3.18E+15
3275	9.71E+14	4925	2.53E+15	6650	5.18E+15	9950	7.49E+15	32500	2.87E+15
3325	8.97E+14	4975	2.48E+15	6750	5.14E+15	10150	2.11E+16	33500	2.70E+15
3375	9.44E+14	5025	2.49E+15	6850	5.09E+15	10750	1.68E+16	34500	2.47E+15
3425	1.01E+15	5075	2.50E+15	6950	5.04E+15	11250	1.60E+16	35500	2.31E+15
3475	1.03E+15	5125	2.43E+15	7050	4.99E+15	11750	1.50E+16	36500	2.14E+15
3525	1.03E+15	5175	2.43E+15	7150	4.94E+15	12250	1.48E+16	37500	2.01E+15
3575	1.04E+15	5225	2.52E+15	7250	4.90E+15	12750	1.43E+16	38500	1.87E+15
3625	1.18E+15	5275	2.58E+15	7350	4.83E+15	13250	1.32E+16	39500	1.71E+15
3675	1.23E+15	5325	2.64E+15	7450	4.80E+15	13750	1.25E+16	40500	1.60E+15
3725	1.24E+15	5375	2.67E+15	7550	4.67E+15	14250	1.16E+16	41500	1.48E+15
3775	1.17E+15	5425	2.70E+15	7650	4.59E+15	14750	1.12E+16	42500	1.41E+15
3825	1.11E+15	5475	2.68E+15	7750	4.68E+15	15250	1.07E+16	43500	1.33E+15
3875	1.09E+15	5525	2.66E+15	7850	4.54E+15	15750	9.95E+15	44500	1.25E+15
3925	1.19E+15	5575	2.66E+15	7950	4.60E+15	16250	9.72E+15	45500	1.16E+15
3975	1.54E+15	5625	2.67E+15	8050	4.53E+15	16750	9.20E+15	46500	1.06E+15
4025	1.90E+15	5675	2.67E+15	8150	4.41E+15	17250	8.24E+15	47500	9.67E+14
4075	1.99E+15	5725	2.69E+15	8250	4.34E+15	17750	7.70E+15	48500	9.25E+14
4125	1.99E+15	5775	2.71E+15	8350	4.31E+15	18250	6.94E+15	49500	2.84E+15
4175	2.02E+15	5825	2.71E+15	8450	4.03E+15	18750	6.51E+15	52750	6.74E+15
4225	2.01E+15	5875	2.71E+15	8550	4.33E+15	19250	6.19E+15	65000	3.35E+15
4275	1.94E+15	5925	2.72E+15	8650	4.25E+15	19750	7.46E+15	75000	2.22E+15
4325	1.98E+15	5975	2.72E+15	8750	4.27E+15	20375	1.11E+16	85000	1.59E+15
4375	2.25E+15	6025	2.71E+15	8850	4.23E+15	21500	8.28E+15	95000	4.53E+15
4425	2.39E+15	6075	2.70E+15	8950	4.13E+15	22500	7.33E+15	140000	

dissociative ionization. This is immediately apparent from the magnitude of the threshold wavelengths for these processes (see Table I) – although a small photodissociation and a large ionization cross section near the respective thresholds can invalidate such an oversimplified prediction. Predissociation and autoionization significantly increase rate coefficients (decrease lifetimes) and, if known, are included in the evaluations presented here.

Dissociation rate coefficients presented in the literature are often based only on broad averages over bandwidths of 100 Å or more, and at wavelengths not below that of the hydrogen L α line (1215.7 Å). Details about branching ratios are usually also ignored. For terrestrial atmospheric constituents, cross sections have been compiled by Huffman (1971) and rate coefficients by Bauer and Bortner (1978). Preferred cross sections, branching ratios, and threshold wavelengths for neutral species occurring in middle atmosphere chemistry have been evaluated by the CODATA Task Group on Chemical Kinetics (Baulch *et al.*, 1980, 1982, 1984), while NASA has evaluated and compiled preferred cross sections for use in stratospheric modeling (DeMore *et al.*, 1982). Whenever possible, we have gone to the original references for these data and supplemented them with additional data when available. For the extreme UV and X-ray region we have supplemented the cross sections for molecules from the sum of the cross sections of the atomic constituents. Cross sections with resonances have been tabulated to the greatest detail possible and rate coefficients are calculated for small wavelength bins. Most of the known branching ratios are taken into account as a function of wavelength, but where necessary, some values have been estimated. In addition cross sections are estimated for some metastable states.

In Section 2 the solar spectrum is presented for the nonflaring Sun at medium activity. Also the ratio of the irradiances for the Sun near solar maximum to that of the nonflaring Sun at medium activity as presented by Lean (1987) based on the Atmospheric Explorer E (AE-E) data of Hinteregger *et al.* (1981) is shown, prorated to the wavelength grid used here. In the following we will refer to these simply as the quiet and the active Sun. Section 3 presents the computed rate coefficients for each photo process together with the sources for the cross sections, the thresholds, the branching ratios, and the excess energies. For easy reference the rate coefficients for each process and the sum for all the processes operating on a mother species are presented in Table II in Section 4. Also presented in this Table are a quality rating of the cross section data and the mean excess energies of the solar photolysis products. These energies are relevant for the heating of an atmosphere or the escape from it. The mother species are listed in order of the number of atoms in the species: monatomic, diatomic, etc. In each of these groups, species are listed in increasing order with total atomic number. Species without state designation refer to the ground state. Since cross sections are measured typically at temperatures around 300 K, rotationally excited levels in the ground state of molecules will in effect lower the photo threshold compared to that at 0 K. The molecular rate coefficients presented here include the contribution caused by the shift to this effective threshold. Larger contributions from excited states occur at higher temperatures. The theoretical cross sections correspond to 0 K.

The rate constants scale approximately with the solar flux, i.e., with r^{-2} , where r is the heliocentric distance in AU. At small r the rate constants can increase more rapidly than r^{-2} because of the contributions from thermally excited states.

2. Solar Flux

The solar flux for the quiet Sun has been compiled from many publications. To provide better resolution, it was sometimes necessary to interpolate by prorating the unresolved portions of flux measured in large wavelength intervals to smaller bins and then add the measured flux from emission lines with wavelengths that fall into these bins. From 0 to 10 Å, data from Swider (1969) were used. In the interval 10 to 280 Å measured fluxes were taken from Hinteregger (1970). From 270 to 1163 Å the data from Hall and Hinteregger (1970) were interpolated. In the range from 1163 to 7350 Å data from Ackerman (1971) were used with a correction by Simon (1974) in the interval 1961 to 2299 Å. Finally, from 7350 to 140 000 Å the data published by Iqbal (1983) were used. There are 324 solar flux bins. Figure 1 presents this solar flux as number of photons $\text{cm}^{-2} \text{s}^{-1} \text{\AA}^{-1}$. Figure 2 shows the solar flux for the quiet Sun in the UV part of the spectrum and Figure 3 presents the ratio of the irradiances of the active to that of the quiet Sun from Hinteregger *et al.* (1981), as presented by Lean (1987), in the same spectrum range.

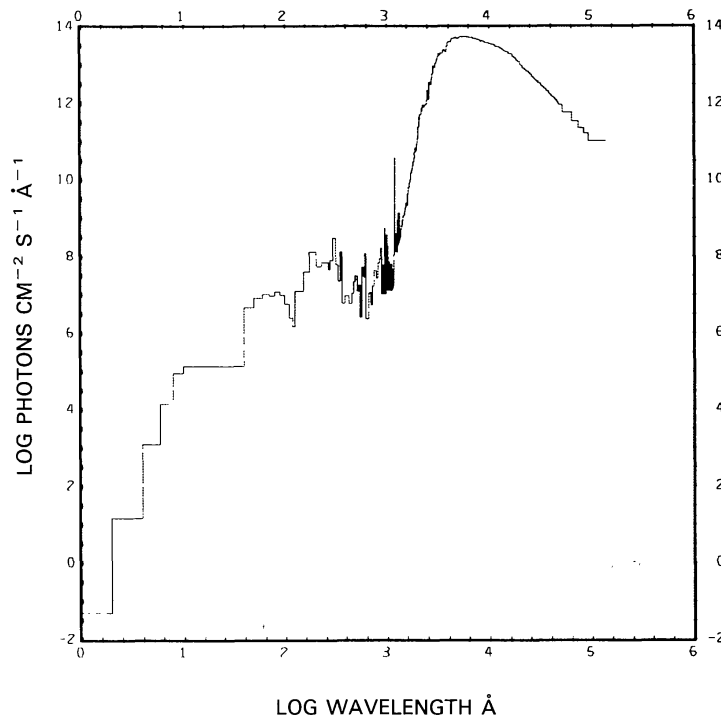


Fig. 1. The solar flux at 1 AU heliocentric distance for the quiet Sun presented as log number of photons $\text{cm}^{-2} \text{s}^{-1} \text{\AA}^{-1}$ vs log wavelength in Å.

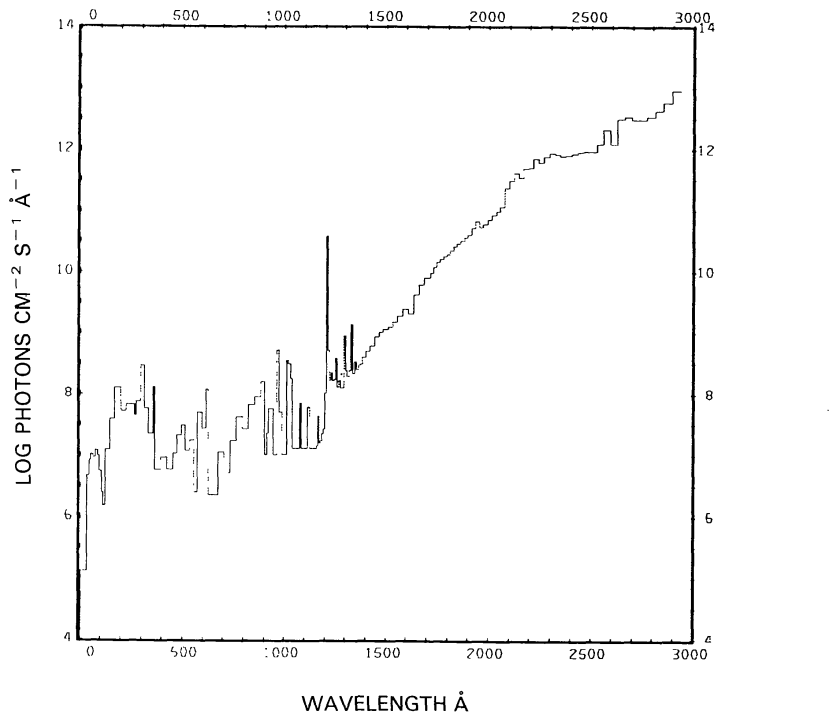


Fig. 2. The solar UV flux at 1 AU heliocentric distance for the quiet Sun presented as log number of photons $\text{cm}^{-2} \text{s}^{-1} \text{\AA}^{-1}$ vs wavelength in \AA up to 2941 \AA .

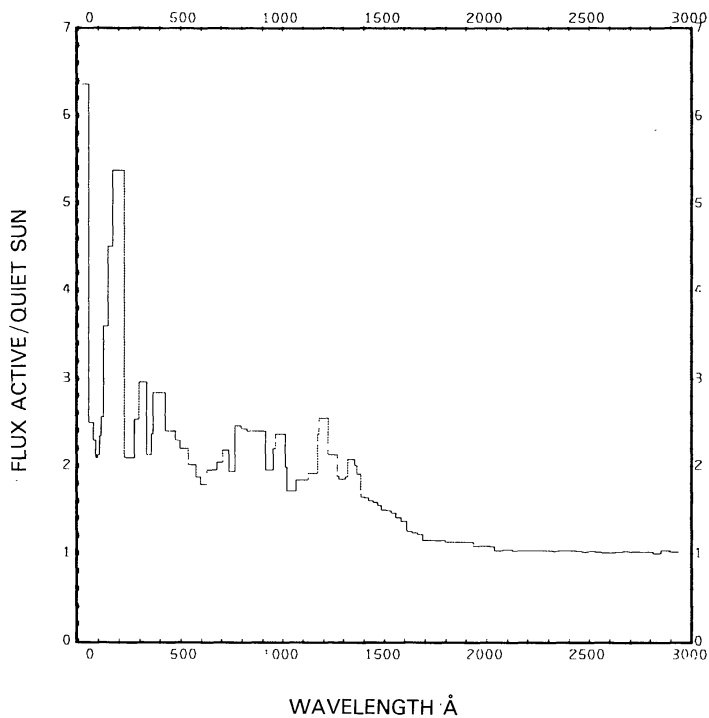


Fig. 3. The ratio of the flux of the active Sun to that of the quiet Sun vs wavelength in \AA up to 2941 \AA .

3. Photo Rate Coefficients and Excess Energies

The rate coefficient for the wavelength interval between λ_i and $\lambda_i + \Delta\lambda$ is

$$k_i(\tau_i) = \int_{\lambda_i}^{\lambda_i + \Delta\lambda} \sigma(\lambda)\Phi(\lambda) e^{-\tau(\lambda)} d\lambda, \quad (1)$$

where $\sigma(\lambda)$ is a photo cross section and $\Phi(\lambda)$ is the unattenuated solar photon flux at wavelength λ . Since neither $\sigma(\lambda)$ nor $\Phi(\lambda)$ are known as a continuous function of λ , the rate coefficients are approximated by

$$k_i(\tau_i) = \sigma_i \Phi_i(\tau_i), \quad (2)$$

where σ_i denotes the wavelength-averaged photo cross section in a bin of width $\Delta\lambda$ and $\Phi_i(\tau_i)$ is the attenuated and wavelength-integrated photon flux in the same bin

$$\Phi_i(\tau_i) = \int_{\lambda_i}^{\lambda_i + \Delta\lambda} \Phi(\lambda) e^{-\tau(\lambda)} d\lambda. \quad (3)$$

In the following discussions the photon flux $\Phi_i(0)$ is the unattenuated solar flux at 1 AU heliocentric distance as presented in Table I (photons $\text{cm}^{-2} \text{s}^{-1} \text{bin}^{-1}$) (the same flux is presented in Figures 1 and 2, but in photons $\text{cm}^{-2} \text{s}^{-1} \text{\AA}^{-1}$) for the quiet Sun, or when multiplied by the enhancement factor (see Figure 3) for the active Sun, except in those bins that contain the threshold of a cross section. In those cases $\Phi_i(0)$ is linearly prorated to the threshold wavelength. The unattenuated rate coefficients ($\text{s}^{-1} \text{\AA}^{-1}$) in each bin (Equation (2), but with $\tau_i = 0$) are presented in figures for each reaction of each species for the quiet Sun and for many cases also for the active Sun. The rate coefficient for a bin must be multiplied by the width of the bin (see Table I for bin widths).

The mean excess energy of the solar photolysis products is

$$E(\tau) = \int_0^{\lambda_{th}} hc \left(\frac{1}{\lambda} - \frac{1}{\lambda_{th}} \right) \sigma(\lambda)\Phi(\lambda) e^{-\tau(\lambda)} d\lambda / \int_0^{\lambda_{th}} \sigma(\lambda)\Phi(\lambda) e^{-\tau(\lambda)} d\lambda = \\ = \sum_i hc \{ (\lambda_i + \Delta\lambda/2)/[\lambda_i(\lambda_i + \Delta\lambda)] - 1/\lambda_{th} \} k_i(\tau_i)/k(\tau), \quad (4)$$

where the summation is over all wavelength bins, λ_{th} is the threshold wavelength, e.g., the wavelength equivalent for the dissociation or ionization energy, and

$$k(\tau) = \sum_i k_i(\tau_i), \quad (5)$$

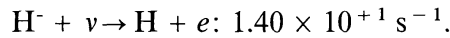
is the photo rate coefficient. Results for the unattenuated rate coefficients $k(0)$ and the corresponding excess energies $E(0)$ are summarized in Table II in columns 5 and 7 for the quiet Sun. Column 6 contains the sum of the rate coefficients for all branches of a species. Columns 8, 10, and 9, respectively, contain the equivalent quantities for the active Sun. Unless indicated otherwise, the photolysis products are in their ground states.

NEGATIVE ATOMIC HYDROGEN ION, H⁻

Cross section: From 180 to 16640 Å the cross section was calculated by Broad and Reinhardt (1976). These values were supplemented with the calculated data from Geltman (1962).

Threshold: The detachment threshold at $\lambda = 16640 \text{ \AA}$ is given by Broad and Reinhardt (1962).

Rate coefficient:



See Figure 4. This value is not sensitive to the activity of the Sun.

Excess energy: The excess energy, 0.93 eV, is also not sensitive to the activity of the Sun.

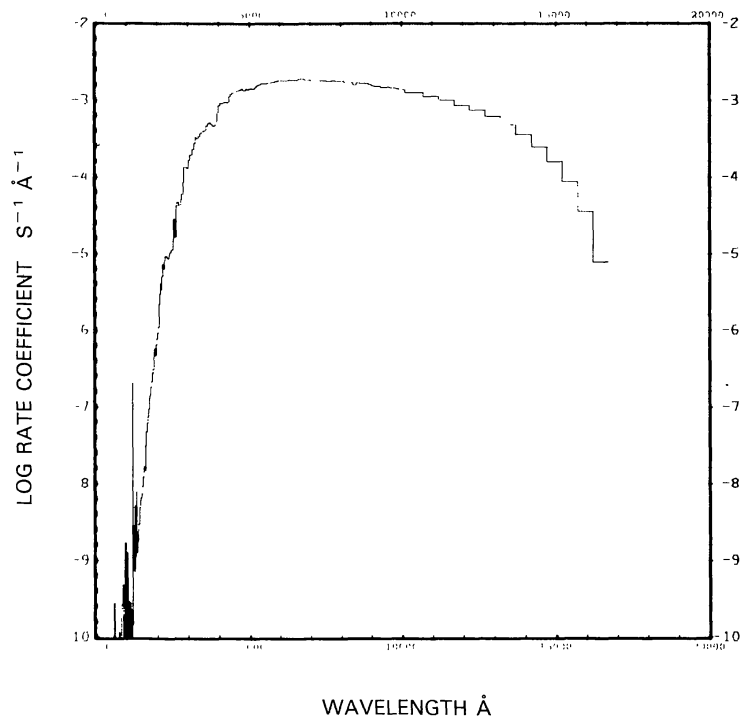


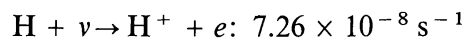
Fig. 4. $\text{H}^- + v \rightarrow \text{H} + e$, for the quiet Sun.

ATOMIC HYDROGEN, H

Cross section: In the long wavelength region the Stobbe (1930) formula is used and in the short wavelength region the cross section is based on the Sauter (1931) formula. The transition from one to the other is made by a modification that further improves a formula suggested by Bethe and Salpeter (1957).

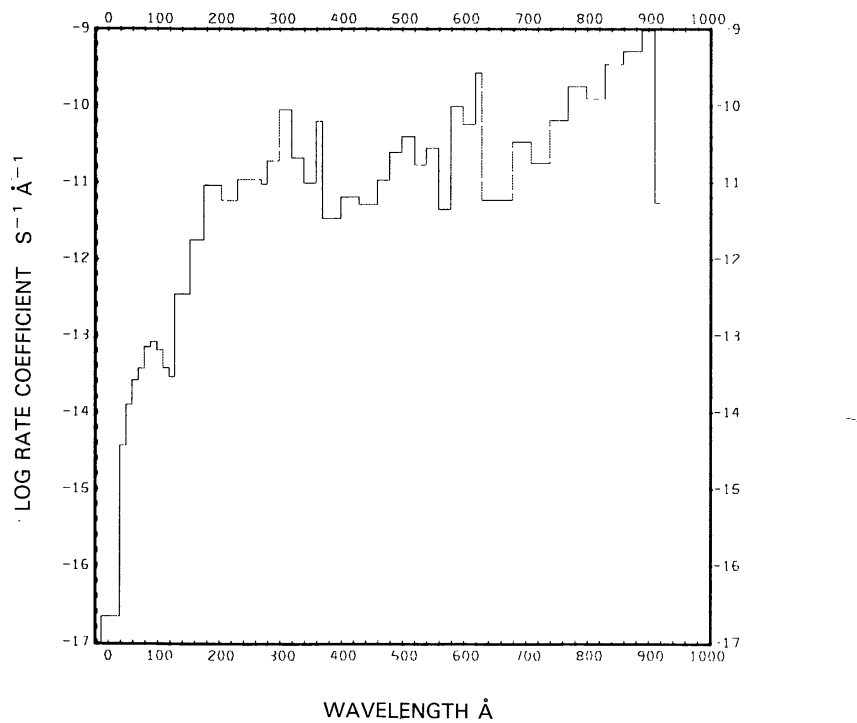
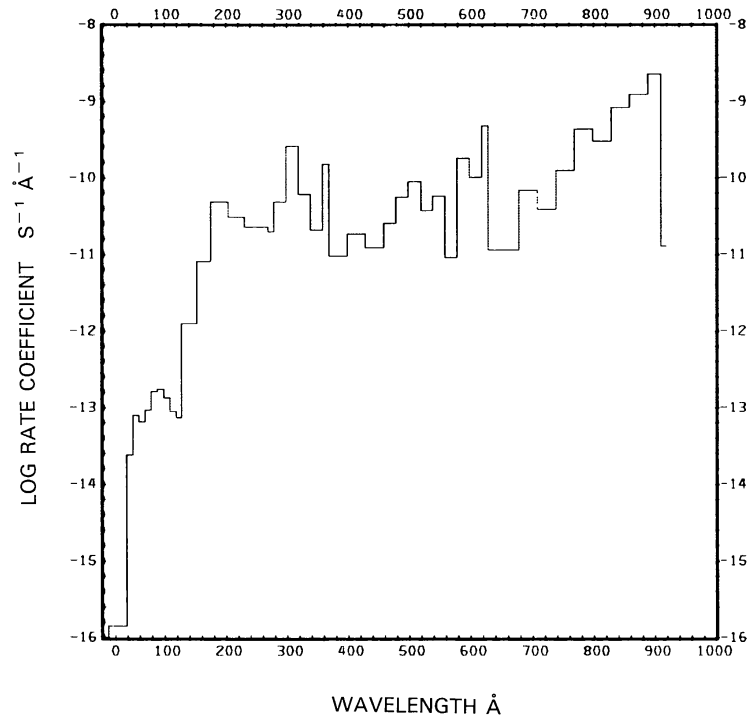
Threshold: $\lambda = 911.75 \text{ \AA}$, as given by Moore (1970).

Rate coefficient:



for the quiet Sun (see Figure 5(a)) and $1.72 \times 10^{-7} \text{ s}^{-1}$ for the active Sun (see Figure 5(b)). The value for the quiet Sun compares well with $7.1 \times 10^{-8} \text{ s}^{-1}$ obtained by Keller (1971) and $7.0 \times 10^{-8} \text{ s}^{-1}$ obtained by Bertaux *et al.* (1973). The values $1.5 \times 10^{-7} \text{ s}^{-1}$ quoted by Axford (1972) and $4.5 \times 10^{-7} \text{ s}^{-1}$ obtained by Siscoe and Mukherjee (1972) are too high.

Excess energy: The excess energy is 3.54 eV for the quiet Sun and 3.97 eV for the active Sun.

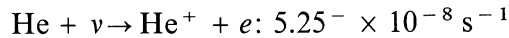
Fig. 5a. $H + v \rightarrow H^+ + e$, for the quiet Sun.Fig. 5b. $H + v \rightarrow H^+ + e$, for the active Sun.

ATOMIC HELIUM, He

Cross section: The cross section for helium is obtained from fits made by Barfield *et al.* (1972).

Threshold: $\lambda = 504.27 \text{ \AA}$, as given by Moore (1970).

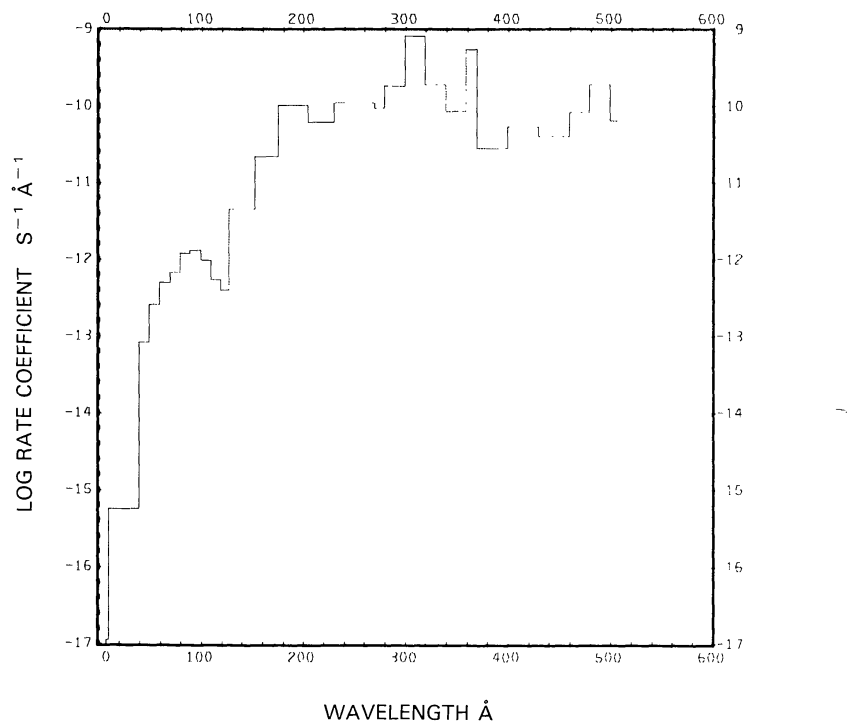
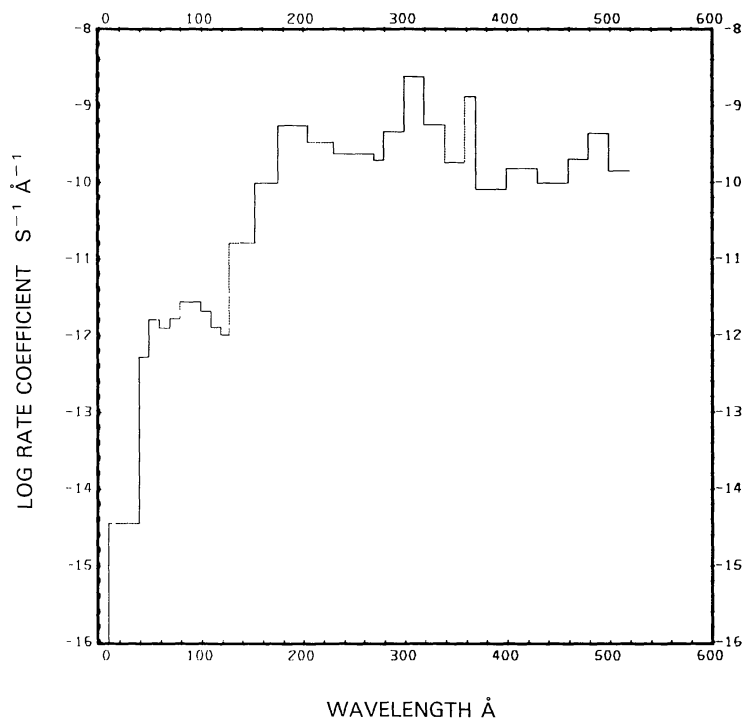
Rate coefficient:



for the quiet Sun (see Figure 6(a)) and $1.51 \times 10^{-7} \text{ s}^{-1}$ for the active Sun (see Figure 6(b))*.

Excess energy: The excess energy is 15.5^- eV for the quiet Sun and 17.8 eV for the active Sun.

* A value ending in 5^- indicates that the value should be rounded down, if it is to be rounded further.

Fig. 6a. $\text{He} + \nu \rightarrow \text{He}^+ + e$, for the quiet Sun.Fig. 6b. $\text{He} + \nu \rightarrow \text{He}^+ + e$, for the active Sun.

ATOMIC CARBON, C(3P), C(1D), C(1S)

Cross sections: From $\lambda = 110 \text{ \AA}$ to threshold the cross sections are calculated from fits made by Henry (1970). At shorter wavelengths cross sections are based on fits made by Barfield *et al.* (1972).

Thresholds: The threshold values, as given by Moore (1970), are:

$$\text{C}({}^3P) : \lambda = 1101.07 \text{ \AA},$$

$$\text{C}({}^1D) : \lambda = 1240.27 \text{ \AA},$$

$$\text{C}({}^1S) : \lambda = 1445.66 \text{ \AA}.$$

Rate coefficients:

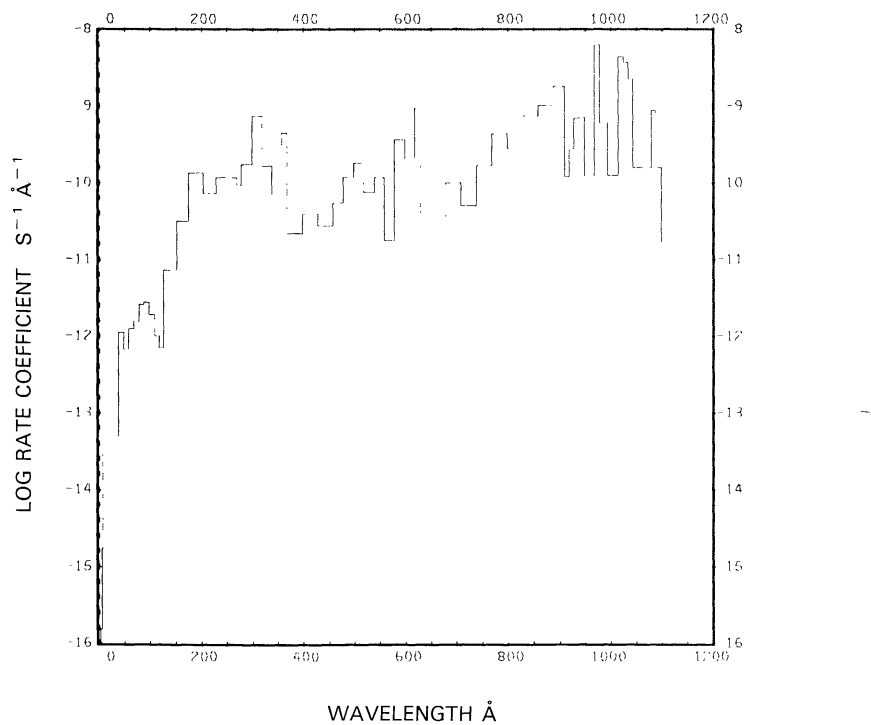
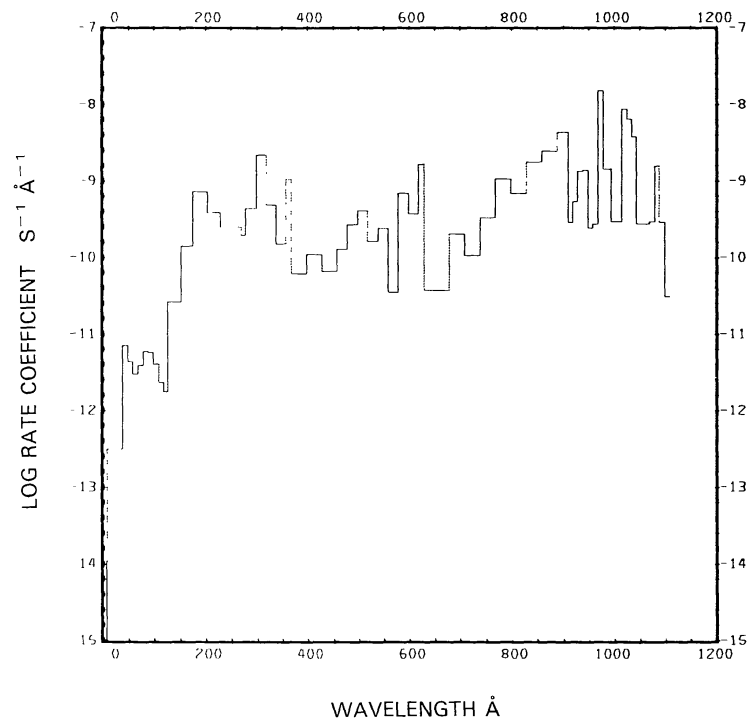
$$\text{C}({}^3P) + v \rightarrow \text{C}^+ + e : 4.10 \times 10^{-7} \text{ s}^{-1}, 9.20 \times 10^{-7} \text{ s}^{-1},$$

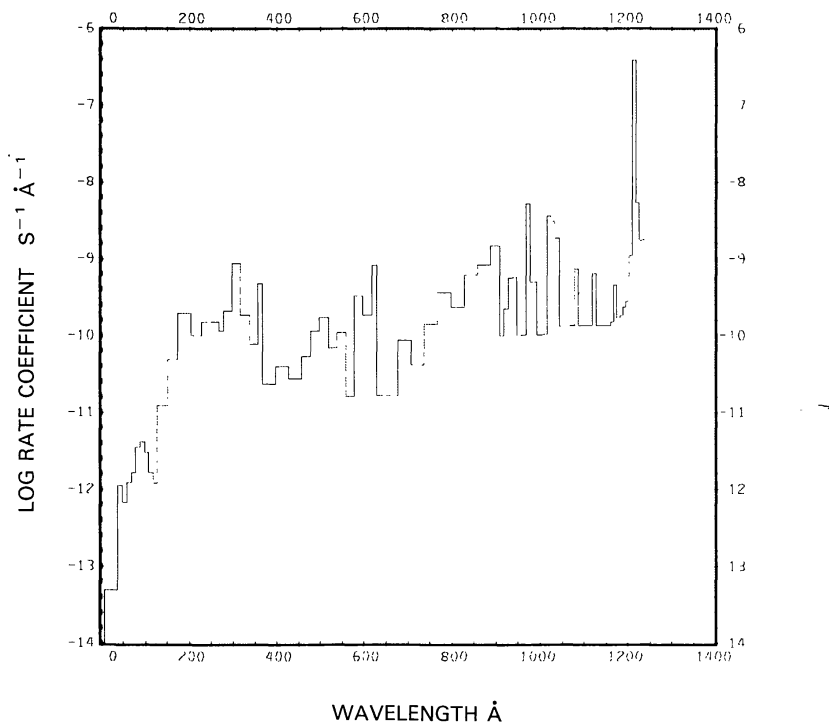
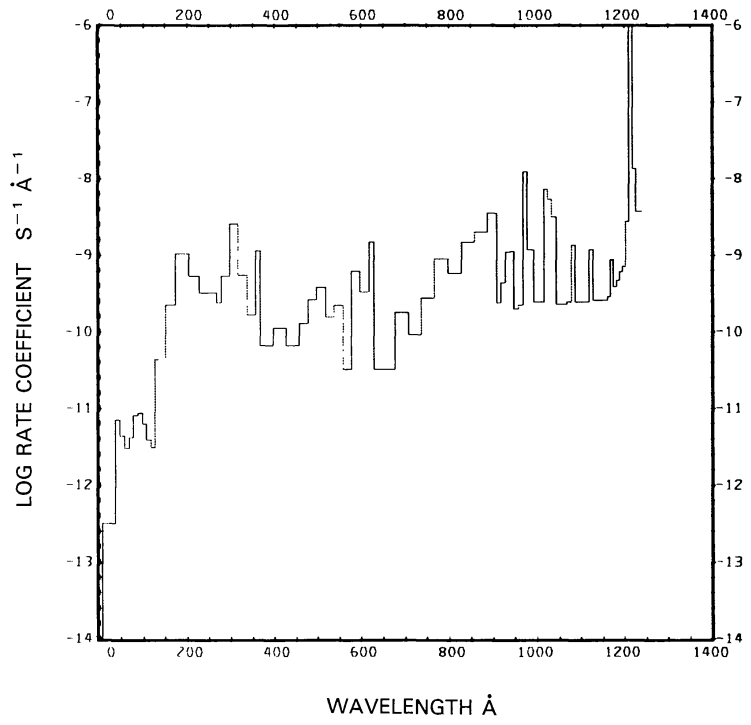
$$\text{C}({}^1D) + v \rightarrow \text{C}^+ + e : 3.58 \times 10^{-6} \text{ s}^{-1}, 9.00 \times 10^{-6} \text{ s}^{-1},$$

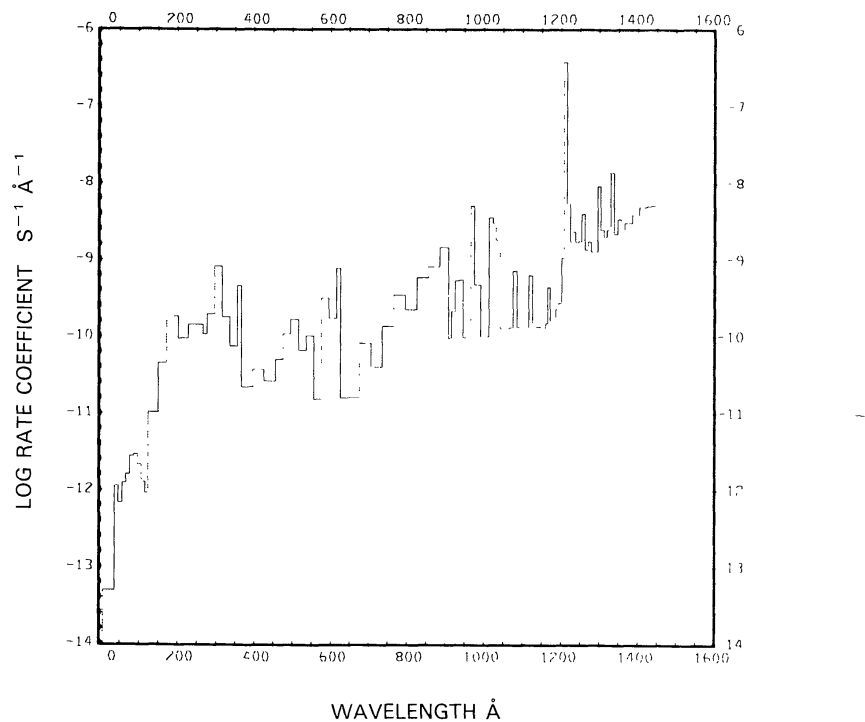
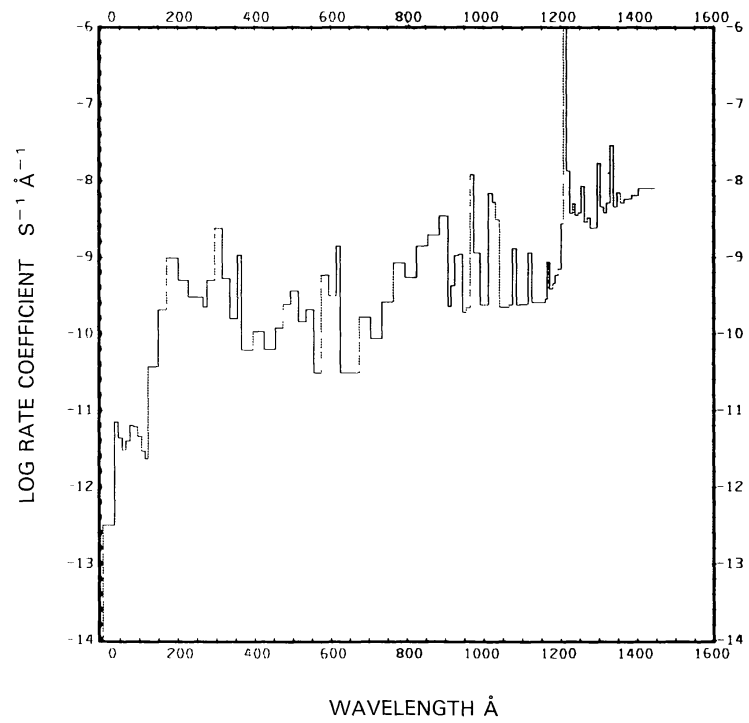
$$\text{C}({}^1S) + v \rightarrow \text{C}^+ + e : 4.34 \times 10^{-6} \text{ s}^{-1}, 1.04 \times 10^{-5} \text{ s}^{-1}.$$

Here the first value is for the quiet Sun (see Figures 7(a) to 9(a)) and the second value is for the active Sun (see Figures 7(b) to 9(b)). The rate coefficient for the quiet Sun, quoted for the ground state by Axford (1972) ($4.0 \times 10^{-6} \text{ s}^{-1}$) is wrong. The large rates for the metastable states are caused by the solar hydrogen L α flux.

Excess energies: The excess energies for the quiet and the active Sun are, respectively, 5.86 and 7.41 eV for the first of the above ionizations, 1.04 and 1.17 eV for the second, and 2.08 and 2.27 eV for the third.

Fig. 7a. $\text{C}({}^3P) + \nu \rightarrow \text{C}^+ + e$, for the quiet Sun.Fig. 7b. $\text{C}({}^3P) + \nu \rightarrow \text{C}^+ + e$, for the active Sun.

Fig. 8a. C(1D) + $\nu \rightarrow C^+ + e$, for the quiet Sun.Fig. 8b. C(1D) + $\nu \rightarrow C^+ + e$, for the active Sun.

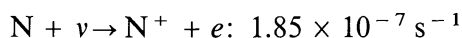
Fig. 9a. $\text{C}({}^1\text{S}) + \nu \rightarrow \text{C}^+ + e$, for the quiet Sun.Fig. 9b. $\text{C}({}^1\text{S}) + \nu \rightarrow \text{C}^+ + e$, for the active Sun.

ATOMIC NITROGEN, N

Cross section: From $\lambda = 110 \text{ \AA}$ to threshold the cross section is calculated from fits made by Henry (1970). At shorter wavelengths the cross section is based on fits made by Barfield *et al.* (1972).

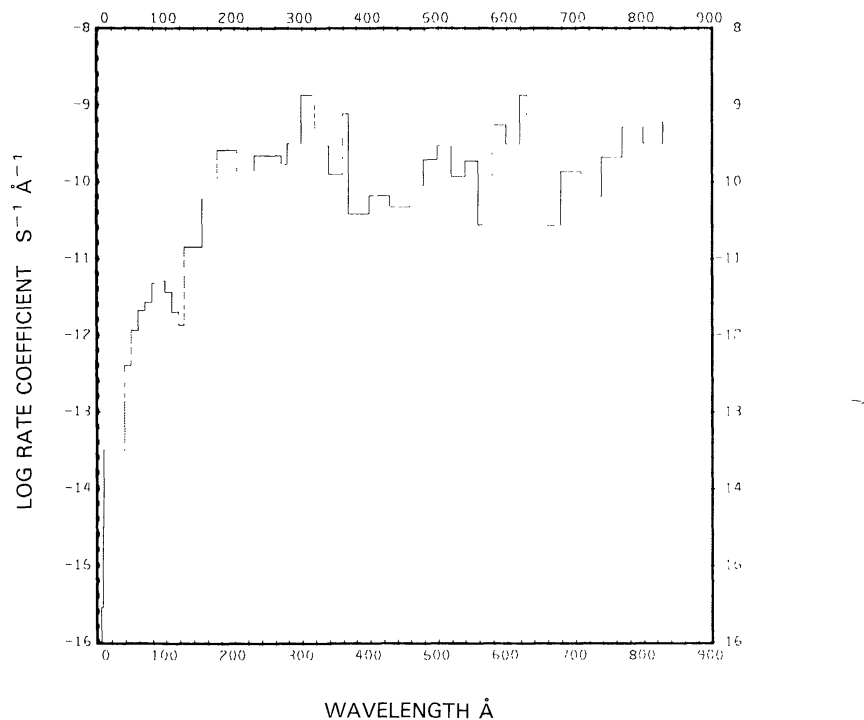
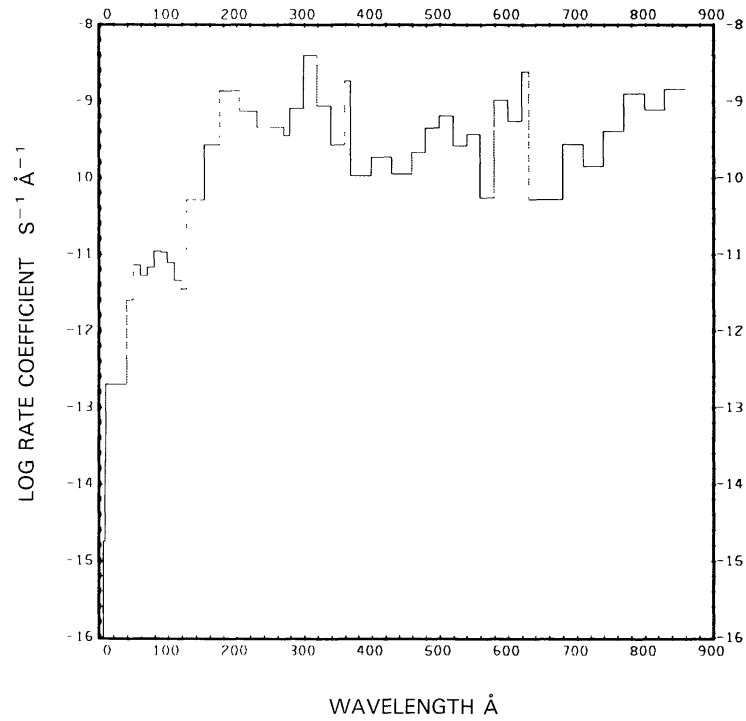
Threshold: $\lambda = 853.06 \text{ \AA}$, as given by Moore (1970).

Rate coefficient:



for the quiet Sun (see Figure 10(a)) and $4.72 \times 10^{-7} \text{ s}^{-1}$ for the active Sun (see Figure 10(b)). The value for the quiet Sun is in good agreement with $1.89 \times 10^{-7} \text{ s}^{-1}$ obtained by Siscoe and Mukherjee (1972), $1.7 \times 10^{-7} \text{ s}^{-1}$ reported by Axford (1972), and $1.9 \times 10^{-7} \text{ s}^{-1}$ quoted by Torr (private communication).

Excess energy: The excess energy is 14.9 eV for the quiet Sun and 18.4 eV for the active Sun.

Fig. 10a. N + ν → N⁺ + e⁻, for the quiet Sun.Fig. 10b. N + ν → N⁺ + e⁻, for the active Sun.

ATOMIC OXYGEN, O(3P), O(1D), O(1S)

Cross sections: From $\lambda = 600 \text{ \AA}$ to threshold the cross sections are calculated from fits made by Henry (1970). At shorter wavelengths cross sections are based on fits made by Barfield *et al.* (1972).

Thresholds: The threshold values as given by Moore (1970) are:

$$\text{O}({}^3P): \lambda = 910.44 \text{ \AA},$$

$$\text{O}({}^1D): \lambda = 827.9 \text{ \AA},$$

$$\text{O}({}^1S): \lambda = 858.3 \text{ \AA}.$$

Rate coefficients:

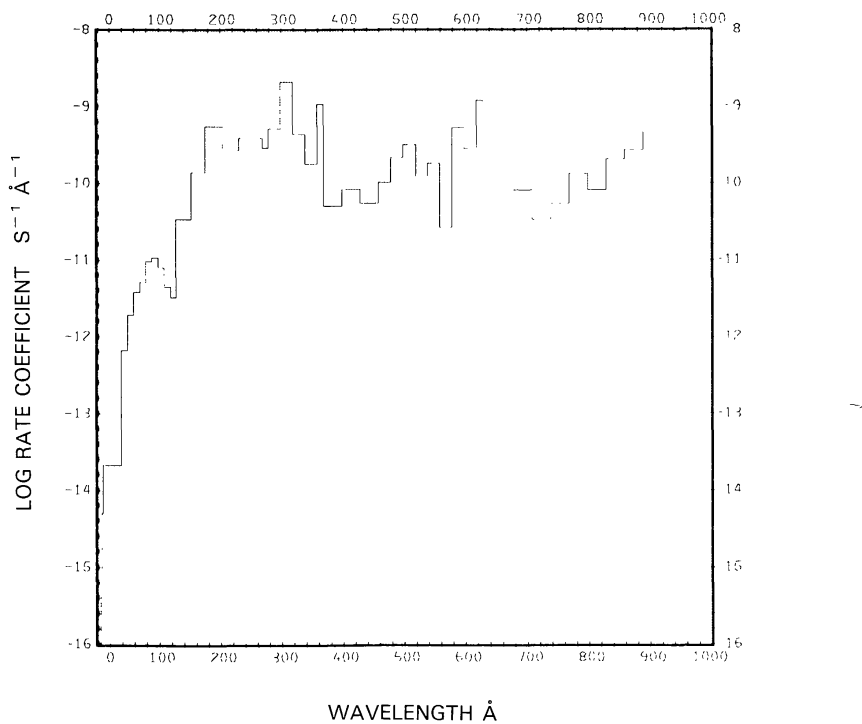
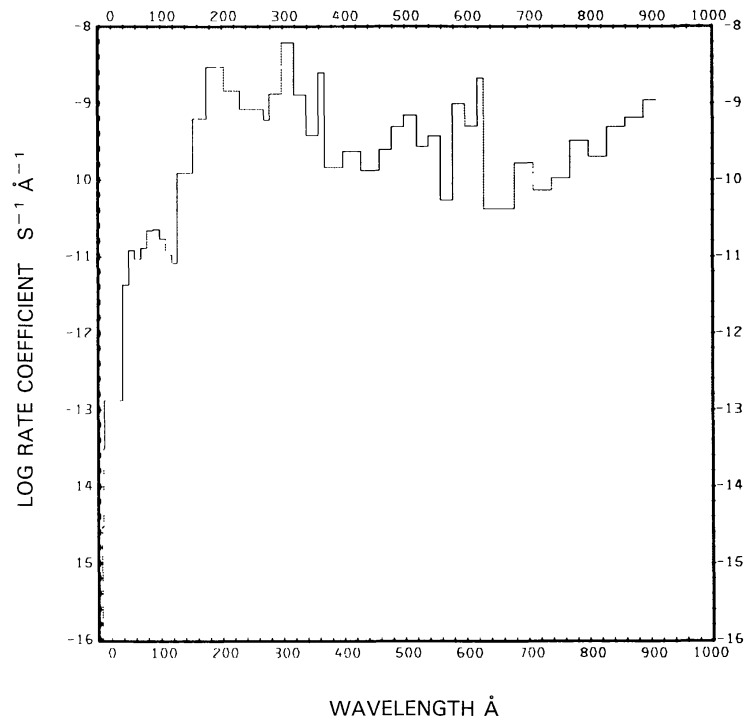
$$\text{O}({}^3P) + v \rightarrow \text{O}^+ + e: 2.12 \times 10^{-7} \text{ s}^{-1}, 5.88 \times 10^{-7} \text{ s}^{-1},$$

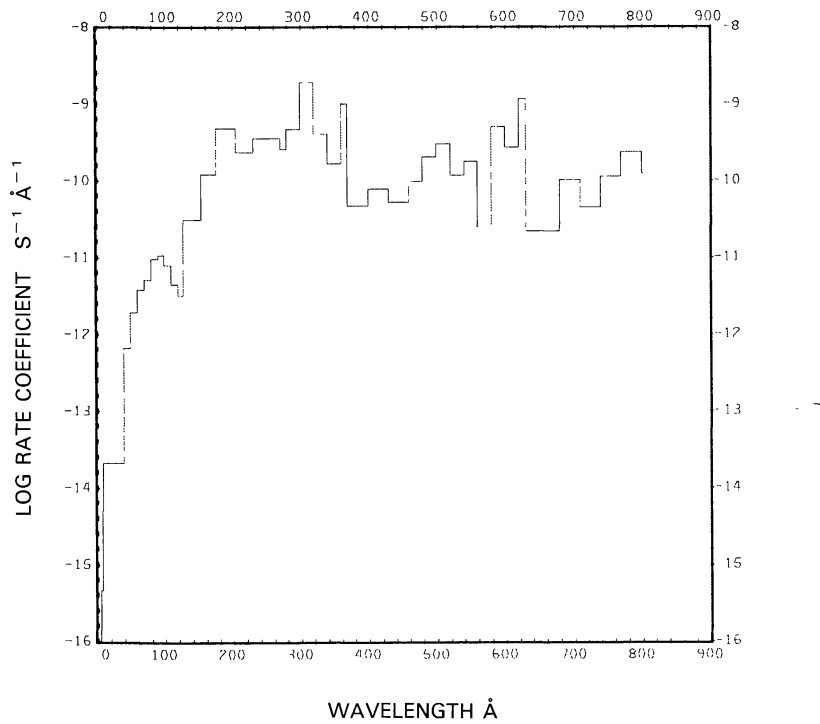
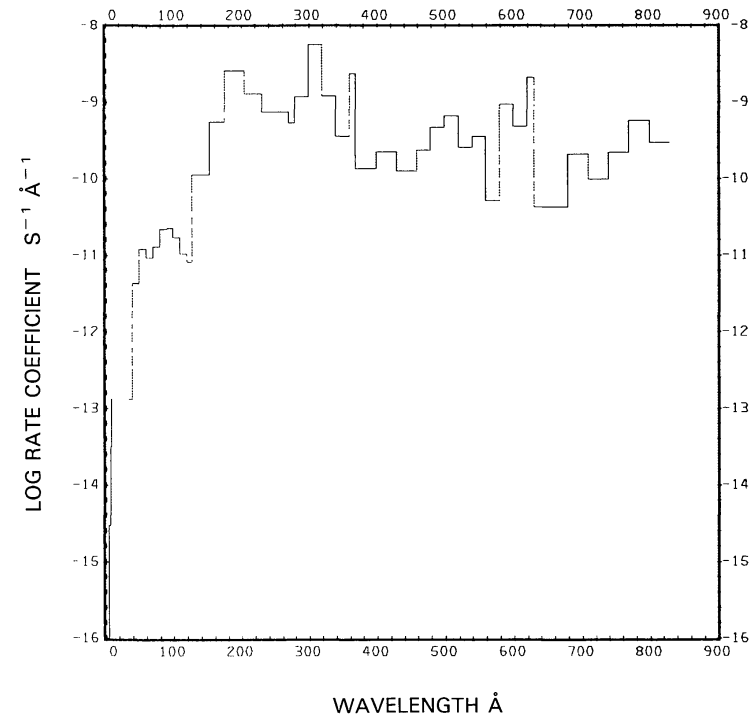
$$\text{O}({}^1D) + v \rightarrow \text{O}^+ + e: 1.82 \times 10^{-7} \text{ s}^{-1}, 5.04 \times 10^{-7} \text{ s}^{-1},$$

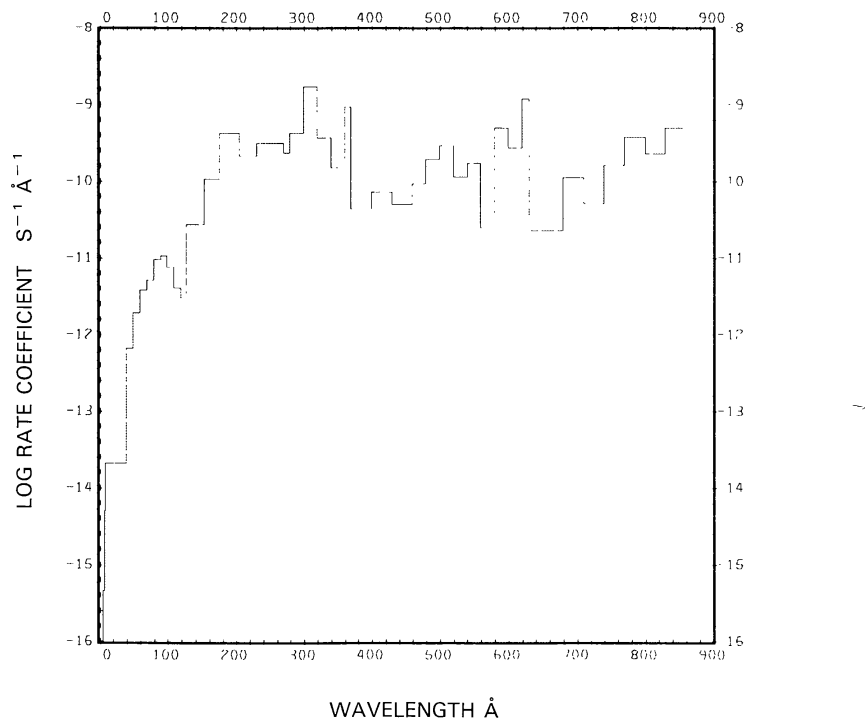
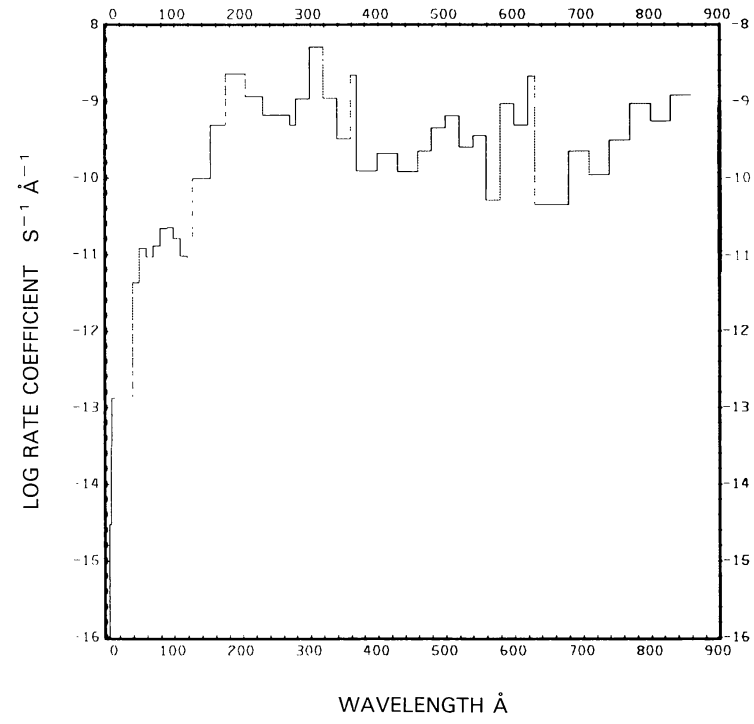
$$\text{O}({}^1S) + v \rightarrow \text{O}^+ + e: 1.96 \times 10^{-7} \text{ s}^{-1}, 5.28 \times 10^{-7} \text{ s}^{-1}.$$

Here the first value is for the quiet Sun (see Figures 11(a) to 13(a)) and the second value for the active Sun (see Figures 11(b) to 13(b)). The rate coefficient for the quiet Sun obtained by Torr ($2.4 \times 10^{-7} \text{ s}^{-1}$, private communication) is 14% higher than our value for O(3P), the value obtained by Siscoe and Mukherjee (1972) ($2.49 \times 10^{-7} \text{ s}^{-1}$) is 17% higher than our value, the rate obtained by Baurer and Bortner (1978) ($2.83 \times 10^{-7} \text{ s}^{-1}$) is 33% higher than ours, while the value computed by McElroy *et al.* (1976) ($6.3 \times 10^{-7} \text{ s}^{-1}$, corrected to 1 AU), is much too high. (The value they quote for Mars orbit is $2.7 \times 10^{-7} \text{ s}^{-1}$.) Kumar (1982) quotes $3.0 \times 10^{-7} \text{ s}^{-1}$ (presumably for ionization of O(3P)) when his value is scaled from 5.2 to 1 AU.

Excess energies: The excess energies for the quiet Sun are 21.6 eV for each of the first and the second of the above ionizations and 18.9 eV for the third. For the active Sun the corresponding excess energies are 26.1 eV for each of the first and the second ionizations, and 23.1 eV for the third.

Fig. 11a. $O(^3P) + \nu \rightarrow O^+ + e$, for the quiet Sun.Fig. 11b. $O(^3P) + \nu \rightarrow O^+ + e$, for the active Sun.

Fig. 12a. $O(^1D) + v \rightarrow O^+ + e$, for the quiet Sun.Fig. 12b. $O(^1D) + v \rightarrow O^+ + e$, for the active Sun.

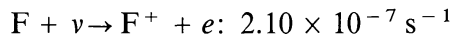
Fig. 13a. $\text{O}(^1S) + \nu \rightarrow \text{O}^+ + e$, for the quiet Sun.Fig. 13b. $\text{O}(^1S) + \nu \rightarrow \text{O}^+ + e$, for the active Sun.

ATOMIC FLUORINE, F

Cross section: From 130 Å to threshold the cross section from Manson *et al.* (1979) was used. For shorter wavelengths the cross section is based on a fit by Barfield *et al.* (1972).

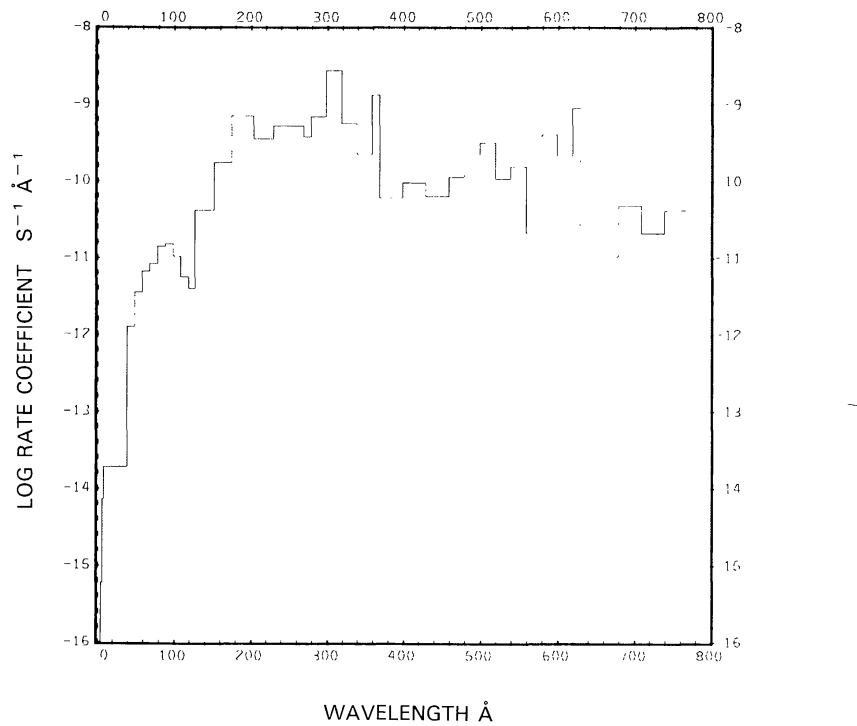
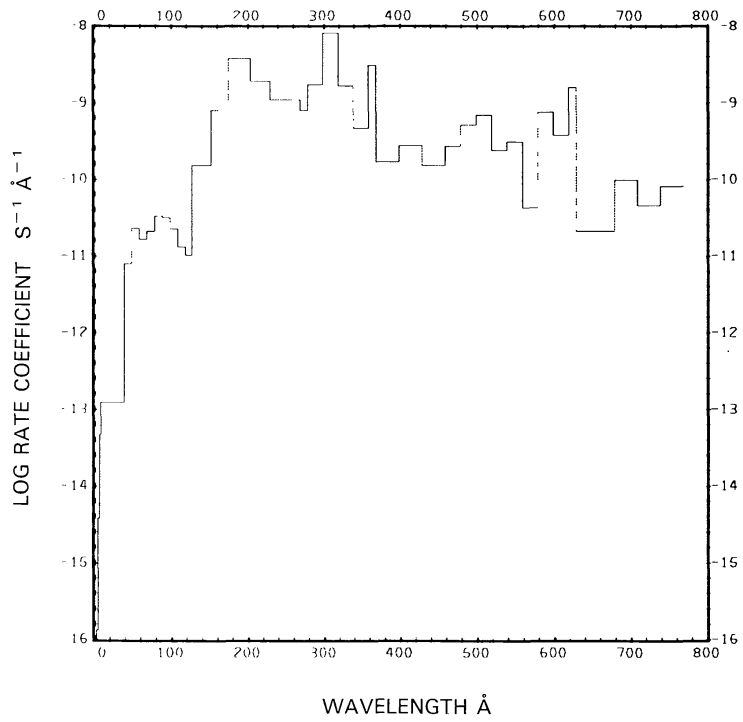
Threshold: $\lambda = 759.44 \text{ \AA}$, as given by Moore (1970).

Rate coefficient:



for the quiet Sun (see Figure 14(a)) and $6.19 \times 10^{-7} \text{ s}^{-1}$ for the active Sun (see Figure 14b).

Excess energy: The excess energy for the quiet Sun is 24.7 eV and for the active Sun 28.9 eV.

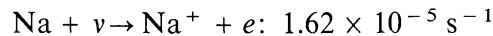
Fig. 14a. $F + \nu \rightarrow F^+ + e$, for the quiet Sun.Fig. 14b. $F + \nu \rightarrow F^+ + e$, for the active Sun.

ATOMIC SODIUM, Na

Cross section: For wavelengths less than 334 Å the fit from Barfield *et al.* (1972) was used. At longer wavelengths the cross section is controversial. Between about 500 and 1200 Å the experimental cross section is bigger than the theoretical cross section and shows a broad feature that cannot be explained by theory. For this reason we have used an experimental and a theoretical cross section alternatively to compute rate coefficients. The experimental cross section comes from Hudson and Carter (1967, 1968) for wavelengths from 500 Å to threshold. The theoretical cross section, in about the same wavelength region, comes from Chang and Kelly (1975). We believe that the theoretical cross section is more nearly correct (Samson, 1982).

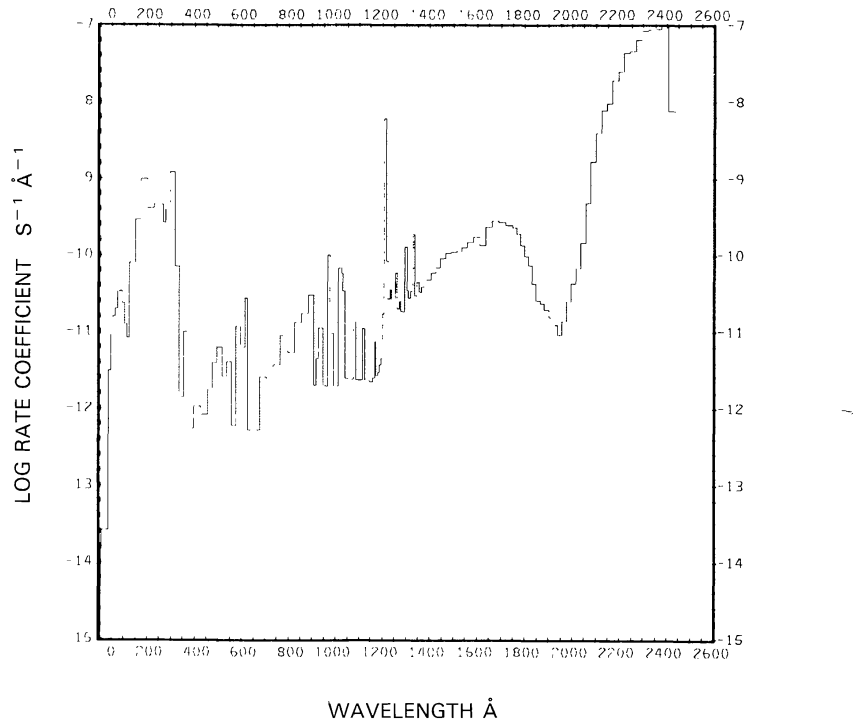
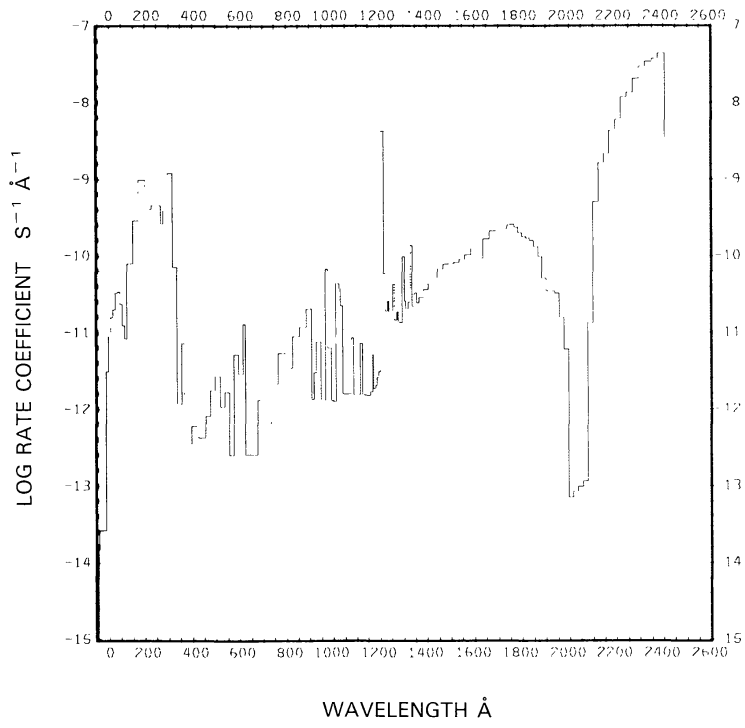
Threshold: $\lambda = 2412.57 \text{ \AA}$, as given by Moore (1970).

Rate coefficient:



from the experimental cross section and $5.92 \times 10^{-6} \text{ s}^{-1}$ from the theoretical cross section, both for the quiet Sun (see Figures 15 and 16, respectively). For the active Sun the corresponding values are $1.72 \times 10^{-5} \text{ s}^{-1}$ and $6.52 \times 10^{-6} \text{ s}^{-1}$. In spite of the discrepancy of the cross section between 500 and 1200 Å, the rate coefficient is dominated by the cross section near threshold.

Excess energy: The excess energy for the quiet Sun is 0.57 eV using the experimental cross section and 1.13 eV using the theoretical cross section. For the active Sun the corresponding values are 1.49 and 3.52 eV.

Fig. 15. $\text{Na} + \nu \rightarrow \text{Na}^+ + e$, for the quiet Sun from the experimental cross section.Fig. 16. $\text{Na} + \nu \rightarrow \text{Na}^+ + e$, for the quiet Sun from the theoretical cross section.

ATOMIC SULFUR, S(3P), S(1D), S(1S)

Cross sections: For S(3P) the cross section up to 122 Å is based on the fit from Barfield *et al.* (1972). From 160 to 1190 Å the cross section fit of Chapman and Henry (1971) was used. For S(1D) the fit from Barfield *et al.* (1972) was used up to 74 Å and the fit from Chapman and Henry (1971) was used from 100 to 1120 Å. For S(1S) the fit from Barfield *et al.* (1972) was used up to 122 Å and the fit from Chapman and Henry (1971) was used from 200 to 1160 Å.

Thresholds: The threshold values as given by Moore (1970) are:

$$S(^3P): 1196.75 \text{ \AA},$$

$$S(^1D): 1121.43 \text{ \AA},$$

$$S(^1S): 1164.12 \text{ \AA}.$$

Rate coefficients:

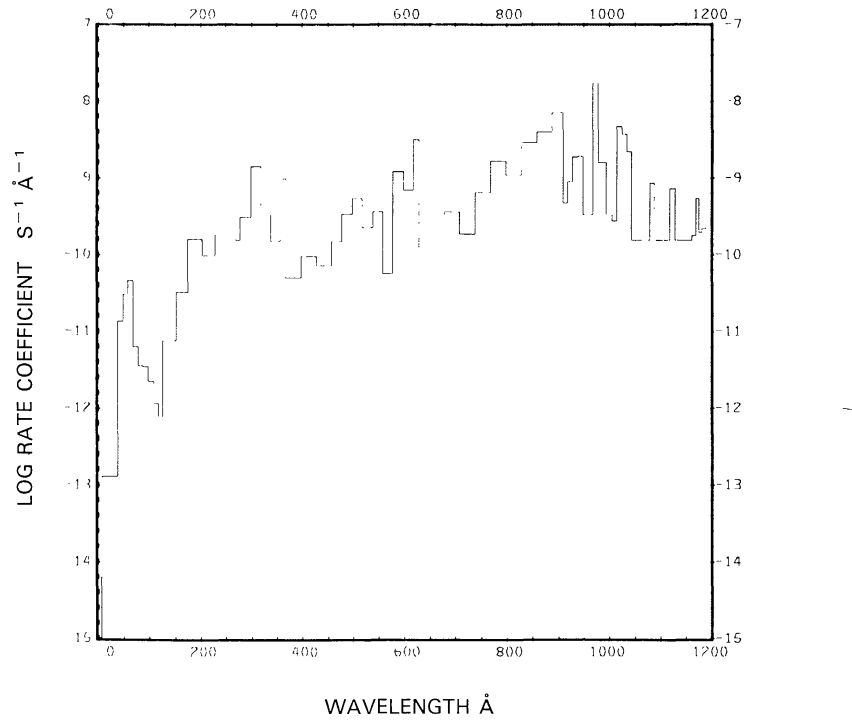
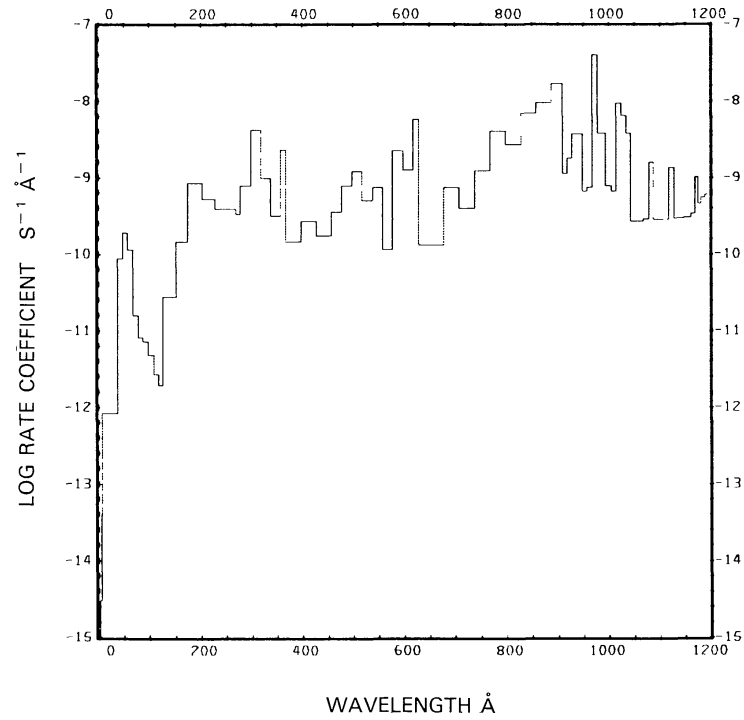
$$S(^3P) + \nu \rightarrow S^+ + e: 1.07 \times 10^{-6} \text{ s}^{-1}, 2.44 \times 10^{-6} \text{ s}^{-1},$$

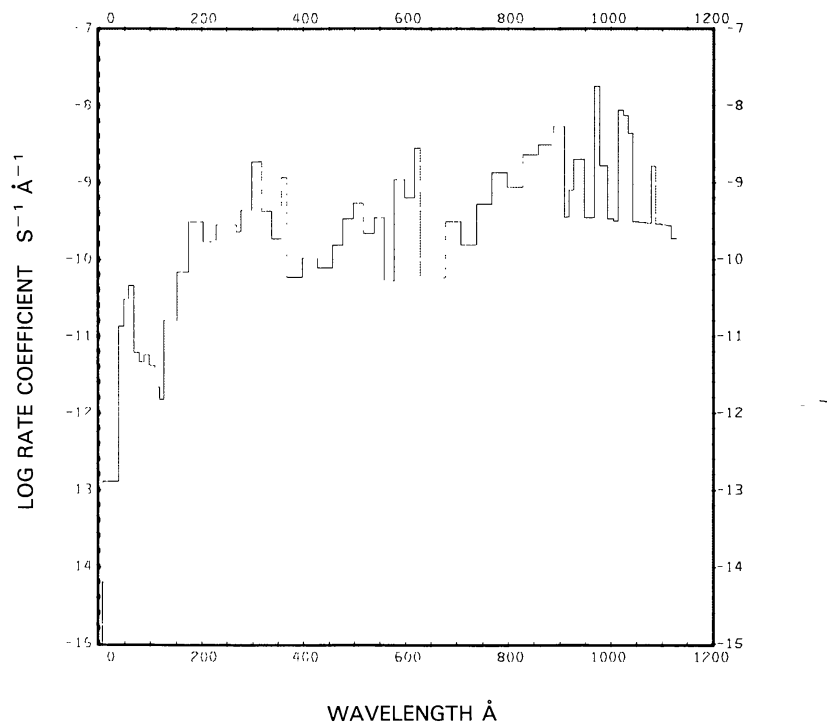
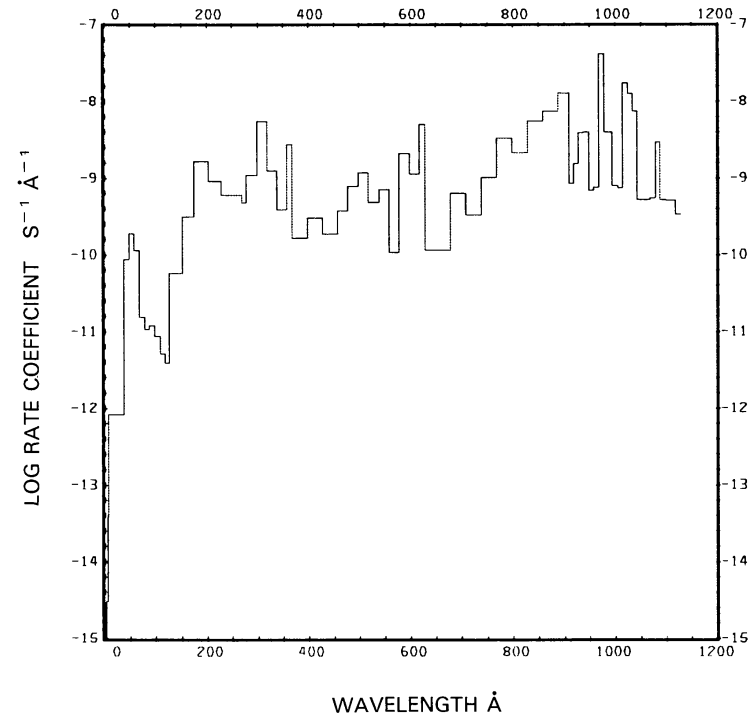
$$S(^1D) + \nu \rightarrow S^+ + e: 1.08 \times 10^{-6} \text{ s}^{-1}, 2.46 \times 10^{-6} \text{ s}^{-1},$$

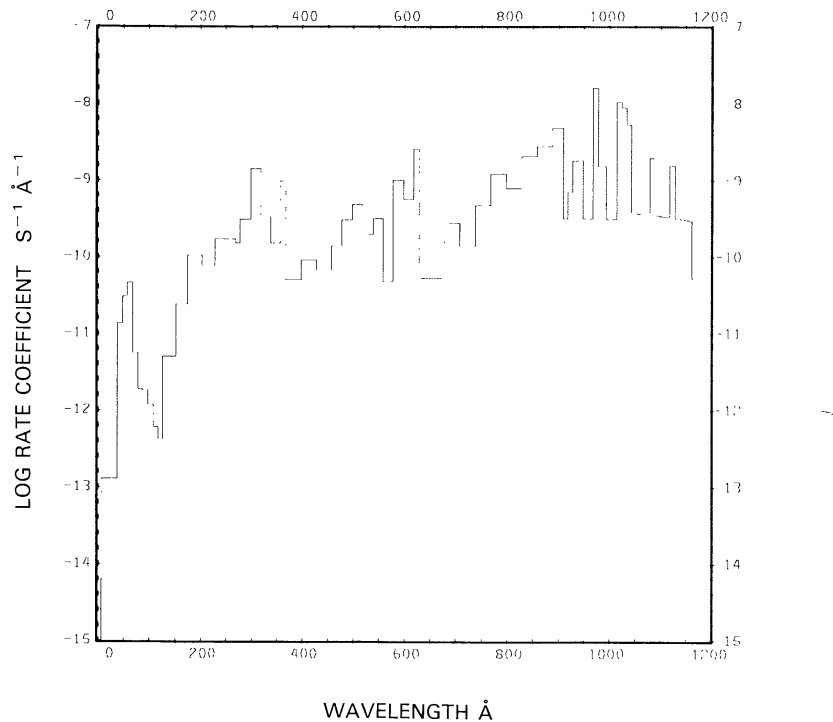
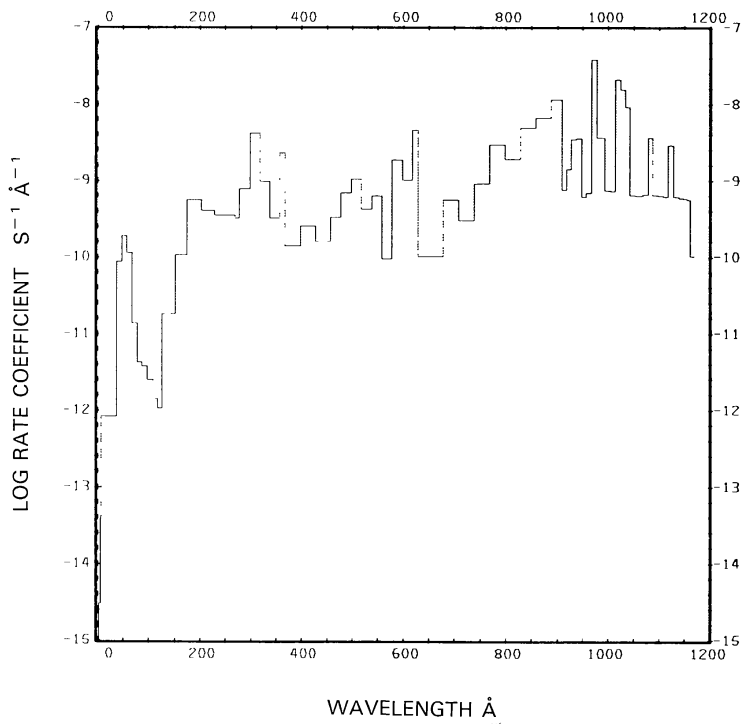
$$S(^1S) + \nu \rightarrow S^+ + e: 1.05 \times 10^{-6} \text{ s}^{-1}, 2.31 \times 10^{-6} \text{ s}^{-1}.$$

Here the first value is for the quiet Sun (see Figures 17(a) to 19(a)) and the second for the active Sun (see Figures 17(b) to 19(b)). Kumar (1982) quotes $1.6 \times 10^{-6} \text{ s}^{-1}$ (presumably for ionization of S(3P) and the quiet Sun) when his value is scaled from 5.2 to 1 AU. His value is about 50% higher than ours.

Excess energies: The excess energies for the quiet Sun are 6.30 eV for the first of the above ionizations, 6.21 eV for the second, and 5.42 eV for the third. The corresponding values for the active Sun are 7.19, 7.68, and 6.38 eV.

Fig. 17a. $S(^3P) + \nu \rightarrow S^+ + e$, for the quiet Sun.Fig. 17b. $S(^3P) + \nu \rightarrow S^+ + e$, for the active Sun.

Fig. 18a. $S(^1D) + \nu \rightarrow S^+ + e$, for the quiet Sun.Fig. 18b. $S(^1D) + \nu \rightarrow S^+ + e$, for the active Sun.

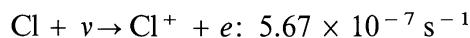
Fig. 19a. $\text{S}(^1S) + v \rightarrow \text{S}^+ + e$, for the quiet Sun.Fig. 19b. $\text{S}(^1S) + v \rightarrow \text{S}^+ + e$, for the active Sun.

ATOMIC CHLORINE, Cl

Cross section: From 275.5 to 950.1 Å, the cross section from Brown *et al.* (1980) was used. For shorter wavelengths the cross section is obtained from fits made by Barfield *et al.* (1972).

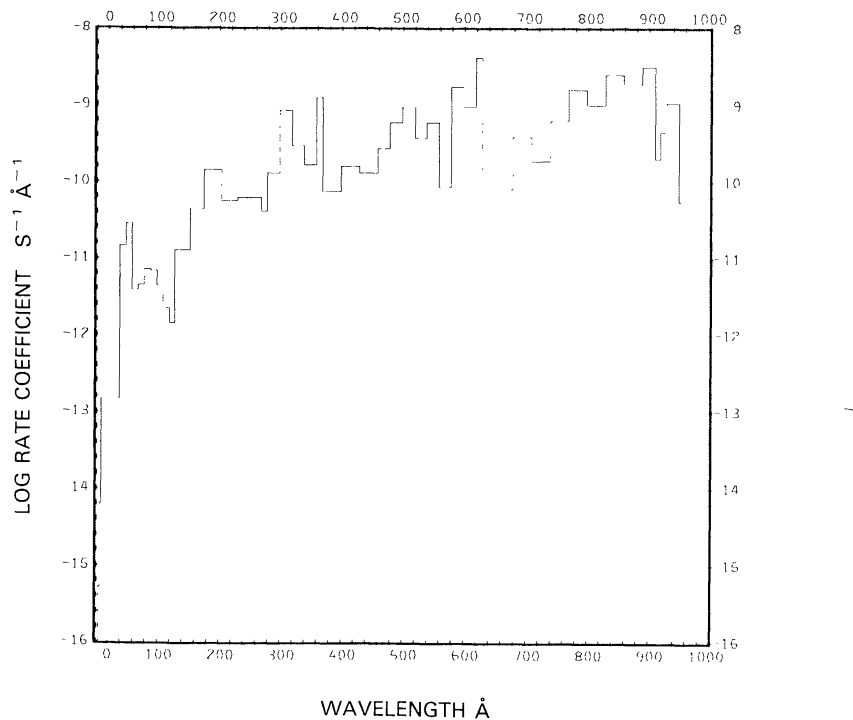
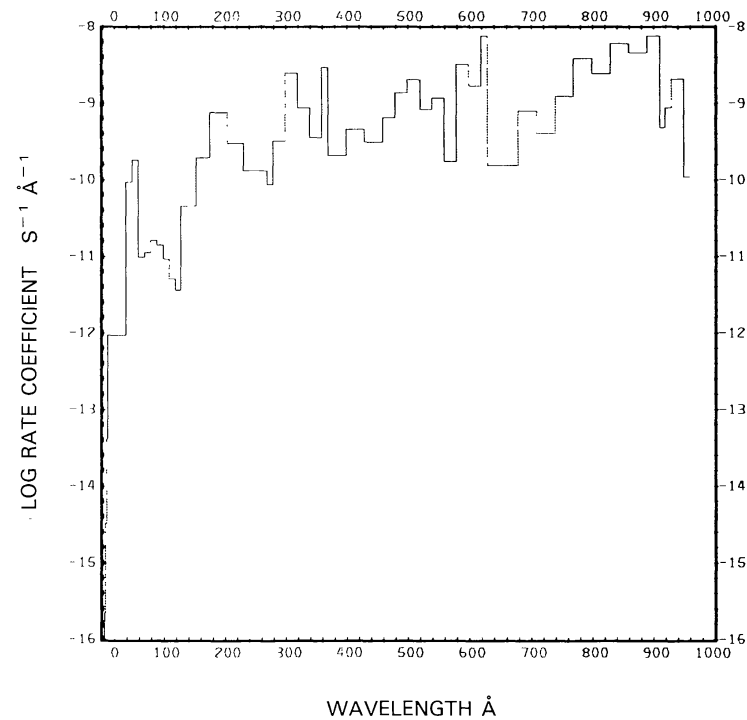
Threshold: $\lambda = 953 \text{ Å}$, as given by Moore (1970).

Rate coefficient:



for the quiet Sun (see Figure 20(a)) and $1.30 \times 10^{-6} \text{ s}^{-1}$ for the active Sun (see Figure 20(b)).

Excess energy: The excess energy is 6.71 eV for the quiet Sun and 7.90 eV for the active Sun.

Fig. 20a. $\text{Cl} + \nu \rightarrow \text{Cl}^+ + e$, for the quiet Sun.Fig. 20b. $\text{Cl} + \nu \rightarrow \text{Cl}^+ + e$, for the active Sun.

ATOMIC ARGON, Ar

Cross section: Up to 783 Å the cross section fits of Marr and West (1976) were used. From 783 Å to the threshold wavelength we used the cross section measured by Huffman *et al.* (1963a).

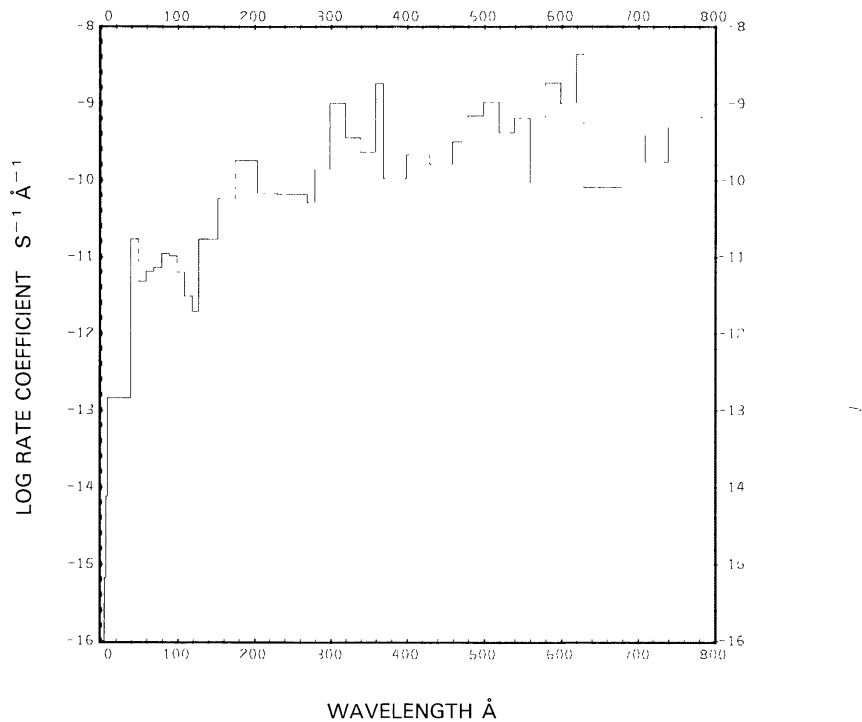
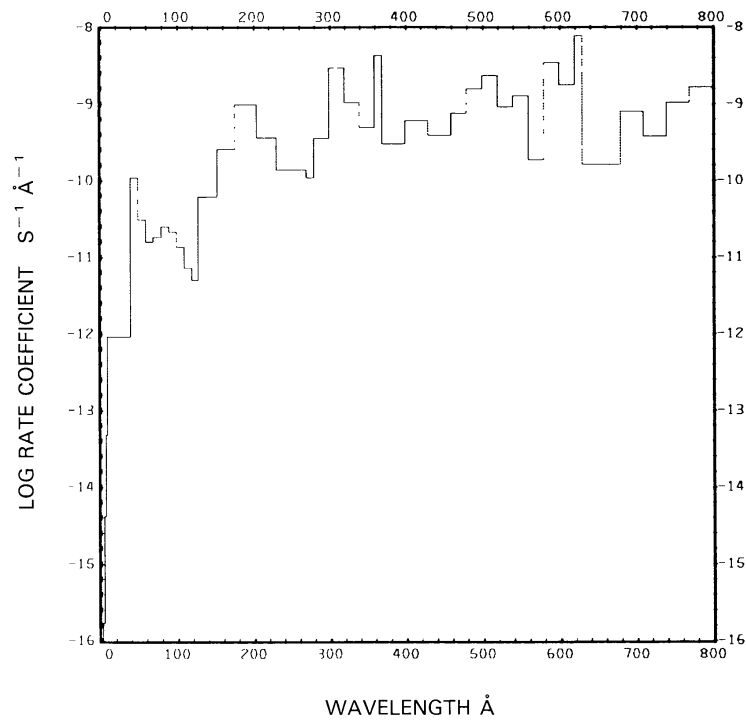
Threshold: The ionization threshold is at $\lambda = 786 \text{ \AA}$ (Huffman *et al.*, 1963a).

Rate coefficient:



for the quiet Sun (see Figure 21(a)) and $6.90 \times 10^{-7} \text{ s}^{-1}$ for the active Sun (see Figure 21(b)).

Excess energy: The excess energy for the quiet Sun is 10.1 eV and 12.8 eV for the active Sun.

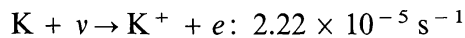
Fig. 21a. $\text{Ar} + \nu \rightarrow \text{Ar}^+ + e$, for the quiet Sun.Fig. 21b. $\text{Ar} + \nu \rightarrow \text{Ar}^+ + e$, for the active Sun.

ATOMIC POTASSIUM, K

Cross section: Up to 1128.2 Å the cross section from the fit of Barfield *et al.* (1972) was used. In the interval from 1200 to 2856 Å we used the cross section from Hudson and Carter (1965). Similar to their Na measurements, the measured K cross section is high compared to the theoretical cross section. However, here the difference is smaller. We have slightly modified the cross section between 915 and 1600 Å to obtain a better fit between the two sources. The results are not sensitive to this modification.

Threshold: The ionization threshold at $\lambda = 2856$ Å is given by Hudson and Carter.

Rate coefficient:



for the quiet Sun (see Figure 22) and $2.36 \times 10^{-5} \text{ s}^{-1}$ for the active Sun.

Excess energy: The excess energy is 1.36 eV for the quiet Sun and 1.78 eV for the active Sun.

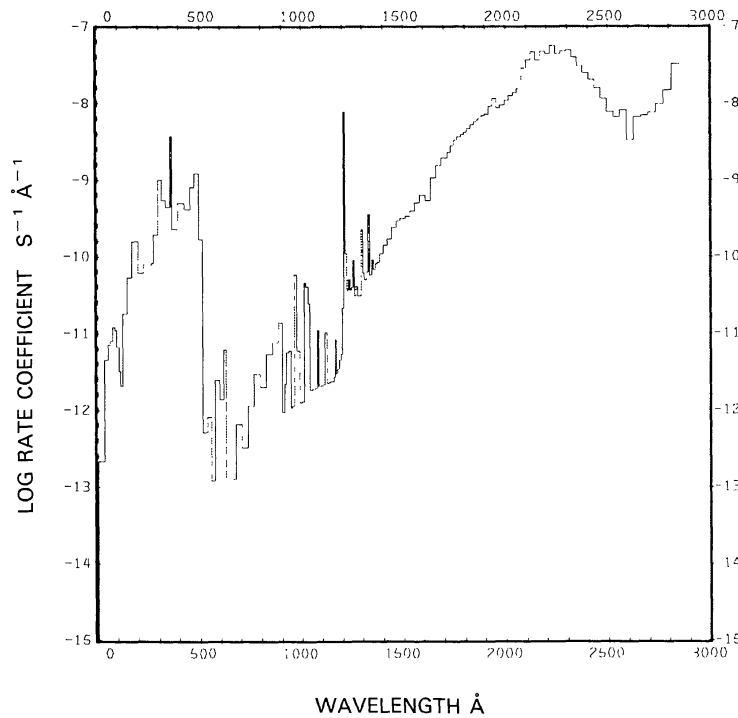


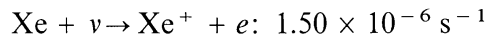
Fig. 22. $K + \nu \rightarrow K^+ + e$, for the quiet Sun.

ATOMIC XENON, Xe

Cross section: Up to 922 Å the cross section of West and Morton (1978) was used. From 922 Å to threshold we used the measured cross section of Huffman *et al.* (1963a).

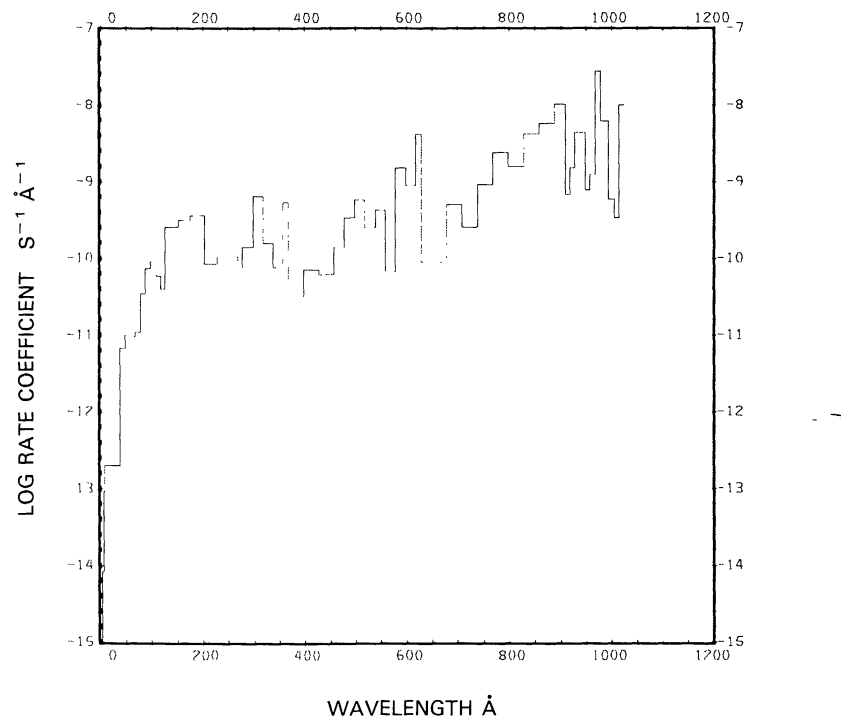
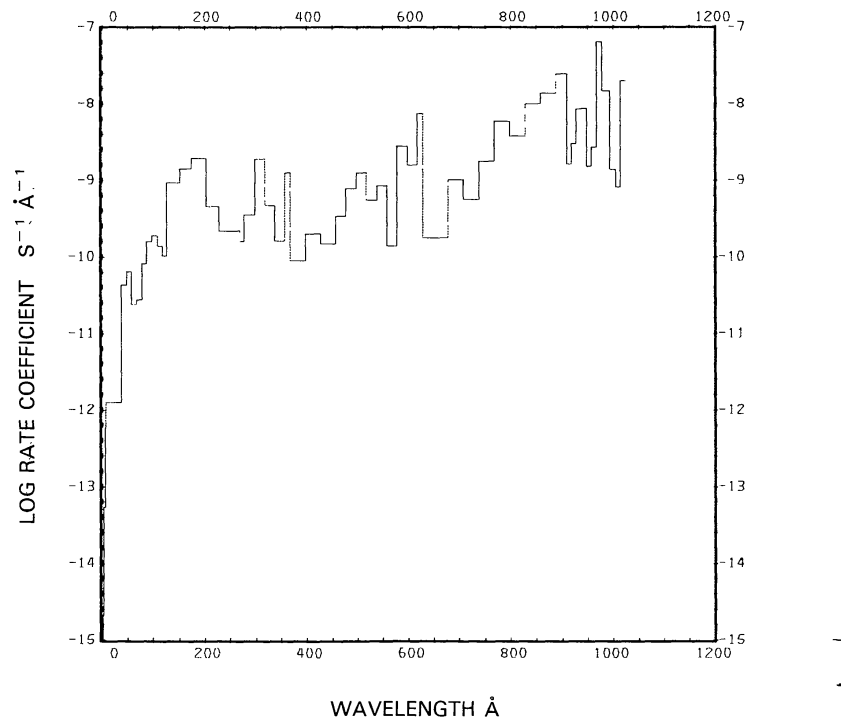
Threshold: The ionization threshold is at $\lambda = 1023 \text{ \AA}$ (Huffman *et al.*, 1963a).

Rate coefficient:



for the quiet Sun (see Figure 23a) and $3.49 \times 10^{-6} \text{ s}^{-1}$ for the active Sun (see Figure 23b).

Excess energy: The excess energy for the quiet Sun is 4.16 eV and 5.22 eV for the active Sun.

Fig. 23a. $\text{Xe} + \nu \rightarrow \text{Xe}^+ + e$, for the quiet Sun.Fig. 23b. $\text{Xe} + \nu \rightarrow \text{Xe}^+ + e$, for the active Sun.

MOLECULAR HYDROGEN, H₂

Cross sections: Up to 200 Å the molecular cross section is approximated by twice the cross section for atomic hydrogen. From $\lambda = 209.3$ to 452.2 Å we used values measured by Samson and Cairns (1965). Between 500 and 844.79 Å the cross section measured by Cook and Metzger (1964) was used. A value at 584 Å is taken from Brolley *et al.* (1973). The line positions between 930.9 and 1108.6 Å for the predissociation in the H₂ Lyman system are given by Herzberg and Howe (1959), while the cross sections are calculated from the oscillator strengths of Allison and Dalgarno (1969).

Branching ratios: The branching ratio for ionization and dissociation is determined from the data of Cook and Metzger (1964), for dissociative ionization it is taken from Browning and Fryar (1973). The branching ratios for predissociation of the Lyman system are from Stephens and Dalgarno (1972).

Thresholds: For dissociation the $v = 0, J = 0$ threshold producing H(1s) and H(2s or 2p) was determined by Herzberg and Monfils (1960) at $\lambda = 844.79$ Å. The dissociation limit leading to H(1s) + H(1s) is 2768.85 Å (Sharp, 1971). The ionization threshold was determined by Beutler and Jünger (1936) for $J = 0$ to $J = 0$ at $\lambda = 803.67$ Å. The threshold for photodissociative ionization according to Browning and Fryar (1973) is at $\lambda = 695.8$ Å.

Rate coefficients:

$$\begin{aligned}
 \text{H}_2 + v \rightarrow & \text{H}(1s) + \text{H}(1s) : 4.80 \times 10^{-8} \text{ s}^{-1}, 1.09 \times 10^{-7} \text{ s}^{-1}, \\
 & \rightarrow \text{H}(1s) + \text{H}(2s, 2p) : 3.44 \times 10^{-8} \text{ s}^{-1}, 8.21 \times 10^{-8} \text{ s}^{-1}, \\
 & \rightarrow \text{H}_2^+ + e : 5.41 \times 10^{-8} \text{ s}^{-1}, 1.15 \times 10^{-7} \text{ s}^{-1}, \\
 & \rightarrow \text{H} + \text{H}^+ + e : 9.52 \times 10^{-9} \text{ s}^{-1}, 2.79 \times 10^{-8} \text{ s}^{-1}.
 \end{aligned}$$

Here the first value corresponds to the quiet Sun (see Figures 24(a) to 27(a)) and the second value to the active Sun (see Figures 24(b) to 27(b)). The rate coefficient for dissociation is sensitive to the cross section at threshold. Thus, vibrational excitation will increase the rate coefficient. For the quiet Sun, our rate for ionization is smaller than the corresponding rate of $8.4 \times 10^{-8} \text{ s}^{-1}$ obtained by Siscoe and Mukherjee (1972).

Excess energies:

$$\begin{aligned}
 \text{H}_2 + v \rightarrow & \text{H}(1s) + \text{H}(1s) : 8.23 \text{ eV}, 8.22 \text{ eV}, \\
 & \rightarrow \text{H}(1s) + \text{H}(2s, 2p) : 0.44 \text{ eV}, 0.42 \text{ eV}, \\
 & \rightarrow \text{H}_2^+ + e : 6.56 \text{ eV}, 7.17 \text{ eV}, \\
 & \rightarrow \text{H} + \text{H}^+ + e : 24.8 \text{ eV}, 27.0 \text{ eV}.
 \end{aligned}$$

The first of each of these values is for the quiet Sun; the second value is for the active Sun. Vibrational excitation will decrease the excess energies.

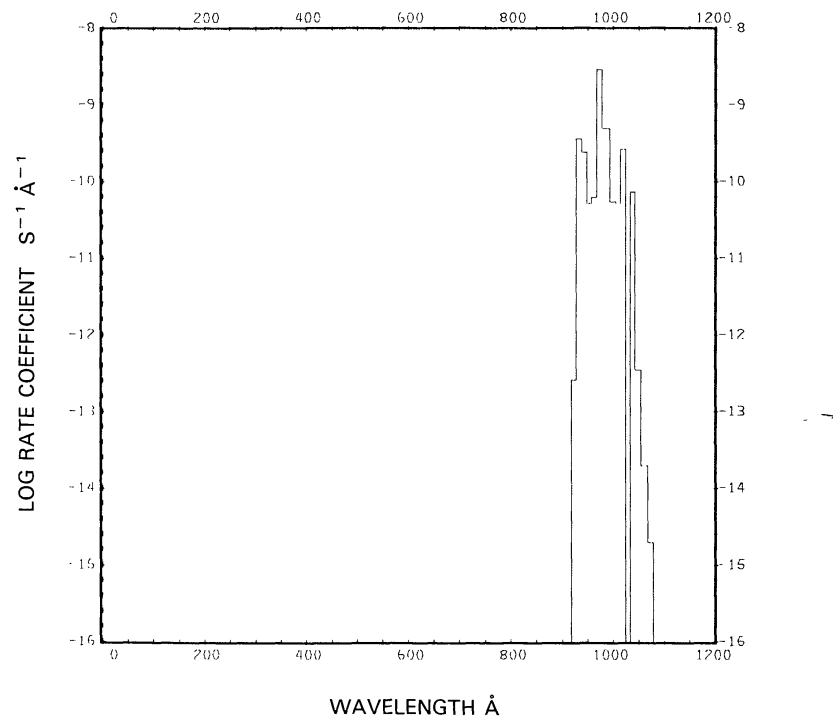


Fig. 24a. H₂ + ν → H(1s) + H(1s), for the quiet Sun.

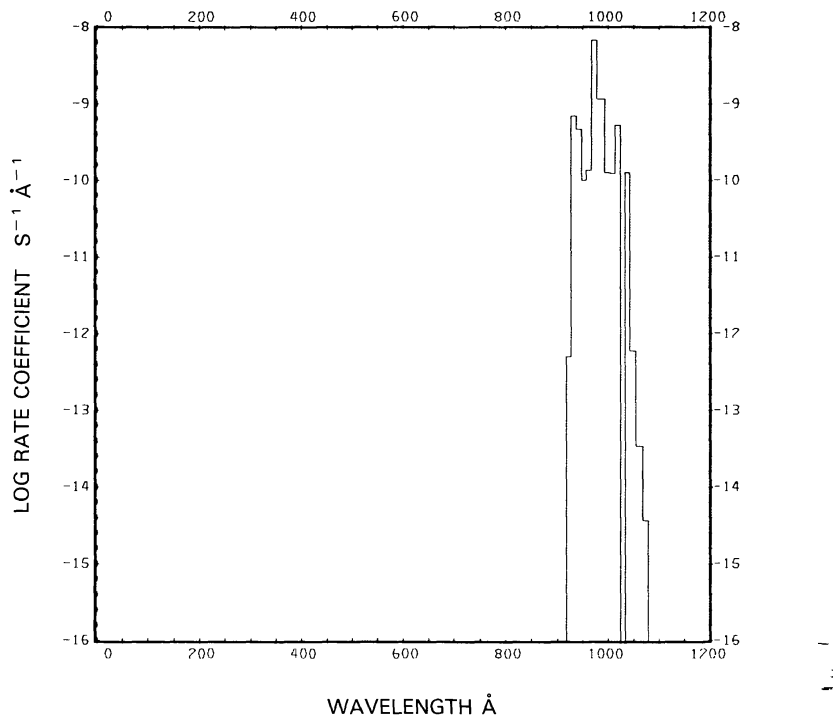
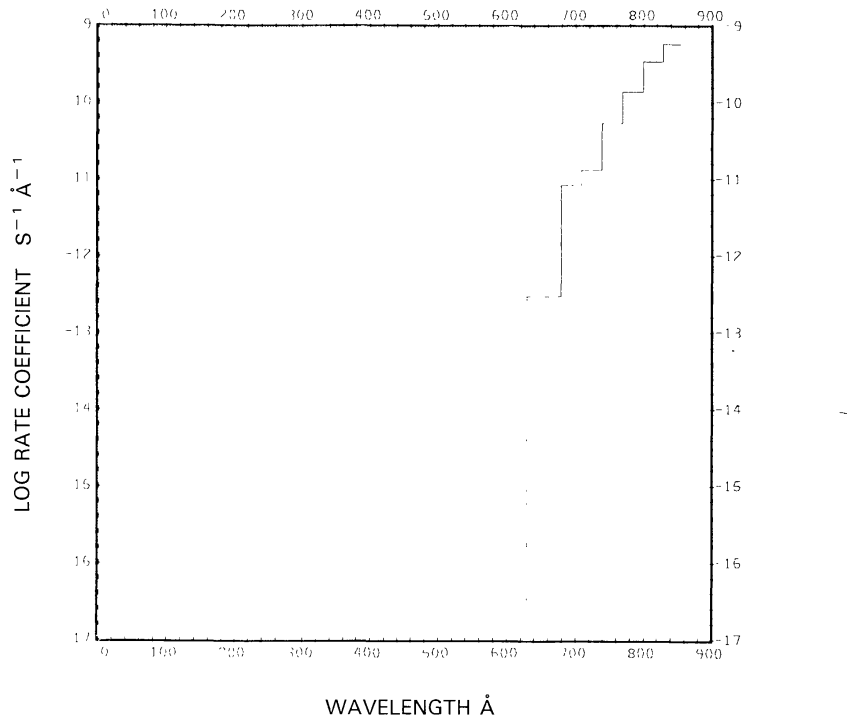
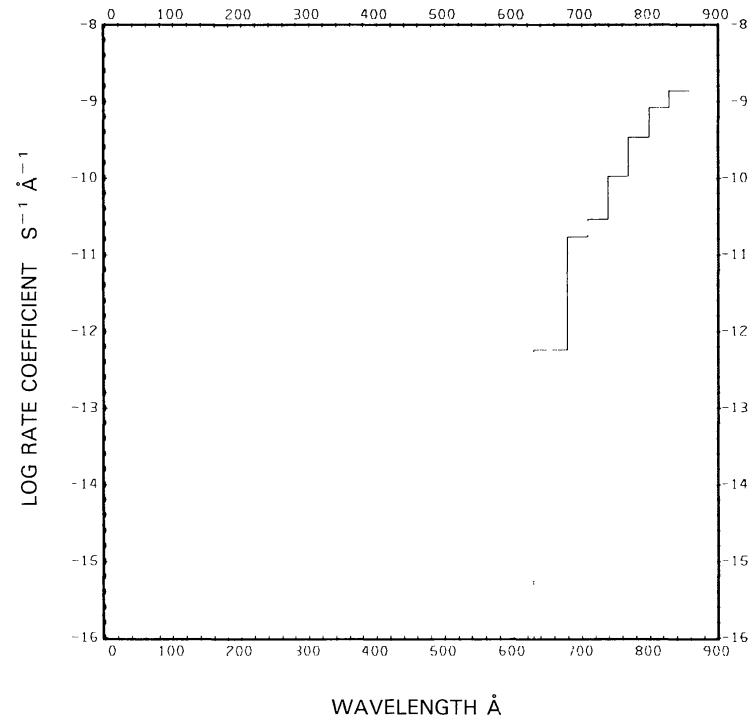
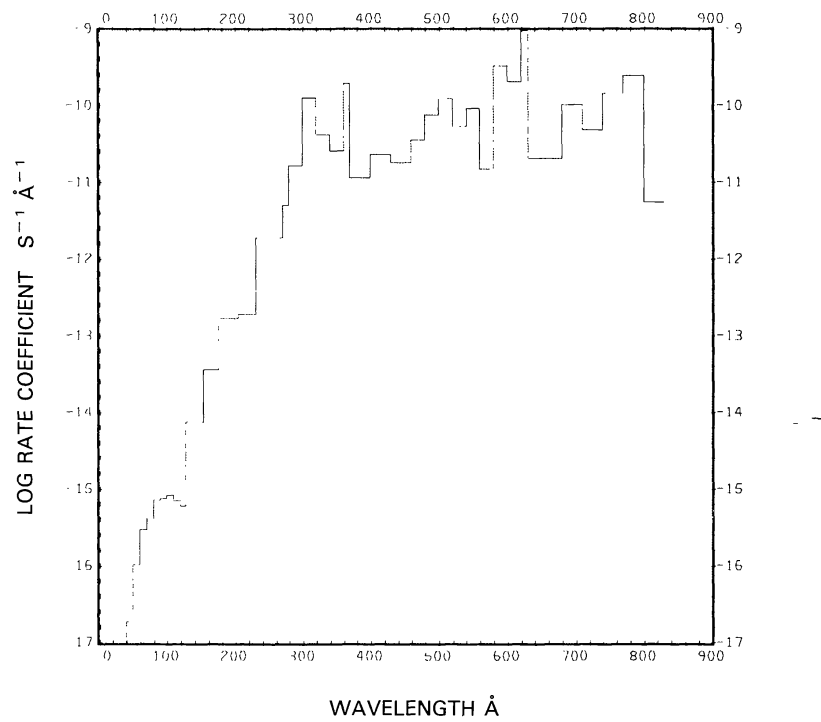
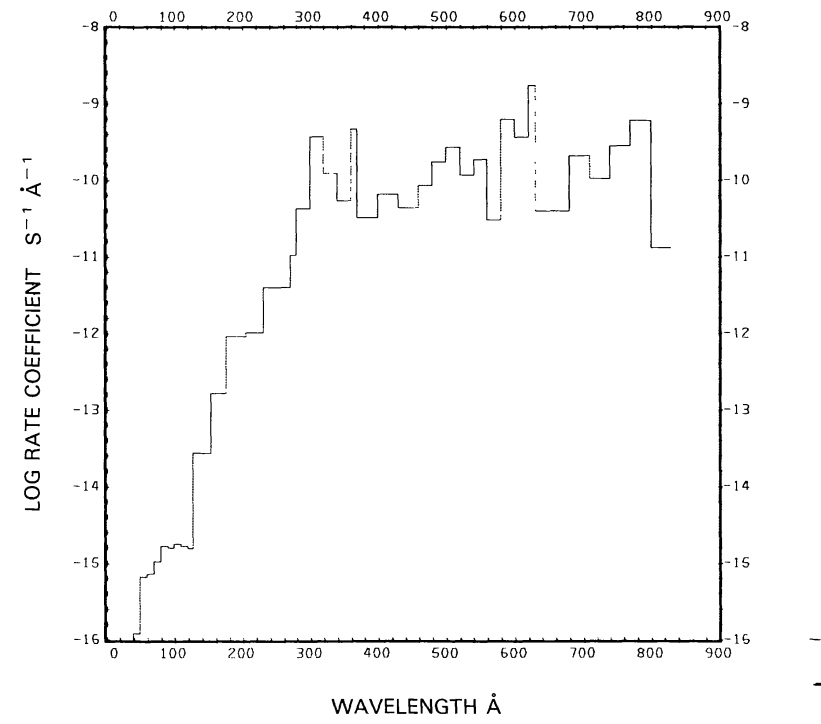
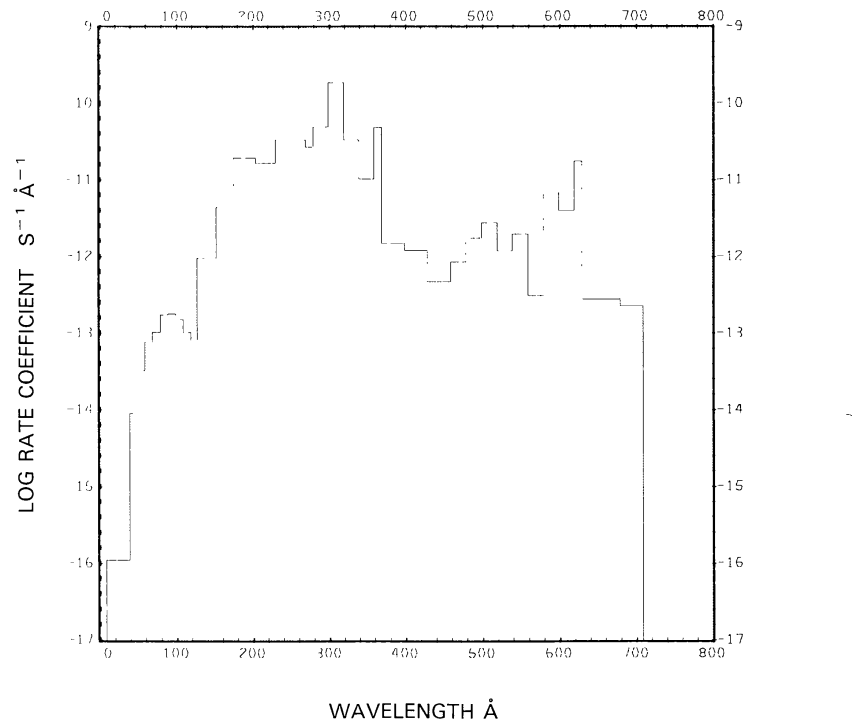
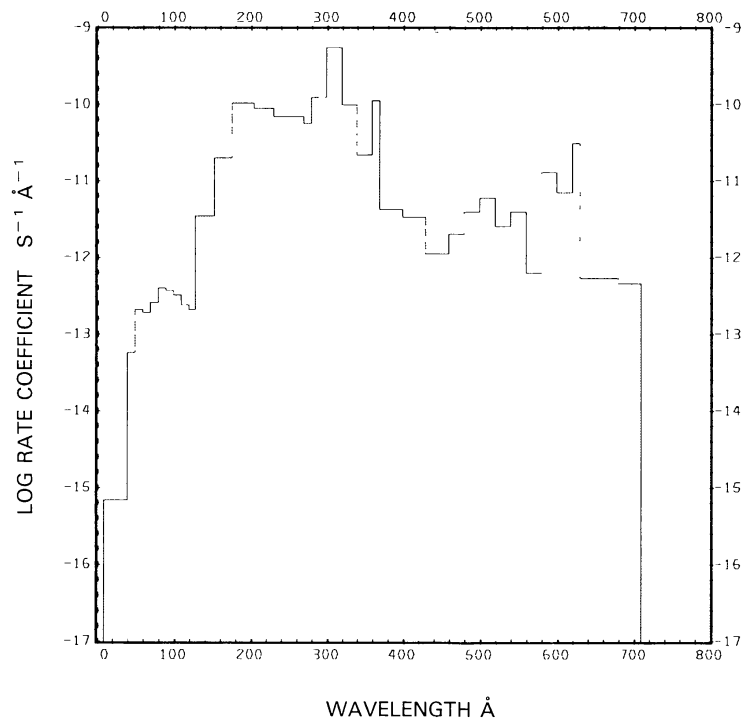


Fig. 24b. H₂ + ν → H(1s) + H(1s), for the active Sun.

Fig. 25a. $H_2 + v \rightarrow H(1s) + H(2s, 2p)$, for the quiet Sun.Fig. 25b. $H_2 + v \rightarrow H(1s) + H(2s, 2p)$, for the active Sun.

Fig. 26a. H₂ + ν → H₂⁺ + e, for the quiet Sun.Fig. 26b. H₂ + ν → H₂⁺ + e, for the active Sun.

Fig. 27a. $\text{H}_2 + \nu \rightarrow \text{H} + \text{H}^+ + e$, for the quiet Sun.Fig. 27b. $\text{H}_2 + \nu \rightarrow \text{H} + \text{H}^+ + e$, for the active Sun.

METHYLIDYNE, CH

Cross sections: Between $\lambda = 12$ and 617 \AA the cross section comes from calculations by Walker and Kelly (1972) and between $\lambda = 827$ and 1170 \AA it comes from calculations by Barsuhn and Nesbet (1978). The cross section was supplemented with the predissociation data at about $\lambda = 1000 \text{ \AA}$ from the theoretical calculations of van Dishoeck (1987). In the region $\lambda = 1170 \text{ \AA}$ to the dissociation threshold the cross sections for the dissociation continuum and predissociation lines of van Dishoeck (1987) were used.

Branching ratios: The branching ratio for ionization was obtained from the work of Barsuhn and Nesbet (1978). The main branch of predissociation is through the $v'' = 0$ level of the $C(^2\Sigma^+)$ electronic state. Although this state is associated with dissociation into $C(^1D) + H$, it predissociates into $C(^3P) + H$ (van Dishoeck, 1987). This predissociation is very sensitive to Doppler shifts relative to the solar spectrum (Singh and Dalgarno, 1987). The $2(^2\Sigma^+)$ electronic state is associated with dissociation into $C(^1S) + H$. Although dissociation through this state can also lead to $C(^1D)$ and $C(^3P)$ states, we have assumed a branching ratio of 1 for dissociation into $C(^1S) + H$. All other dissociation is into $C(^1D) + H$ up to its threshold.

Thresholds: The threshold for dissociation, based on the predissociation limit, is given by Herzberg and Johns (1969) as $\lambda = 3589.9 \text{ \AA}$. This is also in good agreement with the wavelength equivalent for the heats of formation $\lambda = 3540 \pm 20 \text{ \AA}$ as obtained by Linevsky (1967). Thresholds for dissociation into $C(^1D) + H$ and into $C(^1S) + H$ are 2603.3 and 2005.3 \AA , respectively. The ionization limit determined by Barsuhn and Nesbet (1978) is at $\lambda = 1170 \text{ \AA}$.

Rate coefficients:

$$\begin{aligned}
 \text{CH} + v &\rightarrow \text{C} + \text{H} : 9.20 \times 10^{-3} \text{ s}^{-1}, 9.20 \times 10^{-3} \text{ s}^{-1}, \\
 &\rightarrow \text{C}(^1D) + \text{H} : 5.12 \times 10^{-6} \text{ s}^{-1}, 7.61 \times 10^{-6} \text{ s}^{-1}, \\
 &\rightarrow \text{C}(^1S) + \text{H} : 5.03 \times 10^{-5} \text{ s}^{-1}, 5.55 \times 10^{-5} \text{ s}^{-1}, \\
 &\rightarrow \text{CH}^+ + e^- : 7.58 \times 10^{-7} \text{ s}^{-1}, 1.70 \times 10^{-6} \text{ s}^{-1}.
 \end{aligned}$$

The first value of each branch is for the quiet Sun (see Figures 28 to 30 and 31(a)), the second for the active Sun (see Figure 31(b)). The dissociation is dominated by predissociation around $\lambda = 3147 \text{ \AA}$. The largest branches of the rate coefficients are not sensitive to solar activity. For the quiet Sun, our dissociation rates for the various branches agree well with those of Singh and Dalgarno (1987), but our total dissociation rate is almost 50% higher than that of Wyckoff and Wehinger (1976) ($6.4 \times 10^{-3} \text{ s}^{-1}$), while our ionization rate agrees well with their value of $7.9 \times 10^{-7} \text{ s}^{-1}$.

Excess energies:

$\text{CH} + \nu \rightarrow \text{C} + \text{H}$: 0.45 eV, 0.45 eV,
 $\rightarrow \text{C}(^1D) + \text{H}$: 3.60 eV, 3.82 eV,
 $\rightarrow \text{C}(^1S) + \text{H}$: 0.18 eV, 0.18 eV,
 $\rightarrow \text{CH}^+ + e^-$: 6.35 eV, 7.80 eV.

The first value for each branch is for the quiet Sun, the second is for the active Sun

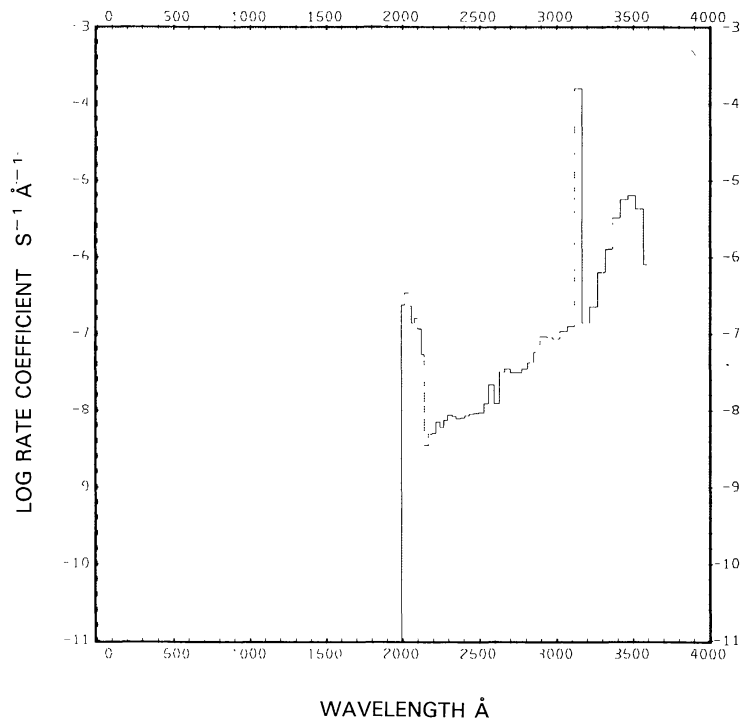
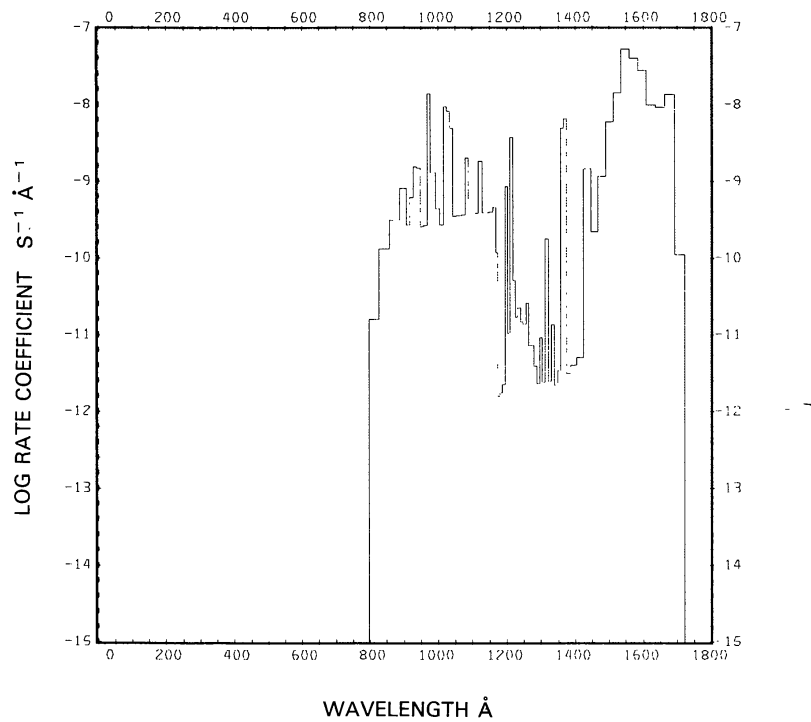
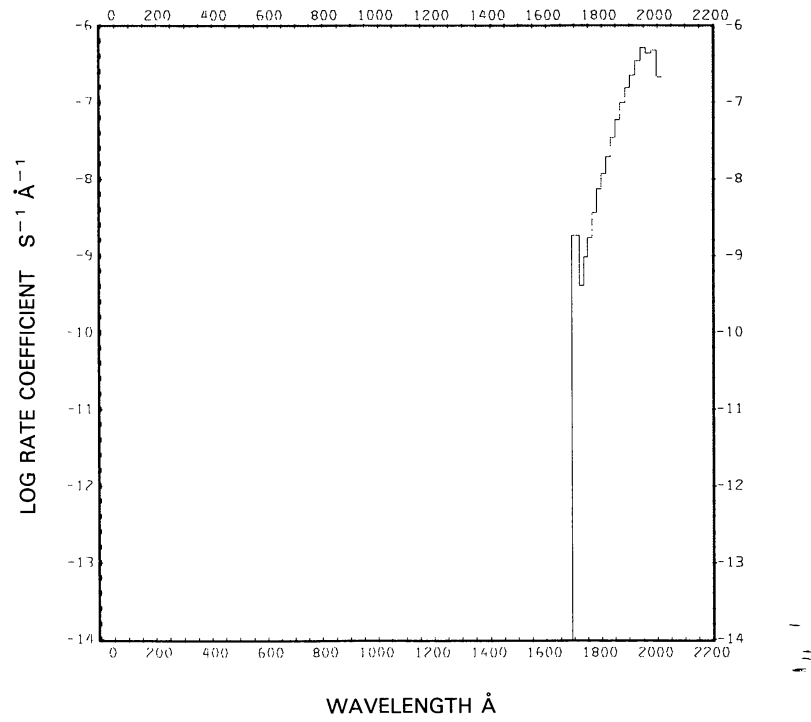
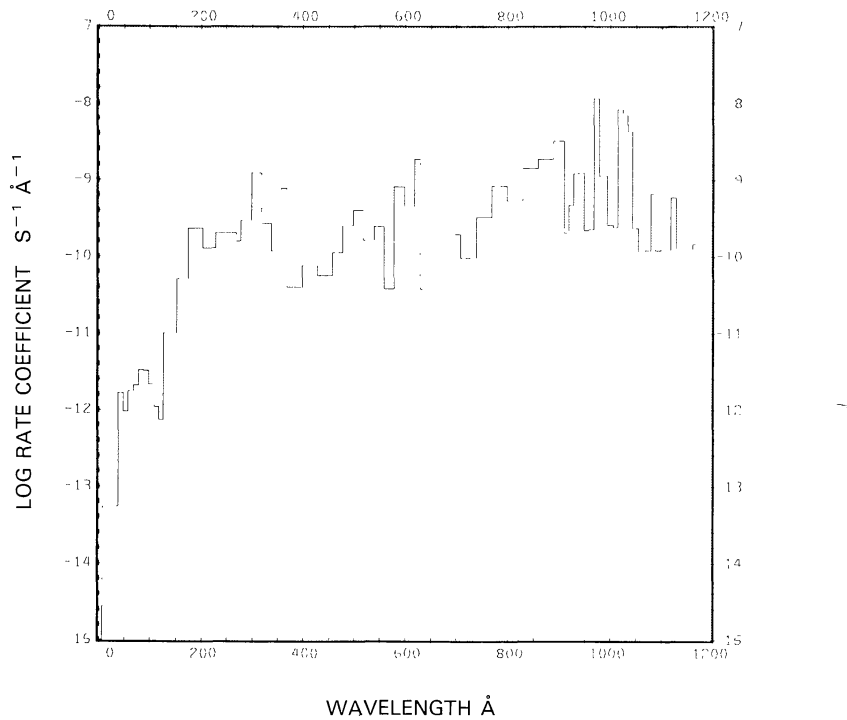
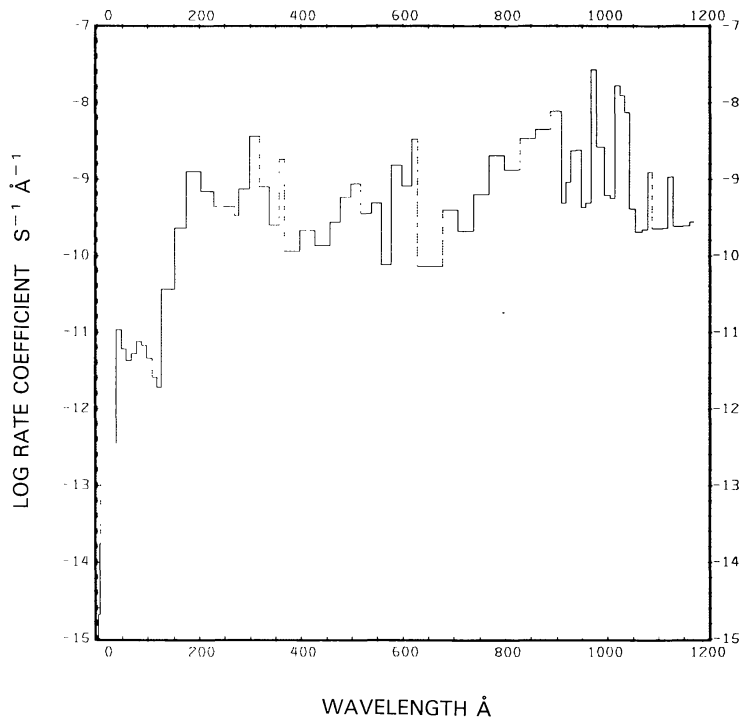


Fig. 28. $\text{CH} + \nu \rightarrow \text{C} + \text{H}$, for the quiet Sun.

Fig. 29. $\text{CH} + \nu \rightarrow \text{C}({}^1\text{D}) + \text{H}$, for the quiet Sun.Fig. 30. $\text{CH} + \nu \rightarrow \text{C}({}^1\text{S}) + \text{H}$, for the quiet Sun.

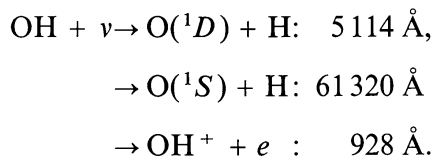
Fig. 31a. $\text{CH} + \nu \rightarrow \text{CH}^+ + e$, for the quiet Sun.Fig. 31b. $\text{CH} + \nu \rightarrow \text{CH}^+ + e$, for the active Sun.

HYDROXYL RADICAL, OH

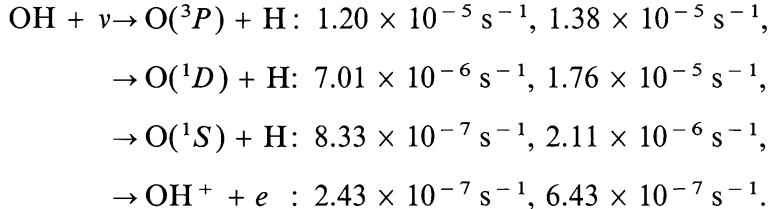
Cross sections: Up to 625.8 Å the cross section for OH is approximated by the sum of the atomic cross sections for O and H taken from fits by Barfield *et al.* (1972). We have used the experimental cross section from $\lambda = 1150$ to 1830 Å of Nee and Lee (1984) and alternatively the theoretical cross section from $\lambda = 939.3$ to 1907 Å of van Dishoeck (1984). The experimental cross section is larger than the theoretical cross section and probably too large (Nee and Lee, 1984).

Branching ratios: Branching ratios are given by Van Dishoeck (1984).

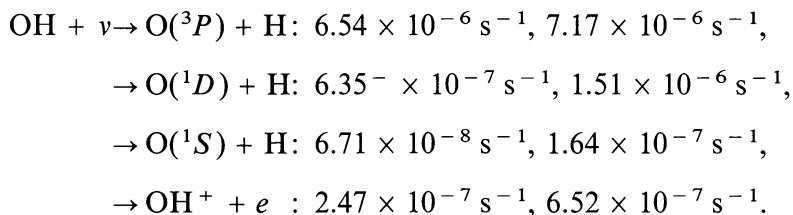
Thresholds: The threshold wavelength for dissociation into the ground state of oxygen is 2823 Å, as given by Huber and Herzberg (1979). Other threshold wavelengths, leading to excited states of atomic oxygen and to ionization, are



Rate coefficients:



These values are for the experimental cross sections. The first values are for the quiet Sun (see Figures 32 and 33(a) to 35(a)), the second for the active Sun (see Figures 33(b) to 35(b)).

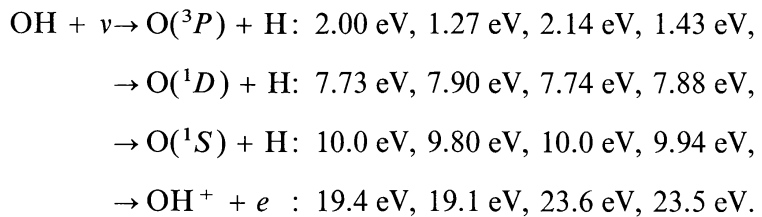


These values are for the theoretical cross sections. The first values are again for the quiet Sun (see Figures 36 and 37(a) to 39(a)), the second for the active Sun (see Figures 37(b) to 39(b)).

For comparison, at solar minimum and zero Doppler shift relative to the Sun, Singh *et al.* (1983) obtain $6.7 \times 10^{-6} \text{ s}^{-1}$ for the total dissociation rate and van Dishoeck and Dalgarno (1984) obtain for the above three dissociation branches $6.4 \times 10^{-6} \text{ s}^{-1}$,

$4.0 \times 10^{-7} \text{ s}^{-1}$, and $5.0 \times 10^{-8} \text{ s}^{-1}$, respectively. The first of these values is an average, since it is sensitive to the Doppler shift of the predissociation lines relative to the solar spectrum. The predissociation lines alone, in the production of $\text{O}({}^3P)$, give a rate coefficient of $3.9 \times 10^{-6} \text{ s}^{-1}$ as an average value, not considering any Doppler shifts resulting in coincidences or anti-coincidences with the solar spectrum. We have assumed that the total absorption cross section below 928 Å leads to photoionization. Our rate for ionization is smaller than the rate of $3.49 \times 10^{-7} \text{ s}^{-1}$ quoted by Siscoe and Mukherjee (1972).

Excess energies: The excess energies are:



The first values for each branch are obtained from the experimental cross section for the quiet Sun, the second from the theoretical cross section for the quiet Sun, the third from the experimental cross section for the active Sun, and the fourth from the theoretical cross section for the active Sun. For the production of $\text{O}({}^3P)$ from predissociation alone, the excess energy is 0.35 eV.

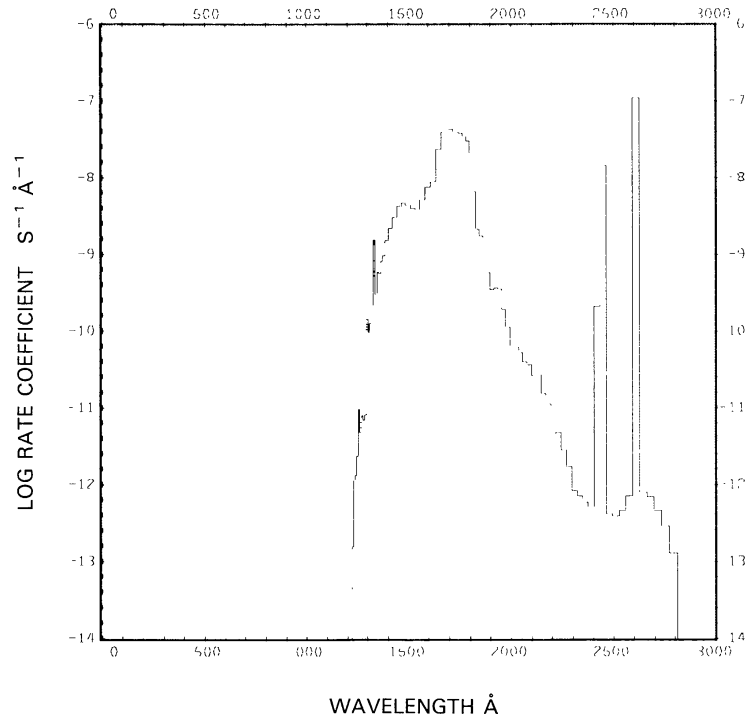


Fig. 32. $\text{OH} + \nu \rightarrow \text{O}({}^3P) + \text{H}$, for the quiet Sun from the experimental cross section.

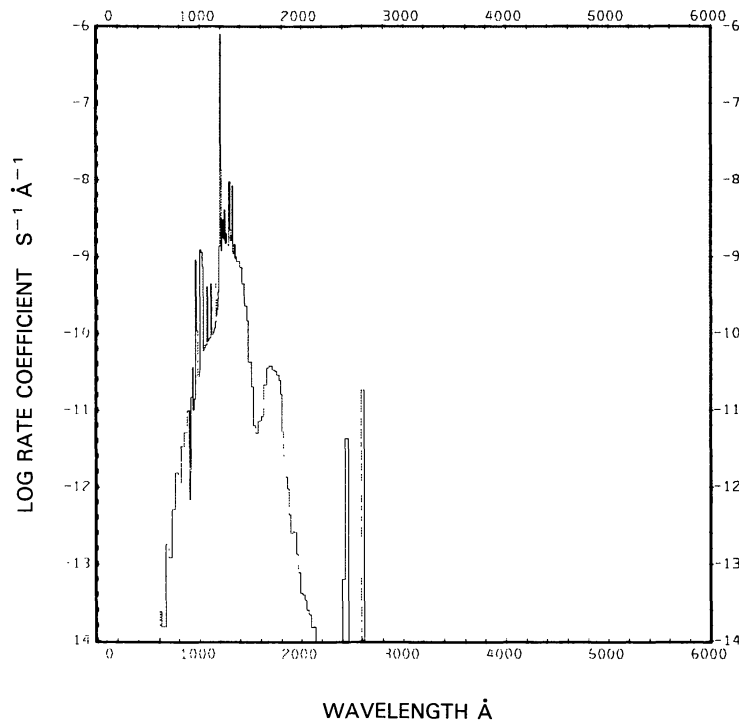


Fig. 33a. $\text{OH} + \nu \rightarrow \text{O}({}^1\text{D}) + \text{H}$, for the quiet Sun from the experimental cross section.

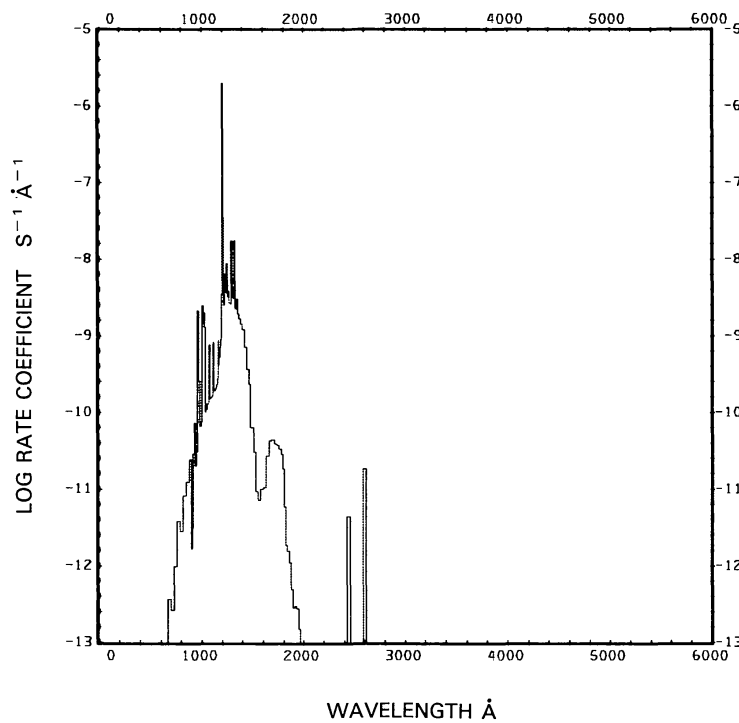


Fig. 33b. $\text{OH} + \nu \rightarrow \text{O}({}^1\text{D}) + \text{H}$, for the active Sun from the experimental cross section.

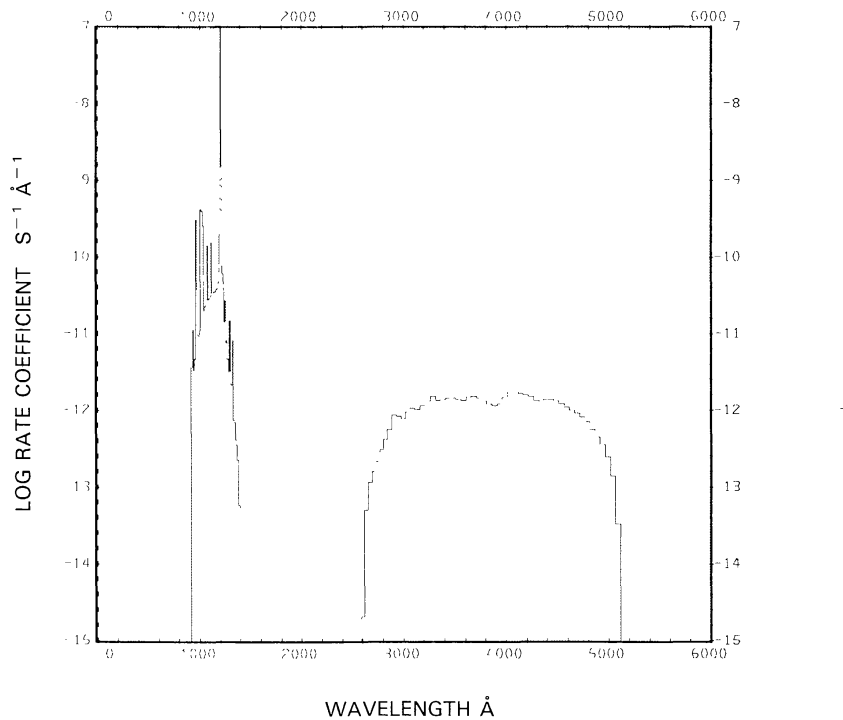


Fig. 34a. $\text{OH} + \nu \rightarrow \text{O}({}^1\text{S}) + \text{H}$, for the quiet Sun from the experimental cross section.

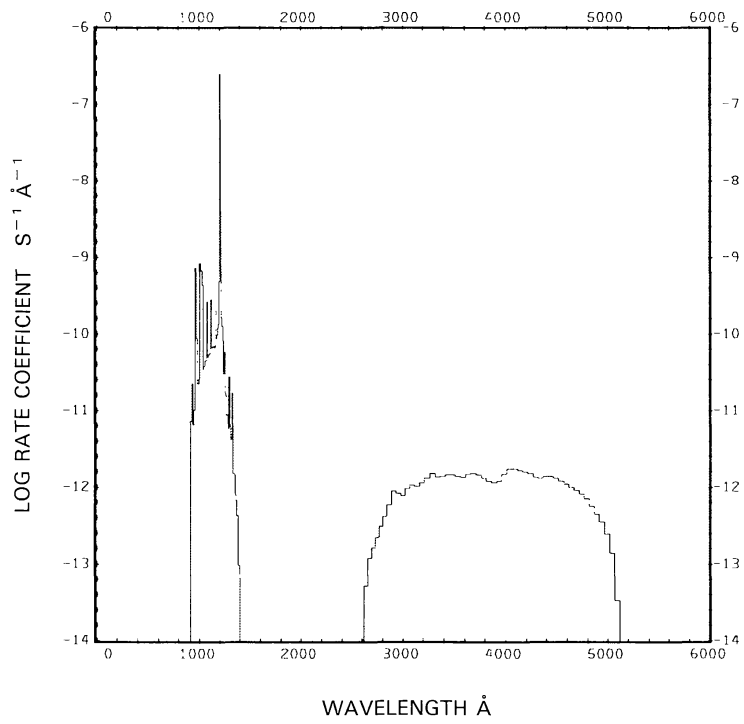


Fig. 34b. $\text{OH} + \nu \rightarrow \text{O}({}^1\text{S}) + \text{H}$, for the active Sun from the experimental cross section.

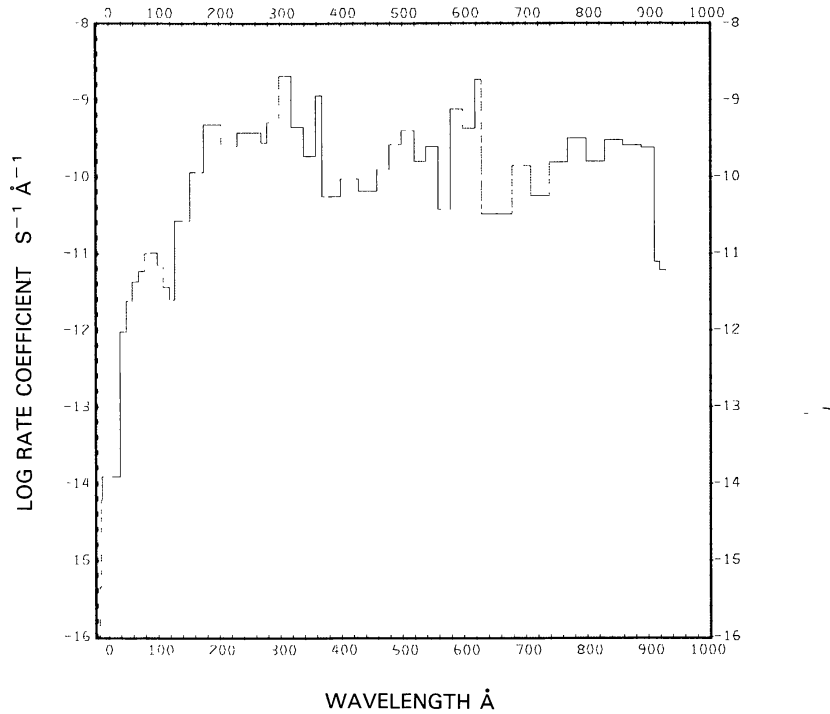


Fig. 35a. $\text{OH} + \nu \rightarrow \text{OH}^+ + e$, for the quiet Sun from the experimental cross section.

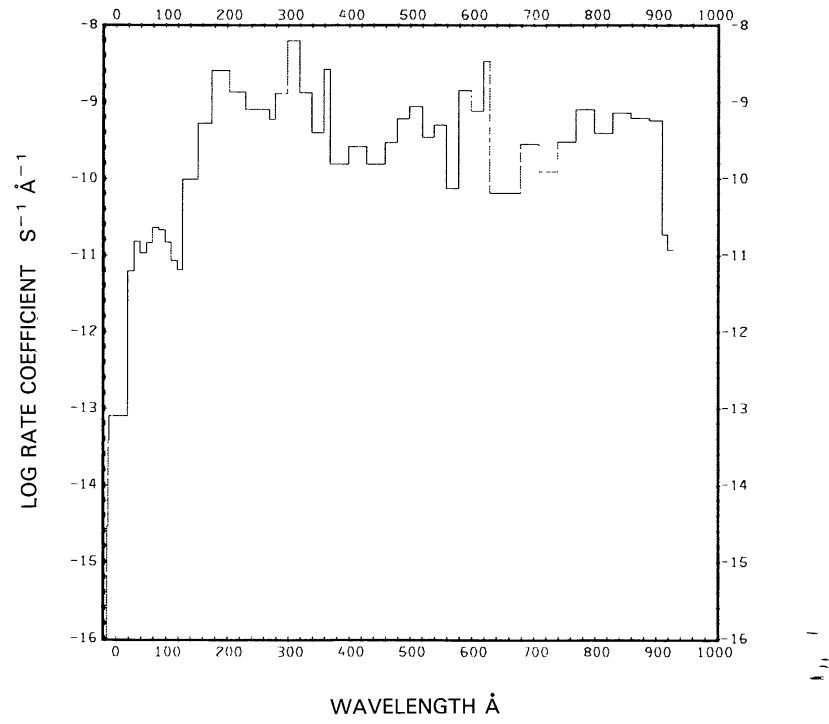


Fig. 35b. $\text{OH} + \nu \rightarrow \text{OH}^+ + e$, for the active Sun from the experimental cross section.

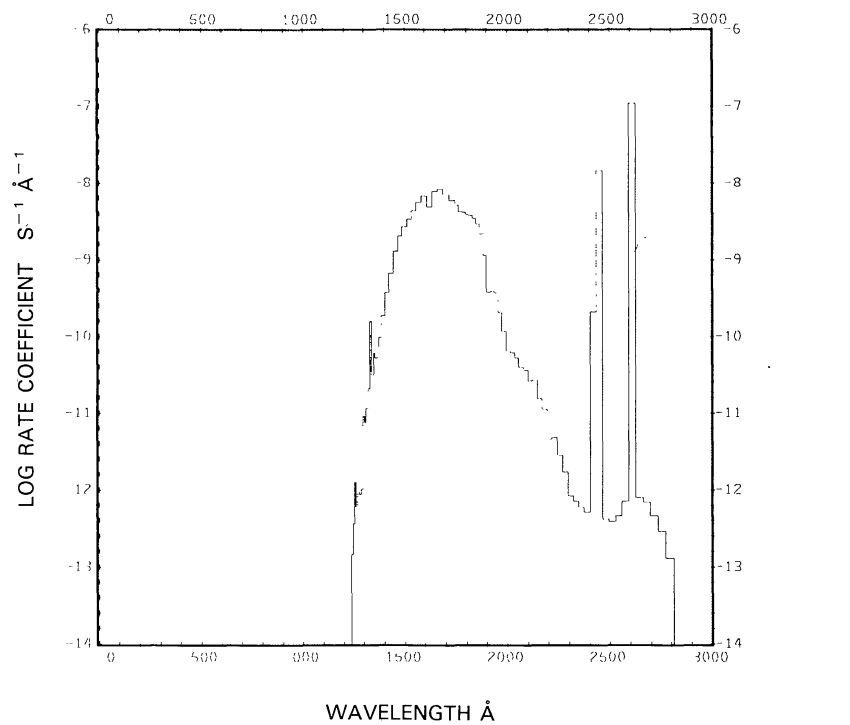


Fig. 36. $\text{OH} + \nu \rightarrow \text{O}(^3\text{P}) + \text{H}$, for the quiet Sun from the theoretical cross section.

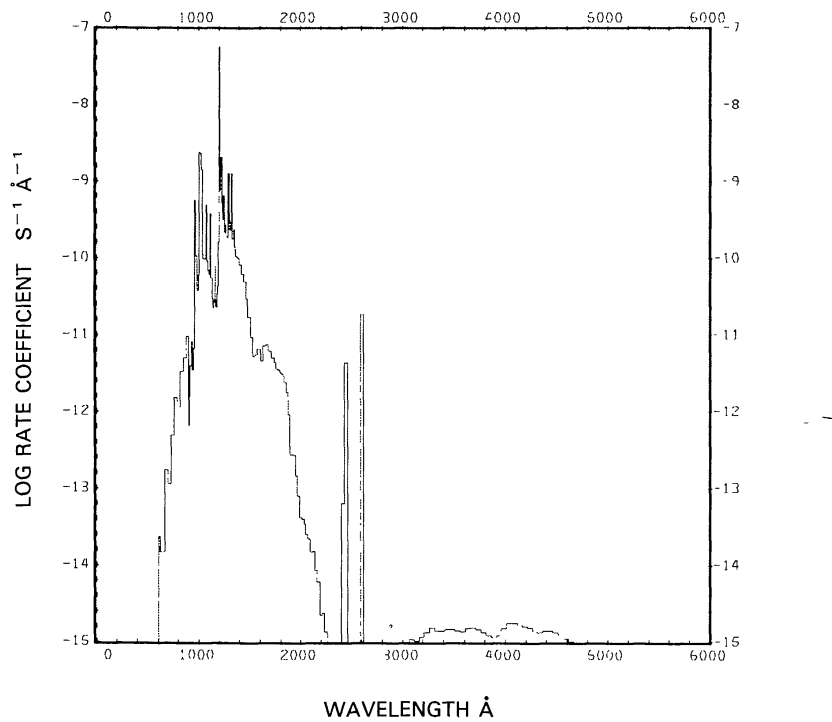


Fig. 37a. $\text{OH} + v \rightarrow \text{O}({}^1\text{D}) + \text{H}$, for the quiet Sun from the theoretical cross section.

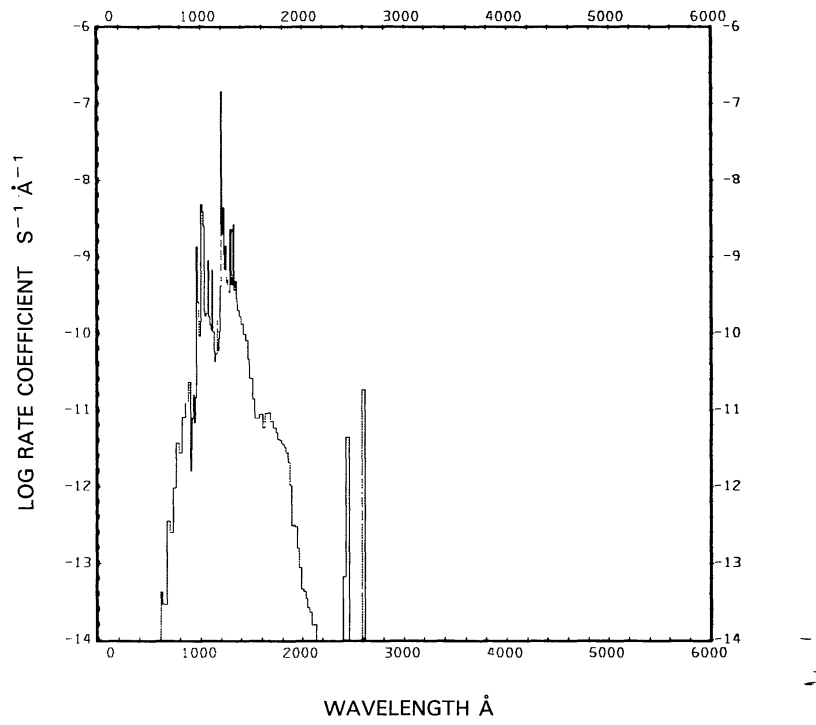


Fig. 37b. $\text{OH} + v \rightarrow \text{O}({}^1\text{D}) + \text{H}$, for the active Sun from the theoretical cross section.

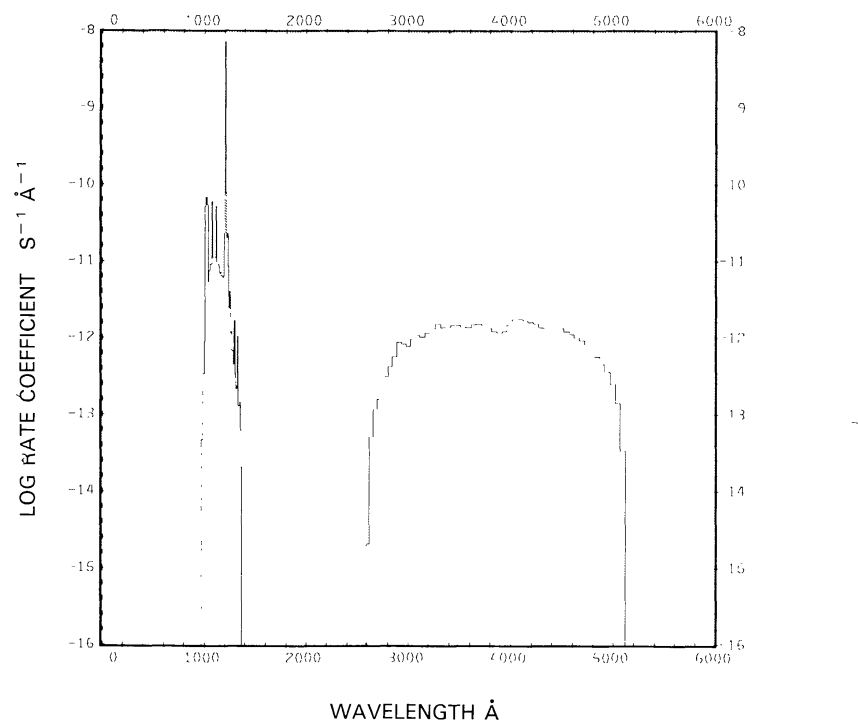


Fig. 38a. $\text{OH} + \nu \rightarrow \text{O}({}^1\text{S}) + \text{H}$, for the quiet Sun from the theoretical cross section.

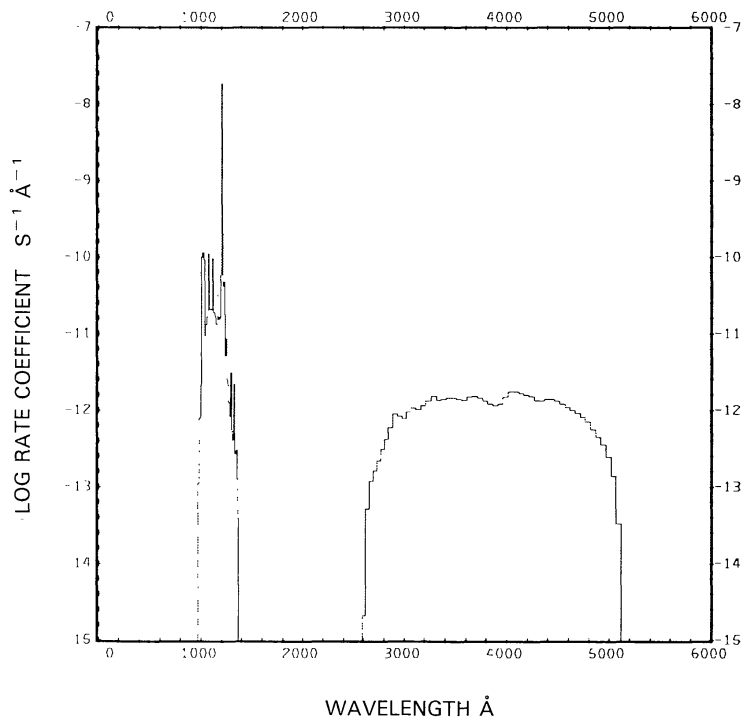


Fig. 38b. $\text{OH} + \nu \rightarrow \text{O}({}^1\text{S}) + \text{H}$, for the active Sun from the theoretical cross section.

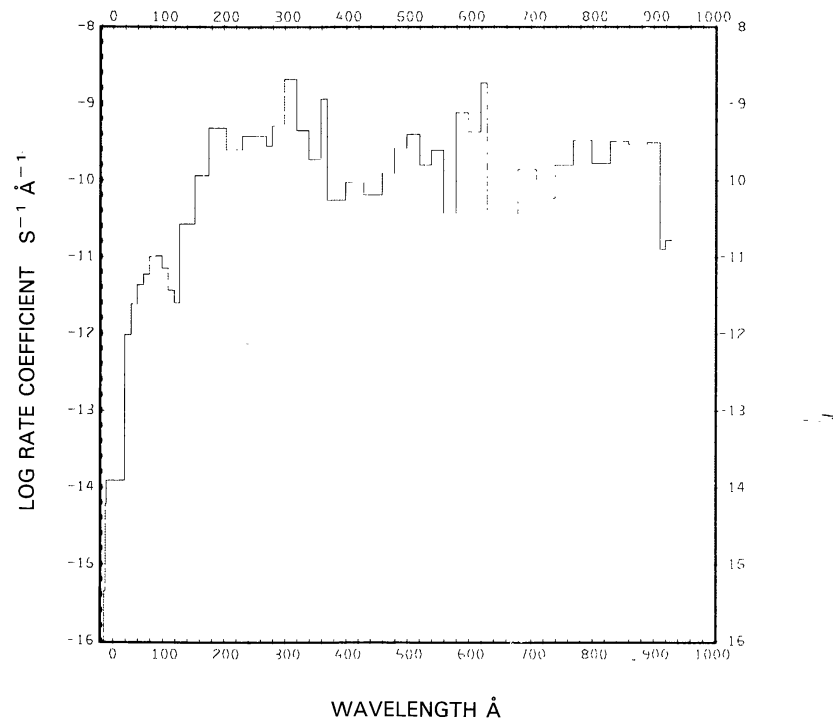


Fig. 39a. $\text{OH} + \nu \rightarrow \text{OH}^+ + e^-$, for the quiet Sun from the theoretical cross section.

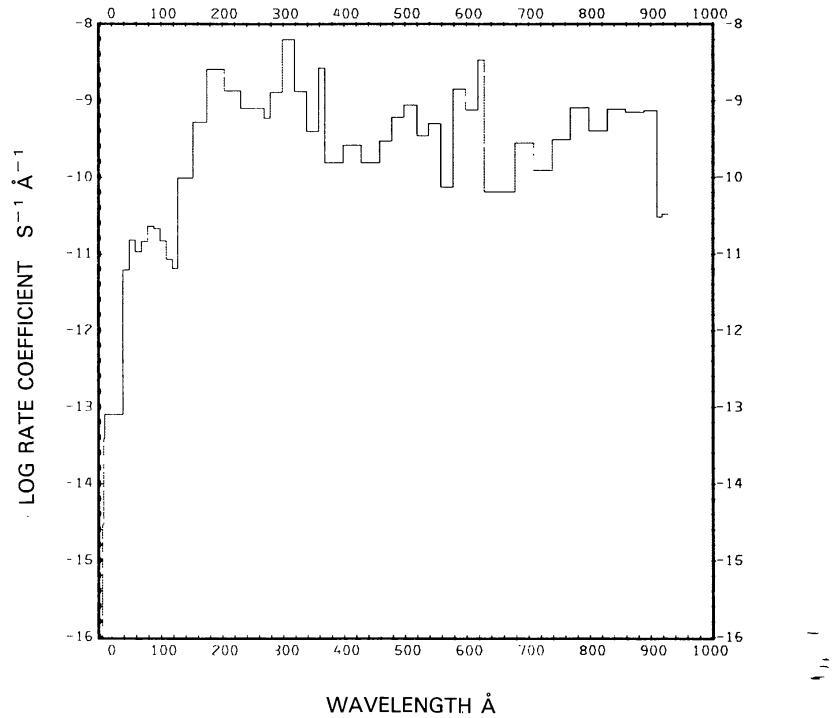


Fig. 39b. $\text{OH} + \nu \rightarrow \text{OH}^+ + e^-$, for the active Sun from the theoretical cross section.

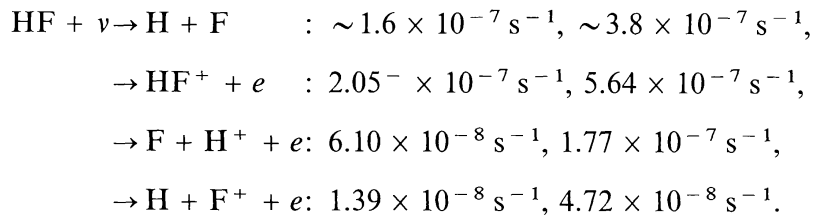
HYDROGEN FLUORIDE, HF

Cross sections: Below 122 Å the cross section is synthesized from the cross sections of the constituent atoms from the fits of Barfield *et al.* (1972). From 206.6 to 774.9 Å the cross section of Carnovale and Brion (1983) was used. Between 1480 and 1610 Å the cross section of Safary *et al.* (1951) was used.

Branching ratios: The branching ratios between ionization and the various dissociative ionizations are given by Carnovale and Brion (1983). We assumed no dissociation below the wavelength of the ionization threshold.

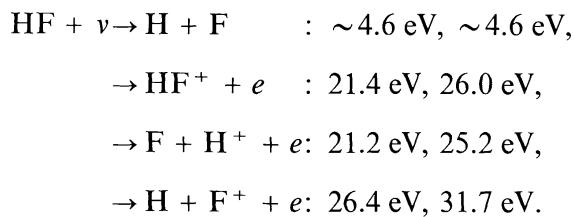
Thresholds: The threshold wavelength for dissociation, $\lambda = 2110 \text{ \AA}$, was taken from Baulch *et al.* (1982). The thresholds for ionization ($\lambda = 774.9 \text{ \AA}$) and dissociative ionization ($\lambda = 652.55 \text{ \AA}$ for both branches) were taken from Carnovale and Brion (1983).

Rate coefficients:



The first values for each branch are for the quiet Sun (see Figures 40(a) to 43(a)), the second for the active Sun (see Figures 40(b) to 43(b)).

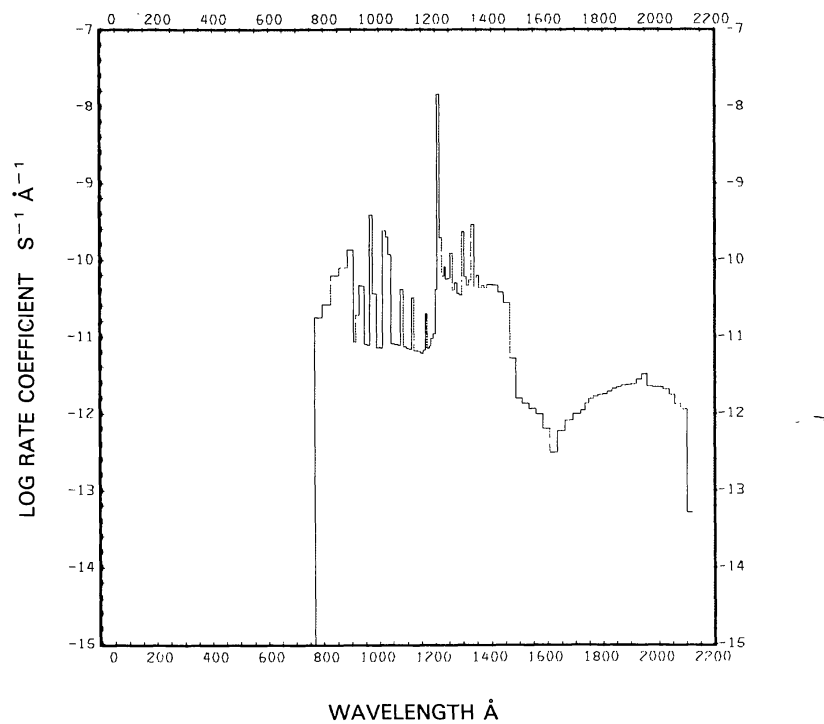
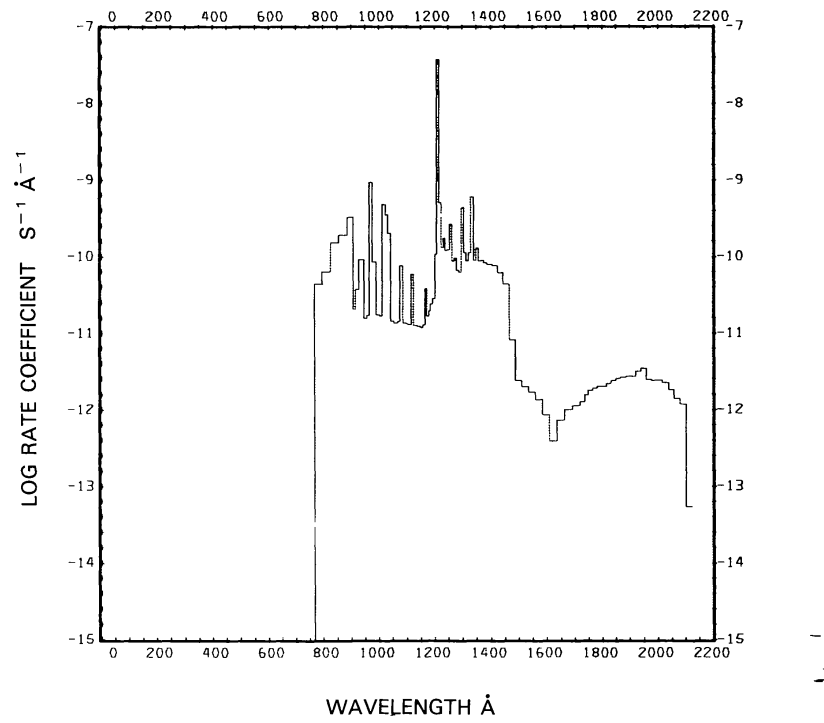
Excess energies: The excess energies are:

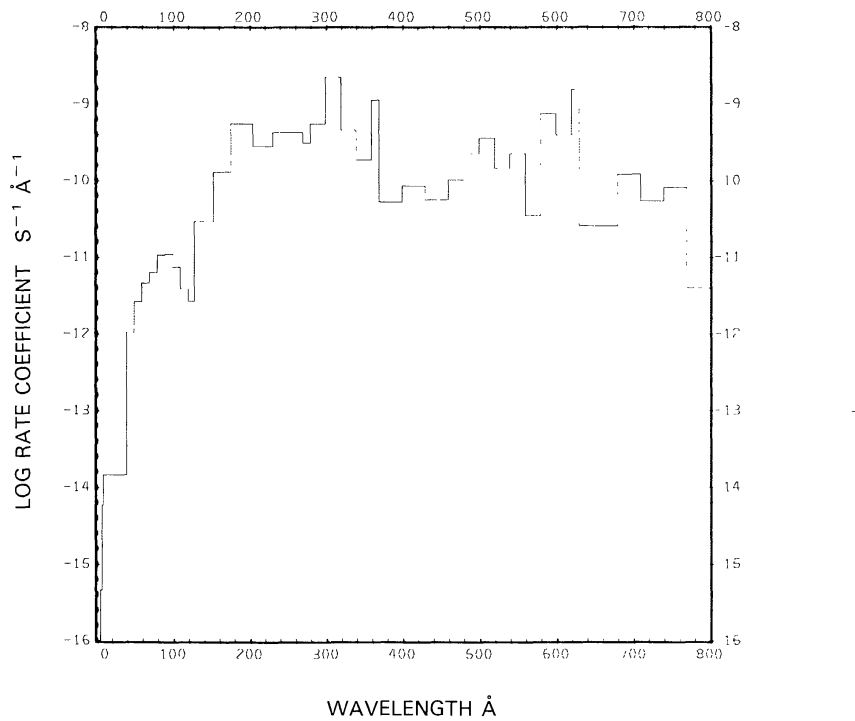
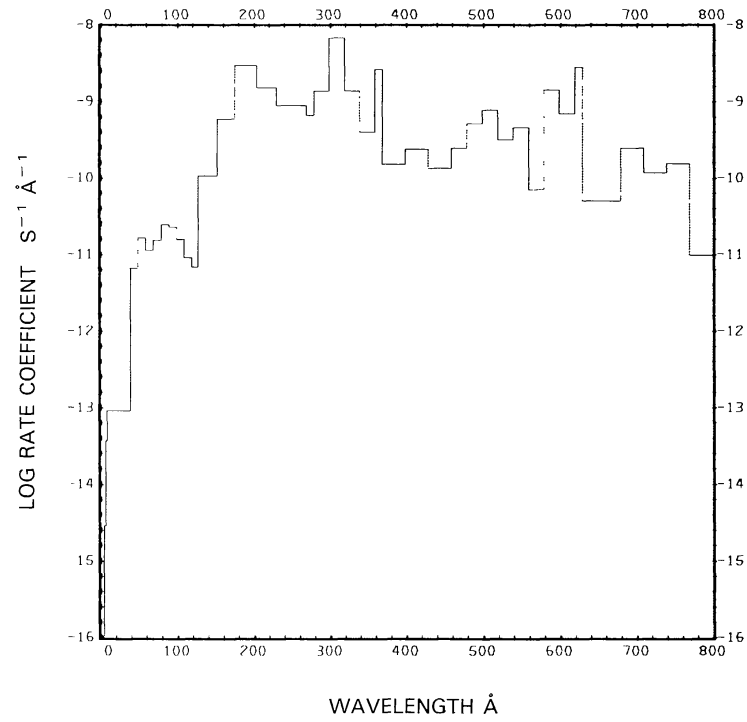


The first entries for each branch are for the quiet Sun, the second for the active Sun.

HYDROGEN FLUORIDE, HF

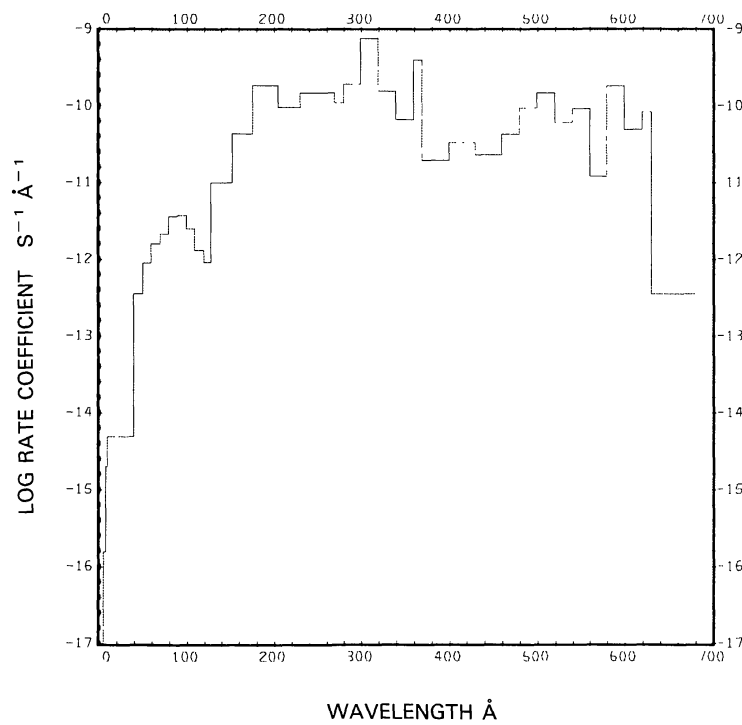
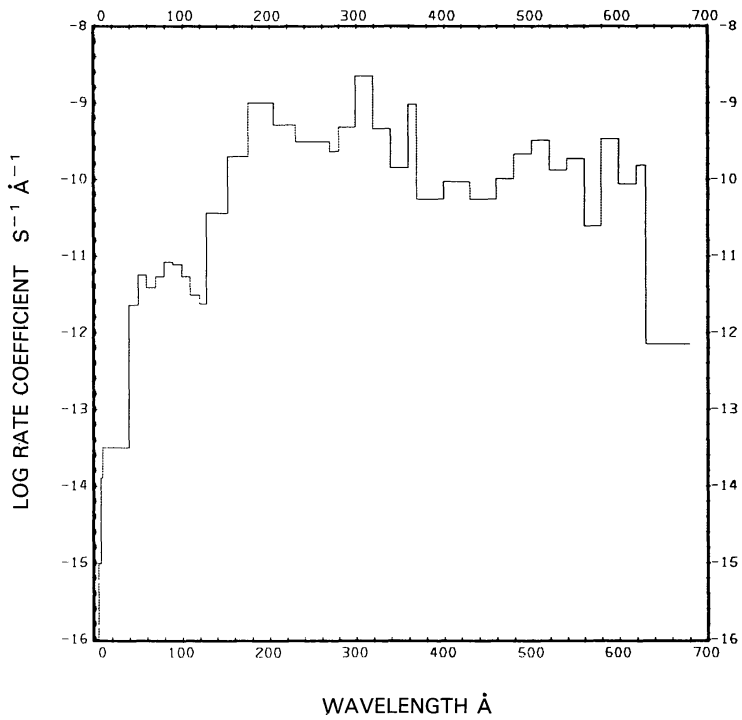
57

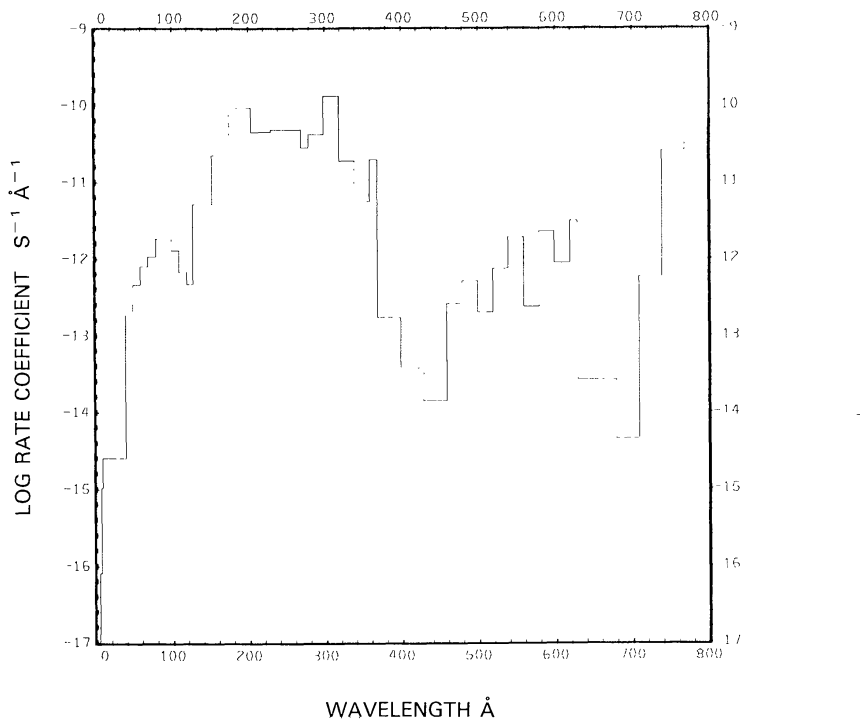
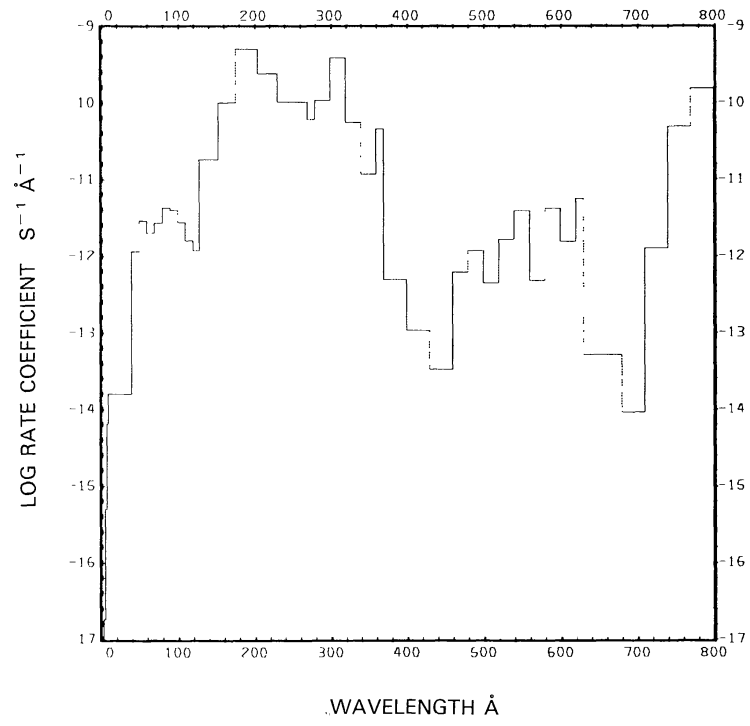
Fig. 40a. $\text{HF} + \nu \rightarrow \text{H} + \text{F}$, for the quiet Sun.Fig. 40b. $\text{HF} + \nu \rightarrow \text{H} + \text{F}$, for the active Sun.

Fig. 41a. $\text{HF} + \nu \rightarrow \text{HF}^+ + e$, for the quiet Sun.Fig. 41b. $\text{HF} + \nu \rightarrow \text{HF}^+ + e$, for the active Sun.

HYDROGEN FLUORIDE, HF

59

Fig. 42a. $\text{HF} + \nu \rightarrow \text{F} + \text{H}^+ + e$, for the quiet Sun.Fig. 42b. $\text{HF} + \nu \rightarrow \text{F} + \text{H}^+ + e$, for the active Sun.

Fig. 43a. HF + $\nu \rightarrow$ H + F⁺ + e, for the quiet Sun.Fig. 43b. HF + $\nu \rightarrow$ H + F⁺ + e, for the active Sun.

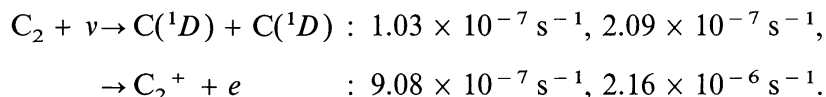
DIATOMIC CARBON, C₂

Cross sections: Up to $\lambda = 248 \text{ \AA}$ the cross section is approximated by twice the atomic cross section for C taken from fits made by Barfield *et al.* (1972). From 248 to 954 \AA the ionization cross section has been calculated by Padial *et al.* (1985) and from 918 to 1210 \AA the dissociation cross section from Pouilly *et al.* (1983) has been used. There is excellent agreement between the cross sections by Barfield *et al.* and Padial *et al.* above 248 \AA . In the overlap region from $\lambda = 918$ to 954 \AA the total cross section is the sum of the ionization and dissociation cross sections. From $\lambda = 1210 \text{ \AA}$ to threshold the cross section is negligibly small.

Branching ratios: We assumed the branching ratio to reflect the cross sections as mentioned above.

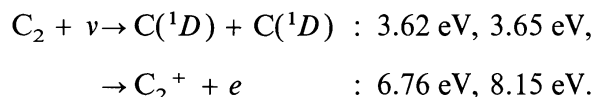
Thresholds: The wavelength equivalent of the dissociation energy into two C(³P) atoms is 2030 \AA (Okabe, 1978). For dissociation into two carbon atoms in the ¹D state, the threshold is at 1436 \AA . The threshold for ionization is at about 1000 \AA .

Rate coefficients:

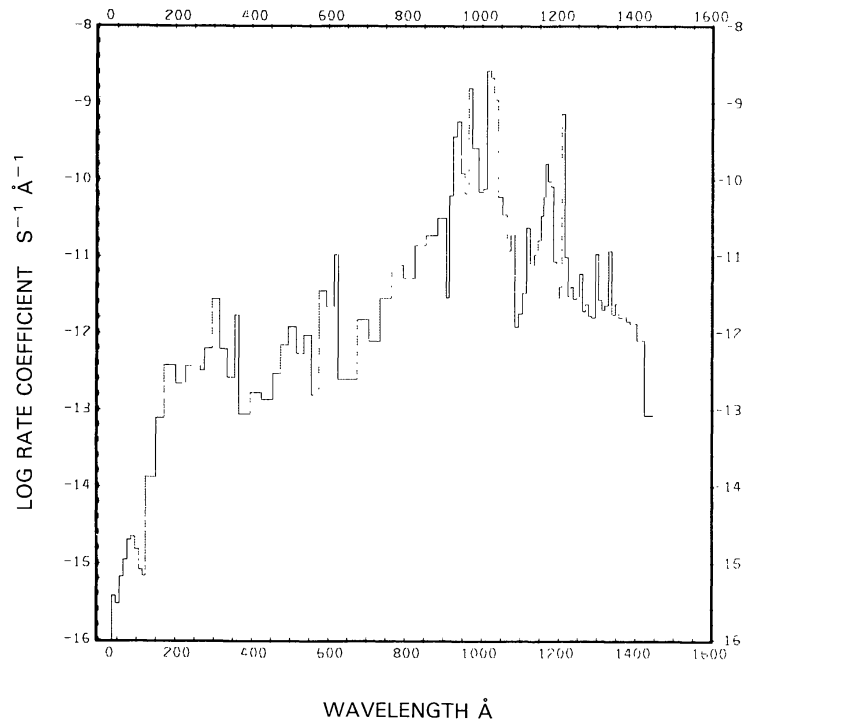
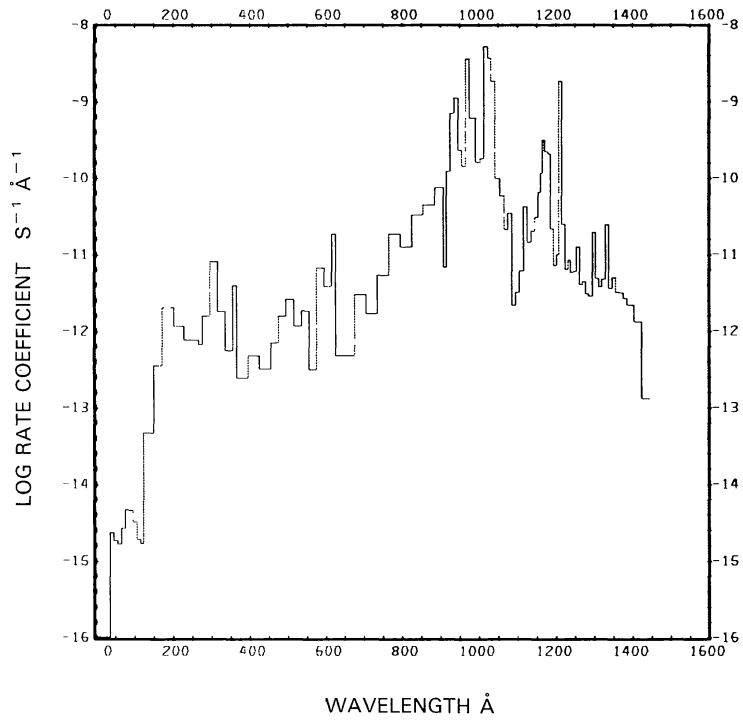


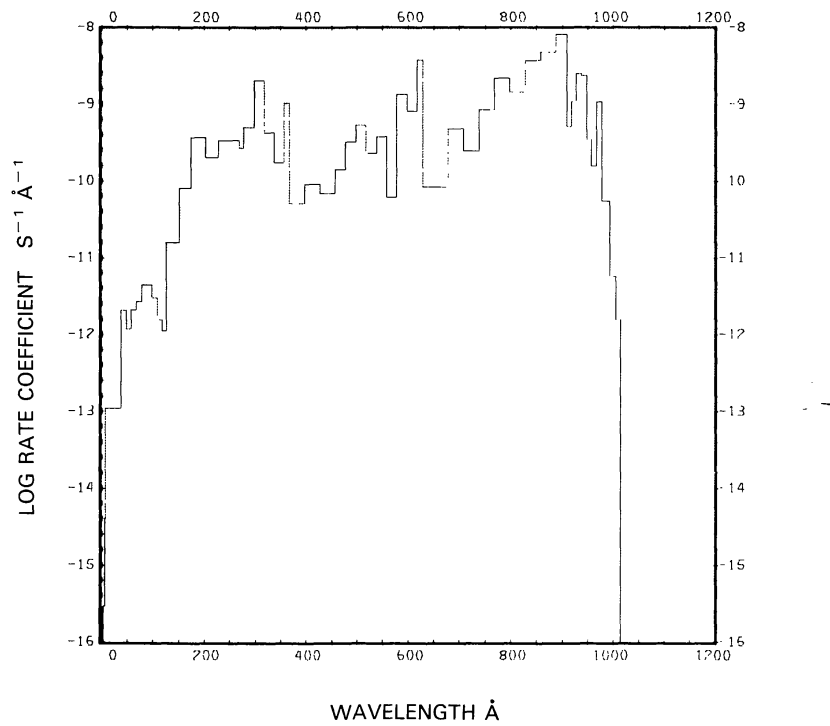
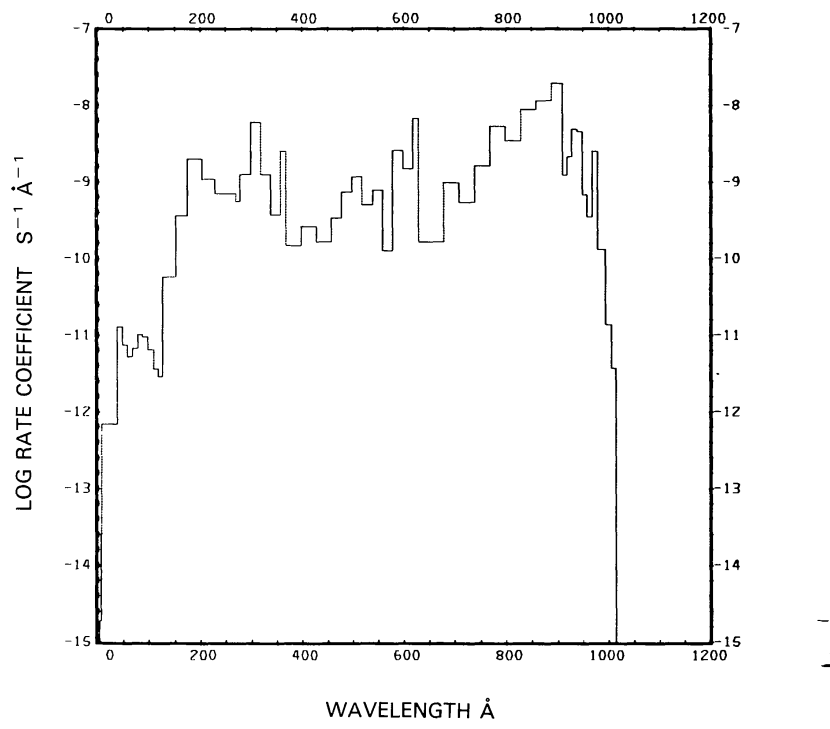
The first values are the rate coefficients for the quiet Sun (see Figures 44(a) and 45(a)), the second values are for the active Sun (see Figures 44(b) and 45(b)). These rate coefficients are for the ground state of C₂ only. There is an electronically excited state with only a small energy difference above the ground state.

Excess energies:



The first values are the excess energies for the quiet Sun, the second values are for the active Sun.

Fig. 44a. $C_2 + \nu \rightarrow C(^1D) + C(^1D)$, for the quiet Sun.Fig. 44b. $C_2 + \nu \rightarrow C(^1D) + C(^1D)$, for the active Sun.

Fig. 45a. C₂ + $\nu \rightarrow$ C₂⁺ + e, for the quiet Sun.Fig. 45b. C₂ + $\nu \rightarrow$ C₂⁺ + e, for the active Sun.

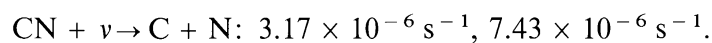
CYANO, CN

Cross sections: Up to $\lambda = 626.8 \text{ \AA}$ the cross section was synthesized from fits by Barfield *et al.* (1972) for the atomic constituents C and N. From $\lambda = 905.8$ to 1171 \AA the cross section was calculated by Lavendy *et al.* (1984) with modifications by Lavendy *et al.* (1987).

Branching ratios: The branching ratios are not known.

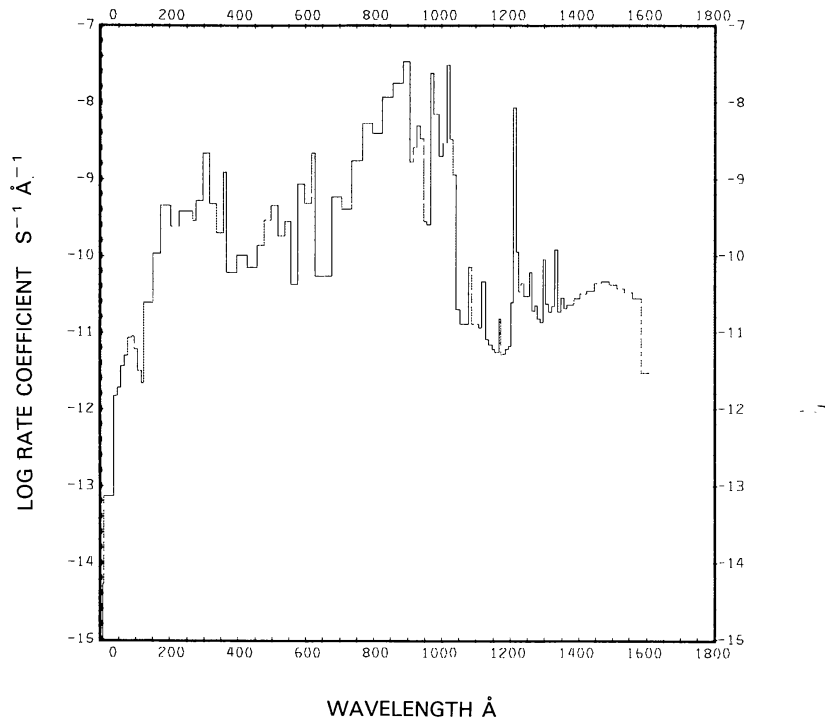
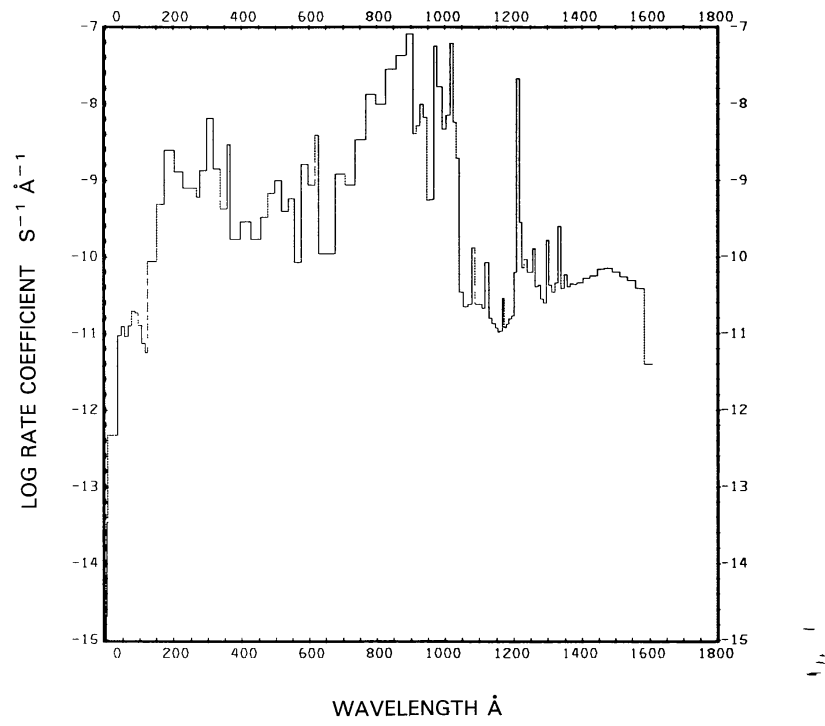
Threshold: $\lambda = 1600 \text{ \AA}$ from Huber and Herzberg (1979).

Rate coefficient:



The first value is for the quiet Sun (see Figure 46(a)), the second for the active Sun (see Figure 46(b)).

Excess energy: The excess energy for the quiet Sun is 7.41 eV and for the active Sun it is 7.97 eV.

Fig. 46a. $\text{CN} + \nu \rightarrow \text{C} + \text{N}$, for the quiet Sun.Fig. 46b. $\text{CN} + \nu \rightarrow \text{C} + \text{N}$, for the active Sun.

CARBON MONOXIDE, CO($X^1\Sigma^+$), CO($a^3\Pi$)

Cross sections: Up to $\lambda = 303.8 \text{ \AA}$ cross sections from many sources, averaged by Henry and McElroy (1968), were used. From $\lambda = 303.8 \text{ \AA}$ the cross section was taken from Cairns and Samson (1965) and supplemented with values from Cook *et al.* (1965) in the wavelength region from 600 to 1002.5 \AA . No dissociation or ionization cross sections for any of the three metastable triplet states $a^3\Pi$, $a'^3\Sigma^+$, and $d^3\Delta y_i$ are available; but since the potential curve for the lowest of these, the $a^3\Pi$, is very similar to that of the ground state $X^1\Sigma^+$ (see Hall *et al.*, 1973), Collins (personal communication) suggested scaling the ground state cross sections with respect to λ^{-1} such that the thresholds are shifted by 6.00 eV to longer wavelengths. The 6.00 eV shift corresponds to the energy difference between $a^3\Pi$ and $X^1\Sigma^+$ states.

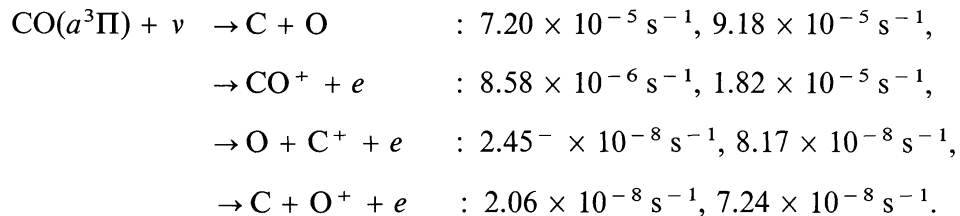
Branching ratios: The branching ratio between dissociation and all ionization processes was determined from the data of Cairns and Samson (1965). Since no branching ratios are available for dissociation into the 1S and 1D metastable states of C and O, we followed the suggestion of McElroy and McConnell (1971) that all such dissociations end up in 1D states, i.e., C(1D) and O(1D), and estimated the branching ratio from data of Cook *et al.* (1965). The branching ratios for ionization and dissociative ionizations was taken from Kronebusch and Berkowitz (1976).

Thresholds: The threshold for dissociation of CO($X^1\Sigma^+$) into the ground states of C and O is at $\lambda = 1117.8 \text{ \AA}$ as given by Krupenie (1966) and into the metastable states C(1D) and O(1D) it is at $\lambda = 863.4 \text{ \AA}$ as tabulated by Cook *et al.* (1965). The ionization threshold, also from Krupenie, is $\lambda = 884.79 \text{ \AA}$. For dissociative ionization into O + C $^+$ + e the threshold is $\lambda = 554.7 \text{ \AA}$ and into C + O $^+$ + e it is $\lambda = 501.8 \text{ \AA}$. Both values are from Kronebusch and Berkowitz (1976).

For CO($a^3\Pi$) dissociation, $\lambda = 2431.8 \text{ \AA}$ and for ionization $\lambda = 1549.1 \text{ \AA}$; both from Krupenie (1966). The dissociative ionization thresholds have been obtained by subtracting 6.00 eV from corresponding ground state values; for the products O + C $^+$ + e the threshold is therefore at $\lambda = 758.3 \text{ \AA}$ and for C + O $^+$ + e it is at $\lambda = 662.7 \text{ \AA}$.

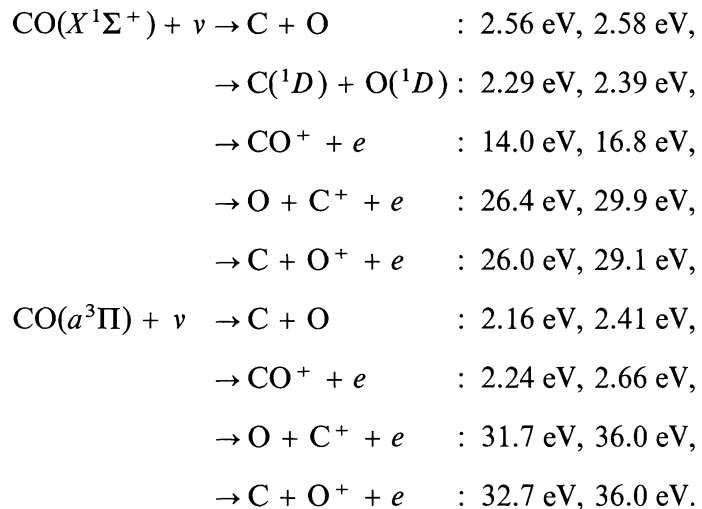
Rate coefficients:

$$\begin{aligned}
 \text{CO}(\textit{X}^1\Sigma^+) + v &\rightarrow \text{C} + \text{O} : 2.81 \times 10^{-7} \text{ s}^{-1}, 6.60 \times 10^{-7} \text{ s}^{-1}, \\
 &\rightarrow \text{C}({}^1D) + \text{O}({}^1D) : 3.47 \times 10^{-8} \text{ s}^{-1}, 7.87 \times 10^{-8} \text{ s}^{-1}, \\
 &\rightarrow \text{CO}^+ + e : 3.80 \times 10^{-7} \text{ s}^{-1}, 9.59 \times 10^{-7} \text{ s}^{-1}, \\
 &\rightarrow \text{O} + \text{C}^+ + e : 2.94 \times 10^{-8} \text{ s}^{-1}, 9.88 \times 10^{-8} \text{ s}^{-1}, \\
 &\rightarrow \text{C} + \text{O}^+ + e : 2.42 \times 10^{-8} \text{ s}^{-1}, 8.31 \times 10^{-8} \text{ s}^{-1},
 \end{aligned}$$

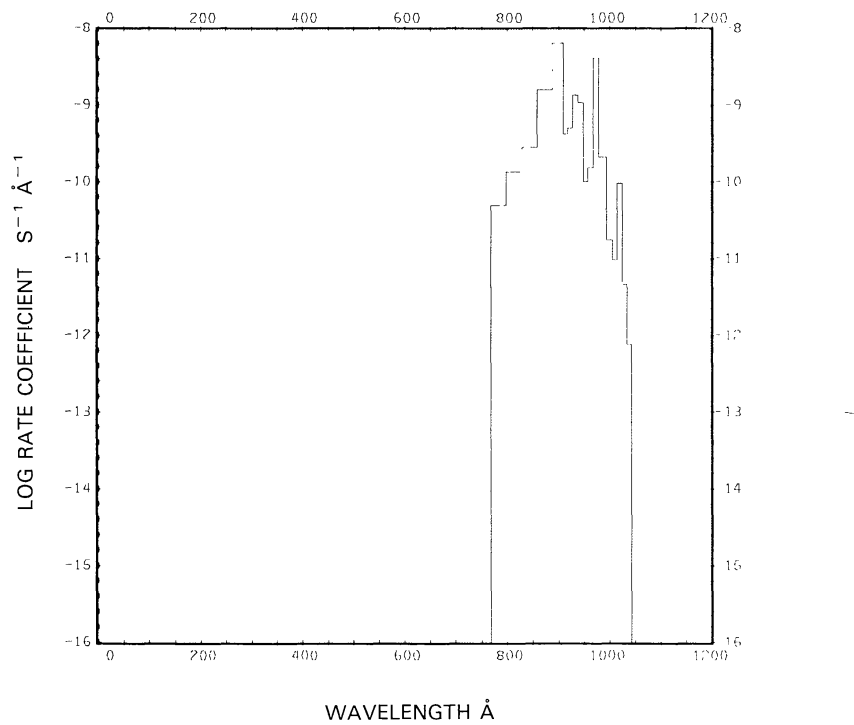
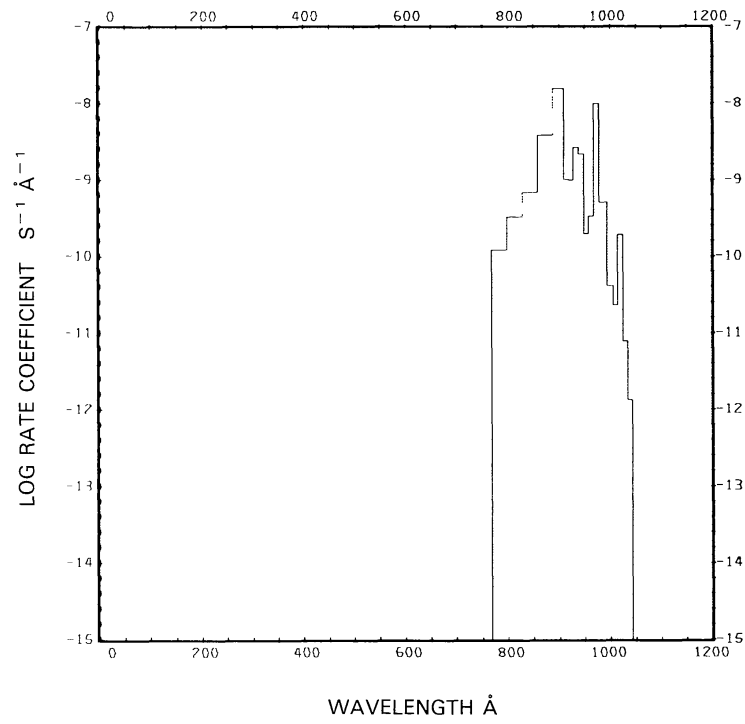


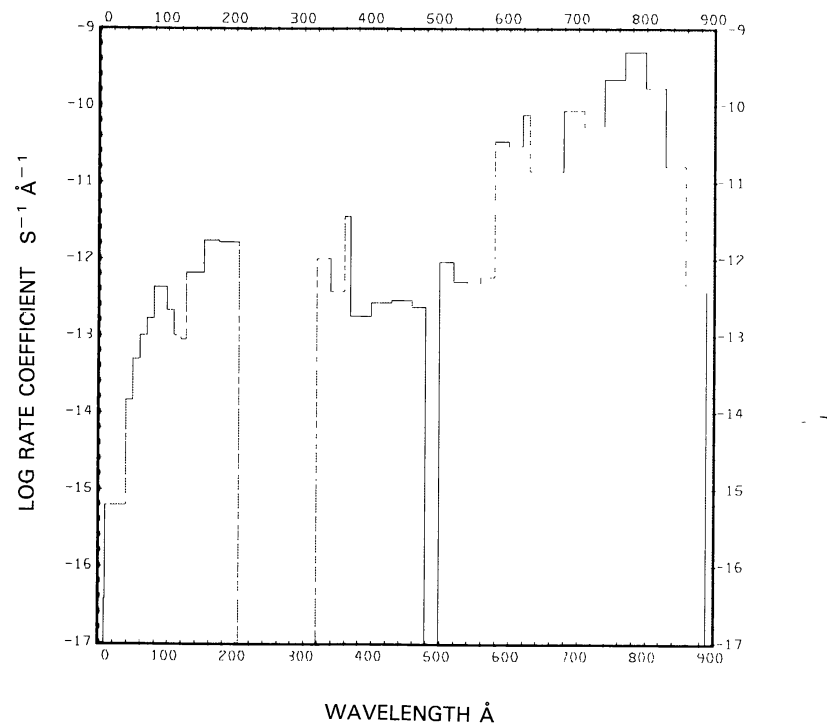
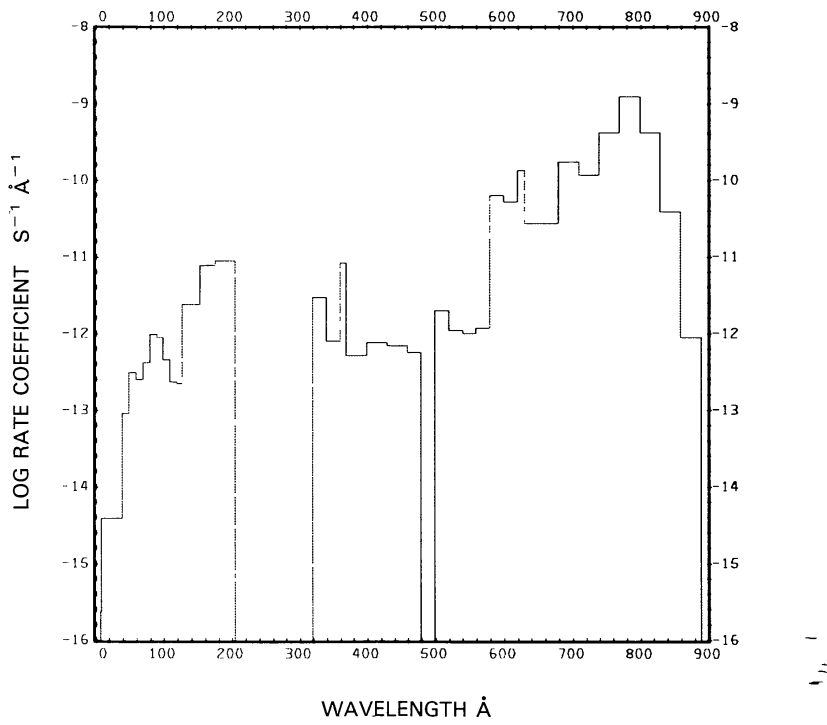
The first of each of these values is for the quiet Sun (see Figures 47(a) to 51(a), 52, and 53(a) to 55(a)), the second is for the active Sun (see Figures 47(b) to 51(b) and 53(b) to 55(b)). For the quiet Sun, McElroy and McConnell (1971) obtain $6.0 \times 10^{-7} \text{ s}^{-1}$ for the first dissociation branch (after scaling to 1 AU heliocentric distance), which is about twice our value, and $5.8 \times 10^{-8} \text{ s}^{-1}$ for the second dissociation branch. On the other hand, Wyckoff and Wehinger (1976) computed $1.9 \times 10^{-7} \text{ s}^{-1}$ for the total dissociation rate, or about 40% less than our value ($3.1 \times 10^{-7} \text{ s}^{-1}$). Our combined rate for ionization and dissociative ionization out of the ground state ($4.3 \times 10^{-7} \text{ s}^{-1}$) is larger than the value obtained by Wyckoff and Wehinger (1976) ($2.7 \times 10^{-7} \text{ s}^{-1}$), but smaller than the ionization rates obtained by Siscoe and Mukherjee (1972) ($7.81 \times 10^{-7} \text{ s}^{-1}$) or by McElroy *et al.* (1976) ($1.0 \times 10^{-6} \text{ s}^{-1}$ after scaling to 1 AU heliocentric distance; they quote $4.4 \times 10^{-7} \text{ s}^{-1}$ at Mars orbit). For the dissociative ionization branch that leads to $\text{C} + \text{O}^+ + e$, McElroy and McConnell (1971) give $1.6 \times 10^{-8} \text{ s}^{-1}$, after scaling to 1 AU, 67% of our value. (They give $6.9 \times 10^{-9} \text{ s}^{-1}$ at Mars orbit). The rate coefficients for the metastable state of CO should be considered to be estimates only.

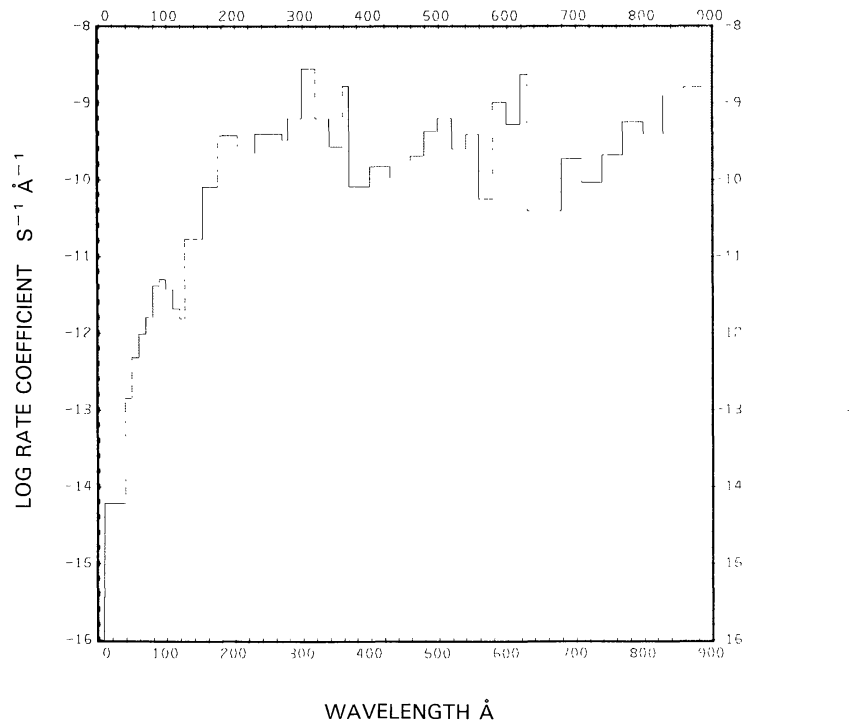
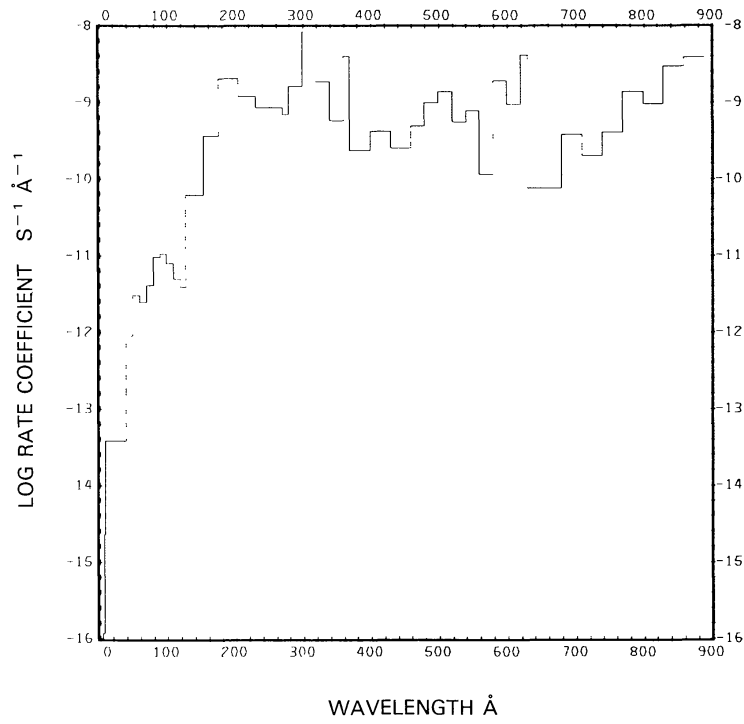
Excess energies:

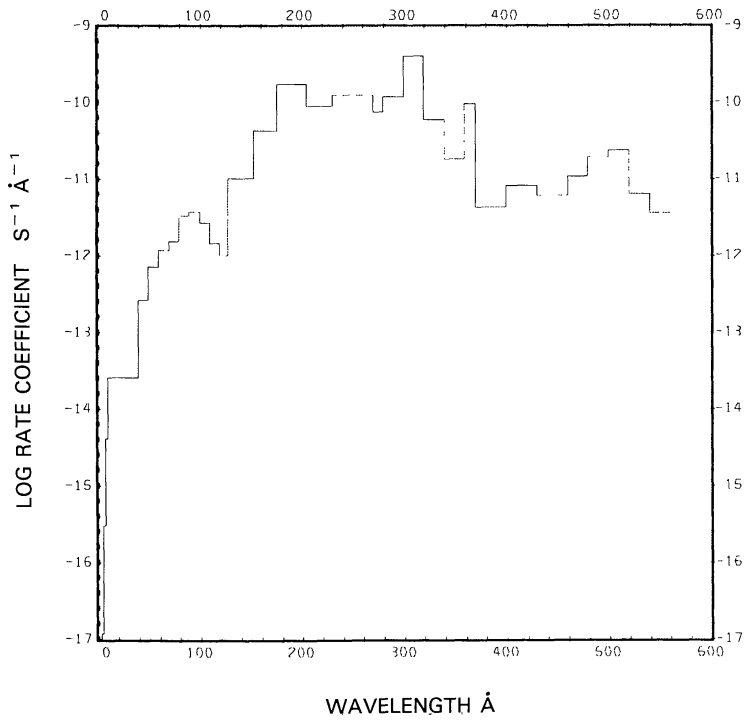
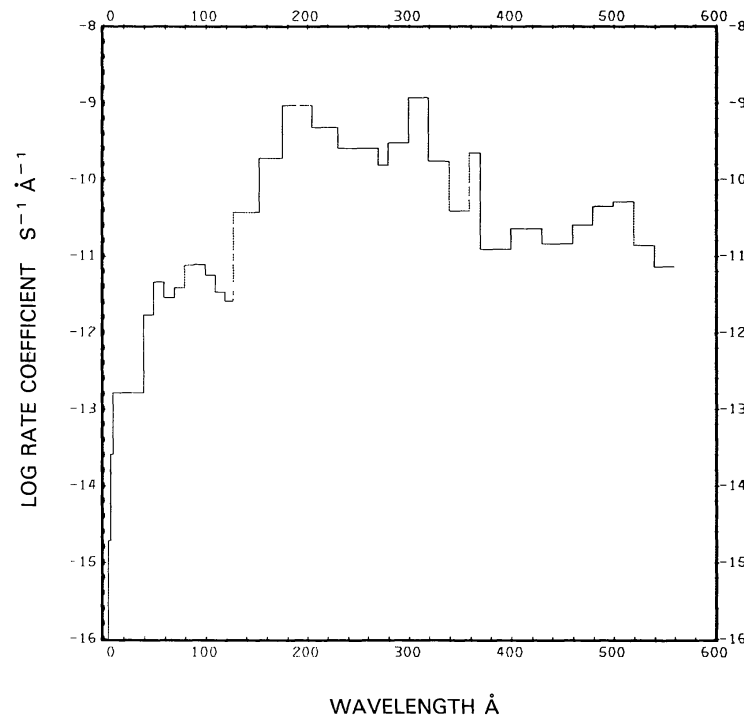


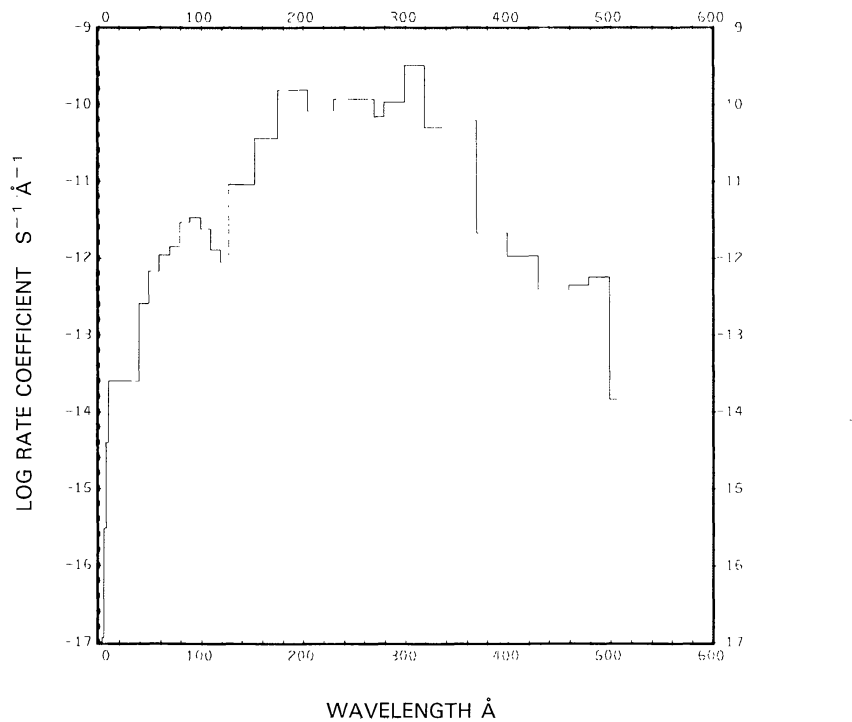
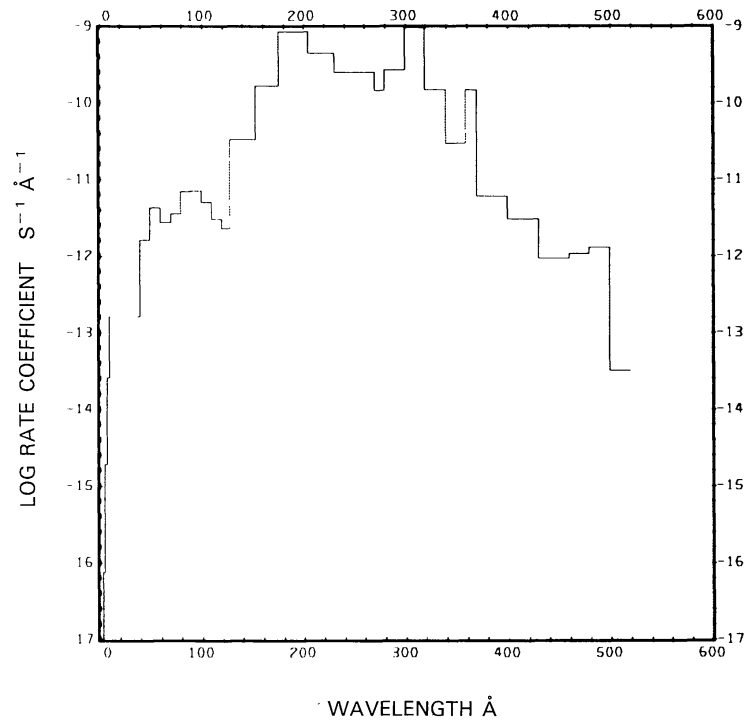
The first of each of these values is for the quiet Sun, the second is for the active Sun.

Fig. 47a. CO($X^1\Sigma^+$) + $\nu \rightarrow C + O$, for the quiet Sun.Fig. 47b. CO($X^1\Sigma^+$) + $\nu \rightarrow C + O$, for the active Sun.

Fig. 48a. CO($X^1\Sigma^+$) + $\nu \rightarrow$ C(1D) + O(1D), for the quiet Sun.Fig. 48b. CO($X^1\Sigma^+$) + $\nu \rightarrow$ C(1D) + O(1D), for the active Sun.

Fig. 49a. $\text{CO}(X^1\Sigma^+) + v \rightarrow \text{CO}^+ + e$, for the quiet Sun.Fig. 49b. $\text{CO}(X^1\Sigma^+) + v \rightarrow \text{CO}^+ + e$, for the active Sun.

Fig. 50a. CO($X^1\Sigma^+$) + $\nu \rightarrow O + C^+ + e$, for the quiet Sun.Fig. 50b. CO($X^1\Sigma^+$) + $\nu \rightarrow O + C^+ + e$, for the active Sun.

Fig. 51a. $\text{CO}(X^1\Sigma^+) + \nu \rightarrow \text{C} + \text{O}^+ + e$, for the quiet Sun.Fig. 51b. $\text{CO}(X^1\Sigma^+) + \nu \rightarrow \text{C} + \text{O}^+ + e$, for the active Sun.

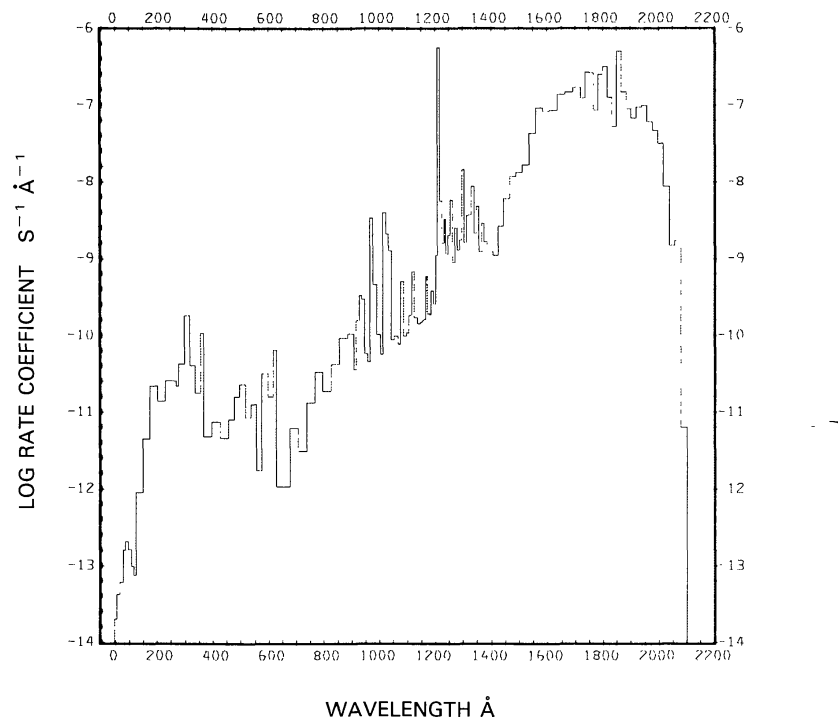
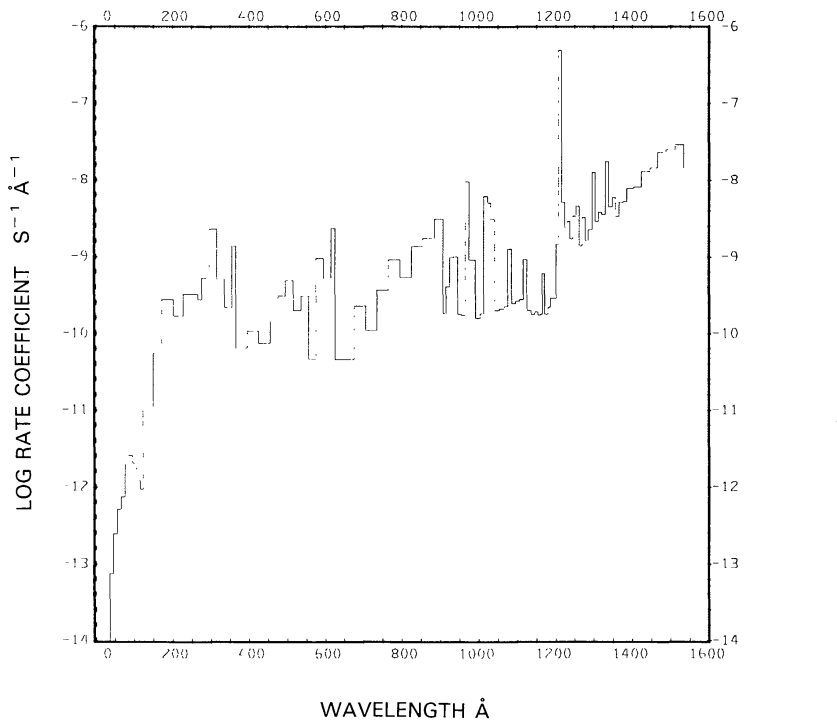
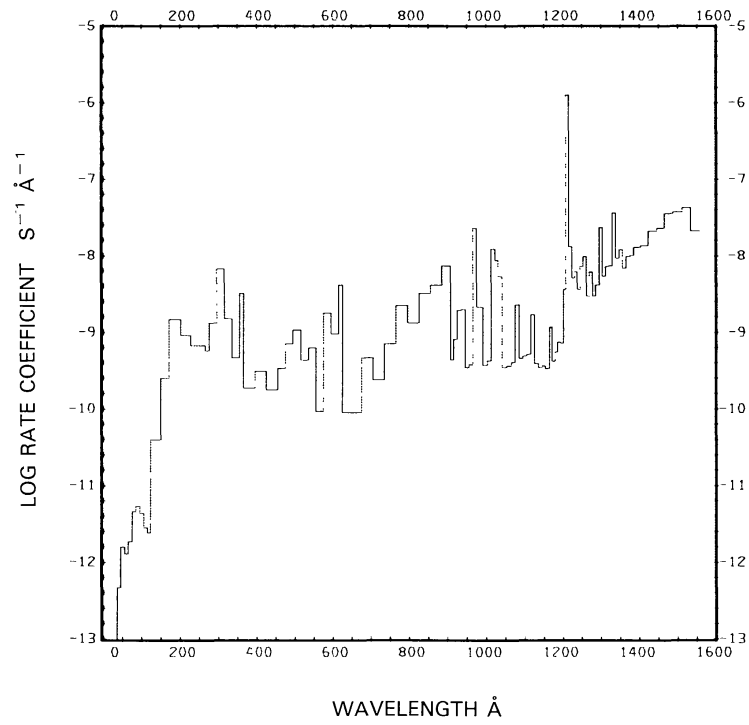
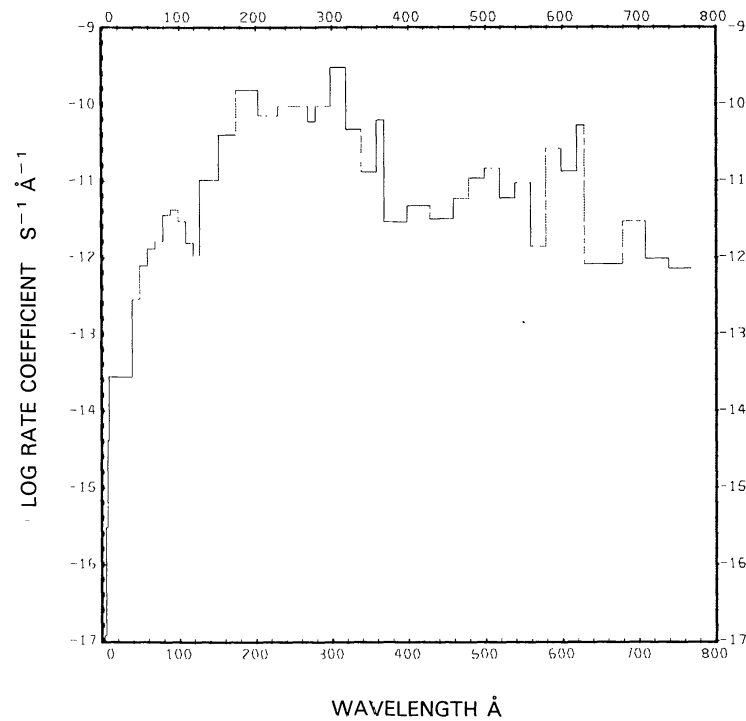
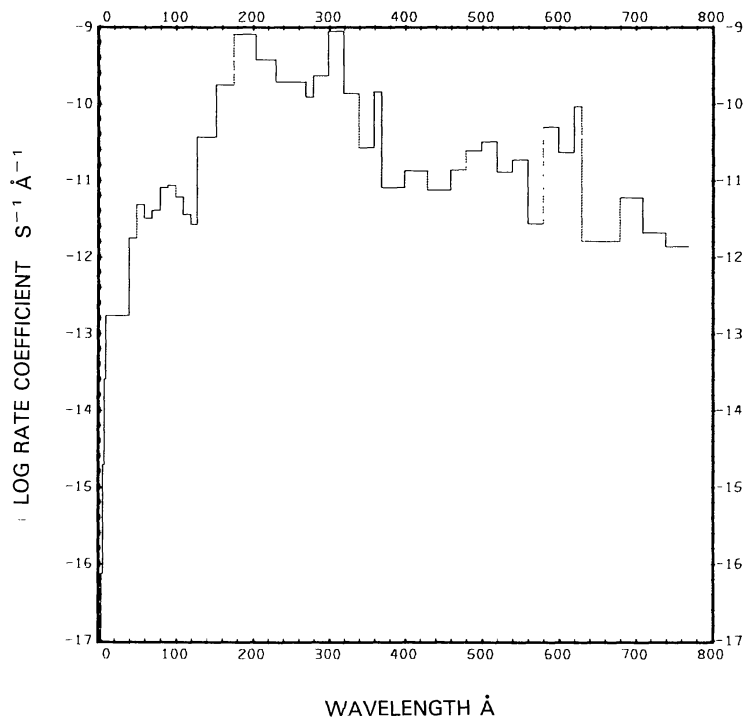
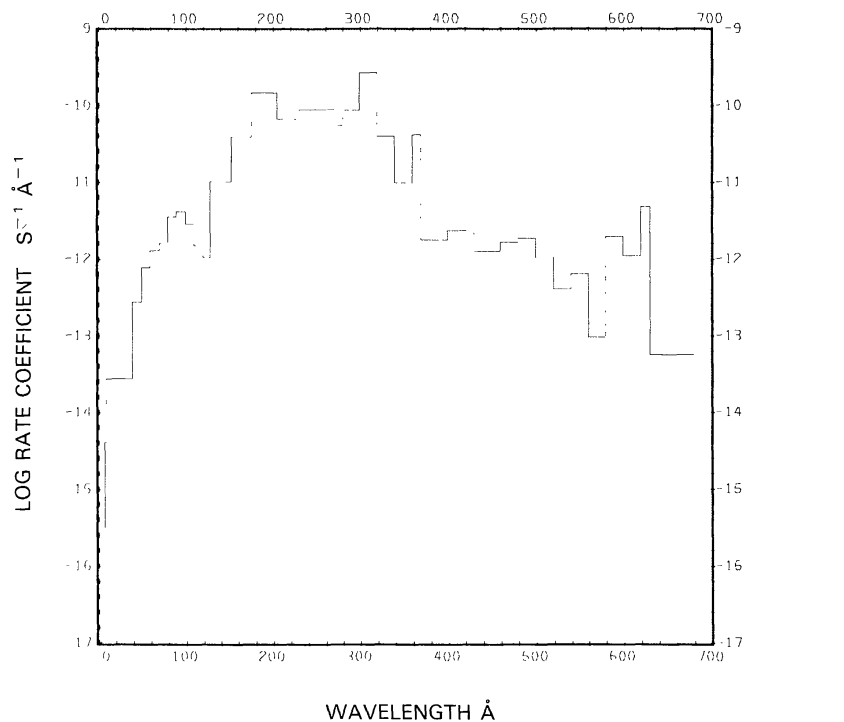
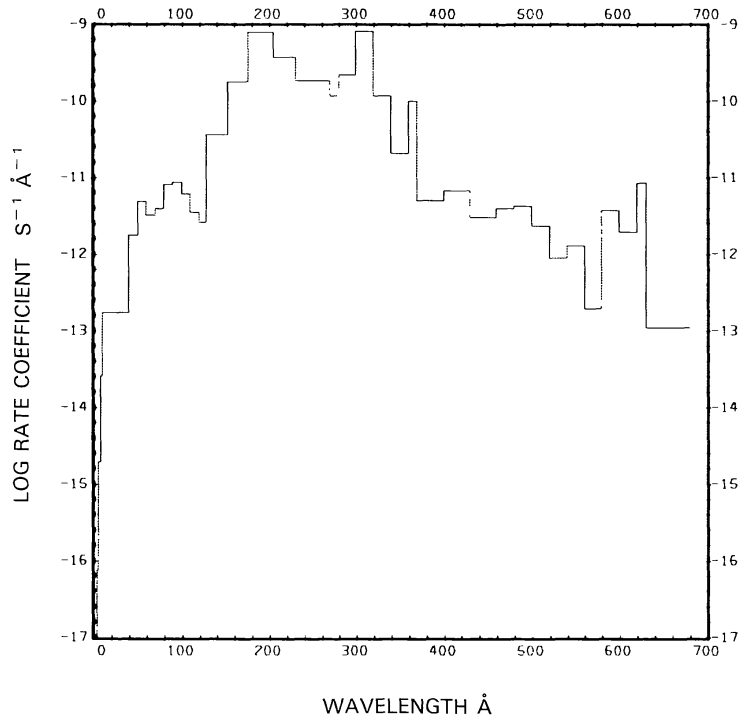


Fig. 52. CO($a^3\Pi$) + $v \rightarrow C + O$, for the quiet Sun.

Fig. 53a. $\text{CO}(a^3\Pi) + v \rightarrow \text{CO}^+ + e$, for the quiet Sun.Fig. 53b. $\text{CO}(a^3\Pi) + v \rightarrow \text{CO}^+ + e$, for the active Sun.

Fig. 54a. CO($a^3\Pi$) + ν → O + C⁺ + e, for the quiet Sun.Fig. 54b. CO($a^3\Pi$) + ν → O + C⁺ + e, for the active Sun.

Fig. 55a. $\text{CO}(\alpha^3\Pi) + v \rightarrow \text{C} + \text{O}^+ + e$, for the quiet Sun.Fig. 55b. $\text{CO}(\alpha^3\Pi) + v \rightarrow \text{C} + \text{O}^+ + e$, for the active Sun.

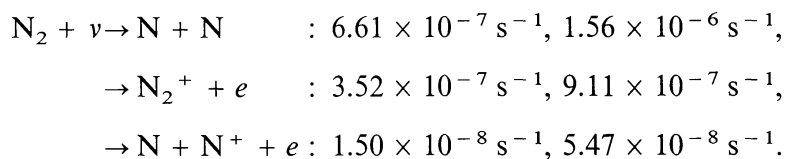
DIATOMIC NITROGEN, N₂

Cross sections: From $\lambda = 9.9$ to 247.2 Å cross sections from various sources have been summarized by Huffman (1971). In the range from 303.8 to 1037.6 Å the cross section was taken from Samson and Cairns (1964) and was supplemented with data from Cook and Metzger (1964) in the range 600 to 978 Å and from Huffman *et al.* (1963b) in the range 798 to 1000 Å. A very broad and strong absorption line of N₂ at 972.5 Å overlaps the solar L γ emission line. The measured cross section of this N₂ line varies widely: Clark (1952) obtained $\sigma = 1.45 \times 10^{-16}$ cm², Watanabe and Marmo (1956) gave $\sigma = 1.12 \times 10^{-17}$ cm², and Itamoto and McAllister (1961) reported $\sigma = 3.72 \times 10^{-16}$ cm² (these values quoted by Huffman *et al.*, 1963b). Huffman *et al.* (1963b) reported $\sigma = 3.02 \times 10^{-16}$ cm², Cook and Metzger (1964) gave $\sigma = 1.94 \times 10^{-16}$ cm², Samson and Cairns (1964) measured $\sigma = 3.56 \times 10^{-16}$ cm², Huffman (1971) reported $\sigma = 3.70 \times 10^{-16}$ cm², while Geiger and Schröder (1969) gave $\sigma = 1.51 \times 10^{-16}$ cm², and Gürtler *et al.* (1977) measured $\sigma = 3.57 \times 10^{-16}$ cm². The average is $\sigma = 2.51 \times 10^{-16}$ cm², which is the value that was adopted here. The line corresponds to the $b^1\Pi_u - X^1\Sigma_g^+$, $v' = 3$ transition (see Gürtler *et al.*, 1977). Cook and Metzger (1964) had identified the line as the $v' = 2$ transition. According to Lofthus and Krupenie (1977) these levels are predissociating.

Branching ratios: The branching ratio for dissociation and ionization is based on the data obtained by Huffman (1971), Samson and Cairns (1964), and Cook and Metzger (1964). The branching ratio for dissociative ionization comes from Kronebusch and Berkowitz (1976).

Thresholds: The threshold for dissociation as given by Huber and Herzberg (1979) is $\lambda = 1270.4$ Å. Lofthus and Krupenie (1977) give the ionization threshold at $\lambda = 796$ Å and Kronebusch and Berkowitz (1976) give the threshold for dissociative ionization at $\lambda = 510.4$ Å.

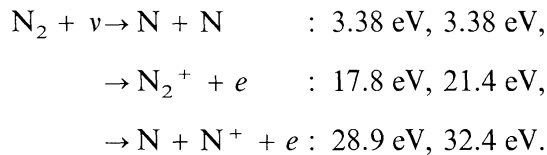
Rate coefficients:



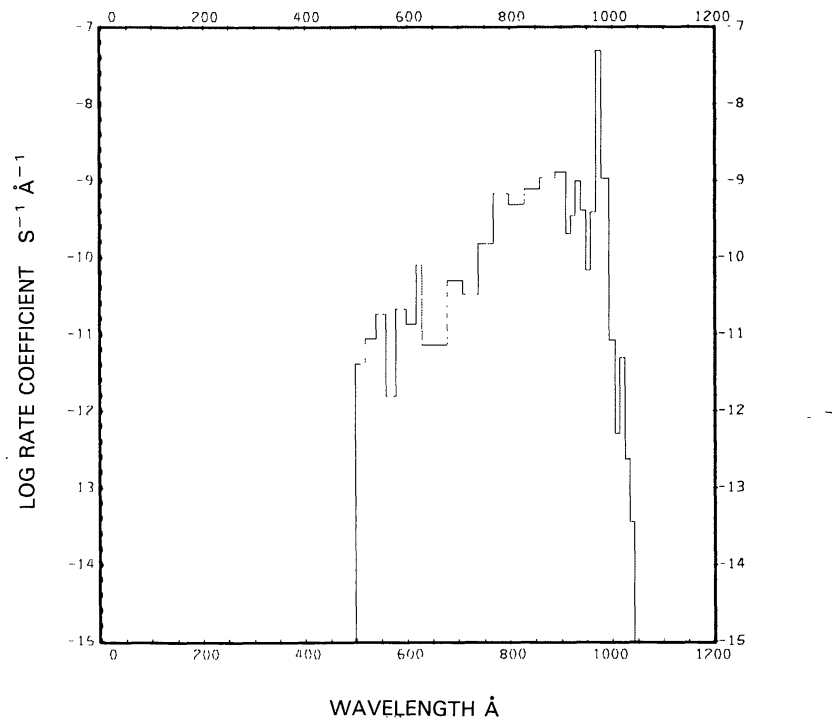
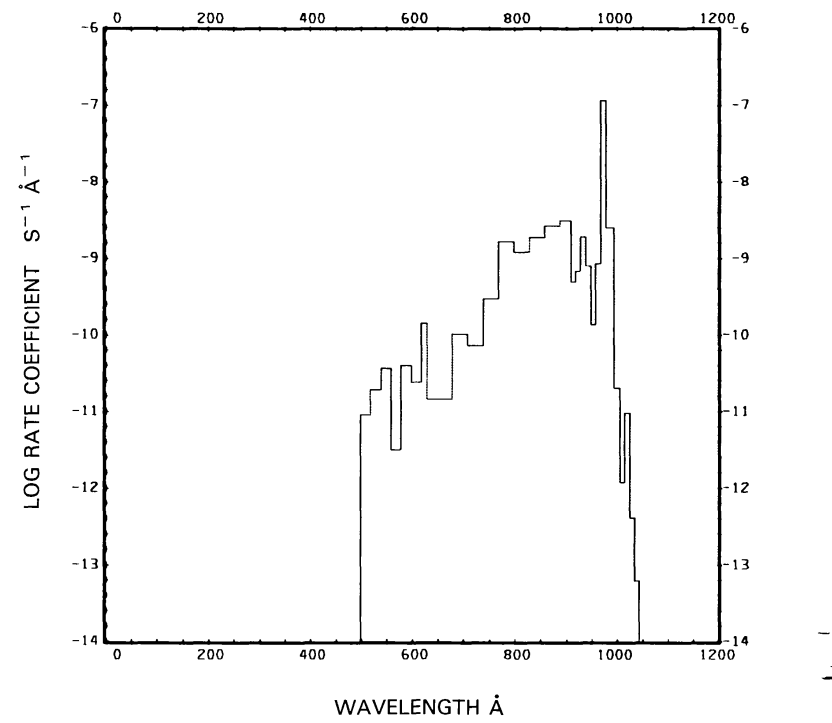
The first of each of these values is for the quiet Sun (see Figures 56(a) to 58(a)), the second is for the active Sun (see Figures 56(b) to 58(b)). The rate coefficient for dissociation is dominated by the predissociation line at $\lambda = 972.5$ Å. Thus this rate coefficient will be drastically reduced if the N₂ molecule's radial velocity with respect to the Sun Doppler shifts the predissociation line out of coincidence with the solar L γ emission line. Between the extreme values of the cross section for the N₂ line (see above) the rate coefficient for the quiet Sun varies from $8.5 \times 10^{-7} \text{ s}^{-1}$ to $2.8 \times 10^{-7} \text{ s}^{-1}$.

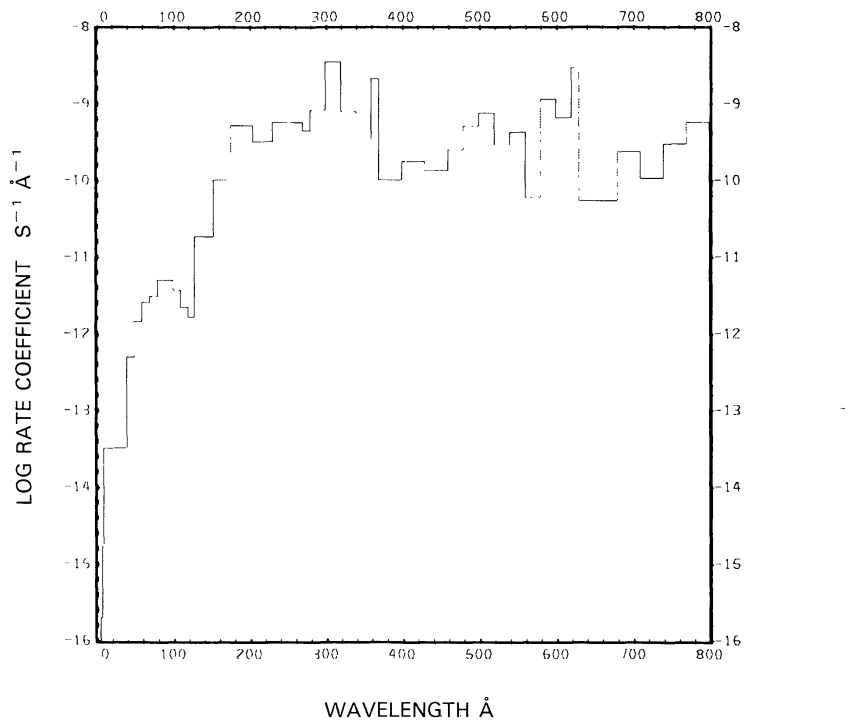
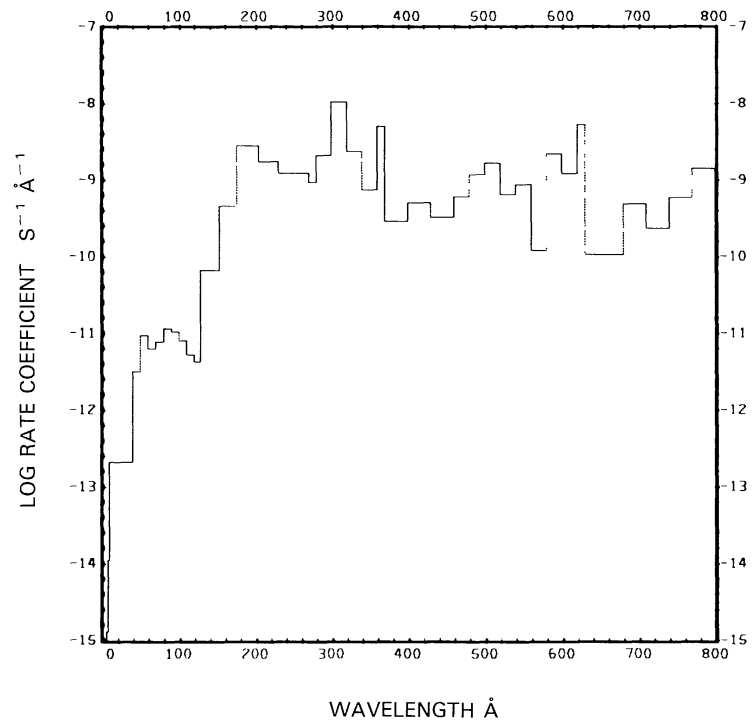
assuming zero Doppler shift. Our combined rate for ionization and dissociative ionization ($3.7 \times 10^{-7} \text{ s}^{-1}$) is about 80% larger than the value reported by McElroy *et al.* (1976) ($2.0 \times 10^{-7} \text{ s}^{-1}$, after scaling their value to 1 AU), but it is equal to the rate quoted by Siscoe and Mukherjee (1972). Bauer and Bortner (1978) quote $4.2 \times 10^{-7} \text{ s}^{-1}$. The rate coefficients of Wyckoff and Wehinger (1976) for dissociation ($1.8 \times 10^{-7} \text{ s}^{-1}$) and for ionization ($1.3 \times 10^{-7} \text{ s}^{-1}$) are much smaller than our values. The ionization rate coefficient is sensitive to the cross section around $\lambda = 300 \text{ \AA}$, where data are sparse.

Excess energies:



The first of each of these values is for the quiet Sun, the second is for the active Sun.

Fig. 56a. $N_2 + \nu \rightarrow N + N$, for the quiet Sun.Fig. 56b. $N_2 + \nu \rightarrow N + N_2$, for the active Sun.

Fig. 57a. $\text{N}_2 + \nu \rightarrow \text{N}_2^+ + e$, for the quiet Sun.Fig. 57b. $\text{N}_2 + \nu \rightarrow \text{N}_2^+ + e$, for the active Sun.

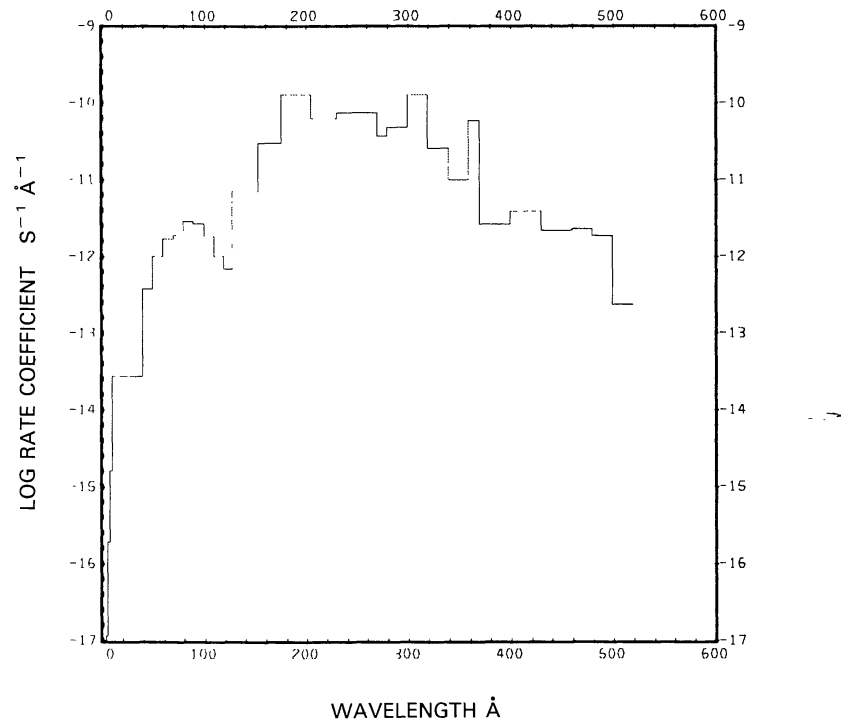


Fig. 58a. N₂ + v → N + N⁺ + e, for the quiet Sun.

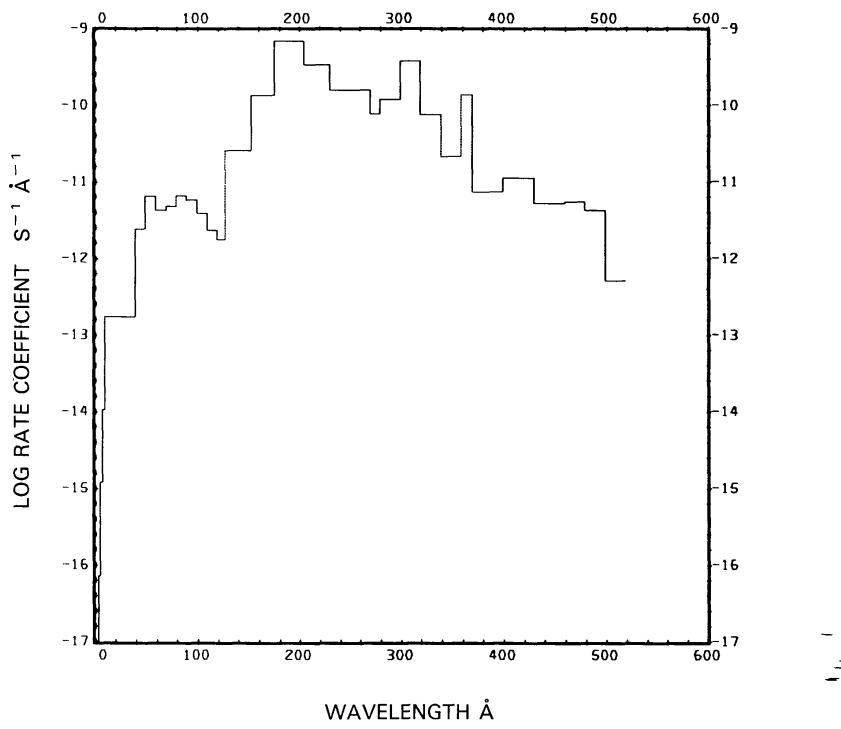


Fig. 58b. N₂ + v → N + N⁺ + e, for the active Sun.

NITRIC OXIDE, NO

Cross sections: Up to 180 Å the cross section is synthesized from the atomic cross sections of N and O, determined from fits by Barfield *et al.* (1972). Between $\lambda = 180$ and 580 Å the cross section data from Lee *et al.* (1973) were used. In the range 580 to 1350 Å the cross section comes from Watanabe *et al.* (1967) and between $\lambda = 1350$ and 2271 Å it comes from Marmo (1953).

Branching ratios: The data for the branching between dissociation and all ionization processes come from Watanabe *et al.* (1967). The branching ratios for photodissociative ionization are given by Kronebusch and Berkowitz (1976).

Thresholds: Marmo (1953) and Mc Nesby and Okabe (1964) give the threshold for dissociation at $\lambda = 1910$ Å. The threshold for ionization is given by Watanabe *et al.* (1967) as $\lambda = 1340$ Å. The thresholds for dissociative ionization into $N + O^+ + e$ and $N^+ + O + e$ are $\lambda = 616.2$ Å and $\lambda = 589.3$ Å, respectively.

Rate coefficients:

$$\begin{aligned}
 NO + v \rightarrow N + O & : 2.20 \times 10^{-6} \text{ s}^{-1}, 3.21 \times 10^{-6} \text{ s}^{-1}, \\
 & \rightarrow NO^+ + e : 1.28 \times 10^{-6} \text{ s}^{-1}, 3.19 \times 10^{-6} \text{ s}^{-1}, \\
 & \rightarrow N + O^+ + e : 1.81 \times 10^{-9} \text{ s}^{-1}, 5.09 \times 10^{-9} \text{ s}^{-1}, \\
 & \rightarrow O + N^+ + e : 3.18 \times 10^{-8} \text{ s}^{-1}, 1.02 \times 10^{-7} \text{ s}^{-1}.
 \end{aligned}$$

The first of each of these values is for the quiet Sun (see Figures 59 and 60(a) to 62(a)), the second is for the active Sun (see Figures 60(b) to 62(b)). Our rate for dissociation for the quiet Sun is smaller than the value quoted by Bauer and Bortner (1978) ($6.10 \times 10^{-6} \text{ s}^{-1}$). Our rate coefficient for all ionization processes ($1.3 \times 10^{-6} \text{ s}^{-1}$) is in very good agreement with the value obtained by Siscoe and Mukherjee (1972) ($1.348 \times 10^{-6} \text{ s}^{-1}$) but is about double the value quoted by Bauer and Bortner (1978) ($6.24 \times 10^{-7} \text{ s}^{-1}$).

Excess energies:

$$\begin{aligned}
 NO + v \rightarrow N + O & : 1.84 \text{ eV}, 2.72 \text{ eV}, \\
 & \rightarrow NO^+ + e : 8.23 \text{ eV}, 9.89 \text{ eV}, \\
 & \rightarrow N + O^+ + e : 18.6 \text{ eV}, 22.5 \text{ eV}, \\
 & \rightarrow O + N^+ + e : 25.2 \text{ eV}, 28.5 \text{ eV}.
 \end{aligned}$$

The first of each of these entries is for the quiet Sun, the second is for the active Sun.

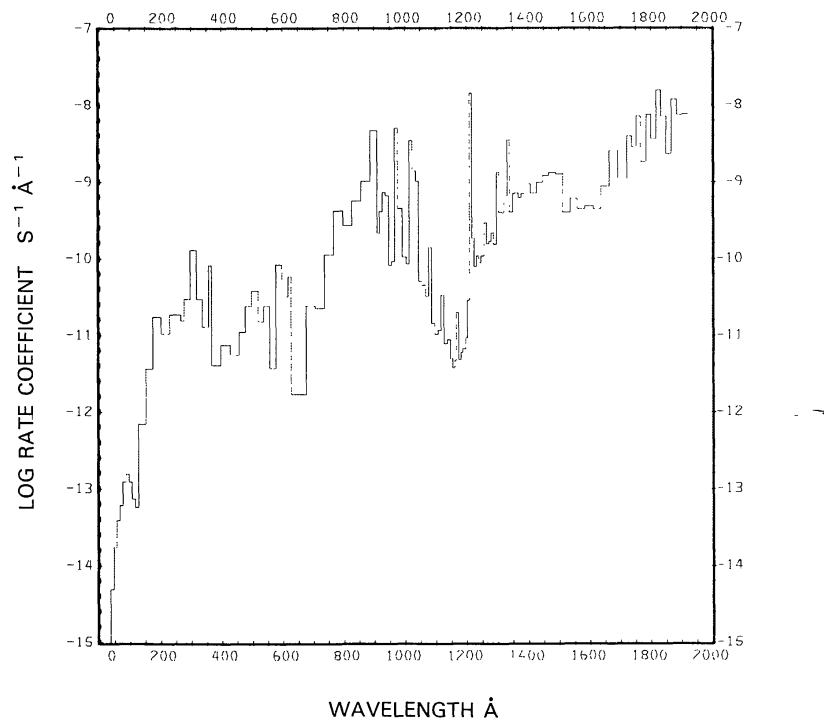
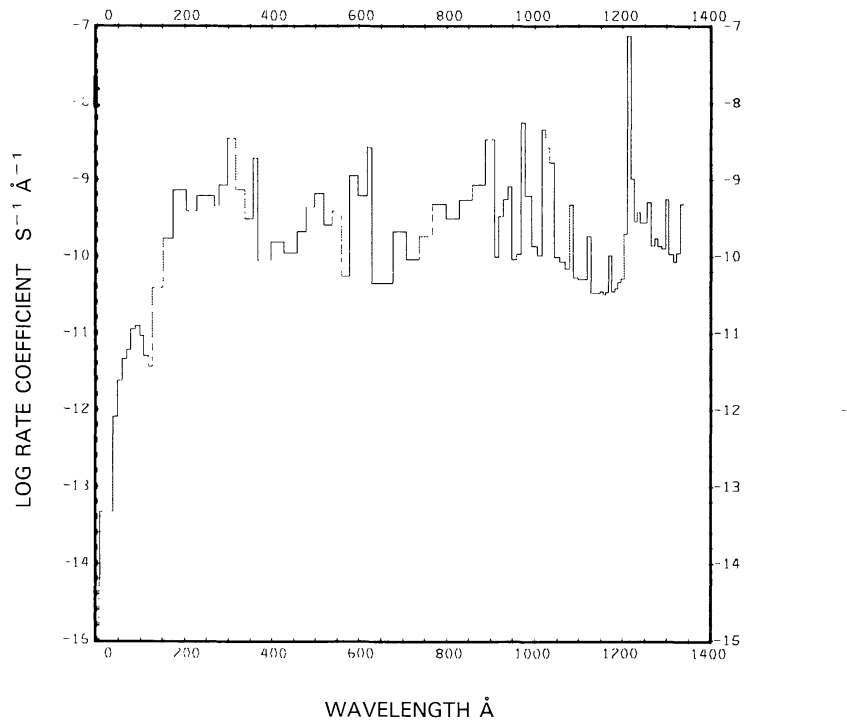
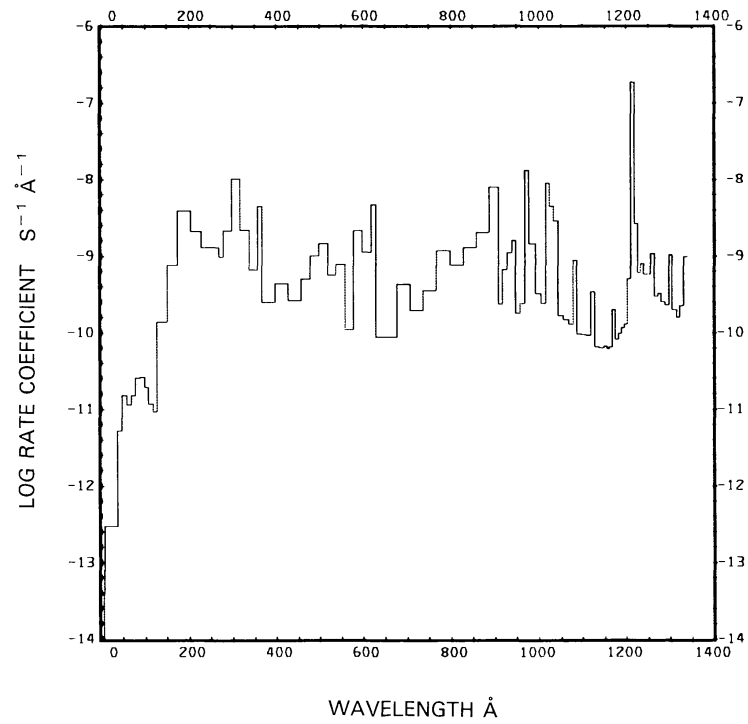
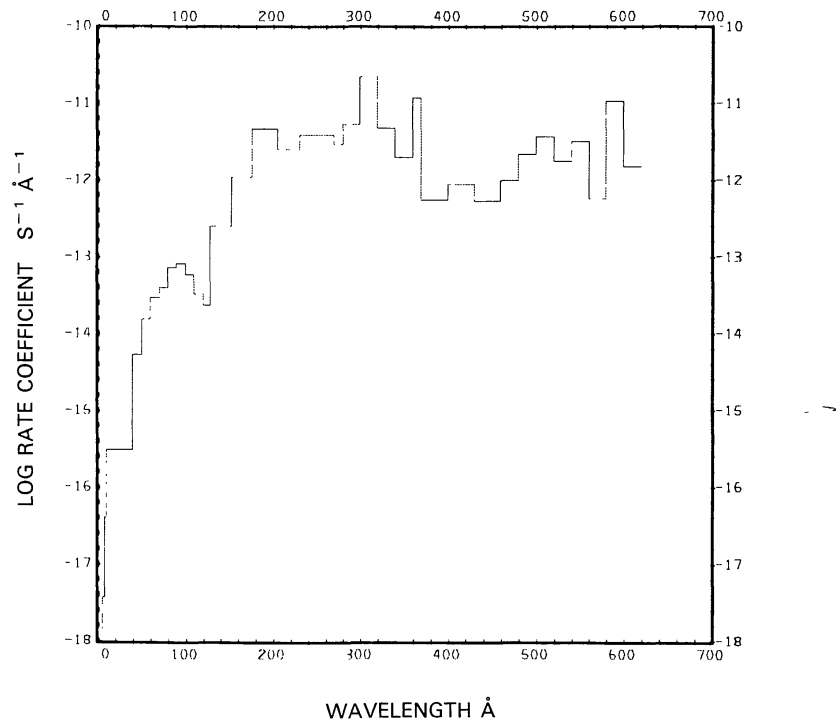
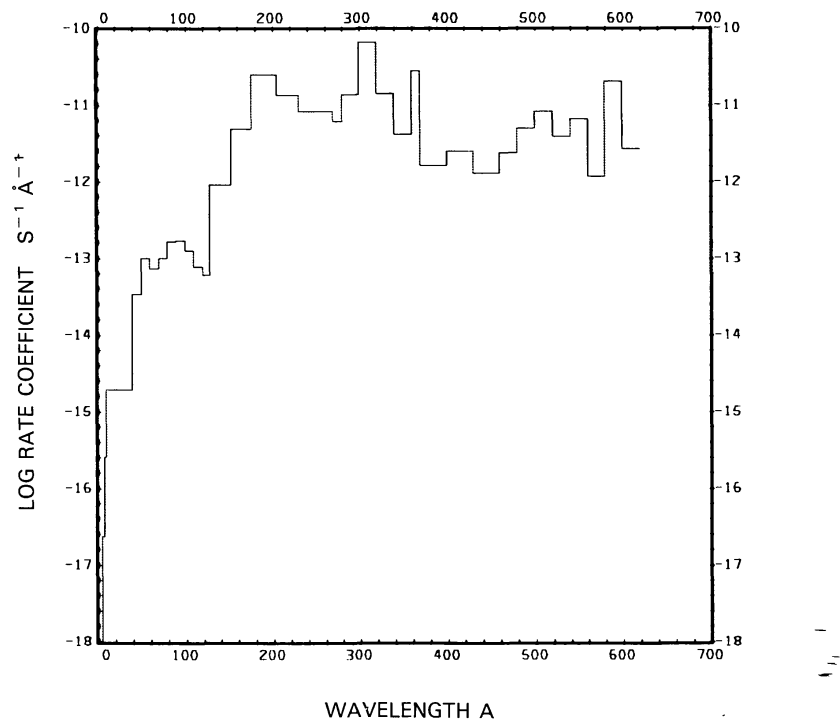
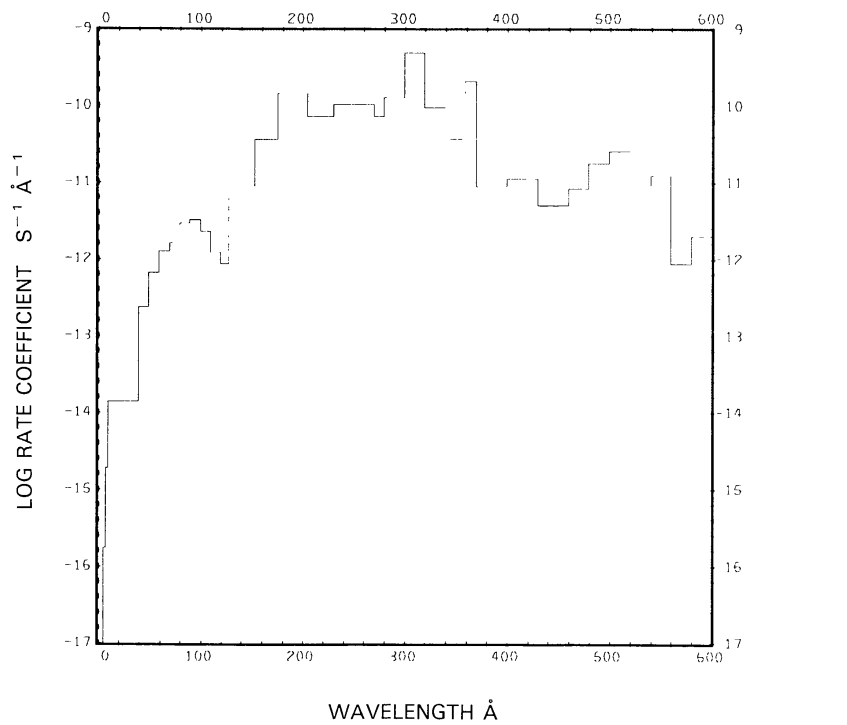
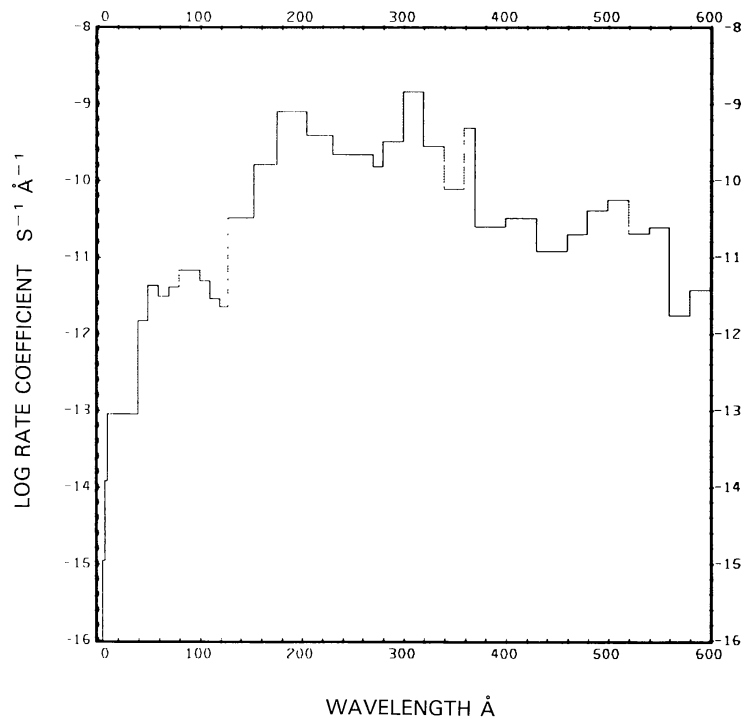


Fig. 59. $\text{NO} + \nu \rightarrow \text{N} + \text{O}$, for the quiet Sun.

Fig. 60a. $\text{NO} + \nu \rightarrow \text{NO}^+ + e$, for the quiet Sun.Fig. 60b. $\text{NO} + \nu \rightarrow \text{NO}^+ + e$, for the active Sun.

Fig. 61a. $\text{NO} + \nu \rightarrow \text{N} + \text{O}^+ + e$, for the quiet Sun.Fig. 61b. $\text{NO} + \nu \rightarrow \text{N} + \text{O}^+ + e$, for the active Sun.

Fig. 62a. $\text{NO} + \nu \rightarrow \text{O} + \text{N}^+ + e$, for the quiet Sun.Fig. 62b. $\text{NO} + \nu \rightarrow \text{O} + \text{N}^+ + e$, for the active Sun.

DIATOMIC OXYGEN, O₂

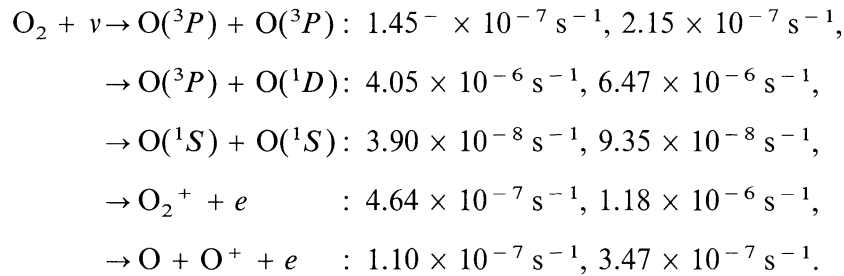
Cross sections: Up to 295 Å the cross section is based on fits made by Barfield *et al.* (1972) for atomic oxygen multiplied by 2; it is supplemented by values taken from Huffman (1971). From 41.33 to 1771.2 Å the data of Brion and Tan (1979) were used, supplemented with data from many other sources. Between 140.3 and 1740 Å data from Gibson *et al.* (1983) were used. Between 209.3 and 1037.6 Å data are taken from Samson and Cairns (1964, 1965) and are supplemented with the cross section from Cook and Metzger (1964) in the interval $\lambda = 600$ to 912 Å. Data are also taken from Matsunaga and Watanabe (1967a) in the range from 580 to 1077 Å. Between 1062 and 1751 Å the data from Watanabe (1958) are used. From 1163 to 1414.5 Å cross sections were used that had been compiled by Ackerman (1971) and Ackerman *et al.* (1970) from many sources. Very detailed cross section data from Yoshino *et al.* (1984) were used between $\lambda = 1792.3$ and 1998.0 Å. Between 2250 and 2423 Å we used the cross section data of Shardanand and Rao (1977).

Branching ratios: Branching ratios for the sum of processes leading to dissociation and the sum of processes leading to ionization are obtained from data of Huffman (1971), Samson and Cairns (1964), Cook and Metzger (1964), and Matsunaga and Watanabe (1967a). Dissociation into O(³P) + O(³P), O(³P) + O(¹D), and O(¹S) + O(¹S) is given by branching ratios of Lee *et al.* (1977), Hudson (1971), Ackerman *et al.* (1970), and Ditchburn and Young (1962). Photodissociative ionization branching ratios are obtained from Comes *et al.* (1968), Weissler *et al.* (1959), and Kronebusch and Berkowitz (1976).

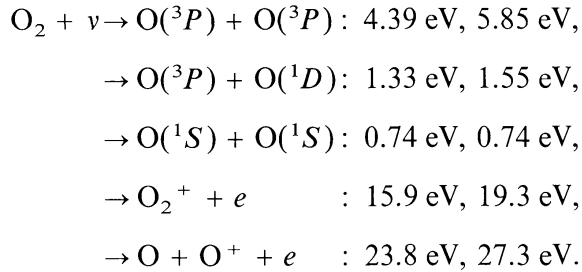
Thresholds: Threshold wavelengths for dissociation, as given by Huber and Herzberg (1979) for the first dissociation branch and by McNesby and Okabe (1964) for the other dissociation branches, are:

$$\begin{aligned}
 \text{O}_2 + \nu \rightarrow & \text{O}(\text{P}^3) + \text{O}(\text{P}^3) : 2423.7 \text{ Å}, \\
 \rightarrow & \text{O}(\text{P}^3) + \text{O}(\text{D}^1) : 1759 \text{ Å}, \\
 \rightarrow & \text{O}(\text{P}^3) + \text{O}(\text{S}^1) : 1342 \text{ Å}, \\
 \rightarrow & \text{O}(\text{S}^1) + \text{O}(\text{S}^1) : 923 \text{ Å}.
 \end{aligned}$$

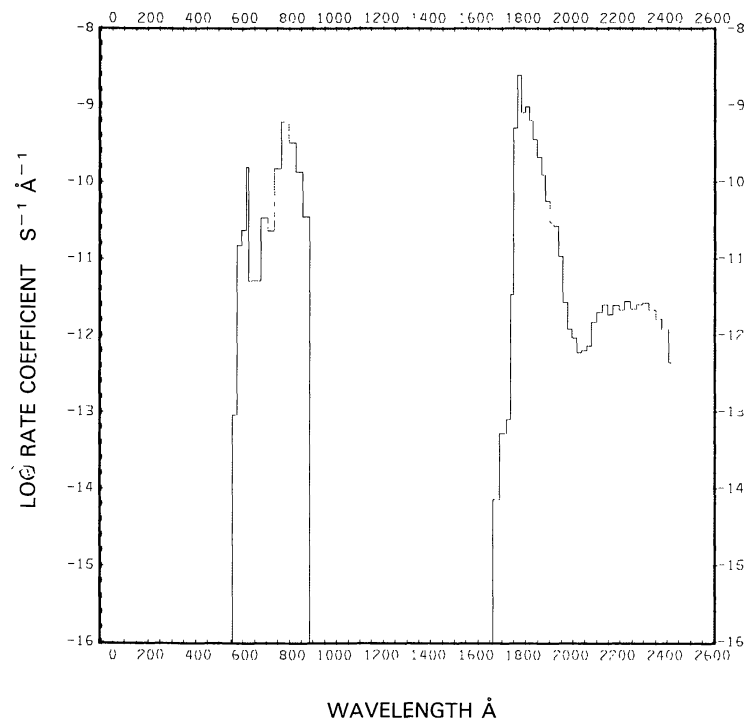
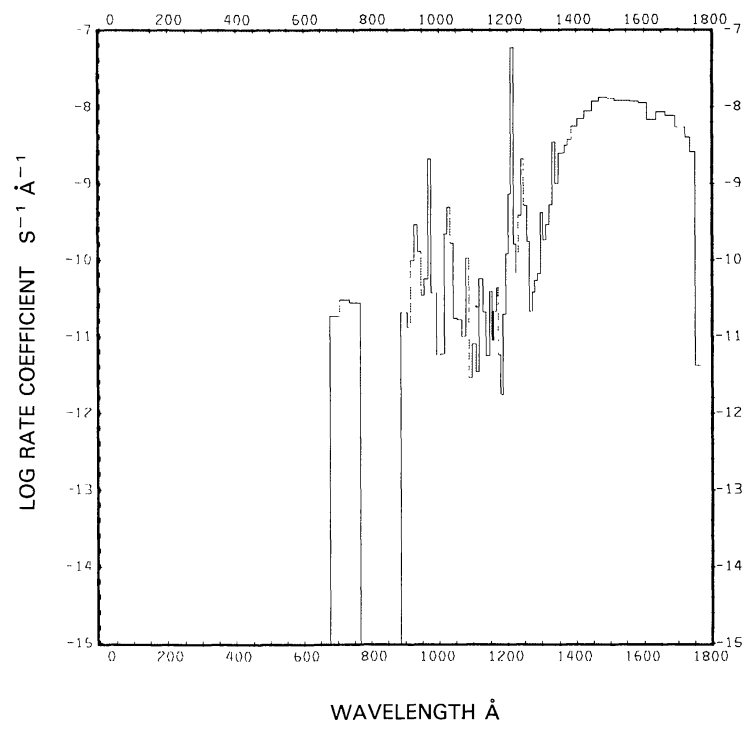
Huffman (1971) quotes 1027.8 Å for the ionization threshold. The threshold for dissociative ionization is at 585 Å, as given by Kronebusch and Berkowitz (1976).

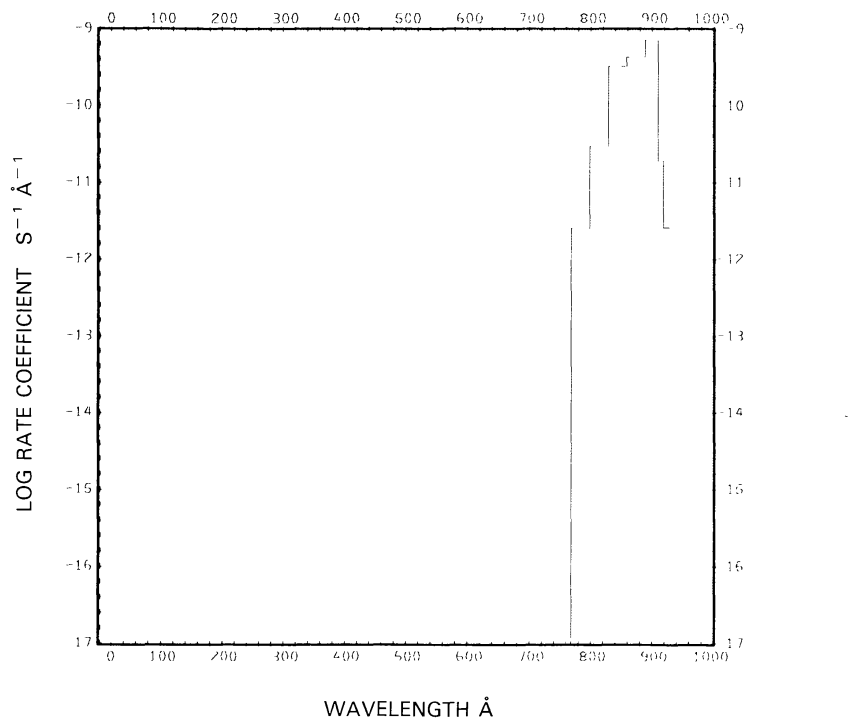
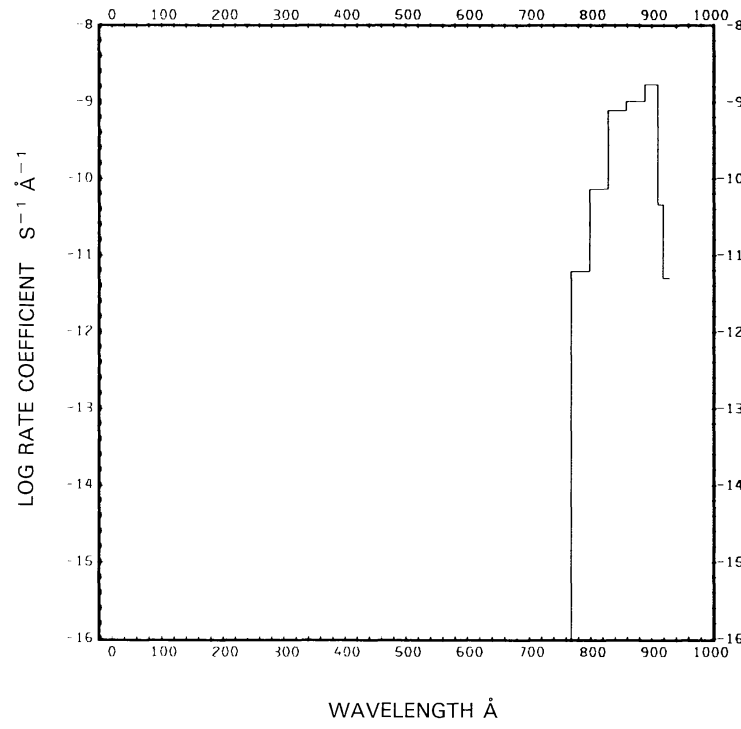
Rate coefficients:

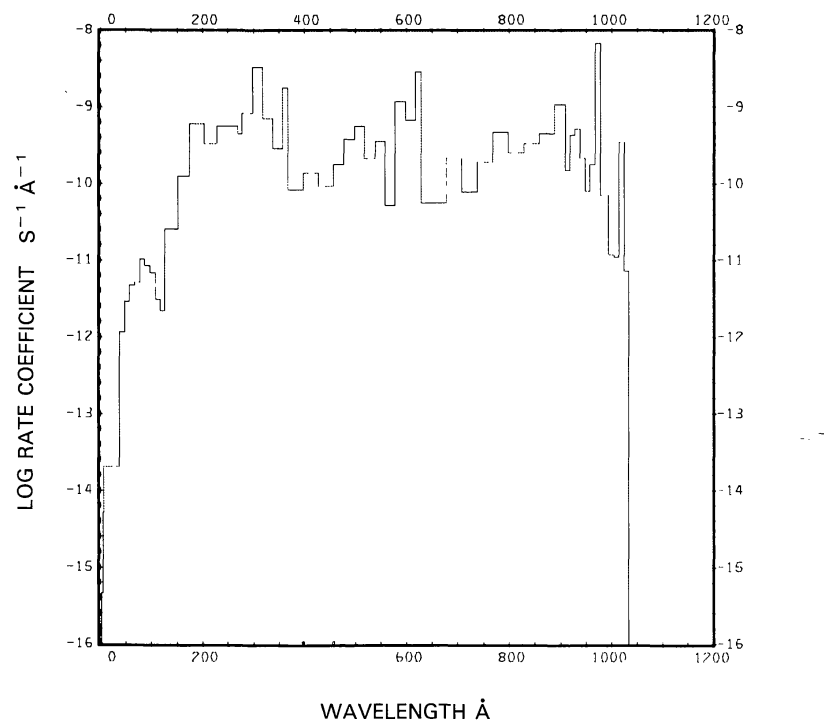
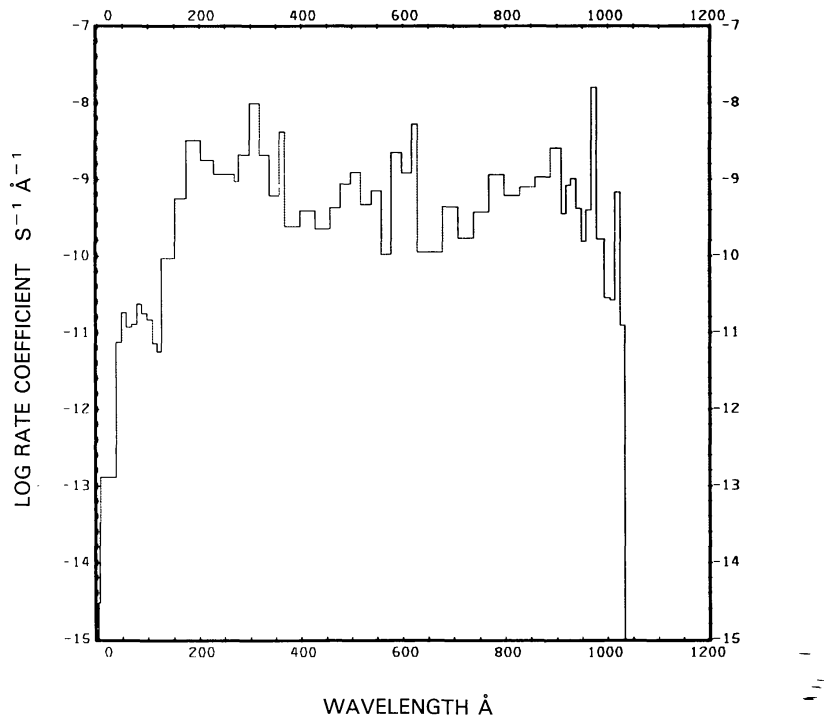
The first of each of these values is for the quiet Sun (see Figures 63, 64, and 65(a) to 67(a)), the second is for the active Sun (see Figures 65(b) to 67(b)). For comparison, the rate coefficients for the quiet Sun quoted by Bauer and Bortner (1978) for the first of these dissociations is $8.4 \times 10^{-8} \text{ s}^{-1}$, for the second it is $2.2 \times 10^{-6} \text{ s}^{-1}$, and for all ionizations combined it is $5.91 \times 10^{-7} \text{ s}^{-1}$. They give no rate coefficient for the third dissociation branch. McElroy and Hunten (1970) give $1.3 \times 10^{-9} \text{ s}^{-1}$ for the first dissociation branch and $6.0 \times 10^{-6} \text{ s}^{-1}$ for the second branch (after scaling their values to 1 AU heliocentric distance). Kumar (1982) quotes $2.6 \times 10^{-6} \text{ s}^{-1}$ for the sum of all dissociations and $6.2 \times 10^{-7} \text{ s}^{-1}$ for ionization, when his values are scaled from 5.2 to 1 AU. Siscoe and Mukherjee (1972) give $7.0 \times 10^{-7} \text{ s}^{-1}$ for the ionization rate.

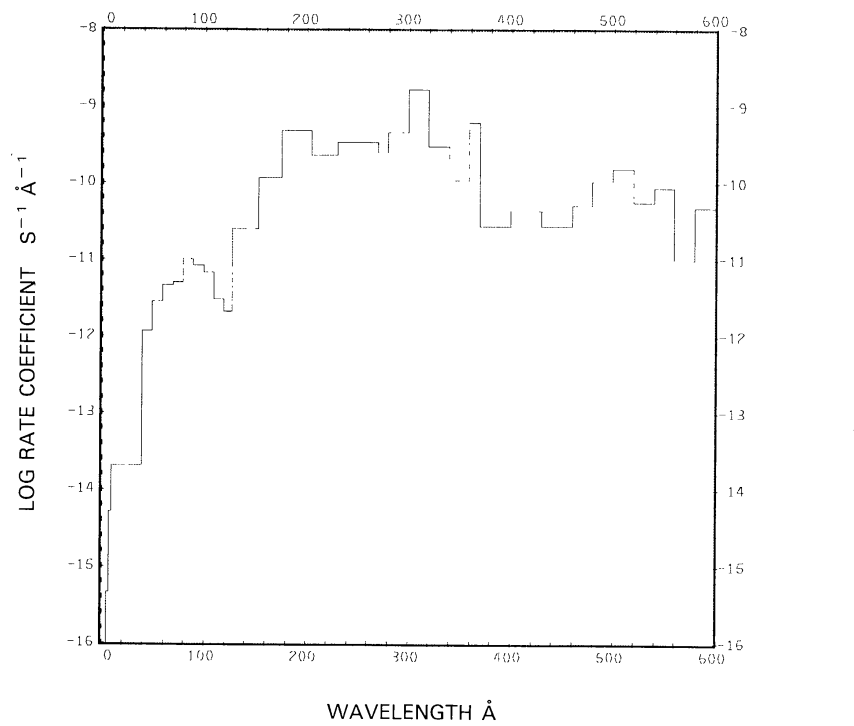
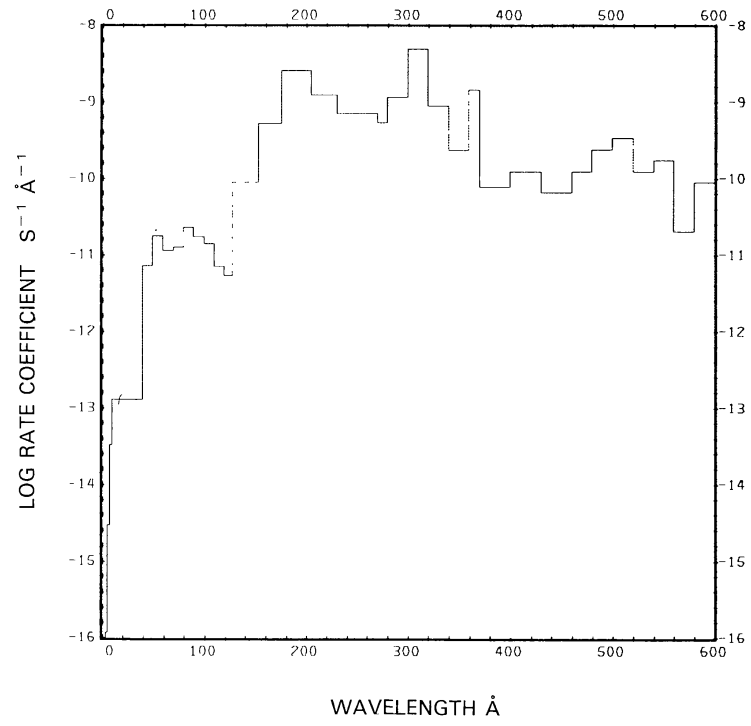
Excess energies:

The first of each of these values is for the quiet Sun, the second is for the active Sun.

Fig. 63. O₂ + ν → O(³P) + O(³P), for the quiet Sun.Fig. 64. O₂ + ν → O(³P) + O(¹D), for the quiet Sun.

Fig. 65a. $O_2 + \nu \rightarrow O(^1S) + O(^1S)$, for the quiet Sun.Fig. 65b. $O_2 + \nu \rightarrow O(^1S) + O(^1S)$, for the active Sun.

Fig. 66a. O₂ + v → O₂⁺ + e, for the quiet Sun.Fig. 66b. O₂ + v → O₂⁺ + e, for the active Sun.

Fig. 67a. $\text{O}_2 + \nu \rightarrow \text{O} + \text{O}^+ + e$, for the quiet Sun.Fig. 67b. $\text{O}_2 + \nu \rightarrow \text{O} + \text{O}^+ + e$, for the active Sun.

HYDROGEN CHLORIDE, HCl

Cross sections: Up to 877.5 Å the cross section is synthesized from the fits for H and Cl made by Barfield *et al.* (1972). For $\lambda = 1050$ to 1350 Å the cross section from Myer and Samson (1970) is used. In the region from 1400 to 2200 Å the cross section comes from Inn (1975). From 2200 Å to threshold the cross section is negligibly small. The theoretical cross section of van Dishoeck *et al.* (1982) are in satisfactory agreement with the measured cross sections below 1460 Å, but at longer wavelengths the discrepancy between theory and experiment has not been resolved. Although the cross section above 1460 Å is rapidly decreasing, the theoretical values are larger than the experimental values and will lead to a larger rate coefficient.

Branching ratios: Branching ratios are not known.

Thresholds: $\lambda = 2798$ Å as given by Rosen (1970).

Rate coefficients:

$$\text{HCl} + \nu \rightarrow \text{H} + \text{Cl}: 7.21 \times 10^{-6} \text{ s}^{-1}$$

for the quiet Sun (see Figure 68) and $1.16 \times 10^{-5} \text{ s}^{-1}$ for the active Sun.

Excess energies: The excess energy is 4.41 eV for the quiet Sun and 5.30 eV for the active Sun.

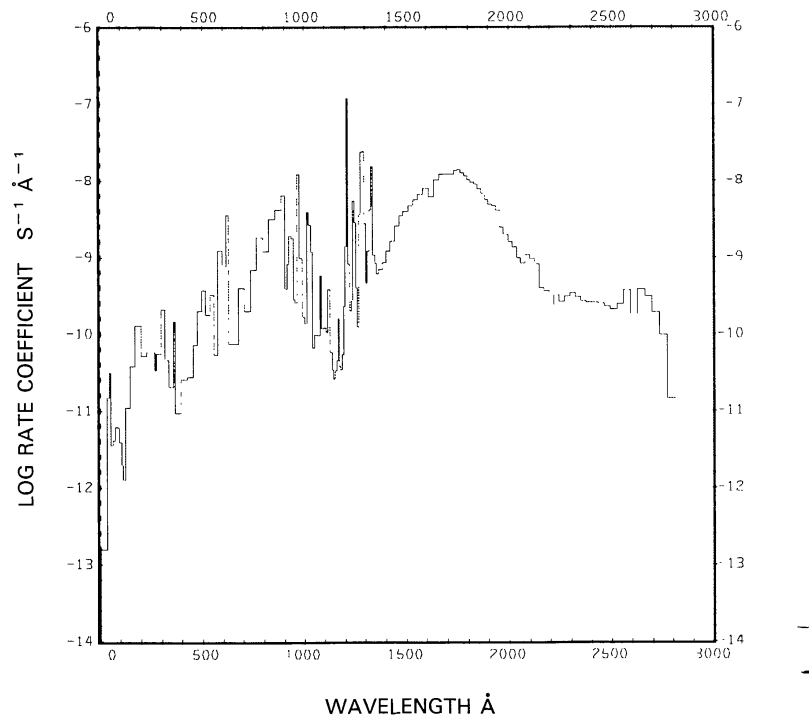


Fig. 68. $\text{HCl} + \nu \rightarrow \text{H} + \text{Cl}$, for the quiet Sun.

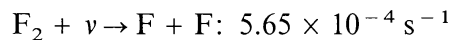
DIATOMIC FLUORINE, F₂

Cross sections: Up to 653.6 Å the cross section is taken to be twice that of atomic fluorine as obtained from fits by Barfield *et al.* (1972). From $\lambda = 2100$ to 3700 Å the cross section is given by Okabe (1978). Between 3700 Å and threshold the cross section is negligibly small.

Branching ratios: Branching ratios are not known.

Thresholds: $\lambda = 7950$ Å from Stull and Prophet (1971).

Rate coefficients:



for the quiet Sun (see Figure 69) and $5.81 \times 10^{-4} \text{ s}^{-1}$ for the active Sun.

Excess energies: The excess energy is 1.78 eV for the quiet Sun and 1.98 eV for the active Sun.

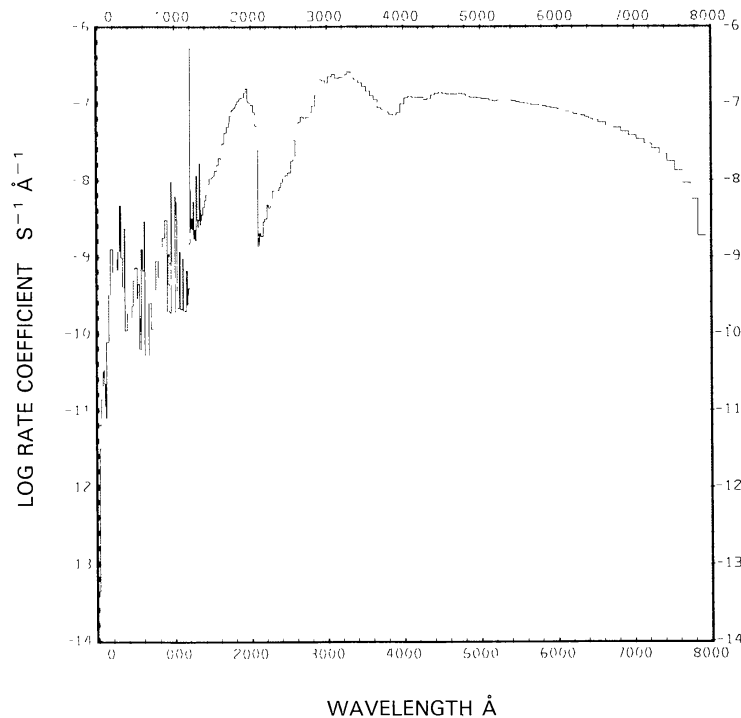


Fig. 69. $F_2 + v \rightarrow F + F$, for the quiet Sun.

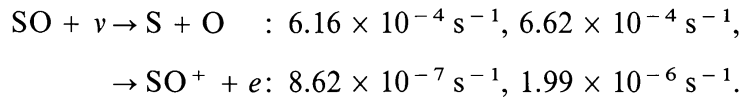
SULFUR MONOXIDE, SO

Cross sections: Up to 800 Å the cross section is synthesized from fits (Barfield *et al.*, 1972) to the cross sections of its atomic constituents. From 1900 to 2314 Å the cross section from Phillips (1981) is used.

Branching ratios: The branching ratio is unknown. We assumed that the entire cross section results in ionization at wavelengths less than the ionization threshold, and in dissociation at wavelengths above that threshold.

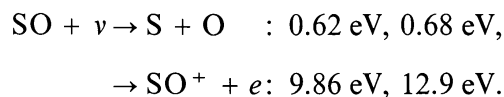
Thresholds: Huber and Herzberg (1979) give the threshold for dissociation at 2314 Å and for ionization at 1205 Å.

Rate coefficients:



The first of each of these values is for the quiet Sun (see Figures 70 and 71(a)), the second is for the active Sun (see Figure 71(b)). For the quiet Sun, Kumar (1982) quotes a rate coefficient of $1.6 \times 10^{-4} \text{ s}^{-1}$ for dissociation and $6.2 \times 10^{-7} \text{ s}^{-1}$ for ionization after his values for Jupiter's satellite Io are scaled from 5.2 AU heliocentric distance to 1 AU. Our rate coefficient for dissociation is about 4 times higher than his, while our ionization rate coefficient is in good agreement with his, considering the uncertainties in the cross section.

Excess energies:



The first of each of these values is for the quiet Sun, the second is for the active Sun.

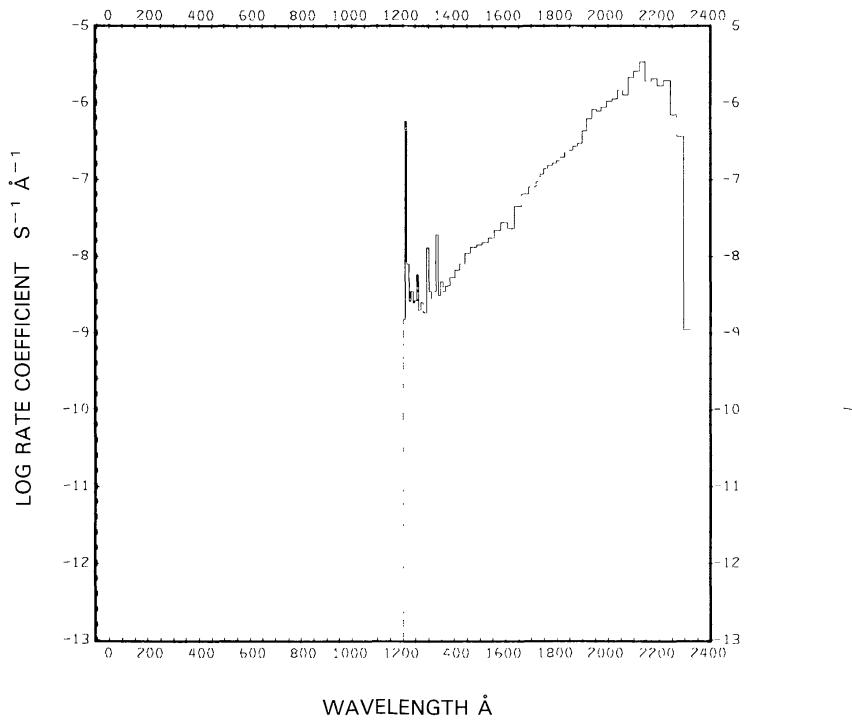
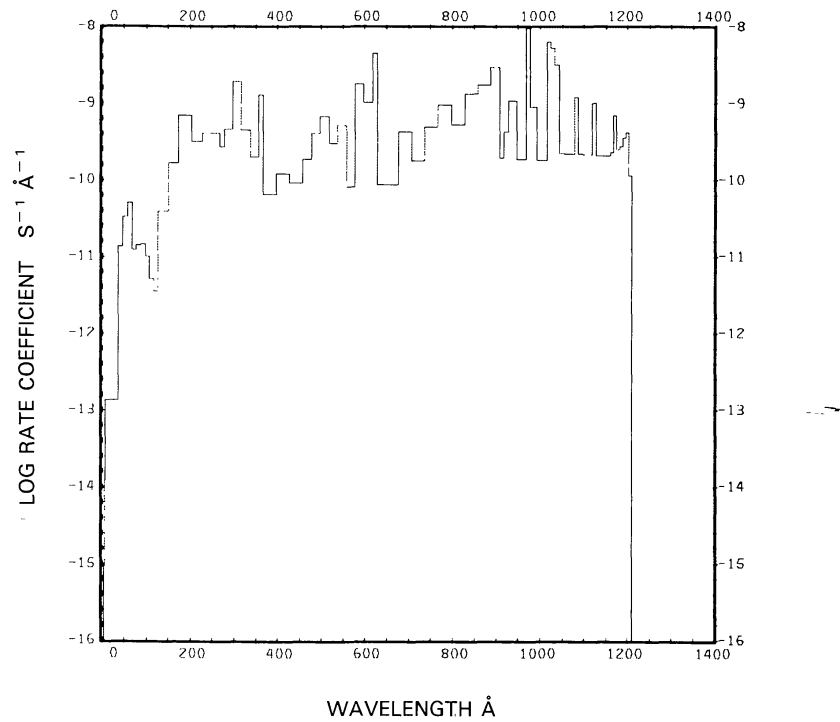
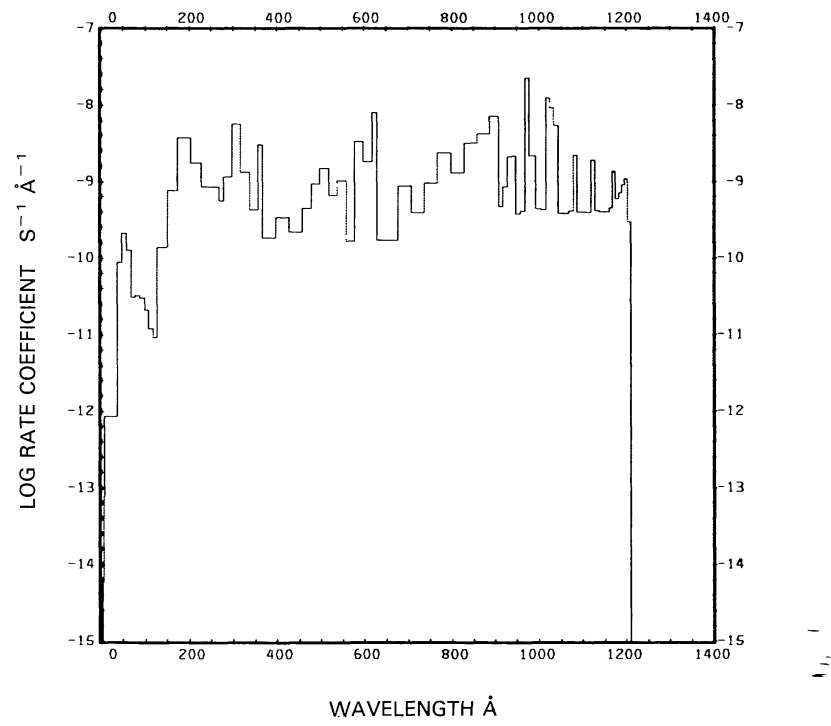


Fig. 70. $\text{SO} + \nu \rightarrow \text{S} + \text{O}$, for the quiet Sun.

Fig. 71a. $\text{SO} + \nu \rightarrow \text{SO}^+ + e^-$, for the quiet Sun.Fig. 71b. $\text{SO} + \nu \rightarrow \text{SO}^+ + e^-$, for the active Sun.

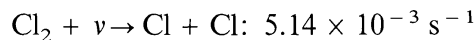
DIATOMIC CHLORINE, Cl_2

Cross sections: Up to 878 Å the cross section is approximated to be twice the atomic cross section for chlorine obtained from fits by Barfield *et al.* (1972). From 2400 to 4500 Å the cross section was measured by Seery and Britton (1964). There are no cross sections available between 878 and 2400 Å. A linear interpolation was used for the cross section between $1.0 \times 10^{-16} \text{ cm}^2$ at 878 Å and $8.0 \times 10^{-22} \text{ cm}^2$ at 2400 Å.

Branching ratios: Branching ratios are not known.

Thresholds: $\lambda = 5000.68 \text{ \AA}$ from Huber and Herzberg (1979).

Rate coefficients:



for the quiet Sun (see Figure 72) and $5.31 \times 10^{-3} \text{ s}^{-1}$ for the active Sun.

Excess energies: The excess energy is 2.10 eV for the quiet Sun and 2.19 eV for the active Sun.

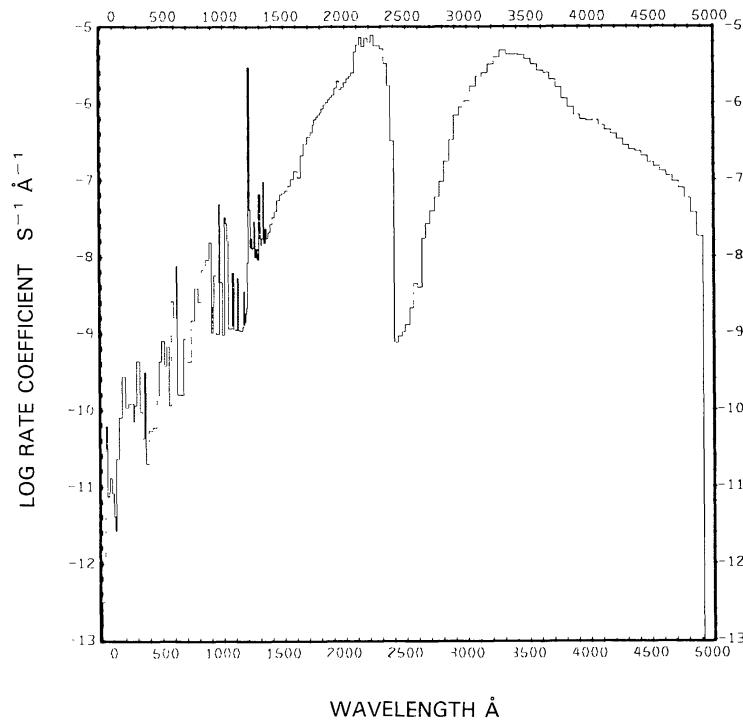


Fig. 72. $\text{Cl}_2 + \nu \rightarrow \text{Cl} + \text{Cl}$, for the quiet Sun.

BROMINE MONOXIDE, BrO

Cross sections: Up to 7.1 Å the cross section of Hubbell and Veigle (1976) was used. From 12 to 1127 Å the cross section was synthesized from our cross sections for the atomic constituents. Additional values between $\lambda = 3208$ Å and $\lambda = 3383$ Å come from Baulch *et al.* (1980). The cross-section data are sparse and uncertain.

Branching ratios: Above $\lambda = 2830$ Å the branching ratio to produce $\text{Br} + \text{O}({}^3P)$ is 1 as given by Baulch *et al.* (1980). No other branching ratio data are available. We assumed a branching ratio of 0.5 below $\lambda = 2830$ Å.

Thresholds: For $\text{BrO} + v \rightarrow \text{Br} + \text{O}({}^3P)$ the threshold is at $\lambda = 5150$ Å and for $\text{BrO} + v \rightarrow \text{Br} + \text{O}({}^1D)$ it is at $\lambda = 2830$ Å, as given by Baulch *et al.* (1980).

Rate coefficients:

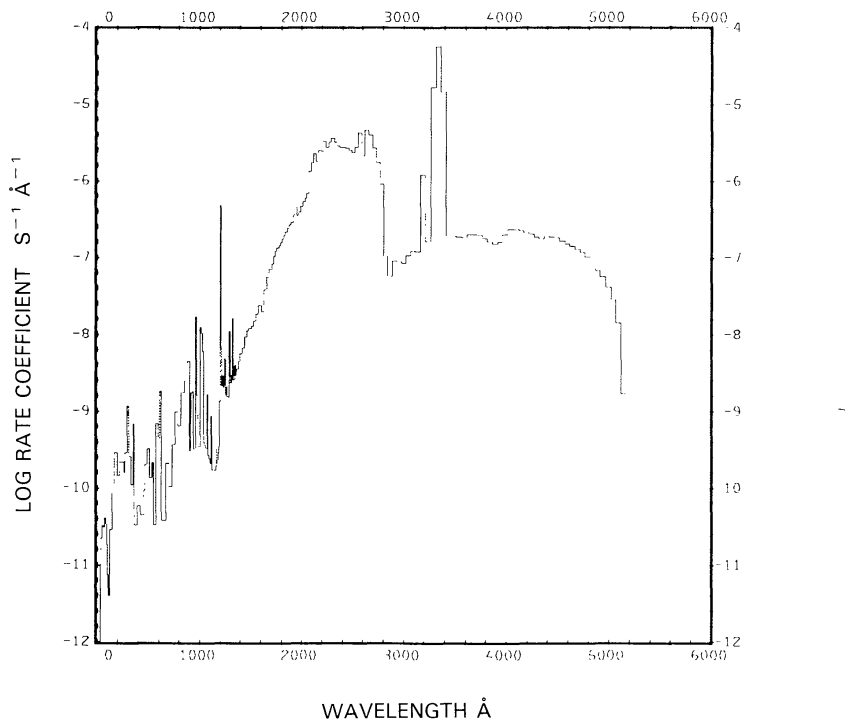
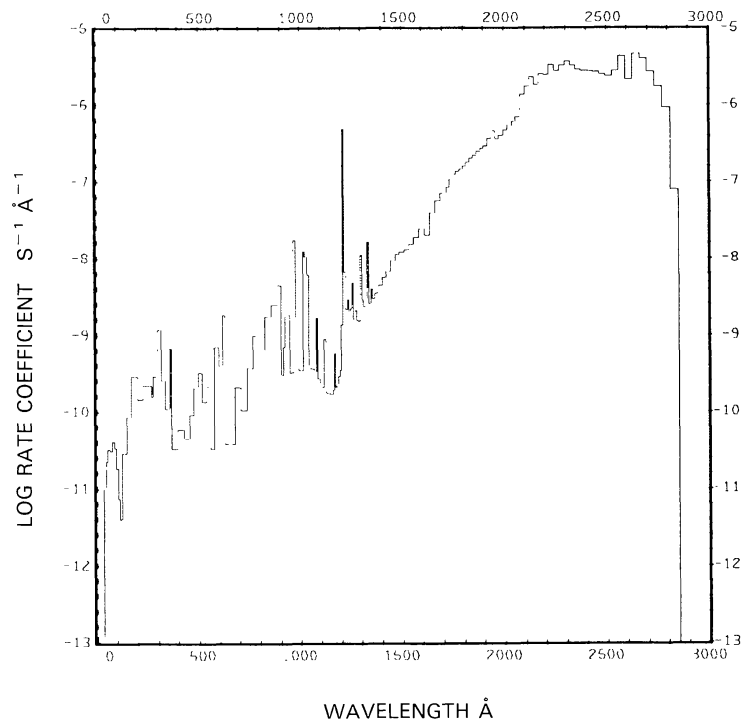
$$\begin{aligned}\text{BrO} + v \rightarrow \text{Br} + \text{O}({}^3P) : & \sim 6.9 \times 10^{-3} \text{ s}^{-1}, \sim 7.0 \times 10^{-3} \text{ s}^{-1}, \\ & \rightarrow \text{Br} + \text{O}({}^1D) : \sim 2.1 \times 10^{-3} \text{ s}^{-1}, \sim 2.2 \times 10^{-3} \text{ s}^{-1}.\end{aligned}$$

The first of each of these values is for the quiet Sun (see Figures 73 and 74), the second is for the active Sun.

Excess energies:

$$\begin{aligned}\text{BrO} + v \rightarrow \text{Br} + \text{O}({}^3P) : & \sim 1.7 \text{ eV}, \sim 1.8 \text{ eV}, \\ & \rightarrow \text{Br} + \text{O}({}^1D) : \sim 0.80 \text{ eV}, \sim 0.83 \text{ eV}.\end{aligned}$$

These approximate excess energies are nearly insensitive to solar activity.

Fig. 73. $\text{BrO} + \nu \rightarrow \text{Br} + \text{O}({}^3P)$, for the quiet Sun.Fig. 74. $\text{BrO} + \nu \rightarrow \text{Br} + \text{O}({}^1D)$, for the quiet Sun.

AMIDOGEN, NH₂

Cross sections: Up to 840 Å the cross section is synthesized from the fits to the constituent atomic cross sections prepared by Barfield *et al.* (1972). From $\lambda = 1215$ to 1970.5 Å the cross section was calculated by Saxon (1983). It does not include predissociation.

Branching ratios: Branching ratios are not known.

Thresholds: The wavelength equivalent to the dissociation threshold obtained from thermodynamic data (Benson, 1976) is $\lambda = 3000$ Å.

Rate coefficients:

$$\text{NH}_2 + v \rightarrow \text{NH} + \text{H}: 2.15^{-} \times 10^{-6} \text{ s}^{-1}$$

for the quiet Sun (see Figure 75), for the active Sun the rate coefficient is $3.40 \times 10^{-6} \text{ s}^{-1}$. This rate coefficient is a minimum value since predissociation was not included in the calculation.

Excess energies: The excess energy is 6.38 eV for the quiet Sun and 8.49 eV for the active Sun.

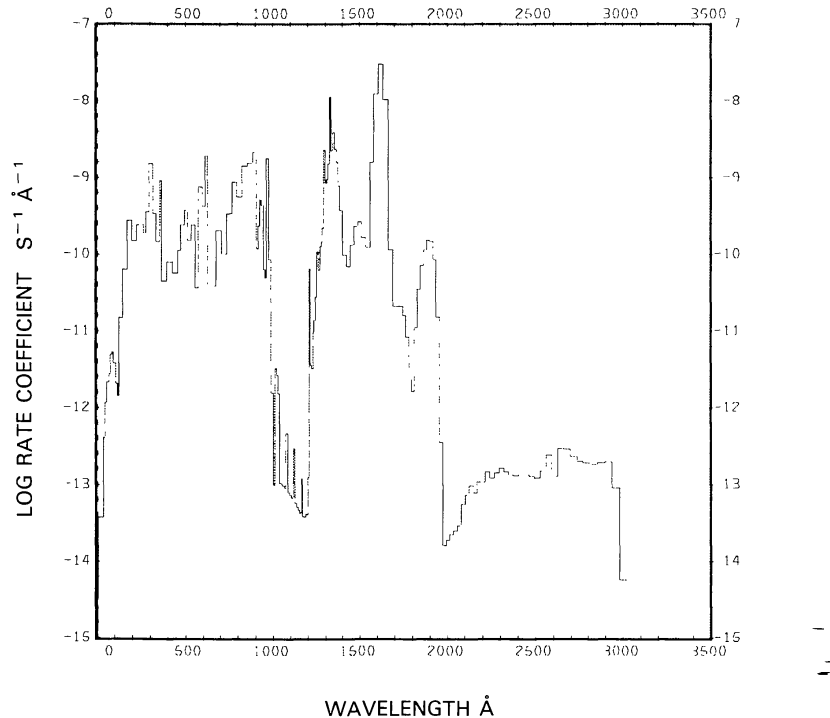


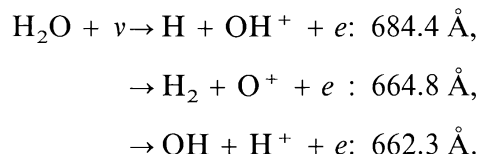
Fig. 75. $\text{NH}_2 + v \rightarrow \text{NH} + \text{H}$, for the quiet Sun.

WATER, H₂O

Cross sections: From $\lambda = 1$ to 100 Å the molecular cross section has been approximated by the sum of the atomic cross sections (Barfield *et al.* 1972). Between 180 and 720 Å, cross section data were taken from Phillips *et al.* (1977), supplemented with data from Dibeler *et al.* (1966). From $\lambda = 700$ to 980.8 Å the cross section was determined by Katayama *et al.* (1973). In the range $\lambda = 850$ to 1110 Å the measurements made by Watanabe and Jursa (1964) were incorporated. Between $\lambda = 1060$ and 1860 Å data are based on measurements made by Watanabe and Zelikoff (1953).

Branching ratios: The branching ratio for dissociation and ionization is obtained from the papers of Katayama *et al.* (1973) and Watanabe and Jursa (1964). Between 982.6 and 1304 Å we assumed the branching ratio for production of H + H + O to be equal to the value found by Slanger and Black (1982) at 1216 Å. Above $\lambda = 1450$ Å the branching ratio to produce H₂ + O(¹D) is zero (McNesby *et al.*, 1962). Branching ratios for dissociative ionization are obtained from Dibeler *et al.* (1966) and from Kronebusch and Berkowitz (1976).

Thresholds: The dissociation into H + OH has a threshold at $\lambda = 2424.6$ Å (Herzberg, 1966), while the threshold for dissociation into H₂ + O(¹D) is at $\lambda = 1770$ Å as assumed from discussions given by McNesby *et al.* (1962). The threshold for dissociation into H + H + O is at $\lambda = 1304$ Å as obtained from the dissociation of OH. The ionization threshold of $\lambda = 984$ Å reported by Katayama *et al.* (1973) is in good agreement with values measured by Dibeler *et al.* (1966) and Watanabe and Jursa (1964). Thresholds for dissociative ionization as reported by Kronebusch and Berkowitz (1976) are:

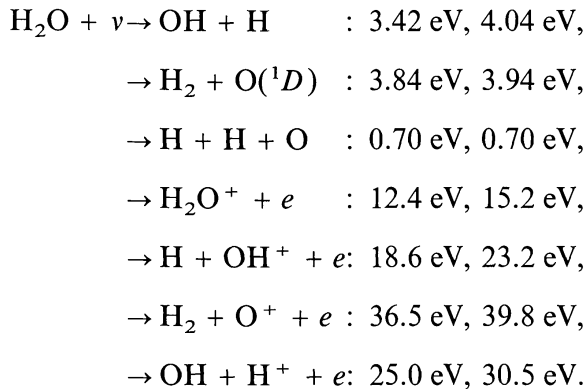
**Rate coefficients:**

$$\begin{aligned} \text{H}_2\text{O} + v \rightarrow & \text{OH} + \text{H} : 1.03 \times 10^{-5} \text{ s}^{-1}, 1.76 \times 10^{-5} \text{ s}^{-1}, \\ \rightarrow & \text{H}_2 + \text{O}(\text{¹D}) : 5.97 \times 10^{-7} \text{ s}^{-1}, 1.48 \times 10^{-6} \text{ s}^{-1}, \\ \rightarrow & \text{H} + \text{H} + \text{O} : 7.55 \times 10^{-7} \text{ s}^{-1}, 1.91 \times 10^{-6} \text{ s}^{-1}, \\ \rightarrow & \text{H}_2\text{O}^+ + e : 3.31 \times 10^{-7} \text{ s}^{-1}, 8.28 \times 10^{-7} \text{ s}^{-1}, \\ \rightarrow & \text{H} + \text{OH}^+ + e: 5.54 \times 10^{-8} \text{ s}^{-1}, 1.51 \times 10^{-7} \text{ s}^{-1}, \\ \rightarrow & \text{H}_2 + \text{O}^+ + e : 5.85 \times 10^{-9} \text{ s}^{-1}, 2.21 \times 10^{-8} \text{ s}^{-1}, \\ \rightarrow & \text{OH} + \text{H}^+ + e: 1.31 \times 10^{-8} \text{ s}^{-1}, 4.07 \times 10^{-8} \text{ s}^{-1}. \end{aligned}$$

The first of each of these values is for the quiet Sun (see Figures 76 and 77(a) to 82(a)),

the second is for the active Sun (see Figures 77(b) to 82(b)). For the quiet Sun, the total photodissociation rate coefficient of $1.16 \times 10^{-5} \text{ s}^{-1}$ is in good agreement with the values reported by Potter and del Duca (1964) ($1.38 \times 10^{-5} \text{ s}^{-1}$), Wyckoff and Wehinger (1976) ($1.1 \times 10^{-5} \text{ s}^{-1}$), Festou (1981) ($1.3 \times 10^{-5} \text{ s}^{-1}$), as well as Crovisier (1989) ($1.21 \times 10^{-5} \text{ s}^{-1}$), but it is larger than the value given by Bauer and Bortner (1978) ($8.3 \times 10^{-6} \text{ s}^{-1}$) and is much smaller than the value quoted by Jackson (1976a,b) ($5 \times 10^{-5} \text{ s}^{-1}$). Our combined ionization rate coefficient of $4.08 \times 10^{-7} \text{ s}^{-1}$ is also in good agreement with the value given by Wyckoff and Wehinger (1976) ($4.4 \times 10^{-7} \text{ s}^{-1}$) but is smaller than the value quoted by Siscoe and Mukherjee (1972) ($6.24 \times 10^{-7} \text{ s}^{-1}$). For the quiet Sun, our total photo rate coefficient for destruction of H₂O is $1.20 \times 10^{-5} \text{ s}^{-1}$. This is in good agreement with the value obtained by Bertaux *et al.* (1973) ($9.3 \times 10^{-6} \text{ s}^{-1}$) and by Festou (1981) ($1.2 \times 10^{-5} \text{ s}^{-1}$).

Excess energies:



The first of each value is for the quiet Sun, the second for the active Sun. Keller (1971) estimated an excess energy of 2.48 eV for the first of the above processes. Crovisier (1989), who also considers partitioning of the excess energy into the states of excitation and translation, gives 3.14 eV for the first of the above dissociation channels for the quiet Sun.

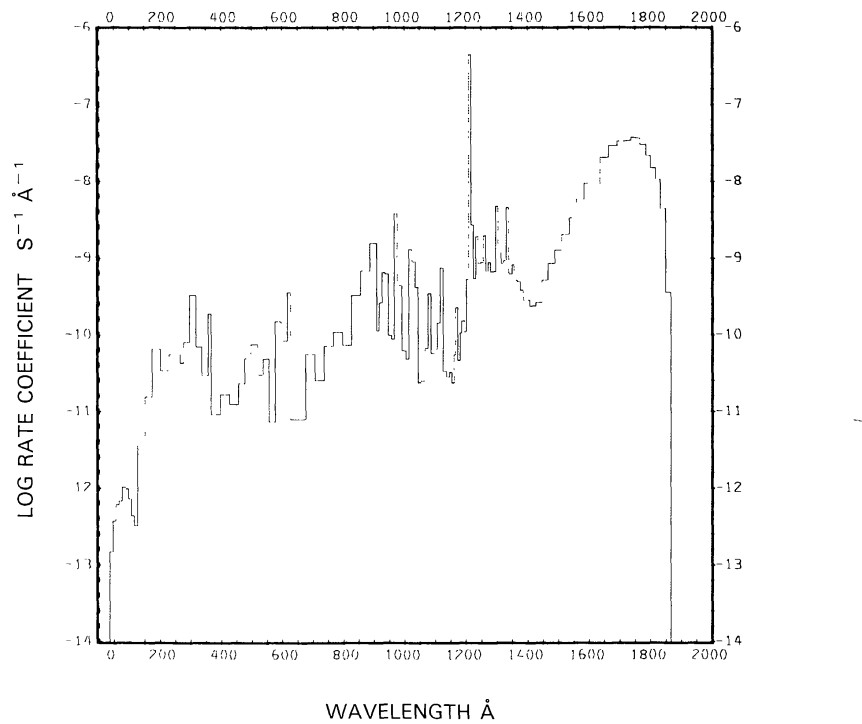
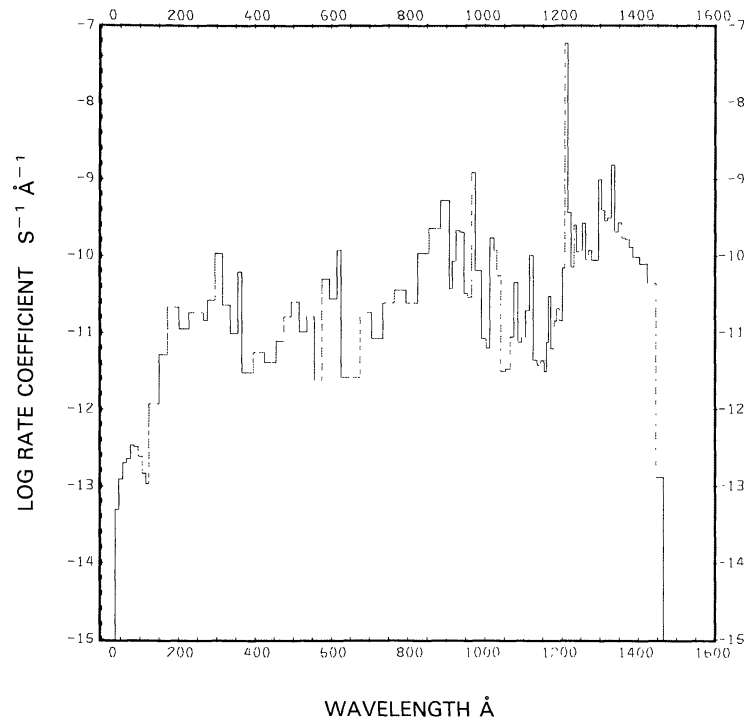
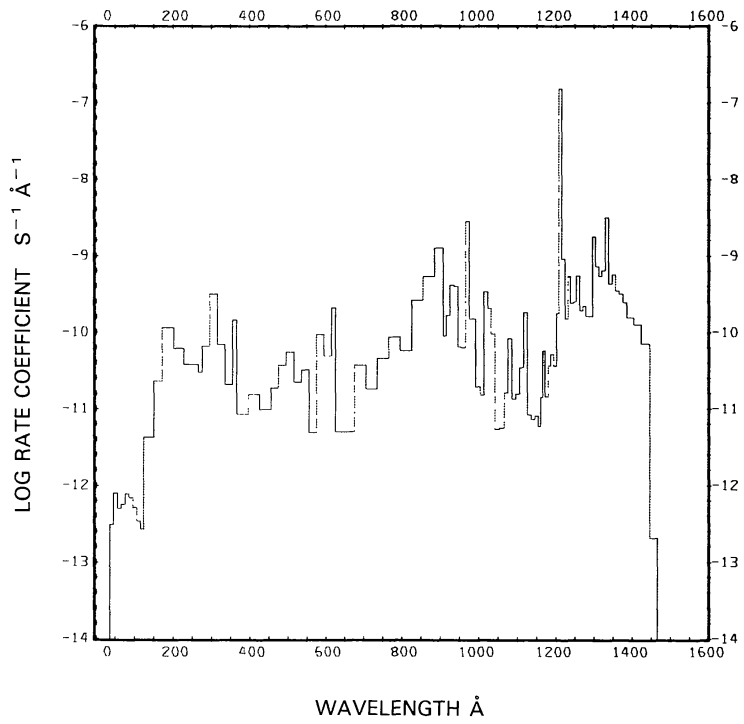
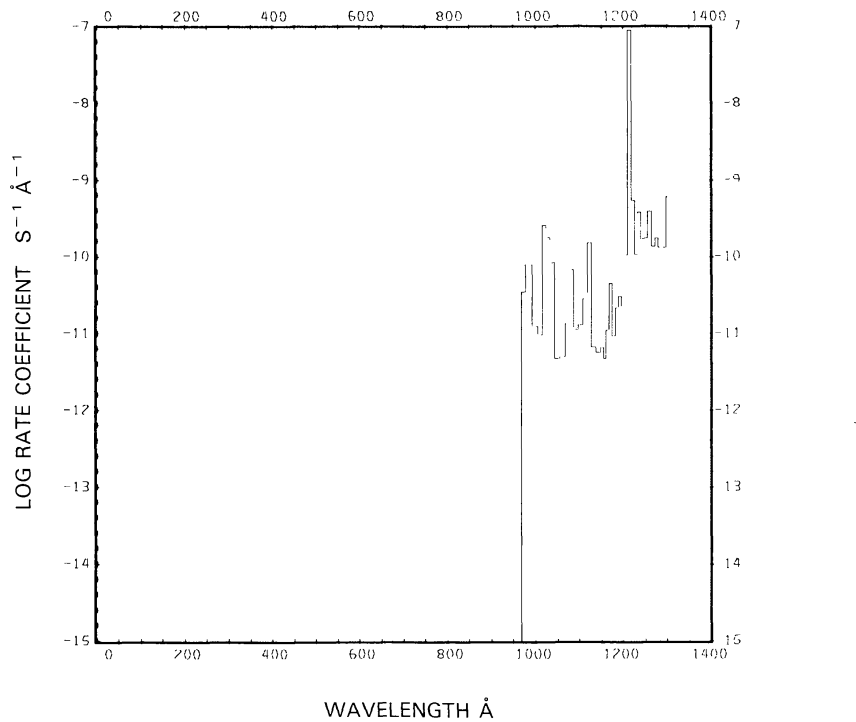
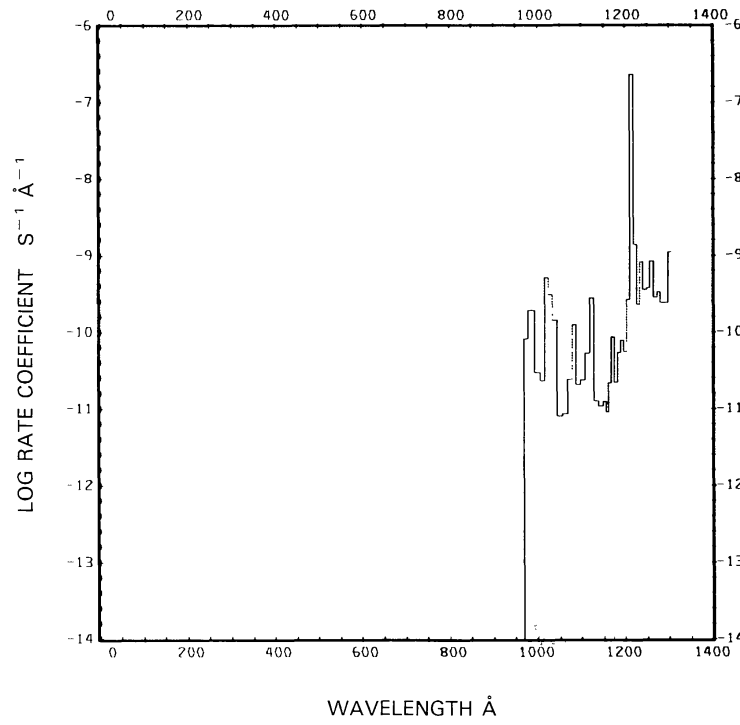
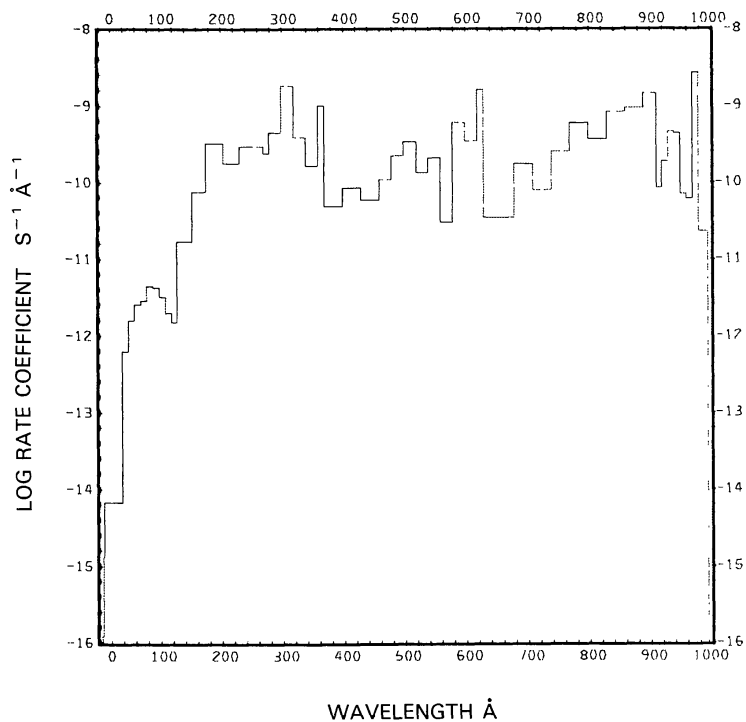
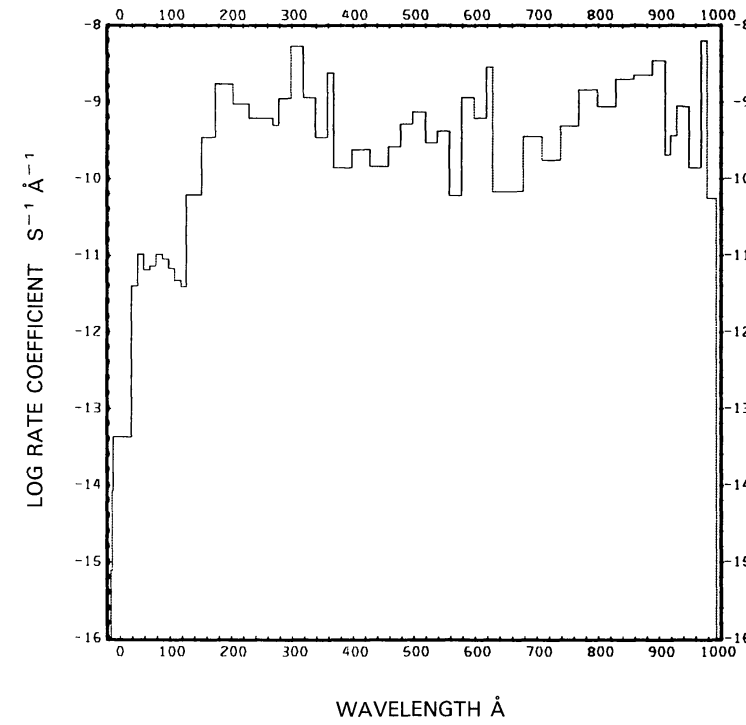
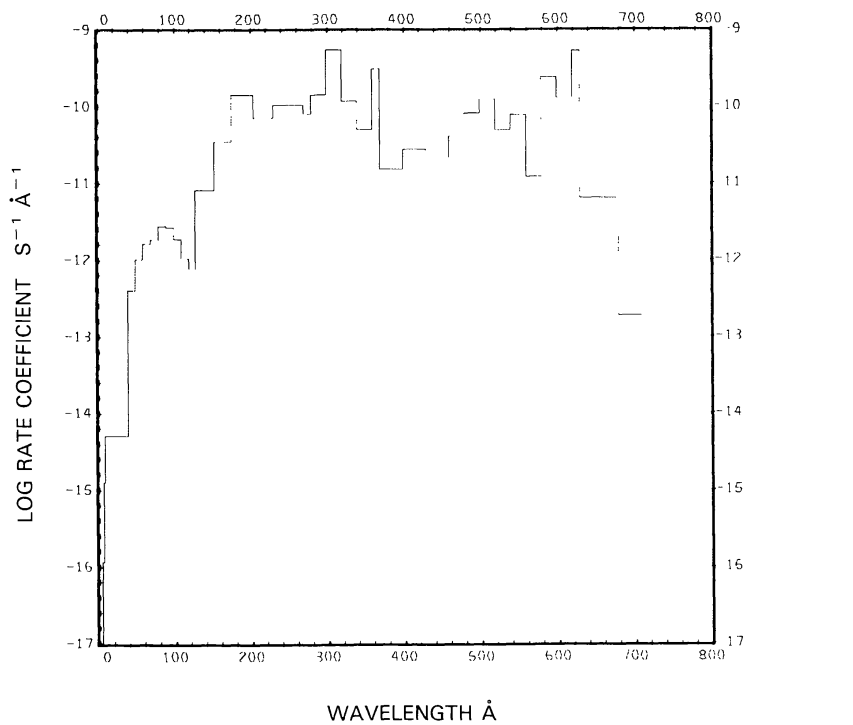
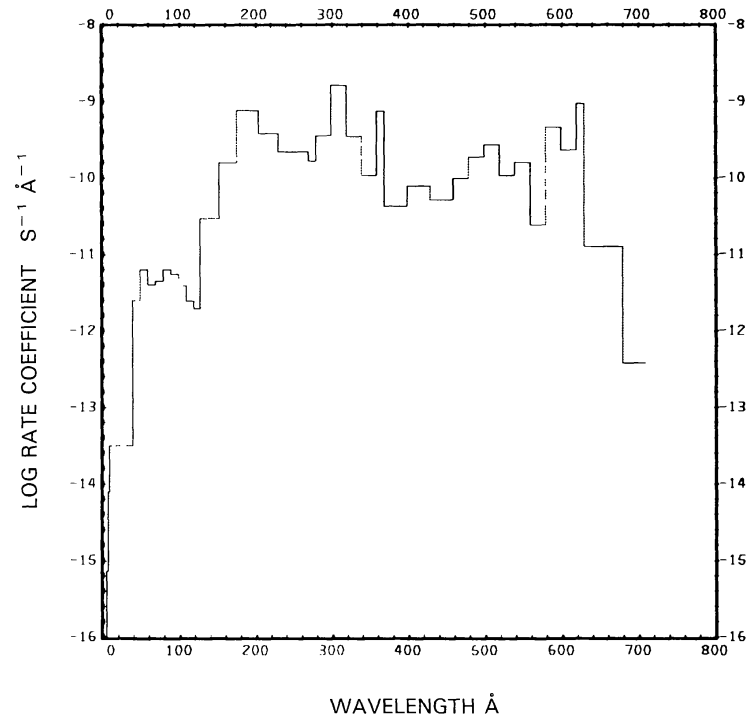


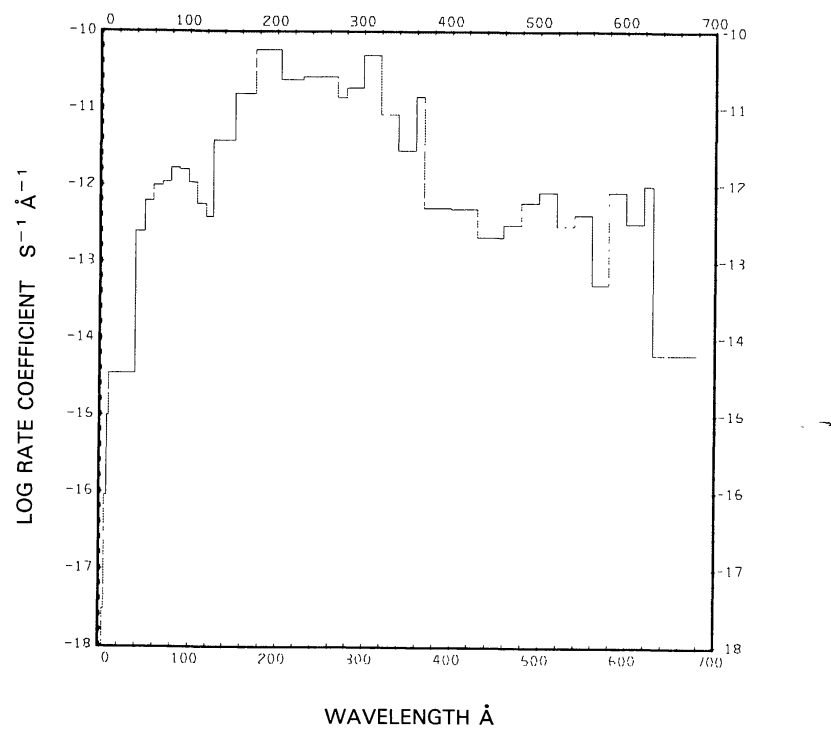
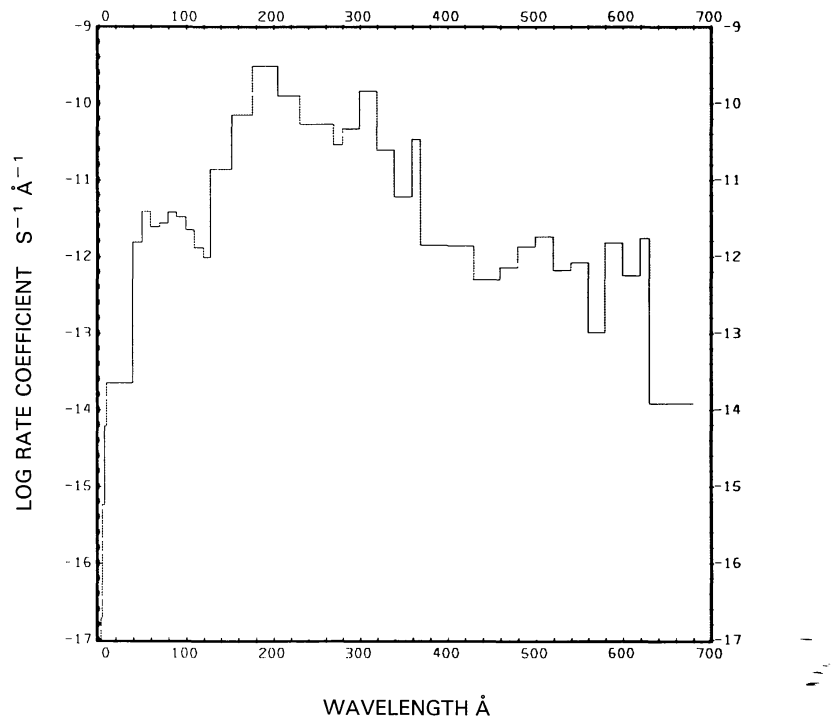
Fig. 76. $\text{H}_2\text{O} + \nu \rightarrow \text{OH} + \text{H}$, for the quiet Sun.

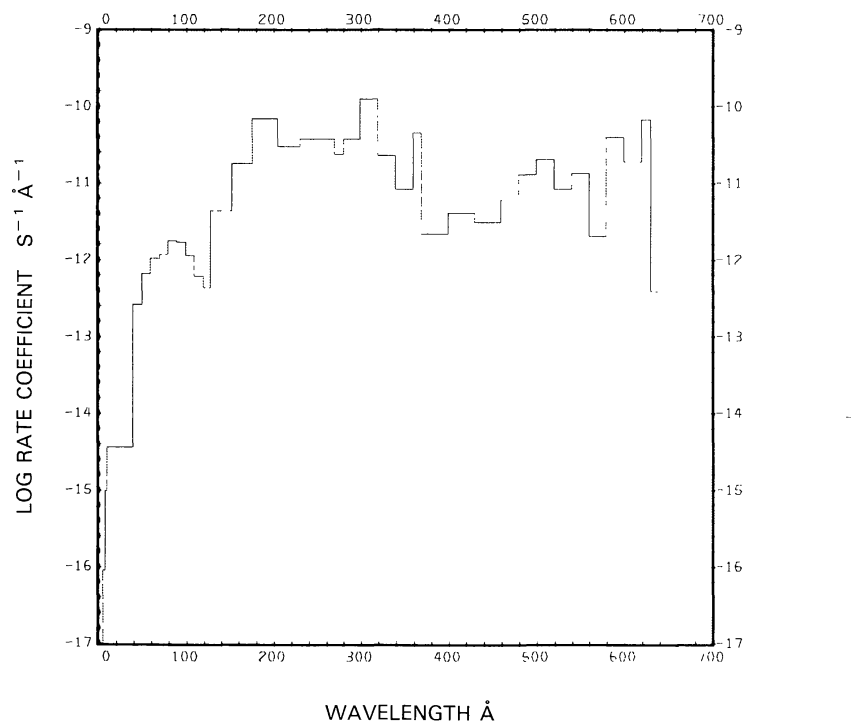
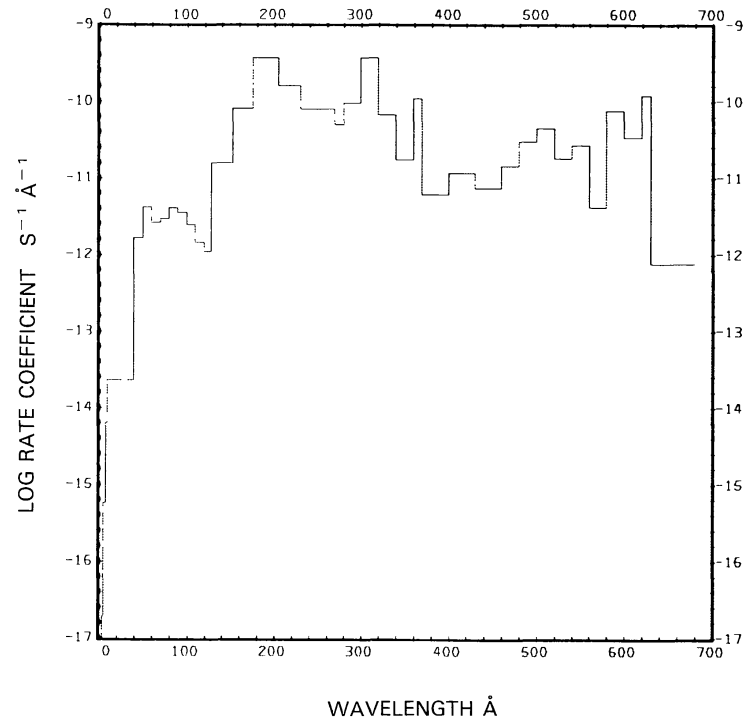
Fig. 77a. H₂O + $\nu \rightarrow$ H₂ + O(¹D), for the quiet Sun.Fig. 77b. H₂O + $\nu \rightarrow$ H₂ + O(¹D), for the active Sun.

Fig. 78a. H₂O + ν → H + H + O, for the quiet Sun.Fig. 78b. H₂O + ν → H + H + O, for the active Sun.

Fig. 79a. H₂O + $\nu \rightarrow$ H₂O⁺ + e, for the quiet Sun.Fig. 79b. H₂O + $\nu \rightarrow$ H₂O⁺ + e, for the active Sun.

Fig. 80a. $\text{H}_2\text{O} + \nu \rightarrow \text{H} + \text{OH}^+ + e$, for the quiet Sun.Fig. 80b. $\text{H}_2\text{O} + \nu \rightarrow \text{H} + \text{OH}^+ + e$, for the active Sun.

Fig. 81a. H₂O + ν → H₂ + O⁺ + e, for the quiet Sun.Fig. 81b. H₂O + ν → H₂ + O⁺ + e, for the active Sun.

Fig. 82a. H₂O + ν → OH + H⁺ + e⁻, for the quiet Sun.Fig. 82b. H₂O + ν → OH + H⁺ + e⁻, for the active Sun.

HYDROGEN CYANIDE, HCN

Cross sections: Up to 900 Å the molecular cross section is synthesized from the atomic cross sections of H, C, and N as obtained from fits by Barfield *et al.* (1972). From $\lambda = 1050$ to 1950 Å the cross section was measured by West (1975).

Branching ratios: The branching ratio is not known. We assume that below the ionization threshold all photoabsorption leads to ionization, and above that threshold to dissociation.

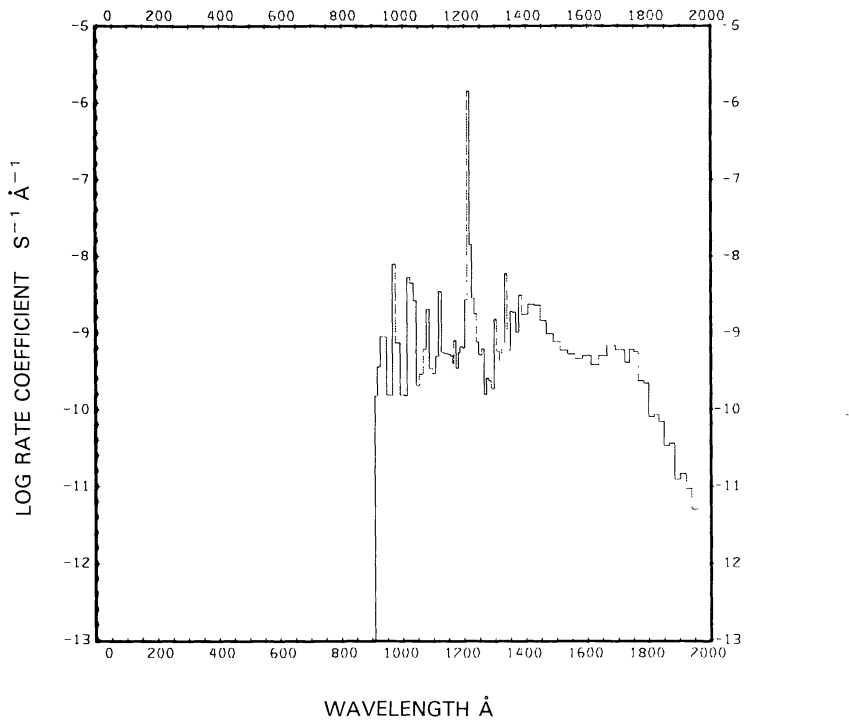
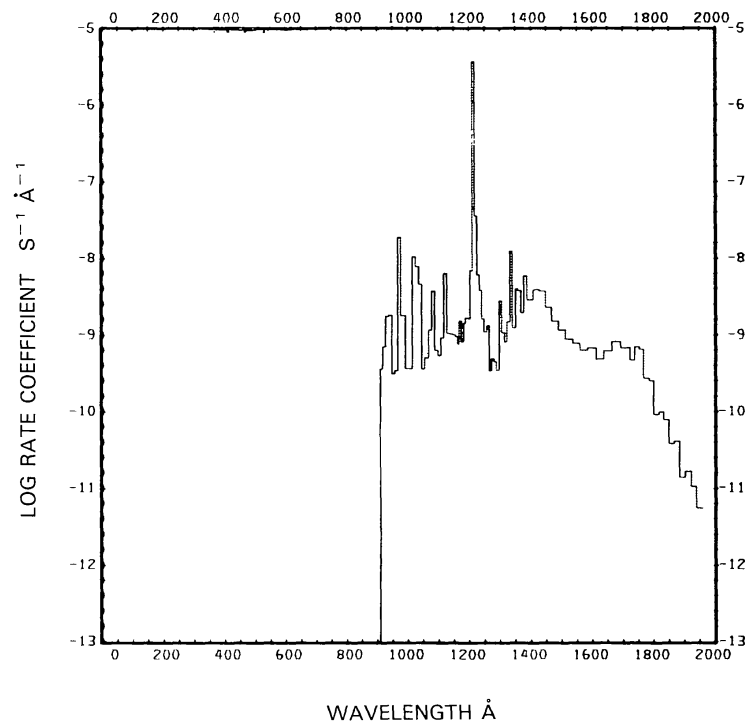
Thresholds: $\lambda = 1950$ Å for dissociation into H and CN($A^2\Pi_i$) is obtained from thermodynamic data (Benson, 1976) and the excitation energy of the $A^2\Pi_i$ state of CN above the ground state $X^2\Sigma^+$ (West, 1975). The threshold for ionization was measured by Fridh and Åsbrink (1975) to be 13.607 eV (911.19 Å).

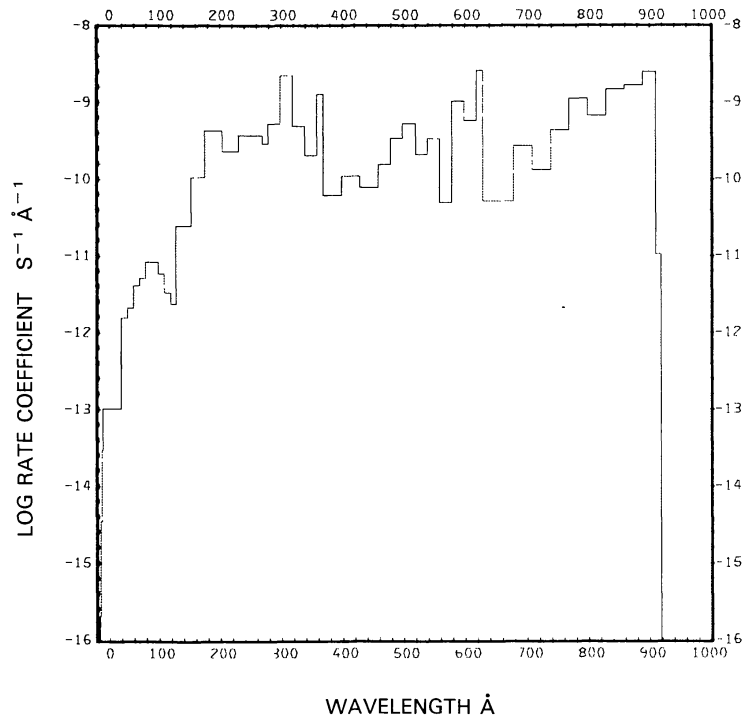
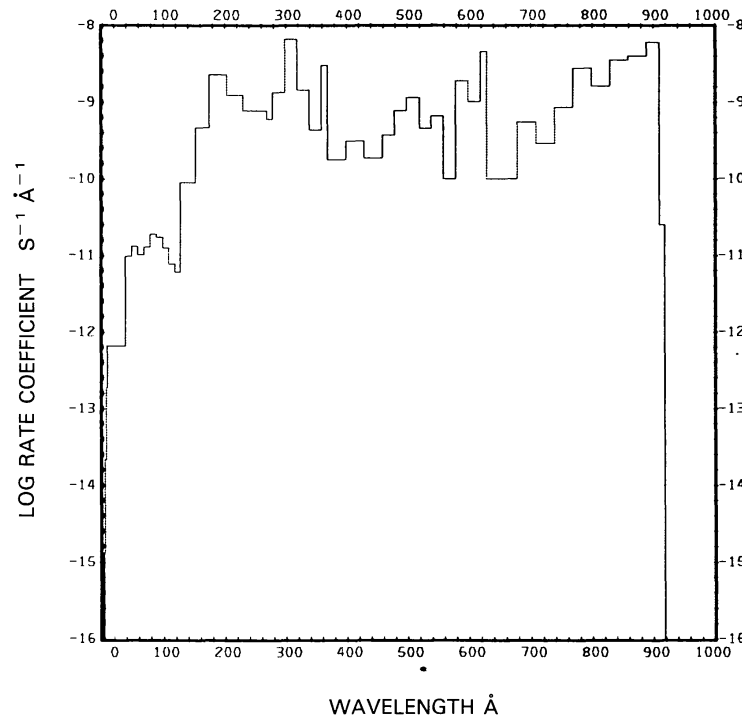
Rate coefficients:

$$\begin{aligned} \text{HCN} + \nu \rightarrow \text{H} + \text{CN}(A^2\Pi_i) : & 1.26 \times 10^{-5} \text{ s}^{-1}, 3.13 \times 10^{-5} \text{ s}^{-1}, \\ \rightarrow \text{HCN}^+ + e^- : & 4.51 \times 10^{-7} \text{ s}^{-1}, 1.12 \times 10^{-6} \text{ s}^{-1}. \end{aligned}$$

The first value of each branch is for the quiet Sun (see Figures 83(a) and 84(a)), the second is for the active Sun (see Figures 83(b) and 84(b)). The dissociation rate coefficient for the quiet Sun agrees well with that obtained by Jackson (1976a, b) ($1.1 \times 10^{-5} \text{ s}^{-1}$) who used the same cross section data for $\lambda > 1050$ Å. The rate coefficient is completely dominated by the solar L α contribution.

Excess energies: For dissociation the excess energy is 3.82 eV for the quiet Sun (3.84 eV for the active Sun) and for ionization it is 11.2 eV for the quiet Sun and 13.9 eV for the active Sun.

Fig. 83a. $\text{HCN} + \nu \rightarrow \text{H} + \text{CN}(A^2\Pi_i)$, for the quiet Sun.Fig. 83b. $\text{HCN} + \nu \rightarrow \text{H} + \text{CN}(A^2\Pi_i)$, for the active Sun.

Fig. 84a. $\text{HCN} + \nu \rightarrow \text{HCN}^+ + e$, for the quiet Sun.Fig. 84b. $\text{HCN} + \nu \rightarrow \text{HCN}^+ + e$, for the active Sun.

HYDROPEROXYL, HO₂

Cross sections: Up to $\lambda = 1000 \text{ \AA}$ the sum of the cross sections of the atomic constituents were used as given by the fits from Barfield *et al.* (1972). Since no data are available between $\lambda = 1000$ and 1850 \AA , we used the cross section for H₂O₂; this cross section may be an overestimate. From $\lambda = 1900$ to 2500 \AA the cross section has been determined by Paukert and Johnston (1972), Hochanadel *et al.* (1972), and Cox and Burrows (1979). We used the average values from these determinations as given by DeMore *et al.* (1982).

Branching ratios: The branching ratios are not known. We assumed that only dissociation into O + OH occurs.

Thresholds: $\lambda = 4395 \text{ \AA}$ for dissociation into O and OH is obtained from thermodynamic data (Benson, 1976).

Rate coefficients:

$$\text{HO}_2 + v \rightarrow \text{O} + \text{OH}: 6.62 \times 10^{-3} \text{ s}^{-1}$$

for the quiet Sun (see Figure 85) and $6.67 \times 10^{-3} \text{ s}^{-1}$ for the active Sun.

Excess energies: The excess energy is 1.02 eV for the quiet Sun and 1.04 eV for the active Sun.

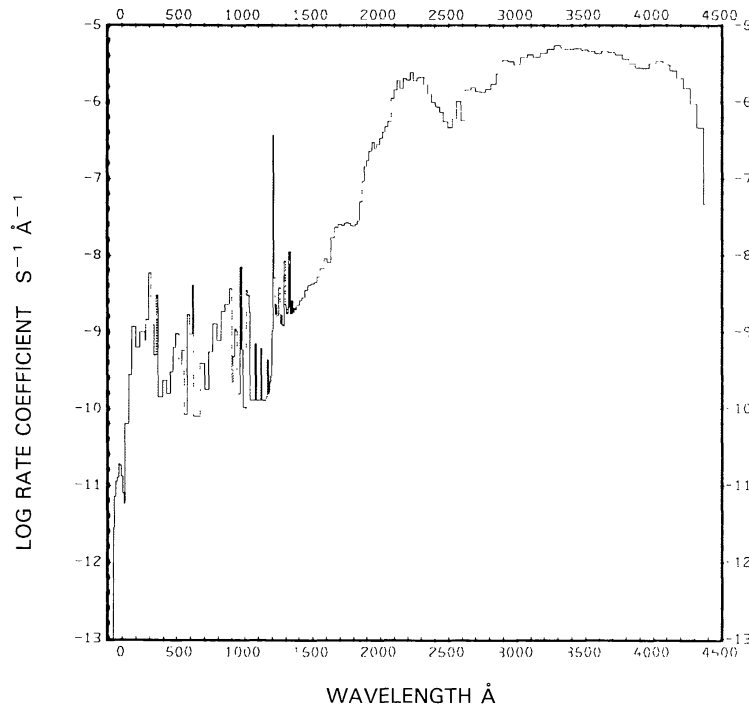


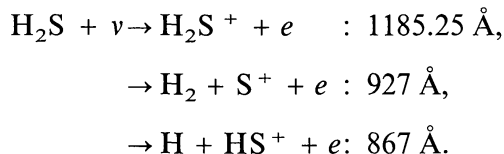
Fig. 85. $\text{HO}_2 + v \rightarrow \text{O} + \text{OH}$, for the quiet Sun.

HYDROGEN SULFIDE, H₂S

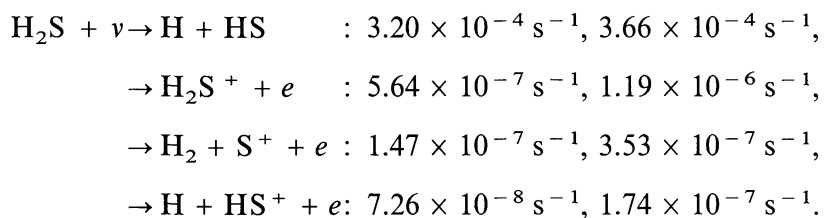
Cross sections: Up to $\lambda = 927 \text{ \AA}$ the cross section is synthesized from the cross sections of the constituent atoms as determined from fits by Barfield *et al.* (1972). From $\lambda = 1060$ to 2100 \AA the cross section was measured by Watanabe and Jursa (1964) and in the range $\lambda = 1850$ to 2700 \AA it was measured by Goodeve and Stein (1931). We used the latter data at wavelengths larger than 2100 \AA . The cross section of Lee *et al.* (1987) between 490 and 2900 \AA are very similar to the above values.

Branching ratios: The branching ratio between dissociation and the combined ionization processes comes from the data of Watanabe and Jursa (1964), while the branching ratios between ionization and the two dissociative ionization branches come from the measurements of Prest *et al.* (1983).

Thresholds: $\lambda = 3170 \text{ \AA}$ for dissociation into H and SH is given by Okabe (1978) as obtained from thermodynamic data. The thresholds for ionization and dissociative ionizations, as given by Prest *et al.* (1983), are:

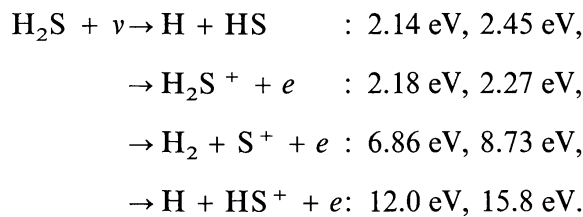


Rate coefficients:



The first of each value is for the quiet Sun (see Figures 86 and 87(a) to 89(a)), the second is for the active Sun (see Figures 87(b) to 89(b)). The rate coefficients are sensitive to the cross section in the region of the L α flux and the wavelength region from 1900 to 2400 \AA .

Excess energies:



The first of each value is for the quiet Sun, the second is for the active Sun.

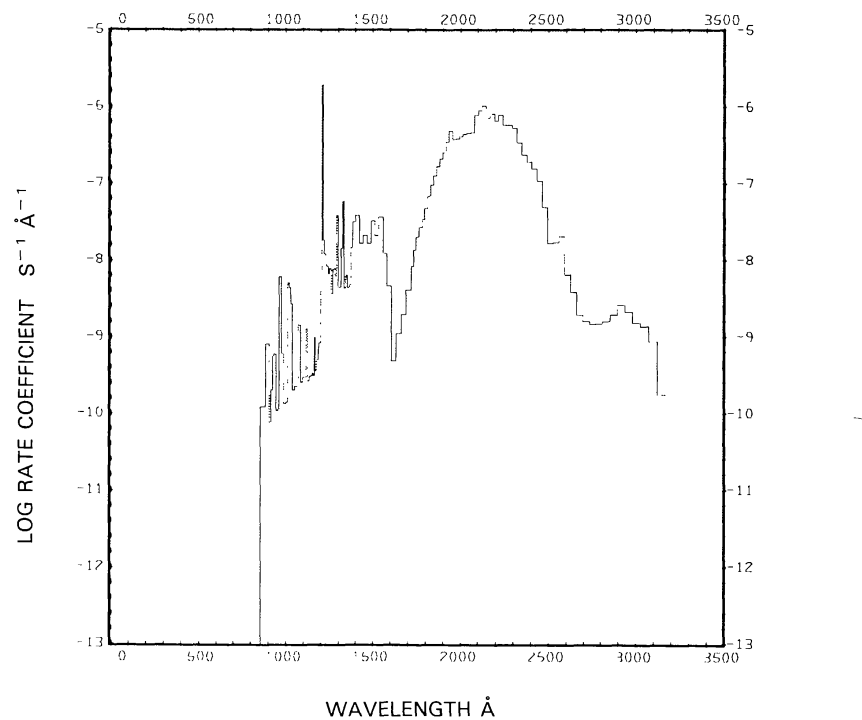


Fig. 86. $\text{H}_2\text{S} + \nu \rightarrow \text{H} + \text{HS}$, for the quiet Sun.

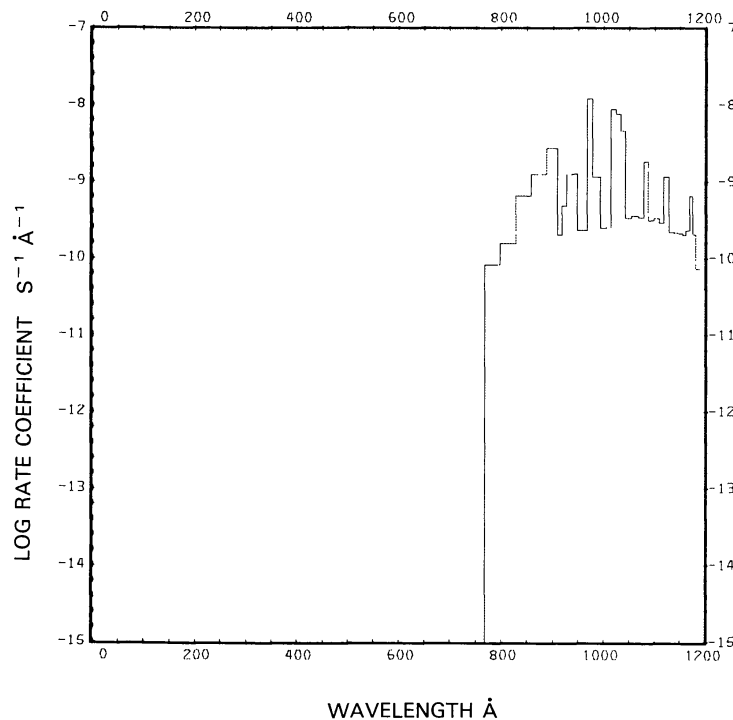


Fig. 87a. H₂S + ν → H₂S⁺ + e⁻, for the quiet Sun.

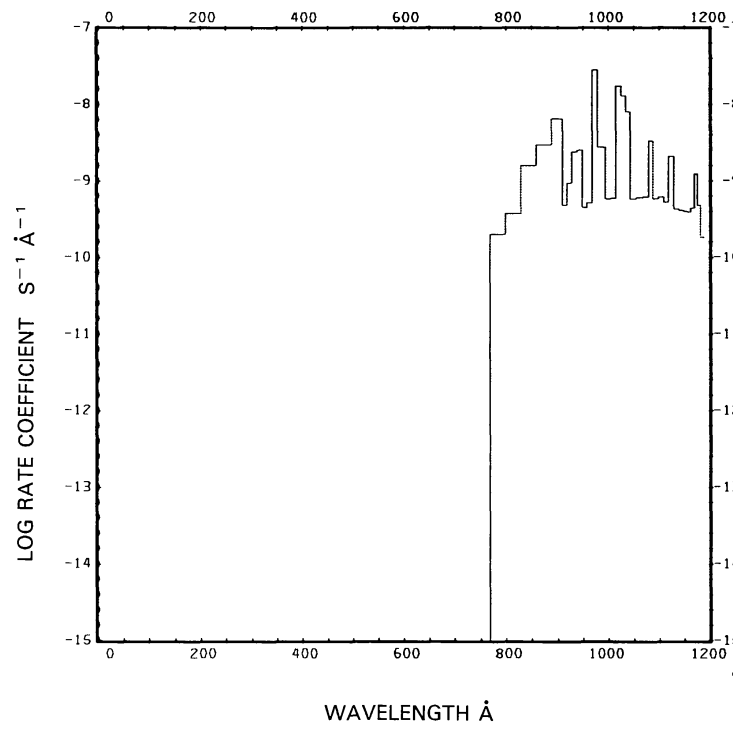
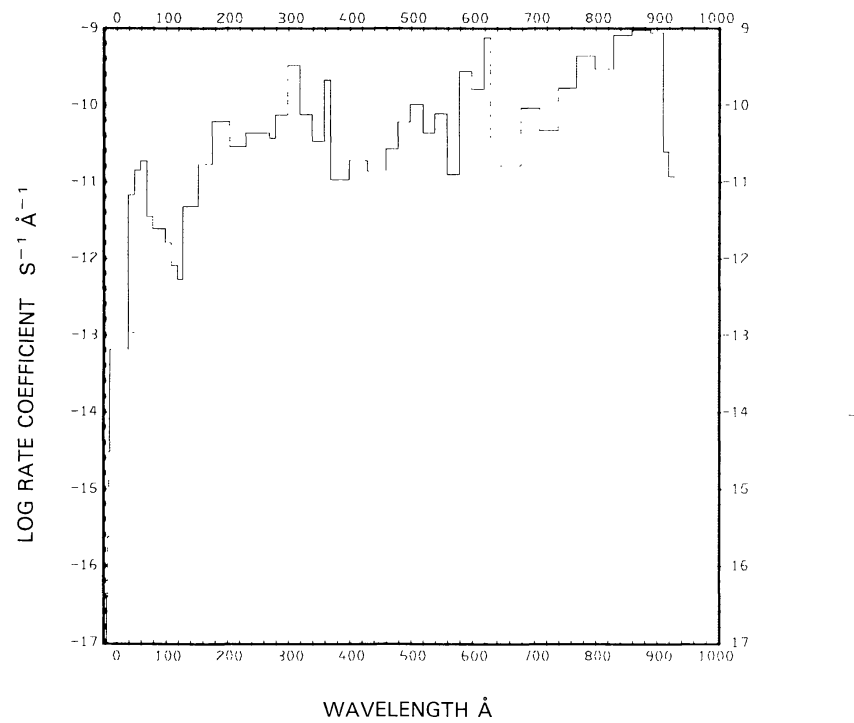
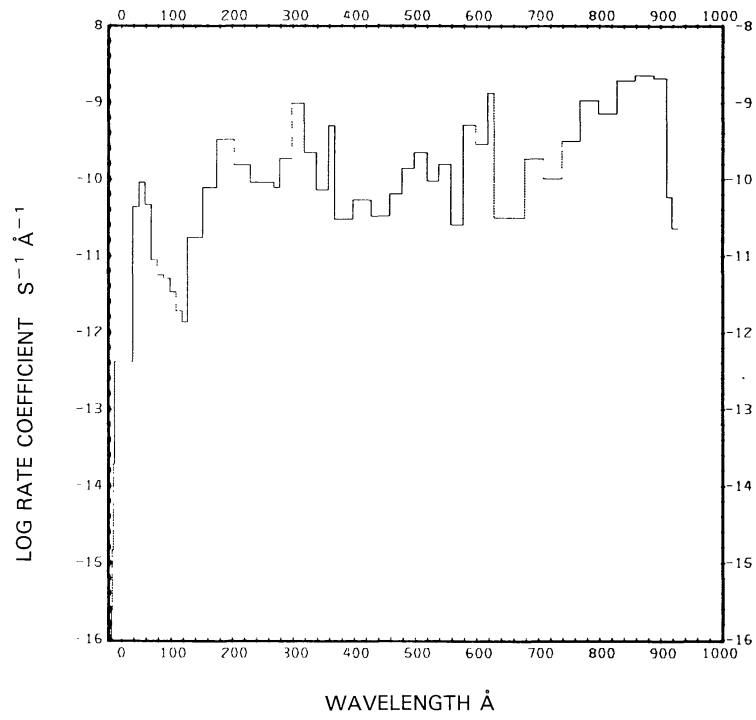


Fig. 87b. H₂S + ν → H₂S⁺ + e⁻, for the active Sun.

Fig. 88a. H₂S + ν → H₂ + S⁺ + e⁻, for the quiet Sun.Fig. 88b. H₂S + ν → H₂ + S⁺ + e⁻, for the active Sun.

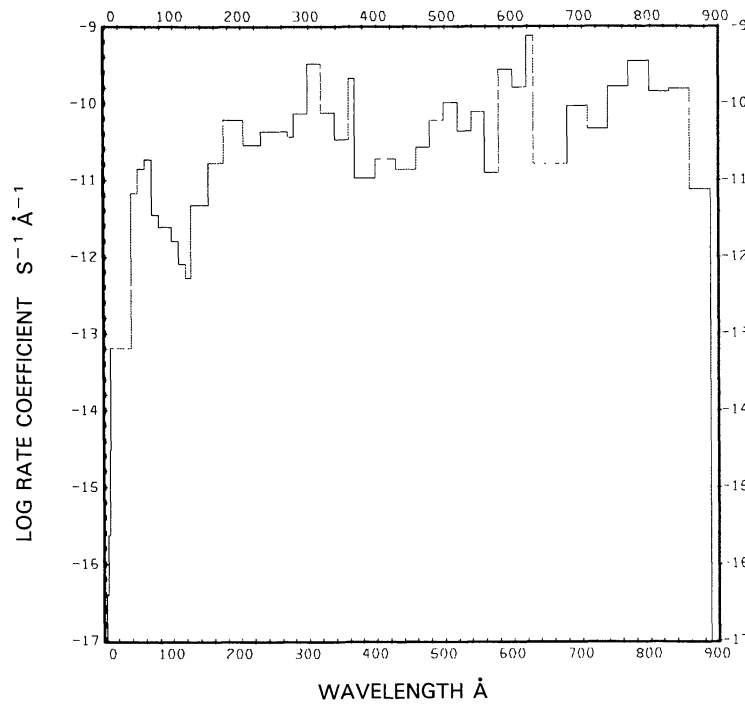


Fig. 89a. H₂S + $\nu \rightarrow$ H + HS⁺ + e, for the quiet Sun.

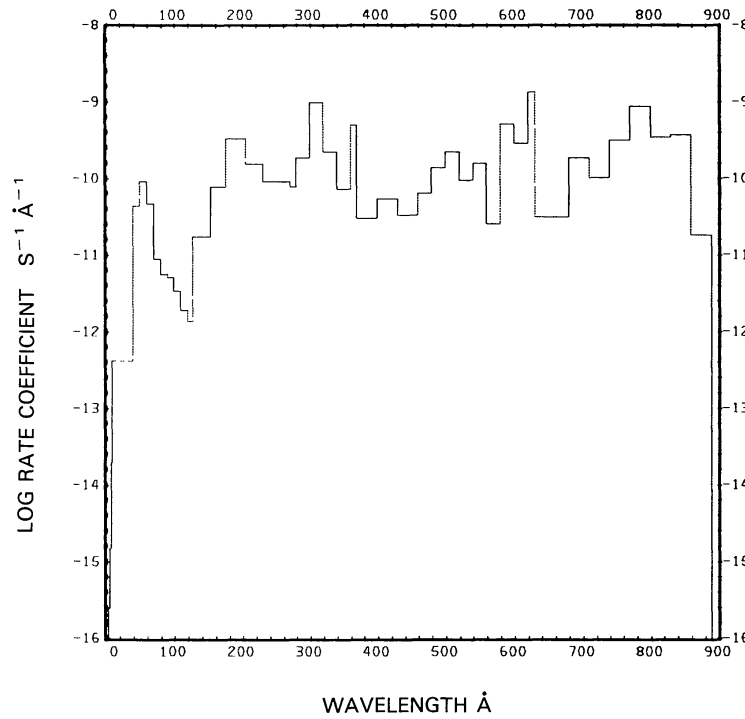


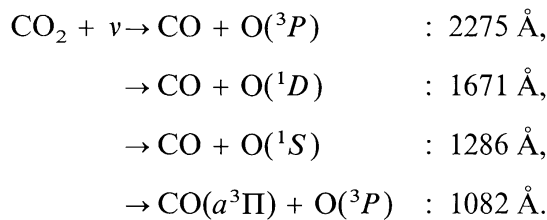
Fig. 89b. H₂S + $\nu \rightarrow$ H + HS⁺ + e, for the active Sun.

CARBON DIOXIDE, CO₂

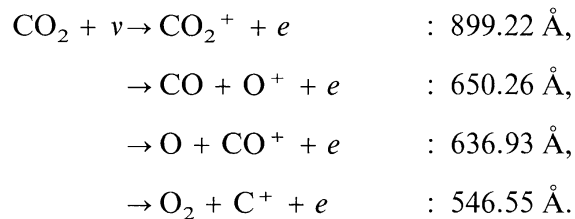
Cross sections: Up to $\lambda = 270 \text{ \AA}$ the cross section compiled by Henry and McElroy (1968) was used. Between $\lambda = 303.7$ and 555.26 \AA the cross section comes from the measurements made by Cairns and Samson (1965). The range from $\lambda = 580$ to 1670 \AA is covered by the data from Nakata *et al.* (1965). From $\lambda = 1670$ to 1990 \AA the compiled cross section from Huffman (1971) was used.

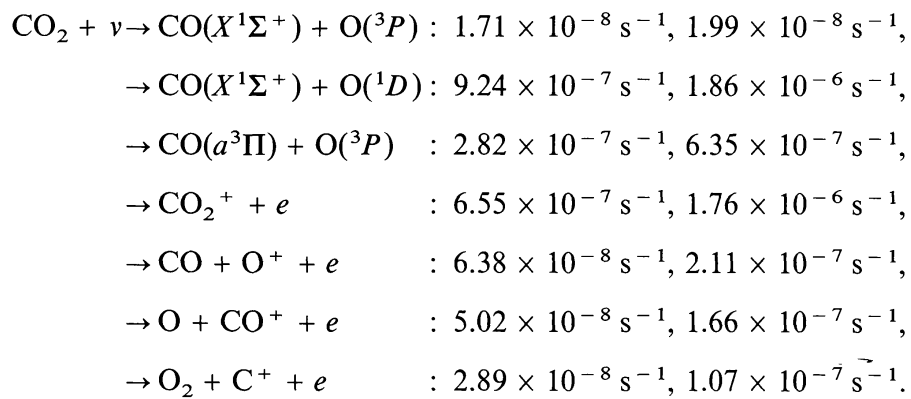
Branching ratios: The branching ratio for all ionization processes versus all dissociation processes was obtained from the data of Nakata *et al.* (1965). The dissociation branching ratio for production of CO in the $X^1\Sigma^+$ or in the $a^3\Pi$ states from $\lambda = 851$ to 1090 \AA was determined from the data of Lawrence (1972). The structural features of this data are in excellent agreement with the total absorption coefficients of Nakata *et al.* (1965). Ionization and dissociative ionization branching ratios are given by Kronebusch and Berkowitz (1976).

Thresholds: Some important threshold values for dissociation are given by Okabe (1978):

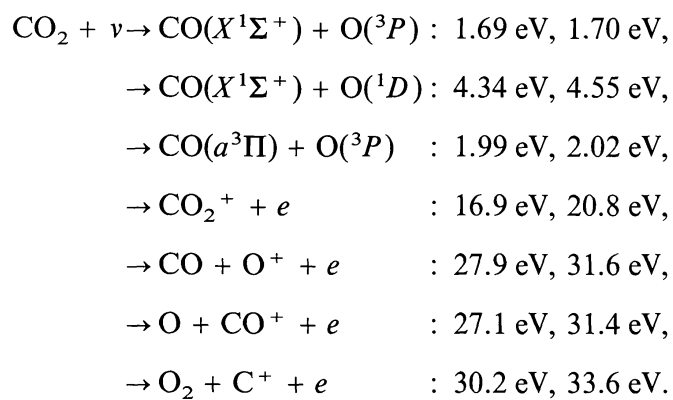


Here CO without further notation stands for the ground state. Since the first of these dissociations is spin forbidden, the total dissociation cross section between $\lambda = 1650$ and 2275 \AA is very small. Thresholds for ionization are given by Kronebusch and Berkowitz (1976):



Rate coefficients:

The first of each value is for the quiet Sun (see Figures 90 and 91(a) to 96(a)), the second is for the active Sun (see Figures 91(b) to 96(b)). For the quiet Sun our value for the sum of the first two dissociation processes is a factor of ten larger than the equivalent value quoted by Baurer and Bortner (1978) ($9.4 \times 10^{-8} \text{ s}^{-1}$). For the first process alone they obtain $1.1 \times 10^{-8} \text{ s}^{-1}$, about 35% less than our value. McElroy and Hunten (1970) obtain $2.8 \times 10^{-8} \text{ s}^{-1}$ for the first process and $1.5 \times 10^{-6} \text{ s}^{-1}$ for the second process (after scaling their values to 1 AU heliocentric distance); higher than our values by more than 50% and 60%, respectively. Their rate for the O(³P) branch appears to come from the small cross section ($\sim 10^{-20} \text{ cm}^2$) between $\lambda = 1650$ and 1990 \AA and not from the branch yielding CO(^a Π) + O(³P). Our rate coefficient for all ionization processes is $8.0 \times 10^{-7} \text{ s}^{-1}$. This is half way between the rate coefficients given by Siscoe and Mukherjee (1972) who obtain $1.038 \times 10^{-6} \text{ s}^{-1}$, and McElroy *et al.* (1976) who obtain $5.6 \times 10^{-7} \text{ s}^{-1}$ (after scaling to 1 AU heliocentric distance).

Excess energies:

The first of each value is for the quiet Sun, the second is for the active Sun.

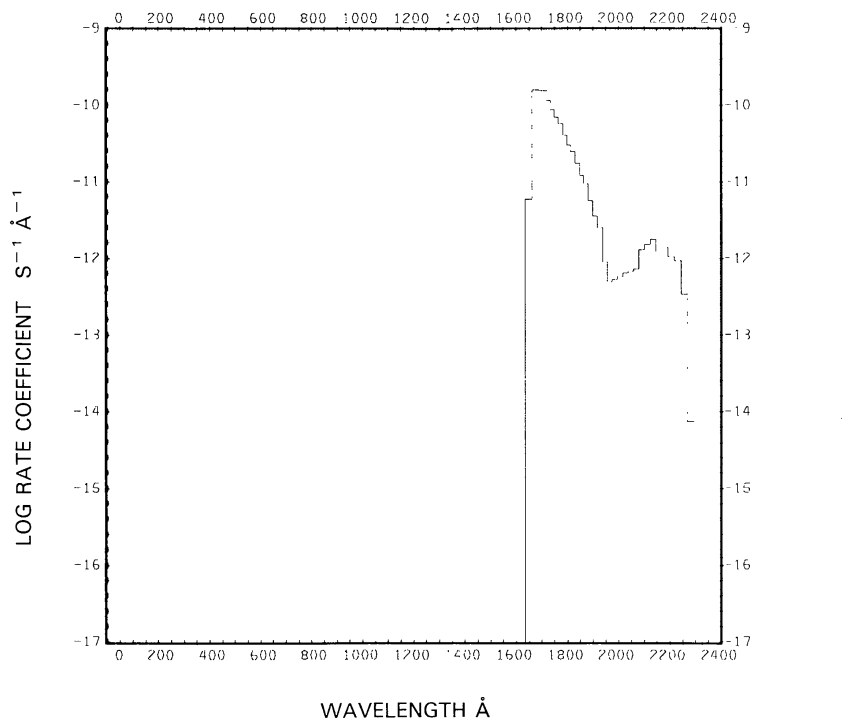


Fig. 90. $\text{CO}_2 + \nu \rightarrow \text{CO}(X^1\Sigma^+) + \text{O}({}^3P)$, for the quiet Sun.

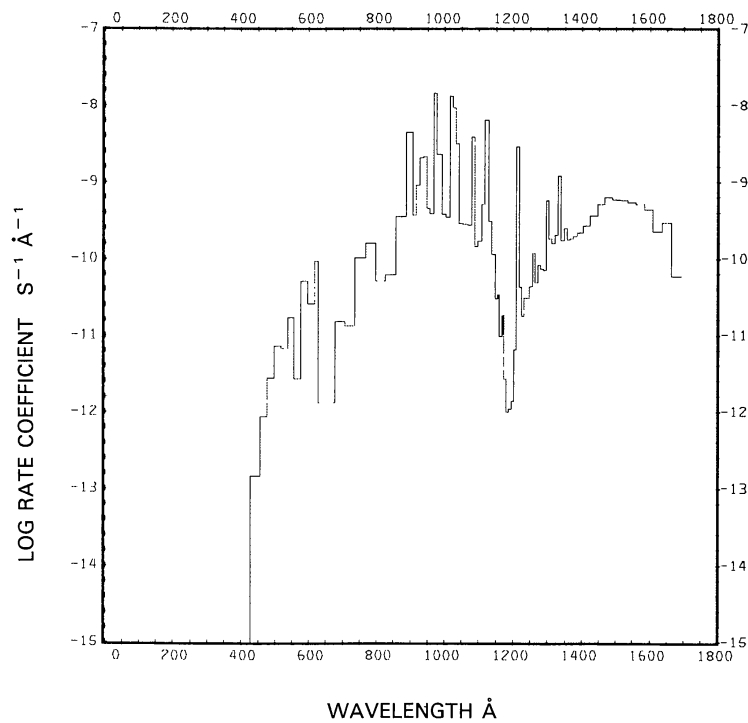


Fig. 91a. $\text{CO}_2 + \nu \rightarrow \text{CO}(X^1\Sigma^+) + \text{O}({}^1D)$, for the quiet Sun.

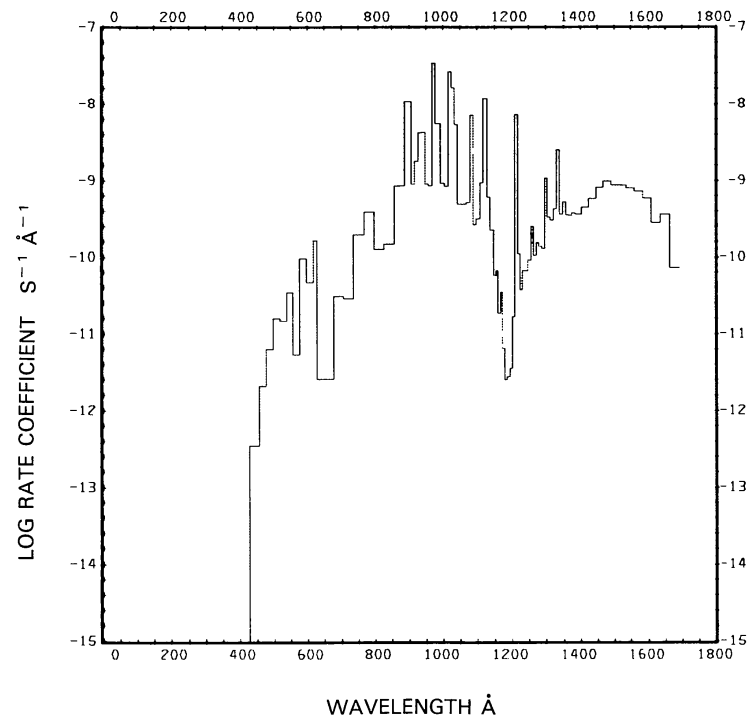
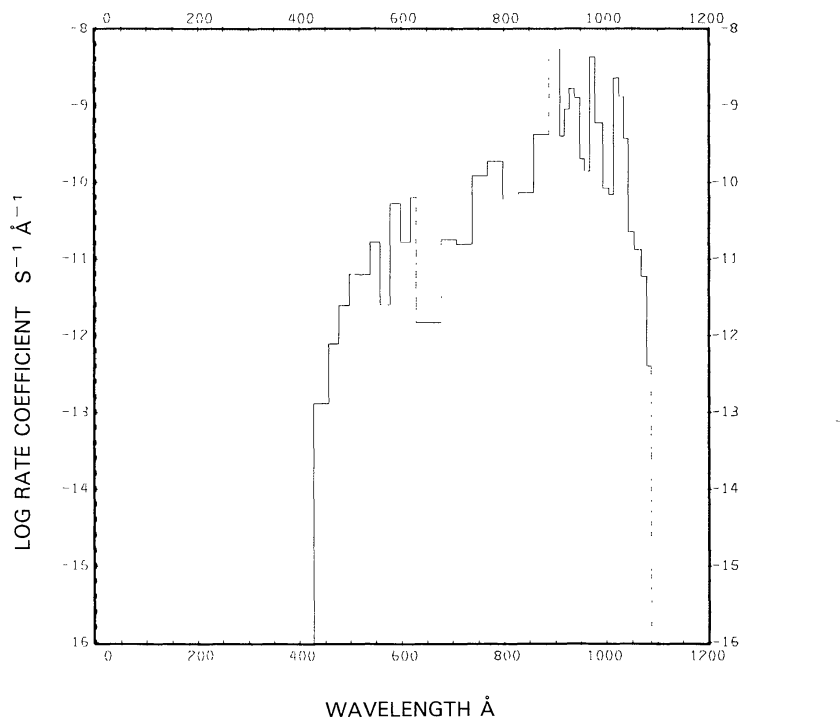
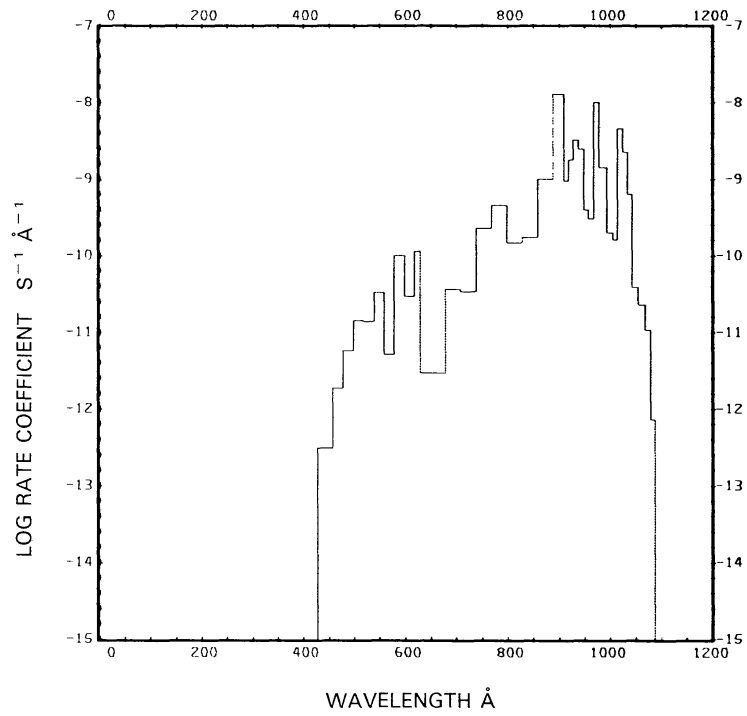
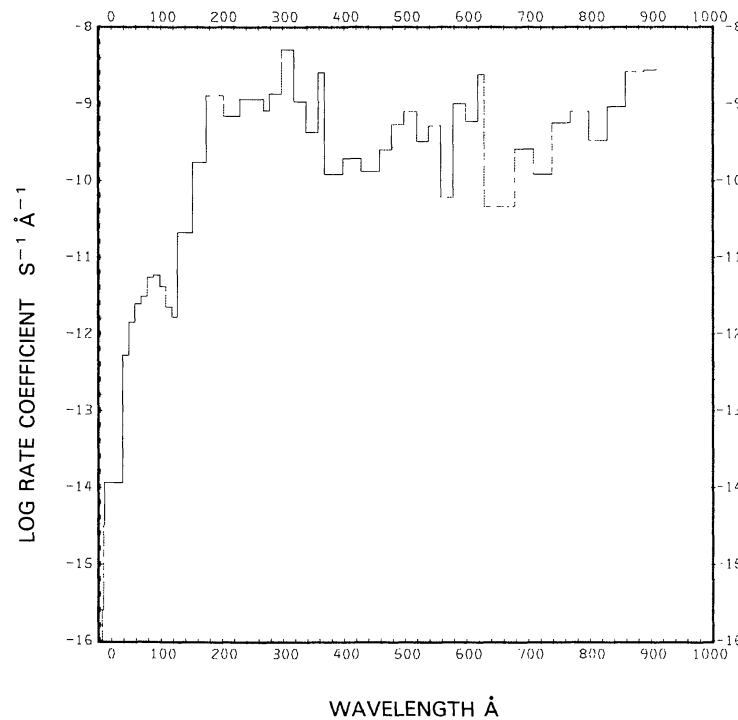
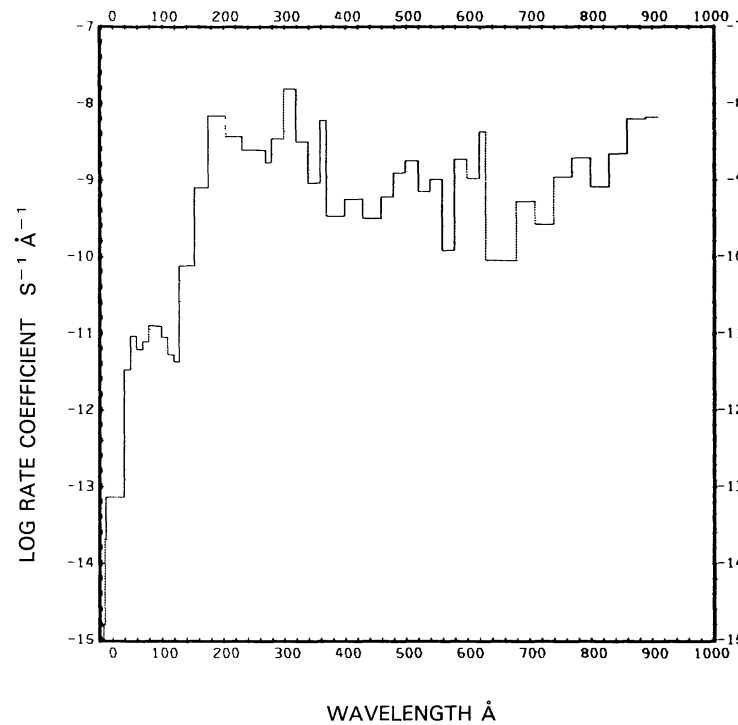
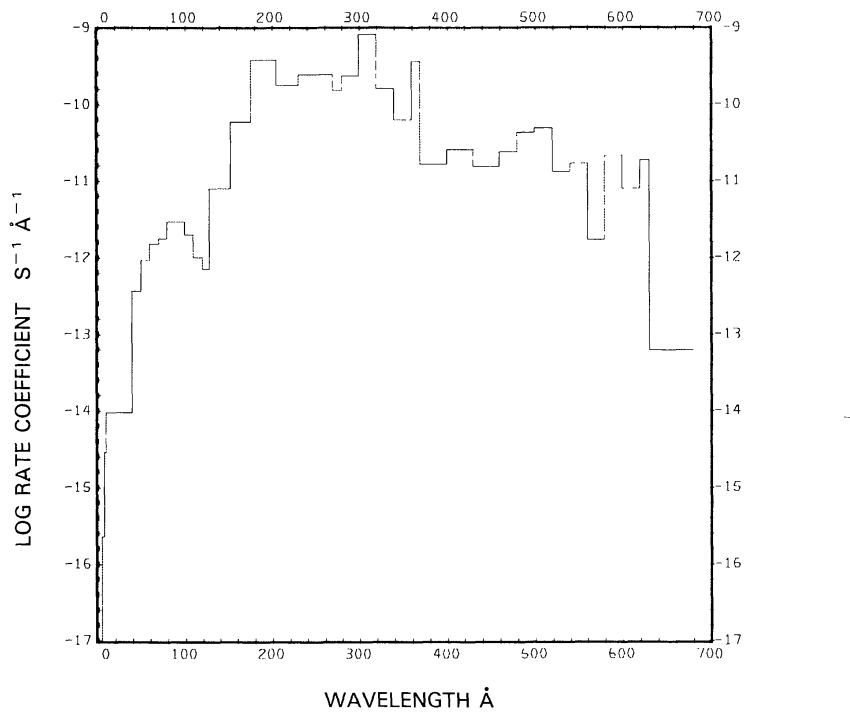
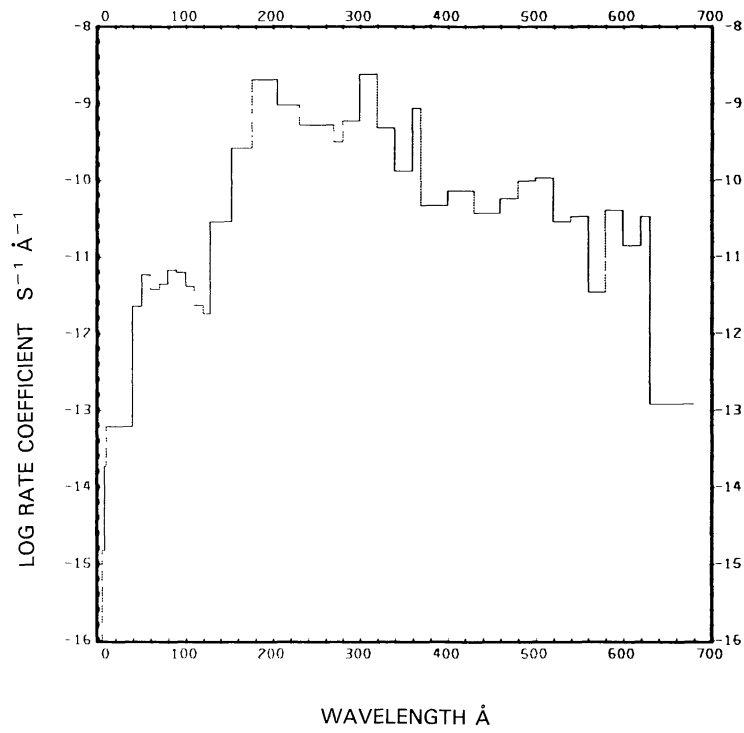


Fig. 91b. $\text{CO}_2 + \nu \rightarrow \text{CO}(X^1\Sigma^+) + \text{O}({}^1D)$, for the active Sun.

Fig. 92a. $\text{CO}_2 + \nu \rightarrow \text{CO}(\alpha^3\Pi) + \text{O}({}^3P)$, for the quiet Sun.Fig. 92b. $\text{CO}_2 + \nu \rightarrow \text{CO}(\alpha^3\Pi) + \text{O}({}^3P)$, for the active Sun.

Fig. 93a. CO₂ + $\nu \rightarrow$ CO₂⁺ + e^- , for the quiet Sun.Fig. 93b. CO₂ + $\nu \rightarrow$ CO₂⁺ + e^- , for the active Sun.

Fig. 94a. CO₂ + ν → CO + O⁺ + e⁻, for the quiet Sun.Fig. 94b. CO₂ + ν → CO + O⁺ + e⁻, for the active Sun.

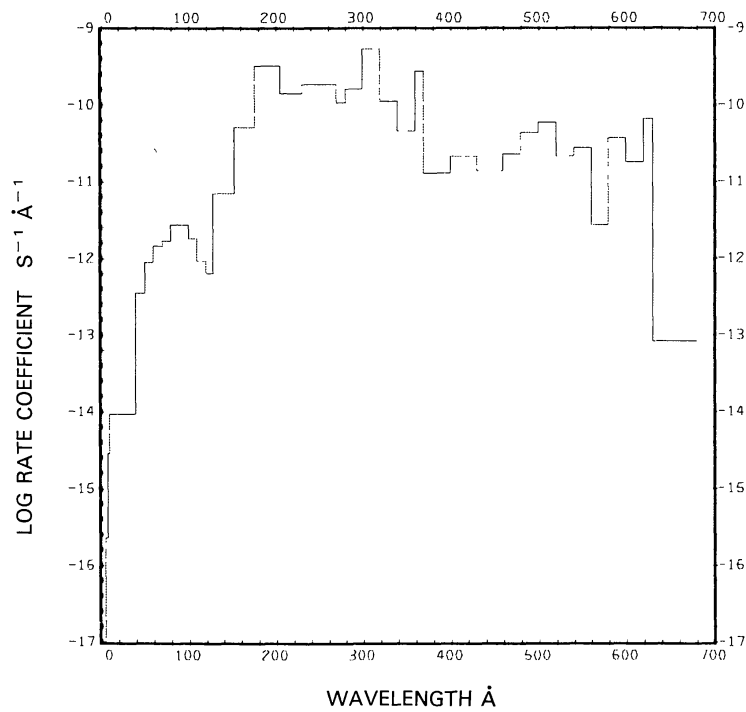


Fig. 95a. $\text{CO}_2 + \nu \rightarrow \text{O} + \text{CO}^+ + e^-$, for the quiet Sun.

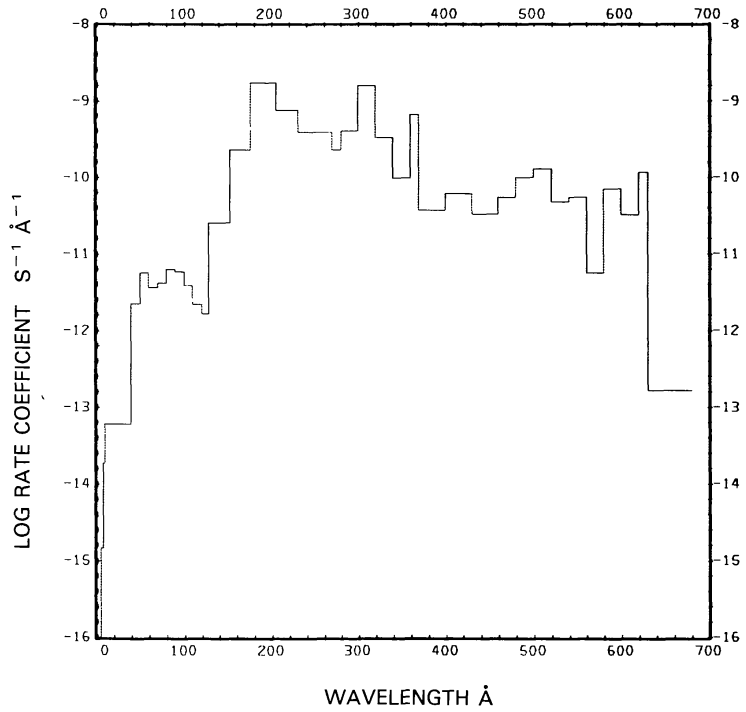
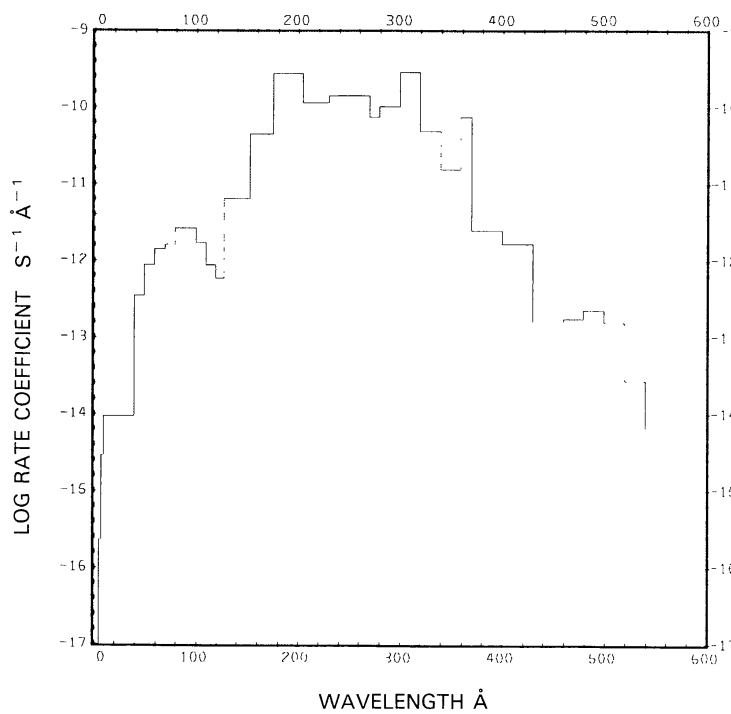
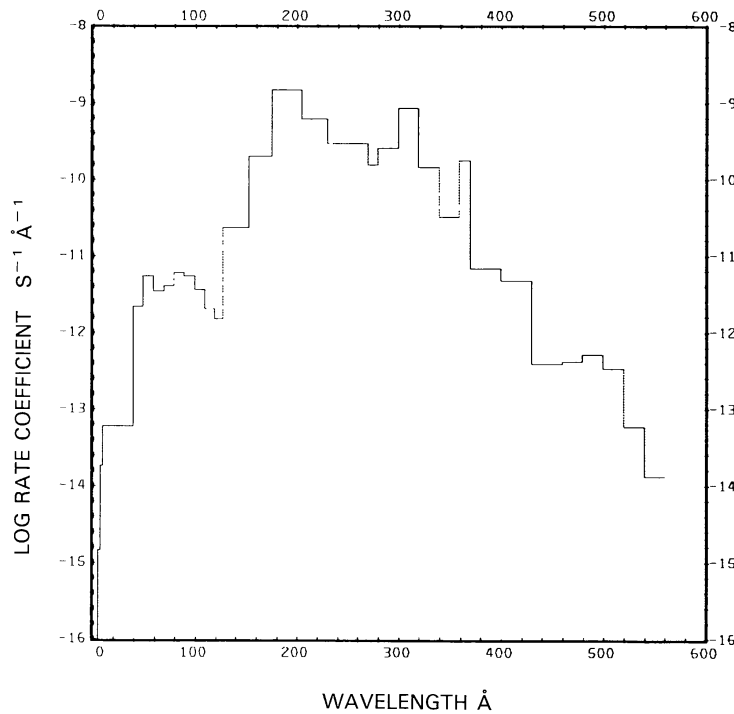


Fig. 95b. $\text{CO}_2 + \nu \rightarrow \text{O} + \text{CO}^+ + e^-$, for the active Sun.

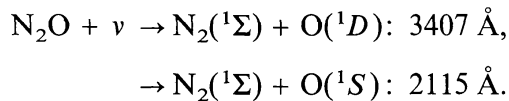
Fig. 96a. $\text{CO}_2 + \nu \rightarrow \text{O}_2 + \text{C}^+ + e$, for the quiet Sun.Fig. 96b. $\text{CO}_2 + \nu \rightarrow \text{O}_2 + \text{C}^+ + e$, for the active Sun.

NITROUS OXIDE, N₂O

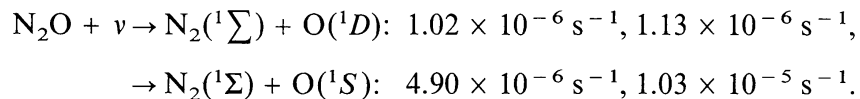
Cross sections: Up to $\lambda = 625 \text{ \AA}$ the cross section is synthesized from the cross sections of the atomic constituents as presented by fits from Barfield *et al.* (1972). From $\lambda = 1080$ to 1700 \AA the cross section was measured by Zelikoff *et al.* (1953). Between $\lambda = 1730$ and 2400 \AA the cross section was determined by Selwyn *et al.* (1977), while Johnston and Selwyn (1975) have determined the cross section in an overlap region between $\lambda = 2100$ and 2500 \AA .

Branching ratios: There are two branches for the dissociation of N₂O that are significant, but the branching ratio for them is only an estimate (Okabe, 1978).

Thresholds: Threshold wavelengths for the two most important branches are given by Okabe (1978) as

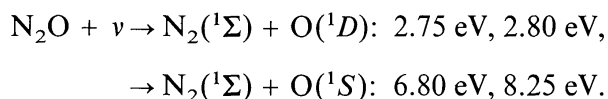


Rate coefficients:



The first of each value is for the quiet Sun (see Figures 97 and 98(a)), the second is for the active Sun (see Figure (98)).

Excess energies:



The first of each value is for the quiet Sun, the second is for the active Sun.

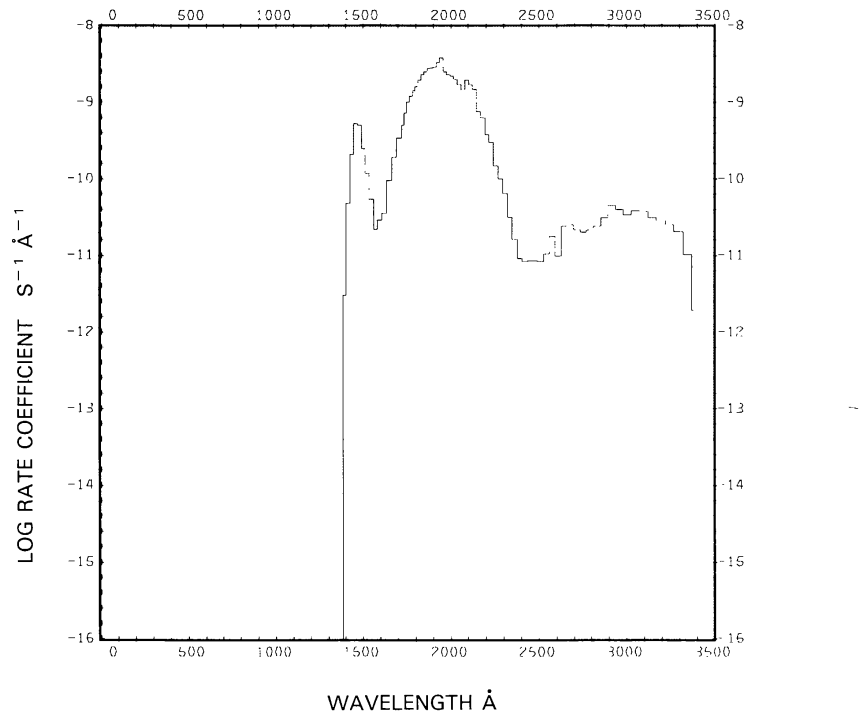


Fig. 97. $\text{N}_2\text{O} + v \rightarrow \text{N}_2(^1\Sigma) + \text{O}(^1D)$, for the quiet Sun.

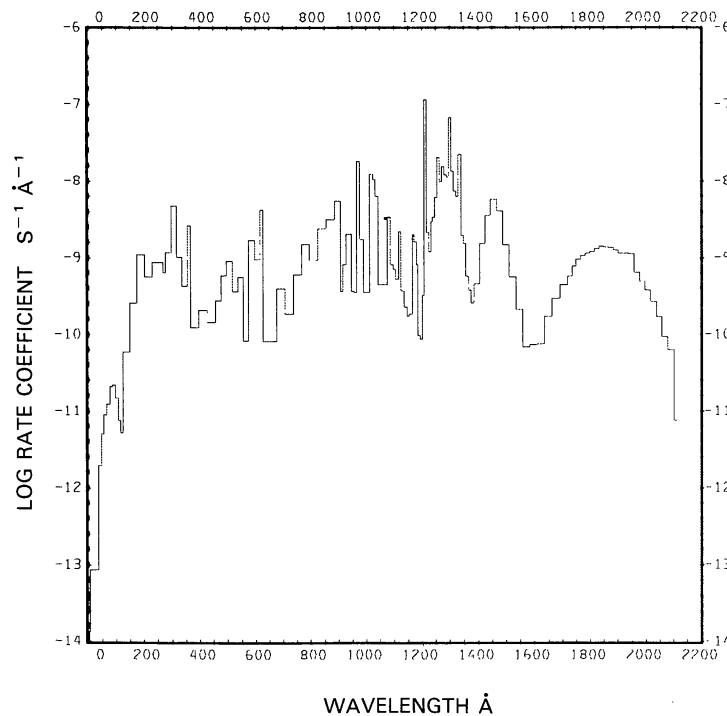


Fig. 98a. N₂O + $\nu \rightarrow$ N₂(¹ Σ) + O(¹S), for the quiet Sun.

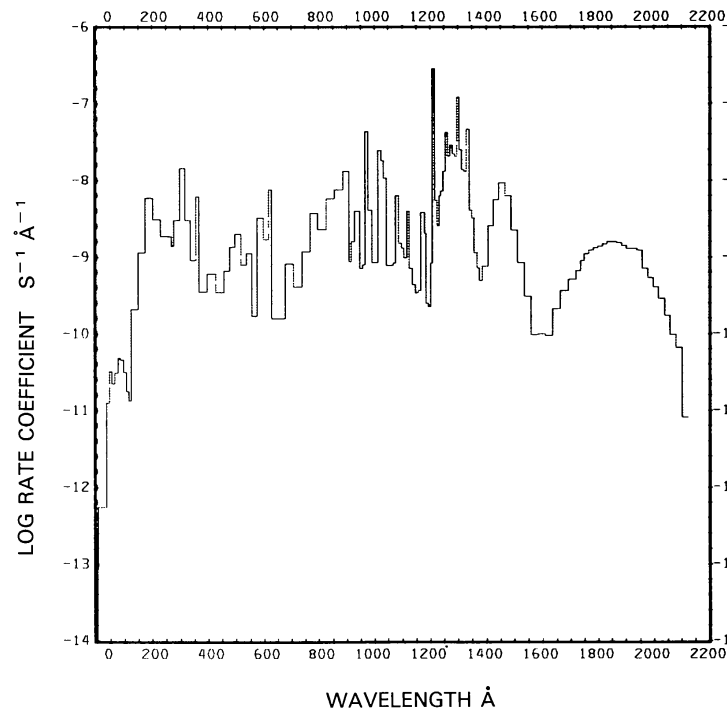


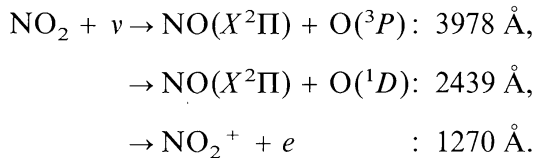
Fig. 98b. N₂O + $\nu \rightarrow$ N₂(¹ Σ) + O(¹S), for the active Sun.

NITROGEN DIOXIDE, NO₂

Cross sections: Up to $\lambda = 940 \text{ \AA}$ the cross section is synthesized from the fits to the cross sections for the constituent elements made by Barfield *et al.* (1972). From $\lambda = 1080$ to 1800 \AA the cross section measured by Nakayama *et al.* (1959) was used. From $\lambda = 1850 \text{ \AA}$ to threshold we used the data compiled by DeMore *et al.* (1982), but we have supplemented it with the data from Hall and Blacet (1952) and Bass *et al.* (1976).

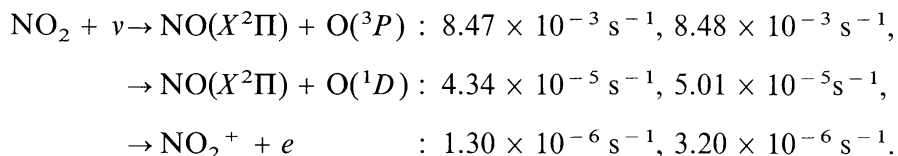
Branching ratios: The branching ratio between dissociation and ionization was taken from the cross section data of Nakayama *et al.* (1959). The branching ratio between formation of O(³P) and O(¹D) is based on the data of Jones and Bayes (1973) and Harker *et al.* (1977).

Thresholds:



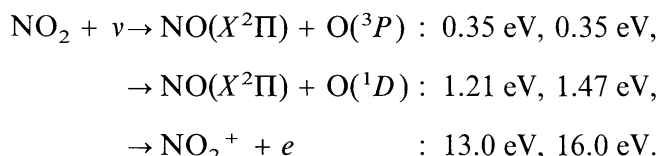
The dissociation thresholds are given by Okabe (1978) and the ionization threshold is given by Nakayama *et al.* (1959).

Rate coefficients:

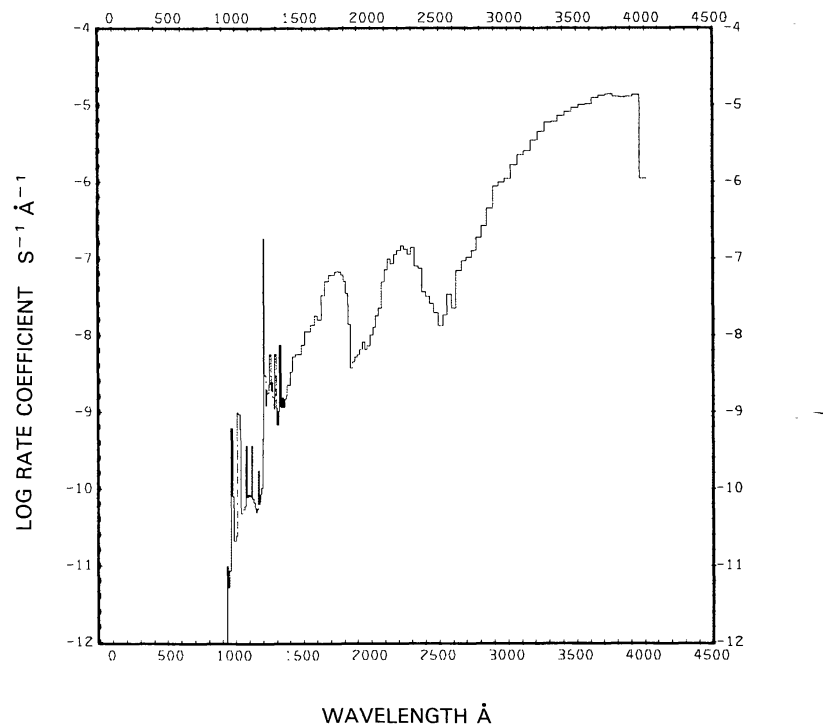
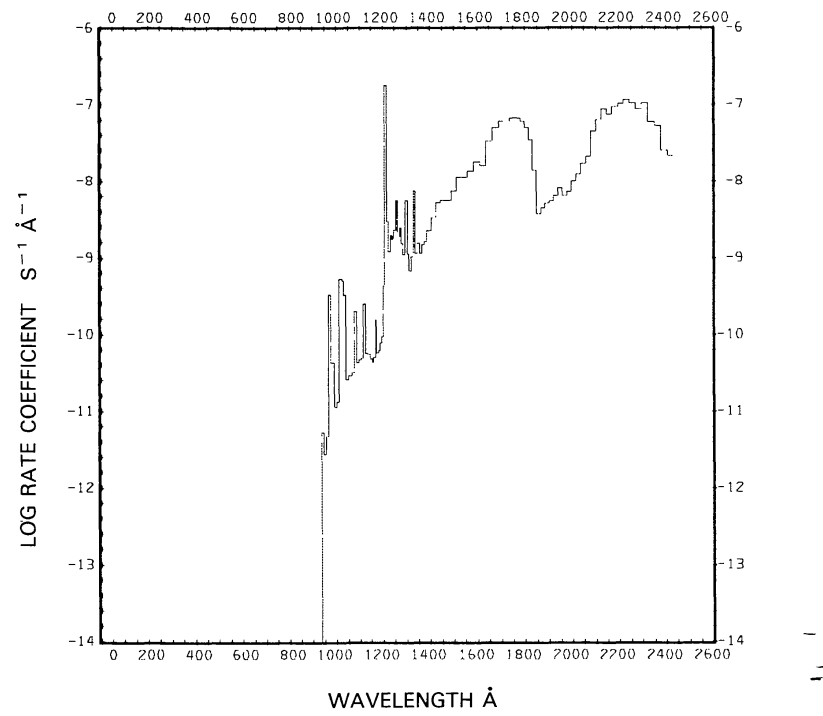


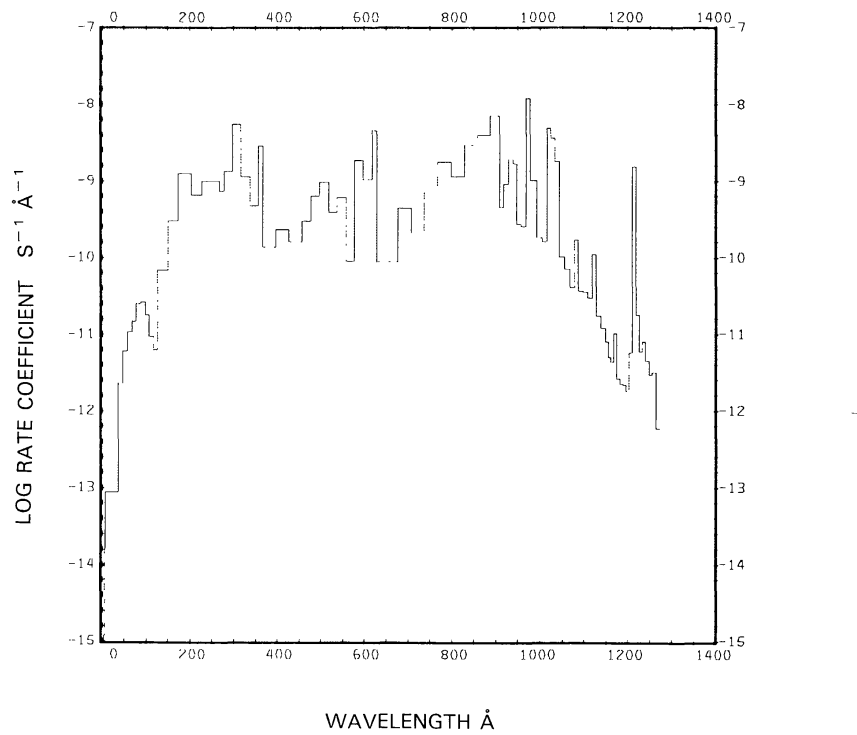
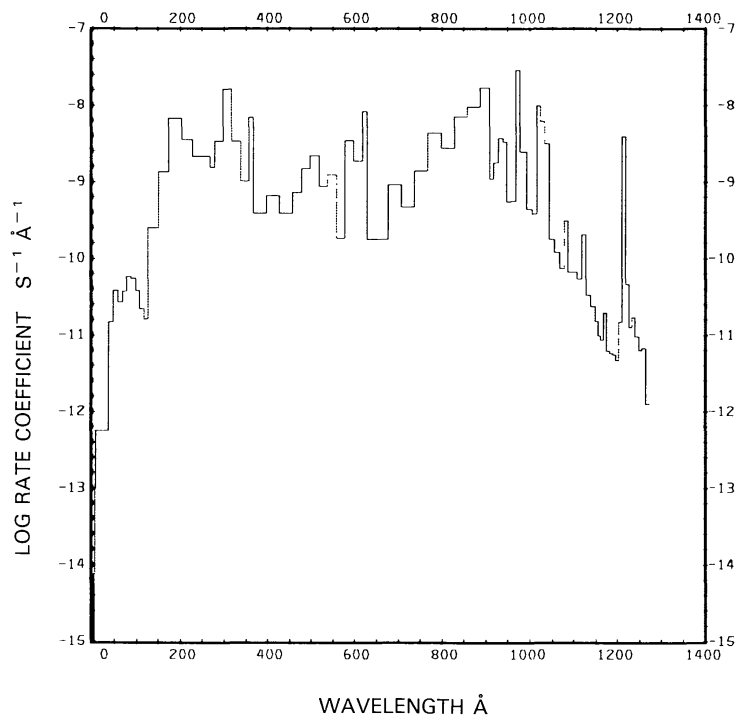
The first of each entry corresponds to the quiet Sun (see Figures 99 to 100 and 101(a)), the second to the active Sun (see Figure 101(b)). Our rate coefficient for the quiet Sun for the first process compares well with that calculated by Stedman *et al.* (1975) who get about 8.4 or $8.5 \times 10^{-3} \text{ s}^{-1}$.

Excess energies:



The first of each value is for the quiet Sun, the second is for the active Sun.

Fig. 99. NO₂ + ν → NO($X^2\Pi$) + O(3P), for the quiet Sun.Fig. 100. NO₂ + ν → NO($X^2\Pi$) + O(1D), for the quiet Sun.

Fig. 101a. $\text{NO}_2 + \nu \rightarrow \text{NO}_2^+ + e$, for the quiet Sun.Fig. 101b. $\text{NO}_2 + \nu \rightarrow \text{NO}_2^+ + e$, for the active Sun.

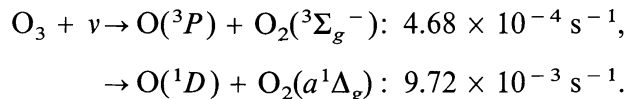
OZONE, O₃

Cross sections: Up to 742 Å the cross section is synthesized from three times the atomic cross section of oxygen as presented by fits from Barfield *et al.* (1972). From 1060 to 1360 Å the cross section was measured by Tanaka *et al.* (1953). Between 1360 and 2000 Å we used the value compiled by Ackerman (1971). From 2000 to 2900 Å and from 3310 to 8500 Å we used the values measured by Griggs (1968). In the region from 2975 to 3300 Å we used the measurements of Moortgat and Warneck (1975).

Branching ratios: The ratio leading to the O(³P) and O(¹D) branches was measured by Moortgat and Warneck (1975).

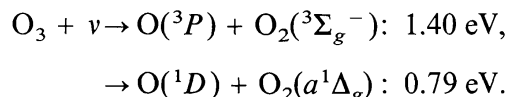
Thresholds: The threshold leading to O(³P) and O₂(³Σ_g⁻) is at 11 790 Å from heats of formation, in good agreement with values quoted by Okabe (1978) and Baulch *et al.* (1982). The threshold leading to O(¹D) and O₂(^a1Δ_g) is assumed to be at 3195 Å based on the branching ratios measured by Moortgat and Warneck (1975). This is at a longer wavelength than given by Okabe (1972) and Baulch *et al.* (1982) who quote 3100 Å.

Rate coefficients:



See Figures 102 and 103. Only the second branch is slightly influenced by the activity of the Sun. Its value for the active Sun is $9.94 \times 10^{-3} \text{ s}^{-1}$.

Excess energies:



Only the second branch changes for the active Sun; its value becomes 0.81 eV.

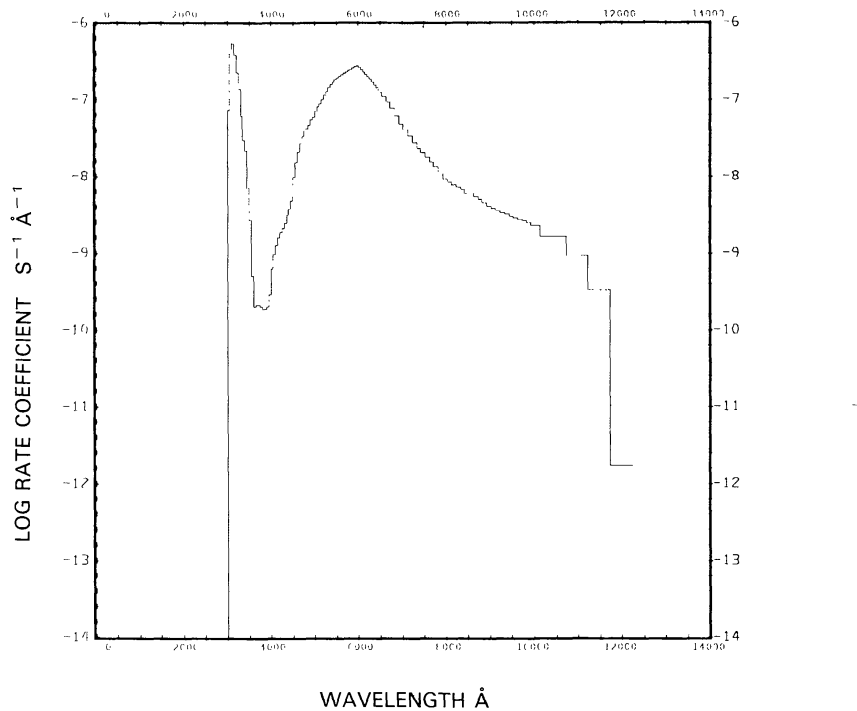


Fig. 102. $O_3 + \nu \rightarrow O(^3P) + O_2(^3\Sigma_g^-)$, for the quiet Sun.

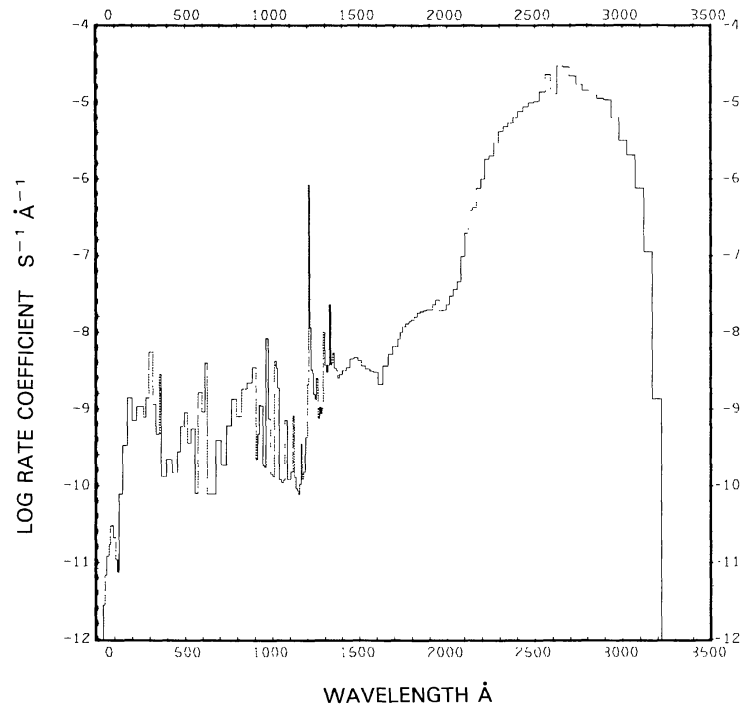


Fig. 103. $O_3 + \nu \rightarrow O(^1D) + O_2(a^1\Delta_g)$, for the quiet Sun.

HYDROGEN OXYCHLORIDE, HOCl

Cross sections: Up to 780 Å the cross section is synthesized from the cross sections of the atomic constituents as obtained from fits by Barfield *et al.* (1972). Between 2000 and 4200 Å we used the measurements from Knauth *et al.* (1979). No data are available between 780 and 2000 Å. To fill this gap we used the data from HCl in this region; the fit is quite smooth at both end points without further adjustment.

Branching ratios: No branching ratios are available. We assumed that only dissociation into OH + Cl takes place.

Thresholds: The threshold wavelength leading to dissociation into OH and Cl is at $\lambda = 5130$ Å as obtained from heats of formation (Benson, 1976). This is in good agreement with the value quoted by Baulch *et al.* (1982) (5200 Å).

Rate coefficients:

$$\text{HOCl} + \nu \rightarrow \text{OH} + \text{Cl}: 5.58 \times 10^{-4} \text{ s}^{-1}$$

for the quiet Sun (see Figure 104), for the active Sun it is $5.67 \times 10^{-4} \text{ s}^{-1}$.

Excess energies: The excess energy for the quiet Sun is 1.71 eV, for the active Sun it is 1.79 eV.

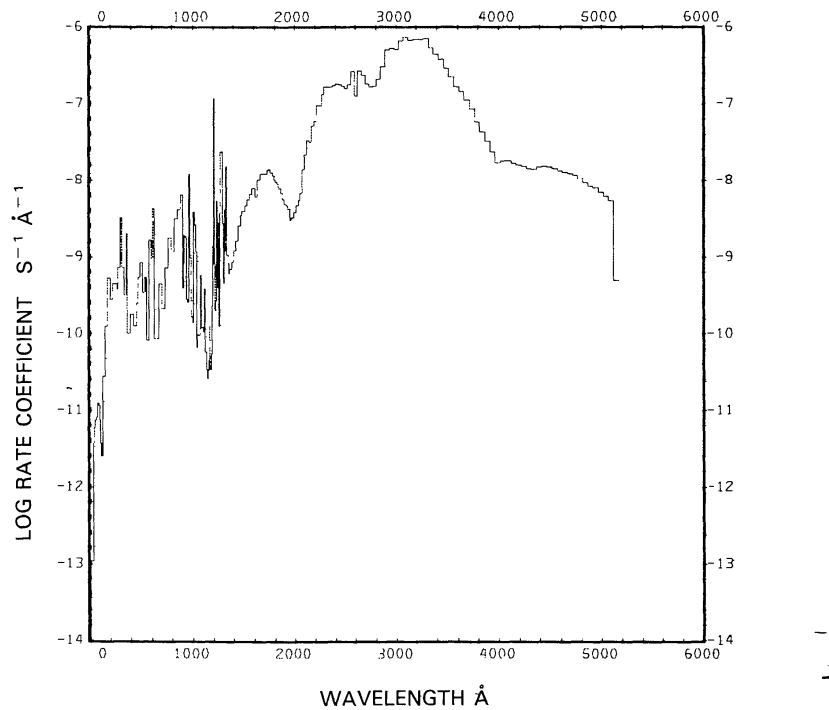


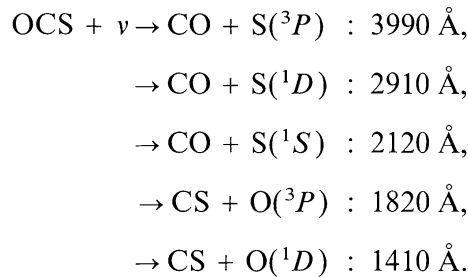
Fig. 104. $\text{HOCl} + \nu \rightarrow \text{OH} + \text{Cl}$, for the quiet Sun.

CARBON OXYSULFIDE, OCS

Cross sections: Up to 122 Å the cross section is synthesized from the cross sections of the atomic constituents as obtained from fits by Barfield *et al.* (1972). From 248 to 954 Å the cross sections were measured by Carnovale *et al.* (1982). Between 1060 and 1240 Å the measurements of Lee and Chiang (1982) were used. In the wavelength range $\lambda = 1240$ to 1700 Å the cross sections were measured by Matsunaga and Watanabe (1967b). From $\lambda = 1850$ to 3000 Å cross section values for $T = 225$ K from Molina *et al.* (1981) have been used. At longer wavelengths the cross section is too small to be measured.

Branching ratios: In the wavelength region $\lambda = 248$ to 954 Å branching ratios for the various ionization and dissociative ionization processes are obtained from Carnovale *et al.* (1982). The branching ratios for dissociation are given by Black *et al.* (1975) and Okabe (1978).

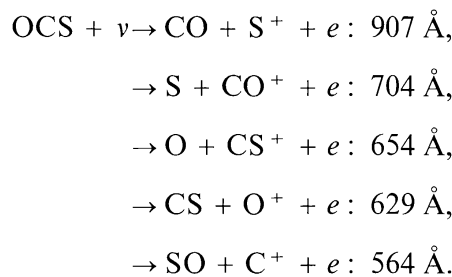
Thresholds: Thresholds for dissociation are given by Black *et al.* (1975):

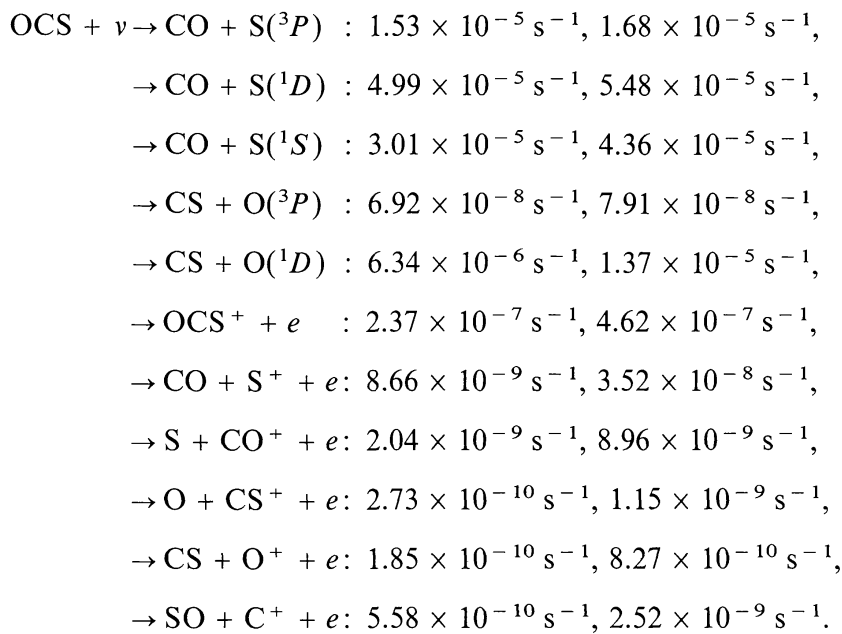


Thresholds for ionization and dissociative ionizations were calculated from the average of the values quoted by Carnovale *et al.* (1982):

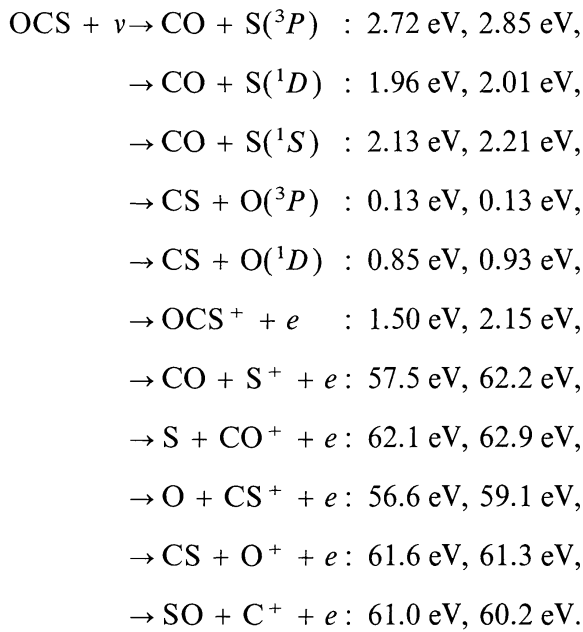


which agrees with the value found by Matsunaga and Watanabe (1967b),

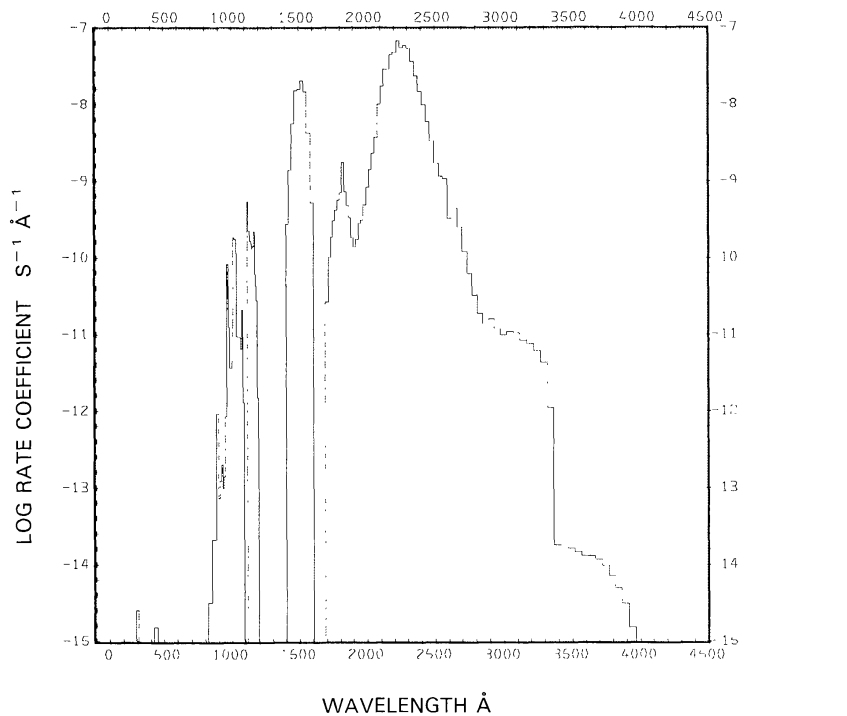
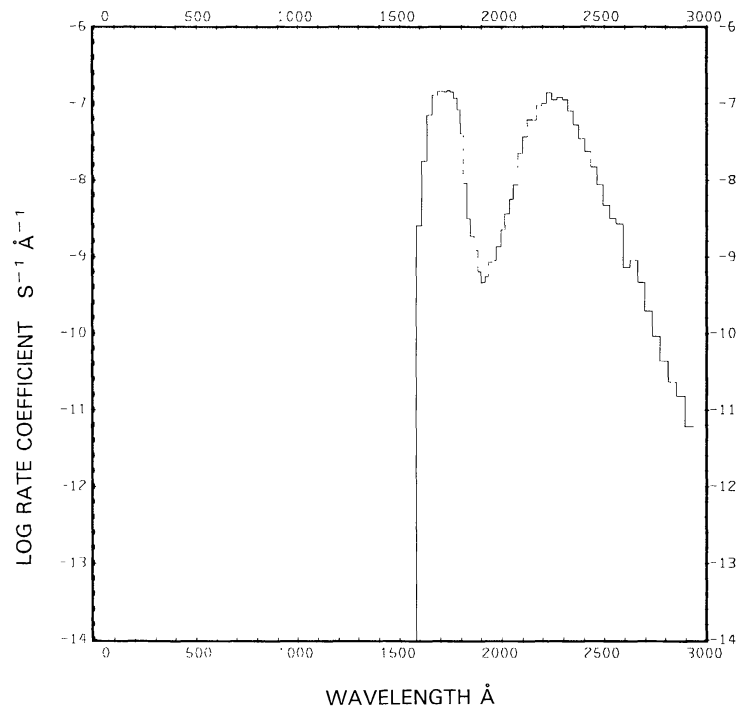


Rate coefficients:

The first of each value is for the quiet Sun (see Figures 105 to 108 and 109(a) to 115(a)) and the second is for the active Sun (see Figures 109(b) to 115(b)). Molina *et al.* (1981) estimate the ‘upper limit’ to the dissociation rate coefficient for the quiet Sun to be about $4 \times 10^{-9} \text{ s}^{-1}$, but this is for a strongly attenuated atmosphere.

Excess energies:

The first value for each branch is for the quiet Sun, the second is for the active Sun.

Fig. 105. $\text{OCS} + \nu \rightarrow \text{CO} + \text{S}({^3P})$, for the quiet Sun.Fig. 106. $\text{OCS} + \nu \rightarrow \text{CO} + \text{S}({^1D})$, for the quiet Sun.

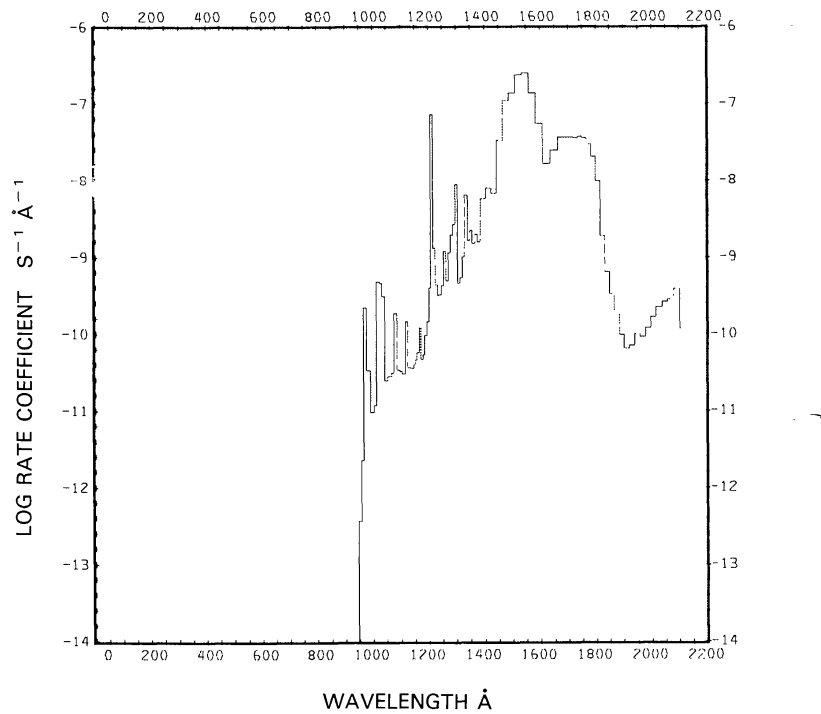


Fig. 107. OCS + $\nu \rightarrow$ CO + S(1S), for the quiet Sun.

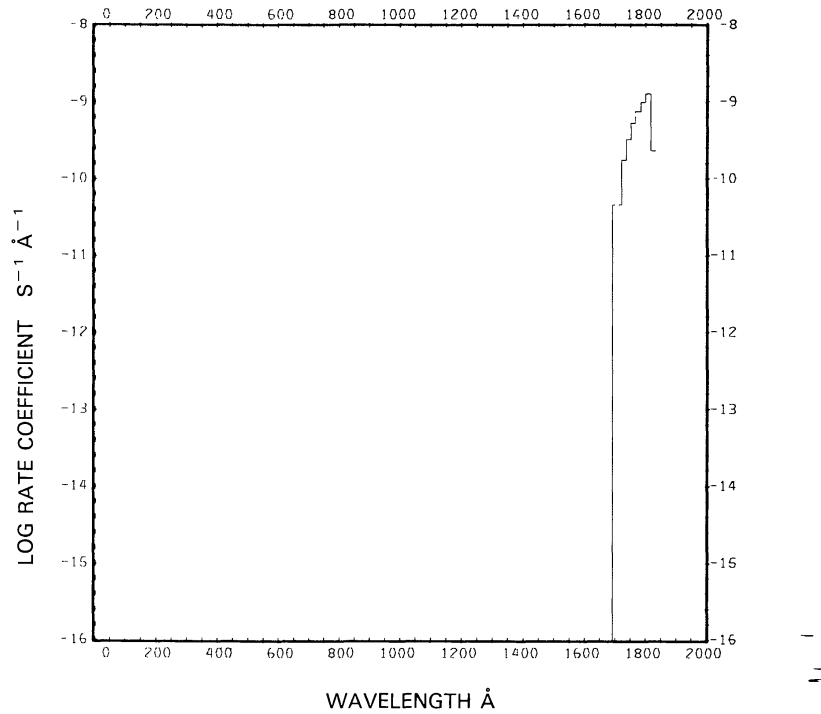
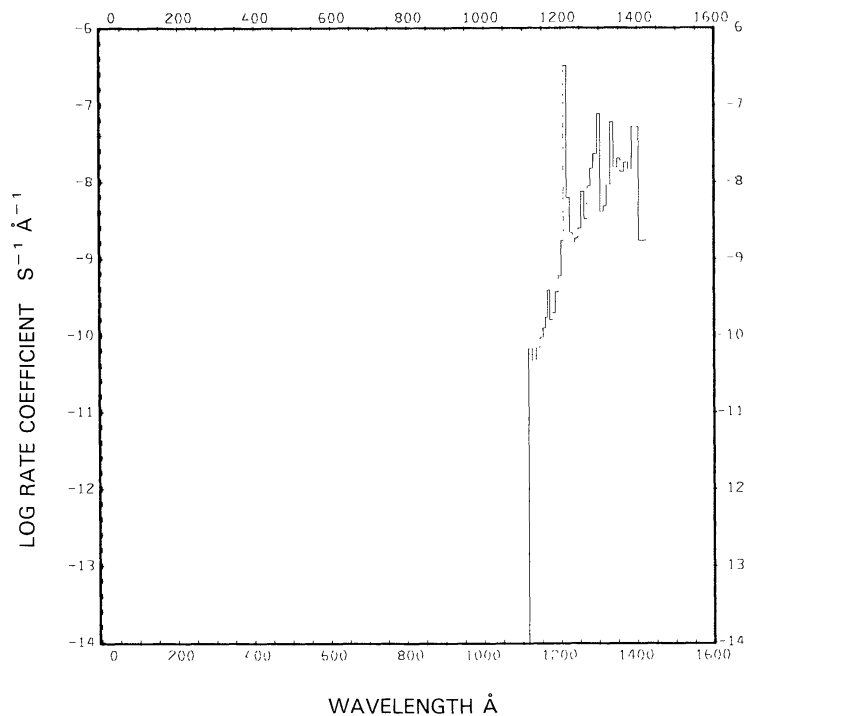
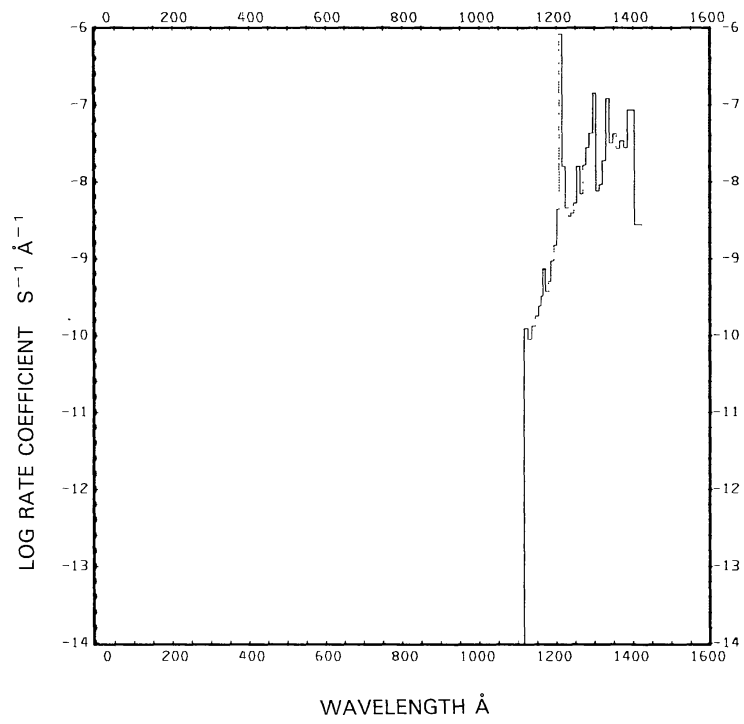


Fig. 108. OCS + $\nu \rightarrow$ CS + O(3P), for the quiet Sun.

Fig. 109a. OCS + $v \rightarrow$ CS + O(1D), for the quiet Sun.Fig. 109b. OCS + $v \rightarrow$ CS + O(1D), for the active Sun.

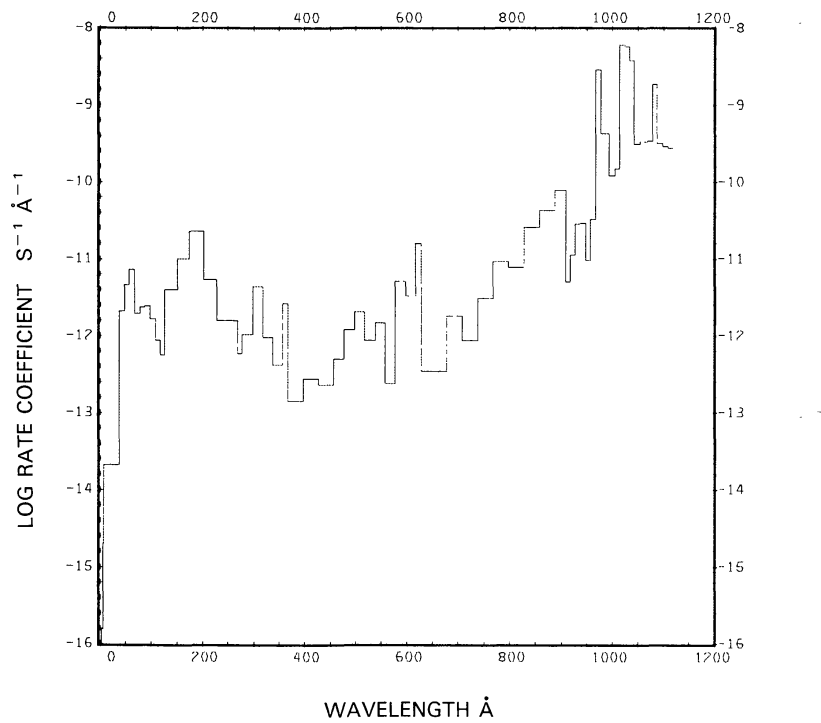


Fig. 110a. $\text{OCS} + \nu \rightarrow \text{OCS}^+ + e$, for the quiet Sun.

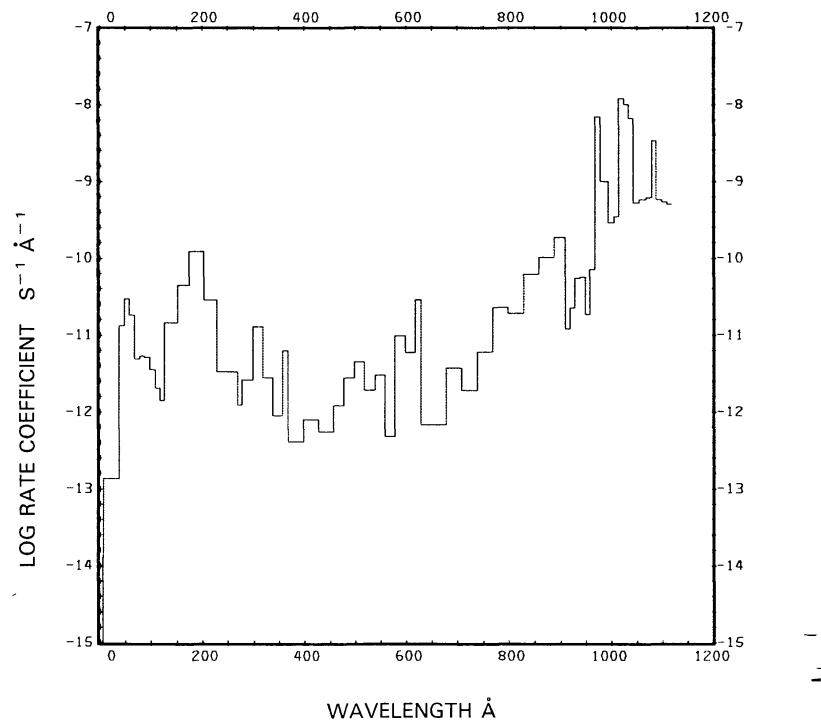
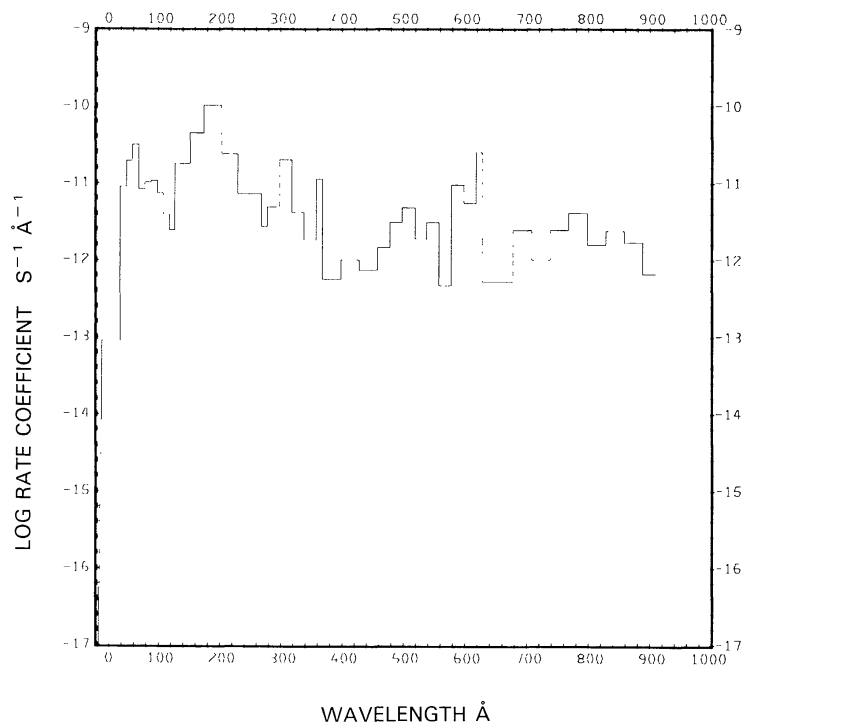
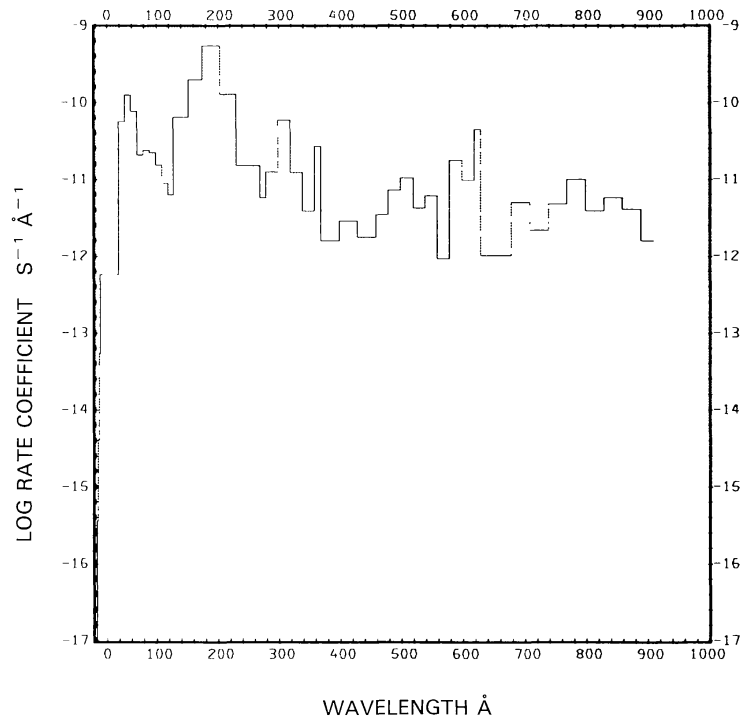


Fig. 110b. $\text{OCS} + \nu \rightarrow \text{OCS}^+ + e$, for the active Sun.

Fig. 111a. OCS + ν → CO + S⁺ + e, for the quiet Sun.Fig. 111b. OCS + ν → CO + S⁺ + e, for the active Sun.

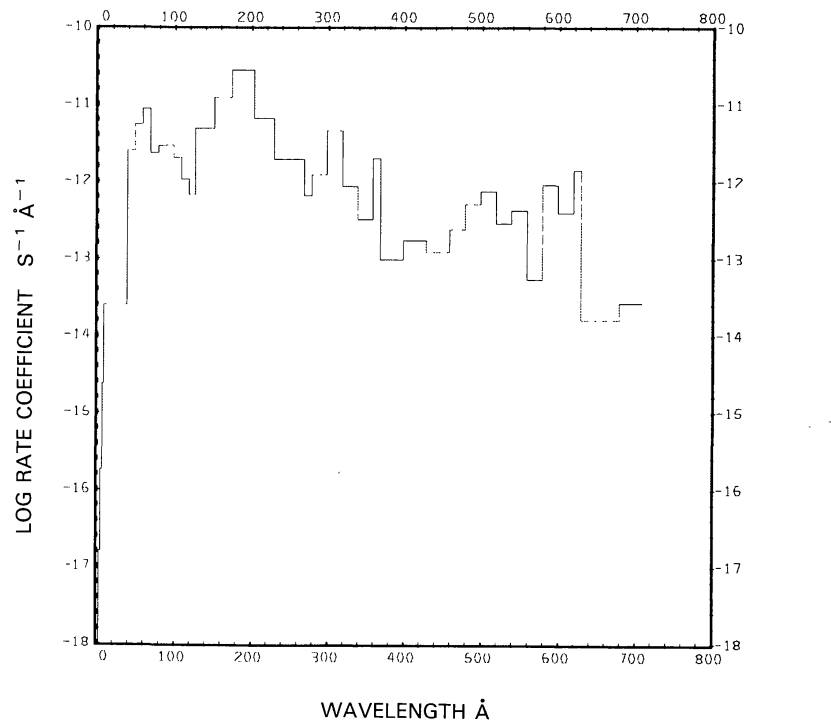


Fig. 112a. $\text{OCS} + \nu \rightarrow \text{S} + \text{CO}^+ + e^-$, for the quiet Sun.

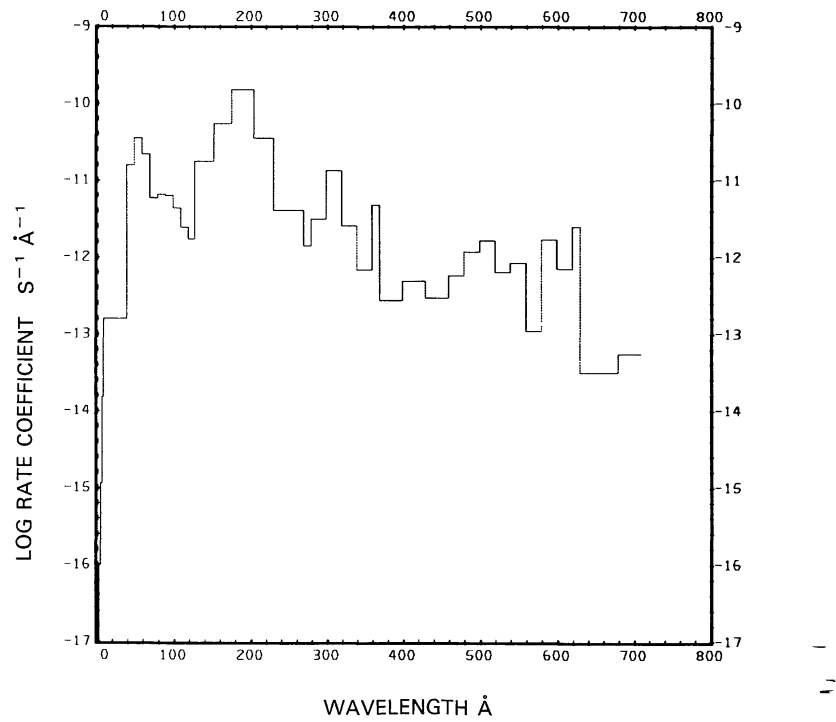
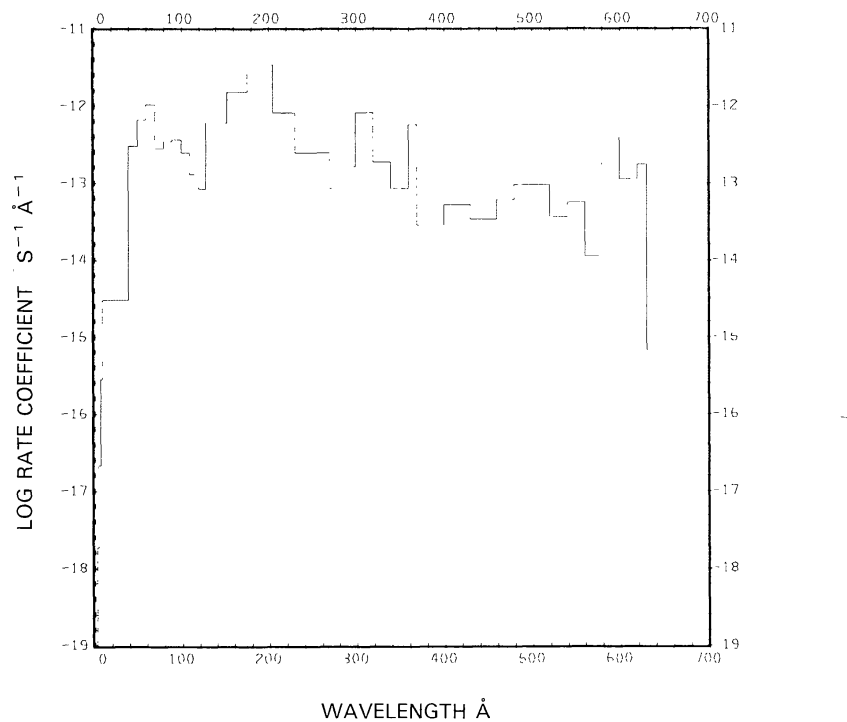
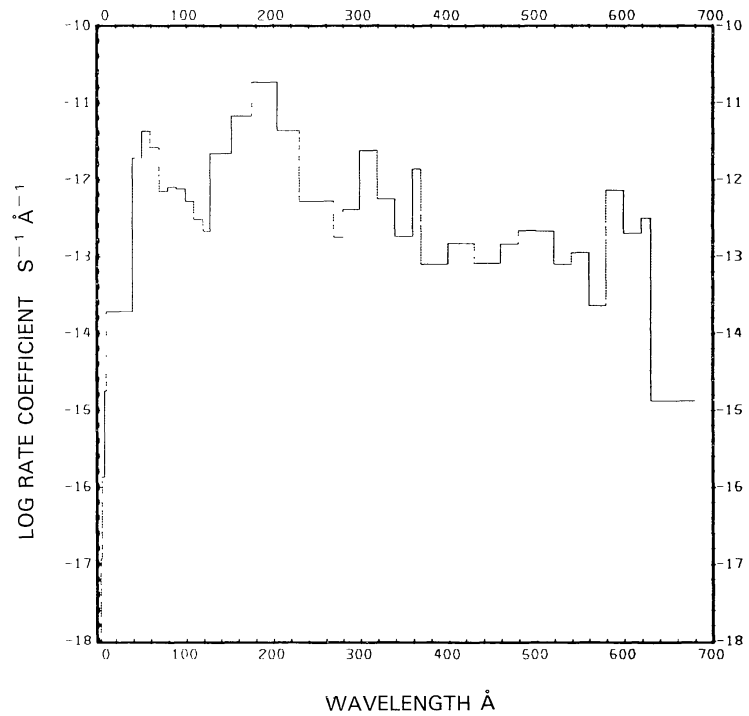
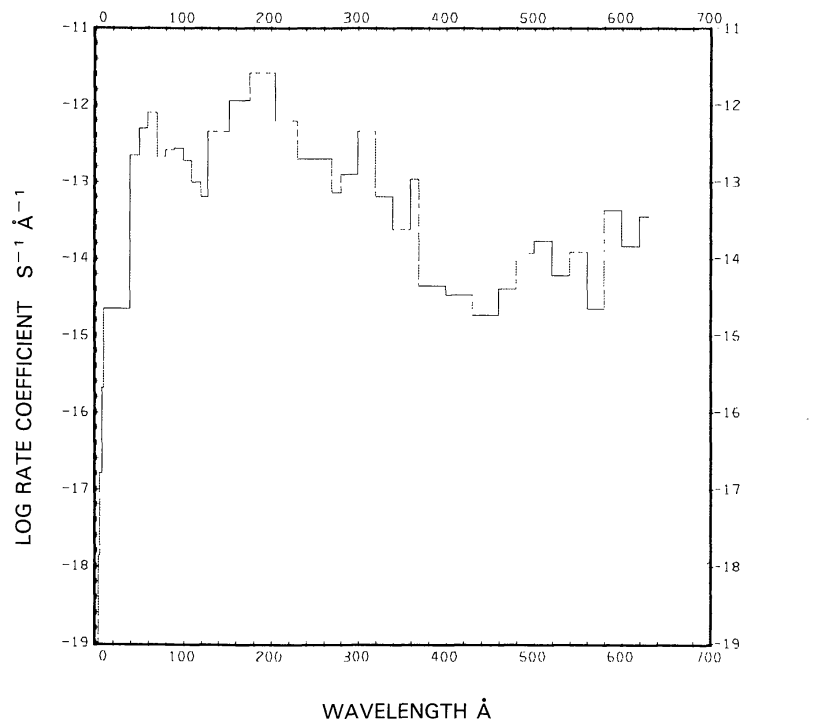
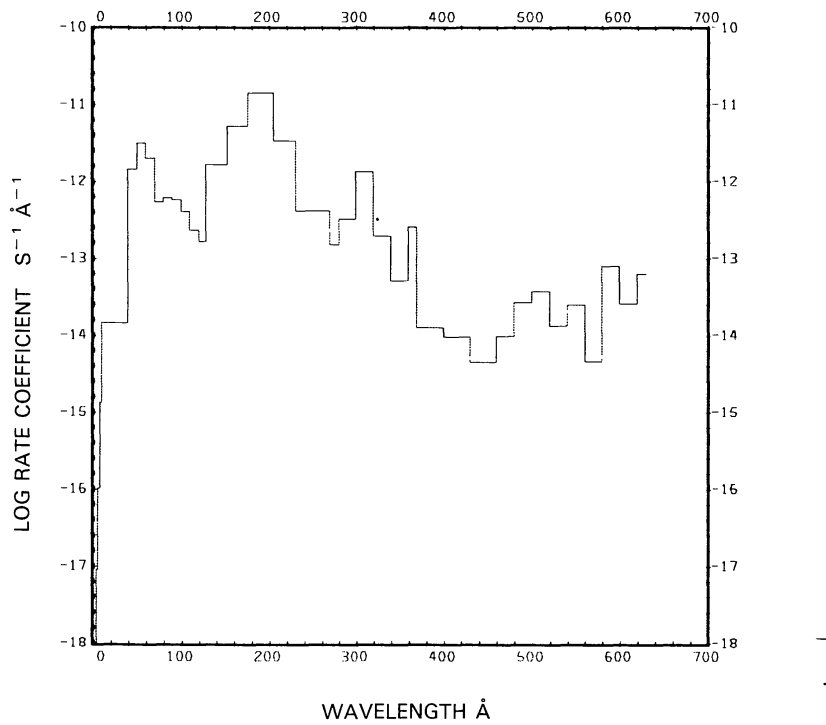
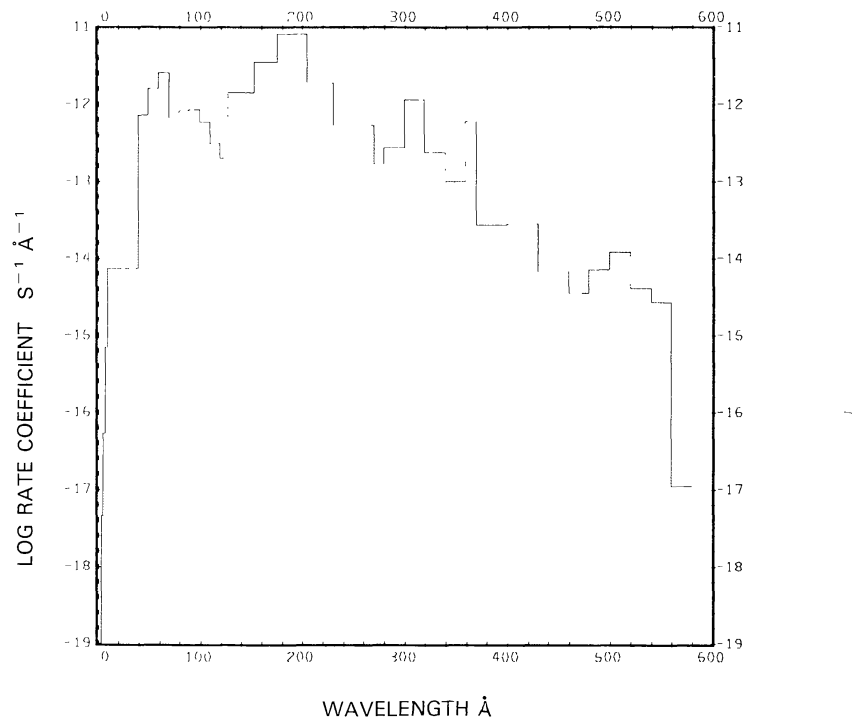
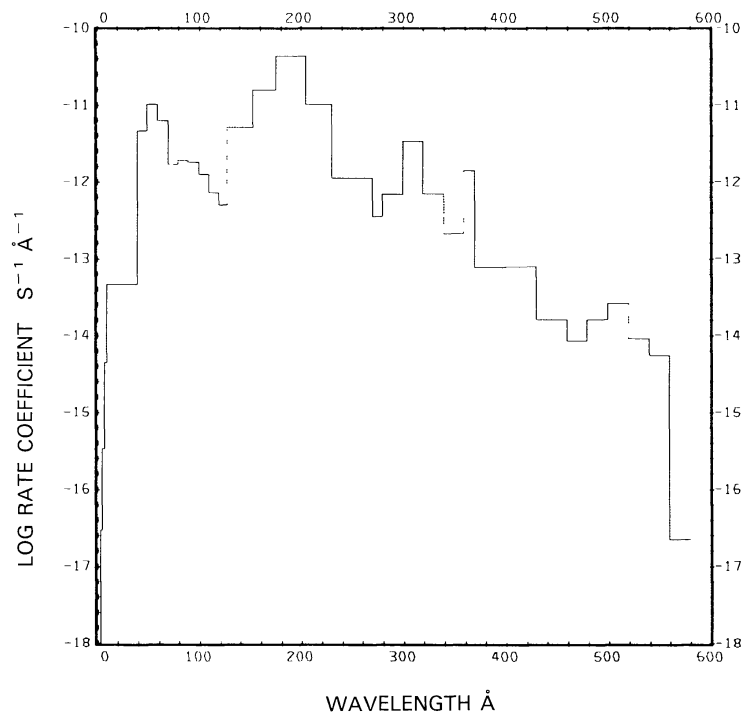


Fig. 112b. $\text{OCS} + \nu \rightarrow \text{S} + \text{CO}^+ + e^-$, for the active Sun.

Fig. 113a. OCS + ν → O + CS⁺ + e, for the quiet Sun.Fig. 113b. OCS + ν → O + CS⁺ + e, for the active Sun.

Fig. 114a. OCS + $\nu \rightarrow$ CS + O⁺ + e, for the quiet Sun.Fig. 114b. OCS + $\nu \rightarrow$ CS + O⁺ + e, for the active Sun.

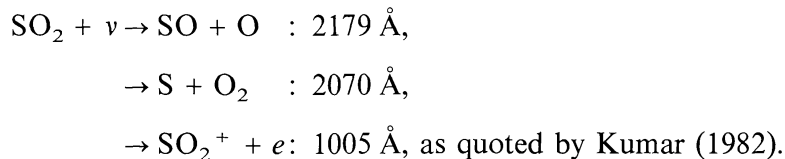
Fig. 115a. $\text{OCS} + \nu \rightarrow \text{SO} + \text{C}^+ + e^-$, for the quiet Sun.Fig. 115b. $\text{OCS} + \nu \rightarrow \text{SO} + \text{C}^+ + e^-$, for the active Sun.

SULFUR DIOXIDE, SO₂

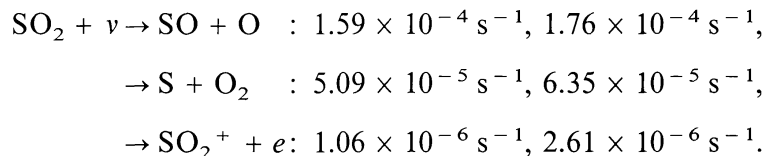
Cross sections: Up to 122 Å the cross section is synthesized from the fits made by Barfield *et al.* (1972) for the cross sections of the atomic constituents. From 170 to 830 Å the cross section was measured by Wu and Judge (1981). Golomb *et al.* (1962) measured the cross section in the wavelength range from 1065 to 2175 Å. We used the very detailed cross sections of Freeman *et al.* (1984) from $\lambda = 1710$ to 2179 Å.

Branching ratios: The branching ratio for dissociation into SO + O and S + O₂ is about 0.5 at 1849 Å (Driscoll and Warneck, 1968). We assumed this value for the branching ratio in the wavelength range from $\lambda = 1005$ to 2065 Å.

Thresholds: Thresholds for dissociation are quoted by Freeman *et al.* (1984) for the first branch and by Welge (1974) for the second branch:

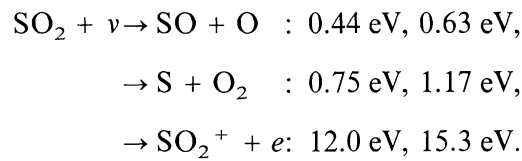


Rate coefficients:

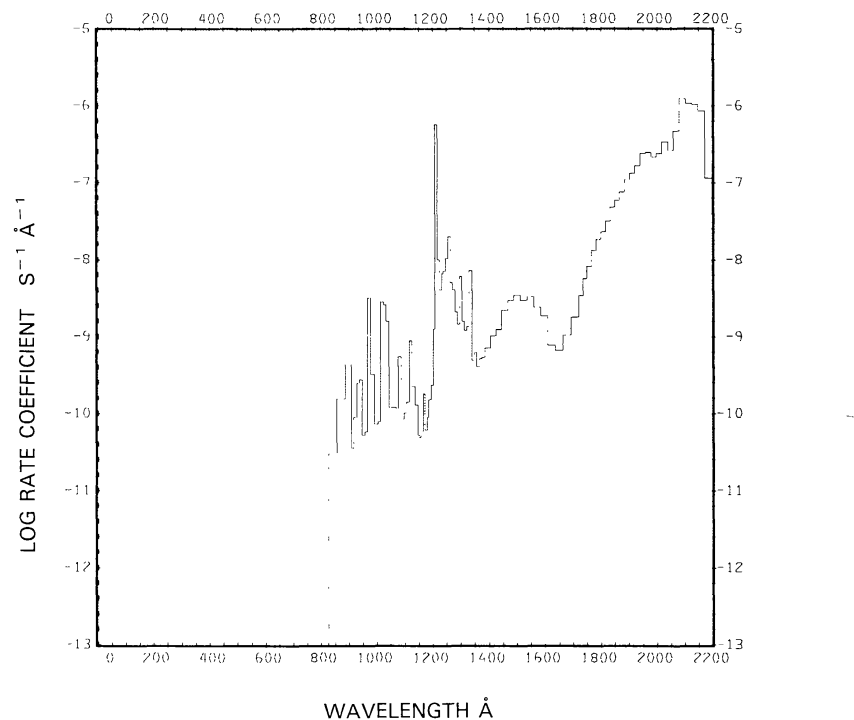
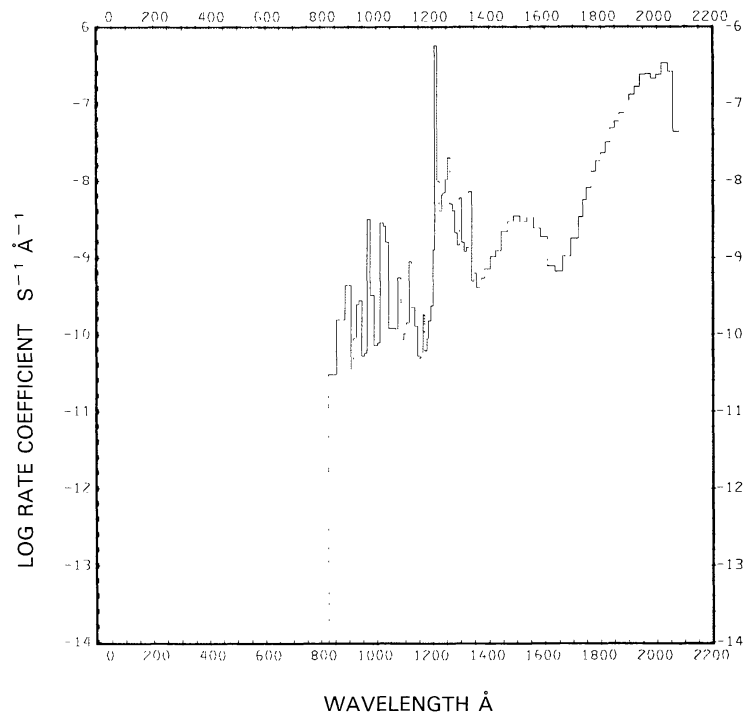


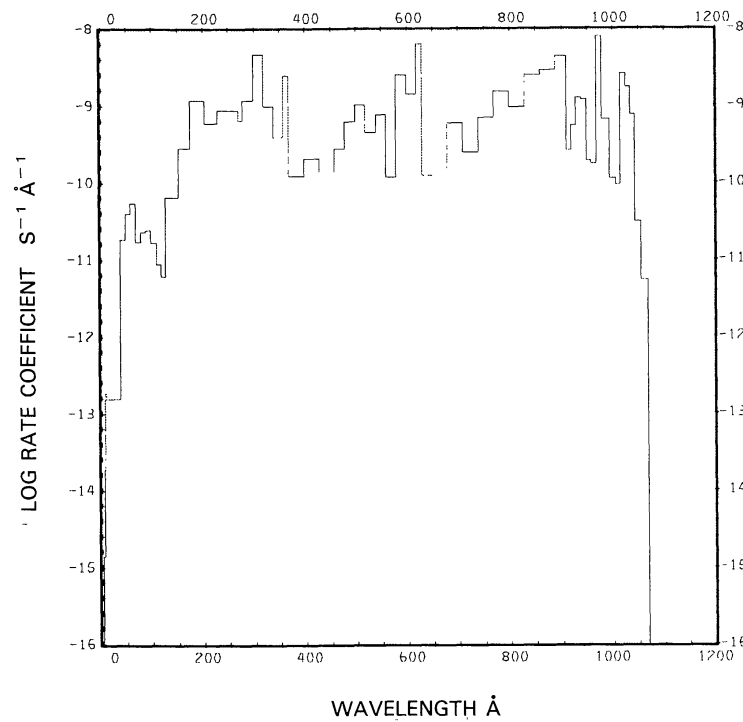
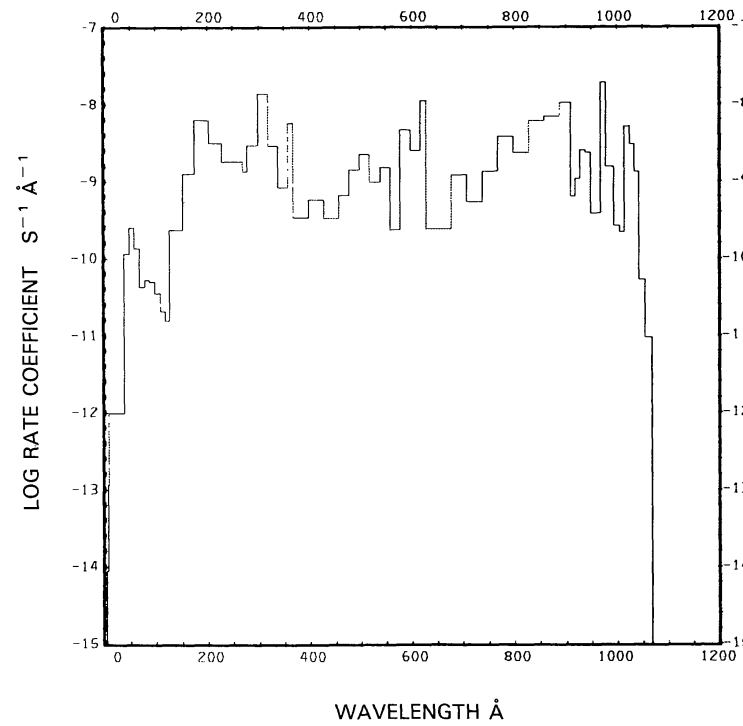
The first value for each branch is for the quiet Sun (see Figures 116, 117, and 118(a)), the second is for the active Sun (see Figure 118(b)). For the quiet Sun, Kumar (1982) quotes the following rate coefficients for the Jupiter moon Io at 5.2 AU heliocentric distance: $5.6 \times 10^{-6} \text{ s}^{-1}$, $2.9 \times 10^{-6} \text{ s}^{-1}$, and $4.8 \times 10^{-8} \text{ s}^{-1}$. Scaled to 1 AU, these values are $1.5 \times 10^{-4} \text{ s}^{-1}$, $7.8 \times 10^{-5} \text{ s}^{-1}$, and $1.3 \times 10^{-6} \text{ s}^{-1}$, respectively; all within 35% of our values. Golomb *et al.* (1962) quote a life time of 4700 s, i.e., a total rate coefficient of $2.1 \times 10^{-4} \text{ s}^{-1}$, for SO₂. This value is in excellent agreement with our value for the quiet Sun.

Excess energies:



The first value for each branch is for the quiet Sun, the second is for the active Sun.

Fig. 116. $\text{SO}_2 + \nu \rightarrow \text{SO} + \text{O}$, for the quiet Sun.Fig. 117. $\text{SO}_2 + \nu \rightarrow \text{S} + \text{O}_2$, for the quiet Sun.

Fig. 118a. $\text{SO}_2 + \nu \rightarrow \text{SO}_2^+ + e$, for the quiet Sun.Fig. 118b. $\text{SO}_2 + \nu \rightarrow \text{SO}_2^+ + e$, for the active Sun.

NITROSYL CHLORIDE, ClNO

Cross sections: Up to 878 Å the cross section is synthesized from the fits by Barfield *et al.* (1972) to the cross sections of the constituent atoms. From 1150 to 1850 Å the cross section was measured by Lenzi and Okabe (1967) and in the wavelength range from 1900 to 4000 Å by Illies and Takacks (1976). The cross section in the range from 4000 to 5400 Å was measured by Ballash and Armstrong (1974). In the range from 5400 to 6700 Å the cross sections were measured by Goodeve and Katz (1939).

Branching ratios: Branching ratios are not known.

Thresholds: Lenzi and Okabe (1968) quote the threshold for dissociation to be at $\lambda = 7748 \text{ Å}$.

Rate coefficients:



for the quiet Sun (see Figure 119), for the active Sun the rate coefficient is $6.50 \times 10^{-3} \text{ s}^{-1}$.

Excess energies: The excess energy for the quiet Sun is 2.73 eV, for the active Sun it is 2.79 eV.

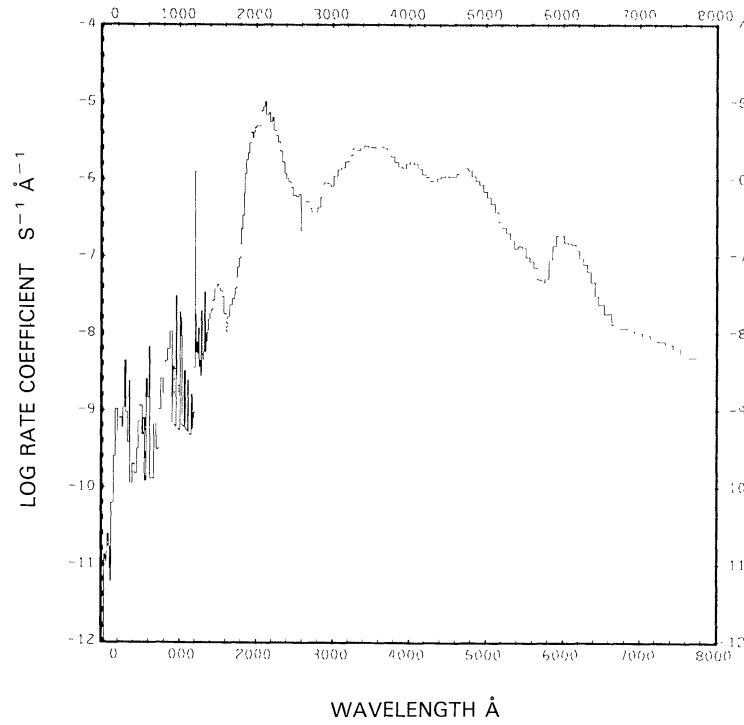


Fig. 119. $\text{ClNO} + \nu \rightarrow \text{Cl} + \text{NO}$, for the quiet Sun.

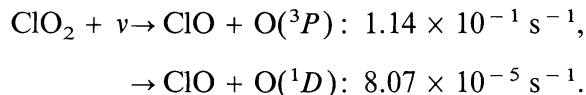
CHLORINE DIOXIDE, ClO₂ (OCLO)

Cross sections: Up to $\lambda = 878 \text{ \AA}$ the cross section is synthesized from the cross sections for the constituent atoms, using the fits by Barfield *et al.* (1972). The cross section is not known in the region from $\lambda = 880$ to 1450 \AA ; we used the cross section of ClNO to fill this gap. From 1470 to 1850 \AA the cross section was measured by Basco and Morse (1974). The cross section for the wavelength range from $\lambda = 2998$ to 4202 \AA was obtained from Birks *et al.* (1977) with a normalization for the cross section at $\lambda = 3515 \text{ \AA}$ to be $1.5 \times 10^{-17} \text{ cm}^2$ from Clyne and Coxon (1968) as quoted by Birks *et al.* In the range from $\lambda = 4404.06$ to 4758.19 \AA we used the data from Coon *et al.* (1962), assuming that this small cross section leads to predissociation as pointed out by Okabe (1978).

Branching ratios: As suggested by Watson (1977) the branching ratio for dissociation leading to O(³P) by predissociation is unity above $\lambda = 2760 \text{ \AA}$ and is unity below that wavelength for dissociation leading to O(¹D).

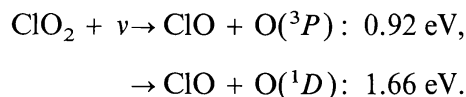
Thresholds: Okabe (1978) quotes the dissociation threshold equivalent wavelength for dissociation into ClO + O(³P) to be $\lambda = 4960 \text{ \AA}$. A second dissociation path to form ClO + O(¹D) is at $\lambda = 2760 \text{ \AA}$ (Watson, 1977).

Rate coefficients:

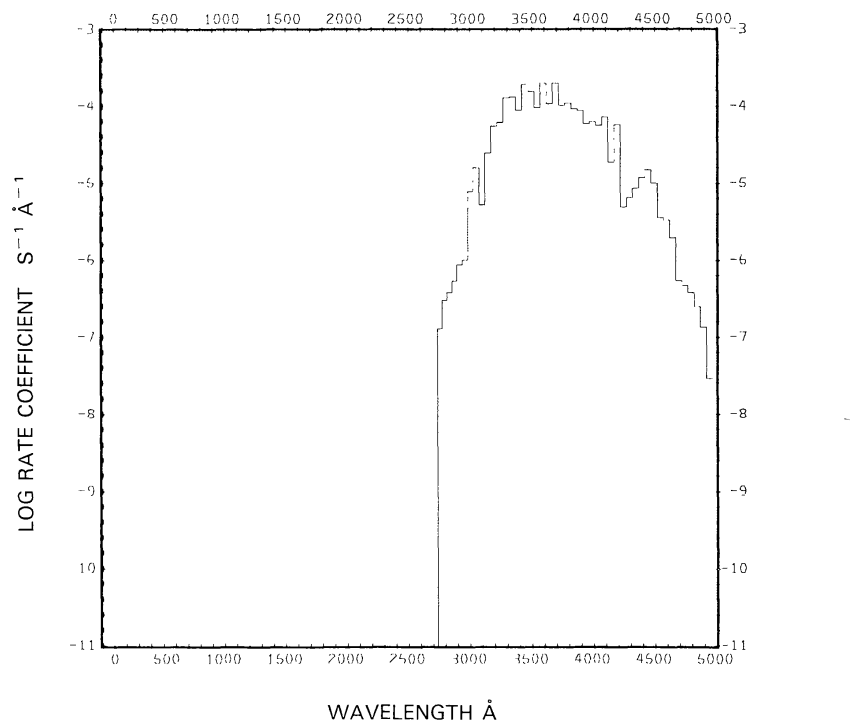
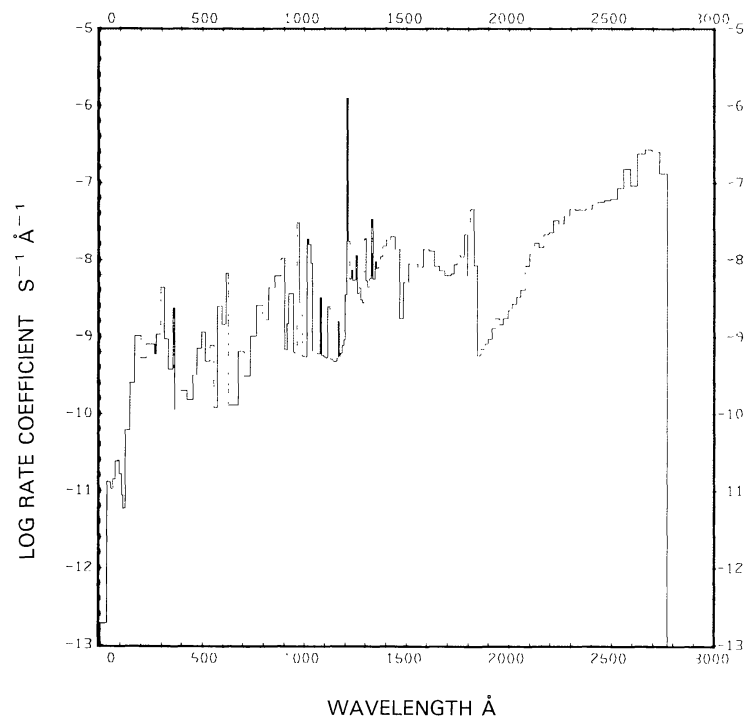


See Figures 120 and 121. Only the second branch is influenced by the activity of the Sun; the rate coefficient for the active Sun is $1.04 \times 10^{-4} \text{ s}^{-1}$. The rate coefficient for the quiet Sun compares reasonably well with the approximated smaller value $7.6 \times 10^{-2} \text{ s}^{-1}$ obtained by Birks *et al.* (1977) who used a more restricted wavelength range from $\lambda = 2960 \text{ \AA}$ to 4640 \AA .

Excess energies:



The first branch is not influenced by the activity of the Sun, the excess energy for the second branch becomes 2.75 eV for the active Sun.

Fig. 120. $\text{ClO}_2 + \nu \rightarrow \text{ClO} + \text{O}({}^3P)$, for the quiet Sun.Fig. 121. $\text{ClO}_2 + \nu \rightarrow \text{ClO} + \text{O}({}^1D)$, for the quiet Sun.

CHLORINE PEROXYL, ClOO

Cross sections: Up to 1850 Å we used the cross section from chlorine dioxide. In the wavelength region from 2250 to 2800 Å the cross section was measured by Johnston *et al.* (1969). For longer wavelengths we assumed that the cross section goes to zero at threshold.

Branching ratios: The branching ratios are unknown. We assumed only dissociation into ClO and O.

Threshold: The threshold is not known. We assumed it to be the same as for chlorine dioxide (~ 4960 Å).

Rate coefficients:



See Figure 122. This very approximate rate coefficient is not sensitive to the activity of the Sun. It is $\sim 9.2 \times 10^{-3} \text{ s}^{-1}$ for the active Sun.

Excess energies: The very approximate value of the excess energy is about 2.2 eV and is not sensitive to the activity of the Sun.

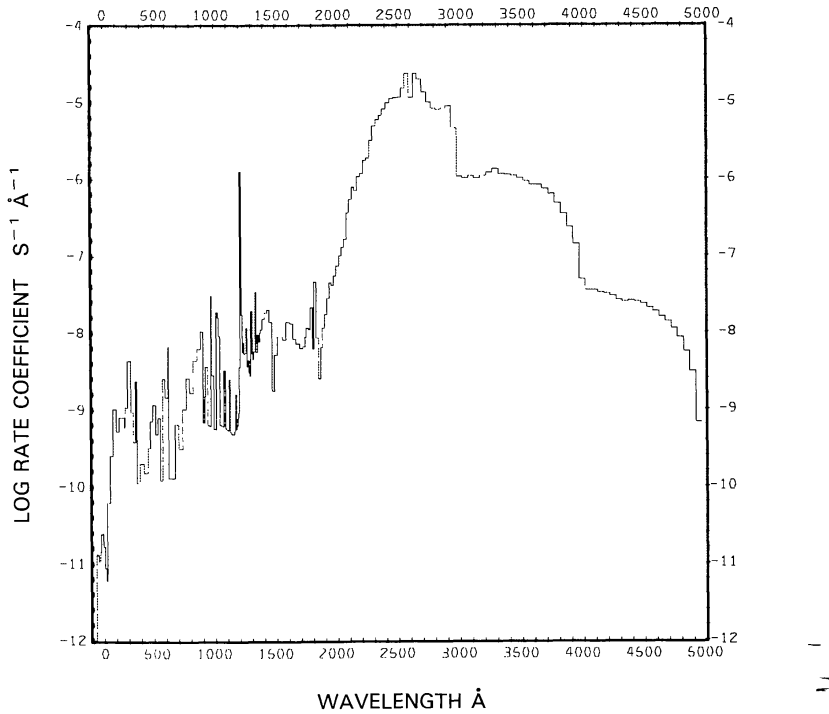


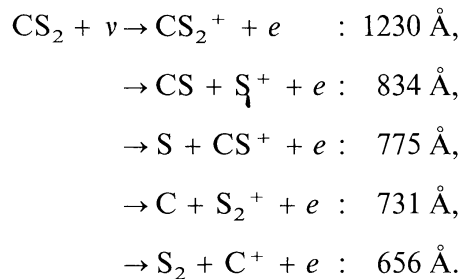
Fig. 122. $\text{ClOO} + h\nu \rightarrow \text{ClO} + \text{O}$, for the quiet Sun.

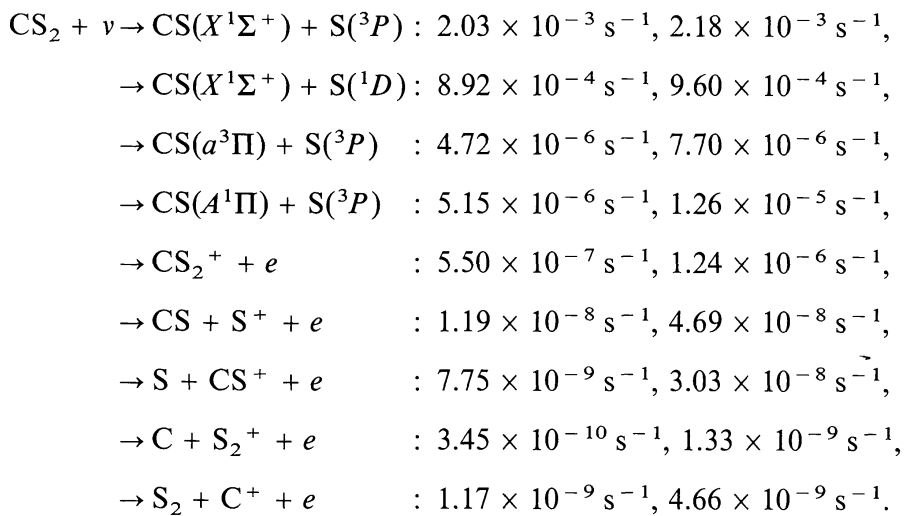
CARBON DISULFIDE, CS₂

Cross sections: Up to 249 Å the cross section is synthesized from the cross sections of the atomic constituents, using the fits of Barfield *et al.* (1972). The cross section was measured by Carnovale *et al.* (1982) in the wavelength range from 310 to 954 Å and by Day *et al.* (1982) in the region from 1060 to 1520 Å. A strong absorption region exists between 1850 and 2300 Å, the cross sections of Molina *et al.* (1981) were used in this region.

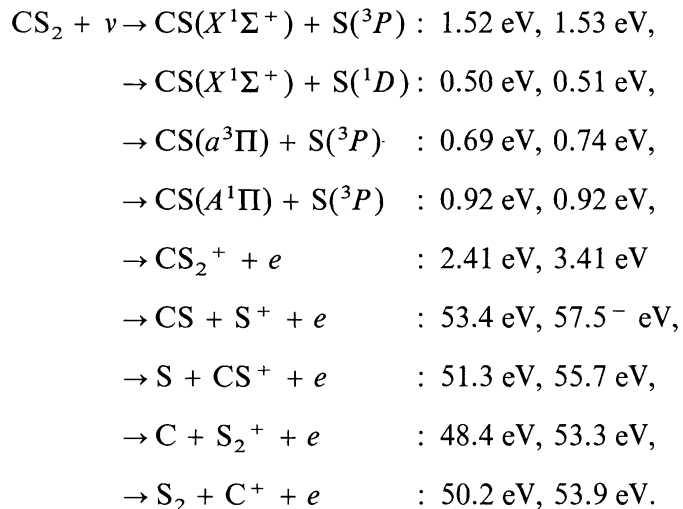
Branching ratios: The branching ratio for dissociation at 1930 Å was determined by Jackson and Okabe (1985) who find the branching ratio for S(³P) to S(¹D) to be 0.67: 0.33. Black *et al.* (1977) find production of CS(*a*³Π) in the region 1250 to 1400 Å; we assumed a branching ratio of one between 1337 and 1572 Å, and 0.5 between 1230 and 1337 Å. Okabe (1972) found production of CS(*A*¹Π) to be an important process; we assumed a branching ratio of 0.5 between 1230 and 1337 Å.

Thresholds: The wavelength equivalent to dissociation into the ground states of CS and S is at $\lambda = 2778$ Å (Okabe, 1978). The threshold wavelength to produce CS in the ground state and S(¹D) is therefore 2211 Å and to produce CS(*a*³Π) + S(³P) the threshold wavelength is 1572 Å, in good agreement with the values given by Fournier *et al.* (1977). The threshold for dissociation into CS(*A*¹Π) and S(³P) is at 1337 Å as determined by Okabe (1972). For the ionization and dissociative ionization thresholds we took the averages of the values quoted by Carnovale *et al.* (1982):

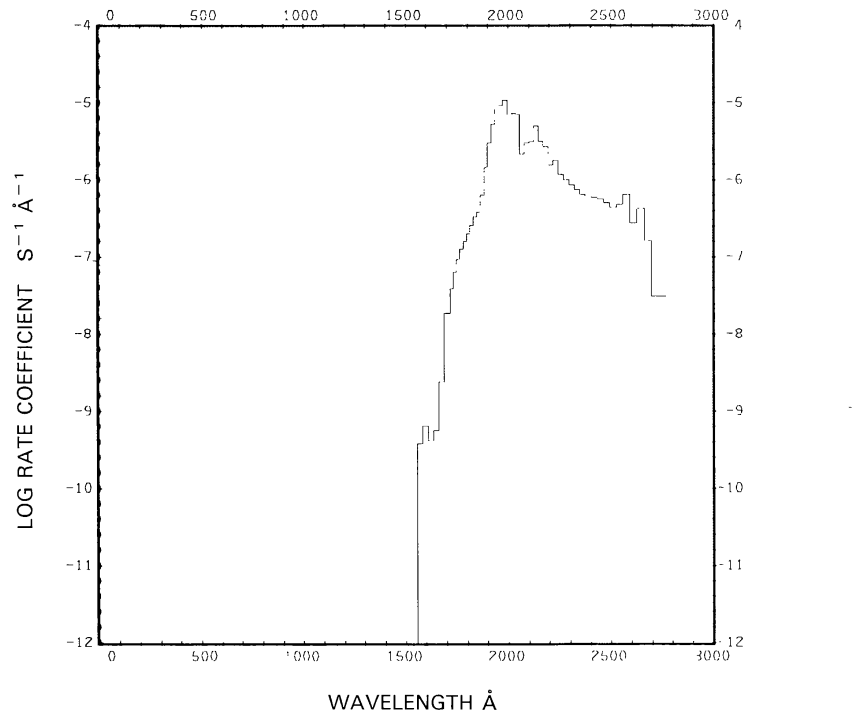
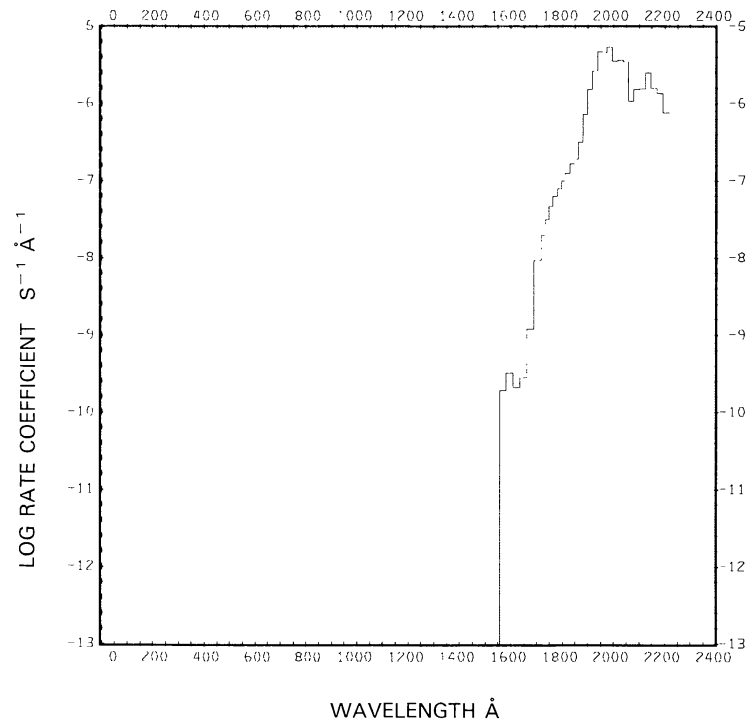


Rate coefficients:

The first value for each of the branches is for the quiet Sun (see Figures 123 to 125 and 126(a) to 131(a)), the second value is for the active Sun (see Figures 127(b) to 131(b)). For the quiet Sun, Jackson *et al.* (1982) quote a total rate coefficient for photo destruction of $9.8 \times 10^{-3} \text{ s}^{-1}$. For comparison, our total rate coefficient is $2.9 \times 10^{-3} \text{ s}^{-1}$.

Excess energies:

The first value for each branch is for the quiet Sun, the second is for the active Sun.

Fig. 123. $\text{CS}_2 + \nu \rightarrow \text{CS}(X^1\Sigma^+) + \text{S}(^3P)$, for the quiet Sun.Fig. 124. $\text{CS}_2 + \nu \rightarrow \text{CS}(X^1\Sigma^+) + \text{S}(^1D)$, for the quiet Sun.

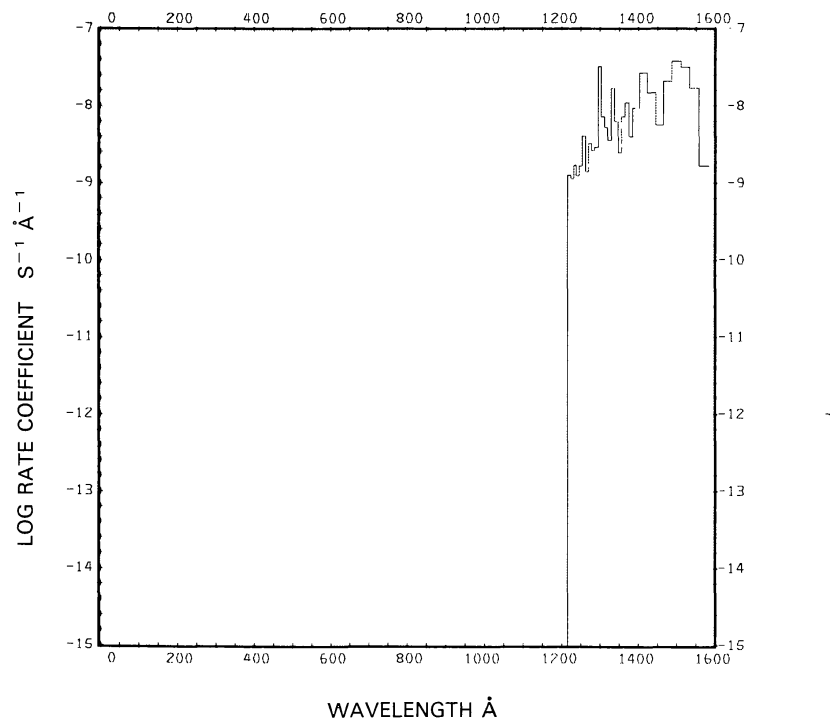
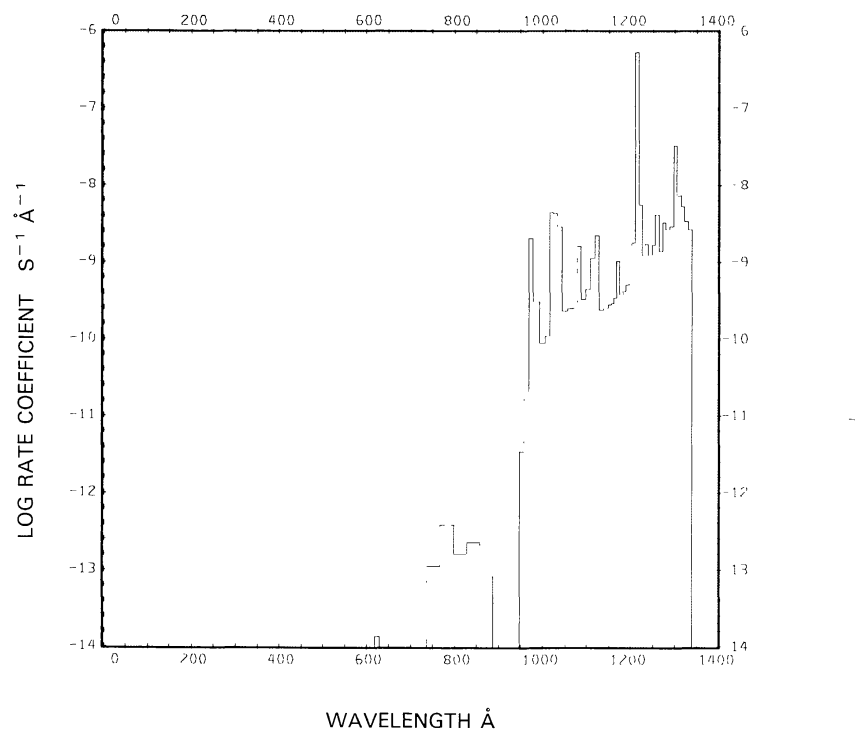
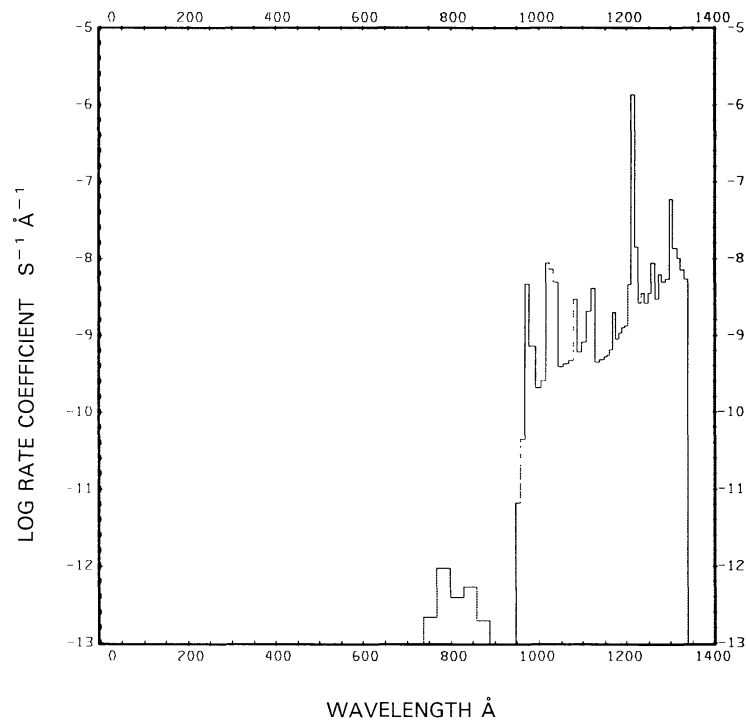
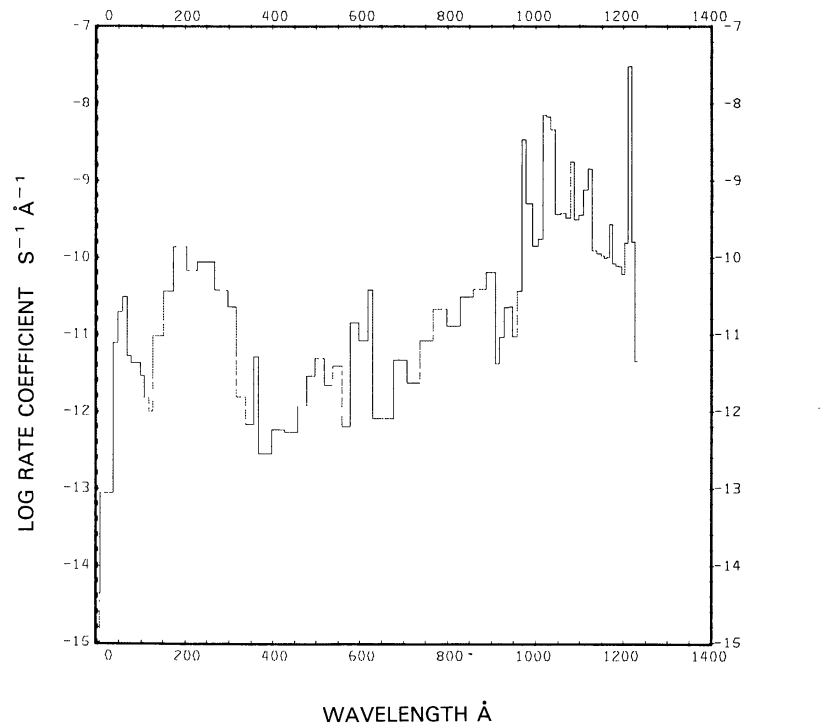
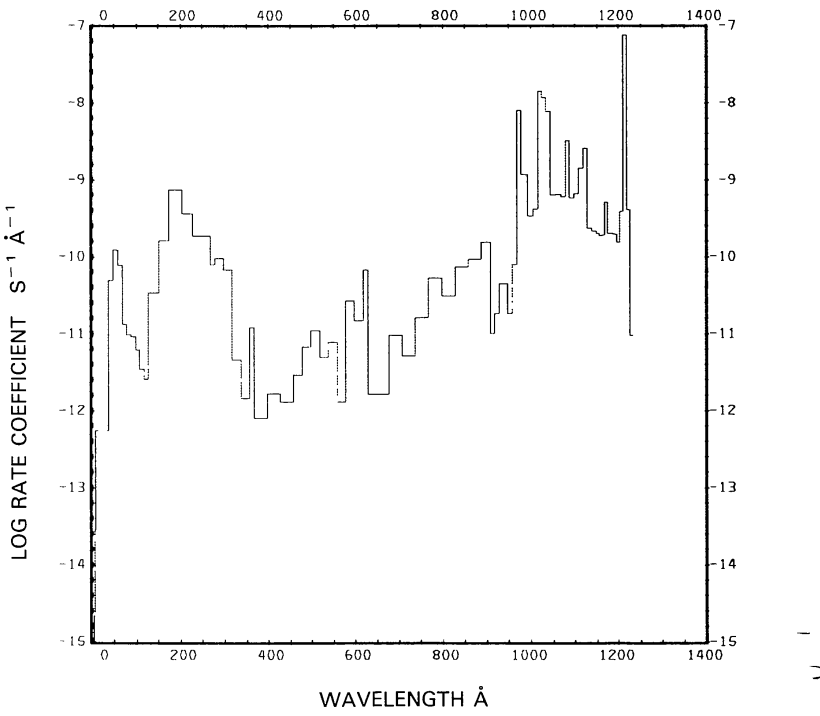
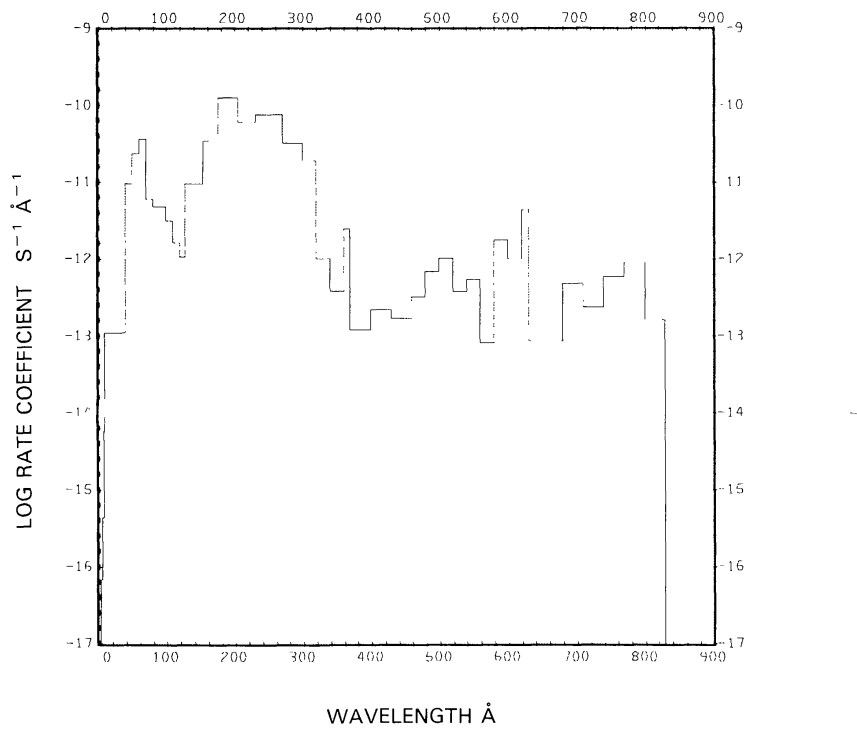
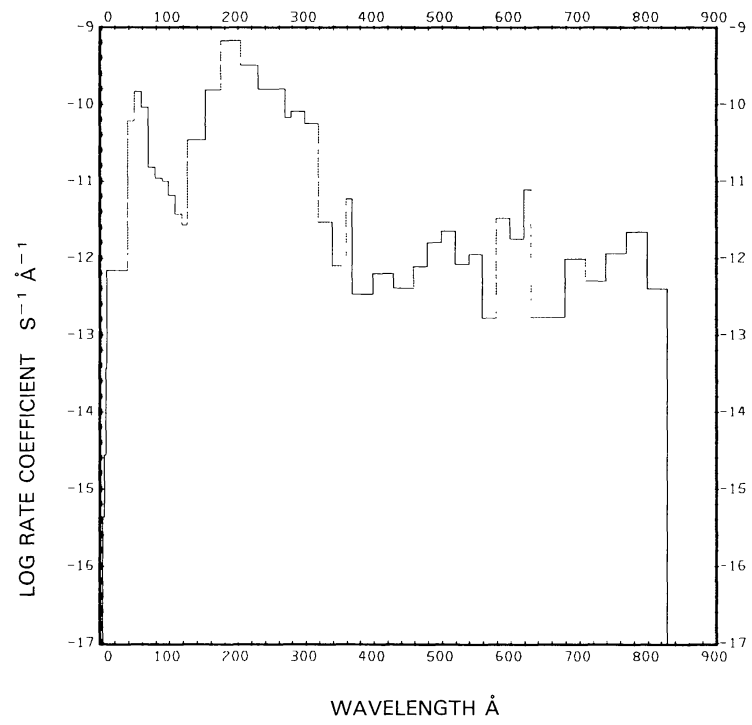
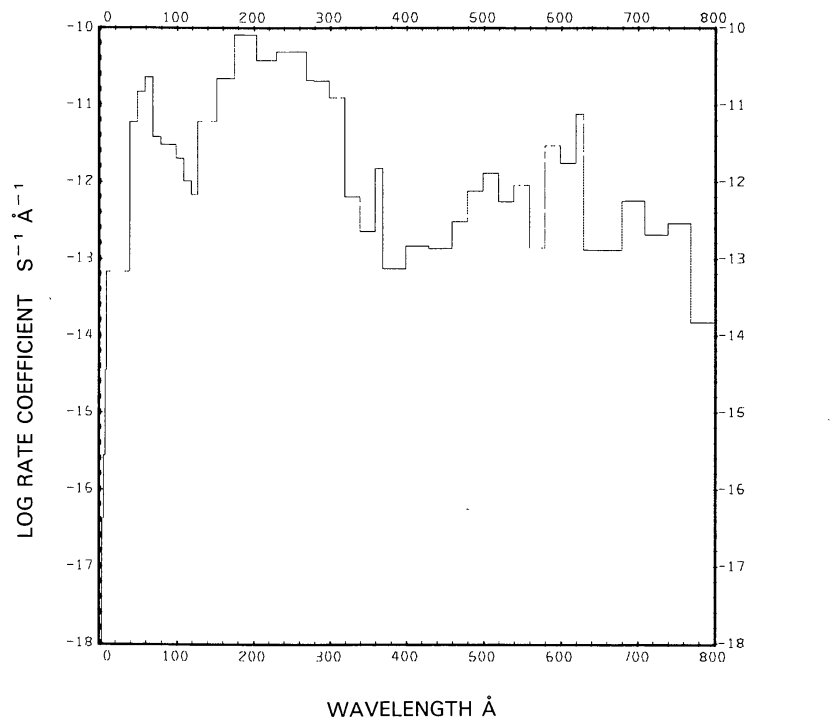
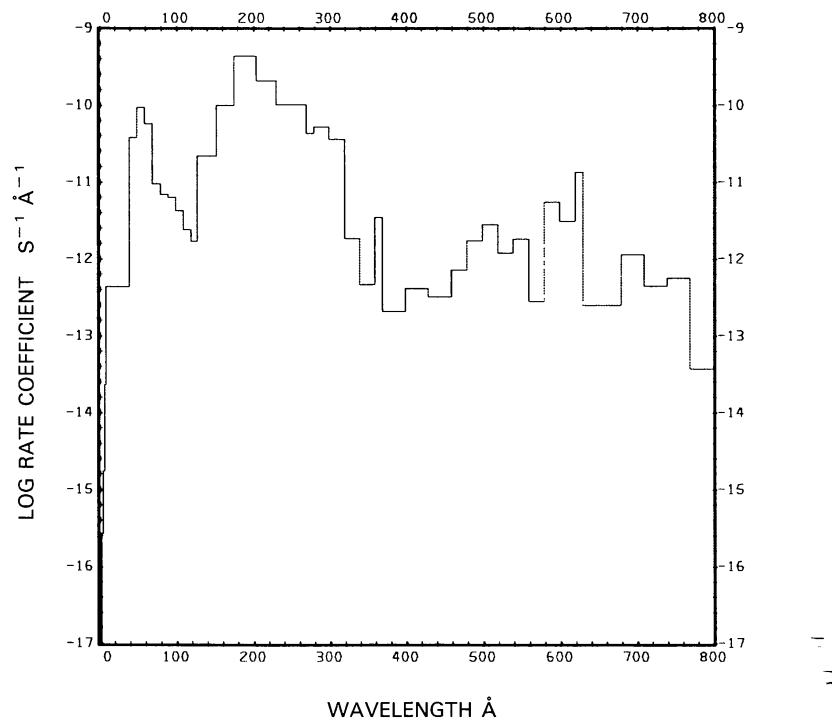


Fig. 125. CS₂ + ν → CS(*a*³Π) + S(³P), for the quiet Sun.

Fig. 126a. $\text{CS}_2 + v \rightarrow \text{CS}(A^1\Pi) + \text{S}(^3P)$, for the quiet Sun.Fig. 126b. $\text{CS}_2 + v \rightarrow \text{CS}(A^1\Pi) + \text{S}(^3P)$, for the active Sun.

Fig. 127a. CS₂ + $\nu \rightarrow$ CS₂⁺ + e^- , for the quiet Sun.Fig. 127b. CS₂ + $\nu \rightarrow$ CS₂⁺ + e^- , for the active Sun.

Fig. 128a. $\text{CS}_2 + v \rightarrow \text{CS} + \text{S}^+ + e$, for the quiet Sun.Fig. 128b. $\text{CS}_2 + v \rightarrow \text{CS} + \text{S}^+ + e$, for the active Sun.

Fig. 129a. CS₂ + ν → S + CS⁺ + e, for the quiet Sun.Fig. 129b. CS₂ + ν → S + CS⁺ + e, for the active Sun.

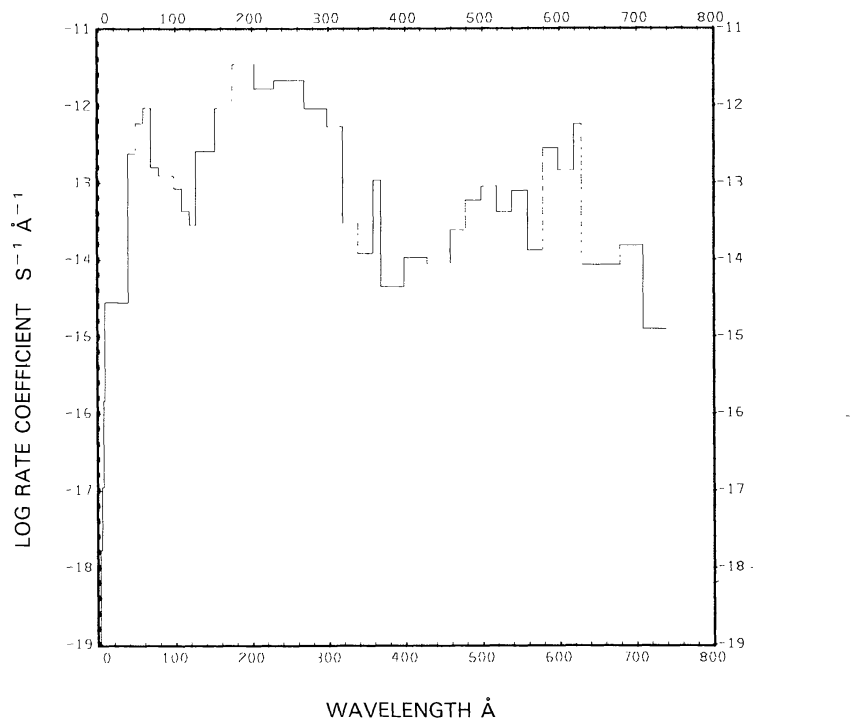


Fig. 130a. $\text{CS}_2 + v \rightarrow \text{C} + \text{S}_2^+ + e$, for the quiet Sun.

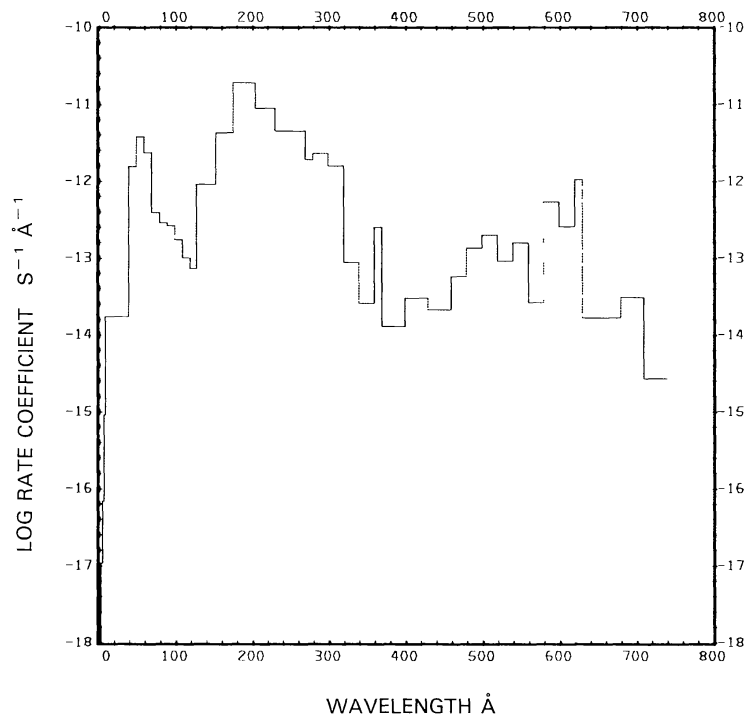
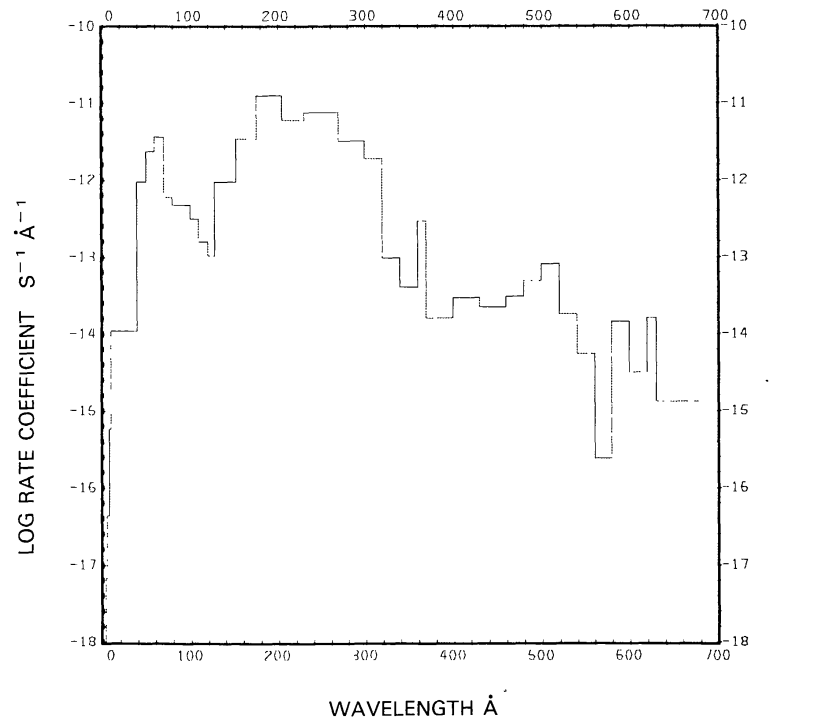
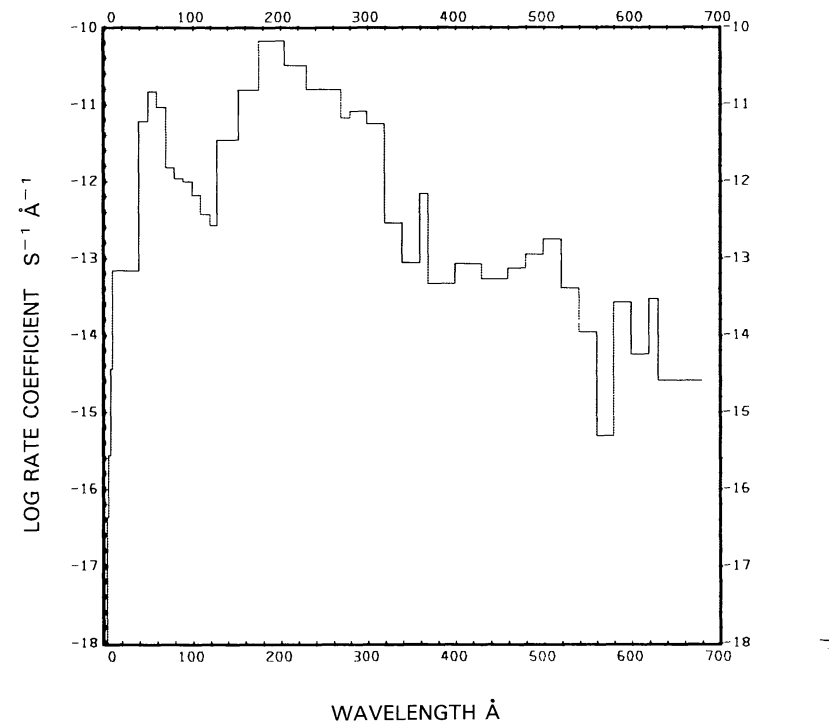


Fig. 130b. $\text{CS}_2 + v \rightarrow \text{C} + \text{S}_2^+ + e$, for the active Sun.

Fig. 131a. CS₂ + $\nu \rightarrow$ S₂ + C⁺ + e, for the quiet Sun.Fig. 131b. CS₂ + $\nu \rightarrow$ S₂ + C⁺ + e, for the active Sun.

HYDROGEN OXYBROMIDE, HOBr

Cross sections: Up to 1127 Å the cross section has been synthesized from our cross sections of the atomic constituents. No cross section data exist beyond this. Baulch *et al.* (1982) suggest scaling the cross section for HOCl so that the observed absorption maxima, at 2300 Å for HOCl and 2600 Å for HOBr, coincide. We have scaled the cross section of HOCl for wavelengths larger than 1127 Å by red-shifting the energy scale by 1/(300 Å) and used it as the cross section for HOBr.

Branching ratios: Branching ratios are not known.

Thresholds: The threshold for dissociation into the main branch forming HO + Br is given by Baulch *et al.* (1982) to be at 5180 Å.

Rate coefficients:



See Figure 132. The rate coefficient is not sensitive to the activity of the Sun.

Excess energies: The excess energy is about 1.3 eV and is not sensitive to the activity of the Sun.

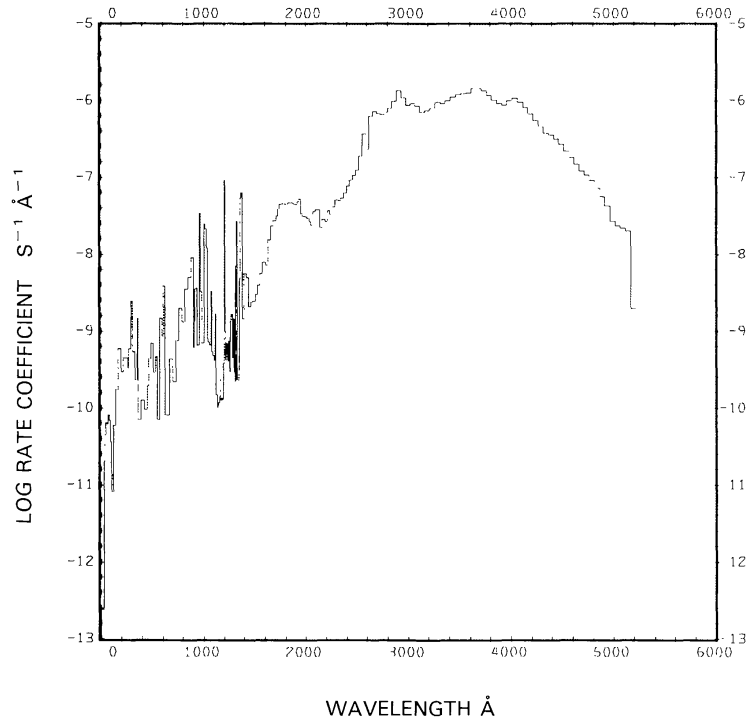


Fig. 132. HOBr + $\nu \rightarrow$ OH + Br, for the quiet Sun.

HYDROGEN OXYIODIDE, HOI

Cross sections: Up to 443 Å the cross section has been synthesized from our cross sections for the atomic constituents. No cross section data exist beyond this. Baulch *et al.* (1982) suggest scaling the cross section to that of HOCl through red-shifting by 100 Å. We have scaled the cross section of HOCl for wavelengths larger than 443 Å by red-shifting the energy scale by 1/(100 Å) and used it as the cross section for HOI, similarly as was done for HOBr.

Branching ratios: Branching ratios are not known.

Thresholds: No threshold data are available. We assumed the threshold to be at 5200 Å which is beyond that of HOCl and HOBr.

Rate coefficients:



See Figure 133. The rate coefficient is not sensitive to the activity of the Sun. It is $\sim 8.8 \times 10^{-4} \text{ s}^{-1}$ for the active Sun.

Excess energies: The excess energy for the quiet Sun is about 1.6 eV and about 1.7 eV for the active Sun.

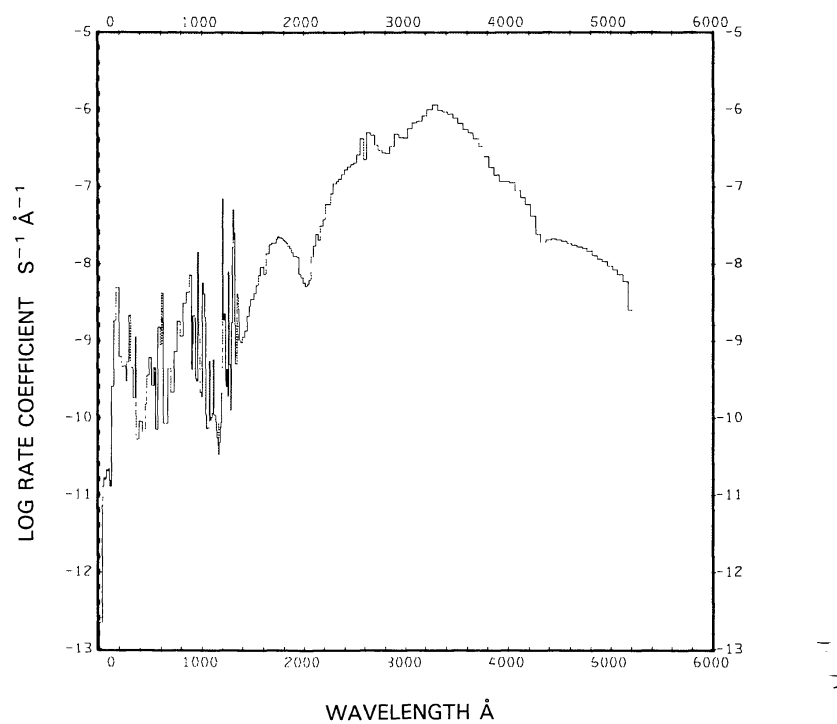


Fig. 133. $\text{HOI} + \nu \rightarrow \text{OH} + \text{I}$, for the quiet Sun.

NITROSYL IODIDE, INO

Cross sections: Up to 443 Å the cross section is synthesized from our cross sections for the atomic constituents. No cross section data exist from there to 2300 Å. Because of this lack of data we used the averaged cross sections, presented by Baulch *et al.* (1982), in the range from 2300 to 4600 Å.

Branching ratios: Branching ratios are not known.

Thresholds: The threshold equivalent wavelength for dissociation into I + NO is given by Baulch *et al.* (1982) to be at 16500 Å.

Rate coefficients:

$$\text{INO} + \nu \rightarrow \text{I} + \text{NO}: \sim 9.8 \times 10^{-2} \text{ s}^{-1}.$$

See Figure 134. The rate coefficient is not sensitive to the activity of the Sun. It is $\sim 9.9 \times 10^{-2} \text{ s}^{-1}$ for the active Sun.

Excess energies: The excess energy is about 2.8 eV and is not sensitive to the activity of the Sun.

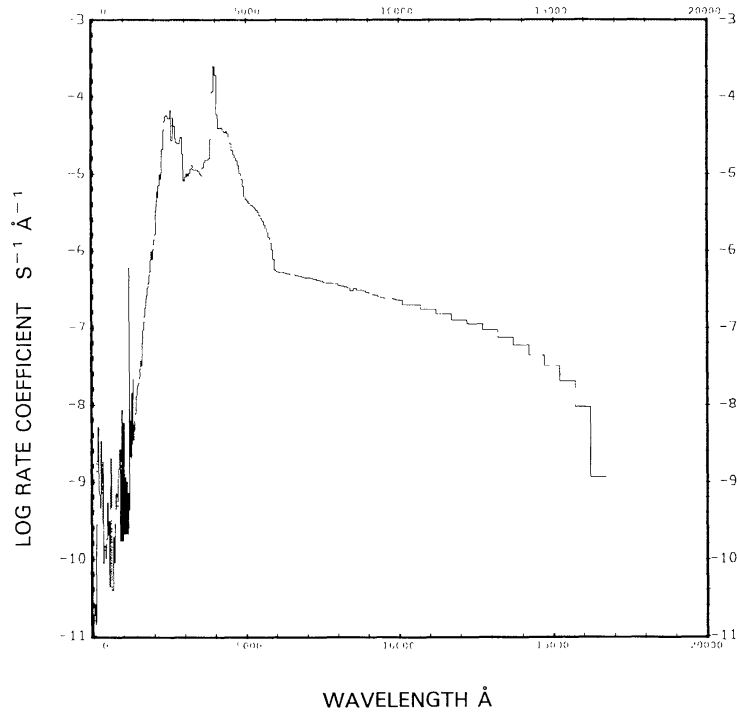


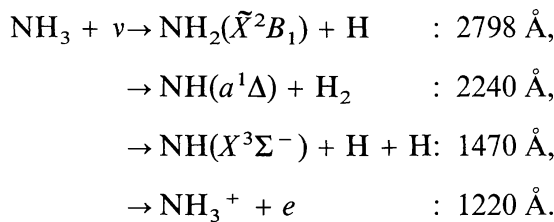
Fig. 134. INO + $\nu \rightarrow \text{I} + \text{NO}$, for the quiet Sun.

AMMONIA, NH₃

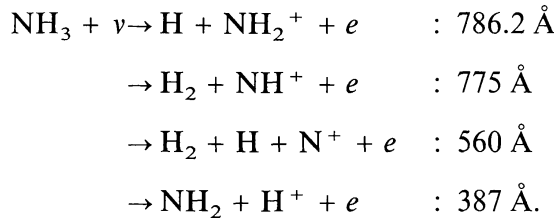
Cross sections: Up to 350 Å the cross section is synthesized from the fits for the atomic constituent cross sections made by Barfield *et al.* (1972). From 374.1 to 1306 Å the cross section was measured by Sun and Weissler (1955). The cross section in the overlap and extension to this wavelength range from 580 to 1650 Å was measured by Watanabe and Sood (1965). From 1650 to 2170 Å the cross section was measured by Watanabe (1954) and in the range from 2140 to 2330 Å it was measured by Thompson *et al.* (1963).

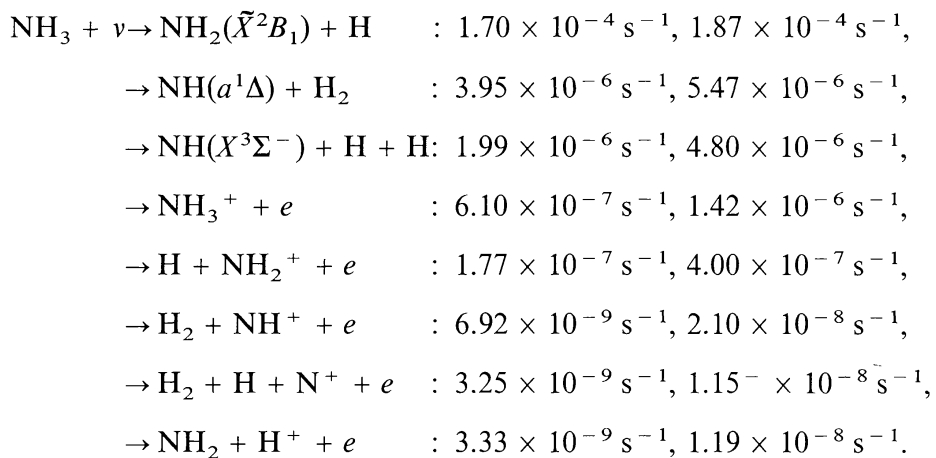
Branching ratios: Branching ratios between the dissociation paths are determined by Lilly *et al.* (1973) between 1048 and 1067 Å and at 1236 and 1470 Å, at 1236 and 1849 Å by McNesby *et al.* (1962), at 1640 Å by Okabe and Lenzi (1967), and at 2062 Å by Groth *et al.* (1968) and Schurath *et al.* (1969). The branching ratios for ionization and dissociative ionization are given by Kronebusch and Berkowitz (1976).

Thresholds: The threshold equivalent wavelengths for the dissociations and for simple ionization are summarized by Okabe (1978):

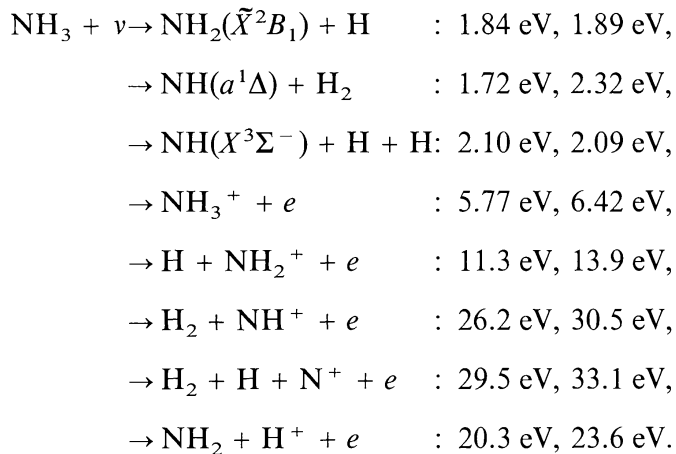


For dissociative ionization thresholds are given by Kronebusch and Berkowitz:



Rate coefficients:

The first value of each branch is for the quiet Sun (see Figures 135, 136, and 137(a) to 142(a)) and the second for the active Sun (see Figures 137(b) to 142(b)). For the quiet Sun, the total rate coefficient ($1.8 \times 10^{-4} \text{ s}^{-1}$) is between the values obtained by Potter and del Duca (1964) ($6.8 \times 10^{-5} \text{ s}^{-1}$) and by Jackson (1976a, b) ($4.8 \times 10^{-4} \text{ s}^{-1}$).

Excess energies:

The first value of each branch is for the quiet Sun, the second for the active Sun. Keller (1971) estimated 1.15 eV for the excess energy of the first of the above dissociation processes for the quiet Sun.

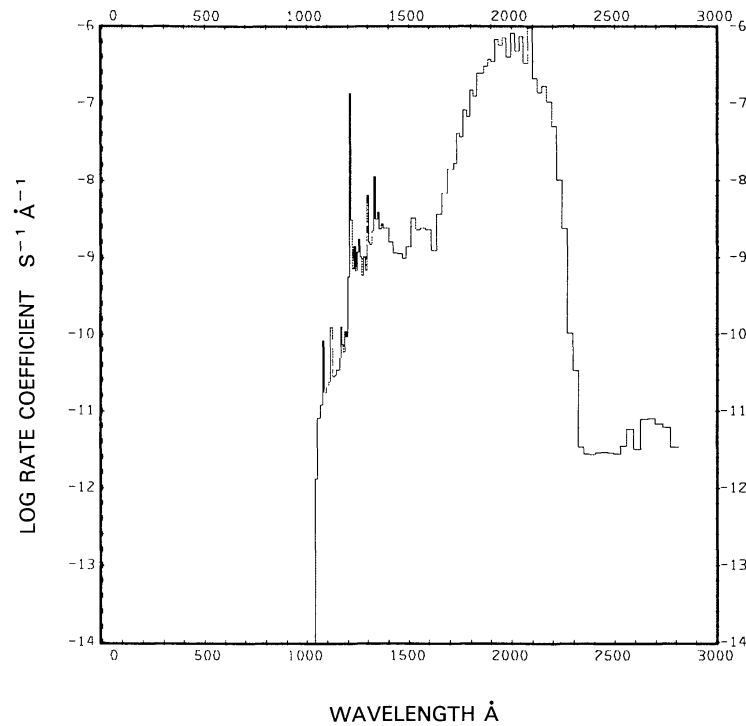


Fig. 135. NH₃ + ν → NH₂(X²B₁) + H, for the quiet Sun.

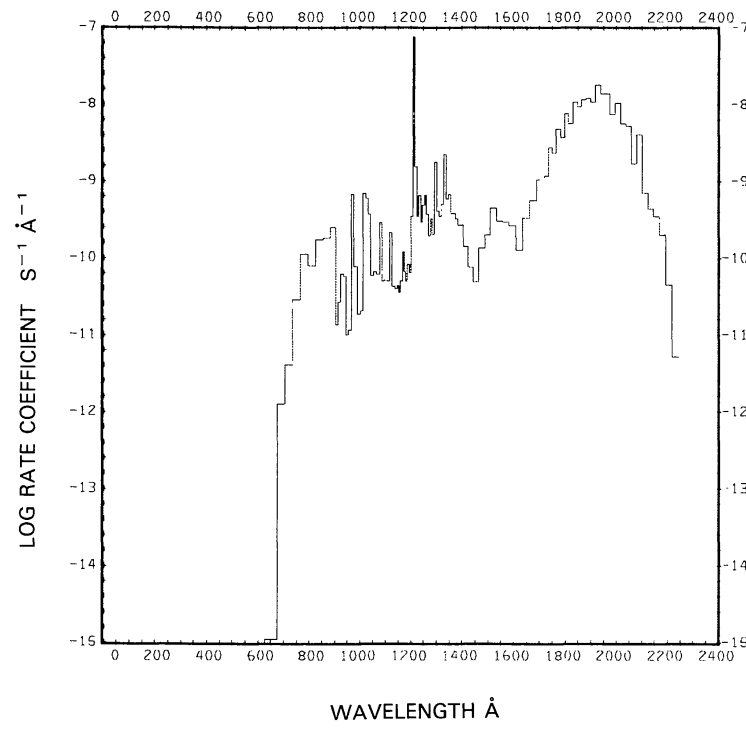
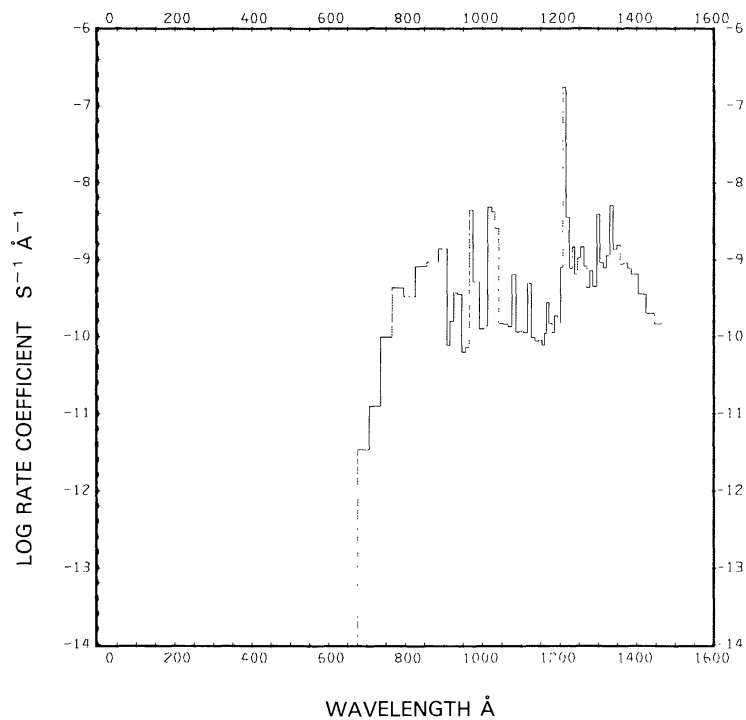
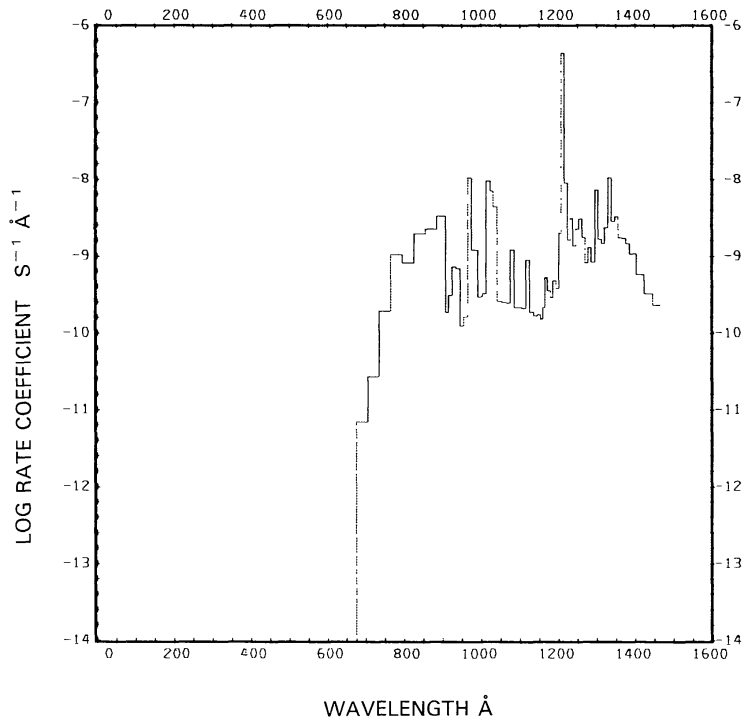


Fig. 136. NH₃ + ν → NH(a¹Δ) + H₂, for the quiet Sun.

Fig. 137a. NH₃ + ν → NH(X³Σ⁻) + H + H, for the quiet Sun.Fig. 137b. NH₃ + ν → NH(X³Σ⁻) + H + H, for the active Sun.

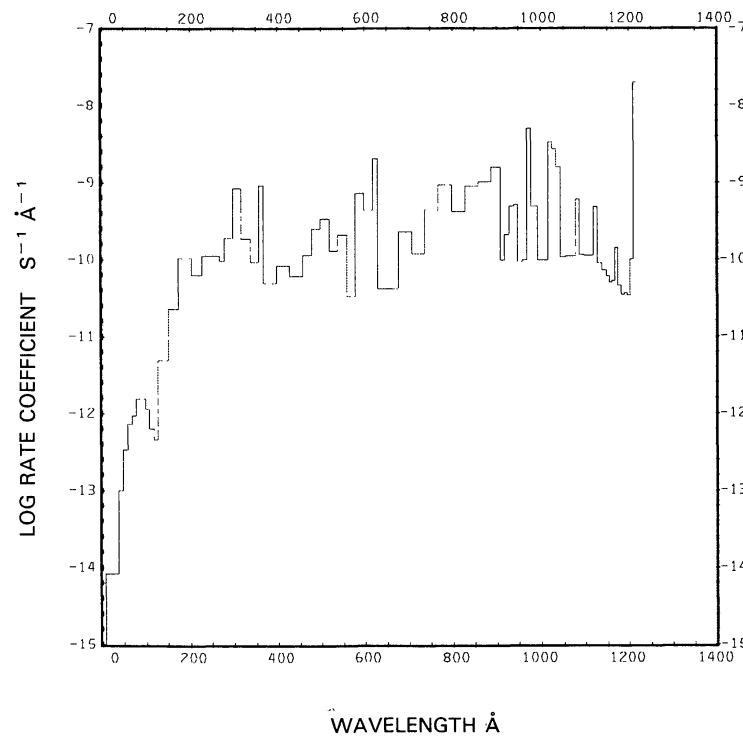


Fig. 138a. NH₃ + ν → NH₃⁺ + e, for the quiet Sun.

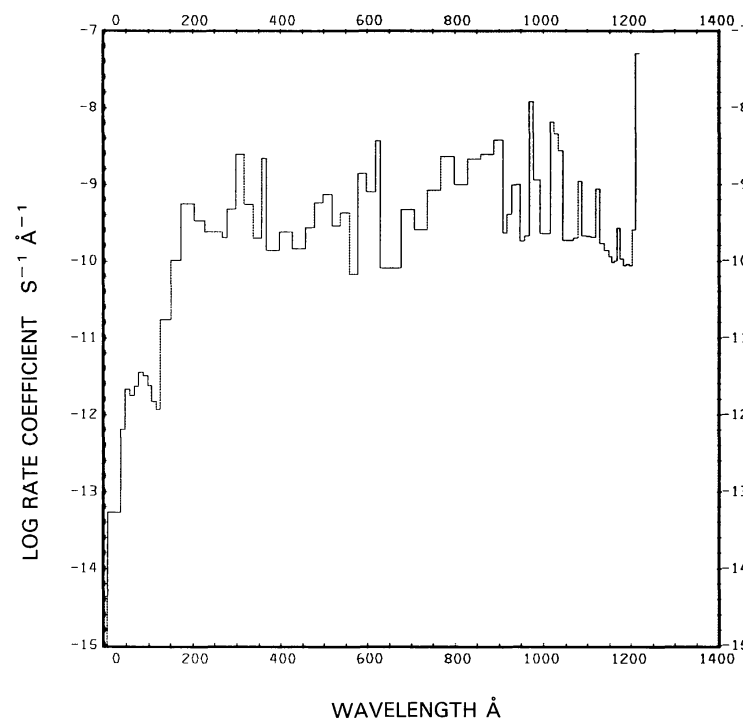
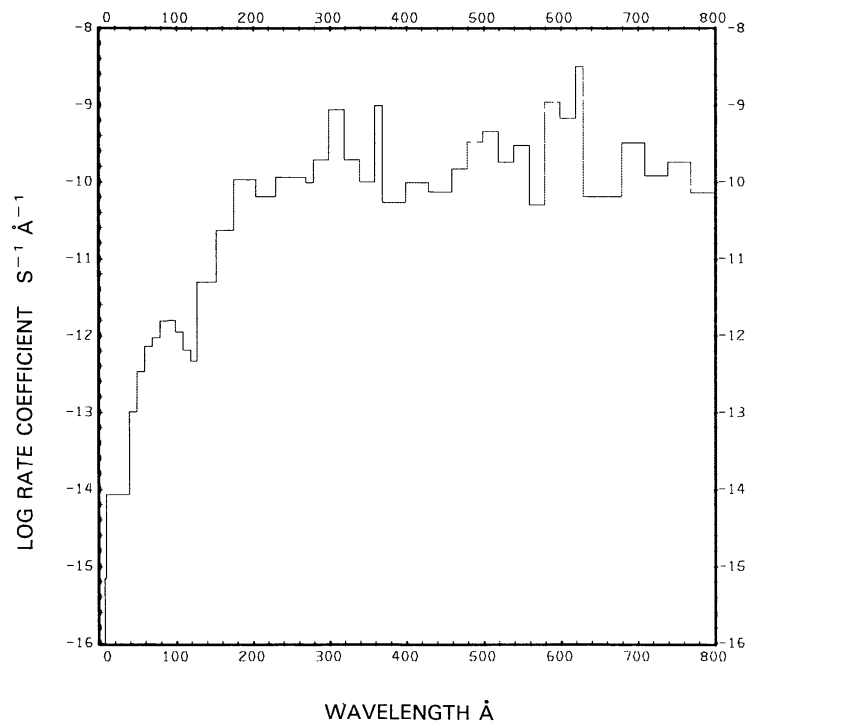
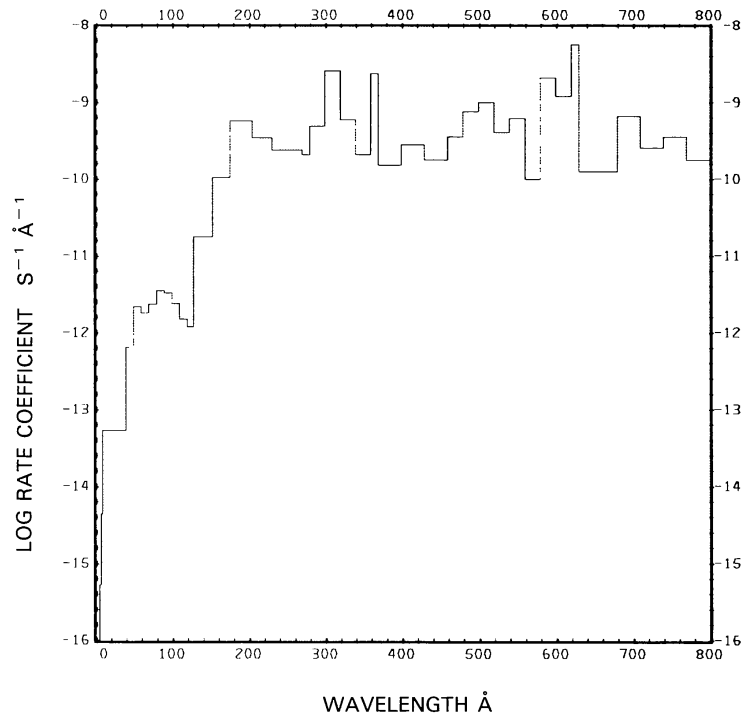
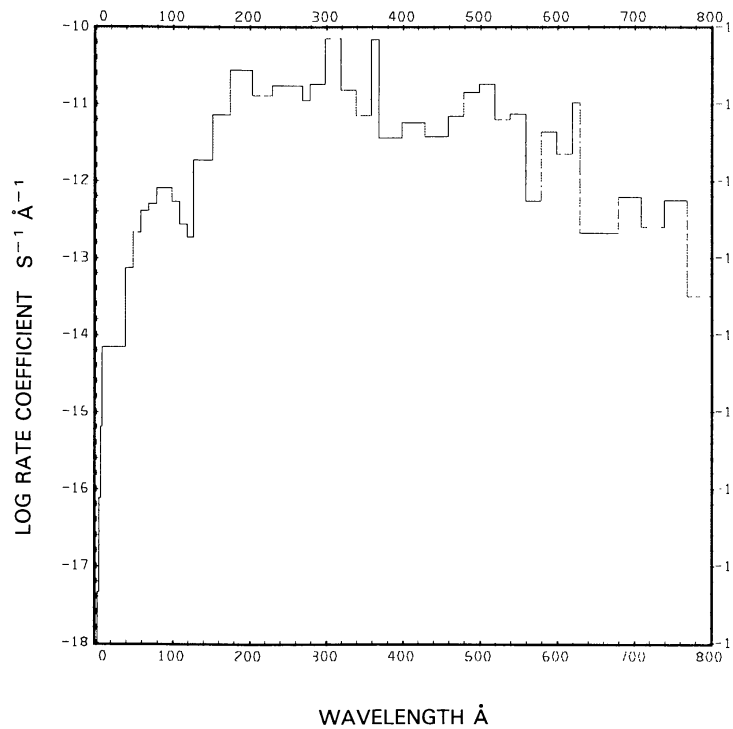
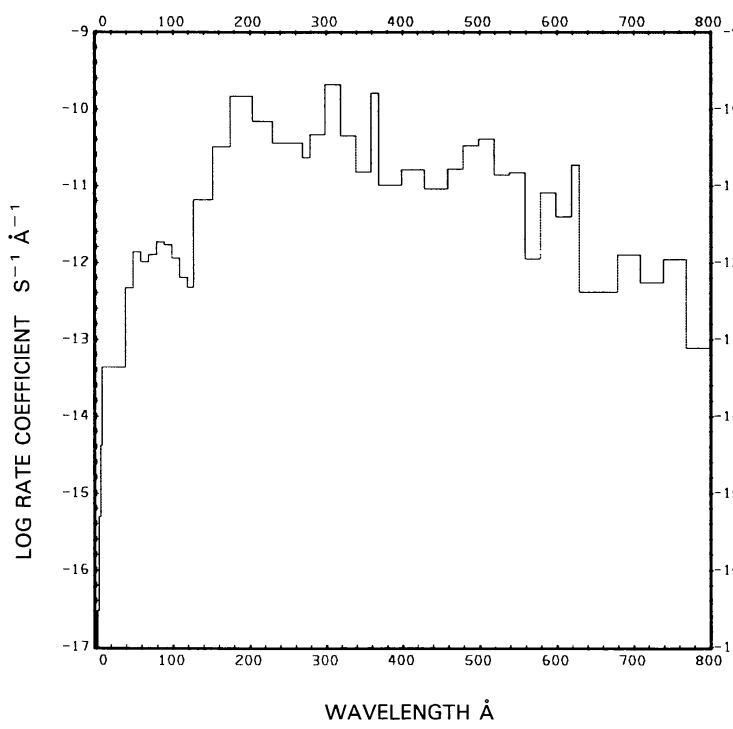
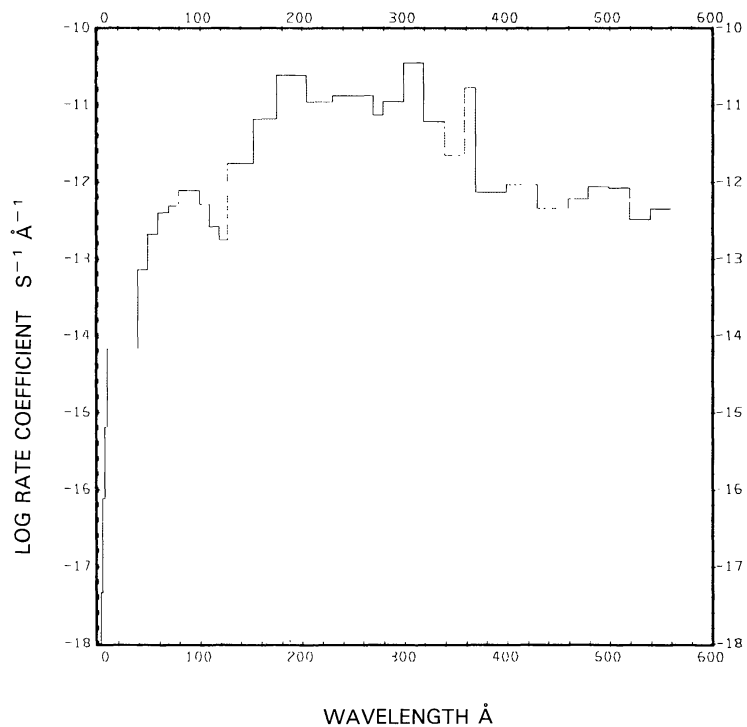
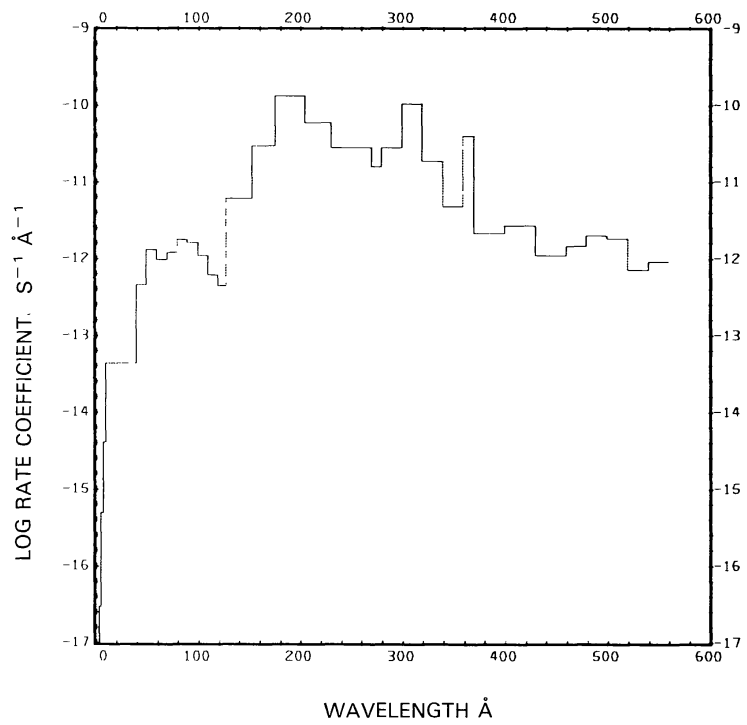
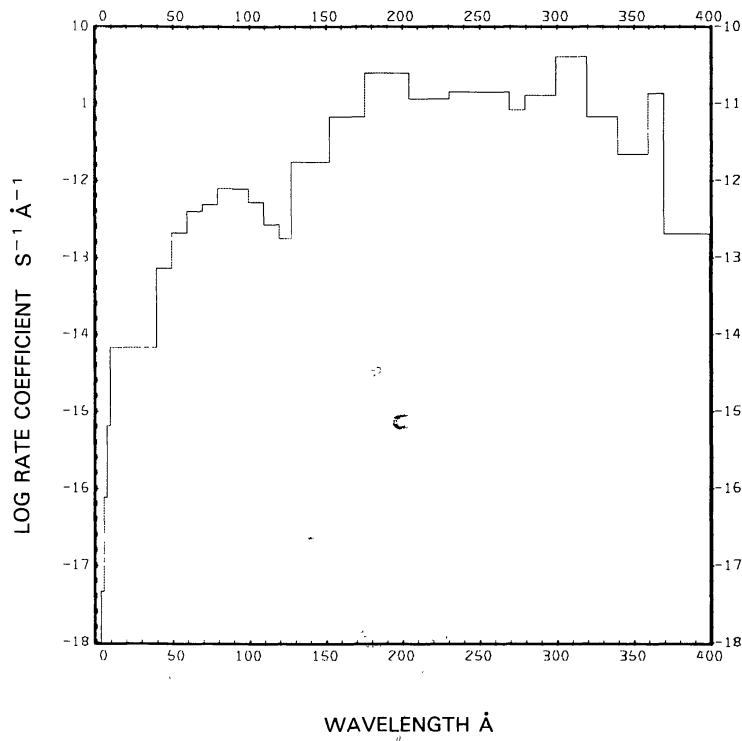
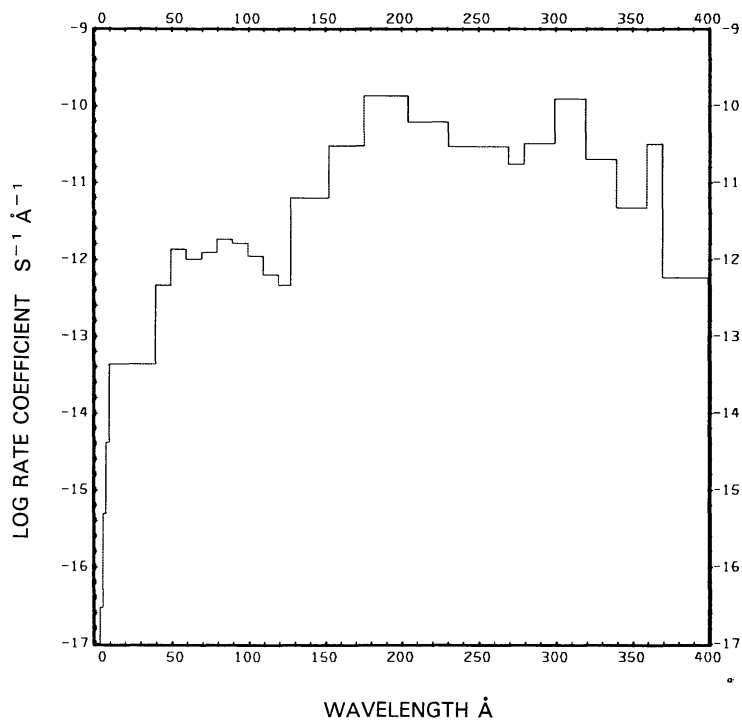


Fig. 138b. NH₃ + ν → NH₃⁺ + e, for the active Sun.

Fig. 139a. $\text{NH}_3 + \nu \rightarrow \text{H} + \text{NH}_2^+ + e$, for the quiet Sun.Fig. 139b. $\text{NH}_3 + \nu \rightarrow \text{H} + \text{NH}_2^+ + e$, for the active Sun.

Fig. 140a. NH₃ + $\nu \rightarrow$ H₂ + NH⁺ + e^- , for the quiet Sun.Fig. 140b. NH₃ + $\nu \rightarrow$ H₂ + NH⁺ + e^- , for the active Sun.

Fig. 141a. $\text{NH}_3 + \nu \rightarrow \text{H}_2 + \text{H} + \text{N}^+ + e$, for the quiet Sun.Fig. 141b. $\text{NH}_3 + \nu \rightarrow \text{H}_2 + \text{H} + \text{N}^+ + e$, for the active Sun.

Fig. 142a. NH₃ + $\nu \rightarrow$ NH₂ + H⁺ + e^- , for the quiet Sun.Fig. 142b. NH₃ + $\nu \rightarrow$ NH₂ + H⁺ + e^- , for the active Sun.

ACETYLENE, C₂H₂

Cross sections: In the range up to 500 Å the sum of the cross sections of the atomic constituents (Barfield *et al.*, 1972) approximates the molecular cross section. From $\lambda = 600$ to 1000 Å the cross section measured by Metzger and Cook (1964) was used. Values between 1050 and 2011 Å come from measurements made by Nakayama and Watanabe (1964).

Branching ratios: The branching ratio between dissociation and all ionization processes from $\lambda = 600$ to 1000 Å is taken from Schoen (1962) and in the range from $\lambda = 1050$ Å to the ionization threshold it is taken from Nakayama and Watanabe (1964). The ratio between branches producing C₂H + H and C₂ + H₂ is given at two wavelengths only: at $\lambda = 1470$ Å (Okabe, 1981) and at $\lambda = 1849$ Å (Okabe, 1983). The branching ratio to produce an excited state of C₂H₂ without dissociating has also been taken into account. For dissociative ionization the branching ratios are obtained from Schoen's data.

Thresholds: For the dissociation into C₂H + H the threshold given by Okabe (1975) is 2306 Å; for dissociation into C₂ + H₂ it is 2006 Å. The threshold for pure ionization is at $\lambda = 1086$ Å as given by Herzberg (1966). These threshold values are also in good agreement with those given by McDonald *et al.* (1978). The threshold for dissociative ionization was determined by Metzger and Cook (1964), it is at $\lambda = 697$ Å.

Rate coefficients:

$$\begin{aligned}
 \text{C}_2\text{H}_2 + v \rightarrow & \text{H} + \text{C}_2\text{H} : 1.02 \times 10^{-5} \text{ s}^{-1}, 1.86 \times 10^{-5} \text{ s}^{-1}, \\
 & \rightarrow \text{C}_2 + \text{H}_2 : 2.74 \times 10^{-6} \text{ s}^{-1}, 5.51 \times 10^{-6} \text{ s}^{-1}, \\
 & \rightarrow \text{C}_2\text{H}_2^+ + e : 7.80 \times 10^{-7} \text{ s}^{-1}, 1.74 \times 10^{-6} \text{ s}^{-1}, \\
 & \rightarrow \text{H} + \text{C}_2\text{H}^+ + e: 7.43 \times 10^{-8} \text{ s}^{-1}, 1.90 \times 10^{-7} \text{ s}^{-1}.
 \end{aligned}$$

The first value of each branch is for the quiet Sun (see Figures 143 and 144(a) to 146(a)), the second is for the active Sun (see Figures 144(b) to 146(b)). For the quiet Sun, the total photo rate coefficient for C₂H₂ is $1.4 \times 10^{-5} \text{ s}^{-1}$; it falls between the values obtained by Potter and del Duca (1964) ($6.5 \times 10^{-6} \text{ s}^{-1}$) and Jackson (1976a, b) ($1.7 \times 10^{-4} \text{ s}^{-1}$).

Excess energies:

$$\begin{aligned}
 \text{C}_2\text{H}_2 + v \rightarrow & \text{H} + \text{C}_2\text{H} : 3.16 \text{ eV}, 3.72 \text{ eV}, \\
 & \rightarrow \text{C}_2 + \text{H}_2 : 3.07 \text{ eV}, 3.36 \text{ eV}, \\
 & \rightarrow \text{C}_2\text{H}_2^+ + e : 5.06 \text{ eV}, 6.10 \text{ eV}, \\
 & \rightarrow \text{H} + \text{C}_2\text{H}^+ + e: 15.9 \text{ eV}, 20.2 \text{ eV}.
 \end{aligned}$$

The first value of each branch is for the quiet Sun, the second is for the active Sun. For the quiet Sun, Keller (1971) estimated 1.3 eV for the first of the above dissociation branches.

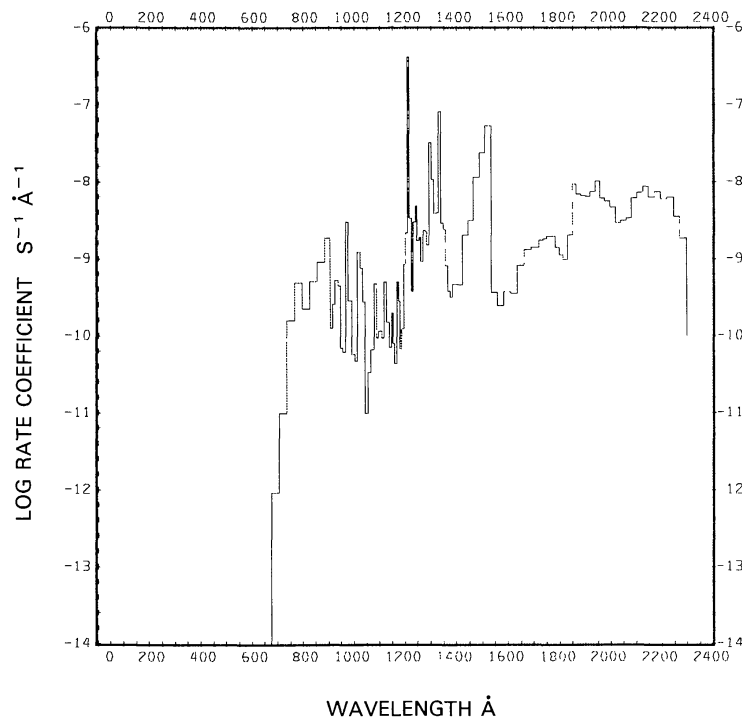
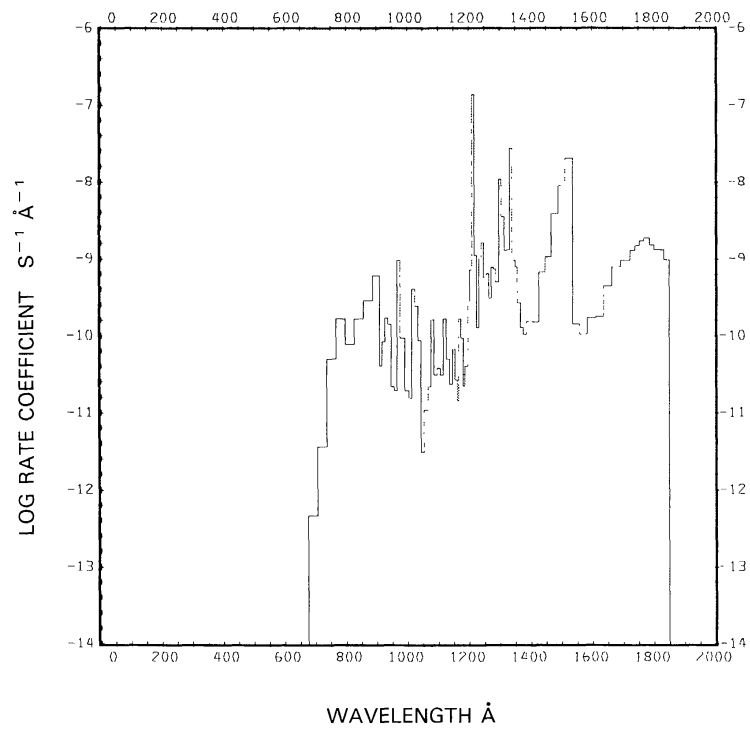
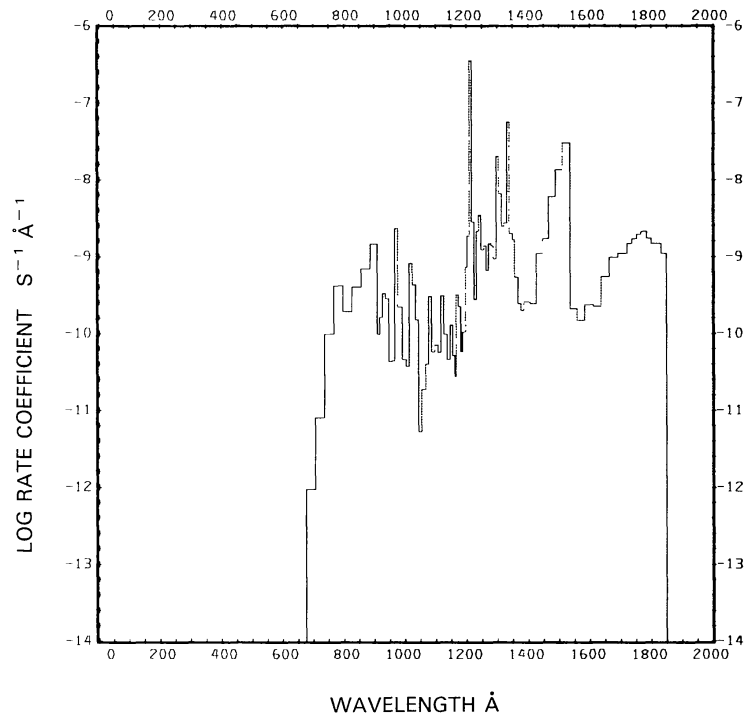


Fig. 143. C₂H₂ + ν → H + C₂H, for the quiet Sun.

Fig. 144a. $\text{C}_2\text{H}_2 + v \rightarrow \text{C}_2 + \text{H}_2$, for the quiet Sun.Fig. 144b. $\text{C}_2\text{H}_2 + v \rightarrow \text{C}_2 + \text{H}_2$, for the active Sun.

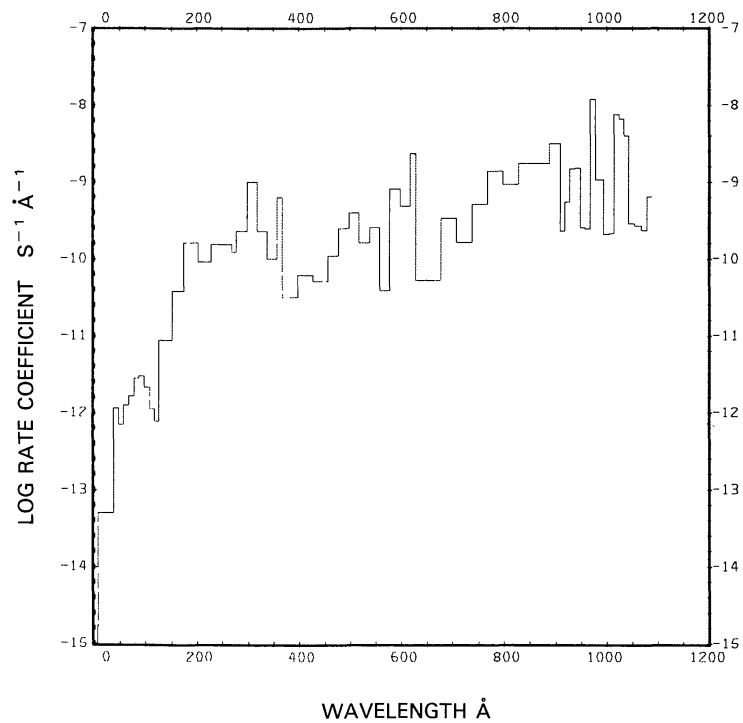


Fig. 145a. $\text{C}_2\text{H}_2 + \nu \rightarrow \text{C}_2\text{H}_2^+ + e$, for the quiet Sun.

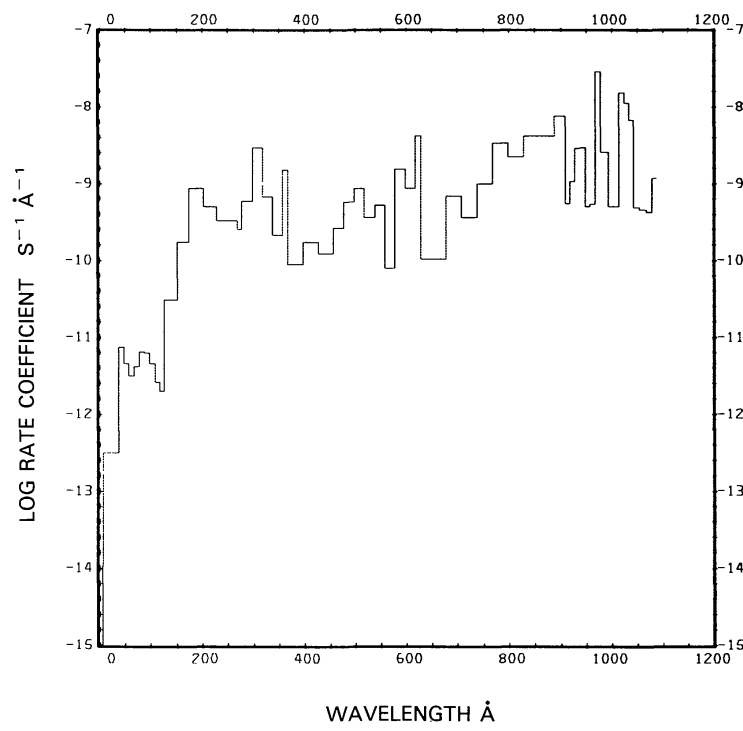


Fig. 145b. $\text{C}_2\text{H}_2 + \nu \rightarrow \text{C}_2\text{H}_2^+ + e$, for the active Sun.

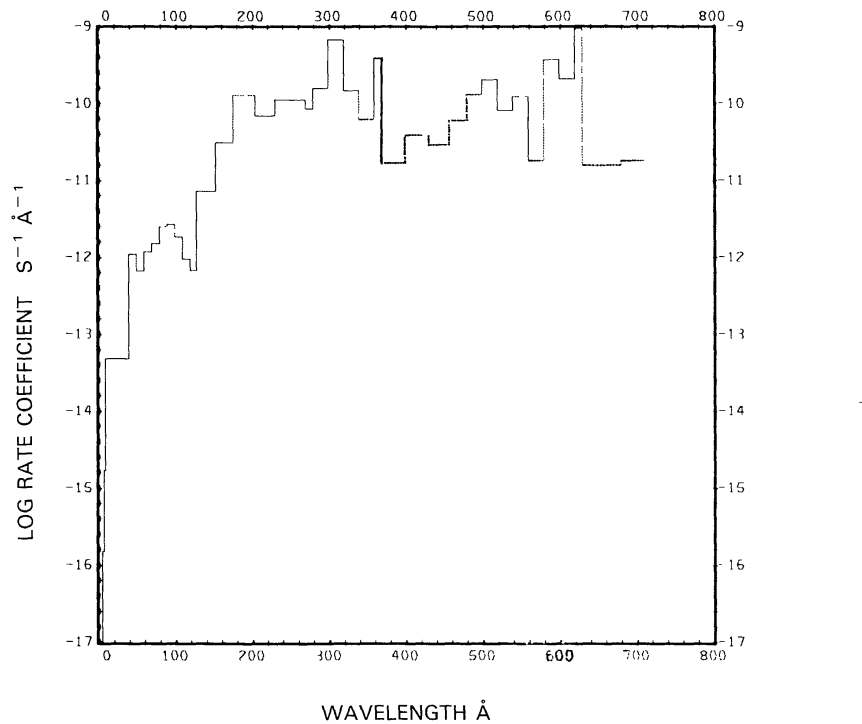


Fig. 146a. $\text{C}_2\text{H}_2 + \nu \rightarrow \text{H} + \text{C}_2\text{H}^+ + e$, for the quiet Sun.

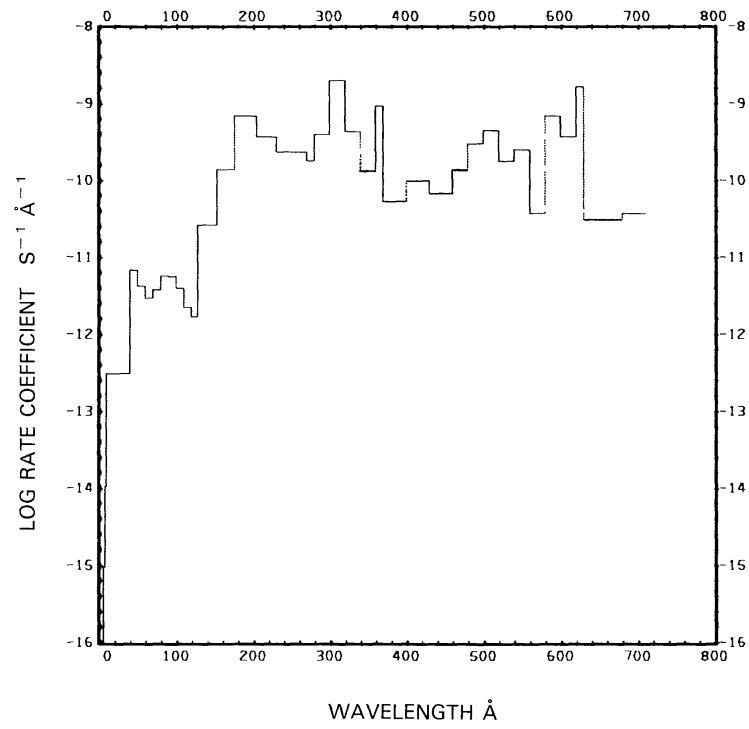


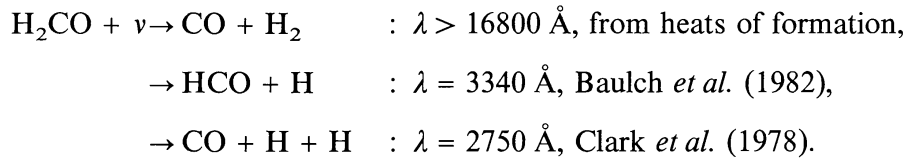
Fig. 146b. $\text{C}_2\text{H}_2 + \nu \rightarrow \text{H} + \text{C}_2\text{H}^+ + e$, for the active Sun.

FORMALDEHYDE, H₂CO

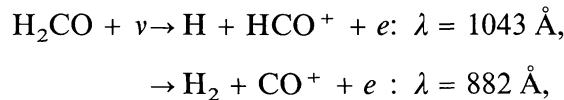
Cross sections: Up to 500 Å the molecular cross section is synthesized from the cross section fits (Barfield *et al.*, 1972) of the atomic constituents. Between $\lambda = 600$ and 1760 Å the cross section reported by Mentall *et al.* (1971) was used. The values of Gentieu and Mentall (1970) were used in the range $\lambda = 1760$ to 1850 Å. They are very similar to those of Suto *et al.* (1987), but preferred because of their higher resolution. The cross section from $\lambda = 2000$ to 2634.7 Å and from 3531.7 to 3740 Å comes from Calvert and Pitts (1966). Between 2634.7 and 3531.7 Å we used the measured cross section of Rogers (1990). Beyond 3740 Å the cross section is negligibly small.

Branching ratios: For dissociation forming CO + H₂ and HCO + H, the branching ratio in the range $\lambda = 2991$ to 3392 Å comes from Clark *et al.* (1978); a few values are also given by Calvert and Pitts (1966). The branching ratio for dissociation into CO + H + H is from Mentall *et al.* (1971) in the range $\lambda = 600$ to 1141.6 Å and from Stief *et al.* (1972) at 1236 and 1470 Å. Branching ratios for ionization and dissociative ionization are from Guyon *et al.* (1976) in the wavelength range 680 to 1043 Å and from Mentall *et al.* (1971) between $\lambda = 600$ and 1141.6 Å.

Thresholds: Dissociation thresholds are:

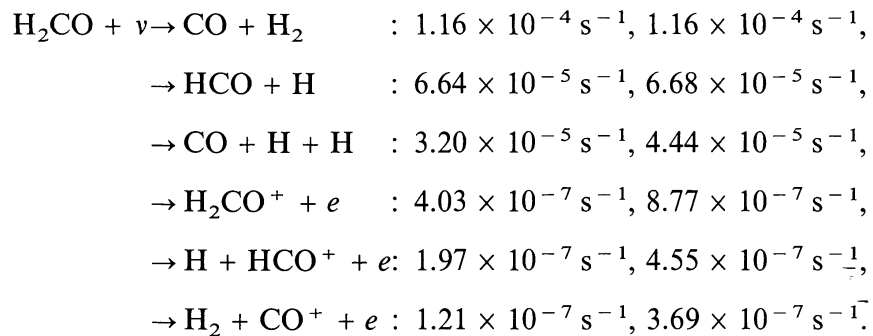


The ionization threshold at $\lambda = 1141.6$ Å and the dissociative ionization thresholds



were determined by Guyon *et al.* (1976).

Rate coefficients:

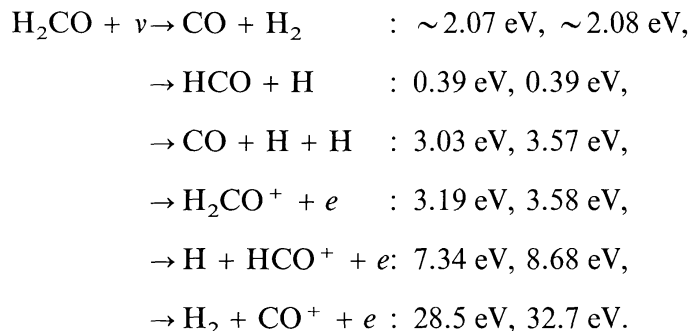


The first value of each branch is for the quiet Sun (see Figures 147 to 149 and 150(a) to 152(a)), the second for the active Sun (see Figures 150(b) to 152(b)). For the quiet Sun, Bauer and Bortner (1978) quote $1.5 \times 10^{-4} \text{ s}^{-1}$ for the first dissociation branch and $1.1 \times 10^{-4} \text{ s}^{-1}$ for the second branch. They do not mention the third branch. Their total dissociation rate coefficient ($2.6 \times 10^{-4} \text{ s}^{-1}$) is in reasonably good agreement with the sum of our three dissociation rates ($2.1 \times 10^{-4} \text{ s}^{-1}$).

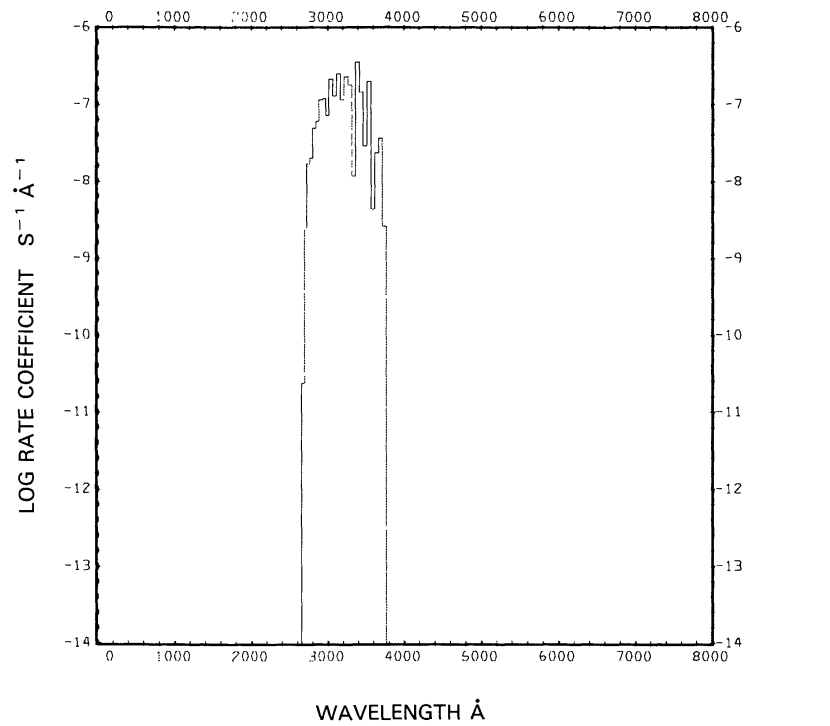
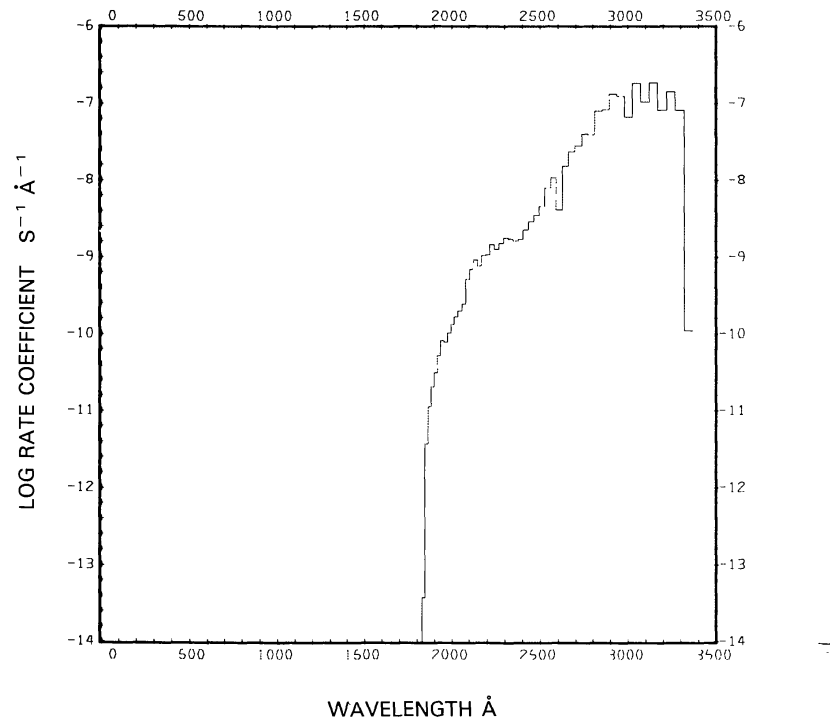
Using the less resolved cross section of Calvert and Pitts (1966) between 2634.7 and 3531.7 Å increases the rate coefficients for the first dissociation branch by about 40% and for the second branch by about 25%. The cross section of Bass *et al.* (1980) for the same wavelength range yields rate coefficients about 25% and 15% lower for the first and second dissociation branches, respectively, at a temperature of 223 K. At 296 K the differences are smaller.

Our total rate coefficient for the quiet Sun ($2.2 \times 10^{-4} \text{ s}^{-1}$) falls between the two values obtained by Jackson (1976a, b) ($5.3 \times 10^{-4} \text{ s}^{-1}$ and $1.8 \times 10^{-4} \text{ s}^{-1}$).

Excess energies:



The first value of each branch is for the quiet Sun, the second is for the active Sun.

Fig. 147. H₂CO + $\nu \rightarrow$ CO + H₂, for the quiet Sun.Fig. 148. H₂CO + $\nu \rightarrow$ HCO + H, for the quiet Sun.

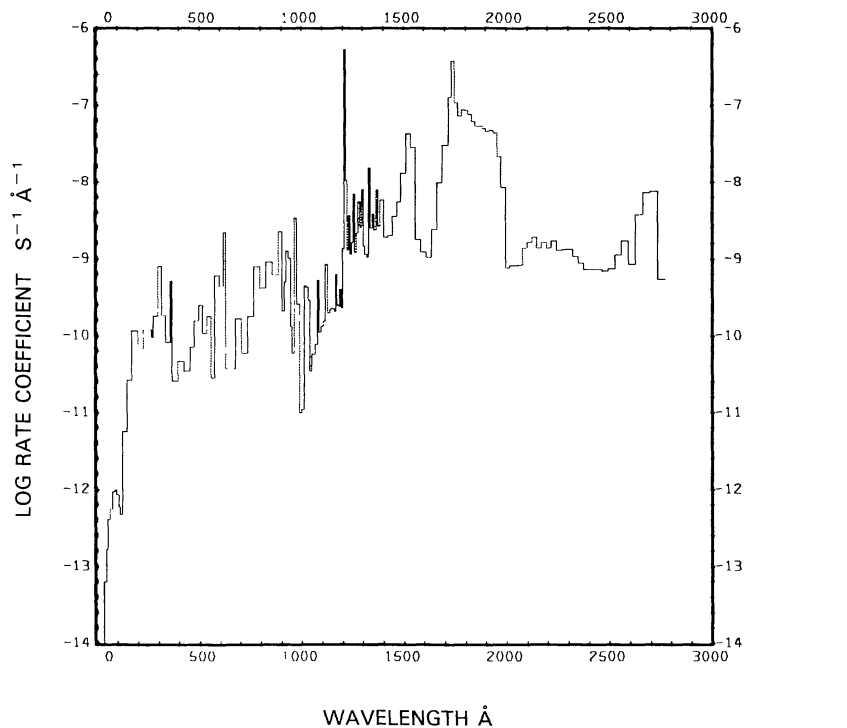
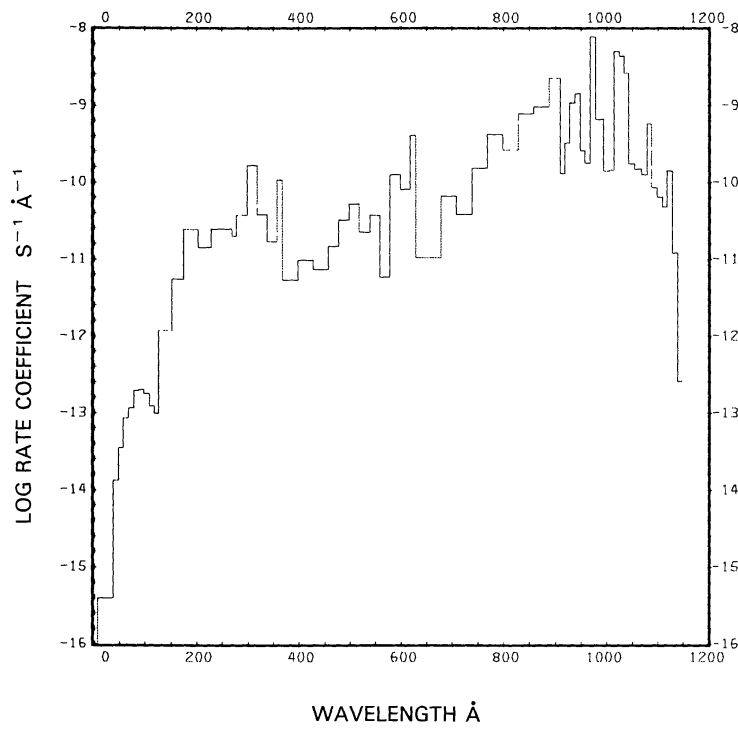
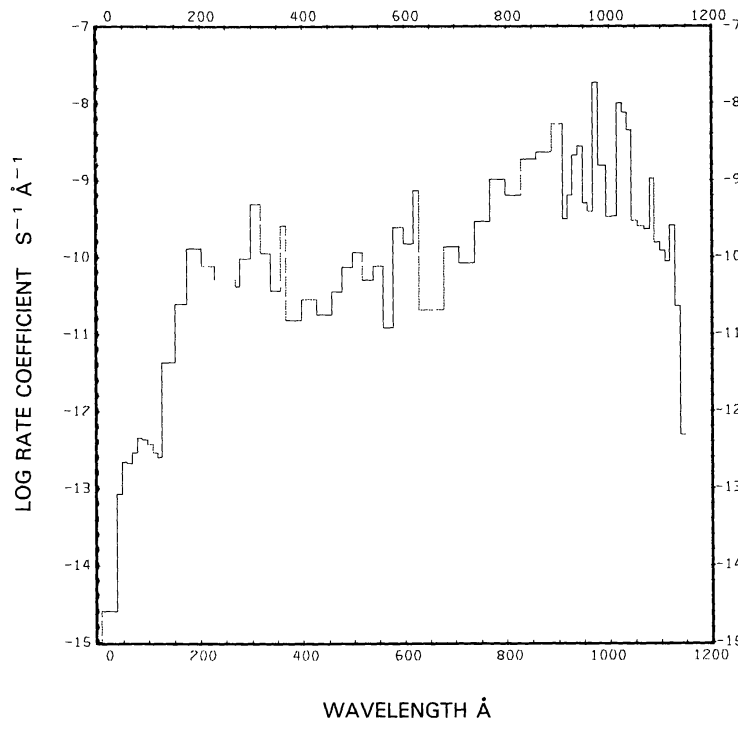
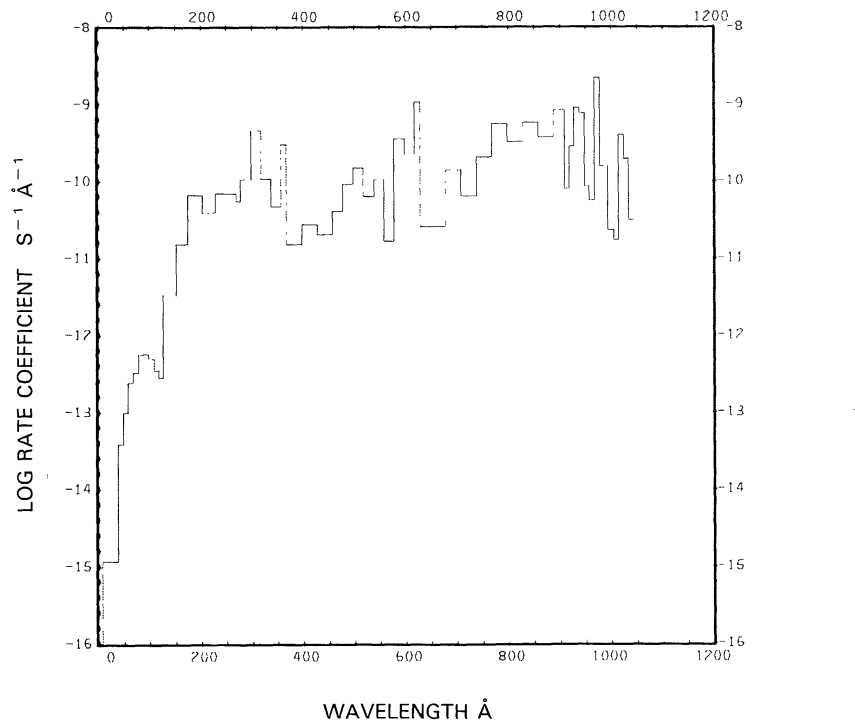
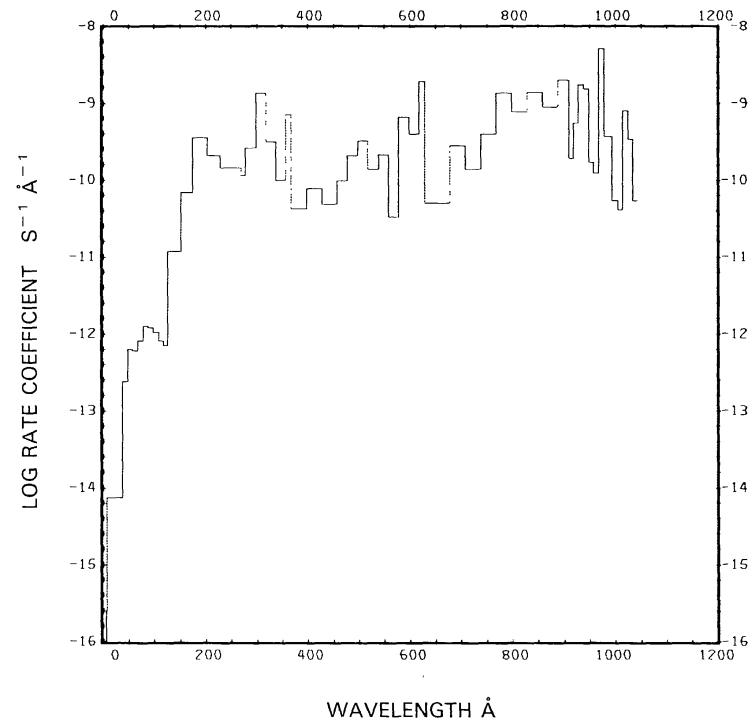
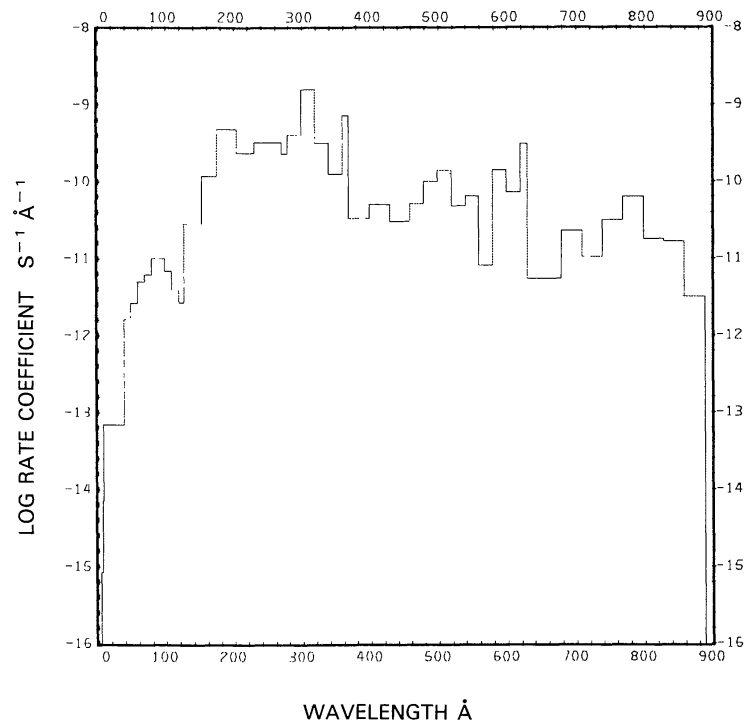
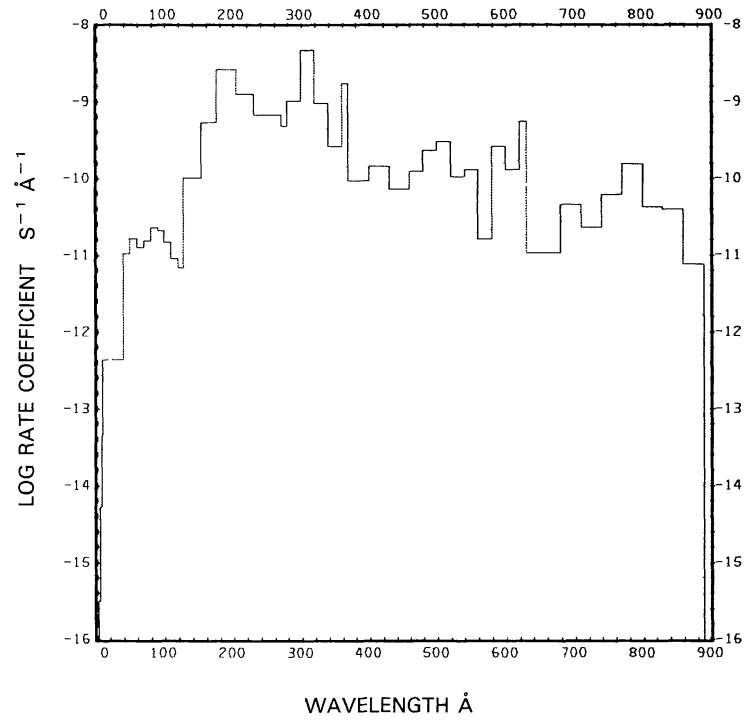


Fig. 149. $\text{H}_2\text{CO} + \nu \rightarrow \text{CO} + \text{H} + \text{H}$, for the quiet Sun.

Fig. 150a. H₂CO + $\nu \rightarrow$ H₂CO⁺ + e, for the quiet Sun.Fig. 150b. H₂CO + $\nu \rightarrow$ H₂CO⁺ + e, for the active Sun.

Fig. 151a. $\text{H}_2\text{CO} + \nu \rightarrow \text{H} + \text{HCO}^+ + e$, for the quiet Sun.Fig. 151b. $\text{H}_2\text{CO} + \nu \rightarrow \text{H} + \text{HCO}^+ + e$, for the active Sun.

Fig. 152a. H₂CO + $\nu \rightarrow$ H₂ + CO⁺ + e, for the quiet Sun.Fig. 152b. H₂CO + $\nu \rightarrow$ H₂ + CO⁺ + e, for the active Sun.

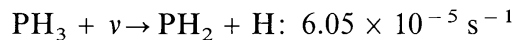
PHOSPHINE, PH₃

Cross sections: Up to 877 Å the cross section is synthesized from the fits for the constituent atomic cross sections of Barfield *et al.* (1972). From $\lambda = 1950$ to 3650 Å we used the cross section measured by Kley and Welge (1965). There is a considerable gap in the cross section below 1950 Å.

Branching ratios: The branching ratios are not known. We assumed that only dissociation into PH₂ + H occurs.

Thresholds: The dissociation energy equivalent wavelength is $\lambda = 3650$ Å as given by Okabe (1978).

Rate coefficients:



for the quiet Sun (see Figure 153) and $7.62 \times 10^{-5} \text{ s}^{-1}$ for the active Sun.

Excess energies: The excess energy for this reaction is 3.52 eV for the quiet Sun and 3.96 eV for the active Sun.

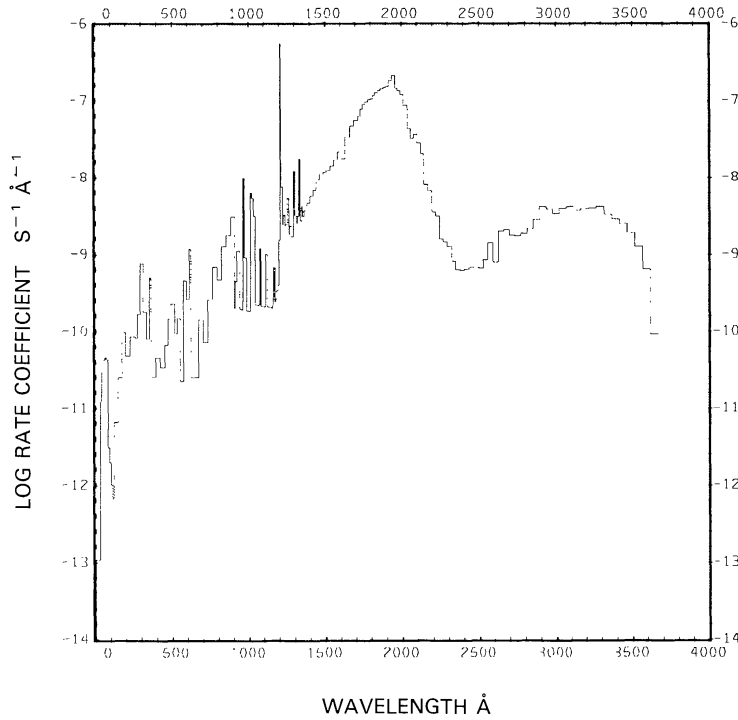


Fig. 153. $\text{PH}_3 + v \rightarrow \text{PH}_2 + \text{H}$, for the quiet Sun.

HYDROGEN PEROXIDE, H₂O₂

Cross sections: Up to 1000 Å the cross section is synthesized from fits for constituent atomic cross sections made by Barfield *et al.* (1972). From 1200 to 1950 Å the cross sections were measured by Lin *et al.* (1978) and from $\lambda = 1950$ to 3500 Å by Schürgers and Welge (1968). From 3500 Å to the dissociation limit the cross section is too small to be measured.

Branching ratios: The branching ratios are not known. We assumed that only dissociation into OH + OH occurs.

Thresholds: The wavelength equivalent for the dissociation energy to produce OH + OH is 5765 Å as quoted by Okabe (1978).

Rate coefficients:



for the quiet Sun (see Figure 154) and $1.48 \times 10^{-4} \text{ s}^{-1}$ for the active Sun.

Excess energies: The excess energy for this reaction is 3.01 eV for the quiet Sun and 3.48 eV for the active Sun.

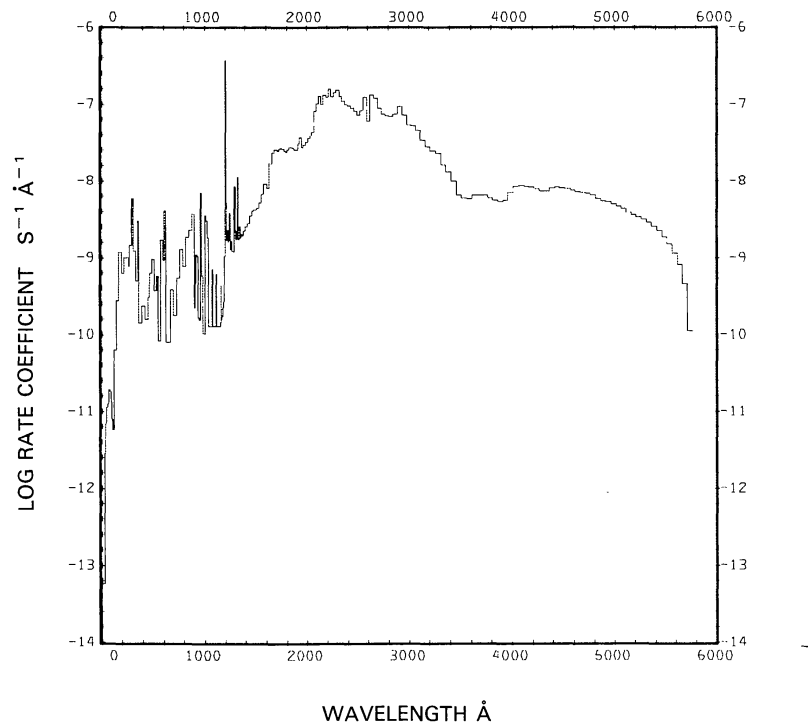


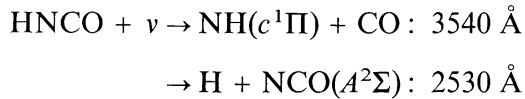
Fig. 154. H₂O₂ + $\nu \rightarrow \text{OH} + \text{OH}$, for the quiet Sun.

HYDROGEN ISOCYANATE (ISOCYANIC ACID), HNCO

Cross sections: Up to $\lambda = 627 \text{ \AA}$ the cross section is synthesized from fits of the constituent atomic cross sections prepared by Barfield *et al.* (1972). No cross section data are available from 627 to 1200 \AA . From $\lambda = 1200 \text{ \AA}$ to 2000 \AA the cross section was measured by Okabe (1970) and from 2100 to 2550 \AA by Dixon and Kirby (1968). The cross section is very small above 2550 \AA to the dissociation threshold.

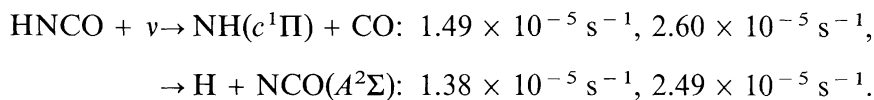
Branching ratios: The dissociation branching ratio is only known at $\lambda = 2062 \text{ \AA}$; there both dissociation processes have equal probability (Woolley and Back, 1968). The branching ratio leading to ionization is not known.

Thresholds: Dissociation energy equivalent wavelengths for the branches



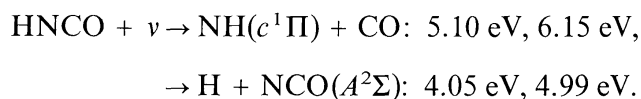
are obtained from Okabe (1978).

Rate coefficients:

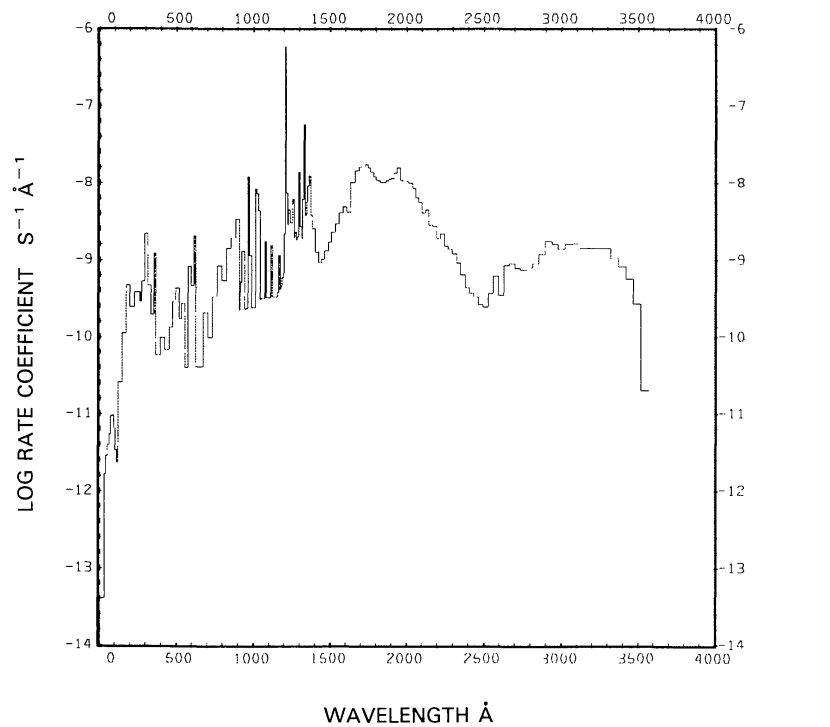
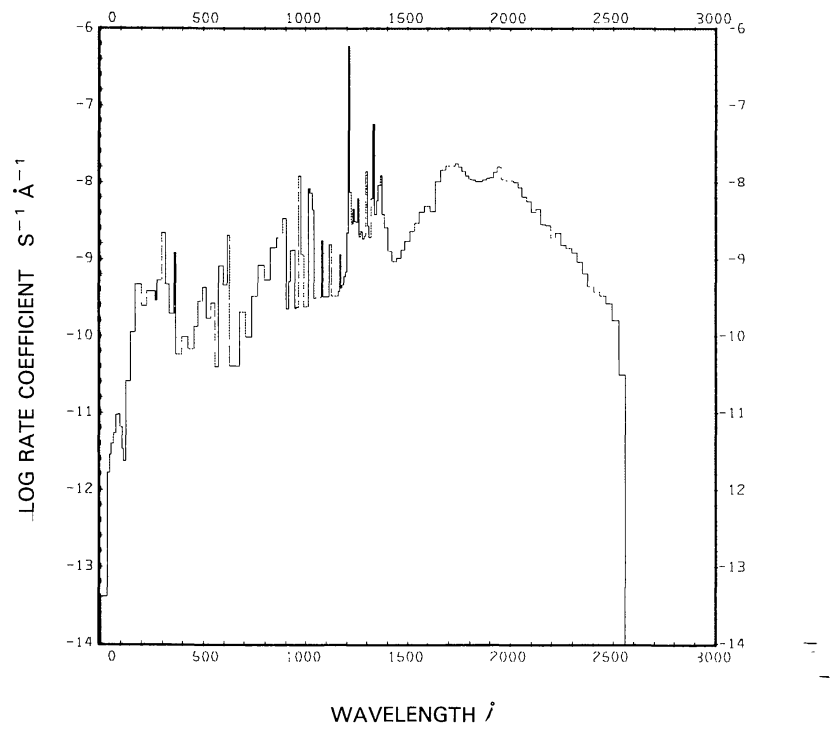


The first value of each branch is for the quiet Sun (see Figures 155 and 156), the second is for the active Sun.

Excess energies:



The first value of each branch is for the quiet Sun, the second is for the active Sun.

Fig. 155. $\text{HNCO} + \nu \rightarrow \text{NH}(c^1\Pi) + \text{CO}$, for the quiet Sun.Fig. 156. $\text{HNCO} + \nu \rightarrow \text{H} + \text{NCO}(A^2\Sigma)$, for the quiet Sun.

NITROUS ACID, HONO

Cross sections: Up to 940 Å the cross section is synthesized from the fits to the atomic constituent cross sections prepared by Barfield *et al.* (1972). In the wavelength ranges from 2000 to 3120 Å and 3900 to 4000 Å, the cross section of Cox and Derwent (1976) were used and from 3120 to 3900 Å the cross section of Stockwell and Calvert (1978) were used. No cross section data are available in the range 940 to 2000 Å; a straight line was used connecting the cross sections between these two values. Above 4000 Å the cross section is assumed to progressively decline to smaller values toward the dissociation threshold.

Branching ratios: The branching ratios are not known. We assumed that only dissociation into OH + NO occurs.

Thresholds: The wavelength equivalent threshold for dissociation into OH and NO is 5910 Å, as quoted by Baulch *et al.* (1982).

Rate coefficients:



See Figure 157. The rate coefficient is not sensitive to the activity of the Sun. It is $\sim 2.4 \times 10^{-3} \text{ s}^{-1}$ for the active Sun.

Excess energies: The excess energy for this reaction is about 1.7 eV for the quiet Sun and about 1.8 eV for the active Sun.

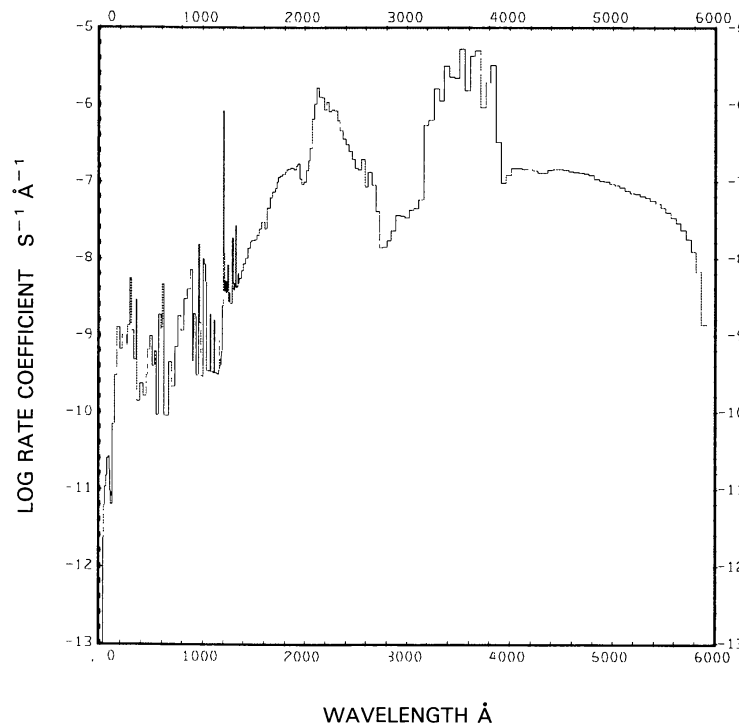


Fig. 157. $\text{HONO} + \nu \rightarrow \text{OH} + \text{NO}$, for the quiet Sun.

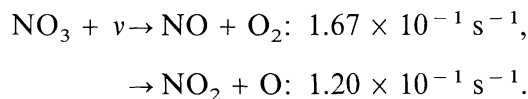
NITROGEN TRIOXIDE, NO₃

Cross sections: Up to 630 Å the cross section is synthesized from the fits prepared by Barfield *et al.* (1972) for the constituent atoms. In the wavelength range $\lambda = 4000$ to 7030 Å the cross section was measured by Graham and Johnston (1978). No cross section data are available in the range from 630 to 4000 Å; we used the cross section for NO₂ as a crude substitution for this range. From 7030 Å to threshold the cross section becomes progressively smaller starting from a value of 1×10^{-20} cm².

Branching ratios: From the data of Magnotta and Johnston (1980), the branching ratio is unity for the dissociation into NO₂ + O for wavelengths up to 5800 Å and then declines to zero at 5900 Å. We assumed the complement to unity for dissociation into NO + O₂. Branching ratios leading to ionization are not known.

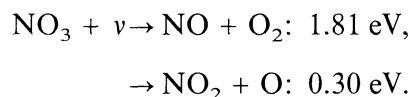
Thresholds: The wavelength equivalent dissociation limit to produce NO and O₂ is at 90 000 Å and to produce NO₂ + O it is 5900 Å according to Okabe (1978). Baulch *et al.* (1982) quote 5800 Å for the latter value, but then quote branching ratios applicable up to 5900 Å. We assumed 5900 Å for the threshold.

Rate coefficients:

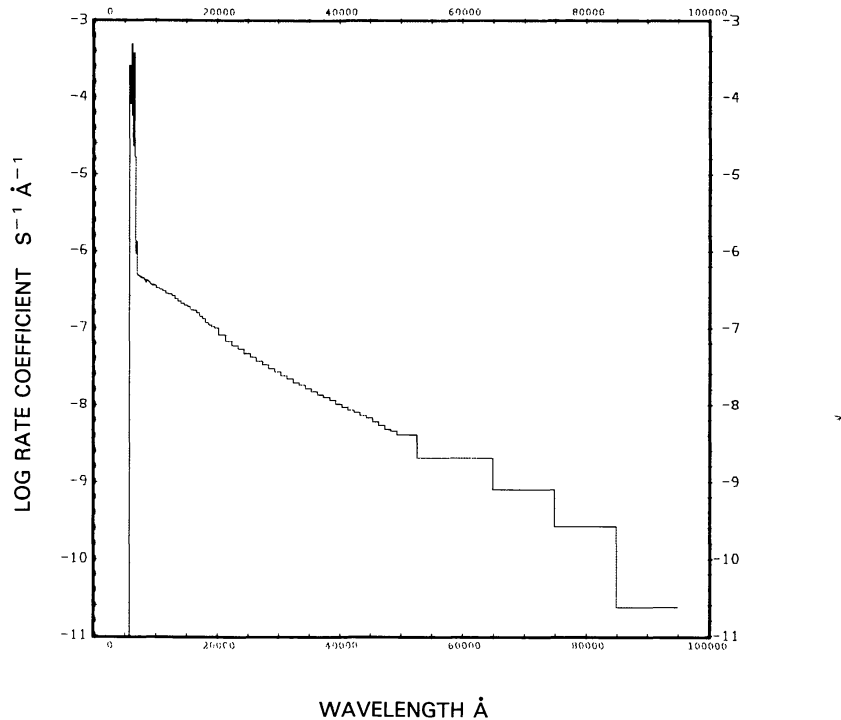
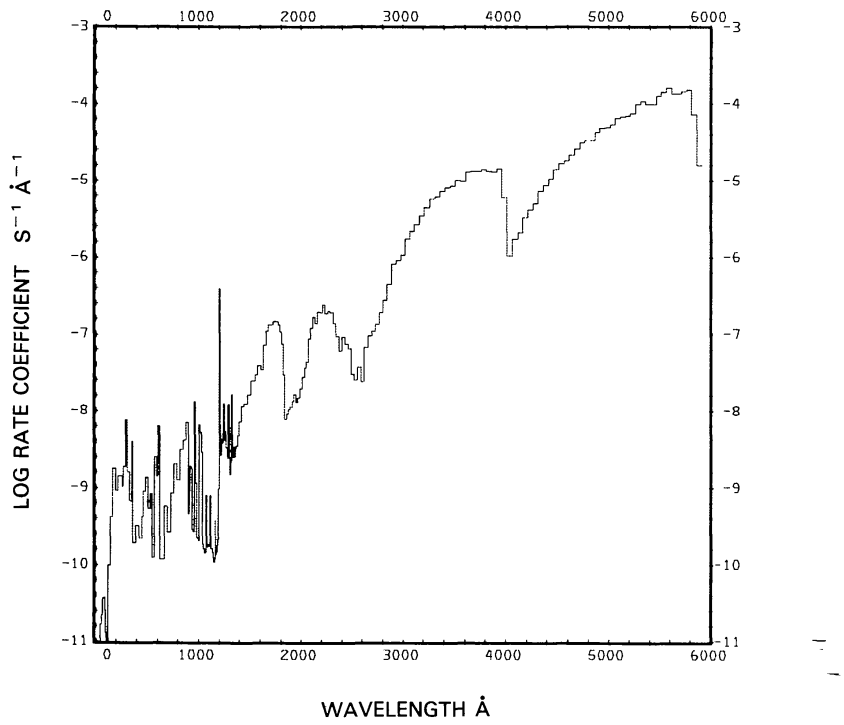


See Figures 158 and 159. The rate coefficients are insensitive to the activity of the Sun. Magnotta and Johnston (1980) quote for the overhead Sun at the Earth's surface $2.2 \times 10^{-2} \text{ s}^{-1}$ for the first of these processes and $1.8 \times 10^{-1} \text{ s}^{-1}$ for the second, limiting the cross sections to the wavelength region from $\lambda = 4700$ to 7000 Å.

Excess energies:



The excess energies are insensitive to the activity of the Sun.

Fig. 158. NO₃ + $\nu \rightarrow$ NO + O₂, for the quiet Sun.Fig. 159. NO₃ + $\nu \rightarrow$ NO₂ + O, for the quiet Sun.

CARBONYL FLUORIDE, COF₂

Cross sections: Up to a wavelength of 625.8 Å the cross section data are synthesized from fits prepared by Barfield *et al.* (1972) for the individual constituent atoms. At 1849 Å we used the value quoted by Baulch *et al.* (1982). In the wavelength region from $\lambda = 1860$ to 2186 Å cross sections published by DeMore *et al.* (1982) were used; these are the same as published by Baulch *et al.* (1984).

Branching ratios: The branching ratios are not known. We assumed that only dissociation into COF + F occurs.

Thresholds: The dissociation threshold to produce COF + F, which is apparently the only branch, is at $\lambda = 2220$ Å as quoted by Baulch *et al.* (1984).

Rate coefficients:



for the quiet Sun (see Figure 160) and $\sim 3.9 \times 10^{-5} \text{ s}^{-1}$ for the active Sun.

Excess energies: The excess energy for this reaction is about 4.1 eV for the quiet Sun and about 5.3 eV for the active Sun.

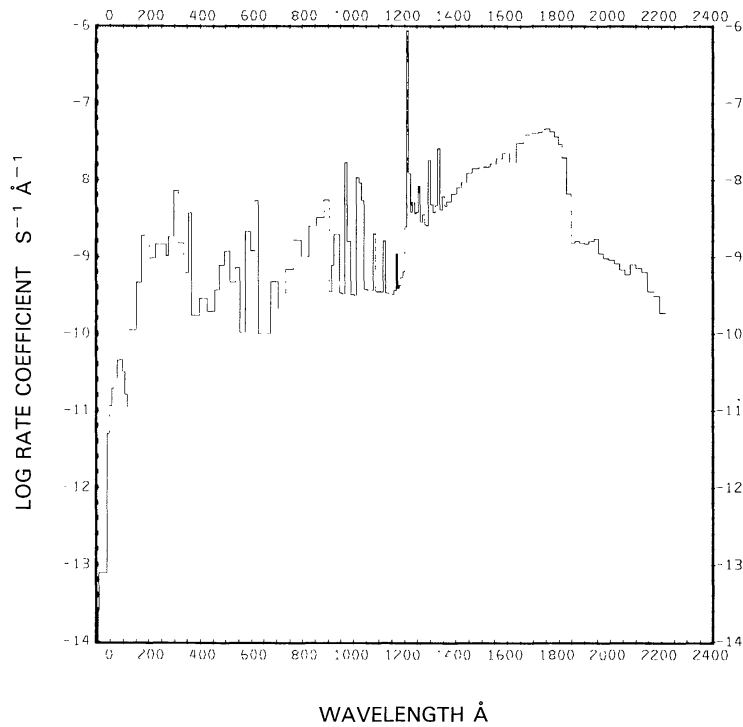


Fig. 160. COF₂ + $\nu \rightarrow$ COF + F, for the quiet Sun.

NITRYL CHLORIDE, ClNO_2

Cross sections: Up to wavelength $\lambda = 622.5 \text{ \AA}$ the cross section is synthesized from the fits of the constituent atomic cross sections prepared by Barfield *et al.* (1972). In the wavelength region from $\lambda = 1850$ to 2600 \AA we used the cross sections from Illies and Takacs (1976) and from $\lambda = 2700$ to 3700 \AA we used the data from Nelson and Johnston (1981). Between 622.5 and 1850 \AA no cross section data are available. We used a straight line to connect these points. Beyond 3700 \AA the cross section becomes very small.

Branching ratios: The branching ratios are not known. We assumed that only dissociation into $\text{Cl} + \text{NO}_2$ occurs.

Thresholds: The wavelength equivalent dissociation energy is given by Illies and Takacs as $\lambda = 8520 \text{ \AA}$.

Rate coefficients:



for the quiet Sun (see Figure 161) and $\sim 3.0 \times 10^{-3} \text{ s}^{-1}$ for the active Sun.

Excess energies: The excess energy for this reaction is about 2.8 eV for the quiet Sun and about 2.9 eV for the active Sun.

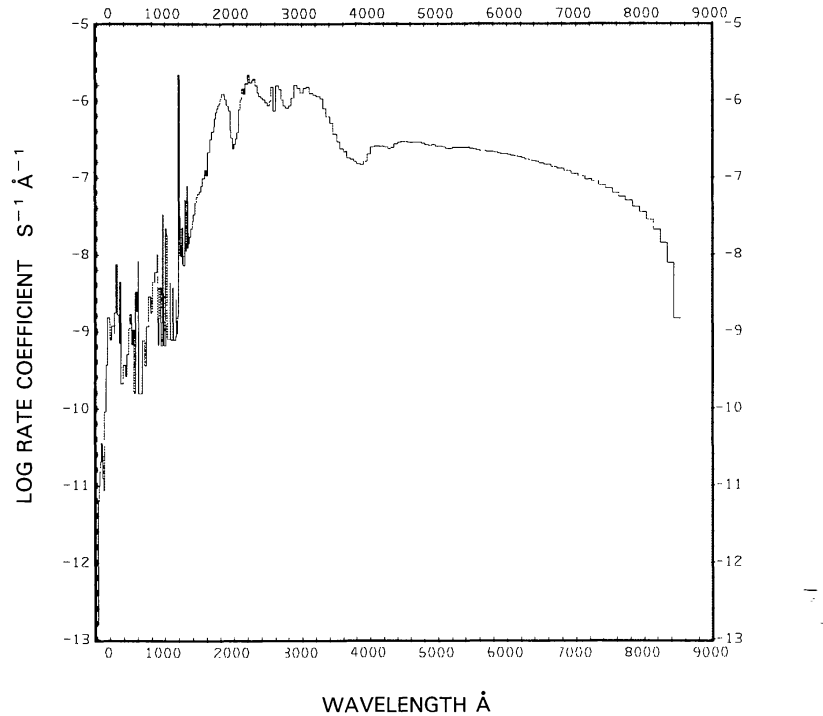


Fig. 161. $\text{ClNO}_2 + v \rightarrow \text{Cl} + \text{NO}_2$, for the quiet Sun.

CHLORINE NITRITE, ClONO

Cross sections: Up to wavelength $\lambda = 622.5 \text{ \AA}$ the cross section is synthesized from fits prepared by Barfield *et al.* (1972) for the constituent atoms. In the wavelength range from 2350 to 4000 \AA the cross section has been measured by Molina and Molina (1977). No cross section data exist between 622.5 and 2350 \AA ; we assumed a straight line connecting cross sections at these points. Above 4000 \AA the cross section becomes very small.

Branching ratios: The branching ratios are not known. We assumed that only dissociation into $\text{Cl} + \text{NO}_2$ occurs.

Thresholds: The wavelength equivalent dissociation energy is about 17000 \AA as obtained from heats of formation.

Rate coefficients:

$$\text{ClONO} + \nu \rightarrow \text{Cl} + \text{NO}_2: \sim 1.1 \times 10^{-2} \text{ s}^{-1}.$$

See Figure 162. The rate coefficient is insensitive to the activity of the Sun. Molina and Molina (1977) quote a rate coefficient for the overhead Sun at the Earth's surface of $5.0 \times 10^{-3} \text{ s}^{-1}$.

Excess energies: The excess energy for this reaction is about 3.4 eV and is insensitive to the activity of the Sun.

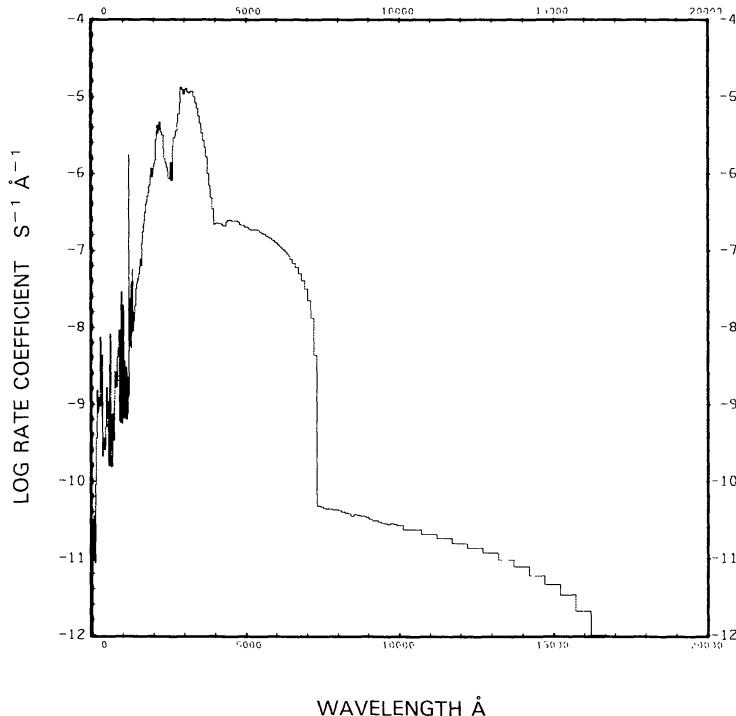


Fig. 162. $\text{ClONO} + \nu \rightarrow \text{Cl} + \text{NO}_2$, for the quiet Sun.

CARBONYL CHLOROFLUORIDE, COFCl

Cross sections: Up to wavelength $\lambda = 625.8 \text{ \AA}$ the cross section is synthesized from fits prepared by Barfield *et al.* (1972) for the constituent atoms. In the range from 1860 to 2260 \AA the cross section has been taken from the compilation of Baulch *et al.* (1982). No data exist in the region from 626 to 1860 \AA . Above 2260 \AA the cross section becomes very small.

Branching ratios: The branching ratios are not known. We assumed that only dissociation into Cl + COF occurs.

Thresholds: The dissociation threshold quoted by Baulch *et al.* (1982) is at $\lambda = 3160 \text{ \AA}$.

Rate coefficients:



for the quiet Sun (see Figure 163) and $\sim 1.0 \times 10^{-4} \text{ s}^{-1}$ for the active Sun.

Excess energies: The excess energy for this reaction is about 2.9 eV for the quiet Sun and about 4.0 eV for the active Sun.

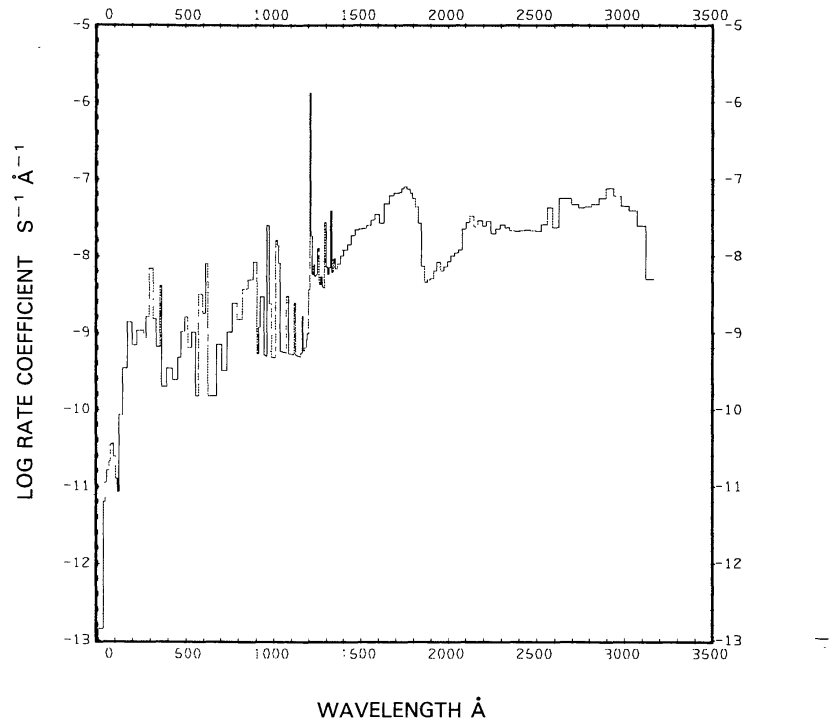


Fig. 163. $\text{COFCl} + v \rightarrow \text{Cl} + \text{COF}$, for the quiet Sun.

CHLORINE TRIOXIDE, ClO_3

Cross sections: Up to 662.5 Å the cross section is synthesized from the fits prepared by Barfield *et al.* (1972) for the constituent atoms. In the wavelength range from $\lambda = 2000$ to 3500 Å the cross section has been measured by Goodeve and Richardson (1937). No cross section values are available between 663 and 2000 Å; we assumed a straight line connecting these values.

Branching ratios: The branching ratios are not known. We assumed that only dissociation into $\text{ClO}_2 + \text{O}$ occurs.

Thresholds: The dissociation energy is unknown, we assumed an equivalent wavelength value of 3500 Å.

Rate coefficients:



See Figure 164. The rate coefficient is insensitive to the activity of the Sun.

Excess energies: The excess energy for this reaction is about 0.59 eV for the quiet Sun and about 0.60 eV for the active Sun.

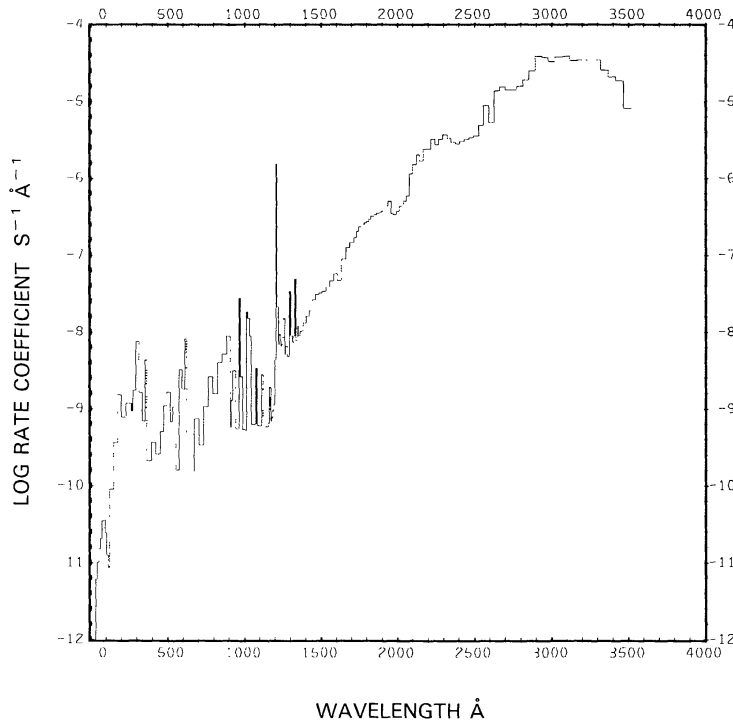


Fig. 164. $\text{ClO}_3 + \nu \rightarrow \text{ClO}_2 + \text{O}$, for the quiet Sun.

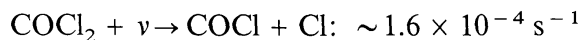
PHOSGENE, COCl_2

Cross sections: Up to 625.8 Å the cross section is synthesized from the fits to the constituent atomic cross sections prepared by Barfield *et al.* (1972). In the wavelength range from $\lambda = 1170$ to 1600 Å the cross section has been measured by Okabe *et al.* (1971). From $\lambda = 1849$ to 2260 Å we used the cross section data compiled by Baulch *et al.* (1982) and from $\lambda = 2300$ to 2900 Å we used the measurements of Moule and Foo (1971).

Branching ratios: The branching ratios are not known. We assumed that only dissociation into $\text{COCl} + \text{Cl}$ occurs.

Thresholds: For the dissociation threshold equivalent wavelength we used $\lambda = 3690$ Å, the value quoted by Baulch *et al.* (1982).

Rate coefficients:



for the quiet Sun (see Figure 165) and $\sim 2.1 \times 10^{-4} \text{ s}^{-1}$ for the active Sun.

Excess energies: The excess energy for this reaction is about 3.3 eV for the quiet Sun and about 4.1 eV for the active Sun.

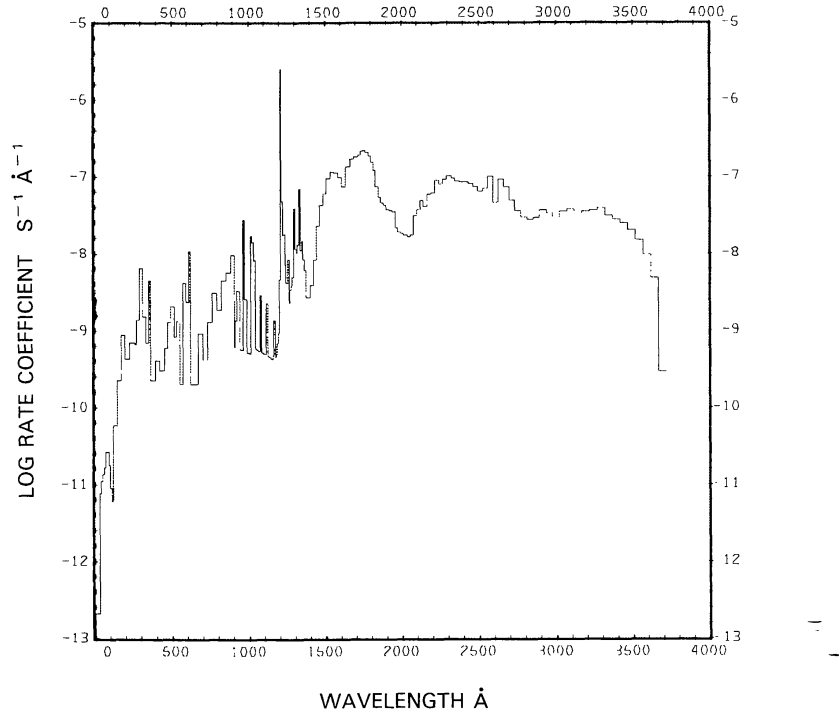


Fig. 165. $\text{COCl}_2 + \nu \rightarrow \text{COCl} + \text{Cl}$, for the quiet Sun.

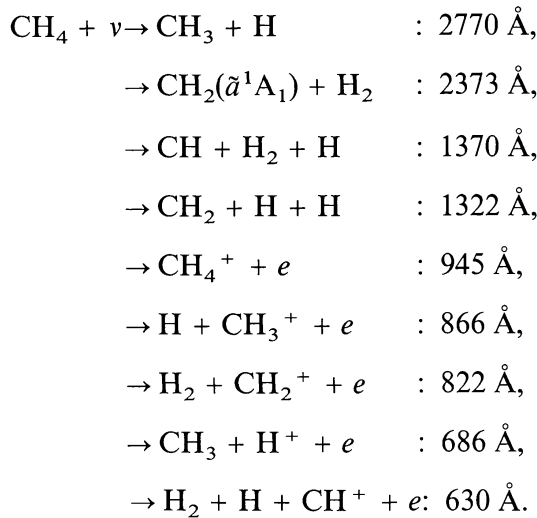
METHANE, CH₄

Cross sections: In the wavelength region from 23.6 to 250 Å the cross section has been measured by Lukirskii *et al.* (1964). These cross section values are in good agreement with values obtained from the fits of Barfield *et al.* (1972) from the constituent atoms. The cross sections synthesized from the constituent atoms were used in the range from 278 to 769.3 Å. From 773 to 1370 Å the cross section was measured by Ditchburn (1955) and supplemented with the cross sections measured by Sun and Weissler (1955) in the range $\lambda = 951.9$ to 1306 Å. In the range from 1370 to 1600 Å the newer and much smaller cross section measurements by Mount *et al.* (1977) were used. Above 1600 Å the cross section is too small to be measured (Thompson *et al.*, 1963).

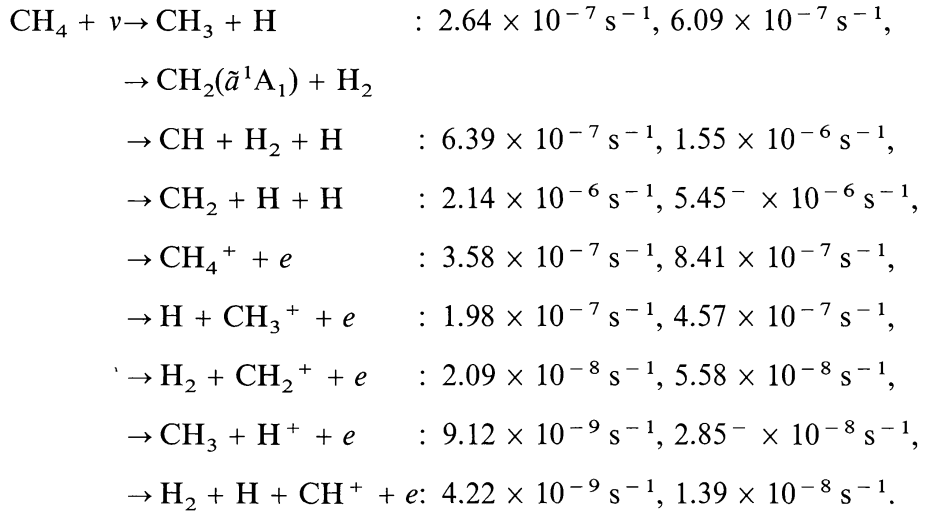
Branching ratios: Because of the many hydrogen atoms in methane, the dissociation branching ratios are very difficult to measure. Where there were several conflicting determinations we have chosen the value closest to the mean. In some cases we had to make other small adjustments to ensure that the sum of the branching ratios is one. The branching ratio data for production of various dissociation products at 1048, 1067, 1216, and 1236 Å is based on investigations and interpretations by Gorden and Ausloos (1967), Rebbert and Ausloos (1972), Rebbert *et al.* (1972), Laufer and McNesby (1968), Slanger and Black (1982), and summaries by Strobel (1973) and Okabe (1978). The values which we finally used are summarized below.

	CH + H ₂ + H	¹ CH ₂ + H ₂	CH ₂ + H + H	CH ₃ + H
1048 Å	0.19	0.723	0.007	0.08
1067 Å	0.188	0.726	0.006	0.08
1216 Å	0.08	0.5	0.4	0.02
1236 Å	0.06	0.8	0.11	0.03

The branching ratio between all dissociation and all ionization products is based on the data of Ditchburn (1955). The branching between ionization and the various dissociative ionization products is based on the data of Kronebusch and Berkowitz (1976).

Thresholds:

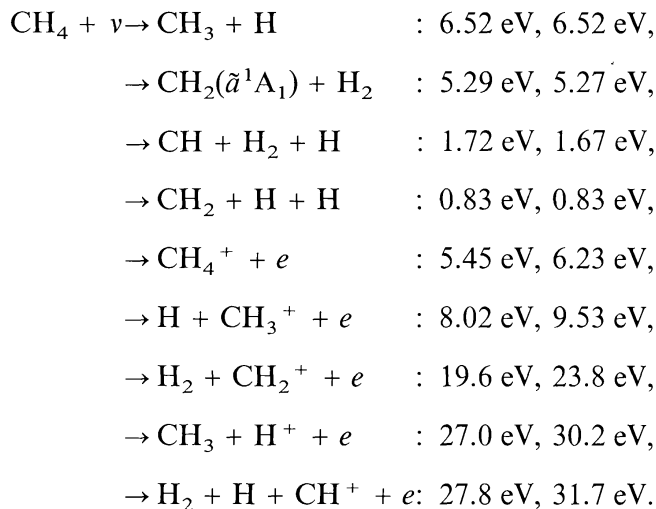
The first of these limits is the wavelength equivalent quoted by Okabe (1978) and is also consistent with heats of formation. The next three thresholds are obtained from heats of formation. The ionization limit is taken from Ditchburn (1955). Dissociative ionization thresholds are quoted by Kronebusch and Berkowitz (1976).

Rate coefficients:

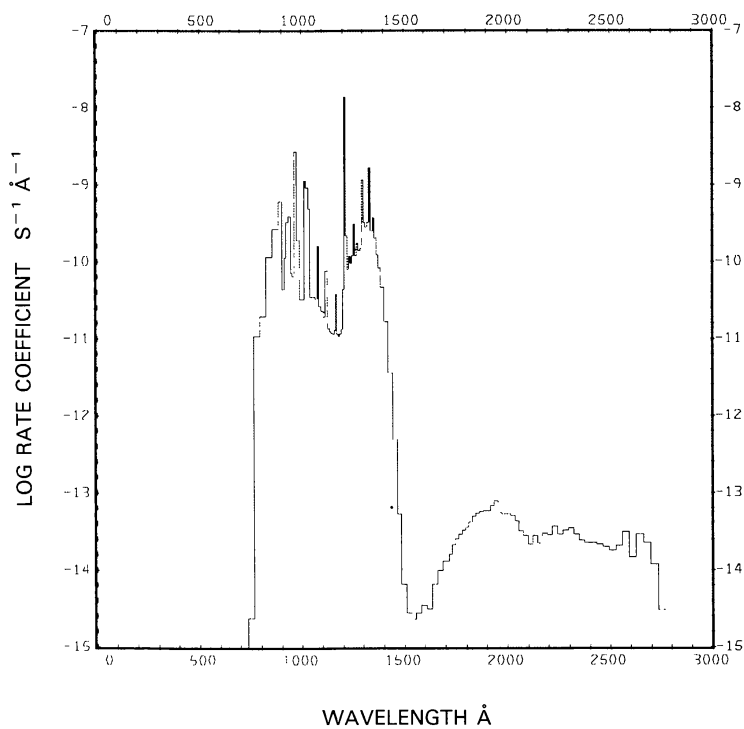
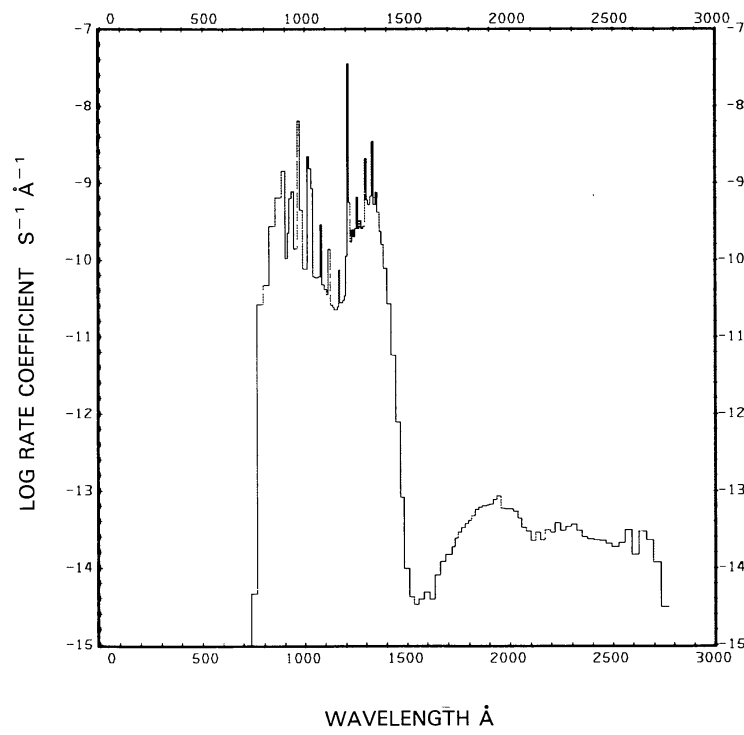
The first value of each branch is for the quiet Sun (see Figures 166(a) to 174(a)), the second for the active Sun (see Figures 166(b) to 174(b)). For the quiet Sun, Yung *et al.* (1984) quote for the second of the above dissociation processes $4.0 \times 10^{-6} \text{ s}^{-1}$ when corrected to 1 AU from the diurnally averaged value at Saturn's heliocentric distance ($2.2 \times 10^{-8} \text{ s}^{-1}$), for the third process $5.8 \times 10^{-7} \text{ s}^{-1}$ ($3.2 \times 10^{-9} \text{ s}^{-1}$ diurnal average at Saturn's orbit), and for the fourth process $3.6 \times 10^{-6} \text{ s}^{-1}$ ($2.0 \times 10^{-8} \text{ s}^{-1}$ diurnal average at Saturn). The sum of their three dissociation processes corrected to 1 AU is $8.2 \times 10^{-6} \text{ s}^{-1}$. From Strobel's (1973) compilation of data the total disso-

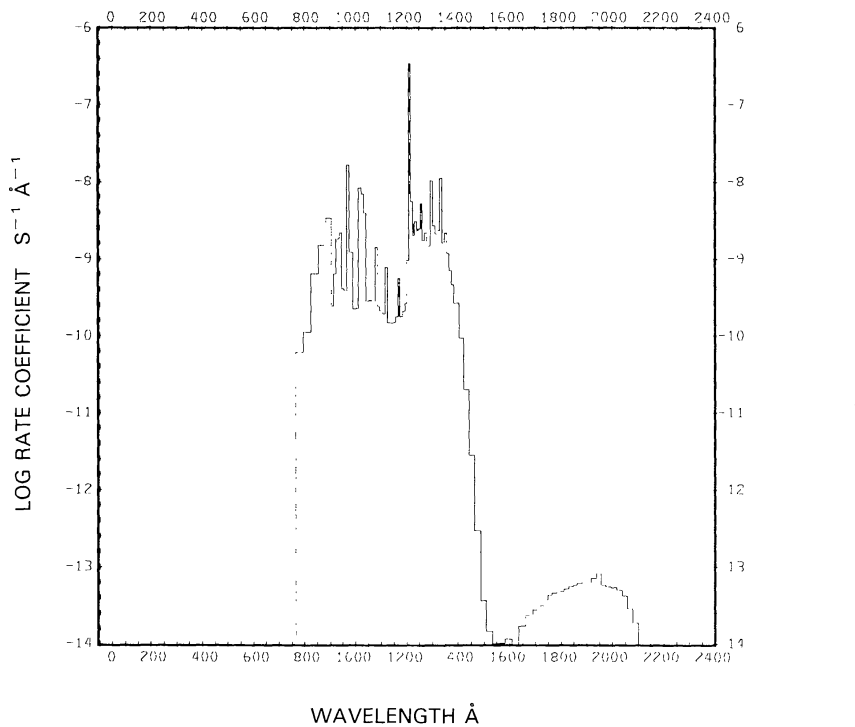
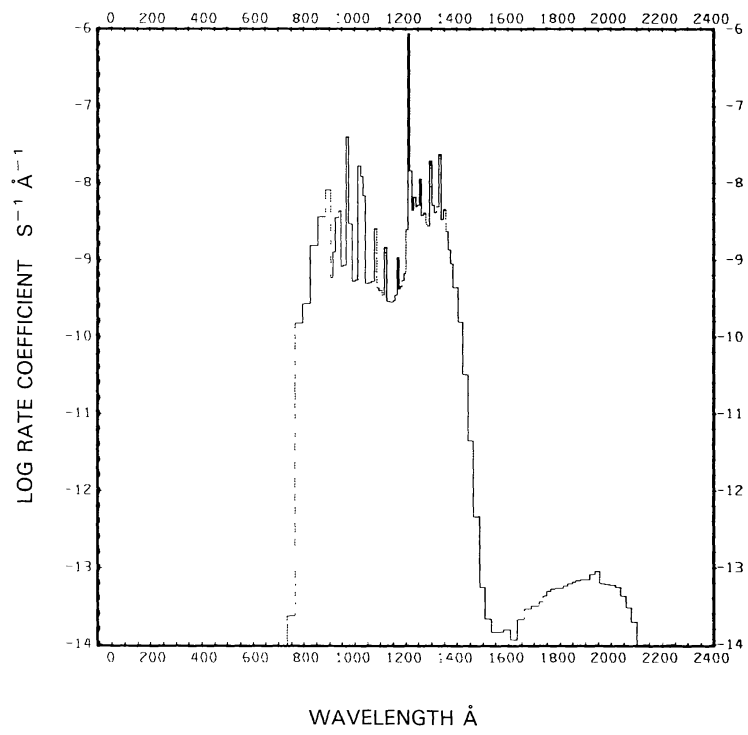
ciation rate coefficient is $6.4 \times 10^{-6} \text{ s}^{-1}$ at 1 AU ($2.4 \times 10^{-7} \text{ s}^{-1}$ at the orbit of Jupiter). This compares to our total dissociation rate coefficient of $7.0 \times 10^{-6} \text{ s}^{-1}$, which falls between that of Yung *et al.* (1984) and that of Strobel (1973). Our rate coefficient for all ionizing processes for the quiet Sun ($5.9 \times 10^{-7} \text{ s}^{-1}$) is somewhat smaller than the ionization rate coefficient quoted by Siscoe and Mukherjee (1972) ($8.74 \times 10^{-7} \text{ s}^{-1}$). Our total rate coefficient for the quiet Sun ($7.6 \times 10^{-6} \text{ s}^{-1}$) is also somewhat smaller than the corresponding rate coefficients reported by Potter and del Duca (1964) ($1.0 \times 10^{-5} \text{ s}^{-1}$) and Jackson (1976a,b) ($8.2 \times 10^{-6} \text{ s}^{-1}$). The dissociation rates are dominated by the hydrogen L α flux.

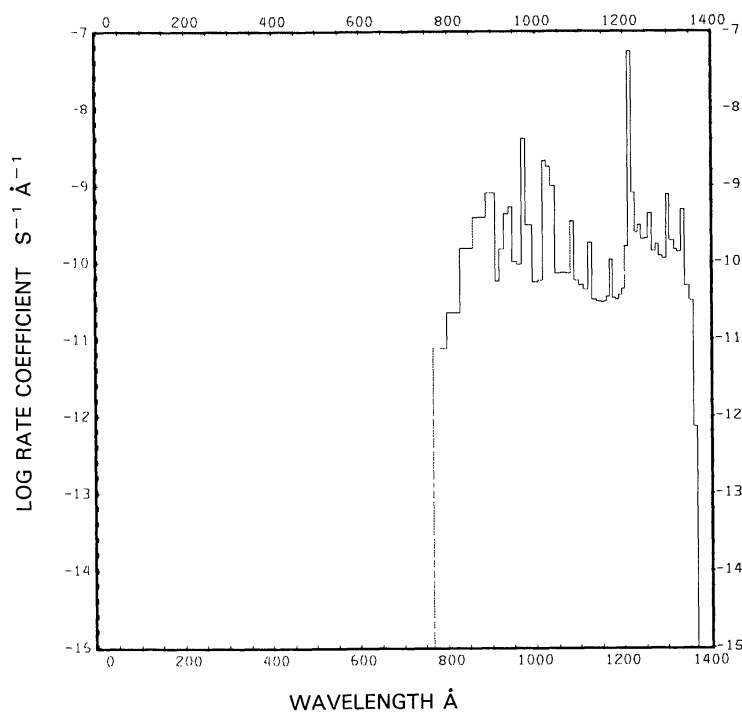
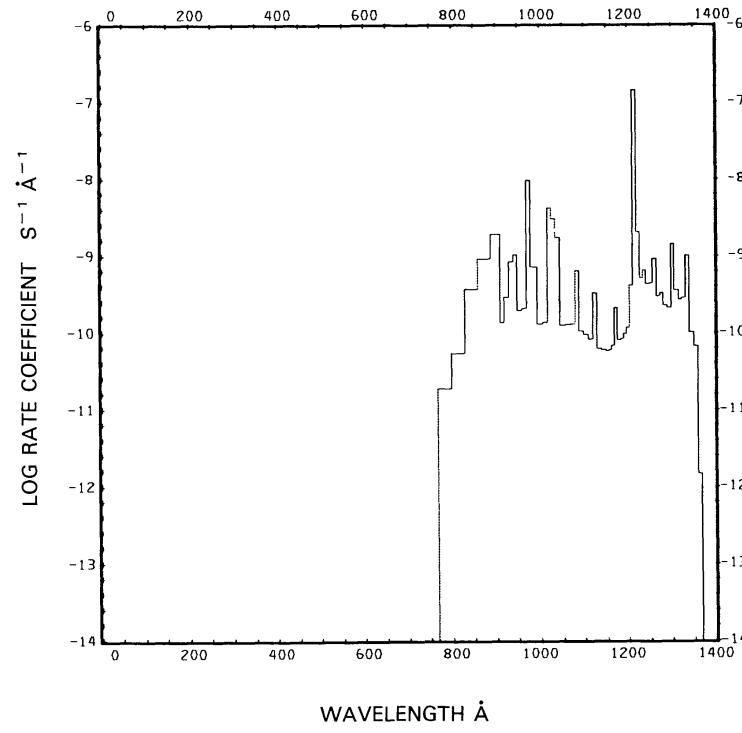
Excess energies:

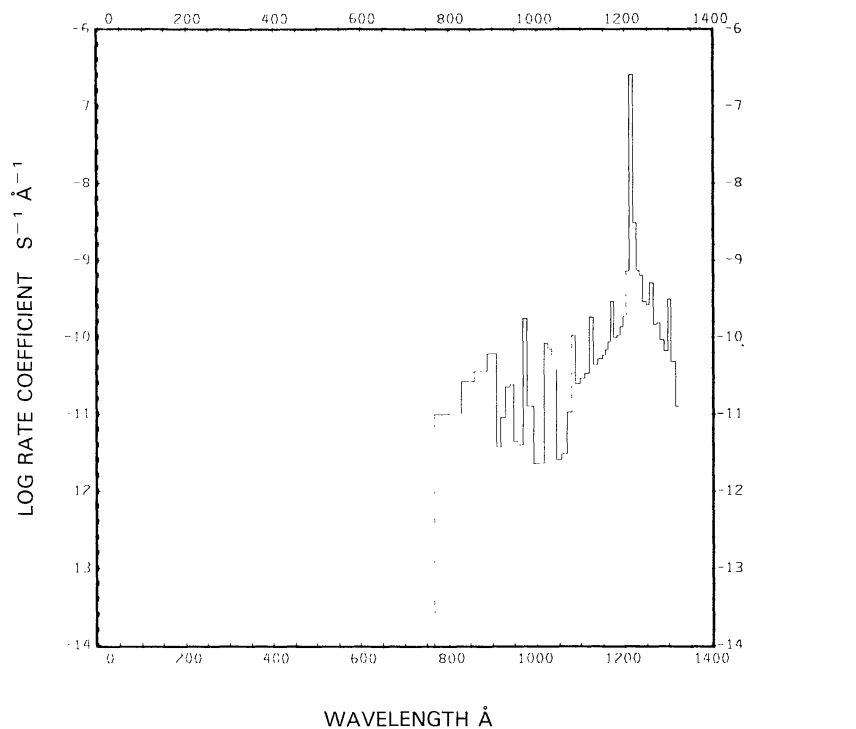
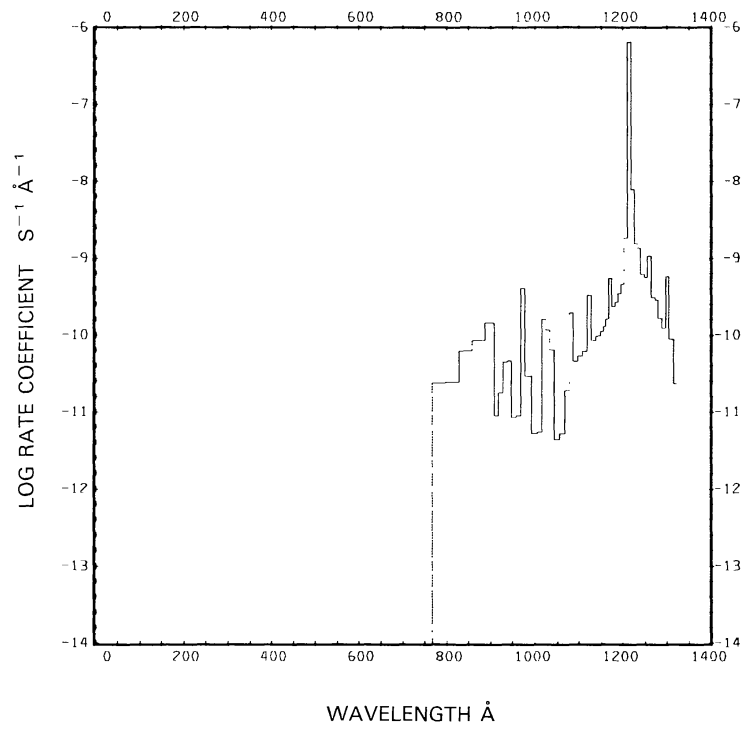


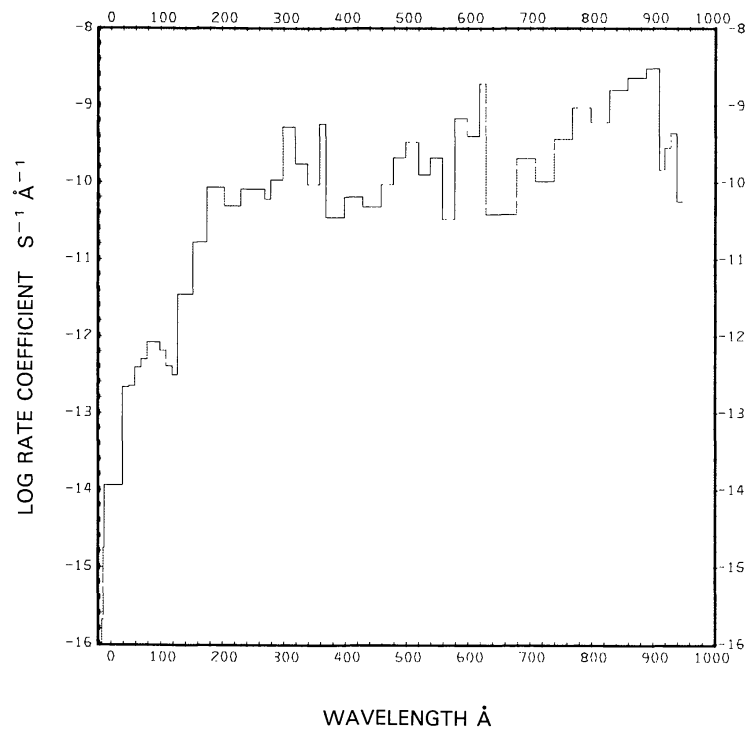
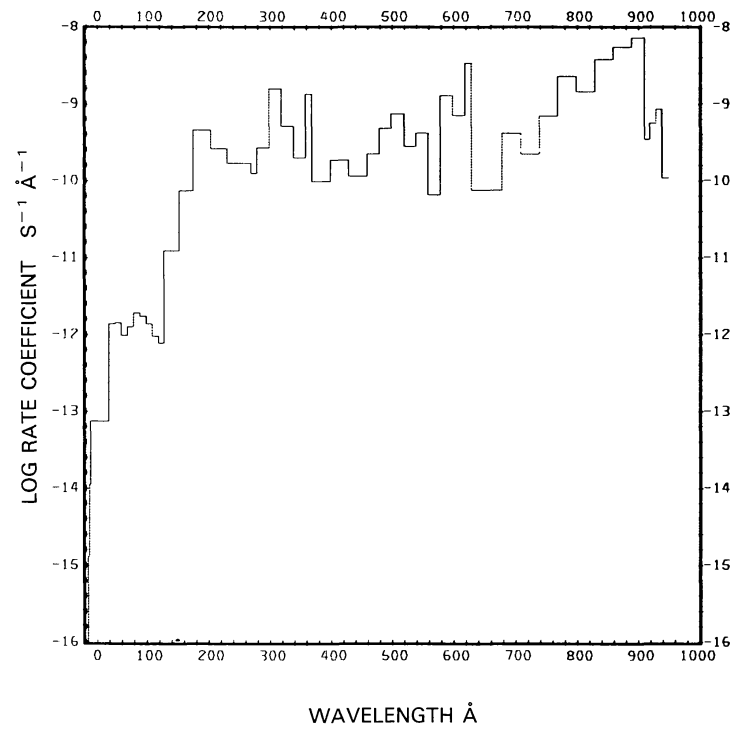
The first value of each branch is for the quiet Sun, the second for the active Sun.

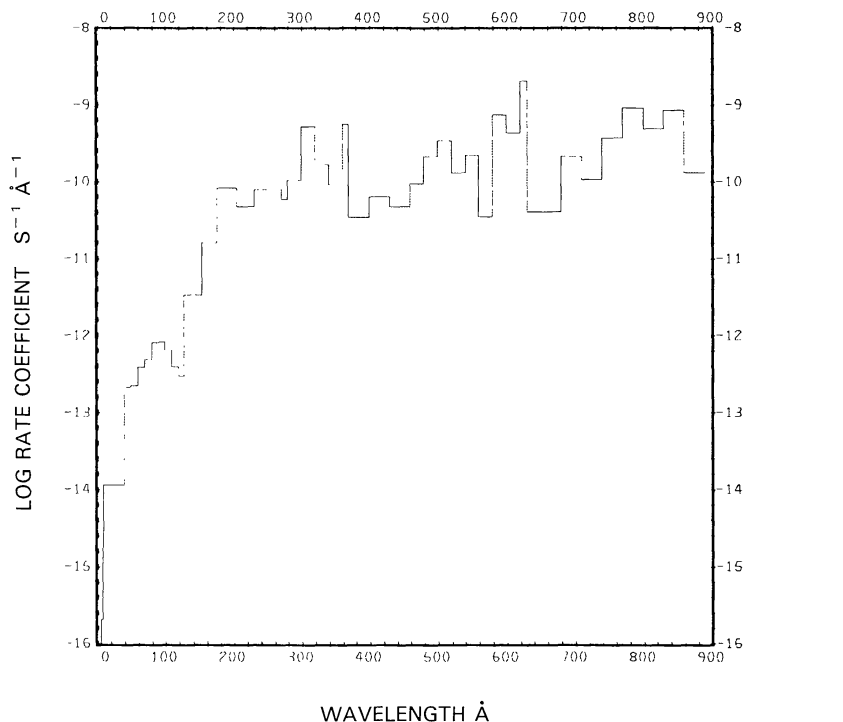
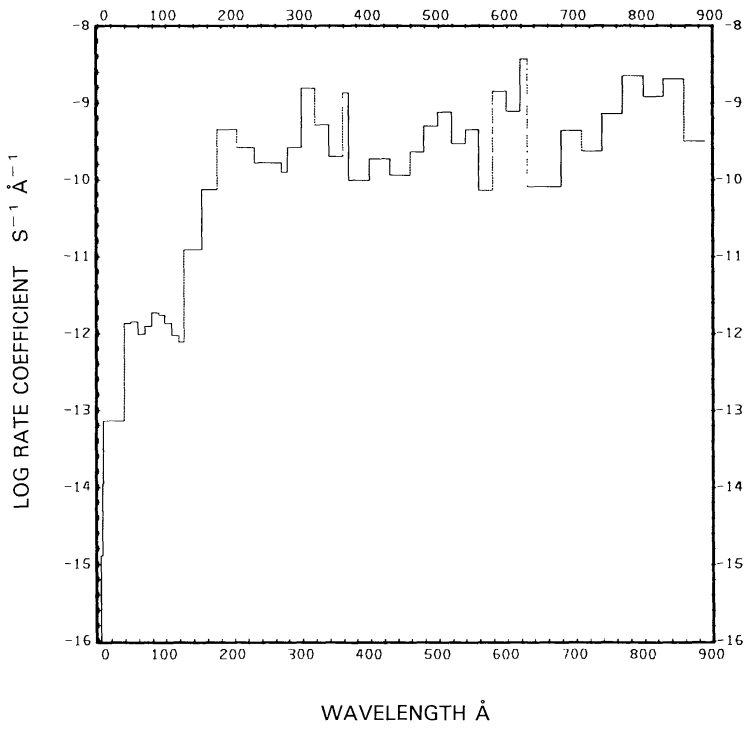
Fig. 166a. CH₄ + $\nu \rightarrow$ CH₃ + H, for the quiet Sun.Fig. 166b. CH₄ + $\nu \rightarrow$ CH₃ + H, for the active Sun.

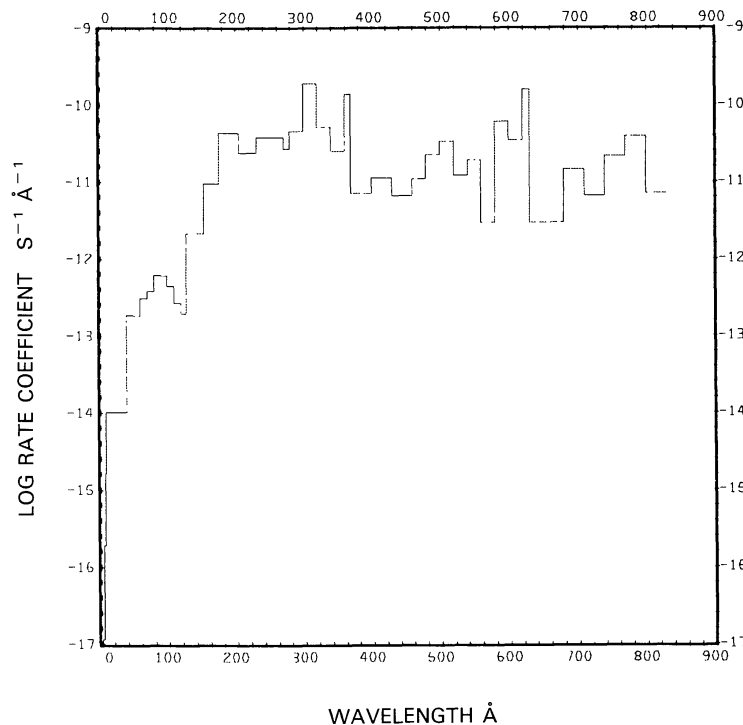
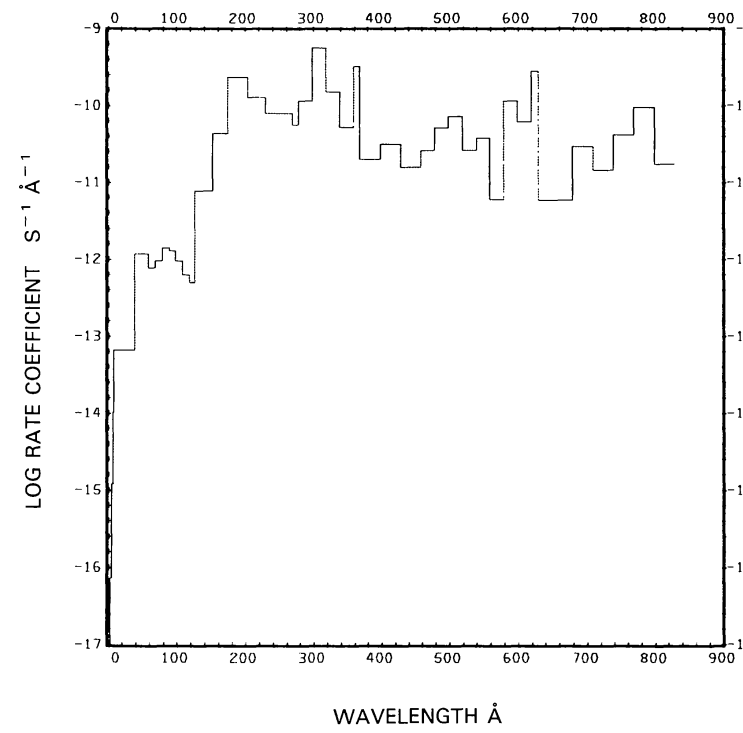
Fig. 167a. $\text{CH}_4 + \nu \rightarrow \text{CH}_2(\tilde{\alpha}^1A_1) + \text{H}_2$, for the quiet Sun.Fig. 167b. $\text{CH}_4 + \nu \rightarrow \text{CH}_2(\tilde{\alpha}^1A_1) + \text{H}_2$, for the active Sun.

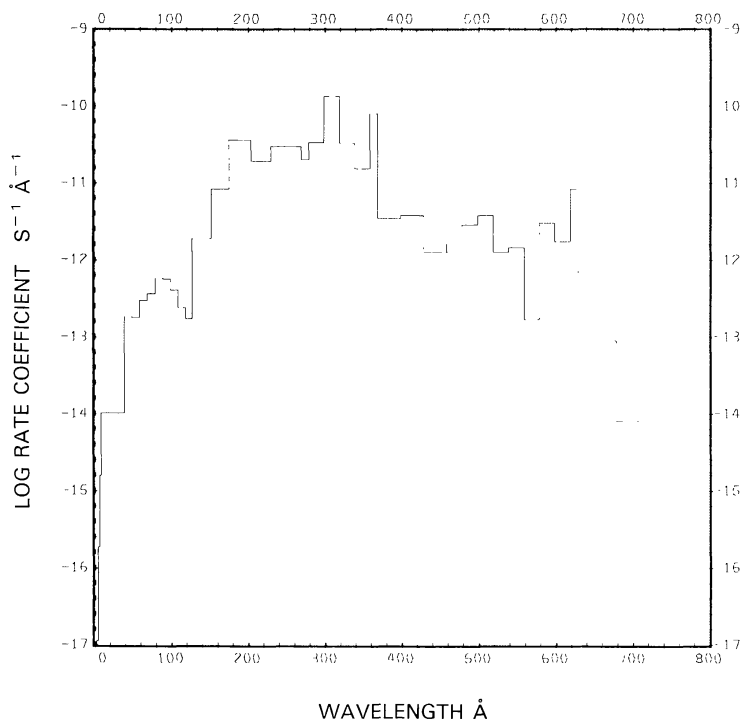
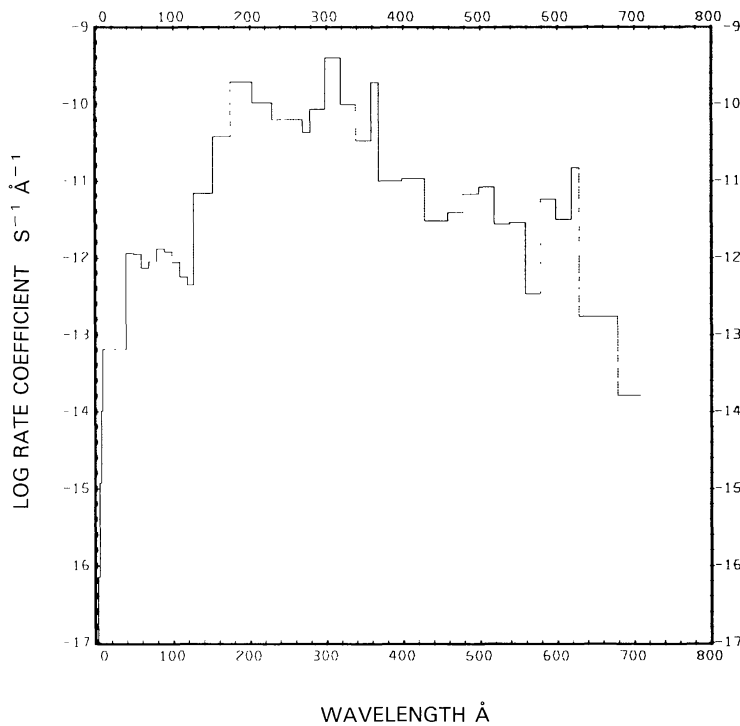
Fig. 168a. CH₄ + $\nu \rightarrow$ CH + H₂ + H, for the quiet Sun.Fig. 168b. CH₄ + $\nu \rightarrow$ CH + H₂ + H, for the active Sun.

Fig. 169a. $\text{CH}_4 + \nu \rightarrow \text{CH}_2 + \text{H} + \text{H}$, for the quiet Sun.Fig. 169b. $\text{CH}_4 + \nu \rightarrow \text{CH}_2 + \text{H} + \text{H}$, for the active Sun.

Fig. 170a. CH₄ + $\nu \rightarrow$ CH₄⁺ + e, for the quiet Sun.Fig. 170b. CH₄ + $\nu \rightarrow$ CH₄⁺ + e, for the active Sun.

Fig. 171a. CH₄ + ν → H + CH₃⁺ + e⁻, for the quiet Sun.Fig. 171b. CH₄ + ν → H + CH₃⁺ + e⁻, for the active Sun.

Fig. 172a. CH₄ + $\nu \rightarrow$ H₂ + CH₂⁺ + e^- , for the quiet Sun.Fig. 172b. CH₄ + $\nu \rightarrow$ H₂ + CH₂⁺ + e^- , for the active Sun.

Fig. 173a. $\text{CH}_4 + \nu \rightarrow \text{CH}_3 + \text{H}^+ + e$, for the quiet Sun.Fig. 173b. $\text{CH}_4 + \nu \rightarrow \text{CH}_3 + \text{H}^+ + e$, for the active Sun.

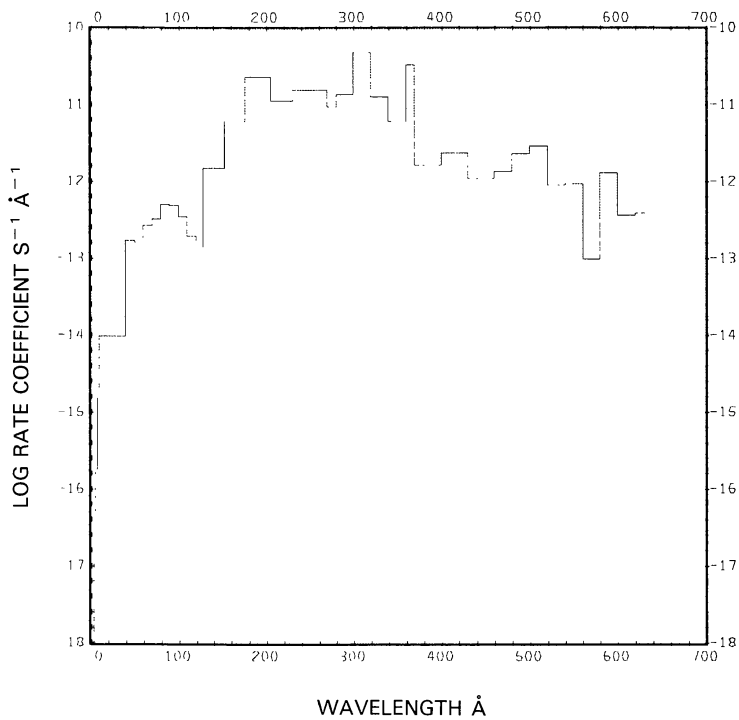


Fig. 174a. CH₄ + ν → H₂ + H + CH⁺ + e, for the quiet Sun.

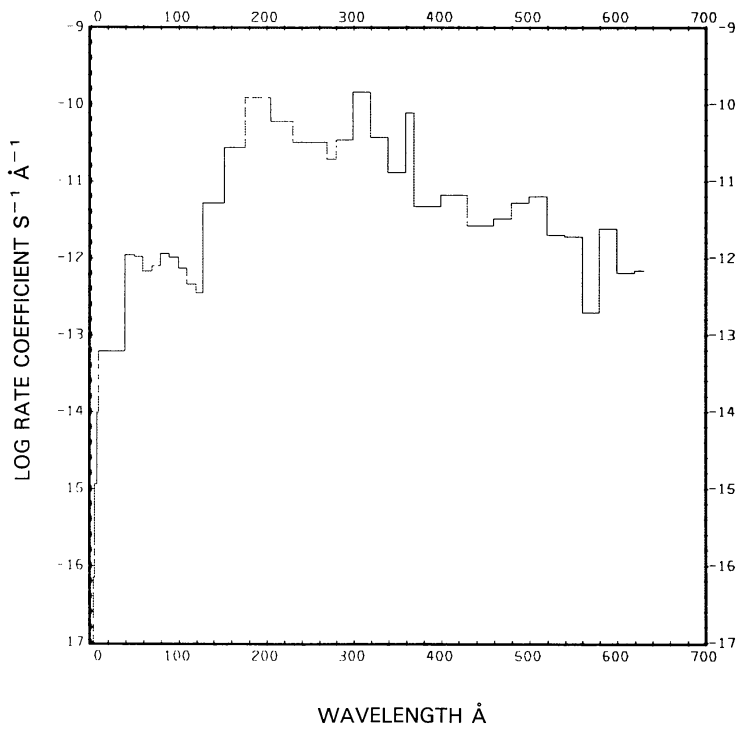


Fig. 174b. CH₄ + ν → H₂ + H + CH⁺ + e, for the active Sun.

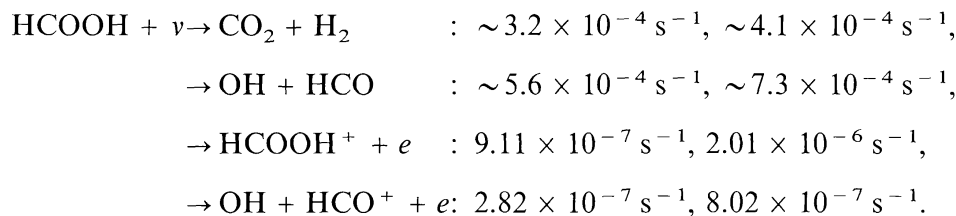
FORMIC ACID, HCOOH

Cross sections: Up to 600 Å the cross section is synthesized from the fits prepared by Barfield *et al.* (1972) for the constituent atoms. In the wavelength range from 1100 to 2500 Å the cross section has been measured by Barnes and Simpson (1963). Above 2500 Å the cross section is very small.

Branching ratios: Branching ratios have been determined by Gorden and Ausloos (1961).

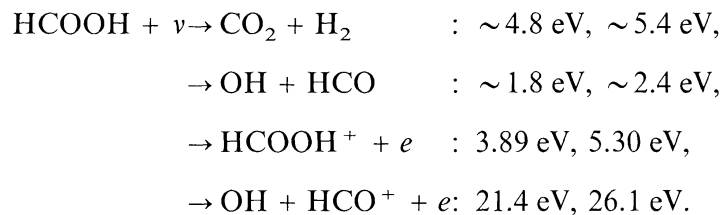
Thresholds: The dissociation energy to produce $\text{H}_2 + \text{CO}_2$ is not known; we have assumed the wavelength equivalent to be 7000 Å. For dissociation into $\text{HCO} + \text{OH}$ it is 2600 Å from heats of formation. The ionization threshold has been measured by Bell *et al.* (1975) to be at $\lambda = 1094.4$ Å. Dissociative ionization has a threshold at 902 Å as listed by Field and Franklin (1970).

Rate coefficients:



The first value of each branch is for the quiet Sun (see Figures 175, 176, 177(a) and 178(a)), the second for the active Sun (see Figures 177(b) to 178(b)). For the quiet Sun, our total rate coefficient ($8.8 \times 10^{-4} \text{ s}^{-1}$) is larger than the value obtained by Jackson (1976a, b) ($1.4 \times 10^{-4} \text{ s}^{-1}$). Because the dissociation threshold is not well known and the branching is incomplete, the rate coefficients are only approximate.

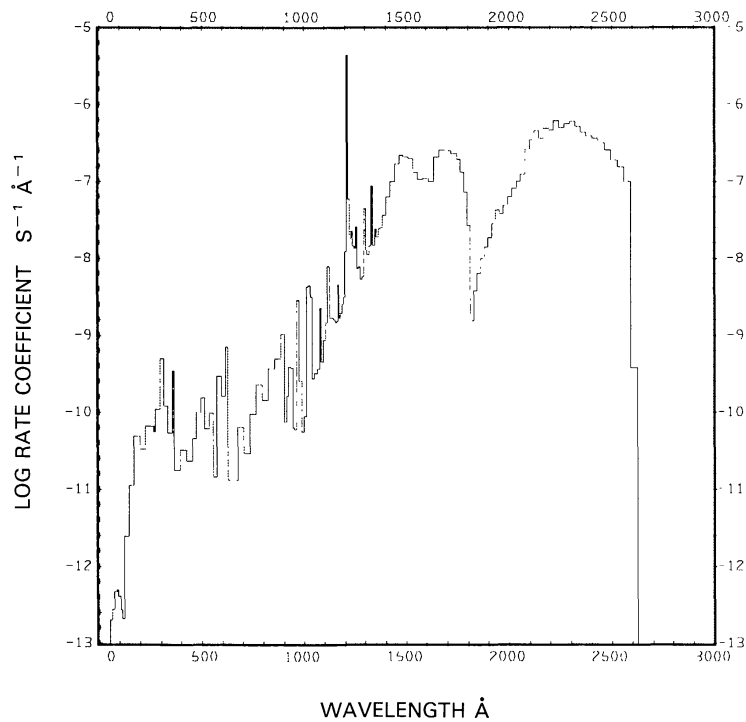
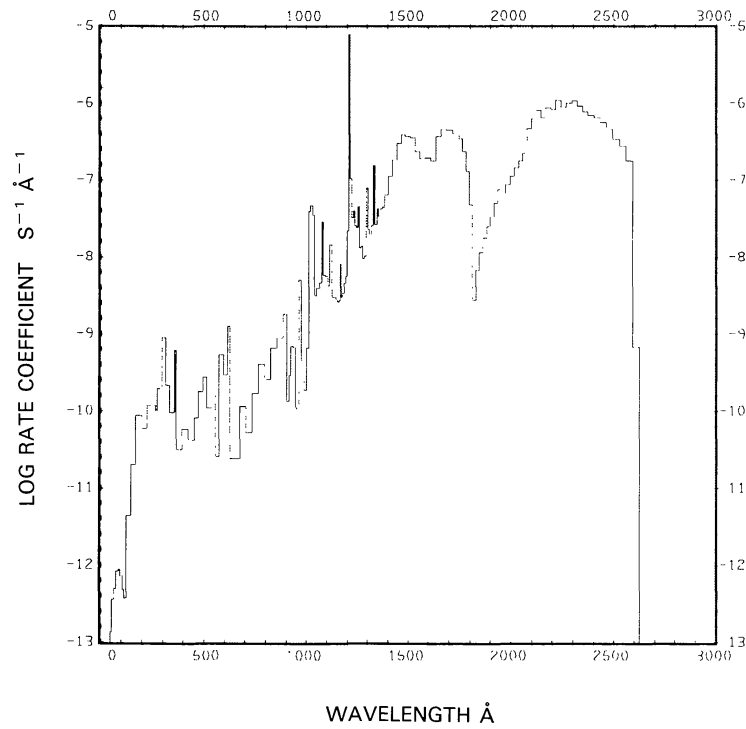
Excess energies:

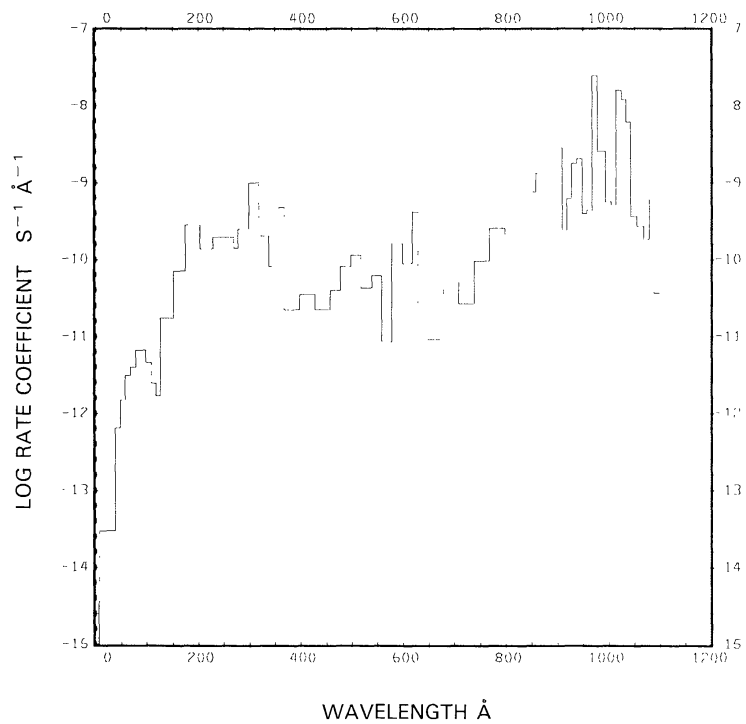
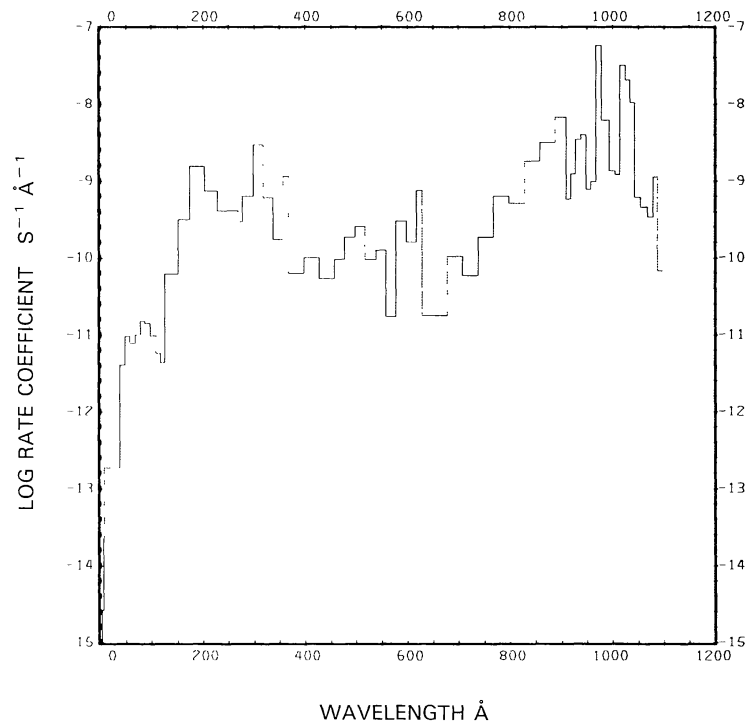


The first value of each branch is for the quiet Sun, the second for the active Sun. The excess energies for dissociation are only approximate.

FORMIC ACID, HCOOH

217

Fig. 175. $\text{HCOOH} + \nu \rightarrow \text{CO}_2 + \text{H}_2$, for the quiet Sun.Fig. 176. $\text{HCOOH} + \nu \rightarrow \text{OH} + \text{HCO}$, for the quiet Sun.

Fig. 177a. $\text{HCOOH} + \nu \rightarrow \text{HCOOH}^+ + e$, for the quiet Sun.Fig. 177b. $\text{HCOOH} + \nu \rightarrow \text{HCOOH}^+ + e$, for the active Sun.

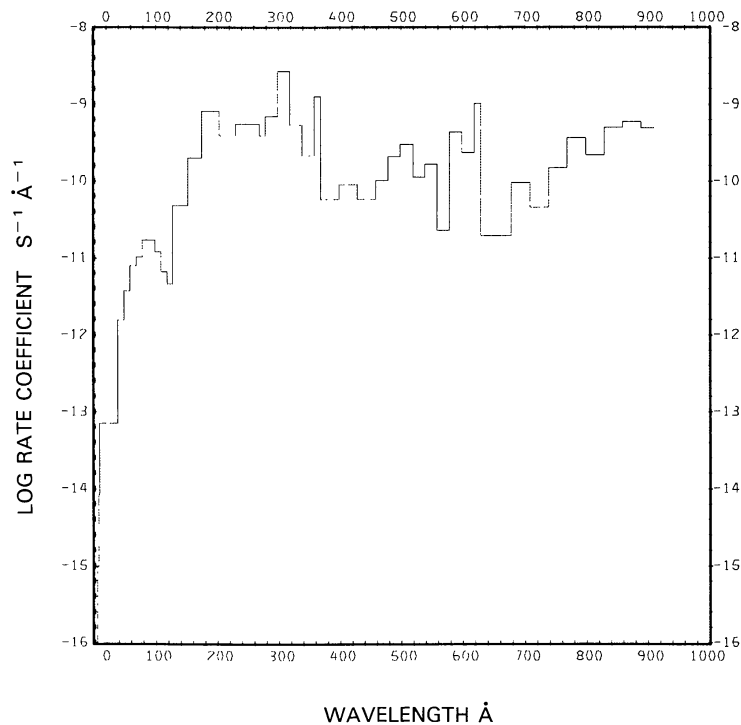


Fig. 178a. $\text{HCOOH} + \nu \rightarrow \text{OH} + \text{HCO}^+ + e$, for the quiet Sun.

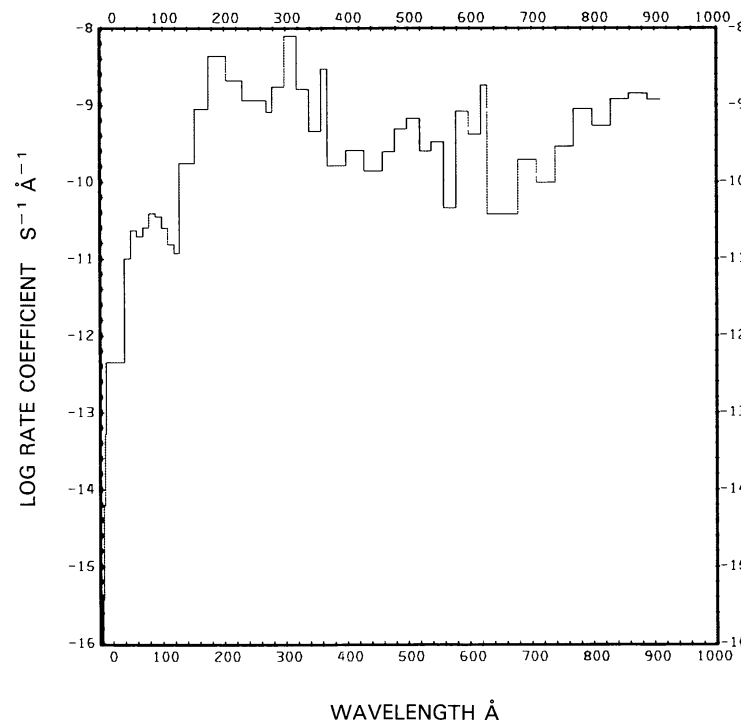


Fig. 178b. $\text{HCOOH} + \nu \rightarrow \text{OH} + \text{HCO}^+ + e$, for the active Sun.

CHLOROMETHANE, CH_3Cl

Cross sections: Up to 625.8 Å the cross section is synthesized from the fits prepared by Barfield *et al.* (1972) for the individual constituent atomic cross sections. In the wavelength region from 1580 to 1733 Å the cross section has been measured by Hubrich *et al.* (1977), from 1740 to 1840 Å it has been measured by Robbins (1976), from 1860 to 2160 Å it was measured by Vanlaethem-Meurée *et al.* (1978), from 2180 to 2200 Å it was measured by Robbins (1976), and from 2200 to 2350 Å it has been measured by Hubrich *et al.* (1977). In the region from 1860 to 2160 Å the Vanlaethem-Meurée *et al.* cross sections are preferred (DeMore *et al.*, 1982) over the Robbins cross sections, although the agreement is quite good.

Branching ratios: The branching ratios are not known. We assumed that only dissociation into $\text{CH}_3 + \text{Cl}$ occurs.

Thresholds: The wavelength equivalent for the dissociation is 3470 Å (Okabe, 1978).

Rate coefficients:



for the quiet Sun (see Figure 179) and $\sim 2.7 \times 10^{-5} \text{ s}^{-1}$ for the active Sun.

Excess energies: The excess energy for this process for the quiet Sun is about 6.2 eV and about 6.9 eV for the active Sun.

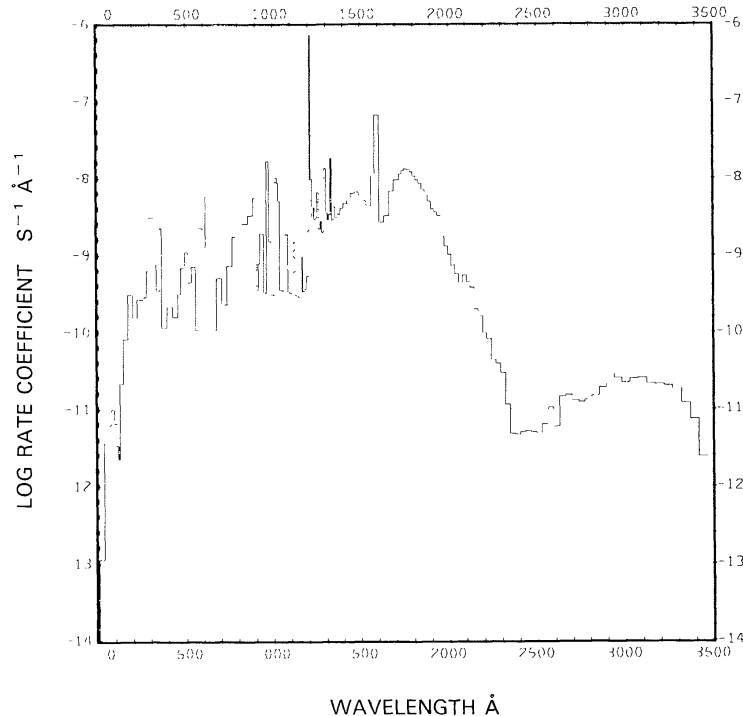


Fig. 179. $\text{CH}_3\text{Cl} + \nu \rightarrow \text{CH}_3 + \text{Cl}$, for the quiet Sun.

CYANOACETYLENE, HC_3N

Cross sections: Up to 800 Å the cross section is synthesized from the fits to the constituent atomic cross sections as prepared by Barfield *et al.* (1972). From $\lambda = 1058$ to 1632 Å cross section data are taken from Connors *et al.* (1974).

Branching ratios: No branching ratios are available. It was assumed that only dissociation into $\text{CN} + \text{C}_2\text{H}$ takes place.

Thresholds: The wavelength equivalent dissociation energy for the above products is ~ 2000 Å (Okabe, 1978).

Rate coefficients:

$$\text{HC}_3\text{N} + v \rightarrow \text{CN} + \text{C}_2\text{H}: \sim 3.9 \times 10^{-5} \text{ s}^{-1}$$

for the quiet Sun (see Figure 180) and $\sim 6.8 \times 10^{-5} \text{ s}^{-1}$ for the active Sun. Our value for the quiet Sun is larger than the one found by Potter and del Duca (1964) who obtained $1.5 \times 10^{-5} \text{ s}^{-1}$, but smaller than that of Jackson (1976a,b) who obtained $7.6 \times 10^{-5} \text{ s}^{-1}$.

Excess energies: The excess energy of this process for the quiet Sun is about 2.7 eV. For comparison, Keller (1971) estimated 1.00 eV. For the active Sun it is about 3.3 eV.

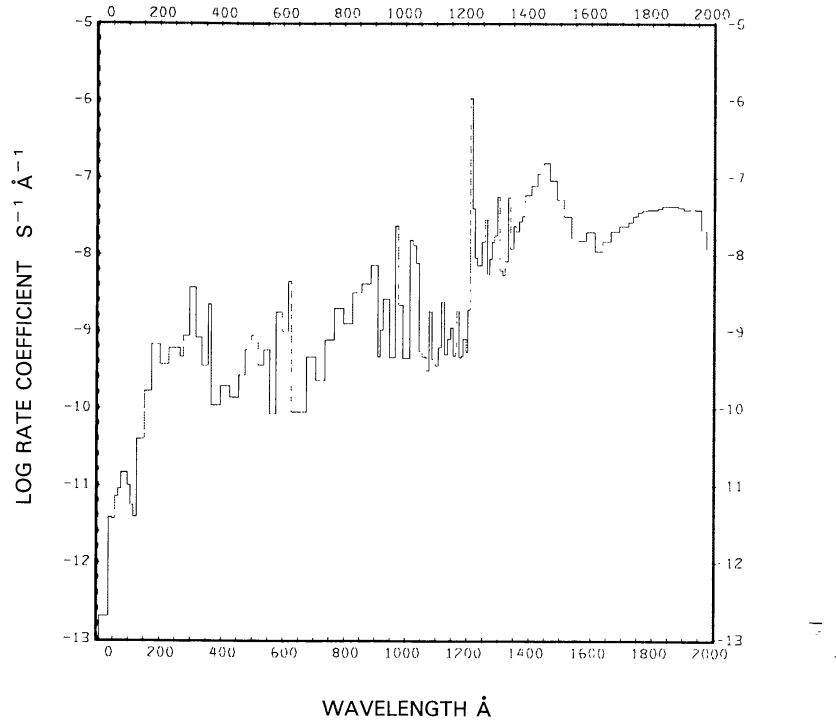


Fig. 180. $\text{HC}_3\text{N} + v \rightarrow \text{CN} + \text{C}_2\text{H}$, for the quiet Sun.

NITRIC ACID, HNO_3

Cross sections: Up to a wavelength of $\lambda = 1100 \text{ \AA}$ the cross section is synthesized from the fits to the constituent atomic cross sections prepared by Barfield *et al.* (1972). From $\lambda = 1100$ to 1900 \AA we used the measured cross section of Okabe (1980) and from $\lambda = 1900$ to 3300 \AA we used the cross section of Molina and Molina (1981). This cross section is also in good agreement with the measurements by Biaume (1973) and Johnston and Graham (1973). The cross section is very small above 3300 \AA .

Branching ratios: The dissociation branching ratio to produce $\text{OH} + \text{NO}_2$ is unity. No branching ratio is known for ionization.

Thresholds: The wavelength equivalent for the dissociation energy as given by Okabe (1978) is 5980 \AA in agreement with Johnston and Graham (1973).

Rate coefficients:



for the quiet Sun (see Figure 181) and $2.39 \times 10^{-4} \text{ s}^{-1}$ for the active Sun. For the quiet Sun this compares well with the value $1.7 \times 10^{-4} \text{ s}^{-1}$ at the top of the atmosphere obtained by Biaume (1973).

Excess energies: The excess energy for the quiet Sun for this process is 4.32 eV and for the active Sun it is 4.70 eV.

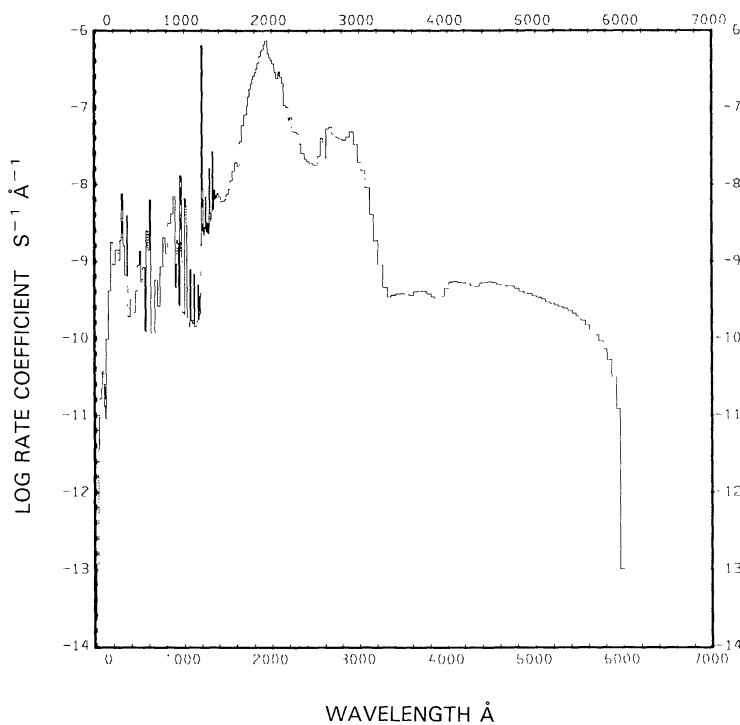


Fig. 181. $\text{HNO}_3 + v \rightarrow \text{OH} + \text{NO}_2$, for the quiet Sun.

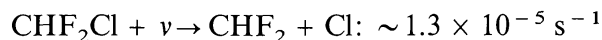
CHLORODIFLUOROMETHANE, CHF₂Cl

Cross sections: Up to 625.8 Å the cross section is synthesized from the fits to the constituent atomic cross sections prepared by Barfield *et al.* (1972). From 1580 to 1733 Å the cross section has been measured by Hubrich *et al.* (1977), from 1740 to 2020 Å the measured cross section of Robbins and Stolarski (1976) is used, and from 2033 to 2200 Å the cross section of Hubrich *et al.* (1977) is used.

Branching ratios: The branching ratio has not been measured. We assume that dissociation produces CHF₂ + Cl.

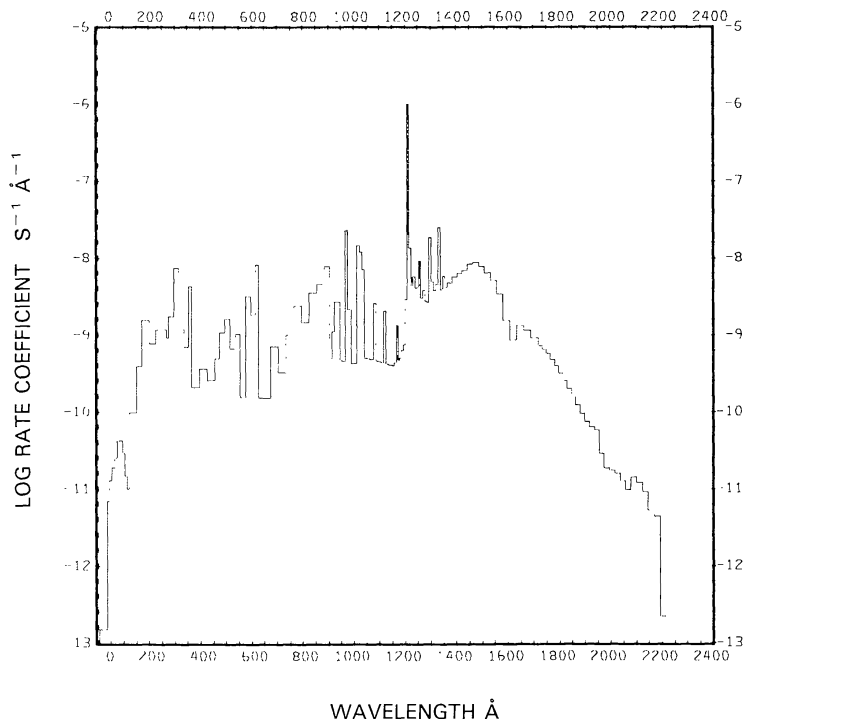
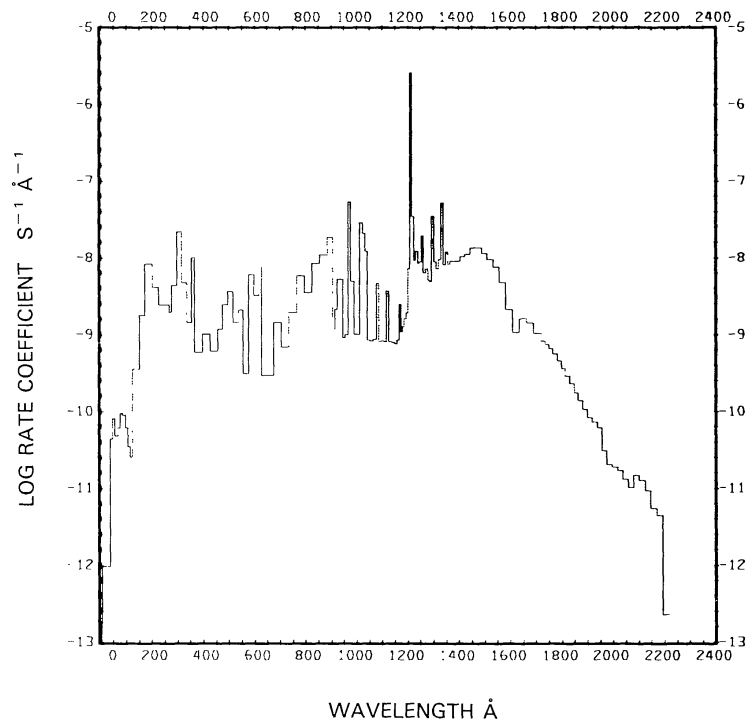
Thresholds: The dissociation energy is not known, but appears to be above 2200 Å; we assume this to be the threshold value.

Rate coefficients:



for the quiet Sun (see Figure 182(a)) and $\sim 3.0 \times 10^{-5} \text{ s}^{-1}$ for the active Sun (see Figure 182(b)).

Excess energies: The excess energy of this process for the quiet Sun is about 6.0 eV and about 6.6 eV for the active Sun.

Fig. 182a. $\text{CHF}_2\text{Cl} + \nu \rightarrow \text{CHF}_2 + \text{Cl}$, for the quiet Sun.Fig. 182b. $\text{CHF}_2\text{Cl} + \nu \rightarrow \text{CHF}_2 + \text{Cl}$, for the active Sun.

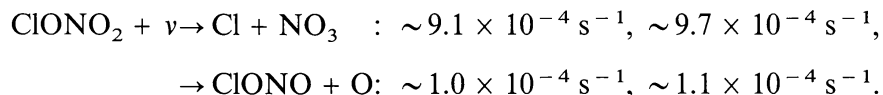
CHLORINE NITRATE, ClONO₂

Cross sections: Up to 622.5 Å the cross section is synthesized from the fits to the atomic constituent cross sections prepared by Barfield *et al.* (1972). Molina and Molina (1979) have measured the cross section in the range $\lambda = 1900$ to 4500 Å. No cross section data are available between 623 and 1900 Å or above 4500 Å.

Branching ratios: Branching ratios have been measured at 2650 and 3130 Å by Knauth and Schindler (1983) and at 2660 and 3550 Å by Margitan (1983). At all of these wavelengths the branching ratio is 0.9 for production of Cl + NO₃ and ~ 0.1 for production of ClONO + O(³P). We have assumed this ratio to apply at all wavelengths up to the threshold of the latter production path. Branching ratios leading to ionization are not known.

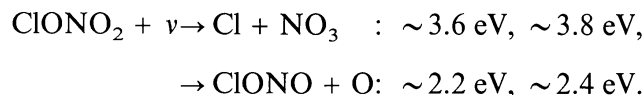
Thresholds: The wavelength equivalent of the dissociation energy to produce Cl + NO₃ is 7210 Å and for production of ClONO + O(³P) it is 3910 Å, as quoted by Baulch *et al.* (1984).

Rate coefficients:

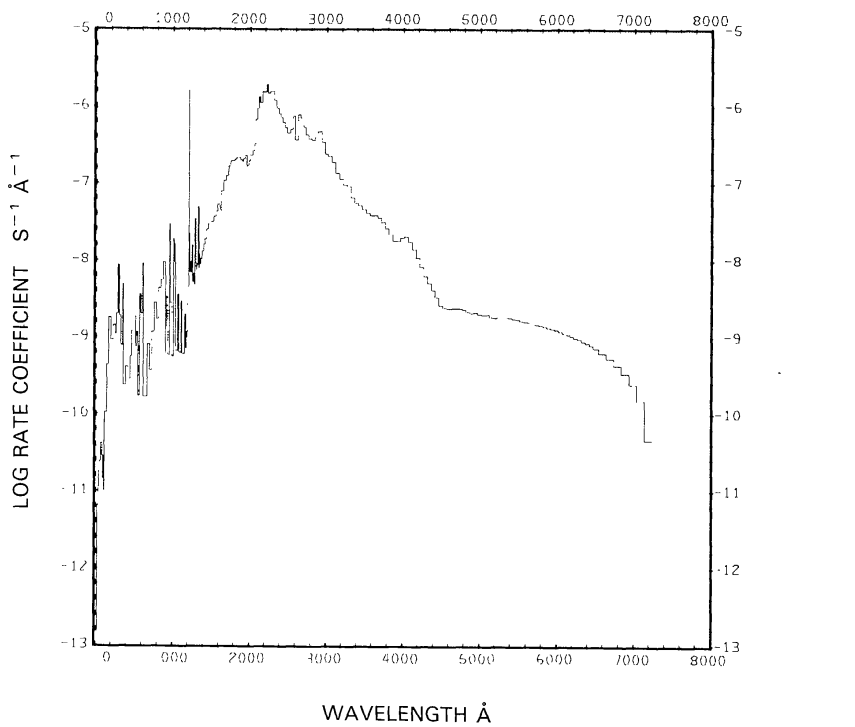
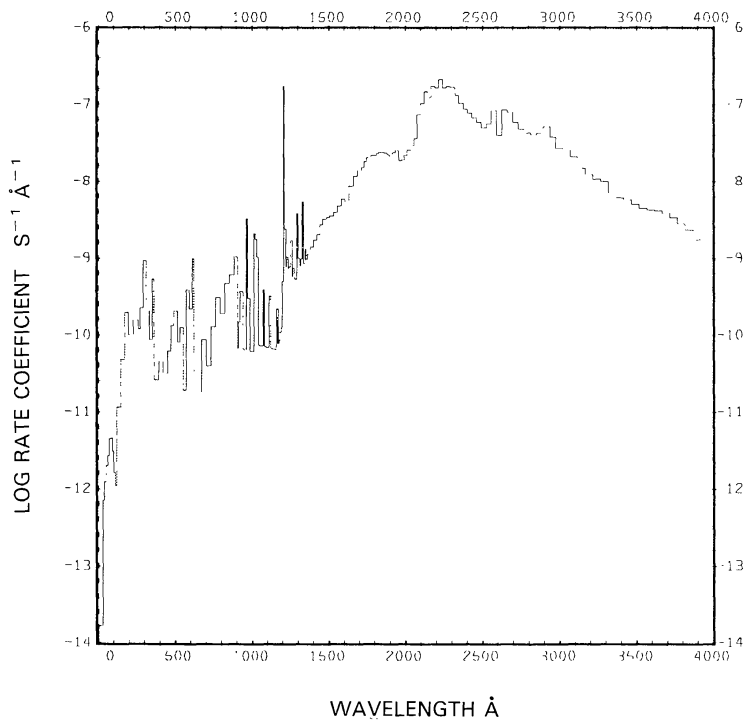


The first value of each branch is for the quiet Sun (see Figures 183 and 184), the second is for the active Sun.

Excess energies:



The first value of each branch is for the quiet Sun, the second is for the active Sun.

Fig. 183. $\text{ClONO}_2 + \nu \rightarrow \text{Cl} + \text{NO}_3$, for the quiet Sun.Fig. 184. $\text{ClONO}_2 + \nu \rightarrow \text{ClONO} + \text{O}$, for the quiet Sun.

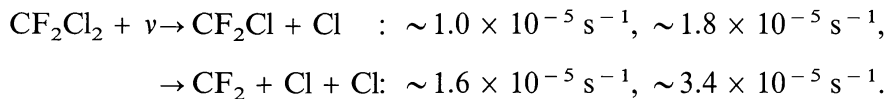
CARBON DIFLUORODICHLORIDE, CF_2Cl_2

Cross sections: Up to 625.8 Å the cross section is synthesized from the atomic cross section fits of the constituent atoms as prepared by Barfield *et al.* (1972). In the wavelength range from 1590 to 1700 Å the cross section has been measured by Hubrich *et al.* (1977). From 1700 to 2400 Å we used the average of the cross sections from many different measurements as presented by Baulch *et al.* (1982). No cross section measurements exist between 626 and 1590 Å.

Branching ratios: The branching ratios as recommended by Baulch *et al.* (1982) have been used for the dominant dissociation path to produce $\text{CF}_2\text{Cl} + \text{Cl}$ and the secondary path to produce $\text{CF}_2 + \text{Cl} + \text{Cl}$.

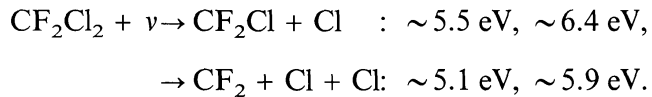
Thresholds: The threshold as given by Baulch *et al.* (1982) for the primary path is 3460 Å and for the secondary path it is 2160 Å.

Rate coefficients:



The first value of each branch is for the quiet Sun (see Figures 185 and 186(a)), the second for the active Sun (see Figure 186(b)).

Excess energies:



The first value of each branch is for the quiet Sun, the second for the active Sun.

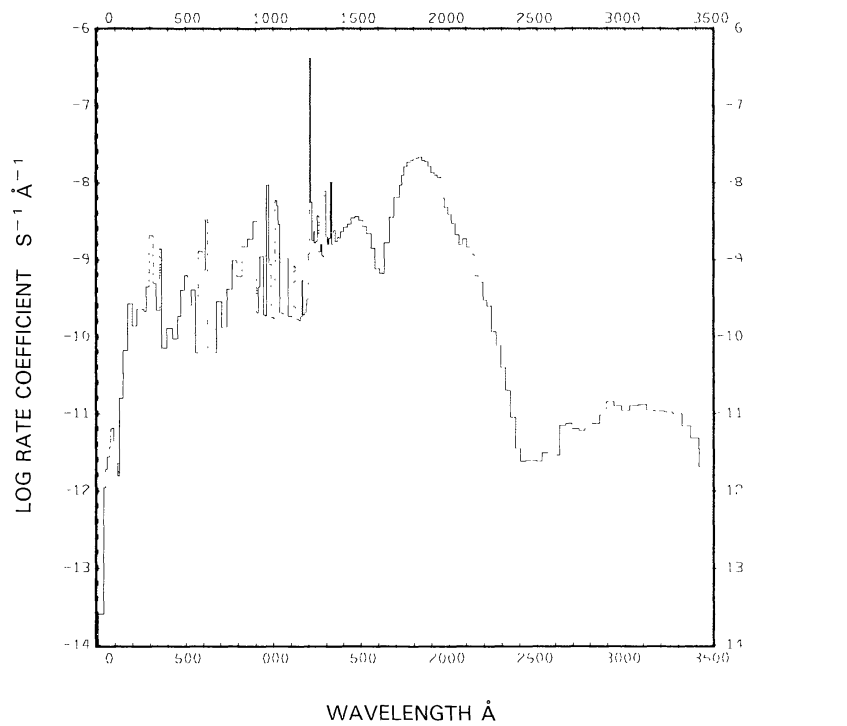


Fig. 185. $\text{CF}_2\text{Cl}_2 + \nu \rightarrow \text{CF}_2\text{Cl} + \text{Cl}$, for the quiet Sun.

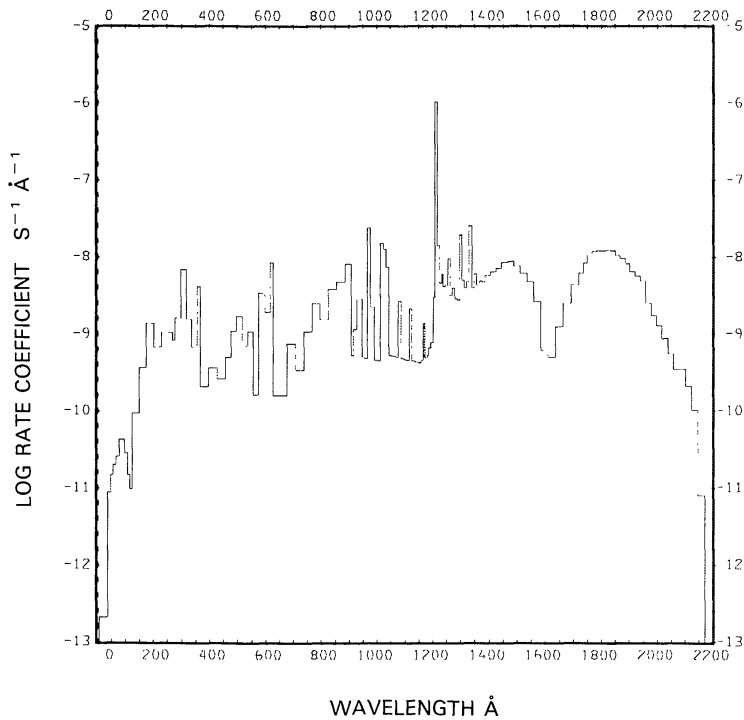


Fig. 186a. $\text{CF}_2\text{Cl}_2 + \nu \rightarrow \text{CF}_2 + \text{Cl} + \text{Cl}$, for the quiet Sun.

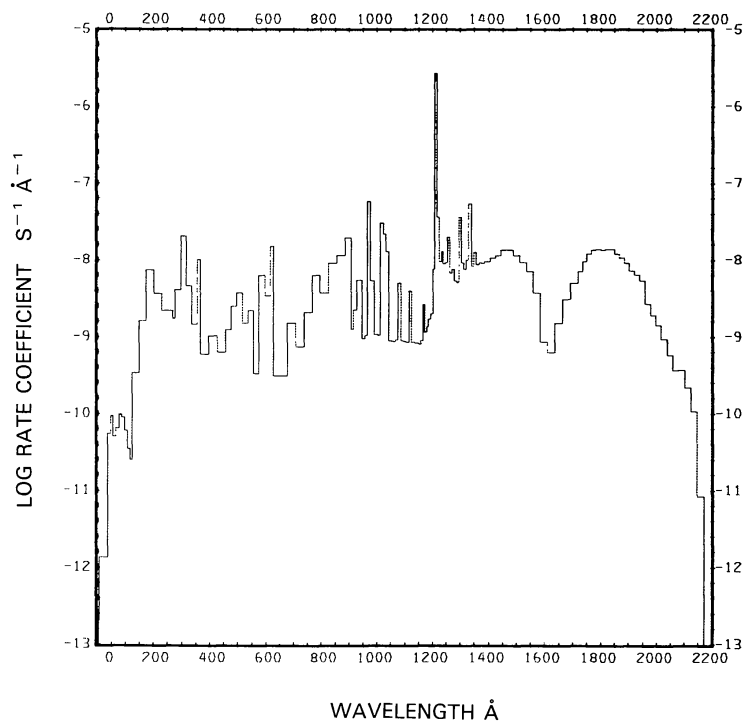


Fig. 186b. $\text{CF}_2\text{Cl}_2 + \nu \rightarrow \text{CF}_2 + \text{Cl} + \text{Cl}$, for the active Sun.

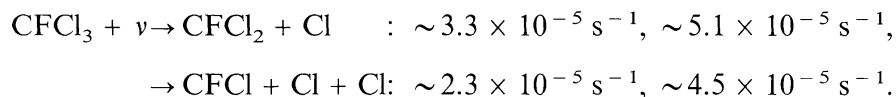
CARBON FLUOROTRICHLORIDE, CFCl_3

Cross sections: Up to 625.8 Å the cross section is synthesized from the fits to the atomic constituent cross sections prepared by Barfield *et al.* (1972). In the wavelength range from 1700 to 2600 Å we used the cross section values recommended by Baulch *et al.* (1982). No cross sections are available in the range from 626 to 1700 Å. The cross section is very small above 2600 Å.

Branching ratios: Production of $\text{CFCl}_2 + \text{Cl}$ and $\text{CFCl} + \text{Cl} + \text{Cl}$ are the primary dissociation processes, with the first one dominating at longer wavelengths. Branching ratios have been compiled by Baulch *et al.* (1982). Branching ratios leading to ionization are not known.

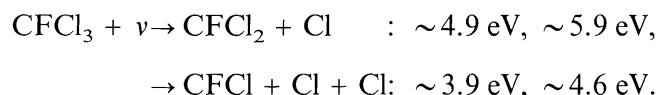
Thresholds: The threshold for the first of the above processes is at 3860 and 2140 Å for the second process (Baulch *et al.*, 1982).

Rate coefficients:

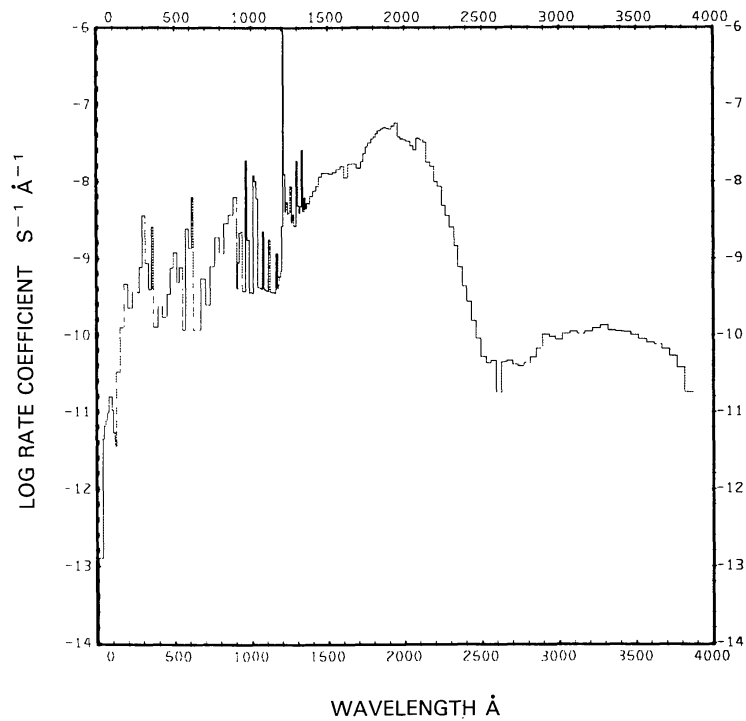
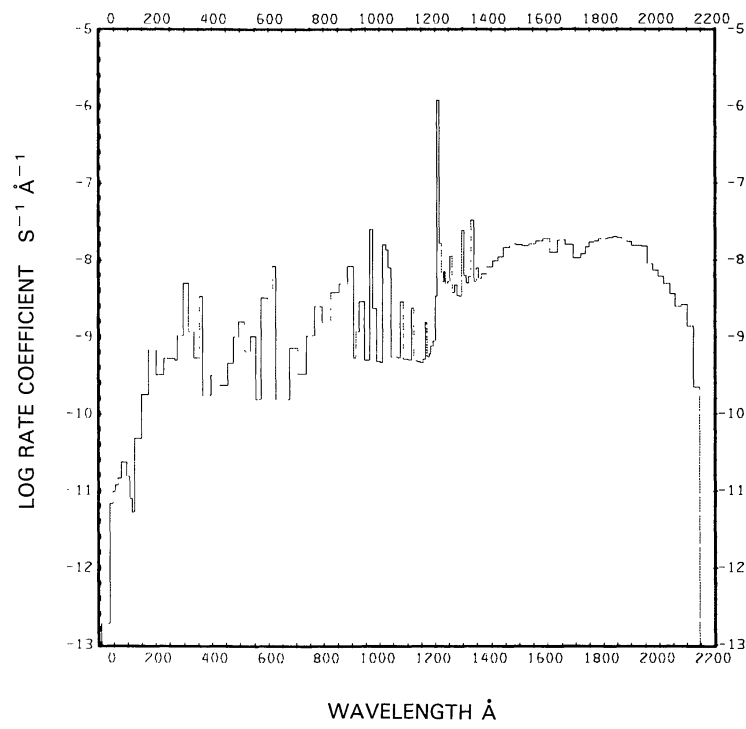


The first value of each branch is for the quiet Sun (see Figures 187 and 188), the second for the active Sun.

Excess energies:



The first value of each branch is for the quiet Sun, the second for the active Sun.

Fig. 187. $\text{CFCl}_3 + \nu \rightarrow \text{CFCl}_2 + \text{Cl}$, for the quiet Sun.Fig. 188. $\text{CFCl}_3 + \nu \rightarrow \text{CFCl} + \text{Cl} + \text{Cl}$, for the quiet Sun.

BROMINE NITRATE, BrONO₂

Cross sections: Up to a wavelength of $\lambda = 1127 \text{ \AA}$ we have estimated the cross section by summing the cross sections for BrO and NO₂. In the wavelength range from 1860 to 3900 \AA the cross section has been measured by Spencer and Rowland (1978). At longer wavelengths the cross section is assumed to be very small.

Branching ratios: Branching ratios are unknown. We assumed that only BrO + NO₂ are produced.

Thresholds: The wavelength equivalent of the dissociation energy for the above products is $\lambda = 8660 \text{ \AA}$ as quoted by Baulch *et al.* (1982).

Rate coefficients:



for the quiet Sun (see Figure 189) and $\sim 3.3 \times 10^{-3} \text{ s}^{-1}$ for the active Sun. These results are somewhat sensitive to the cross section at wavelengths longer than 3900 \AA .

Excess energies: The excess energy for this process is about 2.7 eV for the quiet Sun and about 2.8 eV for the active Sun.

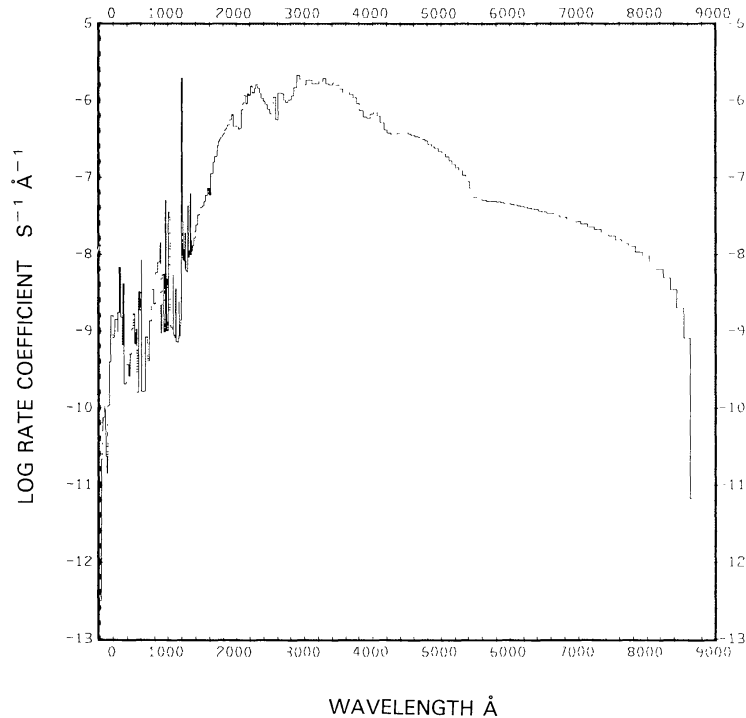


Fig. 189. $\text{BrONO}_2 + v \rightarrow \text{BrO} + \text{NO}_2$, for the quiet Sun.

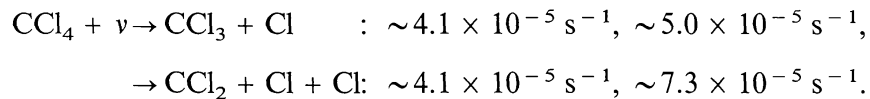
CARBON TETRACHLORIDE, CCl_4

Cross sections: Up to 625.8 Å the cross section is synthesized from the fits to the atomic constituent cross sections prepared by Barfield *et al.* (1972). In the range from 1600 to 1700 Å the cross section has been measured by Hubrich and Stuhl (1980). In the region from 1740 to 2750 Å we used the averaged cross sections recommended by Baulch *et al.* (1982). No cross sections are available between 626 Å and 1600 Å. The cross section is very small above 2750 Å.

Branching ratios: Dissociation leads primarily to $\text{CCl}_3 + \text{Cl}$ and $\text{CCl}_2 + \text{Cl} + \text{Cl}$. The branching ratio for these paths is given by Baulch *et al.* (1982). Branching ratios leading to ionization are not known.

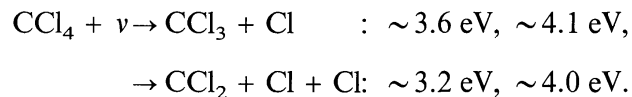
Thresholds: The threshold wavelength for the first of the above dissociation paths is 4070 Å and for the second one 2090 Å, as quoted by Baulch *et al.* (1982).

Rate coefficients:

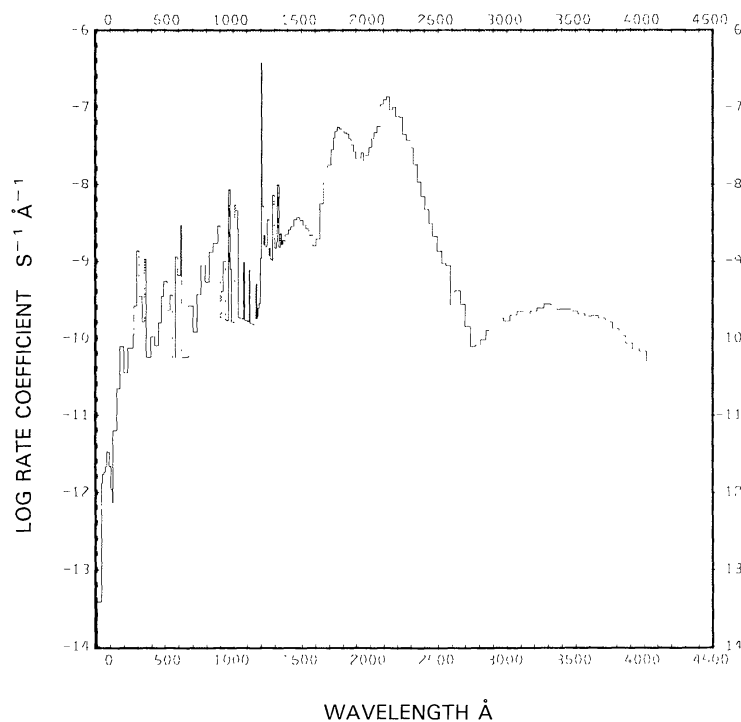
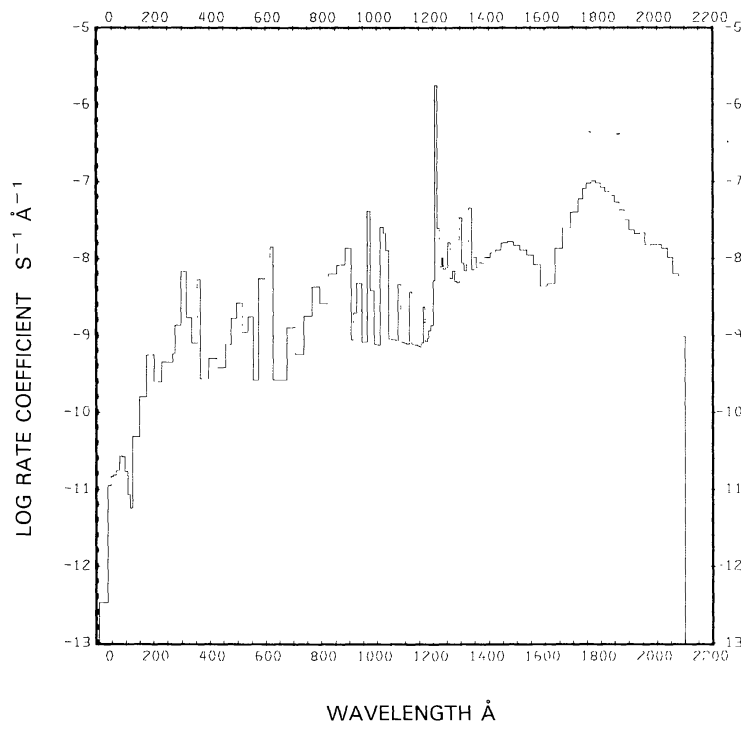


The first value of each branch is for the quiet Sun (see Figures 190 and 191), the second for the active Sun.

Excess energies:



The first value of each branch is for the quiet Sun, the second for the active Sun.

Fig. 190. $\text{CCl}_4 + \nu \rightarrow \text{CCl}_3 + \text{Cl}$, for the quiet Sun.Fig. 191. $\text{CCl}_4 + \nu \rightarrow \text{CCl}_2 + \text{Cl} + \text{Cl}$, for the quiet Sun.

IODINE NITRATE, IONO_2

Cross sections: Up to 443 Å the cross section has been synthesized from the fits to the atomic constituent cross sections prepared by Barfield *et al.* (1972). From 1890 to 4036 Å the cross section for IONO_2 has been obtained from the cross section of BrONO_2 by shifting the photon energy by $1/(500 \text{ Å})$ to the red.

Branching ratios: Branching ratios are unknown. We assumed that only $\text{IO} + \text{NO}_2$ are produced.

Thresholds: The threshold is unknown. We assumed it to be at 7850 Å.

Rate coefficients:

$$\text{IONO}_2 + \nu \rightarrow \text{IO} + \text{NO}_2: \sim 5.9 \times 10^{-3} \text{ s}^{-1}.$$

See Figure 192. The rate coefficient is insensitive to the activity of the Sun. It is $\sim 6.0 \times 10^{-3}$ for the active Sun.

Excess energies: The excess energy for this process is about 1.9 eV and is insensitive to the activity of the Sun.

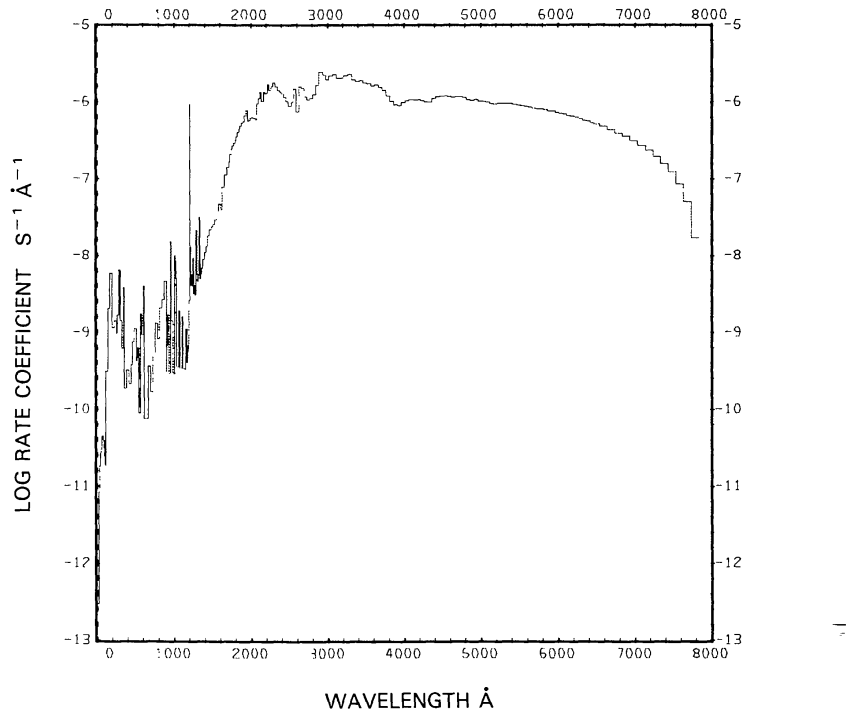


Fig. 192. $\text{IONO}_2 + \nu \rightarrow \text{IO} + \text{NO}_2$, for the quiet Sun.

ETHYLENE, C₂H₄

Cross sections: Up to $\lambda = 100 \text{ \AA}$ the cross section has been synthesized from the fits to the atomic constituent cross sections prepared by Barfield *et al.* (1972). In the wavelength range from $\lambda = 180$ to 700 \AA the cross section was measured by Lee *et al.* (1973). From $\lambda = 500$ to 1200 \AA the cross section data is from Schoen (1962) and in the range $\lambda = 1065$ the measurements of Zelikoff and Watanabe (1953) were used. Above 1973 \AA the cross section is very small.

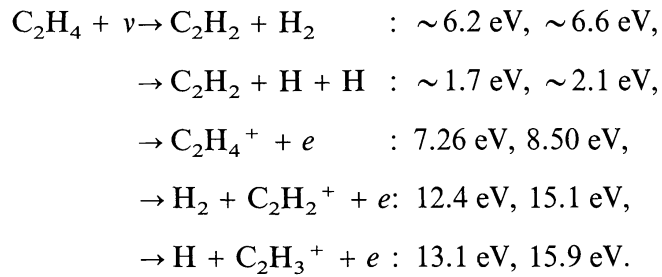
Branching ratios: McNesby and Okabe (1964) state that above $\lambda = 1236 \text{ \AA}$ only dissociation leading to C₂H₂ + H₂ occurs. Strobel (1973) reports that dissociation leading to C₂H₂ + H + H occurs with a probability of 65% at the L α line. We have assumed that below 1226 \AA C₂H₂ + H + H makes up 65% of total dissociation and C₂H₂ + H₂ makes up 35% and above 1226 \AA C₂H₂ + H₂ is the only branch. The branching ratios for ionization and dissociative ionization are from Schoen (1962). The branching ratio for dissociation was estimated.

Thresholds: From heats of formation (Benson, 1976) the wavelength equivalent for dissociation into C₂H₂ + H₂ is 7200 \AA and for dissociation into C₂H₂ + H + H it is 1960 \AA . The ionization threshold as determined by Zelikoff and Watanabe (1953) is at $\lambda = 1180 \text{ \AA}$. Thresholds for photodissociative ionization have been determined by Botter *et al.* (1966) to be at $\lambda = 945 \text{ \AA}$ for production of C₂H₂⁺ + H₂ and at $\lambda = 898 \text{ \AA}$ for production of C₂H₃⁺ + H.

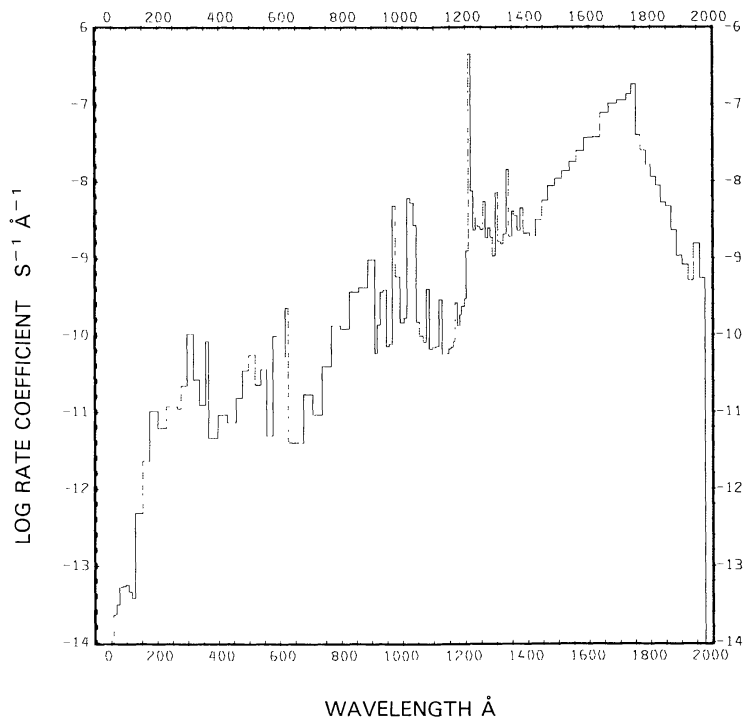
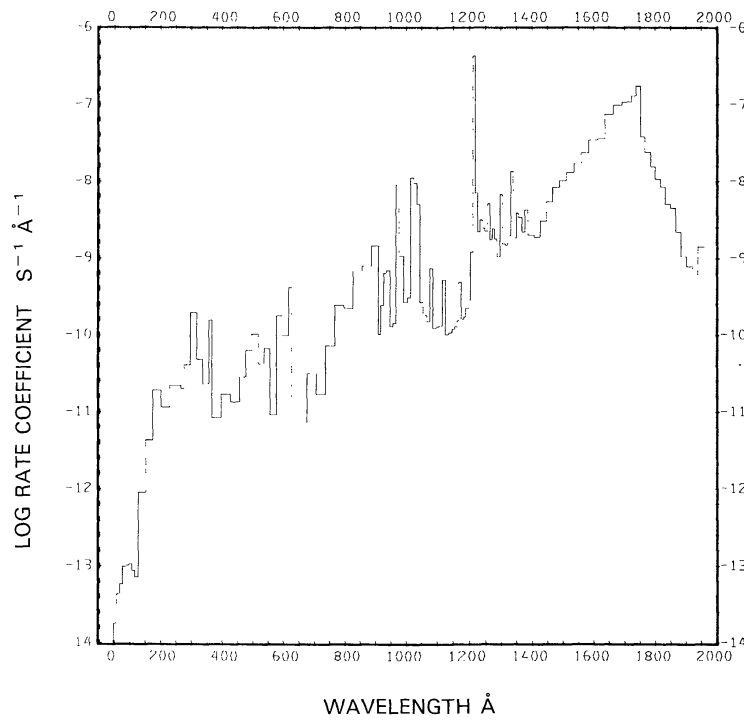
Rate coefficients:

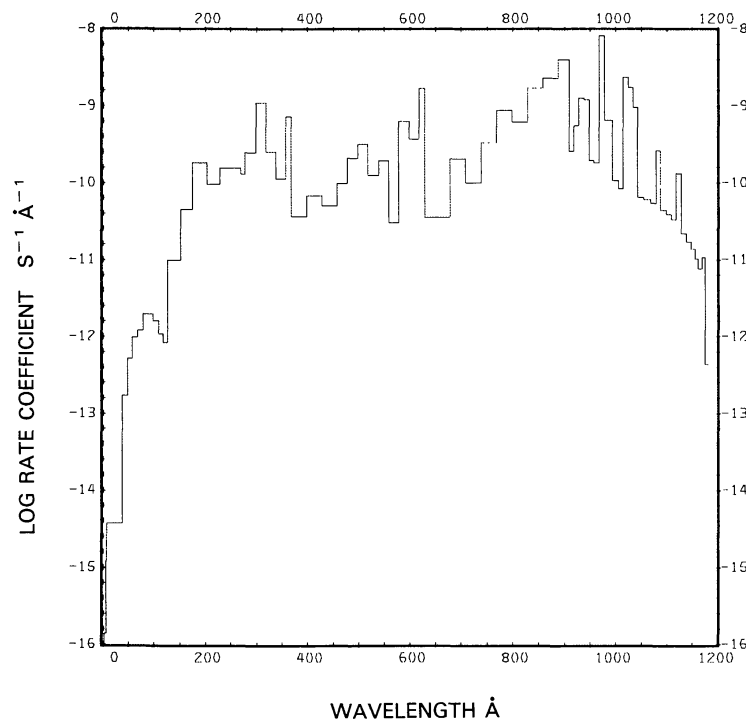
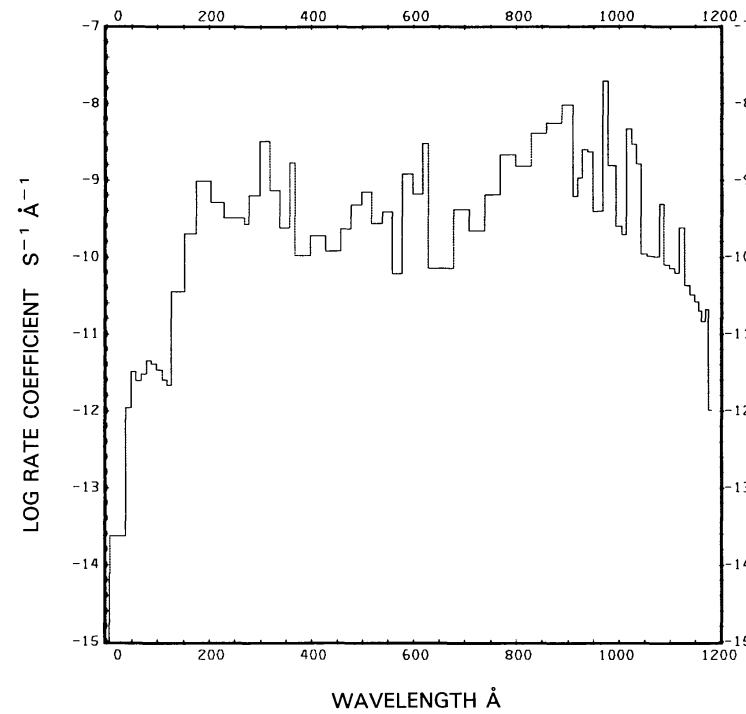
$$\begin{aligned}
 \text{C}_2\text{H}_4 + v \rightarrow & \text{C}_2\text{H}_2 + \text{H}_2 : \sim 2.4 \times 10^{-5} \text{ s}^{-1}, \sim 3.4 \times 10^{-5} \text{ s}^{-1}, \\
 & \rightarrow \text{C}_2\text{H}_2 + \text{H} + \text{H} : \sim 2.3 \times 10^{-5} \text{ s}^{-1}, \sim 3.4 \times 10^{-5} \text{ s}^{-1}, \\
 & \rightarrow \text{C}_2\text{H}_4^+ + e : 5.80 \times 10^{-7} \text{ s}^{-1}, 1.35 \times 10^{-6} \text{ s}^{-1}, \\
 & \rightarrow \text{H}_2 + \text{C}_2\text{H}_2^+ + e : 1.97 \times 10^{-7} \text{ s}^{-1}, 4.89 \times 10^{-7} \text{ s}^{-1}, \\
 & \rightarrow \text{H} + \text{C}_2\text{H}_3^+ + e : 2.26 \times 10^{-7} \text{ s}^{-1}, 5.47 \times 10^{-7} \text{ s}^{-1}.
 \end{aligned}$$

The first value of each branch is for the quiet Sun (see Figures 193, 194, and 195(a) to 197(a)), the second for the active Sun (see Figures 195(b) to 197(b)). For the quiet Sun our total rate coefficient ($4.8 \times 10^{-5} \text{ s}^{-1}$) is smaller than the value obtained by Potter and del Duca (1964) ($6.5 \times 10^{-5} \text{ s}^{-1}$), but considering the uncertainties about the threshold, this is good agreement. The second dissociation path in the above table is sensitive to L α .

Excess energies:

The first value of each branch is for the quiet Sun, the second for the active Sun.

Fig. 193. $\text{C}_2\text{H}_4 + \nu \rightarrow \text{C}_2\text{H}_2 + \text{H}_2$, for the quiet Sun.Fig. 194. $\text{C}_2\text{H}_4 + \nu \rightarrow \text{C}_2\text{H}_2 + \text{H} + \text{H}$, for the quiet Sun.

Fig. 195a. C₂H₄ + ν → C₂H₄⁺ + e⁻, for the quiet Sun.Fig. 195b. C₂H₄ + ν → C₂H₄⁺ + e⁻, for the active Sun.

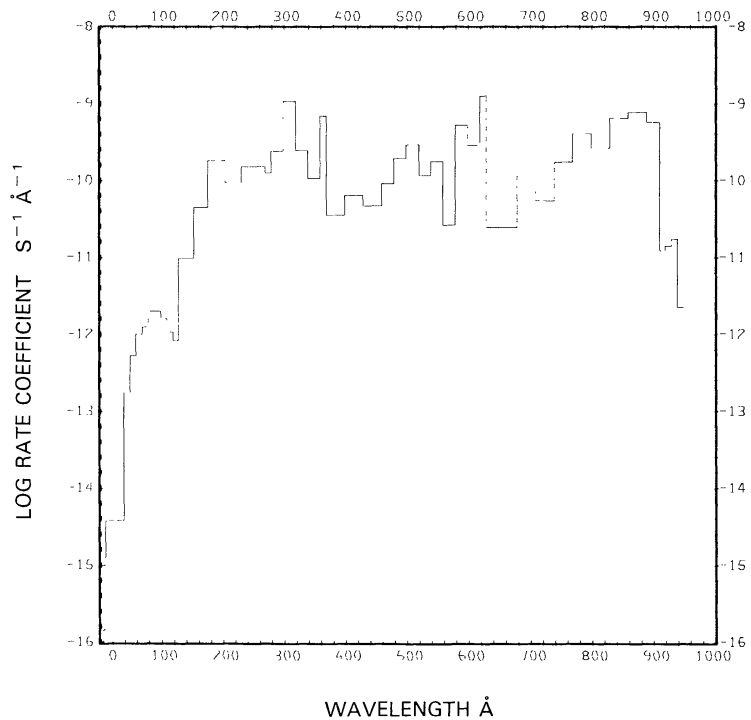


Fig. 196a. $\text{C}_2\text{H}_4 + \nu \rightarrow \text{H}_2 + \text{C}_2\text{H}_2^+ + e^-$, for the quiet Sun.

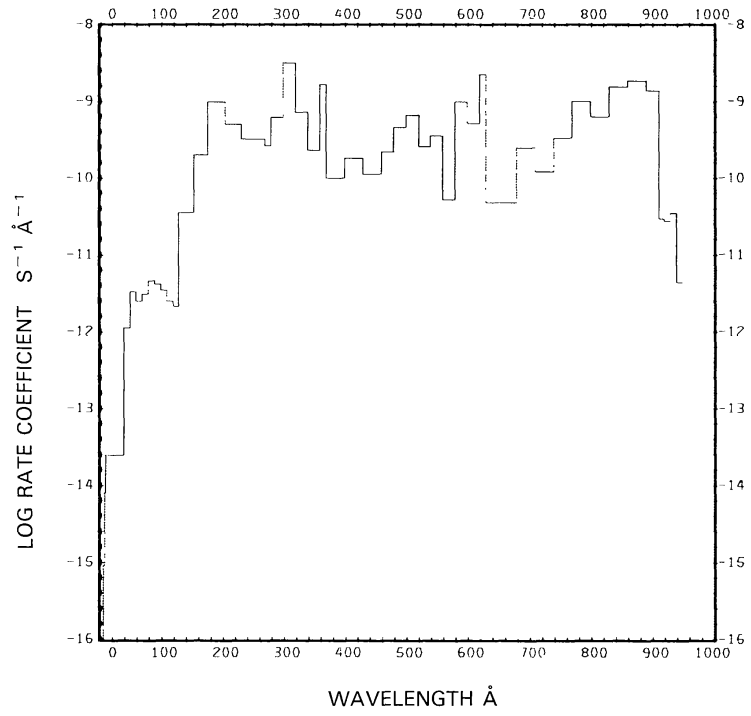
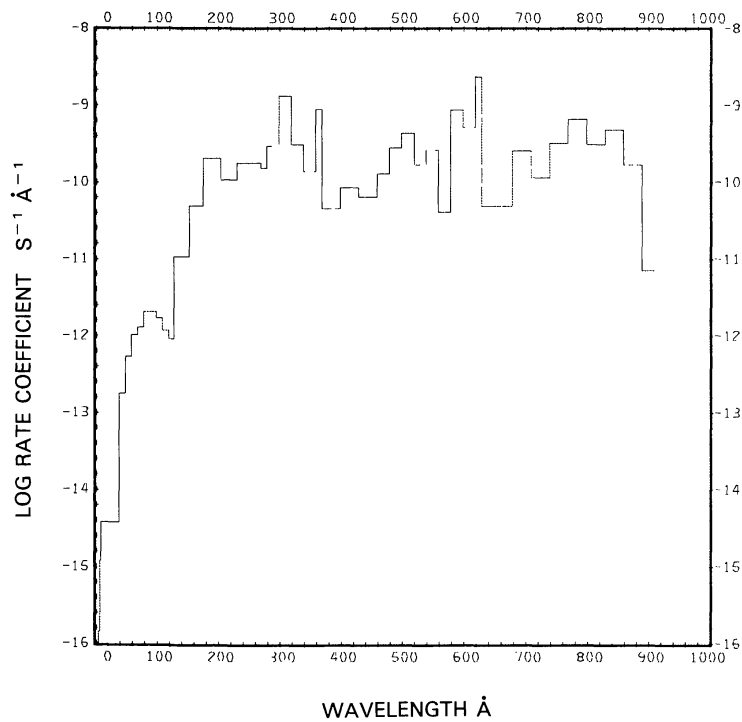
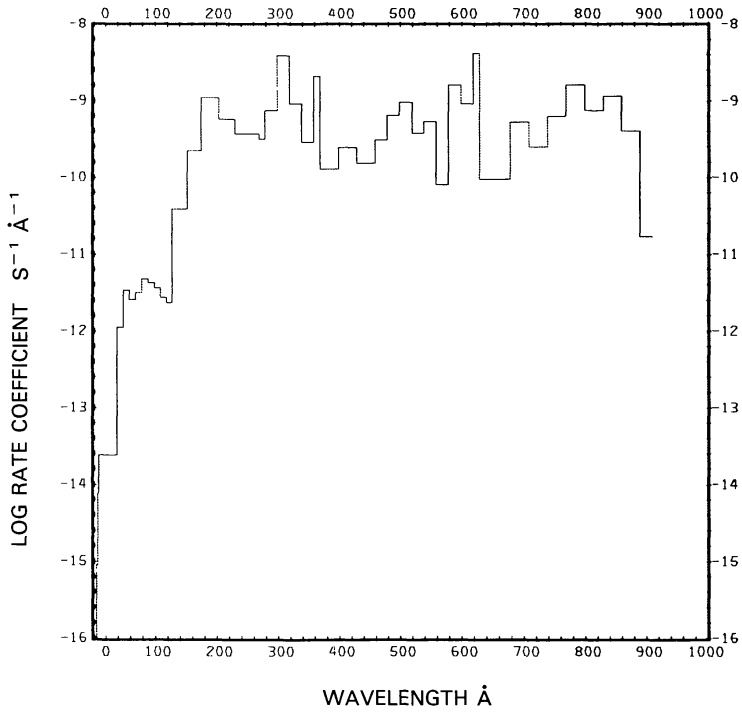


Fig. 196b. $\text{C}_2\text{H}_4 + \nu \rightarrow \text{H}_2 + \text{C}_2\text{H}_2^+ + e^-$, for the active Sun.

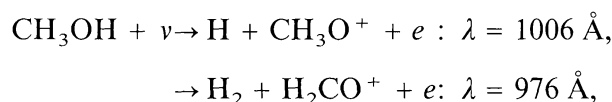
Fig. 197a. C₂H₄ + ν → H + C₂H₃⁺ + e, for the quiet Sun.Fig. 197b. C₂H₄ + ν → H + C₂H₃⁺ + e, for the active Sun.

METHYL ALCOHOL, CH₃OH

Cross sections: Up to 800 Å the cross section is synthesized from the fits to the atomic constituent cross sections as prepared by Barfield *et al.* (1972). In the range from $\lambda = 1060$ to 1980 Å we used the data of Nee *et al.* (1985), supplemented with data of Salahub and Sandorfy (1971) in the range 1200 to 2053 Å. There are no data available between 800 and 1060 Å; we scaled water cross sections into this region. Beyond 2053 Å the cross section is negligibly small. We assume that it decreased from 10^{-22} cm² at 2053 Å to 10^{-25} cm² at threshold.

Branching ratios: The data of Porter and Noyes (1959) indicate that the dissociation branch to form OH + CH₃ contributes less than 5% of all processes. A 5% branching ratio was assumed for this process. We assume that 95% dissociates into H₂ + H₂CO; all ionization branching ratios are guessed, the guesses are based on water data.

Thresholds: Dissociation energies are not available and heats of formation are not well known. From heats of formation we obtain about 13500 Å for dissociation into H₂ + H₂CO and about 3150 Å for dissociation into OH + CH₃. The threshold for ionization $\lambda = 1143$ Å is given by Salahub and Sandorfy (1971); while the threshold wavelengths for dissociative ionizations



are obtained from Field and Franklin (1970).

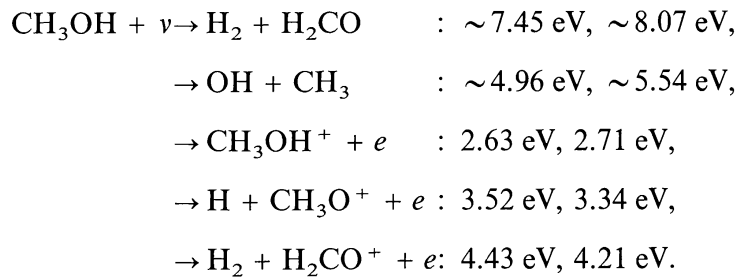
Rate coefficients:

$$\begin{aligned} \text{CH}_3\text{OH} + \nu \rightarrow & \text{H}_2 + \text{H}_2\text{CO} : \sim 1.02 \times 10^{-5} \text{ s}^{-1}, \\ & \sim 1.82 \times 10^{-5} \text{ s}^{-1}, \\ \rightarrow & \text{OH} + \text{CH}_3 : \sim 5.58 \times 10^{-7} \text{ s}^{-1}, \\ & \sim 1.02 \times 10^{-6} \text{ s}^{-1}, \\ \rightarrow & \text{CH}_3\text{OH}^+ + e : 4.88 \times 10^{-7} \text{ s}^{-1}, 1.02 \times 10^{-6} \text{ s}^{-1}, \\ \rightarrow & \text{H} + \text{CH}_3\text{O}^+ + e : 1.20 \times 10^{-7} \text{ s}^{-1}, 2.70 \times 10^{-7} \text{ s}^{-1}, \\ \rightarrow & \text{H}_2 + \text{H}_2\text{CO}^+ + e: 1.15 \times 10^{-7} \text{ s}^{-1}, 2.55 \times 10^{-7} \text{ s}^{-1}. \end{aligned}$$

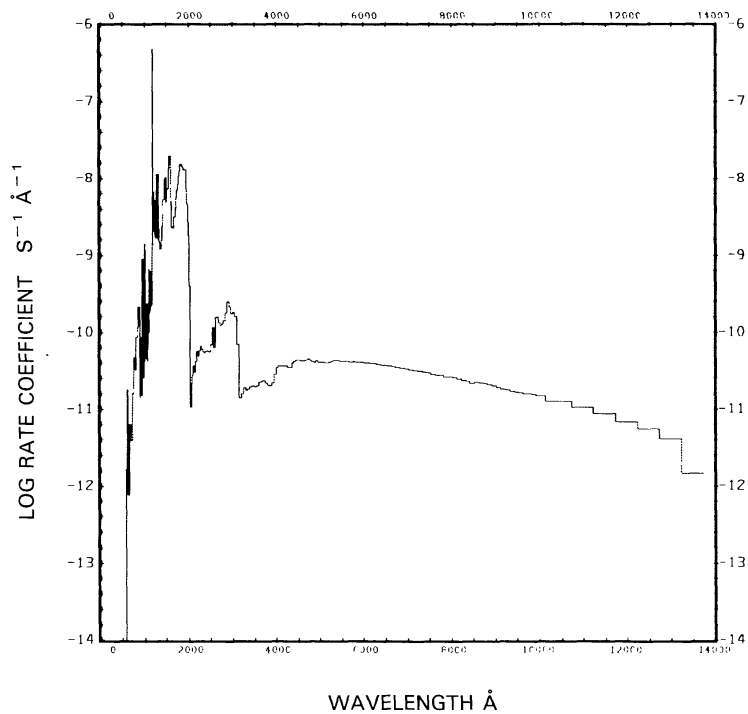
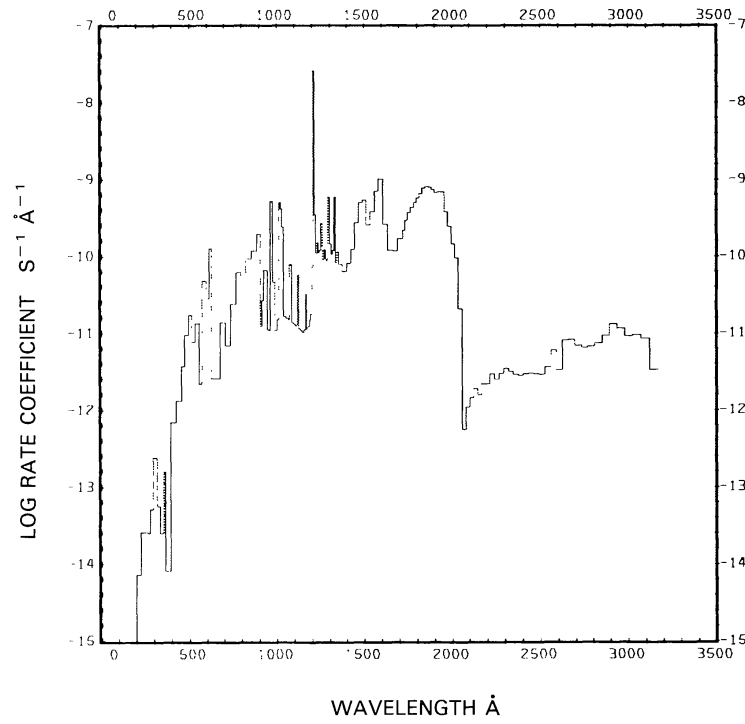
The first value of each branch is for the quiet Sun (see Figures 198, 199, and 200(a) to 202(a)), the second for the active Sun (see Figures 200(b) to 202(b)). The rate coefficient for the first branch (and therefore also the total rate coefficient) is very sensitive to the cross section between 2053 Å and threshold. If the cross section in this range is assumed to be 10^{-22} cm², then the rate coefficient for the first branch is 5.1×10^{-5} s⁻¹ for the quiet Sun and 5.9×10^{-5} s⁻¹ for the active Sun. These could be considered to be

maximum values. For the quiet Sun the total rate coefficient ($5.2 \times 10^{-5} \text{ s}^{-1}$) is then comparable to the value given by Jackson (1976a,b) ($4.7 \times 10^{-5} \text{ s}^{-1}$). The dissociation rates are dominated by L α .

Excess energies:



The first value of each branch is for the quiet Sun, the second for the active Sun.

Fig. 198. $\text{CH}_3\text{OH} + \nu \rightarrow \text{H}_2 + \text{H}_2\text{CO}$, for the quiet Sun.Fig. 199. $\text{CH}_3\text{OH} + \nu \rightarrow \text{OH} + \text{CH}_3$, for the quiet Sun.

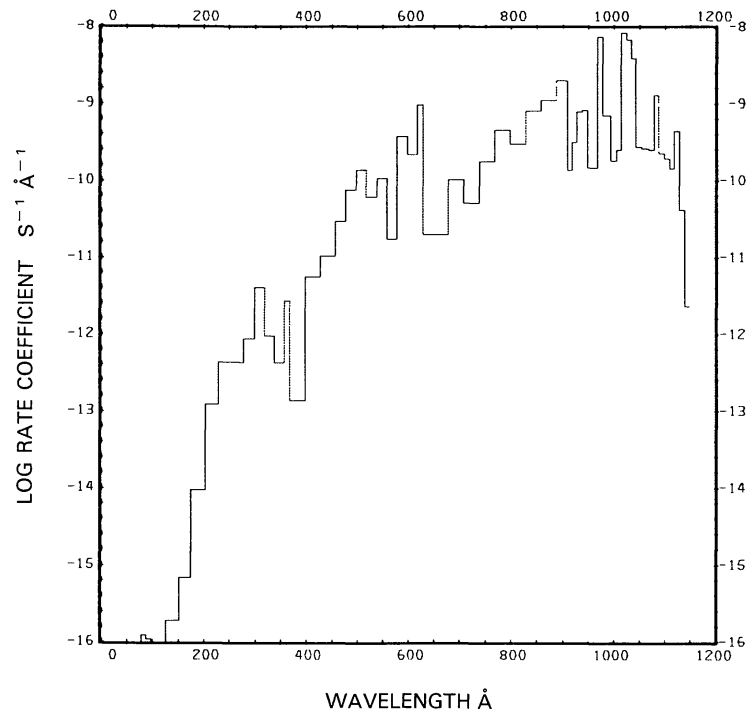


Fig. 200a. CH₃OH + $\nu \rightarrow$ CH₃OH⁺ + e^- , for the quiet Sun.

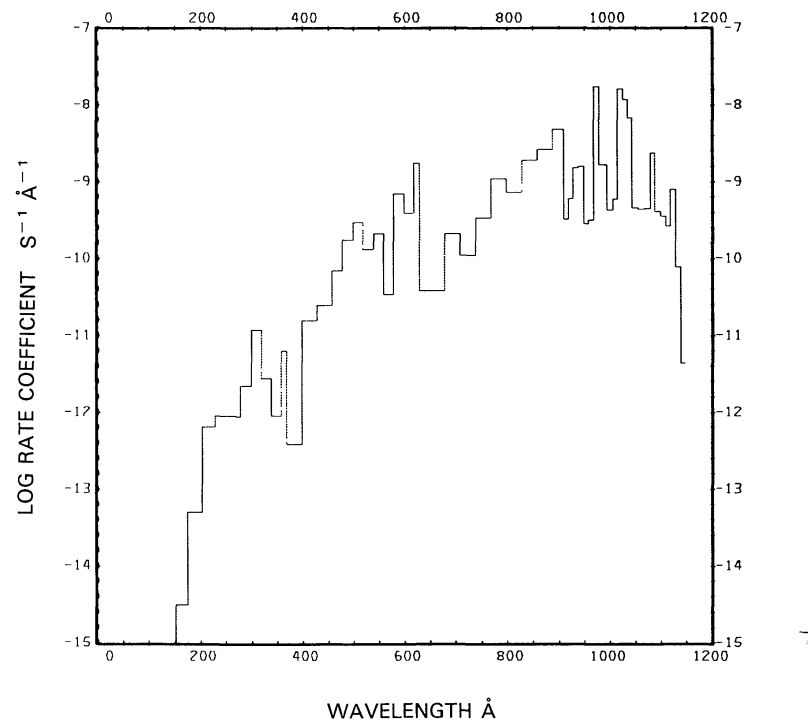
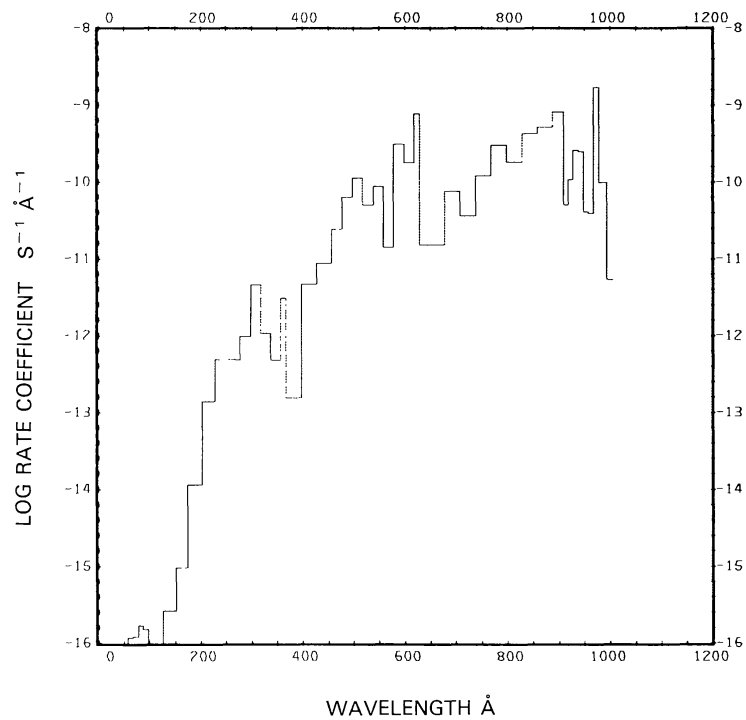
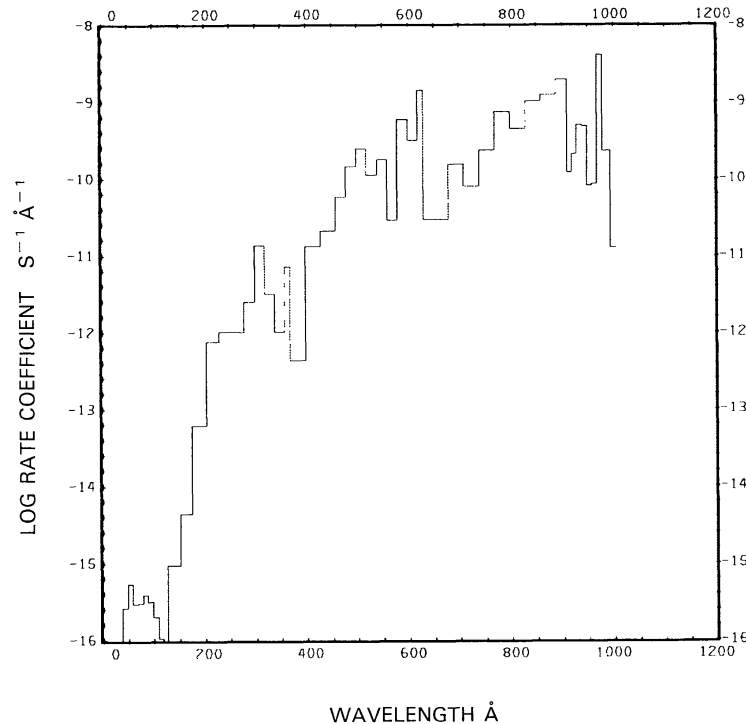
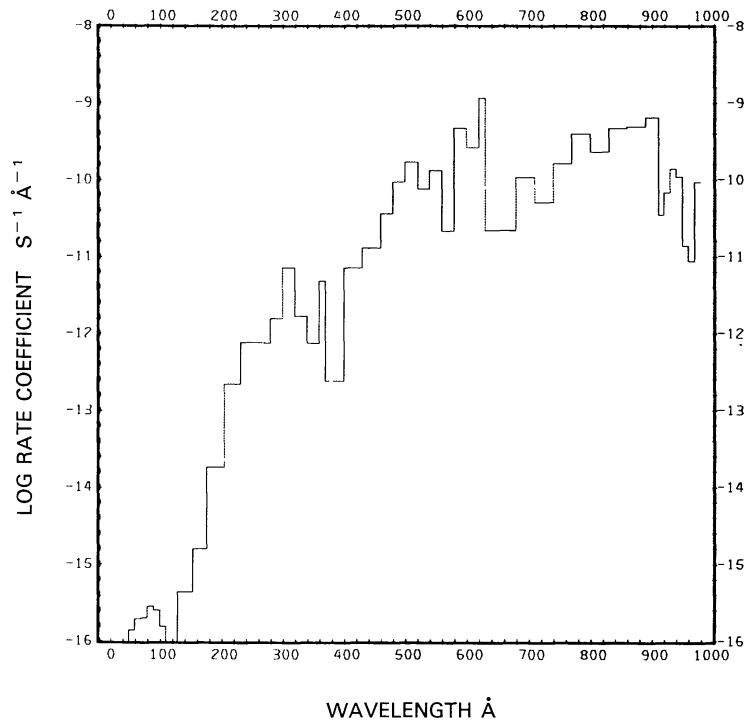
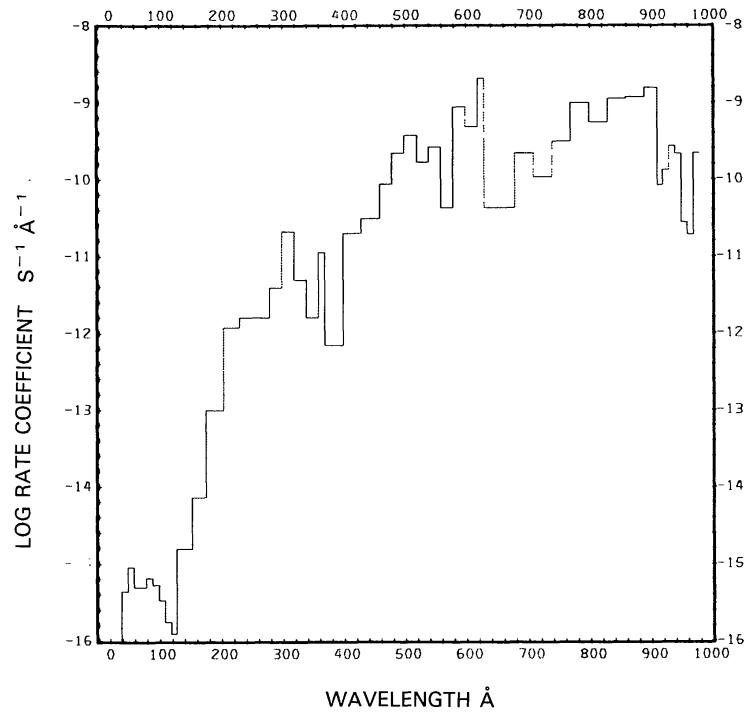


Fig. 200b. CH₃OH + $\nu \rightarrow$ CH₃OH⁺ + e^- , for the active Sun.

Fig. 201a. $\text{CH}_3\text{OH} + \nu \rightarrow \text{H} + \text{CH}_3\text{O}^+ + e$, for the quiet Sun.Fig. 201b. $\text{CH}_3\text{OH} + \nu \rightarrow \text{H} + \text{CH}_3\text{O}^+ + e$, for the active Sun.

Fig. 202a. $\text{CH}_3\text{OH} + \nu \rightarrow \text{H}_2 + \text{H}_2\text{CO}^+ + e$, for the quiet Sun.Fig. 202b. $\text{CH}_3\text{OH} + \nu \rightarrow \text{H}_2 + \text{H}_2\text{CO}^+ + e$, for the active Sun.

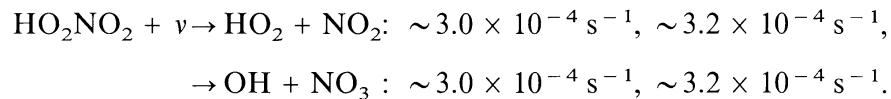
PEROXYNITRIC ACID, HO₂NO₂

Cross sections: Up to 1850 Å we used the combined cross sections of HO₂ and NO₂. In the wavelength range from 1900 to 3300 Å the cross section has been measured by Molina and Molina (1981). From 3400 to 3600 Å the cross section measured by Jesson *et al.* (1977) for an aqueous solution were used; they smoothly match the values determined by Molina and Molina at 3300 Å. Beyond 3600 Å the cross section is very small.

Branching ratios: Branching ratios are unknown. We assumed that 50% of the cross section results in production of HO₂ + NO₂ and 50% in OH + NO₃.

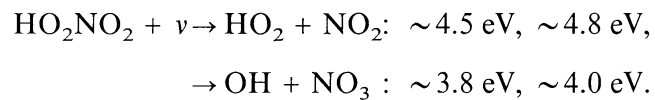
Thresholds: According to Baulch *et al.* (1982) the threshold wavelength for the first of the above processes is at 13400 Å and the second is at 7300 Å.

Rate coefficients:

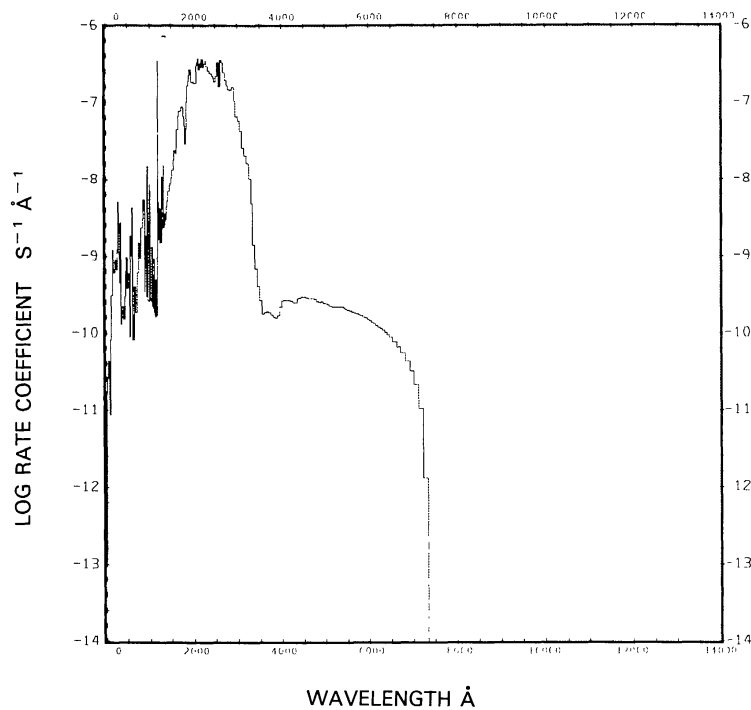
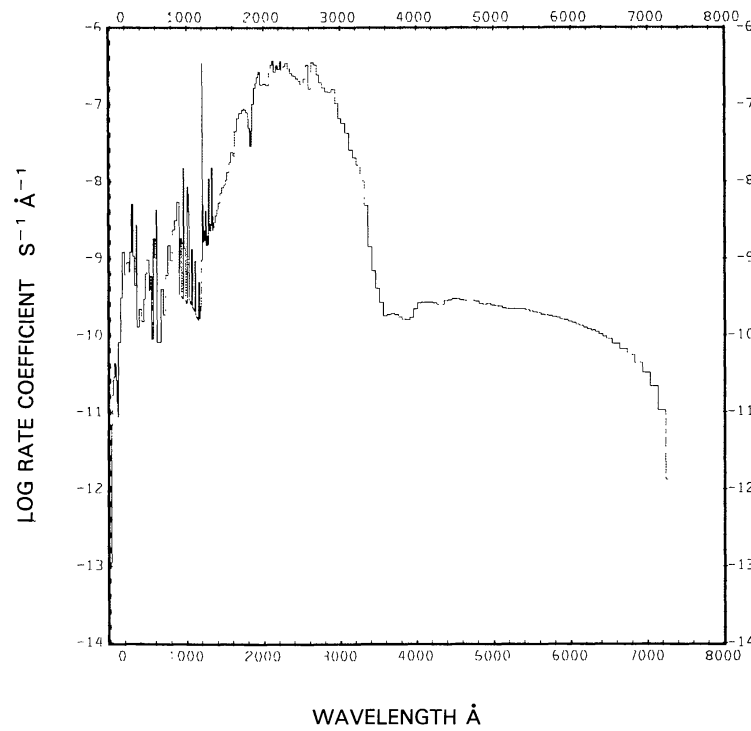


The first value of each branch is for the quiet Sun (see Figures 203 and 204), the second for the active Sun. All rates are very approximate.

Excess energies:



The first value of each branch is for the quiet Sun, the second for the active Sun.

Fig. 203. $\text{HO}_2\text{NO}_2 + \nu \rightarrow \text{HO}_2 + \text{NO}_2$, for the quiet Sun.Fig. 204. $\text{HO}_2\text{NO}_2 + \nu \rightarrow \text{OH} + \text{NO}_3$, for the quiet Sun.

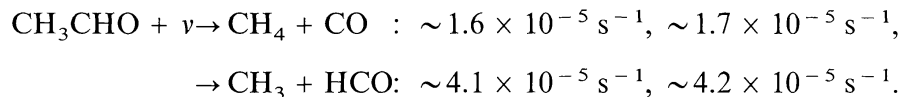
ACETALDEHYDE, CH₃CHO

Cross sections: Up to 625.8 Å the cross section has been synthesized from the fits to the constituent atomic cross sections prepared by Barfield *et al.* (1972). In the wavelength range $\lambda = 2000$ to 3450 Å we used the compiled cross sections of Baulch *et al.* (1982) supplemented with two values from Weaver *et al.* (1976) at $\lambda = 3100$ Å and $\lambda = 3500$ Å. There is no data between 626 and 2000 Å; since there is a significant change in the cross section in this range, we assumed the cross section at $\lambda = 1000$ Å to be 1×10^{-20} cm².

Branching ratios: We adopted the dissociation branching ratios listed by Baulch *et al.* (1982), but adjusted them for discrepancies and forced the sum of the branching ratios (including the production of the triplet state ³CH₃CHO) to be one. We assumed no ionization since that branching ratio is unknown.

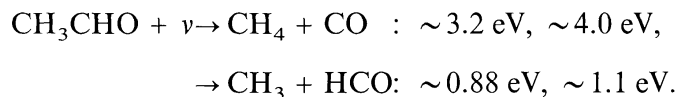
Thresholds: The threshold for production of CH₄ + CO is not known; we assumed it to be 7350 Å. The threshold for production of CH₃ + HCO is at 3501 Å, as quoted by Baulch *et al.* (1982).

Rate coefficients:

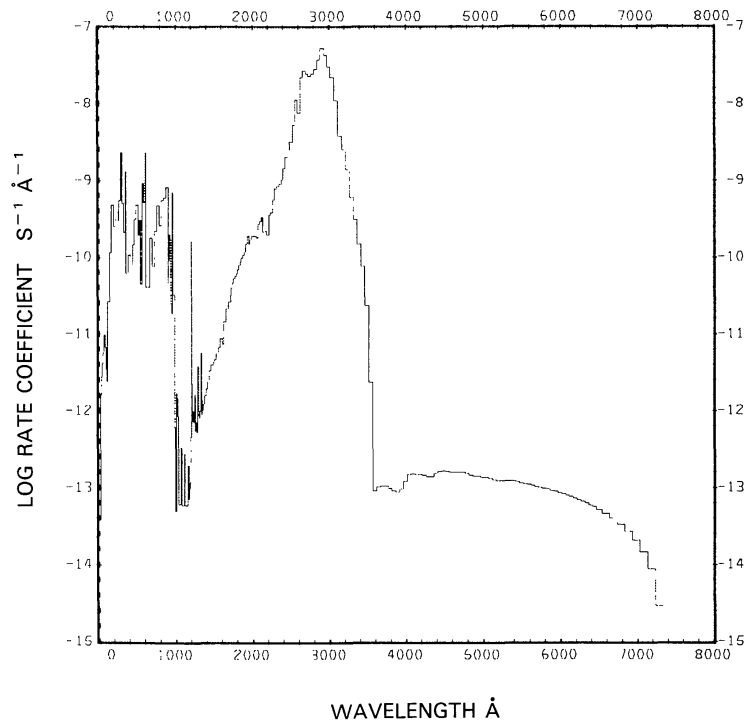
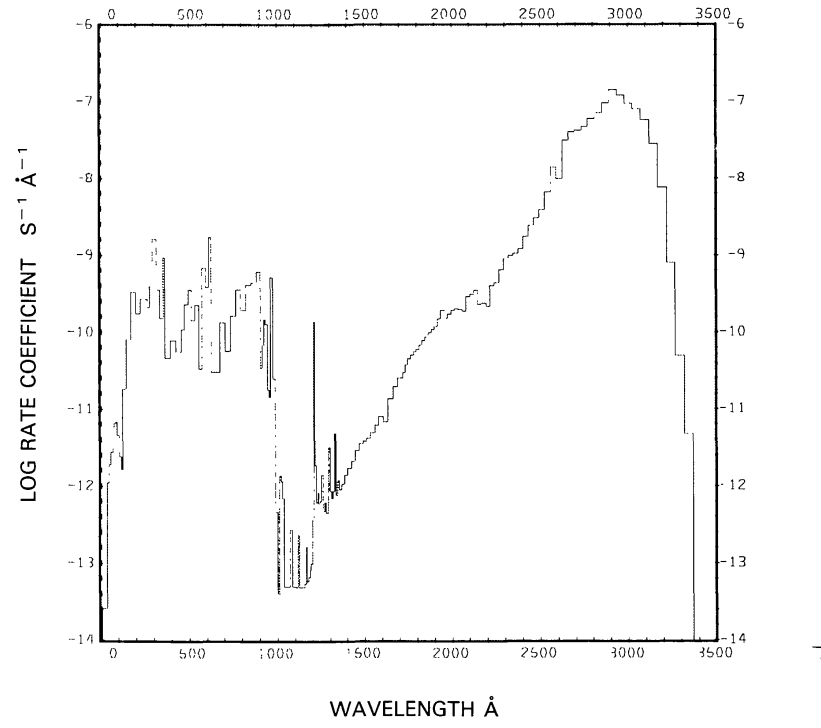


The first value of each branch is for the quiet Sun (see Figures 205 and 206), the second for the active Sun. Because of the uncertainties in the branching ratios, cross sections, and thresholds, there is considerable uncertainty in these rate coefficients. Weaver *et al.* (1976) obtain for an overhead Sun at the surface of the Earth $4.1 \times 10^{-7} \text{ s}^{-1}$ for the first of the above processes, and $2.8 \times 10^{-6} \text{ s}^{-1}$ for the second process. In comparing with our much larger rate coefficients it must be born in mind that our rates are without any attenuation by the Earth atmosphere.

Excess energies:



The first value of each branch corresponds to the quiet Sun, the second to the active Sun.

Fig. 205. $\text{CH}_3\text{CHO} + \nu \rightarrow \text{CH}_4 + \text{CO}$, for the quiet Sun.Fig. 206. $\text{CH}_3\text{CHO} + \nu \rightarrow \text{CH}_3 + \text{HCO}$, for the quiet Sun.

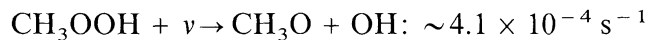
METHYLHYDROPEROXIDE, CH₃OOH

Cross sections: Up to 2000 Å we used the cross section of formic acid as an approximation for the cross section for CH₃OOH; no other cross sections are available for this compound in this wavelength range. From 2100 to 3500 Å the cross section has been measured by Molina and Arguello (1979). At wavelengths longer than 3500 Å the cross section becomes very small.

Branching ratios: Branching ratios have not been measured, but indications are that production of CH₃O + OH is dominant in photodissociation.

Thresholds: The wavelength equivalent of the dissociation energy for production of CH₃O + OH is 6470 Å.

Rate coefficients:



for the quiet Sun (see Figure 207) and $\sim 6.5 \times 10^{-4} \text{ s}^{-1}$ for the active Sun. About one quarter of this value comes from L α radiation, where we have used the H₂COO cross section as an approximation. This rate coefficient is therefore not very reliable. Molina and Arguello (1979) quote $1.0 \times 10^{-6} \text{ s}^{-1}$ for an overhead Sun using the cross section between 2100 and 3500 Å only.

Excess energies: The excess energy for this process is about 5.8 eV for the quiet Sun and about 6.5 eV for the active Sun.

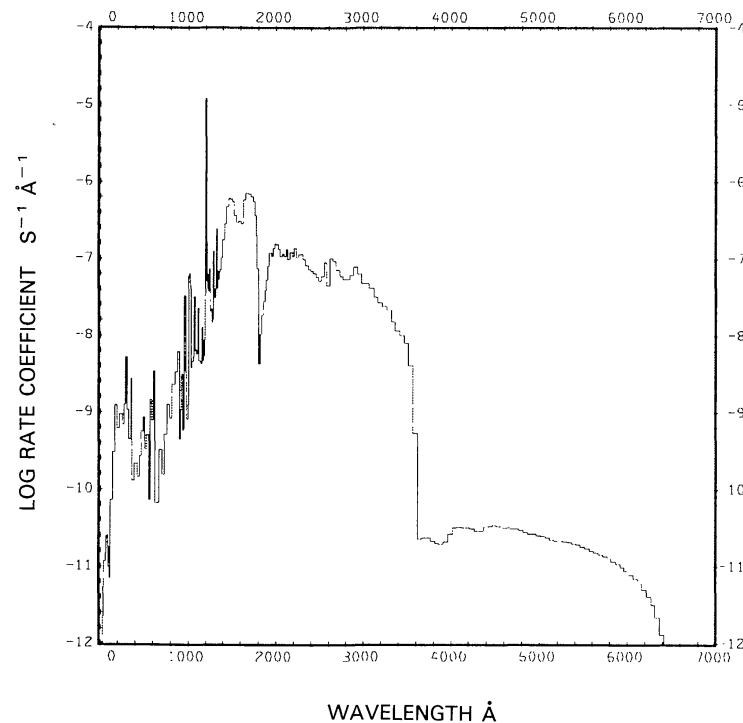


Fig. 207. CH₃OOH + $\nu \rightarrow$ CH₃O + OH, for the quiet Sun.

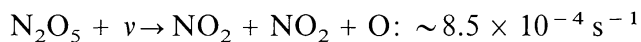
DINITROGEN PENTOXIDE, N_2O_5

Cross sections: Up to 2000 Å we synthesized the cross section from the sum of the NO_2 and NO_3 cross sections. In the wavelength region from 2000 to 4055 Å the cross section has been measured by Yao *et al.* (1982). No cross sections are available beyond 4055 Å; we assumed the cross section to be negligibly small.

Branching ratios: Branching ratios have not been measured, but indications are that N_2O_5 dissociates into $2\text{NO}_2 + \text{O}$.

Thresholds: From heats of formation (Stull and Prophet, 1971) the dissociation wavelength is about 94 100 Å.

Rate coefficients:



for the quiet Sun (see Figure 208) and $\sim 9.0 \times 10^{-4} \text{ s}^{-1}$ for the active Sun.

Excess energies: The excess energy for this process is about 5.2 eV for the quiet Sun and about 5.4 eV for the active Sun.

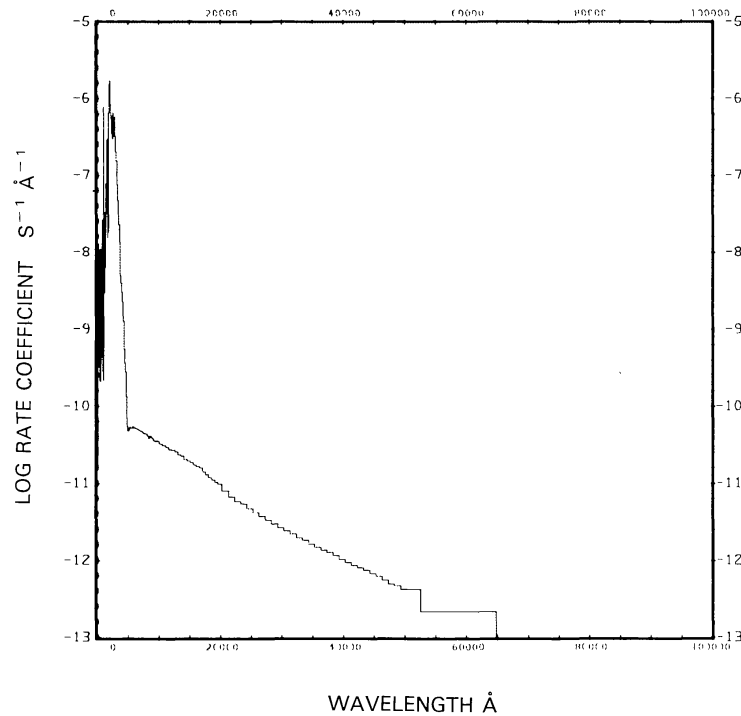


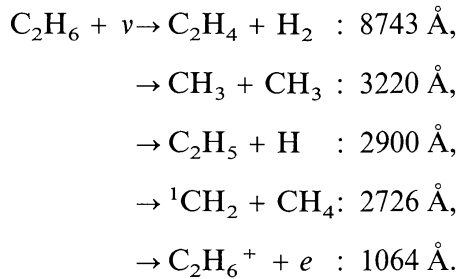
Fig. 208. $\text{N}_2\text{O}_5 + v \rightarrow \text{NO}_2 + \text{NO}_2 + \text{O}$, for the quiet Sun.

ETHANE, C₂H₆

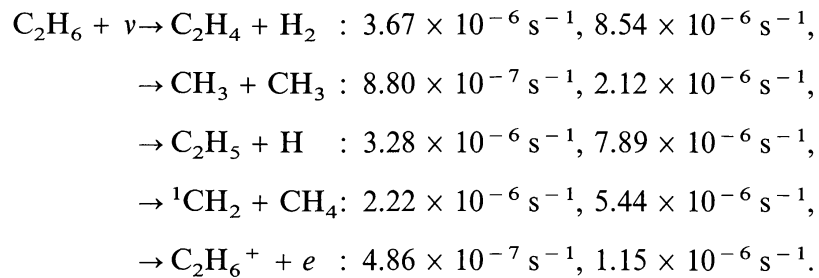
Cross sections: Up to 250 Å the cross section is synthesized from the fits for the atomic cross sections for H and C as prepared by Barfield *et al.* (1972). Koch and Skibowski (1971) have measured the cross section in the wavelength range from $\lambda = 354$ to 1127 Å, Lombos *et al.* (1967) in the range from 1160 to 1200 Å, Okabe and Becker (1963) in the range from 1200 to 1380 Å, and Mount and Moos (1978) in the range from 1380 to 1600 Å. Beyond this wavelength the cross section is very small.

Branching ratios: Branching ratios leading to dissociations and to ionization have been measured by Lias *et al.* (1970) at $\lambda = 1055$, 1236, and 1470 Å.

Thresholds:

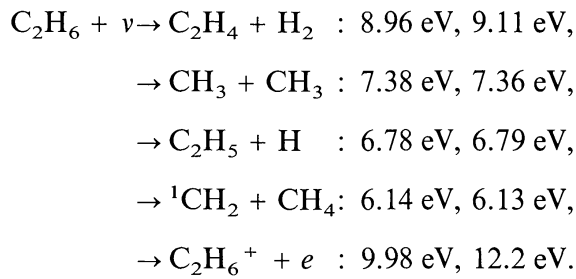


Rate coefficients:

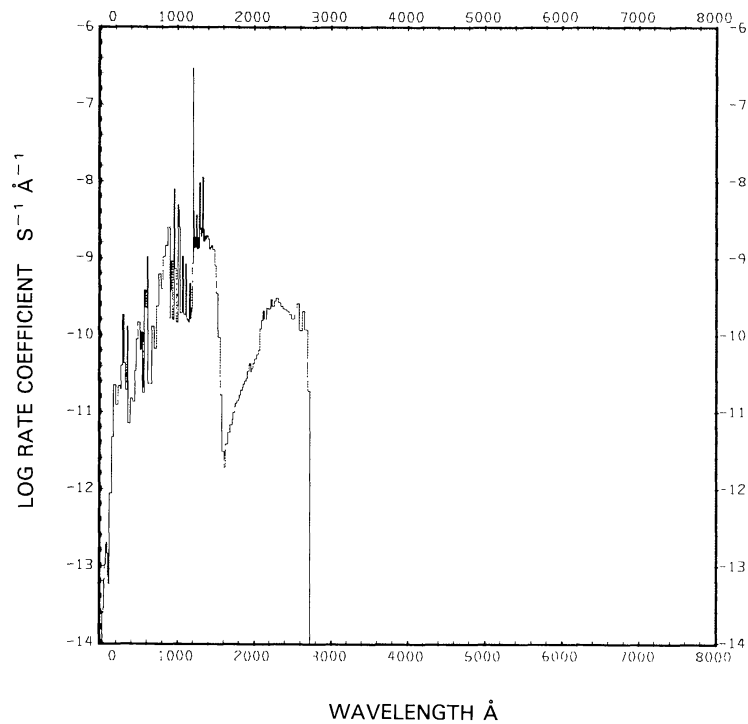
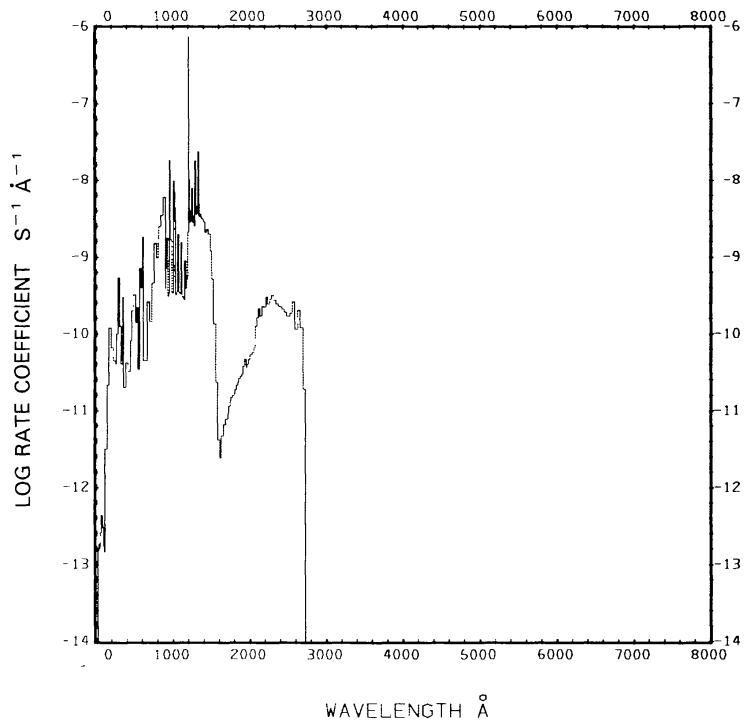


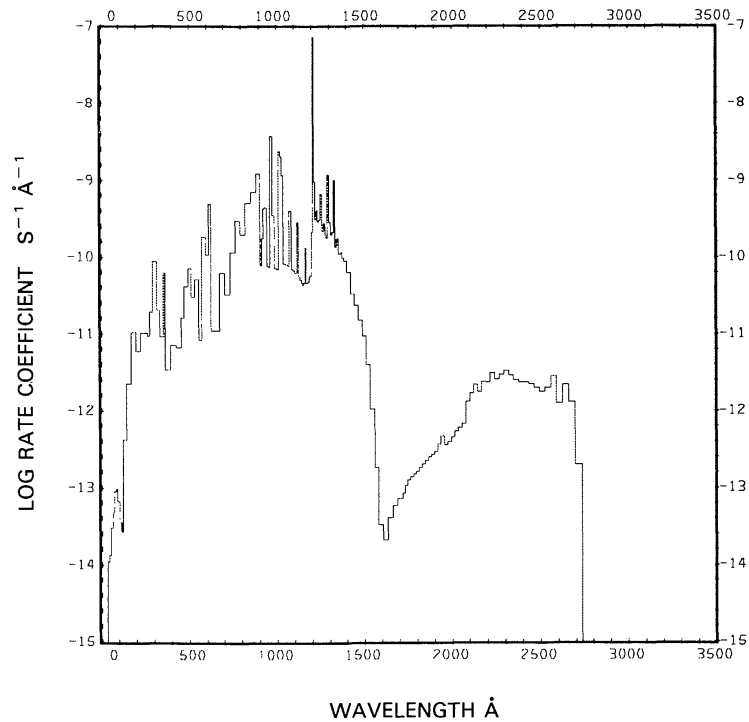
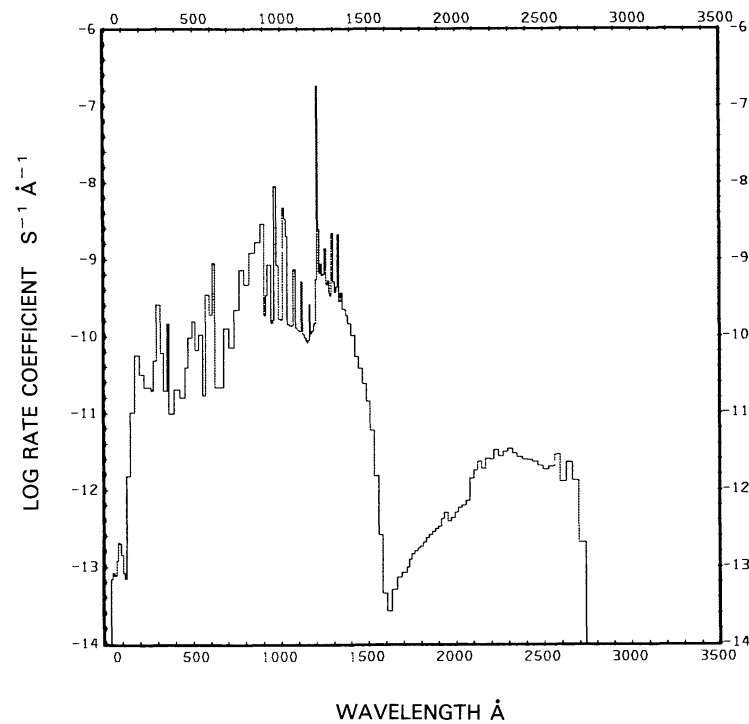
The first value of each branch is for the quiet Sun (see Figures 209(a) to 213(a)), the second for the active Sun (see Figures 209(b) to 213(b)).

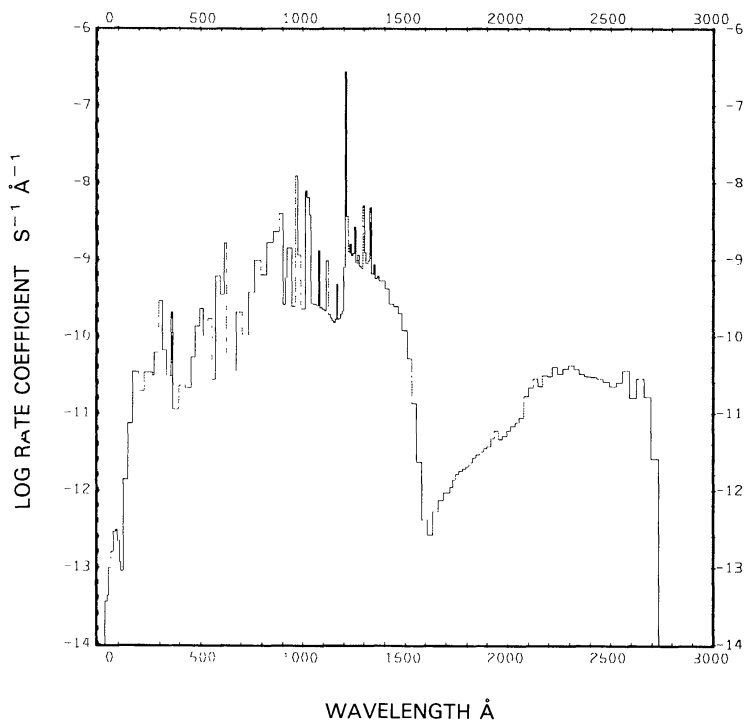
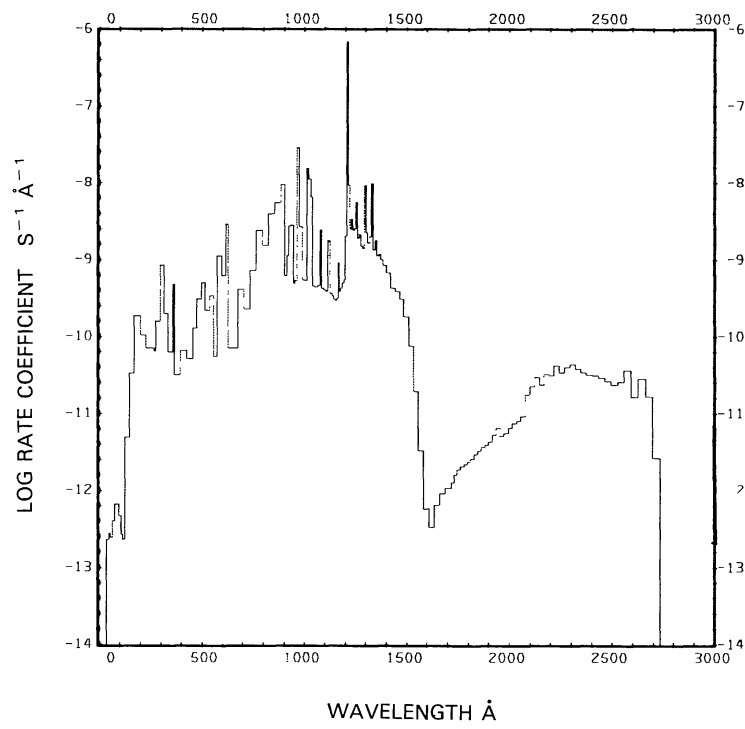
Excess energies:



The first value of each branch is for the quiet Sun, the second for the active Sun.

Fig. 209a. $\text{C}_2\text{H}_6 + \nu \rightarrow \text{C}_2\text{H}_4 + \text{H}_2$, for the quiet Sun.Fig. 209b. $\text{C}_2\text{H}_6 + \nu \rightarrow \text{C}_2\text{H}_4 + \text{H}_2$, for the active Sun.

Fig. 210a. C₂H₆ + ν → CH₃ + CH₃, for the quiet Sun.Fig. 210b. C₂H₆ + ν → CH₃ + CH₃, for the active Sun.

Fig. 211a. $\text{C}_2\text{H}_6 + \nu \rightarrow \text{C}_2\text{H}_5 + \text{H}$, for the quiet Sun.Fig. 211b. $\text{C}_2\text{H}_6 + \nu \rightarrow \text{C}_2\text{H}_5 + \text{H}$, for the active Sun.

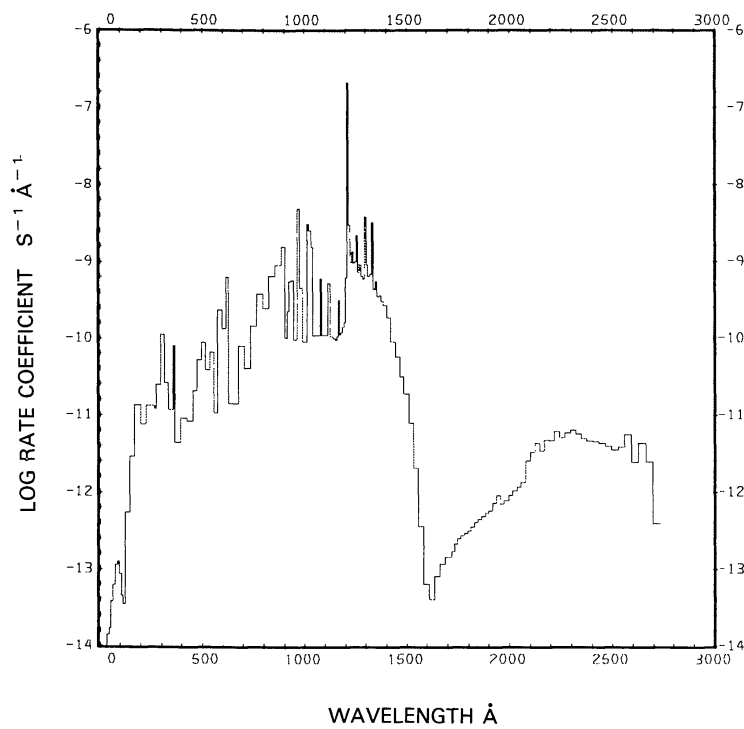


Fig. 212a. C₂H₆ + $\nu \rightarrow$ ¹CH₂ + CH₄, for the quiet Sun.

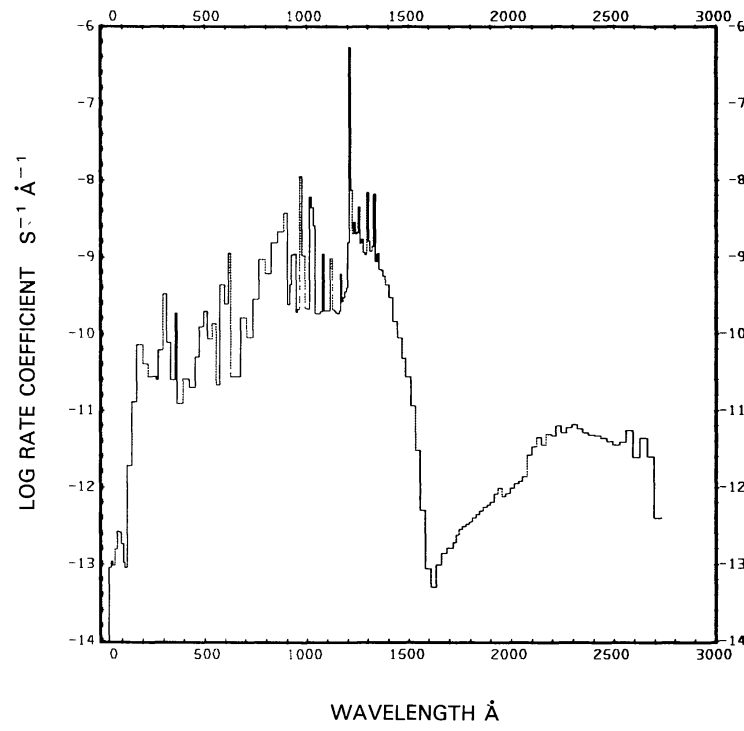
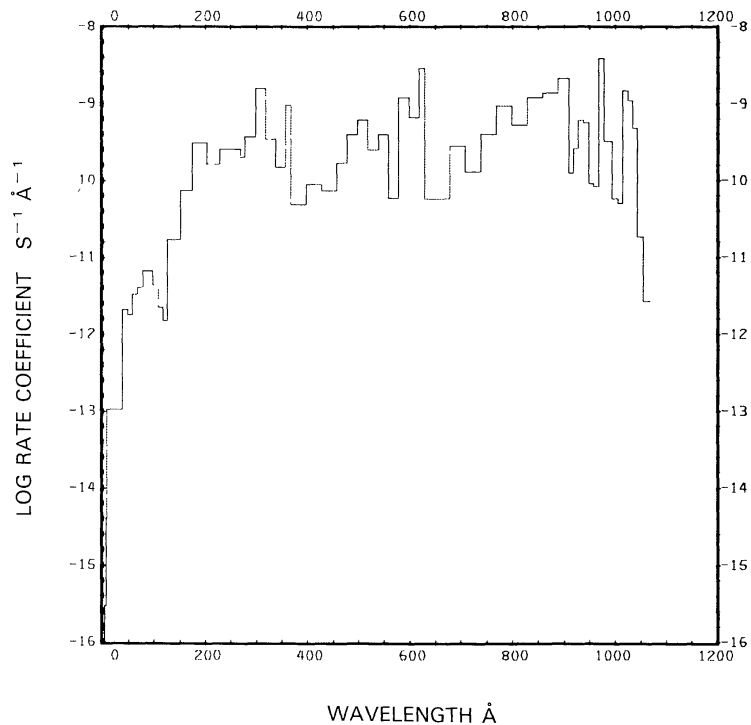
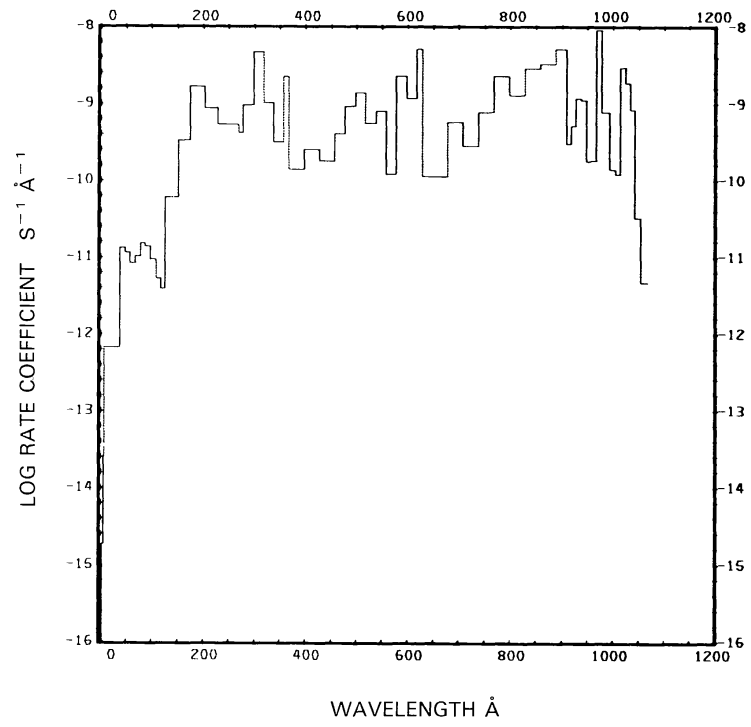


Fig. 212b. C₂H₆ + $\nu \rightarrow$ ¹CH₂ + CH₄, for the active Sun.

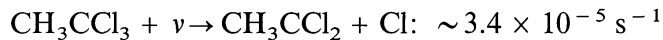
Fig. 213a. C₂H₆ + ν → C₂H₆⁺ + e⁻, for the quiet Sun.Fig. 213b. C₂H₆ + ν → C₂H₆⁺ + e⁻, for the active Sun.

METHYLCHLOROFORM, CH_3CCl_3

Cross sections: Up to 625.8 Å the cross section is synthesized from the data of Barfield *et al.* (1972) for the fits to the cross sections of the elemental constituents. From 1600 to 1800 Å the measured data from Hubrich and Stuhl (1980) were used. In the range from 1820 to 2400 Å the measurements for a temperature of 295 K were used from Vanlaethem-Meurée *et al.* (1979). From 2450 to 2550 Å the data from Hubrich and Stuhl were divided by about a factor of 2 to match to the data of Vanlaethem-Meurée at 2400 Å (see comments by DeMore *et al.* (1982)).

Branching ratios: The branching ratio for dissociation to produce $\text{CH}_3\text{CCl}_2 + \text{Cl}$ is 1 according to Vanlaethem-Meurée (1979).

Thresholds: The threshold for dissociation is unknown. We assumed the value for the longest wavelength (2550 Å) for which a cross section has been measured (Hubrich and Stuhl, 1980).

Rate coefficients:

for the quiet Sun (see Figure 214) and $\sim 4.1 \times 10^{-5} \text{ s}^{-1}$ for the active Sun. Even for the quiet Sun this is higher than the value obtained by Vanlaethem-Meurée *et al.* (1979) who quote $1.14 \times 10^{-5} \text{ s}^{-1}$ for an altitude of 45 km in the Earth's atmosphere assuming a constant temperature of 295 K.

Excess energies: The excess energy is about 2.4 eV for the quiet Sun and about 3.3 eV for the active Sun; but since the threshold for dissociation is not known, these values are quite uncertain.

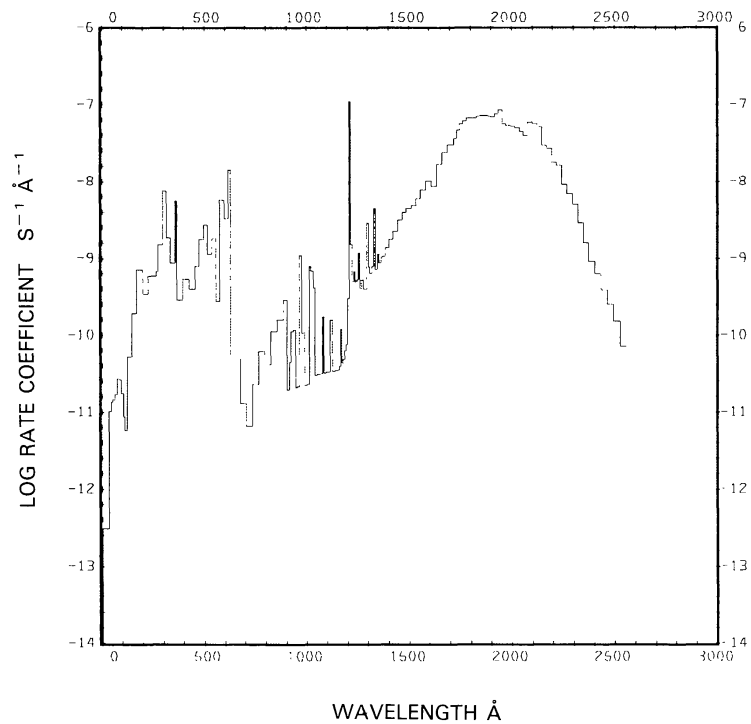


Fig. 214. $\text{CH}_3\text{CCl}_3 + \nu \rightarrow \text{CH}_3\text{CCl}_2 + \text{Cl}$, for the quiet Sun.

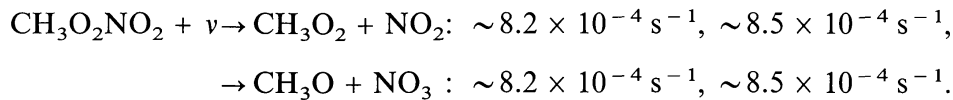


Cross sections: Up to 1850 Å the cross section is the combined cross section of H₂CO and HNO₃. Between 2000 and 3100 Å the cross sections from Baulch *et al.* (1982) were used. Beyond 3100 Å the cross section is very small.

Branching ratios: Two dissociation branches are given by Baulch *et al.* (1982). We used a branching ratio of 0.5 at all wavelengths up to the threshold for dissociation into CH₃O + NO₃. No other branching ratios are known.

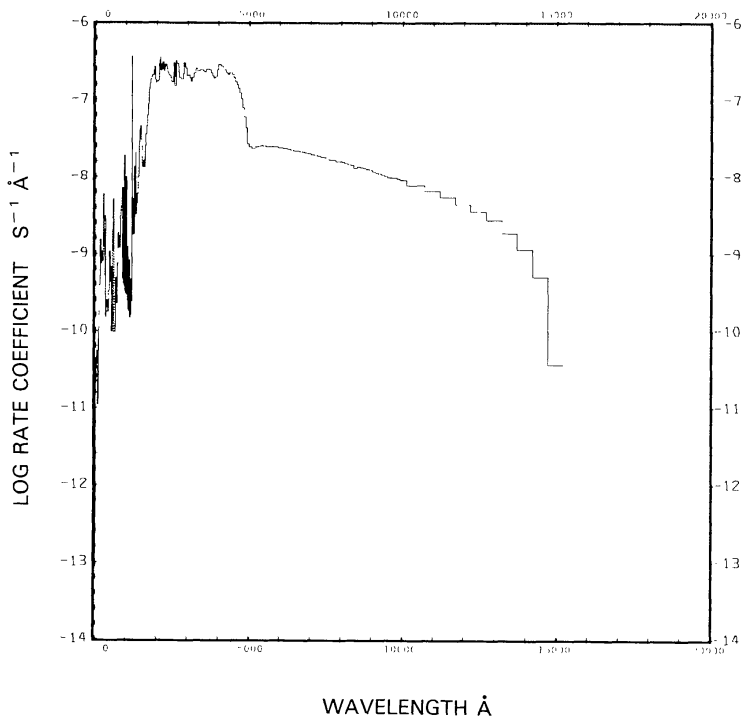
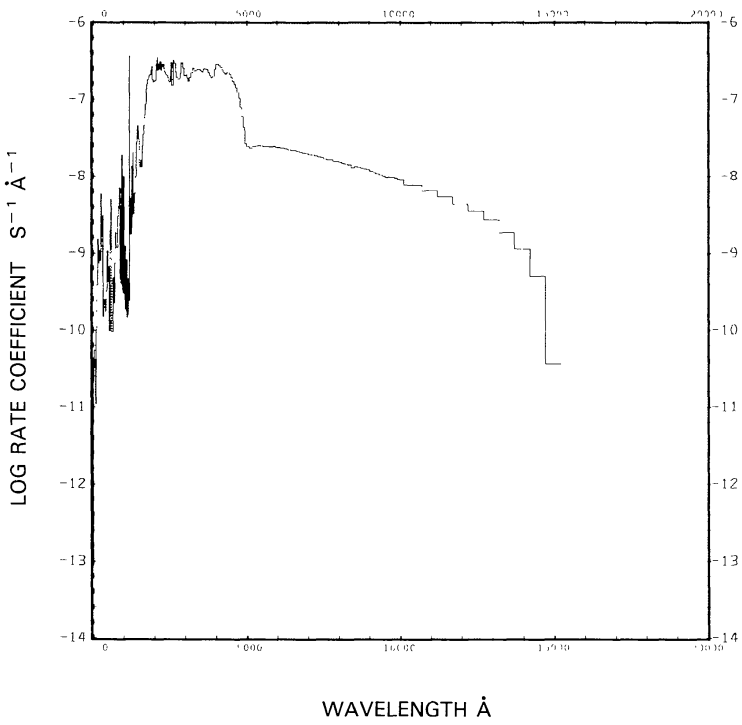
Thresholds: The thresholds for dissociation into CH₃O + NO₃ and CH₃O₂ + NO₂ are $\lambda = 9560 \text{ \AA}$ and $\lambda = 14930 \text{ \AA}$, respectively, as quoted by Baulch *et al.* (1982).

Rate coefficients:



The first value is for the quiet Sun (see Figures 215 and 216) and the second for the active Sun.

Excess energies: The excess energies for the two branches are about 3.0 eV and 2.6 eV, respectively, for the quiet Sun and about 3.2 eV and 2.7 eV for the active Sun.

Fig. 215. $\text{CH}_3\text{O}_2\text{NO}_2 + \nu \rightarrow \text{CH}_3\text{O}_2 + \text{NO}_2$, for the quiet Sun.Fig. 216. $\text{CH}_3\text{O}_2\text{NO}_2 + \nu \rightarrow \text{CH}_3\text{O} + \text{NO}_3$, for the quiet Sun.

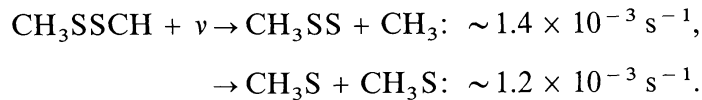


Cross sections: Up to 600 Å the cross section has been synthesized from the fits to the constituent atomic cross sections from Barfield *et al.* (1972). In the wavelength region from 2000 to 3100 Å the cross sections quoted by Baulch *et al.* (1982) have been used. Between 600 and 2000 Å the cross section has been interpolated.

Branching ratios: Two dissociation branches are given by Baulch *et al.* (1982). We used a branching ratio of 0.5 at all wavelengths up to the threshold for dissociation into $\text{CH}_3\text{S} + \text{CH}_3\text{S}$. No other branching ratios are known.

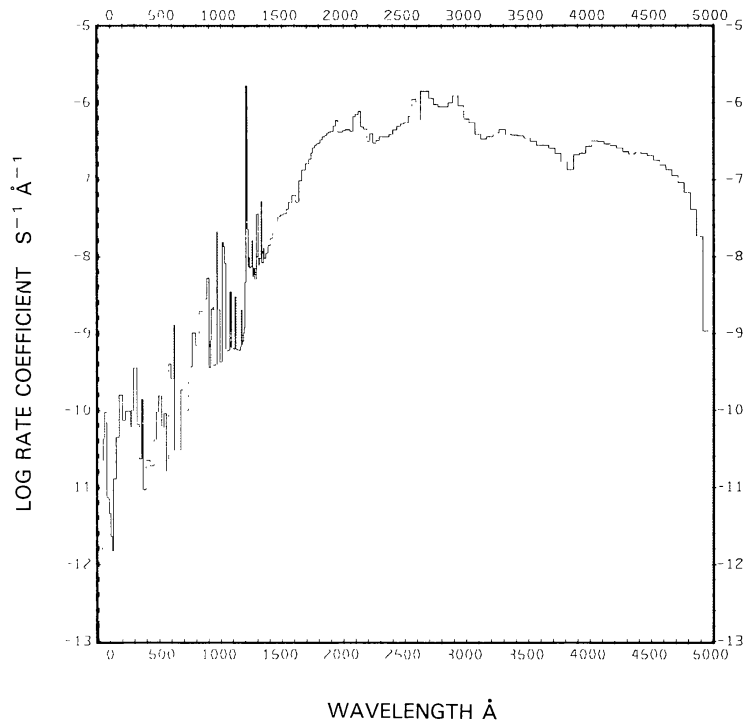
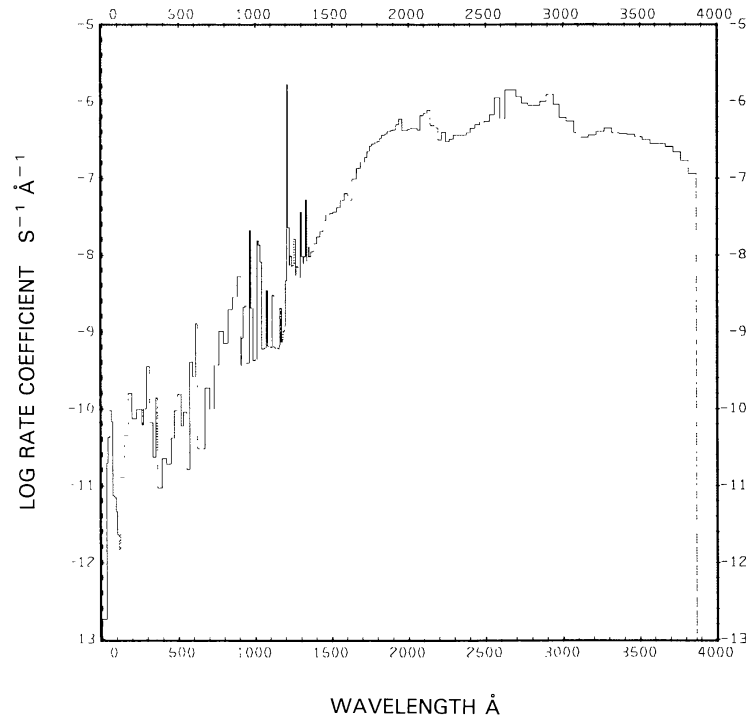
Thresholds: The thresholds for dissociation into $\text{CH}_3\text{S} + \text{CH}_3\text{S}$ and $\text{CH}_3\text{S}\text{S} + \text{CH}_3$ are 3870 Å and 4940 Å, respectively, as quoted by Baulch *et al.* (1982).

Rate coefficients:



See Figures 217 and 218. The rate coefficients are insensitive to the activity of the Sun.

Excess energies: The excess energies for the two branches are about 2.0 eV and 1.6 eV, respectively, for the quiet Sun and about 2.2 eV and 1.8 eV, respectively, for the active Sun.

Fig. 217. CH₃SSCH₃ + ν → CH₃SS + CH₃, for the quiet Sun.Fig. 218. CH₃SSCH₃ + ν → CH₃S + CH₃S, for the quiet Sun.

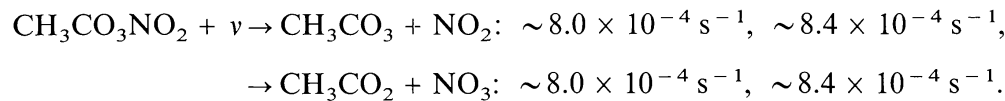


Cross sections: Up to 770 Å the cross section has been synthesized from the fits to the constituent atomic cross sections from Barfield *et al.* (1972). In the wavelength region from 2200 to 2700 Å the cross sections quoted by Baulch *et al.* (1982) have been used. Between 770 and 2200 Å the cross section has been interpolated.

Branching ratios: Two dissociation branches are given by Baulch *et al.* (1982). We used a branching ratio of 0.5 at all wavelengths up to the threshold for dissociation into $\text{CH}_3\text{CO}_2 + \text{NO}_3$. No other branching ratios are known.

Thresholds: The thresholds for dissociation into $\text{CH}_3\text{CO}_3 + \text{NO}_2$ and $\text{CH}_3\text{CO}_2 + \text{NO}_3$ are 10860 and 9140 Å, respectively, as quoted by Baulch *et al.* (1982).

Rate coefficients:



The first value of each branch is for the quiet Sun (see Figures 219 and 220), the second for the active Sun.

Excess energies: The excess energies for the two branches are about 3.4 eV and 3.2 eV, respectively, for the quiet Sun and about 3.7 eV and 3.5 eV, respectively, for the active Sun.

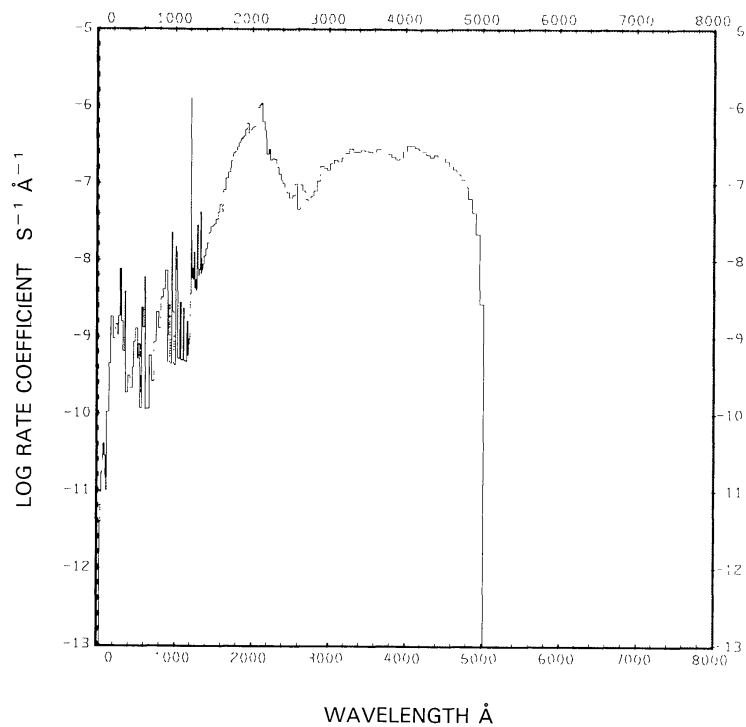


Fig. 219. $\text{CH}_3\text{CO}_3\text{NO}_2 + \nu \rightarrow \text{CH}_3\text{CO}_3 + \text{NO}_2$, for the quiet Sun.

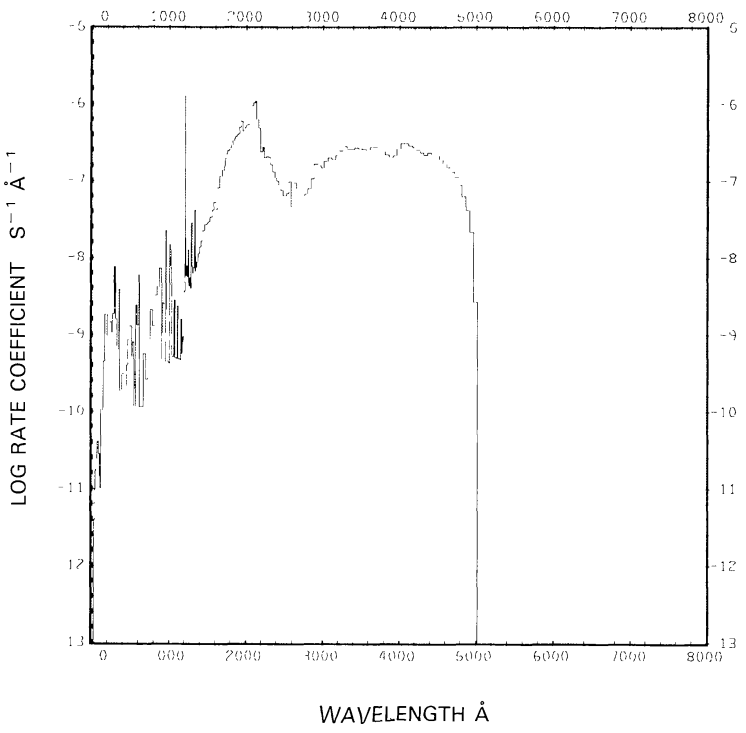


Fig. 220. $\text{CH}_3\text{CO}_3\text{NO}_2 + \nu \rightarrow \text{CH}_3\text{CO}_2 + \text{NO}_3$, for the quiet Sun.

4. Summary

A quantitative measure of the accuracy of the rate coefficients and the excess energies is a desirable goal of this analysis. There are two major sources of uncertainties: The atomic and molecular data and the solar irradiance. The cross sections and branching ratios used in this analysis come from many different sources; many of them without any error indications. For this reason, we must confine ourselves to a qualitative indication of the reliability of the results. Specifically we give a quality scale in Table II for the data of each mother molecule; A indicating the highest quality of atomic and molecular data and F the lowest quality.

The letter B typically means that the threshold is uncertain. For most molecules the cross section at threshold is very small and the rate coefficient for these molecules is therefore not influenced by this uncertainty. For atomic species the cross section is usually large near threshold, but for these species the threshold is known quite accurately. The letter B, therefore, indicates that the rate coefficient is most likely quite accurate, but the excess energy is less accurately known.

The letter C usually means that the branching ratios are not well known. This means that the total rate coefficient is very good, but the rate coefficients and the excess energies for the individual branches are less accurate.

The letter D implies that the cross section is not known for most of the important wavelength regions. In these cases we have interpolated the cross section. The rate coefficients and excess energies are therefore much less accurate than for cases A and B.

The second major source for uncertainties is the solar irradiance. Lean (1987, 1990) discusses short-term and long-term irradiance variations. The irradiance we used for the quiet Sun is described in detail in Section 2. For the active Sun we used the AE-E data of Hinteregger *et al.* (1981) as presented by Lean (1987). As a sensitivity test, we also used the irradiance of Hinteregger (1981). Since the variations in the solar spectrum depend on emissions from different atomic states and species in the solar corona and photosphere and, therefore, are at different frequencies, the irradiance can increase at some frequencies and decrease at others. By use of the Hinteregger (1981) data, we found that for the active Sun the rate coefficients could increase by as much as 80% and decrease by 15%. For the same case, the excess energies varied by about + 50% and - 10%.

TABLE II
Unattenuated solar photo rate coefficients at 1 AU heliocentric distance

$\Sigma_i Z_i$	Mother species	Quality scale	Photolysis products	Binding energy equivalent wavelength (Å)	Quiet Sun		Active Sun	
					Rate coefficient (s^{-1})	Total rate coefficient (s^{-1})	Photolysis products excess energy (eV)	Rate coefficient (s^{-1})
Monatomics								
1	H ⁻	A	H + e	16640	1.4×10^1	0.93	1.4×10^1	1.4×10^1
1	H	A	H ⁺ + e	911.75	7.3×10^{-8}	3.5	1.7×10^{-7}	1.7×10^{-7}
2	He	A	He ⁺ + e	504.27	5.2×10^{-8}	15 ⁻	1.5×10^{-7}	1.7×10^{-7}
6	C(³ P)	A	C ⁺ + e	1101.07	4.1×10^{-7}	5.9	9.2×10^{-7}	1.5×10^{-7}
6	C(¹ D)	A	C ⁺ + e	1240.27	3.6×10^{-6}	1.0	9.0×10^{-6}	9.2×10^{-7}
6	C(¹ S)	A	C ⁺ + e	1445.66	4.3×10^{-6}	2.1	1.0×10^{-5}	9.0×10^{-6}
7	N	A	N ⁺ + e	853.06	1.9×10^{-7}	15	4.7×10^{-7}	1.0×10^{-5}
8	O(³ P)	A	O ⁺ + e	910.44	2.1×10^{-7}	22	5.9×10^{-7}	4.7×10^{-7}
8	O(¹ D)	A	O ⁺ + e	827.9	1.8×10^{-7}	22	5.0×10^{-7}	5.9×10^{-7}
8	O(¹ S)	A	O ⁺ + e	858.3	2.0×10^{-7}	19	5.3×10^{-7}	5.0×10^{-7}
9	F	A	F ⁺ + e	759.44	2.1×10^{-7}	25	6.2×10^{-7}	5.3×10^{-7}
11	Na(exp)	D	Na ⁺ + e	2412.57	1.6×10^{-5}	0.57	1.7×10^{-5}	6.2×10^{-7}
					1.6×10^{-5}		1.7×10^{-5}	1.5×10^{-5}

Table II (continued)

$\Sigma_i Z_i$	Mother species	Quality scale	Photolysis products	Binding energy equivalent wavelength (\AA)	Quiet Sun		Active Sun		
					Rate coefficient (s^{-1})	Total rate coefficient (s^{-1})	Photolysis products excess energy (eV)	Rate coefficient (s^{-1})	Total rate coefficient (s^{-1})
11	Na(theor)	B	$\text{Na}^+ + e$	2412.57	5.9×10^{-6}	1.1	6.5×10^{-6}	6.5×10^{-6}	3.5
16	$\text{S}({}^3P)$	A	$\text{S}^+ + e$	1196.75	1.1×10^{-6}	6.3	2.4×10^{-6}	2.4×10^{-6}	7.2
16	$\text{S}({}^1D)$	A	$\text{S}^+ + e$	1121.43	1.1×10^{-6}	1.1 $\times 10^{-6}$	$2.5^- \times 10^{-6}$	$2.5^- \times 10^{-6}$	7.7
16	$\text{S}({}^1S)$	A	$\text{S}^+ + e$	1164.12	1.0×10^{-6}	5.4	2.3×10^{-6}	2.3×10^{-6}	6.4
17	Cl	A	$\text{Cl}^+ + e$	953	5.7×10^{-7}	6.7	1.3×10^{-6}	2.3×10^{-6}	7.9
18	Ar	A	$\text{Ar}^+ + e$	786	3.1×10^{-7}	10	6.9×10^{-7}	1.3×10^{-6}	13
19	K	A	$\text{K}^+ + e$	2856	2.2×10^{-5}	1.4	2.4×10^{-5}	6.9×10^{-7}	1.8
54	Xe	A	$\text{Xe}^+ + e$	1023	1.5×10^{-6}	4.2	$3.5^- \times 10^{-6}$	2.4×10^{-5}	5.2
					1.5×10^{-6}			3.5×10^{-6}	
							Diatomics		
2	H_2	A	$\text{H}(1s) + \text{H}(1s)$ $\text{H}(1s) + \text{H}(2s, 2p)$ $\text{H}_2^+ + e$ $\text{H} + \text{H}^+ + e$	2768.85 844.79 803.67 685.8	4.8×10^{-8} 3.4×10^{-8} 5.4×10^{-8} 9.5×10^{-9}	8.2 0.44 6.6 25	1.1×10^{-7} 8.2×10^{-8} 1.1×10^{-7} 2.8×10^{-8}	8.2×10^{-8} 0.42 7.2 27	3.3 $\times 10^{-7}$

Table II (continued)

Σ, Z_i	Mother species	Quality scale	Photolysis products	Binding energy equivalent wavelength (\AA)	Quiet Sun		Active Sun	
					Rate coefficient (s^{-1})	Total rate coefficient (s^{-1})	Photolysis products excess energy (eV)	Rate coefficient (s^{-1})
7	CH	A	C + H	3589.9	9.2×10^{-3}	0.45	9.2×10^{-3}	0.45
			C(¹ D) + H	2603.3	5.1×10^{-6}	3.6	7.6×10^{-6}	3.8
			C(¹ S) + H	2005.3	5.0×10^{-5}	0.18	5.6×10^{-5}	0.18
			CH ⁺ + e	1170	7.6×10^{-7}	6.4	1.7×10^{-6}	7.8
8	OH(exp)	D	O(³ P) + H	2823	1.2×10^{-5}	2.0	1.4×10^{-5}	2.1
			O(¹ D) + H	5114	7.0×10^{-6}	7.7	1.8×10^{-5}	7.7
			O(¹ S) + H	61320	8.3×10^{-7}	10	2.1×10^{-6}	10
			OH ⁺ + e	928	2.4×10^{-7}	19	6.4×10^{-7}	24
8	OH(theor)	B	O(³ P) + H	2823	6.5×10^{-6}	1.3	7.2×10^{-6}	1.4
			O(¹ D) + H	5114	6.3×10^{-7}	7.9	1.5×10^{-6}	7.9
			O(¹ S) + H	61320	6.7×10^{-8}	9.8	1.6×10^{-7}	9.9
			OH ⁺ + e	928	2.5×10^{-7}	19	6.5×10^{-7}	26
10	HF	D	H + F	2110	$\sim 1.6 \times 10^{-7}$	~ 4.6	$\sim 3.8 \times 10^{-7}$	~ 4.6
			HF ⁺ + e	774.9	2.0×10^{-7}	21	5.6×10^{-7}	26
			F + H ⁺ + e	652.55	6.1×10^{-8}	21	1.8×10^{-7}	25
			H + F ⁺ + e	652.55	1.4×10^{-8}	26	4.7×10^{-8}	32
12	C ₂	C	C(¹ D) + C(¹ D)	1436	1.0×10^{-7}	3.6	2.1×10^{-7}	3.7
			C ₂ ⁺ + e	1000	9.1×10^{-7}	6.8	2.2×10^{-6}	8.2
13	CN	C	C + N	1600	3.2×10^{-6}	7.4	7.4×10^{-6}	8.0
					3.2×10^{-6}		7.4×10^{-6}	

Table II (continued)

$\Sigma_i Z_i$	Mother species	Quality scale	Photolysis products	Quiet Sun		Active Sun	
				Binding energy equivalent wavelength (Å)	Rate coefficient (s ⁻¹)	Total rate coefficient (s ⁻¹)	Rate coefficient (s ⁻¹)
14	CO($X^1\Sigma^+$)	B	C(3P) + O(3P)	1117.8	2.8×10^{-7}	2.6	6.6×10^{-7}
			C(1D) + O(1D)	863.4	3.5×10^{-8}	2.3	7.9×10^{-8}
			CO ⁺ + e	884.79	3.8×10^{-7}	14	9.6×10^{-7}
			O + C ⁺ + e	554.7	2.9×10^{-8}	26	9.9×10^{-8}
			C + O ⁺ + e	501.8	2.4×10^{-8}	26	8.3×10^{-8}
14	CO($a^3\Pi$)	F	C + O	2431.8	7.5×10^{-7}	7.5	1.9×10^{-6}
			CO ⁺ + e	1549.1	7.2×10^{-5}	2.2	9.2×10^{-5}
			O + C ⁺ + e	758.3	8.6×10^{-6}	2.2	1.8×10^{-5}
			C + O ⁺ + e	662.7	2.4×10^{-8}	32	8.2×10^{-8}
					2.1×10^{-8}	33	7.2×10^{-8}
14	N ₂	C	N + N	1270.4	8.1×10^{-6}	3.4	1.1×10^{-4}
			N ₂ ⁺ + e	796	6.6×10^{-7}	18	1.6×10^{-6}
			N + N ⁺ + e	510.4	3.5×10^{-7}	18	9.1×10^{-7}
					1.5×10^{-8}	29	5.5×10^{-8}
15	NO	A	N + O	1910	1.0×10^{-6}	1.8	2.5×10^{-6}
			NO ⁺ + e	1340	2.2×10^{-6}	1.8	3.2×10^{-6}
			N + O ⁺ + e	616.2	1.3×10^{-6}	8.2	3.2×10^{-6}
			O + N ⁺ + e	589.3	1.8×10^{-9}	19	5.1×10^{-9}
					3.2×10^{-8}	25	1.0×10^{-7}
16	O ₂	A	O(3P) + O(3P)	2423.7	3.5×10^{-6}	4.4	2.2×10^{-7}
			O(3P) + O(1D)	1759	1.4×10^{-7}	4.1	6.5×10^{-6}
			O(1S) + O(1S)	923	4.1×10^{-6}	1.3	9.4×10^{-8}
			O ₂ ⁺ + e	1027.8	3.9×10^{-8}	0.74	1.2×10^{-6}
			O + O ⁺ + e	585	4.6×10^{-7}	16	3.5×10^{-7}
					1.1×10^{-7}	24	8.3×10^{-6}
					4.8×10^{-6}		
							8.3×10^{-6}

Table II (continued)

$\Sigma_i Z_i$	Mother species	Quality scale	Photolysis products	Binding energy equivalent wavelength (Å)	Quiet Sun		Active Sun		
					Rate coefficient (s^{-1})	Total rate coefficient (s^{-1})	Photolysis products excess energy (eV)	Rate coefficient (s^{-1})	Total rate coefficient (s^{-1})
18	HCl	C	H + Cl	2798	7.2×10^{-6}	4.4	1.2×10^{-5}	1.2×10^{-5}	5.3
18	F ₂	C	F + F	7950	5.7×10^{-4}	1.8	5.8×10^{-4}	5.8×10^{-4}	2.0
24	SO	C	S + O SO ⁺ + e	2314 1205	6.2×10^{-4} 8.6×10^{-7}	0.62 9.9	6.6×10^{-4} 2.0×10^{-6}	5.8×10^{-4} 6.6×10^{-4}	0.68 13
34	Cl ₂	C	Cl + Cl	5000.68	5.1×10^{-3}	2.1	5.3×10^{-3}	5.3×10^{-3}	2.2
43	BrO	D	Br + O(³ P) Br + O(¹ D)	5150 2830	$\sim 6.9 \times 10^{-3}$ $\sim 2.1 \times 10^{-3}$	~ 1.7 ~ 0.80	$\sim 7.0 \times 10^{-3}$ $\sim 2.2 \times 10^{-3}$	~ 1.8 ~ 0.83	~ 1.8 ~ 0.83
					$\sim 9.0 \times 10^{-3}$		$\sim 9.2 \times 10^{-3}$		
Triatomics									
9	NH ₂	E	NH + H	3000	2.1×10^{-6}	6.4	3.4×10^{-6}	3.4×10^{-6}	8.5-
10	H ₂ O	A	H + OH H ₂ + O(¹ D) H + H + O(³ P) H ₂ O ⁺ + e H + OH ⁺ + e H ₂ + O ⁺ + e OH + H ⁺ + e	2424.6 1770 1304 984 684.4 664.8 662.3	1.0×10^{-5} 6.0×10^{-7} 7.5×10^{-7} 3.3×10^{-7} 5.5×10^{-8} 5.8×10^{-9} 1.3×10^{-8}	3.4 3.8 0.70 12 19 37 25	1.8×10^{-5} 1.5×10^{-6} 1.9×10^{-6} 8.3×10^{-7} 1.5×10^{-7} 2.2×10^{-8} 4.1×10^{-8}	3.4×10^{-6} 3.4×10^{-6} 0.70 12 19 37 25	4.0 3.9 0.70 15 23 40 31
							1.2×10^{-5}	2.2×10^{-5}	

Table II (continued)

$\Sigma_i Z_i$	Mother species	Quality scale	Photolysis products	Binding energy equivalent wavelength (Å)	Quiet Sun		Active Sun	
					Rate coefficient (s^{-1})	Total rate coefficient (s^{-1})	Photolysis products excess energy (eV)	Rate coefficient (s^{-1})
14	HCN	C	H + CN($A^2\Pi_i$) HCN ⁺ + e	1950 911.19	1.3 × 10 ⁻⁵ 4.5 × 10 ⁻⁷	3.8 11	3.1 × 10 ⁻⁵ 1.1 × 10 ⁻⁶	3.8 14
17	HO ₂	C	OH + O	4395	6.6 × 10 ⁻³	6.6 × 10 ⁻³	1.0	6.7 × 10 ⁻³
18	H ₂ S	A	HS + H H ₂ S ⁺ + e H ₂ + S ⁺ + e H + HS ⁺ + e	3170 1185.25 927 867	3.2 × 10 ⁻⁴ 5.6 × 10 ⁻⁷ 1.5 × 10 ⁻⁷ 7.3 × 10 ⁻⁸	2.1 2.2 6.9 3.2 × 10 ⁻⁴	3.7 × 10 ⁻⁴ 1.2 × 10 ⁻⁶ 3.5 × 10 ⁻⁷ 1.7 × 10 ⁻⁷	2.5 2.3 8.7 16
22	CO ₂	A	CO(X ^{1Σ⁺) + O(^{3P}) CO(X^{1Σ⁺) + O(^{1D}) CO($a^3\Pi$) + O CO₂⁺ + e CO + O⁺ + e O + CO⁺ + e O₂ + C⁺ + e}}	2275 1671 1082 899.22 650.26 636.93 546.55	1.7 × 10 ⁻⁸ 9.2 × 10 ⁻⁷ 2.8 × 10 ⁻⁷ 6.6 × 10 ⁻⁷ 6.4 × 10 ⁻⁸ 5.0 × 10 ⁻⁸ 2.9 × 10 ⁻⁸	1.7 4.3 2.0 17 28 27 30	2.0 × 10 ⁻⁸ 1.9 × 10 ⁻⁶ 6.4 × 10 ⁻⁷ 1.8 × 10 ⁻⁶ 2.1 × 10 ⁻⁷ 1.7 × 10 ⁻⁷ 1.1 × 10 ⁻⁷	1.7 4.6 2.0 21 32 31 34
22	N ₂ O	C	N ₂ + O(^{1D}) N ₂ + O(^{1S})	3407 2115	1.0 × 10 ⁻⁶ 4.9 × 10 ⁻⁶	2.8 6.8	1.1 × 10 ⁻⁶ 1.0 × 10 ⁻⁵	2.8 8.3
23	NO ₂	C	NO + O(^{3P}) NO + O(^{1D}) NO ₂ ⁺ + e	3978 2439 1270	8.5 ⁻ × 10 ⁻³ 4.3 × 10 ⁻⁵ 1.3 × 10 ⁻⁶	0.35 1.2 13	8.5 × 10 ⁻³ 5.0 × 10 ⁻⁵ 3.2 × 10 ⁻⁶	0.35 1.5 ⁻ 16

Table II (continued)

$\Sigma_i Z_i$	Mother species	Quality scale	Photolysis products	Binding energy equivalent wavelength (Å)	Quiet Sun		Active Sun	
					Rate coefficient (s^{-1})	Total rate coefficient (s^{-1})	Photolysis products excess energy (eV)	Rate coefficient (s^{-1})
24	O ₃	C	O + O ₂ O(¹ D) + O ₂ (¹ a'Δ _g)	11790 3195	4.7 × 10 ⁻⁴ 9.7 × 10 ⁻³	1.4 0.79	4.7 × 10 ⁻⁴ 9.9 × 10 ⁻³	1.4 0.81
26	HOC	C	OH + Cl	5130	5.6 × 10 ⁻⁴	1.7	5.7 × 10 ⁻⁴	1.8
30	OCS	A	CO + S(³ P) CO + S(¹ D) CO + S(¹ S) CS + O(³ P) CS + O(¹ D) OCS ⁺ + e	3990 2910 2120 1820 1410 1120	1.5 × 10 ⁻⁵ 5.0 × 10 ⁻⁵ 3.0 × 10 ⁻⁵ 6.9 × 10 ⁻⁸ 6.3 × 10 ⁻⁶ 2.4 × 10 ⁻⁷	2.7 2.0 2.1 0.13 0.85 1.5	1.7 × 10 ⁻⁵ 5.5 × 10 ⁻⁵ 4.4 × 10 ⁻⁵ 7.9 × 10 ⁻⁸ 1.4 × 10 ⁻⁵ 4.6 × 10 ⁻⁷	2.9 2.0 2.2 0.13 0.93 2.2
			CO + S ⁺ + e S + CO ⁺ + e O + CS ⁺ + e CS + O ⁺ + e SO + C ⁺ + e	907 704 654 629 564	8.7 × 10 ⁻⁹ 2.0 × 10 ⁻⁹ 2.7 × 10 ⁻¹⁰ 1.9 × 10 ⁻¹⁰ 5.6 × 10 ⁻¹⁰	58 62 57 62 61	3.5 × 10 ⁻⁸ 9.0 × 10 ⁻⁹ 1.2 × 10 ⁻⁹ 8.3 × 10 ⁻¹⁰ 2.5 × 10 ⁻⁹	62 63 59 61 60
32	SO ₂	C	SO + O S + O ₂ SO ₂ ⁺ + e	2179 2070 1005	1.6 × 10 ⁻⁴ 5.1 × 10 ⁻⁵ 1.1 × 10 ⁻⁶	0.44 0.75 12	1.8 × 10 ⁻⁴ 6.4 × 10 ⁻⁵ 2.6 × 10 ⁻⁶	0.63 1.2 15
32	CINO	C	Cl + NO	7748	6.3 × 10 ⁻³	2.7	6.5 × 10 ⁻³	2.4 × 10 ⁻⁴
33	OClO	C	ClO + O(³ P) ClO + O(¹ D)	4960 2760	1.1 × 10 ⁻¹ 8.1 × 10 ⁻⁵	0.92 1.7	1.1 × 10 ⁻¹ 1.0 × 10 ⁻⁴	0.92 2.8
					1.1 × 10 ⁻¹		1.1 × 10 ⁻¹	

Table II (continued)

$\Sigma_i Z_i$	Mother species	Quality scale	Photolysis products	Binding energy equivalent wavelength (Å)			Quiet Sun			Active Sun		
				Rate coefficient (s ⁻¹)	Total rate coefficient (s ⁻¹)	Photolysis products excess energy (eV)	Rate coefficient (s ⁻¹)	Total rate coefficient (s ⁻¹)	Photolysis products excess energy (eV)	Rate coefficient (s ⁻¹)	Total rate coefficient (s ⁻¹)	Photolysis products excess energy (eV)
33	ClOO	D	ClO + O	~4960	~9.0 × 10 ⁻³	~2.2	~9.2 × 10 ⁻³	~9.2 × 10 ⁻³	~2.2	~9.2 × 10 ⁻³	~9.2 × 10 ⁻³	~2.2
38	CS ₂	C	CS(X ^{1Σ⁺}) + S(^{3P}) CS(X ^{1Σ⁺}) + S(^{1D}) CS(a ^{3Π}) + S(^{3P}) CS(A ^{1Π}) + S(^{3P}) CS ₂ ⁺ + e CS + S ⁺ + e S + CS ⁺ + e C + S ₂ ⁺ + e S ₂ + C ⁺ + e	2778 2211 1572 1337 1230 834 775 731 656	2.0 × 10 ⁻³ 8.9 × 10 ⁻⁴ 4.7 × 10 ⁻⁶ 5.2 × 10 ⁻⁶ 5.5 × 10 ⁻⁷ 1.2 × 10 ⁻⁸ 7.8 × 10 ⁻⁹ 3.5 × 10 ⁻¹⁰ 1.2 × 10 ⁻⁹	1.5 0.50 0.69 0.92 2.4 53 51 48 50	9.6 × 10 ⁻⁴ 7.7 × 10 ⁻⁶ 1.3 × 10 ⁻⁵ 1.2 × 10 ⁻⁶ 4.7 × 10 ⁻⁸ 3.0 × 10 ⁻⁸ 1.3 × 10 ⁻⁹ 4.7 × 10 ⁻⁹	2.2 × 10 ⁻³ 9.6 × 10 ⁻⁴ 7.7 × 10 ⁻⁶ 1.3 × 10 ⁻⁵ 1.2 × 10 ⁻⁶ 57 56 53 54	9.6 × 10 ⁻⁴ 7.7 × 10 ⁻⁶ 1.3 × 10 ⁻⁵ 1.2 × 10 ⁻⁶ 4.7 × 10 ⁻⁸ 3.0 × 10 ⁻⁸ 1.3 × 10 ⁻⁹ 4.7 × 10 ⁻⁹	~9.2 × 10 ⁻³	~9.2 × 10 ⁻³	~9.2 × 10 ⁻³
44	HOB _r	F	OH + Br	5180	~1.8 × 10 ⁻³	~1.3	~1.8 × 10 ⁻³	~1.8 × 10 ⁻³	~1.3	~1.8 × 10 ⁻³	~1.8 × 10 ⁻³	~1.3
62	HOI	F	OH + I	~5200	~8.7 × 10 ⁻⁴	~1.6	~8.7 × 10 ⁻⁴	~8.8 × 10 ⁻⁴	~1.7	~8.8 × 10 ⁻⁴	~8.8 × 10 ⁻⁴	~1.7
68	INO	F	I + NO	16500	~9.8 × 10 ⁻²	~2.8	~9.8 × 10 ⁻²	~9.9 × 10 ⁻²	~2.8	~9.9 × 10 ⁻²	~9.9 × 10 ⁻²	~2.8
			Tetramics									
10	NH ₃	B	NH ₂ + H NH(a ^{1Δ}) + H ₂ NH + H + H NH ₃ ⁺ + e	2798 2240 1470 1220	1.7 × 10 ⁻⁴ 4.0 × 10 ⁻⁶ 2.0 × 10 ⁻⁶ 6.1 × 10 ⁻⁷	1.8 1.7 2.1 5.8	1.9 × 10 ⁻⁴ 5.5 × 10 ⁻⁶ 4.8 × 10 ⁻⁶ 1.4 × 10 ⁻⁶	1.9 2.3 2.1 6.4	1.9 × 10 ⁻⁴ 5.5 × 10 ⁻⁶ 4.8 × 10 ⁻⁶ 1.4 × 10 ⁻⁶	1.9 2.3 2.1 6.4	1.9 2.3 2.1 6.4	

Table II (continued)

$\Sigma_i Z_i$	Mother species	Quality scale	Photolysis products	Binding energy equivalent wavelength (Å)	Quiet Sun		Active Sun	
					Rate coefficient (s^{-1})	Total rate coefficient (s^{-1})	Photolysis products excess energy (eV)	Rate coefficient (s^{-1})
14	C_2H_2	A	$H + NH_2^+ + e^-$	786.2	1.8×10^{-7}	11	4.0×10^{-7}	14
			$H_2 + NH^+ + e^-$	~775	6.9×10^{-9}	26	2.1×10^{-8}	31
			$H_2 + H + N^+ + e^-$	~560	3.3×10^{-9}	30	1.1×10^{-8}	33
			$NH_2 + H^+ + e^-$	~387	3.3×10^{-9}	20	1.2×10^{-8}	24
			$H + C_2H$	2306	1.0×10^{-5}	3.2	1.9×10^{-5}	3.7
16	H_2CO	B	$H_2 + C_2$	2006	2.7×10^{-6}	3.1	5.5×10^{-6}	3.4
			$C_2H_2^+ + e^-$	1086	7.8×10^{-7}	5.1	1.7×10^{-6}	6.1
			$H + C_2H^+ + e^-$	697	7.4×10^{-8}	16	1.9×10^{-7}	20
			$H_2 + CO$	>16800	1.2×10^{-4}	~2.1	1.2×10^{-4}	~2.1
18	PH_3	D	$H + HCO$	3340	6.6×10^{-5}	0.39	6.7×10^{-5}	0.39
			$H + H + CO$	2750	3.2×10^{-5}	3.0	6.7×10^{-5}	3.6
			$H_2CO^+ + e^-$	1141.6	4.0×10^{-7}	3.2	8.8×10^{-7}	3.6
			$H + HCO^+ + e^-$	1043	2.0×10^{-7}	7.3	4.6×10^{-7}	8.7
			$H_2 + CO^+ + e^-$	882	1.2×10^{-7}	29	3.7×10^{-7}	33
			$PH_2 + H$	3650	6.1×10^{-5}	2.8 $\times 10^{-4}$	7.6×10^{-5}	3.1×10^{-4}
			$OH + OH$	5765	1.4×10^{-4}	3.5	$1.5^- \times 10^{-4}$	4.0
			$NH(c^1\Pi) + CO$	3540	$1.5^- \times 10^{-5}$	5.1	2.6×10^{-5}	6.2
22	$HNCO$	C	$H + NCO(A^2\Sigma)$	2530	1.4×10^{-5}	4.1	$2.5^- \times 10^{-5}$	5.0
			$OH + NO$	5910	$\sim 2.3 \times 10^{-3}$	2.9 $\times 10^{-5}$	5.1×10^{-5}	$\sim 2.4 \times 10^{-3}$
					$\sim 2.3 \times 10^{-3}$	~1.7	$\sim 2.4 \times 10^{-3}$	~1.8

Table II (continued)

$\Sigma_i Z_i$	Mother species	Quality scale	Photolysis products	Binding energy equivalent wavelength (Å)		Quiet Sun		Active Sun		
				Rate coefficient (s ⁻¹)	Total rate coefficient (s ⁻¹)	Photolysis products excess energy (eV)	Rate coefficient (s ⁻¹)	Total rate coefficient (s ⁻¹)	Photolysis products excess energy (eV)	Rate coefficient (s ⁻¹)
31	NO ₃	C	NO + O ₂ NO ₂ + O	90000 5900	1.7 × 10 ⁻¹ 1.2 × 10 ⁻¹	1.8 0.30	1.7 × 10 ⁻¹ 1.2 × 10 ⁻¹	1.8 0.30	1.8 0.30	1.8 0.30
32	COF ₂	D	COF + F	2220	~2.1 × 10 ⁻⁵	~4.1	~3.9 × 10 ⁻⁵	~3.9 × 10 ⁻⁵	~3.9 × 10 ⁻⁵	~5.3
40	CINO ₂	D	Cl + NO ₂	8520	~2.9 × 10 ⁻³	~2.8	~3.0 × 10 ⁻³	~3.0 × 10 ⁻³	~3.0 × 10 ⁻³	~2.9
40	CIONO	D	Cl + NO ₂	17000	~1.1 × 10 ⁻²	~2.9	~1.0 × 10 ⁻²	~1.0 × 10 ⁻²	~1.0 × 10 ⁻²	~3.4
40	COFCl	D	COF + Cl	3160	~7.4 × 10 ⁻⁵	~2.9	~1.0 × 10 ⁻⁴	~1.0 × 10 ⁻⁴	~1.0 × 10 ⁻⁴	~4.0
41	ClO ₃	D	ClO ₂ + O	~3500	~2.6 × 10 ⁻²	~0.59	~2.6 × 10 ⁻²	~2.6 × 10 ⁻²	~2.6 × 10 ⁻²	~0.60
48	COCl ₂	D	COCl + Cl	3690	~1.6 × 10 ⁻⁴	~3.3	~2.1 × 10 ⁻⁴	~2.1 × 10 ⁻⁴	~2.1 × 10 ⁻⁴	~4.1
Pentatomics										
10	CH ₄	C	CH ₃ + H CH ₂ (\tilde{a}^1A_1) + H ₂	2770 2372	2.6 × 10 ⁻⁷ 4.0 × 10 ⁻⁶	6.5 5.3	6.1 × 10 ⁻⁷ 9.6 × 10 ⁻⁶	6.5 5.3	6.1 × 10 ⁻⁷ 9.6 × 10 ⁻⁶	6.5 5.3
			CH + H ₂ + H CH ₂ + H + H	1370 1322	6.4 × 10 ⁻⁷ 2.1 × 10 ⁻⁶	1.7 0.83	1.6 × 10 ⁻⁶ 5.4 × 10 ⁻⁶	1.7 0.83	1.6 × 10 ⁻⁶ 5.4 × 10 ⁻⁶	1.7 0.83
			CH ₄ ⁺ + e H + CH ₃ ⁺ + e H ₂ + CH ₂ ⁺ + e	945 866 822	3.6 × 10 ⁻⁷ 2.0 × 10 ⁻⁷ 2.1 × 10 ⁻⁸	5.5 ⁻ 8.0 20	8.4 × 10 ⁻⁷ 4.6 × 10 ⁻⁷ 5.6 × 10 ⁻⁸	8.4 × 10 ⁻⁷ 4.6 × 10 ⁻⁷ 5.6 × 10 ⁻⁸	8.4 × 10 ⁻⁷ 4.6 × 10 ⁻⁷ 5.6 × 10 ⁻⁸	6.2 9.5 24

Table II (continued)

$\Sigma, Z,$	Mother species	Quality scale	Photolysis products	Binding energy equivalent wavelength (Å)	Quiet Sun		Active Sun	
					Rate coefficient (s^{-1})	Total rate coefficient (s^{-1})	Photolysis products excess energy (eV)	Rate coefficient (s^{-1})
24	HCOOH	B	$\text{CH}_3 + \text{H}^+ + e$	686	9.1×10^{-9}	27	2.8×10^{-8}	30
			$\text{H}_2 + \text{H} + \text{CH}^+ + e$	630	4.2×10^{-9}	28	1.4×10^{-8}	32
			$\text{CO}_2 + \text{H}_2$	~7000	$\sim 3.2 \times 10^{-4}$	~4.8	$\sim 4.1 \times 10^{-4}$	~5.4
			$\text{HCO} + \text{OH}$	~2600	$\sim 5.6 \times 10^{-4}$	~1.8	$\sim 7.3 \times 10^{-4}$	~2.4
26	CH ₃ Cl	D	$\text{HCOOH}^+ + e$	1094.4	9.1×10^{-7}	3.9	2.0×10^{-6}	5.3
			$\text{OH} + \text{HCO}^+ + e$	902	2.8×10^{-7}	21	8.0×10^{-7}	26
			$\text{CH}_3 + \text{Cl}$	3470	$\sim 1.4 \times 10^{-5}$	~6.2	$\sim 2.7 \times 10^{-5}$	~6.9
			$\text{HC}_2 + \text{CN}$	2000	$\sim 3.9 \times 10^{-5}$	~2.7	$\sim 2.7 \times 10^{-5}$	~3.3
32	HNO ₃	C	$\text{OH} + \text{NO}_2$	5980	2.1×10^{-4}	4.3	6.8×10^{-5}	6.8×10^{-5}
			$\text{CHF}_2 + \text{Cl}$	~2200	$\sim 1.3 \times 10^{-5}$	~6.0	2.4×10^{-4}	4.7×10^{-4}
			$\text{Cl} + \text{NO}_3$	7210	$\sim 9.1 \times 10^{-4}$	~3.6	3.0×10^{-5}	6.6×10^{-5}
			$\text{ClONO} + \text{O}$	3910	$\sim 1.0 \times 10^{-4}$	~2.2	9.7×10^{-4}	3.8×10^{-4}
48	ClONO ₂	D	$\text{Cl} + \text{NO}_3$	7210	$\sim 1.3 \times 10^{-5}$	~1.0	1.1×10^{-4}	2.4×10^{-4}
			$\text{ClONO} + \text{O}$	3910	$\sim 1.0 \times 10^{-4}$	~1.0	1.1×10^{-4}	2.4×10^{-4}
			$\text{CF}_2\text{Cl}_2 + \text{Cl}$	3460	$\sim 1.0 \times 10^{-5}$	~5.5	1.8×10^{-5}	6.4×10^{-5}
			$\text{CFCl} + \text{Cl} + \text{Cl}$	2160	$\sim 1.6 \times 10^{-5}$	~5.1	3.4×10^{-5}	5.9×10^{-5}
58	CF ₂ Cl ₂	D	$\text{Cl} + \text{Cl} + \text{Cl}$	3860	$\sim 3.3 \times 10^{-5}$	~4.9	5.1×10^{-5}	5.9×10^{-5}
			$\text{CFCl}_2 + \text{Cl}$	2140	$\sim 2.3 \times 10^{-5}$	~3.9	4.5×10^{-5}	4.6×10^{-5}
66	CFCl ₃	D	$\text{CFCl} + \text{Cl} + \text{Cl}$	~	$\sim 5.6 \times 10^{-5}$	~	$\sim 9.6 \times 10^{-5}$	~

Table III (continued)

$\Sigma_i Z_i$	Mother species	Quality scale	Photolysis products	Binding energy equivalent wavelength (Å)	Quiet Sun			Active Sun		
					Rate coefficient (s^{-1})	Total rate coefficient (s^{-1})	Photolysis products excess energy (eV)	Rate coefficient (s^{-1})	Total rate coefficient (s^{-1})	Photolysis products excess energy (eV)
66	BrONO ₂	D	BrO + NO ₂	8600	$\sim 3.2 \times 10^{-3}$	$\sim 3.2 \times 10^{-3}$	~ 2.7	$\sim 3.3 \times 10^{-3}$	$\sim 3.3 \times 10^{-3}$	~ 2.8
74	CCl ₄	D	CCl ₃ + Cl CCl ₂ + Cl + Cl	4070 2090	$\sim 4.1 \times 10^{-5}$ $\sim 4.1 \times 10^{-5}$	~ 3.6 ~ 3.2		$\sim 5.0 \times 10^{-5}$ $\sim 7.3 \times 10^{-5}$	$\sim 3.3 \times 10^{-3}$ $\sim 1.2 \times 10^{-4}$	~ 4.2 ~ 4.0
84	INO ₂	F	IO + NO ₂	~ 7850	$\sim 5.9 \times 10^{-3}$	$\sim 8.1 \times 10^{-5}$	~ 1.9	$\sim 6.0 \times 10^{-3}$	$\sim 1.2 \times 10^{-3}$	~ 1.9
					$\sim 5.9 \times 10^{-3}$			$\sim 6.0 \times 10^{-3}$		
Hexatomics										
16	C ₂ H ₄	B	C ₂ H ₂ + H ₂ C ₂ H ₂ + H + H C ₂ H ₄ ⁺ + e H ₂ + C ₂ H ₂ ⁺ + e H + C ₂ H ₃ ⁺ + e	~7200 1960 1180 945 898	$\sim 2.4 \times 10^{-5}$ $\sim 2.3 \times 10^{-5}$ 5.8×10^{-7} 2.0×10^{-7} 2.3×10^{-7}	~ 6.2 ~ 1.7 7.3 12 13		$\sim 3.4 \times 10^{-5}$ $\sim 3.4 \times 10^{-5}$ 1.4×10^{-6} 4.9×10^{-7} 5.5×10^{-7}	~ 6.6 ~ 2.1 8.5 15 16	
18	CH ₃ OH	B	H ₂ CO + H ₂ CH ₃ + OH CH ₃ OH ⁺ + e H + CH ₃ O ⁺ + e H ₂ + H ₂ CO ⁺ + e	~13500 ~3150 1143 1006 976	$\sim 1.0 \times 10^{-5}$ $\sim 5.6 \times 10^{-7}$ 4.9×10^{-7} 1.2×10^{-7} 1.2×10^{-7}	$\sim 7.5^-$ ~ 5.0 2.6 3.5 4.4		$\sim 1.8 \times 10^{-5}$ $\sim 1.0 \times 10^{-6}$ 1.0×10^{-6} 2.7×10^{-7} 2.5×10^{-7}	~ 8.1 ~ 5.5 2.7 3.3 4.2	
40	, HO ₂ NO ₂	D	HO ₂ + NO ₂ OH + NO ₃	13400 7300	$\sim 3.0 \times 10^{-4}$ $\sim 3.0 \times 10^{-4}$	~ 4.5 ~ 3.8		$\sim 3.2 \times 10^{-4}$ $\sim 6.0 \times 10^{-4}$	~ 4.8 ~ 4.0	
								$\sim 2.1 \times 10^{-5}$	$\sim 6.4 \times 10^{-4}$	

Table III (continued)

$\Sigma_i Z_i$	Mother species	Quality scale	Photolysis products	Binding energy equivalent wavelength (Å)	Rate coefficient (s^{-1})	Quiet Sun	Active Sun	
						Rate coefficient (s^{-1})	Total rate coefficient (s^{-1})	Photolysis products excess energy (eV)
Septatomics								
24	CH_3CHO	D	$CH_4 + CO$ $CH_3 + HCO$	~7350 3501	~1.6 $\times 10^{-5}$ ~4.1 $\times 10^{-5}$	~3.2 ~0.88	~1.7 $\times 10^{-5}$ ~4.2 $\times 10^{-5}$	~4.0 ~1.1
26	CH_3OOH	D	$CH_3O + OH$	6470	~4.1 $\times 10^{-4}$	~5.7 $\times 10^{-5}$	~6.5 $\times 10^{-4}$	~5.9 $\times 10^{-5}$
54	N_2O_5	D	$NO_2 + NO_2 + O$	94100	~8.5 $\times 10^{-4}$	~4.1 $\times 10^{-4}$	~9.0 $\times 10^{-4}$	~6.5 $\times 10^{-5}$
					~8.5 $\times 10^{-4}$	~5.2	~9.0 $\times 10^{-4}$	~5.4
Octatomics								
18	C_2H_6	C	$C_2H_4 + H_2$ $CH_3 + CH_3$ $C_2H_5 + H$ $CH_4 + ^1CH_2$ $C_2H_6^+ + e^-$	8743 3220 2900 2726 1064	3.7 $\times 10^{-6}$ 8.8 $\times 10^{-7}$ 3.3 $\times 10^{-6}$ 2.2 $\times 10^{-6}$ 4.9 $\times 10^{-7}$	9.0 7.4 6.8 6.1 10	8.5 $\times 10^{-6}$ 2.1 $\times 10^{-6}$ 7.9 $\times 10^{-6}$ 5.4 $\times 10^{-6}$ 1.2 $\times 10^{-6}$	9.1 7.4 6.8 6.1 12
66	CH_3CCl_3	D	$CH_3 + CCl_3$	~2550	~3.4 $\times 10^{-5}$	~2.4	~4.1 $\times 10^{-5}$	~3.3
					~3.4 $\times 10^{-5}$		~4.1 $\times 10^{-5}$	
Supraoctatomics								
48	$CH_3O_2NO_2$	F	$CH_3O_2 + NO_2$ $CH_3O + NO_3$	14930 9560	~8.2 $\times 10^{-4}$ ~8.2 $\times 10^{-4}$	~3.0 ~2.6	~8.5 $\times 10^{-4}$ ~8.5 $\times 10^{-4}$	~3.2 ~2.7
							~1.7 $\times 10^{-3}$	~1.7 $\times 10^{-3}$

Table II (continued)

$\Sigma_i Z_i$	Mother species	Quality scale	Photolysis products	Binding energy equivalent wavelength (Å)	Quiet Sun		Active Sun	
					Rate coefficient (s ⁻¹)	Total rate (s ⁻¹)	Photolysis products excess energy (eV)	Rate coefficient (s ⁻¹)
50	CH_3SSCH_3	D	$\text{CH}_3\text{SS} + \text{CH}_3$	4940	$\sim 1.4 \times 10^{-3}$	~ 2.0	$\sim 1.4 \times 10^{-3}$	~ 2.2
			$\text{CH}_3\text{S} + \text{CH}_3\text{S}$	3870	$\sim 1.2 \times 10^{-3}$	~ 1.6	$\sim 1.2 \times 10^{-3}$	~ 1.8
62	$\text{CH}_3\text{CO}_3\text{NO}_2$	D	$\text{CH}_3\text{CO}_3 + \text{NO}_2$	10860	$\sim 8.0 \times 10^{-4}$	$\sim 2.5 \times 10^{-3}$	$\sim 8.4 \times 10^{-4}$	$\sim 2.7 \times 10^{-3}$
			$\text{CH}_3\text{CO}_2 + \text{NO}_3$	9140	$\sim 8.0 \times 10^{-4}$	~ 3.2	$\sim 8.4 \times 10^{-4}$	~ 3.7
					$\sim 1.6 \times 10^{-3}$		$\sim 1.7 \times 10^{-3}$	~ 3.5

References

- Ackerman, M.: 1971, in G. Fiocco (ed.), 'Ultraviolet Solar Radiation Related to Mesospheric Processes', *Mesospheric Models and Related Experiments*, Proc. 4th ESRIN-ESLAB Symp., D. Reidel Publ. Co., Dordrecht, Holland, pp. 149–159.
- Ackerman, M., Biaumé, F., and Kockarts, G.: 1970, *Planetary Space Sci.* **18**, 1639.
- Allison, A. C. and Dalgarno, A.: 1969, *J. Quant. Spectr. Rad. Transfer* **9**, 1543.
- Axford, W. I.: 1972, in C. P. Sonett, P. J. Coleman, Jr., and J. M. Wilcox (eds.), 'The Interaction of the Solar Wind with the Interstellar Medium', *Solar Wind*, Proc. NASA Conf. NASA SP-308, pp. 609–658.
- Ballash, N. M. and Armstrong, D. A.: 1974, *Spectr. Acta* **30A**, 941.
- Banks, P. M. and Kockarts, G.: 1973, *Aeronomy*, Academic Press, New York.
- Barfield, W. D., Koontz, G. D., and Huebner, W. F.: 1972, *J. Quant. Spectr. Rad. Transfer* **12**, 1409.
- Barnes, E. E. and Simpson, W. T.: 1963, *J. Chem. Phys.* **39**, 670.
- Barsuhn, J. and Nesbet, R. K.: 1978, *J. Chem. Phys.* **68**, 2783.
- Basco, N. and Morse, R. D.: 1974, *Proc. Roy. Soc. London A* **336**, 495.
- Bass, A. M., Glasgow, L. C., Miller, C., Jesson, J. P., and Filkin, D. L.: 1980, *Planetary Space Sci.* **28**, 675.
- Bass, A. M., Ledford Jr., A. E., and Laufer, A. H.: 1976, *J. Res. Natl. Bur. Stand.* **A80**, 143.
- Baulch, D. L., Cox, R. A., Hampson R. F., Jr., Kerr, J. A., Troe, J., and Watson, R. T.: 1980, *J. Phys. Chem. Ref. Data* **9**, 295.
- Baulch, D. L., Cox, R. A., Crutzen, P. J., Hampson, R. F., Jr., Kerr, J. A., Troe, J., and Watson, R. T.: 1982, *J. Phys. Chem. Ref. Data* **11**, 327.
- Baulch, D. L., Cox, R. A., Hampson, R. F., Jr., Kerr, J. A., Troe, J., and Watson, R. T.: 1984, *J. Phys. Chem. Ref. Data* **13**, 1259.
- Baurer, T. and Bortner, M. H.: 1978, in M. H. Bortner and T. Baurer (eds.), 'Summary of Suggested Rate Constants', *Defense Nuclear Agency Reaction Rate Handbook*, 2nd ed., DNA 1948H, Revision 7, Ch. 24.
- Bell, S., Ng, T. L., and Walsh, A. D.: 1975, *J. Chem. Soc. (London) Faraday Trans.* **71**(2), 393.
- Benson, S. W.: 1976, *Thermochemical Kinetics: Methods for the Estimation of Thermo-chemical Data and Rate Parameters*, John Wiley and Sons, New York.
- Bertaux, J. L., Blamont, J. E., and Festou, M.: 1973, *Astron. Astrophys.* **25**, 415.
- Bethe, H. A. and Salpeter, E. E.: 1957, *Quantum Mechanics of One- and Two-Electron Atoms*, Springer-Verlag, Berlin, p. 315.
- Beutler, H. and Jünger, H.-O.: 1936, *Z. Phys.* **100**, 80.
- Biaume, F.: 1973, *J. Photochem.* **2**, 139.
- Birks, J. W., Shoemaker, B., Leck, T. J., Borders, R. A., and Hart, L. J.: 1977, *J. Chem. Phys.* **66**, 4591.
- Black, G., Sharpless, R. L., Slanger, T. G., and Lorents, D. C.: 1975, *J. Chem. Phys.* **62**, 4274.
- Black, G., Sharpless, R. L., and Slanger, T. G.: 1977, *J. Chem. Phys.* **66**, 2113.
- Botter, R., Dibeler, V. H., Walker, J. A., and Rosenstock, H. M.: 1966, *J. Chem. Phys.* **45**, 1298.
- Brion, C. E. and Tan, K. H.: 1979, *J. Electron Spectr. Related Phen.* **17**, 101.
- Broad, J. T. and Reinhardt, W. P.: 1976, *Phys. Rev. A* **14**, 2159.
- Brolley, J. E., Porter, L. E., Sherman, R. H., Theobald, J. K., and Fong, J. C.: 1973, *J. Geophys. Res.* **78**, 1627.
- Brown, E. R., Carter, S. L., and Kelly, H. P.: 1980, *Phys. Rev. A* **21**, 1237.
- Browning, R. and Fryar, J.: 1973, *J. Phys. B: Atom. Molec. Phys.* **6**, 364.
- Cairns, R. B. and Samson, J. A. R.: 1965, *J. Geophys. Res.* **70**, 99.
- Calvert, J. G. and Pitts, J. N., Jr.: 1966, *Photochemistry*, John Wiley and Sons, New York.
- Carnovale, F. and Brion, C. E.: 1983, *Chem. Phys.* **74**, 253.
- Carnovale, F., Hitchcock, A. P., Cook, J. P. D., and Brion, C. E.: 1982, *Chem. Phys.* **66**, 249.
- Chang, J.-J. and Kelly, H. P.: 1975, *Phys. Rev. A* **12**, 92.
- Chapman, R. D. and Henry, R. J. W.: 1971, *Astrophys. J.* **168**, 169.
- Clark, J. H., Moore, C. B., and Nogar, N. S.: 1978, *J. Chem. Phys.* **68**, 1264.
- Clark, K. C.: 1952, *Phys. Rev.* **87**, 271.
- Clyne, M. A. A. and Coxon, J. A.: 1968, *Proc. Roy. Soc. London A* **303**, 207.
- Comes, F. J., Speier, F., and Elzer, A.: 1968, *Z. Naturforsch.* **23a**, 125.
- Connors, R. E., Roebber, J. L., and Weiss, K.: 1974, *J. Chem. Phys.* **60**, 5011.
- Cook, G. R. and Metzger, P. H.: 1964, *J. Opt. Soc. Am.* **54**, 968.
- Cook, G. R., Metzger, P. H., and Ogawa, M.: 1965, *Can. J. Phys.* **43**, 1706.

- Coon, J. B., DeWames, R. E., and Lloyd, C. M.: 1962, *J. Mol. Spectr.* **8**, 285.
Cox, R. A. and Burrows, J. P.: 1979, *J. Phys. Chem.* **83**, 2560.
Cox, R. A. and Derwent, R. G.: 1976, *J. Phot. Chem.* **6**, 23.
Crovisier, J.: 1989, *Astron. Astrophys.* **213**, 459.
Day, R. L., Masako, S., and Lee, L. C.: 1982, *J. Phys. B: Atom. Molec. Phys.* **15**, 4403.
DeMore, W. B., Watson, R. T., Golden, D. M., Hampson, R. F., Kurylo, M., Howard, C. J., Molina, M. J., and Ravishankara, A. R.: 1982, *Chemical Kinetics and Photochemical Data for Use in Stratospheric Modeling*, Evaluation No. 5, NASA.
Dibeler, V. H., Walker, J. A., and Rosenstock, H. M.: 1966, *J. Res. Nat. Bur. Stand.* **70A**, 459.
Ditchburn, R. W.: 1955, *Proc. Roy. Soc. London* **229A**, 44.
Ditchburn, R. W. and Young, P. A.: 1962, *J. Atmospheric Terrest. Phys.* **24**, 127.
Dixon, R. N. and Kirby, G. H.: 1968, *Trans. Faraday Soc.* **64**, 2002.
Driscoll, J. N. and Warneck, P.: 1968, *J. Phys. Chem.* **72**, 3736.
Festou, M. C.: 1981, *Astron. Astrophys.* **96**, 52.
Field, F. H. and Franklin, J. L.: 1970, *Electron Impact Phenomena*, Academic Press, New York.
Fournier, J., Lalo, C., Deson, J., and Vermeil, C.: 1977, *J. Chem. Phys.* **66**, 2656.
Freeman, D. E., Yoshino, K., Esmond, J. R., and Parkinson, W. H.: 1984, *Planetary Space Sci.* **32**, 1125.
Fridh, C. and Åsbrink, L.: 1975, *J. Electron Spectr. Related Phen.* **7**, 119.
Geiger, J. and Schröder, B.: 1969, *J. Chem. Phys.* **50**, 7.
Geltman, S.: 1962, *Astrophys. J.* **136**, 935.
Gentieu, E. P. and Mentall, J. E.: 1970, *Science* **169**, 681.
Gibson, S. T., Gies, H. P. F., Blake, A. J., McCoy, D. G., and Rogers, P. J.: 1983, *J. Quant. Spectr. Rad. Transfer* **30**, 385.
Golomb, D., Watanabe, K., and Marmo, F. F.: 1962, *J. Chem. Phys.* **36**, 958.
Goodeve, C. F. and Katz, S.: 1939, *Proc. Roy. Soc. London* **A172**, 432.
Goodeve, C. F. and Richardson, F. D.: 1937, *Trans. Faraday Soc.* **33**, 453.
Goodeve, C. F. and Stein, N. O.: 1931, *Trans. Faraday Soc.* **27**, 393.
Gorden, R., Jr. and Ausloos, P.: 1961, *J. Phys. Chem.* **65**, 1033.
Gorden, R., Jr. and Ausloos, P.: 1967, *J. Chem. Phys.* **46**, 4823.
Graham, R. A. and Johnston, H. S.: 1978, *J. Phys. Chem.* **82**, 254.
Griggs, M.: 1968, *J. Chem. Phys.* **49**, 857.
Groth, W. E., Schurath, U., and Schindler, R. N.: 1968, *J. Phys. Chem.* **72**, 3914.
Gürtler, P., Saile, V., and Koch, E. E.: 1977, *Chem. Phys. Letters* **48**, 245.
Guyon, P. M., Chupka, W. A., and Berkowitz, J.: 1976, *J. Chem. Phys.* **64**, 1419.
Hall, J. A., Schamps, J., Robbe, J. M., and Lefebvre-Brion, H.: 1973, *J. Chem. Phys.* **59**, 3271.
Hall, L. A. and Hinteregger, H. E.: 1970, *J. Geophys. Res.* **75**, 6959.
Hall, T. C., Jr. and Blacet, F. E.: 1952, *J. Chem. Phys.* **20**, 1745.
Harker, A. B., Ho, W., and Ratto, J. J.: 1977, *Chem. Phys. Letters* **50**, 394.
Henry, R. J. W.: 1970, *Astrophys. J.* **161**, 1153.
Henry, R. J. W. and McElroy, M. B.: 1968, in J. C. Brandt and M. B. McElroy (eds.), 'Photoelectrons in Planetary Atmospheres', *The Atmospheres of Venus and Mars*, Gordon and Breach Science Publ., Inc., New York, pp. 251–285.
Herzberg, G.: 1966, *Molecular Spectra and Molecular Structure. III. Electronic Spectra and Electronic Structure of Polyatomic Molecules*, Van Nostrand Reinhold Co., New York.
Herzberg, G. and Howe, L. L.: 1959, *Can. J. Phys.* **37**, 636.
Herzberg, G. and Johns, J. W. C.: 1969, *Astrophys. J.* **158**, 399.
Herzberg, G. and Monfils, A.: 1960, *J. Mol. Spectr.* **5**, 482.
Hinteregger, H. E.: 1970, *Ann. Géophys.* **26**, 547.
Hinteregger, H. E.: 1981, *Adv. Space Res.* **1**, 39.
Hinteregger, H. E., Fukui, K., and Gilson, B. G.: 1981, *Geophys. Res. Letters* **8**, 1147.
Hochanadel, C. J., Ghormley, J. A., and Ogren, P. J.: 1972, *J. Chem. Phys.* **56**, 4426.
Hubbel, J. H. and Veigele, W. J.: 1976, *Comparison of Theoretical and Experimental Photoeffect Data 0.1 keV to 1.5 MeV*, National Bureau of Standards Technical Note 901.
Huber, K. P. and Herzberg, G.: 1979, *Molecular Spectra and Molecular Structure: IV. Constants of Diatomic Molecules*, Van Nostrand Reinhold Co., New York.
Hubrich, C. and Stuhl, F.: 1980, *J. Photochem.* **12**, 93.

- Hubrich, C., Zetzsch, C., and Stuhl, F.: 1977, *Ber. Bunsen-Ges.* **81**, 437.
- Hudson, R. D.: 1971, *Rev. Geophys. Space Phys.* **9**, 305.
- Hudson, R. D. and Carter, V. L.: 1965, *Phys. Rev.* **139**, A1426.
- Hudson, R. D. and Carter, V. L.: 1967, *J. Opt. Soc. Am.* **57**, 651.
- Hudson, R. D. and Carter, V. L.: 1968, *J. Opt. Soc. Am.* **58**, 430.
- Huebner, W. F. and Carpenter, C. W.: 1979, *Solar Photo Rate Coefficients*, Los Alamos Scientific Laboratory Report LA-8085-MS.
- Huffman, R. E.: 1969, *Can. J. Chem.* **47**, 1823.
- Huffman, R. E.: 1971, in M. H. Bortner and T. Baurer (eds.), 'Photochemical Processes: Cross Section Data', *Defense Nuclear Agency Reaction Rate Handbook*, 2nd ed. DNA 1948H, Ch. 12.
- Huffman, R. E., Tanaka, Y., and Larrabee, J. C.: 1963a, *J. Chem. Phys.* **39**, 902.
- Huffman, R. E., Tanaka, Y., and Larrabee, J. C.: 1963b, *J. Chem. Phys.* **39**, 910.
- Illies, A. J. and Takacs, G. A.: 1976, *J. Photochem.* **6**, 35.
- Inn, E. C. Y.: 1975, *J. Atm. Sci.* **32**, 2375.
- Iqbal, M.: 1983, *An Introduction to Solar Radiation*, Academic Press, Toronto, New York.
- Itamoto, F. K. and McAllister, H. C.: 1961, 'Absorption Coefficients of Nitrogen in the Region 850 to 1000 Å', *Hawaii Institute of Geophysics Report 4*; U.S. Dept. Com. Office Tech. Serv. AD 272266.
- Jackson, W. M.: 1976a, *J. Photochem.* **5**, 107.
- Jackson, W. M.: 1976b, in B. Donn, M. Mumma, W. Jackson, M. A'Hearn, and R. Harrington (eds.), *Proc. IAU Colloq. 25*, 679.
- Jackson, W. M. and Okabe, H.: 1985, *Adv. Photochem.* **13**, 1.
- Jackson, W. M., Halpern, J. B., Feldman, F. D., and Rahe, J.: 1982, *Astron. Astrophys.* **107**, 385.
- Jesson, J. P., Glasgow, L. P., Filkin, D. L., and Miller, C.: 1977, *Geophys. Res. Letters* **4**, 513.
- Johnston, H. and Graham, R.: 1973, *J. Phys. Chem.* **77**, 62.
- Johnston, H. S. and Selwyn, G. S.: 1975, *Geophys. Res. Letters* **2**, 549.
- Johnston, H. S., Morris, E. D., Jr., and Van den Bogaerde, J.: 1969, *J. Am. Chem. Soc.* **91**, 7712.
- Jones, I. T. N. and Bayes, K. D.: 1973, *J. Chem. Phys.* **59**, 4836.
- Katayama, D. H., Huffman, R. E., and O'Bryan, C. L.: 1973, *J. Chem. Phys.* **59**, 4309.
- Keller, H. U.: 1971, *Mitt. Astron. Ges.* **30**, 143.
- Kley, D. and Welge, K. H.: 1965, *Naturforsch.* **20a**, 124.
- Knauth, H. D. and Schindler, R. N.: 1983, *Z. Naturforsch.* **38a**, 893.
- Knauth, H.-D., Alberti, H., and Clausen, H.: 1979, *J. Phys. Chem.* **83**, 1604.
- Koch, E. E. and Skibowski, M.: 1971, *Chem. Phys. Letters* **9**, 429.
- Kronebusch, P. L. and Berkowitz, J.: 1976, *Int. J. Mass. Spectr. Ion Phys.* **22**, 283.
- Krupenie, P. H.: 1966, 'The Band Spectrum of Carbon Monoxide', National Bureau of Standards Report NRDS-NBS 5.
- Kumar, S.: 1982, *J. Geophys. Res.* **87**, 1677.
- Laufer, A. H. and McNesby, J. R.: 1968, *J. Chem. Phys.* **49**, 2272.
- Lavendy, H., Gandara, G., and Robbe, J. M.: 1984, *J. Mol. Spectr.* **106**, 395.
- Lavendy, H., Robbe, J. M., and Gandara, G.: 1987, *J. Phys. B: Atom. Molec. Phys.* **20**, 3067.
- Lawerence, G.: 1972, *J. Chem. Phys.* **56**, 3435.
- Lean, J.: 1987, *J. Geophys. Res.* **92**, 839.
- Lean, J.: 1990, *J. Geophys. Res.* **95**, 11933.
- Lee, L. C. and Chiang, C. C.: 1982, *Chem. Phys. Letters* **92**, 425.
- Lee, L. C., Carlson, R. W., Judge, D. L., and Ogawa, M.: *J. Quant. Spectr. Rad. Transfer* **13**, 1023.
- Lee, L. C., Slanger, T. G., Black, G., and Sharpless, R. L.: 1977, *J. Chem. Phys.* **67**, 5602.
- Lee, L. C., Wang, X., and Suto, M.: 1987, *J. Chem. Phys.* **86**, 4353.
- Lenzi, M. and Okabe, H.: 1968, *Ber. Bunsenges. Phys. Chem.* **72**, 168.
- Lias, S. G., Collin, G. J., Rebbert, R. E., and Ausloos, P.: 1970, *J. Chem. Phys.* **52**, 1841.
- Lilly, R. L., Rebbert, R. E., and Ausloos, P.: 1973, *J. Photochem.* **2**, 49.
- Lin, C. L., Rohatgi, N. K., and DeMore, W. B.: 1978, *Geophys. Res. Letters* **5**, 113.
- Linevsky, M. J.: 1967, *J. Chem. Phys.* **47**, 3485.
- Loftus, A. and Krupenie, P. H.: 1977, *J. Phys. Chem. Ref. Data* **6**, 113.
- Lombos, B. A., Sauvageau, P., and Sandorfy, C.: 1967, *Mol. Spectr.* **24**, 253.
- Lukirskii, A. P., Brytov, I. A., and Zimkina, T. M.: 1964, *Opt. Spektr.* **17**, 234 (Engl. Trans.).
- Magnotta, F. and Johnston, H. S.: 1980, *Geophys. Res. Letters* **7**, 769.

- Manson, S. T., Msezane, A., Starace, A. F., and Shahabi, S.: 1979, *Phys. Rev. A* **20**, 1005.
- Margitan, J. J.: 1983, *J. Phys. Chem.* **87**, 674.
- Marmo, F. F.: 1953, *J. Opt. Soc. Am.* **43**, 1186.
- Marr, G. V. and West, J. B.: 1976, *Atom. Data Nucl. Data Tables* **18**, 498.
- Matsunaga, F. M. and Watanabe, K.: 1967a, *Sci. Light* **16**, 31.
- Matsunaga, F. M. and Watanabe, K.: 1967b, *J. Chem. Phys.* **46**, 4457.
- McDonald, J. R., Baronavski, A. P., and Donnelly, V. M.: *Chem. Phys.* **33**, 161.
- McElroy, M. B. and Hunten, D. M.: 1970, *J. Geophys. Res. Space Phys.* **75**, 1188.
- McElroy, M. B. and McConnell, J. C.: 1971, *J. Geophys. Res.* **76**, 6674.
- McElroy, M. B., Kong, T. Y., and Yung, Y. L.: 1976, *Science* **194**, 1295.
- McNesby, J. R. and Okabe, H.: 1964, *Adv. Photochem.* **3**, 157.
- McNesby, J. R., Tanaka, I., and Okabe, H.: 1962, *J. Chem. Phys.* **36**, 605.
- Mentall, J. E., Gentieu, E. P., Krauss, M., and Neumann, D.: 1971, *J. Chem. Phys.* **55**, 5471.
- Metzger, P. H. and Cook, G. R.: 1964, *J. Chem. Phys.* **41**, 642.
- Molina, M. J. and Arguello, G.: 1979, *Geophys. Res. Letters* **6**, 953.
- Molina, L. T. and Molina, M. J.: 1977, *Geophys. Res. Letters* **4**, 83.
- Molina, L. T. and Molina, M. J.: 1979, *J. Photochem.* **11**, 139.
- Molina, L. T. and Molina, M. J.: 1981, *J. Photochem.* **15**, 97.
- Molina, L. T., Lamb, J. J., and Molina, M. J.: 1981, *Geophys. Res. Letters* **8**, 1008.
- Moore, C. E.: 1970, 'Ionization Potentials and Ionization Limits Derived from the Analysis of Optical Spectra', Nat. Stand. Ref. Data Ser., Nat. Bur. Stand. Report NSRDS-NBS 34.
- Moortgat, G. K. and Warneck, P.: 1975, *Z. Naturforsch.* **30a**, 835.
- Moule, D. C. and Foo, P. D.: 1971, *J. Chem. Phys.* **55**, 1262.
- Mount, G. H. and Moos, H. W.: 1978, *Astrophys. J.* **224**, L35.
- Mount, G. H., Warden, E. S., and Moos H. W.: 1977, *Astrophys. J.* **214**, L47.
- Myer, J. A. and Samson, J. A. R.: 1970, *J. Chem. Phys.* **52**, 266.
- Nakata, R. S., Watanabe, K., and Matsunaga, F. M.: 1965, *Sci. Light* **14**, 54.
- Nakayama, T. and Watanabe, K.: 1964, *J. Chem. Phys.* **40**, 558.
- Nakayama, T., Kitamura, M. Y., and Watanabe, K.: 1959, *J. Chem. Phys.* **30**, 1180.
- Nee, J. B. and Lee, L. C.: 1984, *J. Chem. Phys.* **81**, 31.
- Nee, J. B., Suto, M., and Lee, L. C.: 1985, *Chem. Phys.* **98**, 147.
- Nelson, H. H. and Johnston, H. S.: 1981, *J. Phys. Chem.* **85**, 3891.
- Okabe, H.: 1970, *J. Chem. Phys.* **53**, 3507.
- Okabe, H.: 1972, *J. Chem. Phys.* **56**, 4381.
- Okabe, H.: 1975, *J. Chem. Phys.* **62**, 2782.
- Okabe, H.: 1978, *Photochemistry of Small Molecules*, John Wiley and Sons, New York.
- Okabe, H.: 1980, *J. Chem. Phys.* **72**, 6642.
- Okabe, H.: 1981, *J. Chem. Phys.* **75**, 2772.
- Okabe, H.: 1983, *J. Chem. Phys.* **78**, 1312.
- Okabe, H. and Becker, D. A.: 1963, *J. Chem. Phys.* **39**, 2549.
- Okabe, H. and Lenzi, M.: 1967, *J. Chem. Phys.* **47**, 5241.
- Okabe, H., Laufer, A. H., and Ball, J. J.: 1971, *J. Chem. Phys.* **55**, 373.
- Padial, N. T., Collins, L. A., and Schneider, B. I.: 1985, *Astrophys. J.* **298**, 369.
- Paukert, T. T. and Johnston, H. S.: 1972, *J. Chem. Phys.* **56**, 2824.
- Phillips, L. F.: 1981, *J. Phys. Chem.* **85**, 3394.
- Phillips, E., Lee, L. C., and Judge, D. L.: 1977, *J. Quant. Spectr. Rad. Transfer* **18**, 309.
- Porter, R. P. and Noyes, W. A., Jr.: *J. Am. Chem. Soc.* **81**, 2307.
- Potter, A. E. and del Duca, B.: 1964, *Icarus* **3**, 103.
- Pouilly, B., Robbe, J. M., Schamps, J., and Roueff, E.: 1983, *J. Phys. B: Atom. Molec. Phys.* **16**, 437.
- Prest, H. F., Tzeng, W.-B., Brom, J. M., Jr., and Ng, C. Y.: 1983, *Int. J. Mass Spectrom. Ion Phys.* **50**, 315.
- Rebbert, R. E. and Ausloos, P.: 1972, *J. Photochem.* **1**, 171.
- Rebbert, R. E., Lilly, R. L., and Ausloos, P.: 1972, *Am. Chem. Soc. Abstracts* **164**, Phys. Chem. Div. No. 30.
- Robbins, D. E.: 1976, *Geophys. Res. Letters* **3**, 213, 757.
- Robbins, D. E. and Stolarski, R. S.: 1976, *Geophys. Res. Letters* **3**, 603.
- Rogers, J. D.: 1990, *J. Phys. Chem.* **94**, 4011.
- Rosen, B.: 1970, *International Tables of Selected Constants. No. 17, Spectroscopic Data Relative to Diatomic Molecules*, Pergamon Press, Oxford.

- Safary, E., Romand, J., and Vodar, B.: 1951, *J. Chem. Phys.* **19**, 379.
Salahub, D. R. and Sandorfy, C.: 1971, *Chem. Phys. Letters* **8**, 71.
Samson, J. A. R.: 1982, in S. Flügge (ed.), 'Atomic Photoionization', *Handbuch der Physik*, Springer-Verlag, Berlin.
Samson, J. A. R. and Cairns, R. B.: 1964, *J. Geophys. Res.* **69**, 4583.
Samson, J. A. R. and Cairns, R. B.: 1965, *J. Opt. Soc. Am.* **55**, 1035.
Sauter, F.: 1931, *Ann. Physik, Ser. 5* **9**, 217.
Saxon, R. P.: 1983, *J. Chem. Phys.* **78**, 312.
Schoen, R. I.: 1962, *J. Chem. Phys.* **37**, 2032.
Schürgers, M. and Welge, K. H.: 1968, *Z. Naturforsch.* **23a**, 1508.
Schurath, U., Tiedemann, P., and Schindler, R. N.: 1969, *J. Phys. Chem.* **73**, 456.
Seery, D. J. and Britton, D.: 1964, *J. Phys. Chem.* **68**, 2263.
Selwyn, G., Podolske, J., and Johnston, H. S.: 1977, *Geophys. Res. Letters* **4**, 427.
Shardanand, and Rao, A. D. P.: 1977, *J. Quant. Spectr. Rad. Transfer* **17**, 433.
Sharp, T. E.: 1971, *Atom. Data* **2**, 119.
Simon, P.: 1974, in A. J. Broderick and T. M. Hard (eds.), 'Balloon Measurements of Solar Fluxes between 1960 and 2300 Å', *Proceedings of the Third Conference on the Climatic Impact Assessment Program*, Dept. Transportation report DOT-TSC-OST-74-15, pp. 137-141.
Singh, P. D. and Dalgarno, A.: 1987, in E. J. Rolfe and B. Battrick (eds.), 'Photodissociation Lifetimes of CH and CD Radicals in Comets', *Symposium on the Diversity and Similarity of Comets*, ESA SP-278, pp. 177-179.
Singh, P. D., van Dishoeck, E. F., and Dalgarno, A.: 1983, *Icarus* **56**, 184.
Siscoe, G. L. and Mukherjee, N. R.: 1972, *J. Geophys. Res.* **77**, 6042.
Slanger, T. M. and Black, G.: 1982, *J. Chem. Phys.* **77**, 2432.
Spencer, J. E. and Rowland, F. S.: 1978, *J. Phys. Chem.* **82**, 7.
Stedman, D. H., Chameides, W., and Jackson, J. O.: 1975, *Geophys. Res. Letters* **2**, 22.
Stephens, T. L. and Dalgarno, A.: 1972, *J. Quant. Spectr. Rad. Transfer* **12**, 569.
Stief, L. J., Donn, B., Glicker, S., Gentieu, E. P., and Mentall, J. E.: 1972, *Astrophys. J.* **171**, 21.
Stobbe, M.: 1930, *Ann. Physik, Ser. 5* **7**, 661.
Stockwell, W. R. and Calvert, J. G.: 1978, *J. Phot. Chem.* **8**, 193.
Strobel, D. F.: 1973, *J. Atmospheric. Sci.* **30**, 489.
Stull, D. R. and Prophet, H.: 1971, *JANAF Thermodynamic Tables*, 2nd edition, NSRDS-NBS 37, U.S. Government Printing Office, Washington, DC.
Sun, H. and Weissler, G. L.: 1955, *J. Chem. Phys.* **23**, 1160.
Suto, M., Wang, X., and Lee, L. C.: 1987, *J. Chem. Phys.* **85**, 4228.
Swider, W., Jr.: 1969, *Rev. Geophys.* **7**, 573.
Tanaka, Y., Inn, E. C. Y., and Watanabe, K.: 1953, *J. Chem. Phys.* **21**, 1651.
Thompson, B. A., Harteck, P., and Reeves, R. R., Jr.: 1963, *J. Geophys. Res.* **68**, 6431.
Torr, M. R., Torr, D. G., and Ong, R. A.: 1979, *Geophys. Res. Letters* **6**, 771.
Van Dishoeck, E.: 1984, 'Photodissociation and Excitation of Interstellar Molecules, Calculations and Astrophysical Applications', Ph.D. Thesis, University of Leiden.
Van Dishoeck, E. F.: 1987, *J. Chem. Phys.* **86**, 196.
Van Dishoeck, E. F. and Dalgarno, A.: 1984, *Icarus* **59**, 305.
Van Dishoeck, E. F., van Hemert, M. C., and Dalgarno, A.: *J. Chem. Phys.* **77**, 3693.
Vanlaethem-Meurée, N., Wisemberg, J., and Simon, P. C.: 1978, *Bull. Acad. Roy. Belgique, Cl. Sci.* **64**, 31.
Vanlaethem-Meurée, N., Wisemberg, J., and Simon, P. C.: 1979, *Geophys. Res. Letters* **6**, 451.
Walker, T. E. H. and Kelly, H. P.: 1972, *Chem. Phys. Letters* **16**, 511.
Watanabe, K.: 1954, *J. Chem. Phys.* **22**, 1564.
Watanabe, K.: 1958, *Adv. Geophys.* **5**, 153.
Watanabe, K. and Jursa, A. S.: 1964, *J. Chem. Phys.* **41**, 1650.
Watanabe, K. and Marmo, F. F.: 1956, *J. Chem. Phys.* **25**, 965.
Watanabe, K. and Sood, S. P.: 1965, *Sci. Light* **14**, 36.
Watanabe, K. and Zelikoff, M.: 1953, *J. Opt. Soc. Am.* **43**, 753.
Watanabe, K., Matsunaga, F. M., and Sakai, H.: 1967, *Appl. Optics* **6**, 391.
Watson, R. T.: 1977, *J. Phys. Chem. Data* **6**, 871.
Weaver, J., Meagher, J., and Heicklen, J.: 1976, *J. Photochem.* **6**, 111.

- Weissler, G. L., Samson, J. A. R., Ogawa, M., and Cook, G. R.: 1959, *J. Opt. Soc. Am.* **49**, 338.
- Welge, K. H.: 1974, *Can. J. Chem.* **52**, 1424.
- West, G. A.: 1975, 'Cyanide Radical Molecular Electronic and Vibrational Chemical Laser: Hydrogen Cyanide Polyatomic Chemical Laser', Thesis, University of Wisconsin, Madison, WI.
- West, J. B. and Morton, J.: 1978, *Atom. Data Nucl. Data Tables* **22**, 104.
- Whipple, F. L. and Huebner, W. F.: 1976, *Ann. Rev. Astron. Astrophys.* **14**, 143.
- Woolley, W. D. and Back, R. A.: 1968, *Can. J. Chem.* **46**, 295.
- Wu, C. Y. R. and Judge, D. L.: 1981, *J. Chem. Phys.* **74**, 3804.
- Wyckoff, S. and Wehinger, P. A.: 1976, *Astrophys. J.* **204**, 604.
- Yao, F., Wilson, I., and Johnston, H.: 1982, *J. Phys. Chem.* **86**, 3611.
- Yoshino, K., Freeman, D. E., Esmond, J. R., and Parkinson, W. H.: 1984, *Planetary Space Sci.* **31**, 339.
- Yung, Y. L., Allen, M., and Pinto, J. P.: 1984, *Astrophys. J. Suppl. Ser.* **55**, 465.
- Zelikoff, M., Watanabe, K., and Inn, E. C. Y.: 1953, *J. Chem. Phys.* **21**, 1643.

Index of Species – Full Names

- Acetaldehyde, 250
- Acetylene, 178
- Amidogen, 101
- Ammonia, 169
- Atomic argon, 33
- Atomic carbon, 13
- Atomic chlorine, 31
- Atomic fluorine, 23
- Atomic helium, 11
- Atomic hydrogen, 9
- Atomic nitrogen, 17
- Atomic oxygen, 19
- Atomic potassium, 35
- Atomic sodium, 25
- Atomic sulfur, 27
- Atomic xenon, 36

- Bromine monoxide, 99
- Bromine nitrate, 232

- Carbon difluorodichloride, 227
- Carbon dioxide, 120
- Carbon disulfide, 156
- Carbon fluorotrichloride, 230
- Carbon monoxide, 66
- Carbon oxysulfide, 138
- Carbon tetrachloride, 233
- Carbonyl chlorofluoride, 201
- Carbonyl fluoride, 198
- Chlorine dioxide, 153
- Chlorine nitrate, 225
- Chlorine nitrite, 200
- Chlorine peroxy, 155
- Chlorine trioxide, 202
- Chlorodifluoromethane, 223
- Chloromethane, 220
- Cyano, 64
- Cyanoacetylene, 221

- Diatomeric carbon, 61
- Diatomeric chlorine, 98

- Diatomeric fluorine, 94
- Diatomeric hydrogen, 38
- Diatomeric nitrogen, 77
- Diatomeric oxygen, 87
- Dinitrogen pentoxide, 254

- Ethane, 255
- Ethylene, 236

- Formaldehyde, 183
- Formic acid, 216

- Hydrogen chloride, 93
- Hydrogen cyanide, 111
- Hydrogen fluoride, 56
- Hydrogen isocyanate, 192
- Hydrogen oxybromide, 166
- Hydrogen oxyiodide, 167
- Hydrogen oxychloride, 137
- Hydrogen peroxide, 191
- Hydrogen sulfide, 115
- Hydroperoxyl, 114
- Hydroxyl radical, 47

- Iodine nitrate (isocyanic acid), 235

- Methane, 204
- Methyl alcohol, 242
- Methylchloroform, 261
- Methylhydroperoxide, 252
- Methylidyne, 43
- Molecular hydrogen, 38

- Negative atomic hydrogen ion, 8
- Nitric acid, 222
- Nitric oxide, 82
- Nitrogen dioxide, 132
- Nitrogen trioxide, 196
- Nitrosyl chloride, 152
- Nitrosyl iodide, 168
- Nitrous acid, 194

- Nitrous oxide, 129
Nitryl chloride, 199
Ozone, 135
Peroxynitric acid, 248
Phosgene, 203
Phosphine, 190
Sulfur dioxide, 149
Sulfur monoxide, 95
Water, 102

Index of Species – Chemical Structures

Ar,	33	F,	23
		F ₂ ,	94
BrO,	99	H,	9
BrONO ₂ ,	232	H-,	8
C(³ P), (¹ D), C(¹ S),	13	H ₂ ,	38
C ₂ ,	61	H ₂ CO,	183
C ₂ H ₂ ,	178	H ₂ O,	102
C ₂ H ₄ ,	236	H ₂ O ₂ ,	191
C ₂ H ₆ ,	255	H ₂ S,	115
CCl ₄ ,	233	HC ₃ N,	221
CF ₂ Cl ₂ ,	227	HCl,	93
CFCl ₃ ,	230	HCN,	111
CH,	43	HCOOH,	216
CH ₃ CCl ₃ ,	261	He,	11
CH ₃ CHO,	250	HF,	56
CH ₃ Cl,	220	HNCO,	192
CH ₃ CO ₃ NO ₂ ,	267	HNO ₃ ,	222
CH ₃ O ₂ NO ₂ ,	263	HO ₂ ,	114
CH ₃ OH,	242	HO ₂ NO ₂ ,	248
CH ₃ OOH,	252	HOBr,	166
CH ₃ SSCH ₃ ,	265	HOCl,	137
CH ₄ ,	204	HOI,	167
CHF ₂ Cl,	223	HONO,	194
Cl,	31		
Cl ₂ ,	98	INO,	168
CINO,	152	IONO ₂ ,	235
CINO ₂ ,	199	K,	35
ClO ₂ , (OCIO),	153		
ClOO,	155	N,	17
ClO ₃ ,	202	N ₂ ,	77
ClONO,	200	N ₂ O,	129
ClONO ₂ ,	225	N ₂ O ₅	254
CN,	64	Na,	25
CO(X ¹ Σ ⁺), CO(a ³ Π),	66	NH ₂ ,	101
CO ₂ ,	120	NH ₃ ,	169
COCl ₂ ,	203	NO,	82
COF ₂ ,	198	NO ₂ ,	132
COFCl,	201	NO ₃ ,	196
CS ₂ ,	156		

Astrophysics and Space Science **195**: 293–294, 1992.

O(³ P), O(¹ D), O(¹ S),	19	S(³ P), S(¹ D), S(¹ S),	27
O ₂ ,	87	SO,	95
O ₃ ,	135	SO ₂ ,	149
OCS,	138		
OH,	47	Xe,	36
PH ₃ ,	190		